# PROCEEDINGS

# VETERINARY PATHOLOGY SERVICE
# WEDNESDAY SLIDE CONFERENCE
# 2012-2013


**JOINT PATHOLOGY CENTER**
**SILVER SPRING, MD 20910**
**2013**

**ML2013**

**JOINT PATHOLOGY CENTER**
**VETERINARY PATHOLOGY SERVICE**

# WEDNESDAY SLIDE CONFERENCE
# 2012-2013

**100 Cases**

**JOINT PATHOLOGY CENTER**
**SILVER SPRING, MD 20910**
**2013**

**ML2013**

# PREFACE

The Veterinary Pathology Service of the Joint Pathology Center (JPC), formerly known as the Armed Forces Institute of Pathology, has conducted a weekly slide conference during the resident training year since 12 November 1953. This ever-changing educational endeavor has evolved into the annual Wednesday Slide Conference program in which cases are presented on 25 Wednesdays throughout the academic year and distributed to 135 contributing military and civilian institutions from around the world. Many of these institutions provide structured veterinary pathology resident training programs. During the course of the training year, histopathology slides, digital images, and histories from selected cases are distributed to the participating institutions and to the JPC Veterinary Pathology Service. Following the conferences, the case diagnoses, comments, and reference listings are posted online to all participants.

This study set has been assembled in an effort to make Wednesday Slide Conference materials available to a wider circle of interested pathologists and scientists, and to further the education of veterinary pathologists and residents-in-training. The number of histopathology slides that can be reproduced from smaller lesions requires us to limit the number of participating institutions.

For their participation and permission to use their cases in this study set, we wish to thank each institution, and especially the individuals who prepared and submitted the selected cases.

A special note of appreciation is extended to the reviewers who helped edit and review this year's individual case summaries:

A final note of thanks goes to the moderators, who unselfishly gave of their time and expertise to help make each conference both enjoyable and educational.

Gross images and photomicrographs were submitted by contributing institutions where indicated.

**Joint Pathology Center**
**WEDNESDAY SLIDE CONFERENCE 2012-2013**
**Table of Contents**

**WSC 2012-2013 Table of Contents**

**WSC 2012-2013 Table of Contents**

**Joint Pathology Center**
**Veterinary Pathology Services**

# WEDNESDAY SLIDE CONFERENCE 2012-2013

## Conference 1

**19 September 2012**

---

**CASE I:** ITPA Berne 2011/2 (JPC 4002463).

**Signalment:** 15-year-old female alpaca, (*Lama pacos*).

**History:** The patient presented with a history of 2 weeks loss of appetite, apathy and weight loss. An intra-abdominal neoplasia was suspected at ultrasound examination.

**Gross Pathology:** The alpaca was in a poor body condition. At necropsy, in the second compartment of the stomach (C2), there was a 30x20x15 cm, non-encapsulated, infiltrative, and relatively well demarcated mass which on cut surface contained abundant fibrous connective tissue. The mucosa was focally, extensively ulcerated and covered by a thick layer of necrotic material and pus. In the mesentery and intestinal serosa, there were multiple white nodules

*1-1. Stomach, C2, alpaca: In the second compartment of the stomach (C2), there is a non-encapsulated, infiltrative, and relatively well demarcated mass which on the cut surface contained abundant fibrous connective tissue. In the mesentery and intestinal serosa there are multiple white nodules of firm consistency. (Photograph courtesy of Institute of Animal Pathology, University of Berne, Länggasstrasse 122, CH-3001, Berne, Switzerland http://www.itpa.vetsuisse.unibe.ch/fiwi/.)*

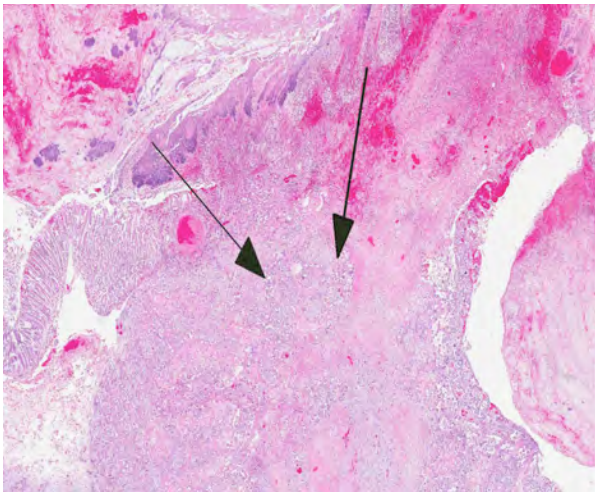

*1-2. Stomach, C2, alpaca: Multifocally and transmurally, the stomach wall is infiltrated by a moderately cellular and poorly demarcated neoplasm (arrows). There is a large coagulum of fibrin, hemorrhage, and entrapped bacterial colonies overlying the ulcerated mucosa. (HE 8X)*

of firm consistency, approximately 1x1x1cm size. White nodules were also present within the liver capsule and parenchyma, approximately 1.5x1x1cm size. In the colon and third compartment of the stomach (C3), there were multiple chronic mucosal ulcerations. The abdomen and thorax contained approximately 500 ml of red, transparent (serosanguinous) fluid.

**Histopathologic Description:** Stomach, C2: The wall of C2 is severely disrupted by an ulcerated, infiltrative growing, non-encapsulated, poorly demarcated, densely cellular neoplasm, projecting from the mucosa and extending transmurally to the serosa, consisting of islands, nests and anastomosing cords of neoplastic epithelial cells separated by a moderate to large amount of fibrovascular stroma. The cells are polygonal, up to 30µm in diameter with abundant eosinophilic to amphophilic fibrillar cytoplasm with a large vesicular, central oval nucleus and prominent, single to multiple nucleoli. Some nests of neoplastic cells exhibit gradual individual cell keratinization, prominent concentrically lamellated keratin "pearls", or contain cellular debris admixed with inflammatory cells, mainly lymphocytes and degenerate neutrophils. Intercellular bridges between keratinized cells are prominent. There are approximately 5 mitoses per 400x field with frequent bizarre mitotic figures. There is severe anisocytosis and anisokaryosis. Multifocally within the neoplasm there are large areas of necrosis, hemorrhage and a mixed inflammatory infiltrate of lymphocytes, plasma cells, neutrophils and some macrophages. Many submucosal and subserosal vessels contain clusters of neoplastic cells (tumor emboli) as well as fibrin thrombi. Overlying the ulcerated mucosa, there is abundant fibrillar eosinophilic material (fibrin exudation) and hemorrhage, admixed with cellular and karyorrhectic debris (necrosis) and bacterial colonies. Throughout the mass, but especially along the serosa, there are multiple nodules or bands of abundant fibrous connective tissue (scirrhous response).

**Contributor's Morphologic Diagnosis:** C2: Gastric squamous cell carcinoma.

**Contributor's Comment:** This was an interesting case of a rare presentation of gastric squamous cell carcinoma (SCC) with carcinomatosis and metastases to the liver and mesenteric lymph nodes in an alpaca. There are numerous reports of neoplasia in South American camelids, including lymphoma, urogenital tumors, cutaneous and mucocutaneous neoplasia, oral, intraocular, gastrointestinal, pulmonary, neuroendocrine and brain neoplasia (Table 1).[5]

| Tumor type | | Total no tumors | Alpacas (no.) | Llamas (no.) | Mean age alpacas (yrs)* | Mean age llamas (yrs) | Location(s) |
|---|---|---|---|---|---|---|---|
| Fibroma/fibropapilloma | | 12 | 8 | 2 | 5.6 | 11.5 | Face; nose; lip; distal limb; gingiva; hard palate |
| Carcinoma | | | | | | | |
| | Cutaneous | 4 | 0 | 4 | — | 13.5 | Perineum; trunk; limb |
| | Ocular | 2 | 1 | 1 | U | 14 | 3rd eyelid |
| | Mammary | 2 | 0 | 2 | — | 17 | Metastatic to local lymph node; disseminated |
| | Un-differentiated | 1 | 1 | 0 | 12 | — | Disseminated |
| Adenocarcinoma | | | | | | | |
| | Biliary | 2 | 0 | 2 | — | 10.5 | Disseminated |
| | Pancreas | 1 | 1 | 0 | 10 | — | Disseminated |
| | Intestine | 1 | 0 | 1 | — | 8 | Disseminated |
| Lymphoma | | 5 | 4 | 1 | 1.5 | 15 | Disseminated |
| Fibrosarcoma | | 4 | 1 | 3 | 6 | 13 | Lip; gingiva; maxilla; cornea |
| Lipoma | | 2 | 0 | 2 | — | 12 | Mesentery; subcutis |
| Melanocytoma | | 1 | 0 | 1 | — | 11 | Pectoral skin |
| Leiomyosarcoma | | 1 | 0 | 1 | — | 12 | Uterus |
| Interstitial cell tumor | | 1 | 1 | 0 | 9 | — | Ovary |
| Primitive stromal tumor | | 1 | 1 | 0 | U | — | Testis |

* U = unknown.

Gastric squamous cell carcinoma in ruminants is usually quite rare and only few have been reported in llamas and alpacas.[3,5] However, in a 5 year (2001-2006) study at Oregon State University it was reported that cutaneous and mucocutaneous squamous cell carcinoma (SCC) was the most frequent malignant neoplasm identified, although in previous studies lymphoma was most commonly reported.[5]

Histologically, C1 and portions of C2 are composed of non-keratinized stratified squamous epithelium, whereas the rest of C2 and all of C3 have a mucinous glandular epithelium.

In previous cases, neoplastic cells most commonly originated from squamous mucosal epithelium of compartments 1 and 2, but it could arise also from the glandular mucosa of compartment 3.[3] In this case, the neoplasm was most closely related to the stratified squamous epithelium of C2. SCC of glandular mucosa could derive from metaplasia of glandular epithelium, from growth of heterotopic squamous cell rests, or from multipotent cells of the crypt gland base, as suggested in prevous reports in dogs.[3]

Commonly described sites of metastases are the liver, diaphragm, mesentery, and myocardium. The mode of metastatic spread is by implantation and vascular dissemination, as seen in horses with gastric SCC.[3]

Several factors have been associated with the development of gastric papillomas and squamous cell carcinomas in humans and other species including host, dietary, genetic, environmental conditions and infectious agents. In cattle, papillomas of the esophagus and reticulorumen are caused by bovine papillomavirus 4 (BPV-4), whereas fibropapillomas of the esophagus, esophageal groove and rumen are caused by bovine papillomavirus 2. It is very seldom for viral particles to be seen in the tumor. Malignant neoplasia of bovine esophagus and forestomach is extremely rare.[2,3] On the contrary, SCC involving male and female genitalia, ocular and periocular tissue and stomach is most commonly reported in the horse. Equine gastric SCC metastasized most frequently to retropharyngeal lymph nodes.[4]

The frequency of llamas and alpacas as patients in the veterinary hospital is increasing; therefore it is important to improve the knowledge about possible lesions, prevalence and predisposing factors causing diseases in these animals.

Table 1. Summary of 40 tumors reported in 20 llamas and 18 alpacas between 2001-2006 at Oregon State University.[5]

**JPC Diagnosis**: C2: Squamous cell carcinoma.

**Conference Comment**: The contributor provided a very good characterization of squamous cell carcinomas (SCC) in alpacas, as well as comparisons to other species such as the horse, in which SCC is the most common gastric tumor. Conference participants readily agreed upon the diagnosis; however, during the discussion a question was raised regarding histological determination of the location of the specimen (C2).

Following is a brief summary of new world camelid gastric anatomy and histology: As the contributor described, new world camelid stomachs are composed of three compartments :C1, C2, and C3, which are sometimes referred to as the proximal compartment (PC), intermediate compartment (IC) and the distal compartment (DC), respectively. C1 is often compared with the rumen, and constitutes the largest chamber (comprising approximately 83% of the gastric volume). C2 is somewhat kidney-shaped and is the smallest of the three compartments. C3 is tubular and elongated and accounts for approximately 11% of the gastric volume. Histologically the majority of C1 is nonglandular, covered by stratified squamous epithelium which is supported by a dense collagenous lamina propria. This tissue is arranged in folds (rather than papillae as in ruminants) which are more prominent when the stomach is contracted. Smaller, more ventral portions of C1 (known as cranial and ventral glandular saccules) are lined by columnar epithelium and deep tubular glands which are supported by a smaller amount of looser connective tissue. C1 communicates with C2 through the ventricular furrow. C2 has thick walls, and histologically is divided into two regions: a dorsal nonglandular and a ventral glandular portion, each of which are similar to those described for C1. Lymphoid tissue may be found in the lamina propria of the glandular portions of C2. The muscularis mucosae is absent in the nonglandular regions of both C1 and C2, and is present in glandular areas, but is incomplete. C2 communicates with C3 via the channel of isthmus, a small tubular continuation of the ventricular furrow that is lined by stratified epithelium. C3 is otherwise covered by a glandular mucosa, with 3 regions differing histologically: the proximal region has abundant lymphoid tissue in the mucosa and submucosa; the central region has simple mucous-secreting tubular glands; and the caudal region has fundic glands in the ventral portion and simple tubular glands in the dorsal (pyloric) region. C3 has a well-developed muscularis mucosae and a thin submucosa. Surrounding all three gastric compartments is a muscularis comprised of inner circular and outer longitudinal layers. [1]

**Contributing Institution**: Institute of Animal Pathology
University of Berne
Länggasstrasse 122, CH-3001
Berne, Switzerland
http://www.itpa.vetsuisse.unibe.ch/fiwi/

**References:**

1. Alzola RH, Ghezzi MD, Gimeno EJ, et al. Topography and morphology of the llama (*Lama galma*) stomach. *Int J Morphol.* 2004;22 (2):155-164.
2. Mckenzie EC, Mills JN, Bolton JR. Gastric squamous cell carcinoma in three horses. *Aust Vet J*. 1997;75(7):480-483.
3. Sartin EA, Waldridge BM, Carter DW, et al. Gastric squamous cell carcinoma in three llamas. *J Vet Diagn Invest.* 1997;9:103-106.
4. Schuh JCL. Squamous cell carcinoma of the oral, pharyngeal and nasal mucosa in the horse. *Vet Pathol*. 1986;23:205-207.
5. Valentine BA, Martin JM. Prevalence of neoplasia in llamas and alpacas (Oregon State University, 2001-2006). *J Vet Diagn Invest*. 2007;19:202-204.

**CASE II:** GC-12 (JPC 4018081).

**Signalment:** Nine-month-old Red Angus steer, *(Bos taurus)*.

**History:** This steer belonged to a herd of 250 animals that were weaned one month prior to presentation. This steer had a brief history of inability to stand up and was treated with 6.5 cc Draxxin® (tulathromycin). Ten other animals in this herd were treated for respiratory disease and twenty were seen limping in the previous week. Another steer in this herd had an enlarged stifle that was tapped and cytology revealed inflammatory arthropathy.

**Gross Pathology:** Brain: There were multifocal random foci of malacia and hemorrhage in the gray and white matter of the cerebrum, cerebellum, and brainstem. The meninges in the ventral aspect of the brain contained a moderate accumulation of fibrinosuppurative material. The thoracic cavity contained approximately 50 mL of serous fluid with fibrin strands. The lungs failed to fully collapse upon opening the thoracic cavity. The right cranial and middle lobes and the left cranial lobe were consolidated and attached to the thoracic wall by a thick mat of fibrin (approximately 50% of the total lung). On cut sections of these lobes, there was exudation of small amounts of whitish suppurative material. Fibrin adhesions were also seen in the caudal portion of the right caudal lobe. The pulmonary parenchyma at this level was grossly normal. Stifle joints in both sides contained increased volume of yellowish and watery synovial fluid with fibrin clots. No gross lesions were found in the heart.

**Laboratory Results:** Bacterial culture from cerebral swabs and fresh samples of brain yielded growth of *Histophilus somni*. *Mycoplasma bovis* culture from joint swab was positive. Polymerase chain reaction (PCR) for detection of *Mycoplasma bovis, Chlamydia* spp., bovine viral diarrhea virus, bovine respiratory syncytial virus, bovine coronavirus, bovine herpesvirus type 1, and parainfluenza type 3 from lung tissue were all negative. Bacterial cultures from the lung yielded no growth of significant pathogens.

**Histopathologic Description:** Brain: Sections of cerebrum, cerebellum, or brainstem contain multiple, variably-sized, and random foci infiltrated by moderate to large numbers of neutrophils and lesser numbers of macrophages associated with hemorrhage, edema, degeneration, necrosis and loss of gray and white matter. The meninges over these areas are expanded by sheets of neutrophils and hemorrhage. The tunica media of numerous small to medium sized blood vessels in the meninges and cerebral parenchyma is necrotic and is often effaced by moderate amounts of fibrin (fibrinoid necrosis), and their lumen contains fibrin thrombi. Colonies of Gram negative bacilli are frequently observed within the blood vessels and in surrounding neuropil.

**Contributor's Morphologic Diagnosis:** Meningoencephalitis, necrosuppurative and hemorrhagic, multifocal, acute, severe, with necrotizing vasculitis, thrombosis, with intralesional colonies of Gram negative bacilli, etiology consistent with *Histophilus somni*.

**Contributor's Comment:** *Histophilus somni* (previously known as *Haemophilus somnus*) is a Gram negative coccobacillus that causes septicemia and a number of clinical signs in cattle, termed altogether as "*Histophilus somni* disease complex" or "histophilosis".[6,7,8] The clinical signs in cattle include

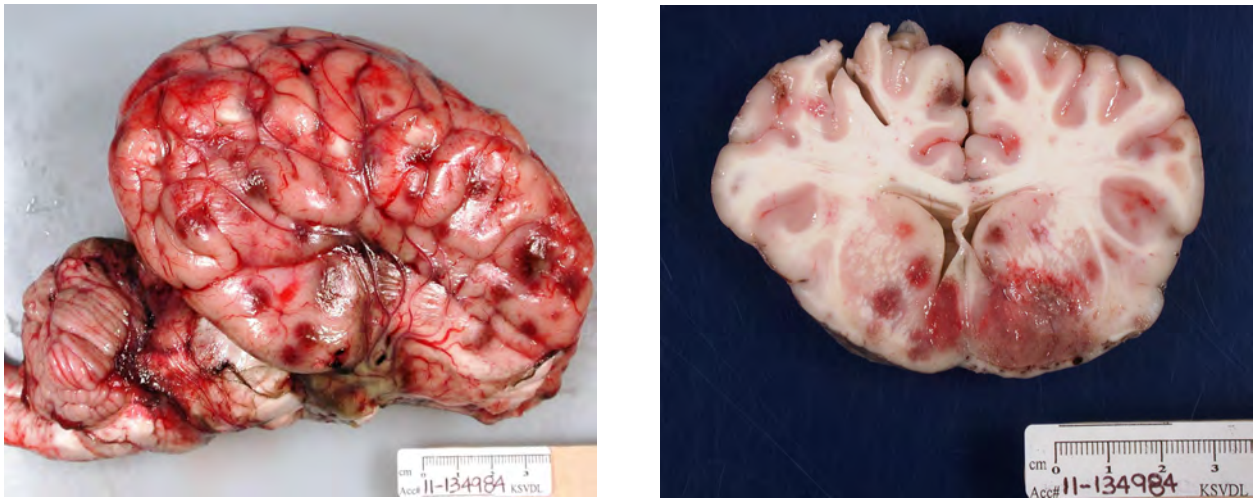


*2-1, 2-2. Brain, ox: There are multifocal, random foci of malacia and hemorrhage in the gray and white matter of the cerebrum, cerebellum, and brain stem. (Photographs courtesy of Department of Diagnostic Medicine/Pathobiology, Kansas State University - College of Veterinary Medicine, 1800 Denison Avenue, Manhattan, KS 66506, www.vet.k-state.edu/depts/dmp/.)*

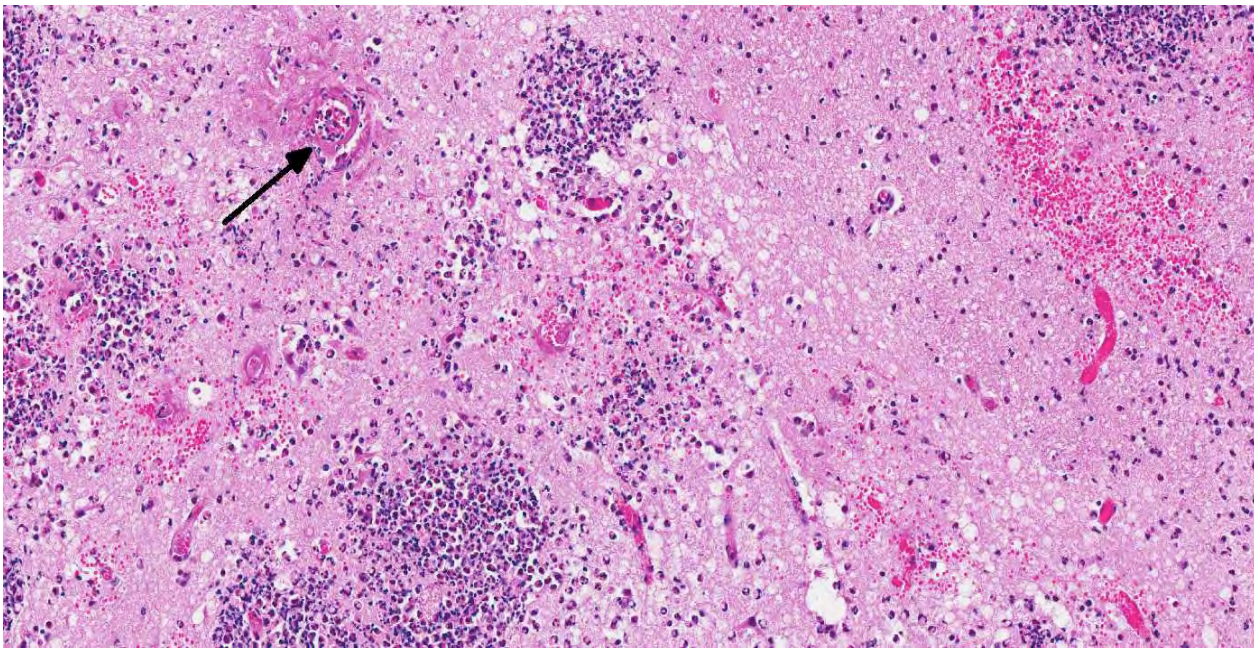

*2-3. Cerebrum, ox: Multifocal areas of lytic necrosis are focus on vessels. Remaining vessels often exhibit thickening of vascular walls by protein and necrotic cells (fibrinoid necrosis). (HE 116X)*

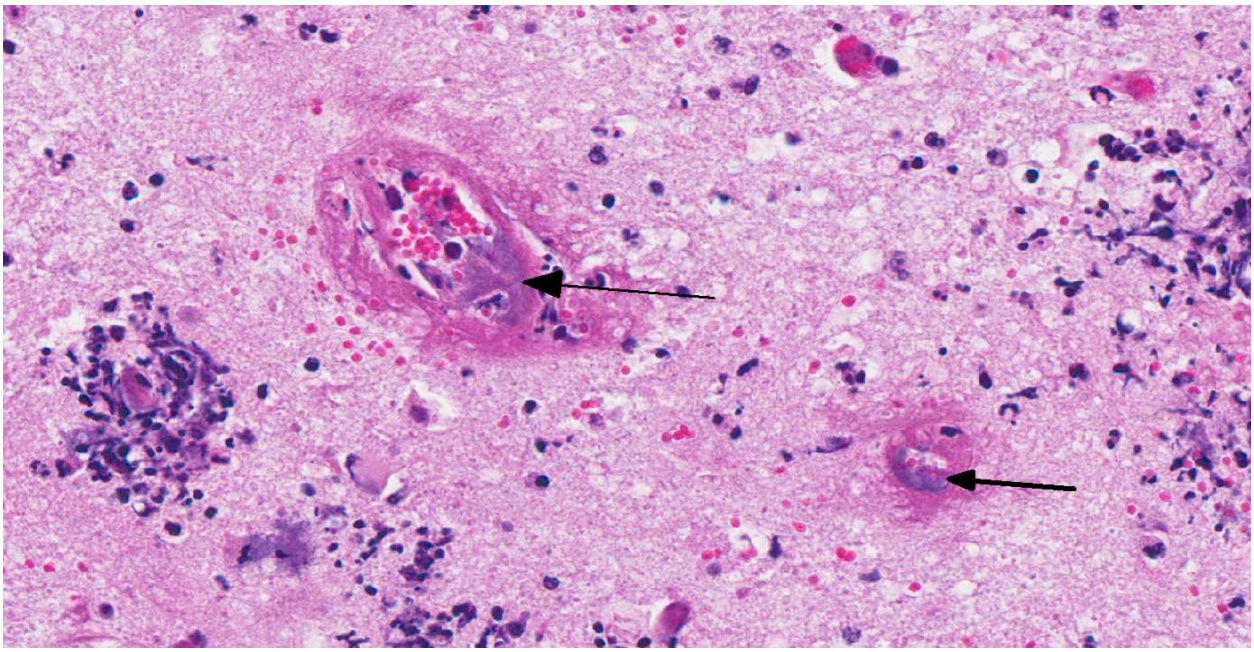

*2-4. Cerebrum, ox: Frequently, vessels exhibit fibrinoid necrosis with extrusion of eosinophilic protein into the perivascular space (as well as perivascular hemorrhage) and often contain colonies of small bacilli (arrows). (HE 360X)*

pneumonia; myocarditis; polyarthritis; mastitis; genital infection; abortion; reproductive failure; and thrombotic meningoencephalitis (TME), the neurological form of the disease.[1,3,6,7] Septicemia caused by *H. somni* develops in cattle in many age groups, but it is more prevalent in young growing cattle in feedlots during the winter time.[3,6,8] Other species that are affected include sheep, bison, and bighorn sheep.[1]

The lesions observed in the central nervous system in this steer are compatible with the neurological form of *H. somni* disease complex, or TME, which was confirmed by bacterial culture from cerebral swabs and

fresh samples of the brain. Historically, TME was the most common disease presentation of the bacterial infection; however, in recent years, the most common presentations are pleuropneumonia and myocarditis.[6,8,9] The gross lesions of TME are random, but most often localized at the cortical gray matter-white matter junction of the cerebral cortex and in the thalamus, where it is presumed that the bacteria can lodge and replicate in the blood vessels due to changes in vessel diameter and flow patterns.[6,7] The lesions consist of multiple variable sized dark red foci of necrosis and hemorrhage.[6,7] The meninges over the hemorrhagic areas are usually affected.[6,7] Similar lesions are also observed in the brainstem and spinal cord.[6,7] Microscopic lesions are characterized by severe vasculitis and thrombosis with infarction, and infiltrates of neutrophils and macrophages in the site.[6,7]

*H. somni* is a commensal of the respiratory and reproductive tracts.[2] The pathogenesis of the septicemia leading to TME in cattle is unknown, but it is believed that some virulent bacterial strains first colonize the surface of the mucous membranes in the upper respiratory tract and invade the circulatory system.[3,7] The bacteria adhere to the endothelial cells, causing vasculitis, thrombosis, and infarction and continue replicating in the thrombus, triggering an inflammatory response.[7] Several studies have shown that virulent strains of *H. somni* produce a multitude of virulence factors aimed at evasion of host defenses for colonization of tissues. Virulence factors in *H. somni* include, but are not limited to, lipooligosaccharides (LOS), attachment and induction of apoptosis in bovine endothelial cells, intraphagocytic survival, immunoglobulin Fc binding proteins (IgBPs), biofilm formation, histamine production, and integration of phosphorylcholine (ChoP) into its LOS.[2,9] Disease in TME likely occurs as a result of apoptosis of endothelial cells and host inflammation due in part to the presence of endotoxin and the activation of the coagulation cascade, and the recruitment of polymorphonuclear leukocytes and macrophages to sites of infection.[3,9]

**JPC Diagnosis**: Cerebrum: Meningoencephalitis, fibrinosuppurative, multifocal, severe, with vasculitis, fibrinoid necrosis, rarefaction, and intravascular bacterial colonies.

**Conference Comment**: The hallmark lesion of TME is vasculitis and thrombus formation due to endothelial cell damage and subsequent exposure of the underlying extracellular matrix. Although the mechanism of vascular injury by *H. somni* is not fully understood, it is thought to be due to apoptosis caused by direct effects of the bacteria and its lipopolysaccharide (LOS) on endothelial cells.[4,5] However, because there is often endothelial damage in areas devoid of bacterial antigen, studies in more recent years have attempted to elucidate additional mechanisms that may contribute to this vasculitis. These studies have suggested that activated platelets likely play an important role in the vascular damage. Although the primary role of platelets lies in maintaining hemostasis, platelets also contribute to vascular inflammation and injury by expressing chemotactic factors (platelet factor 4, lipooxygenase products, RANTES), cytokines (IL-1β), platelet activating factor, and surface molecules (CD40L, FasL, P-selectin)[5] that can interact with leukocytes and endothelial cells.[4,5] Additionally, it has been found that platelets activated by *H. somni* induce endothelial apoptosis via caspases 8 and 9, and promote endothelial cell production of reactive oxygen species (ROS), which further enhances apoptosis. Conversely, inhibitors of either caspase 8 or 9, or the disruption of ROS activity, were found to decrease endothelial apoptosis.[5] Interestingly, bovine (and human) endothelial cells appear to be resistant to Fas-mediated apoptosis, and it has been suggested that activated platelets may induce apoptosis of endothelial cells via a novel pathway that utilizes caspases 8 and 9 as well as ROS.[5] These findings contribute to our developing understanding of mechanisms of endothelial cell damage not only in *H. somni* infections, but in bacterial sepsis in general as well.

**Contributing Institution:** Kansas State University - College of Veterinary Medicine
Department of Diagnostic Medicine/Pathobiology1800 Denison Avenue
Manhattan, KS 66506
www.vet.k-state.edu/depts/dmp/

**References:**

1. Ward Alton CS, Weiser GC, Anderson BC, et al. *Haemophilus somnus* (*Histophilus somni*) in bighorn sheep. *Can J Vet Res*. 2006;70:34-42.
2. Corbeil LB. Histophilus somni host-parasite relationships. *Anim Health Res Rev*. 2008;8:151-160.
3. Fecteau G, George LW. Bacterial meningitis and encephalitis in ruminants. *Vet Clin Food Anim*. 2004;20:363-377.
4. Kuckleburg CJ, McClenahan DJ, Czuprynski CJ. Platelet activation by *Histophilus somni* and its LOS induces endothelial cell pro-inflammatory responses and platelet internalization. *Shock*. 2008;29(2): 189-196.
5. Kuckleburg CJ, Tiwari R, Czuprynski CJ. Endothelial cell apoptosis induced by bacteria-activated platelets requires caspase-8 and -9 and generation of reactive oxygen species. *Thromb Haemost*. 2008;99:363-372.
6. Maxie MG, Youssef S. The Nervous system. In: Maxie MG, ed. *Jubb, Kennedy, and Palmer's Pathology of Domestic Animals*. 5th ed. Vol. 1. Edinburg, Scotland: Elsevier; 2007:281-457.

7. McGavin MD, Zachary JF. *Pathologic Basis of Veterinary Disease*. 4th ed. St Louis, MO: Elsevier; 2007.
8. Radostis OM, Gay CC, Hinchcliff KW, et al. *Veterinary Medicine: A Textbook of the Diseases of Cattle, Horses, Sheep, Pigs and Goats*. 10th ed. Edinburg, Scotland: Elsevier; 2007.
9. Siddaramppa S, Inzana TJ. Haemophilus somnus virulence factors and resistance to host immunity. *Anim Health Res Rev*. 2004;5:79-93.

**CASE III:** V11-07180 (JPC 4003694).

**Signalment:** 5-month-old male Weimaraner, *Canis lupus familiaris*, dog.

**History:** The dog was presented for anorexia. The dog developed melena. Additional abnormalities included severe thrombocytopenia, anemia, and worsening hepatopathy. The owner opted to euthanize due to lack of response to therapy and the poor prognosis.

**Gross Pathology:** The dog was in good body condition with minimal postmortem decomposition. The carcass was icteric. The liver was enlarged and friable. The liver was mottled yellow, tan and dark red in random coalescing foci and in a reticular pattern with small numbers of petechiae. Multiple lymph nodes, including the submandibular, mediastinal, pancreatic, and mesenteric lymph nodes, were dark red with hemorrhage. The lungs were congested and edematous. There were small numbers of petechiae on the endocardium of the heart. There were multiple petechiae in both right and left kidneys and the brain. The mucosal epithelium of the stomach contained rare petechiae with small numbers of erosions and ulcers in the pylorus. The small intestine contained long segments with extensive hemorrhage with smaller segments of the small intestine that contained petechiae. The stomach, small intestine, and large intestine contained digested blood.

**Laboratory Results:** Fluorescent antibody testing was performed at the Colorado State University Veterinary Diagnostic Laboratory. The liver was positive for canine adenovirus using a commercial antibody against canine adenovirus (CAV). Research monoclonal antibodies against canine adenovirus type 1 (CAV-1) and canine adenovirus type 2 (CAV -2) were used to further define the type of CAV present in the liver. Using the research monoclonal antibodies, the liver was positive for CAV-1. CAV-2 was not detected in the liver.

*3-1. Liver, dog: The liver is mottled yellow, tan and dark red in random coalescing foci and in a reticular pattern with small numbers of petechiae. Photograph courtesy of New Mexico Department of Agriculture Veterinary Diagnostic Services, http://www.nmda.nmsu.edu/animal-and-plant-protection/veterinary-diagnostic-services.*

**Histopathologic Description:** The liver contains numerous foci of centrilobular to midzonal necrosis with occasional extension of necrosis from one centrilobular area to another (bridging necrosis). The sinusoids in the foci of necrosis are dilated and filled with blood. There is a sharp distinction between the foci of necrosis in the centrilobular areas and the intact periportal areas that do contain rare apoptotic hepatocytes and swollen vacuolated hepatocytes. The necrotic foci and the adjacent sinusoids contain small numbers of macrophages with lesser numbers of lymphocytes and rare neutrophils. The portal areas contain small numbers of macrophages, lymphocytes, and rare neutrophils. Moderate numbers of Kupffer cells and macrophages and lesser numbers of intact hepatocytes contain magenta to basophilic intranuclear inclusion bodies with occasional karyomegaly. There is apoptosis of small numbers of macrophages and Kupffer cells.

**Contributor's Morphologic Diagnosis:** Severe, acute, centrilobular to midzonal bridging hepatic necrosis with mild lymphohistiocytic hepatitis and magenta to basophilic intranuclear inclusion bodies; etiology consistent with canine adenovirus type 1; infectious canine hepatitis.

**Contributor's Comment:** Canine adenovirus (CAV) is divided into two types: canine adenovirus type 1 (CAV-1) and canine adenovirus type 2 (CAV-2). CAV-1 and CAV-2 are within the genus *Mastadenovirus* in the family *Adenoviridae*, and are antigenically and genetically closely related.[3] CAV-1 is the causative agent of infectious canine hepatitis (ICH) in Canidae and Ursidae. CAV-2 causes respiratory disease (infectious tracheobronchitis) mainly in kenneled dogs.

Infection with CAV-1 in canids can range from subclinical infection to severe clinical infection leading to death.[3,5] In domestic dogs, infectious canine hepatitis is an uncommon clinical disease due to the routine vaccination of domestic dogs. However, there are sporadic individual cases and outbreaks of infectious canine hepatitis in unvaccinated domestic dogs.[1,2,3,5,7] In the wild canid population, subclinical infection with CAV-1 is most likely widespread due to the high incidence of neutralizing antibodies against CAV-1 in this population.[4,6,9]

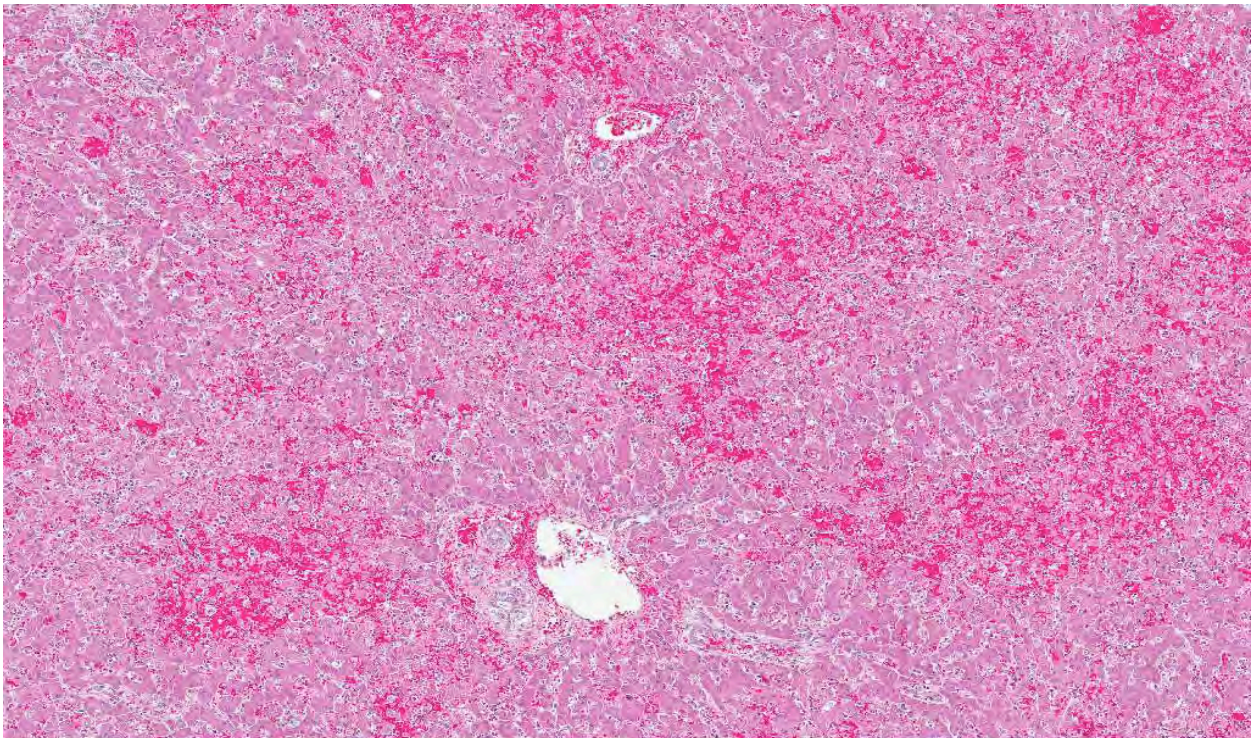

*3-2. Liver, dog: Diffusely, there is a reticular pattern of centrilobular and midzonal hepatocellular necrosis and hemorrhage. (HE 42X)*

When a susceptible dog is oronasally exposed to CAV-1, the virus localizes in the tonsils and travels to the regional lymph nodes.[5,8] The virus then traverses the lymphatic system to the thoracic duct where the virus enters the blood. After the dog becomes viremic, CAV-1 is disseminated to the tissues at which point the virus is shed in body secretions. The viremia usually lasts 4 to 8 days postinfection. During viremia, the hepatocytes and the vascular endothelial cells of many tissues are the prime targets for CAV-1 replication.

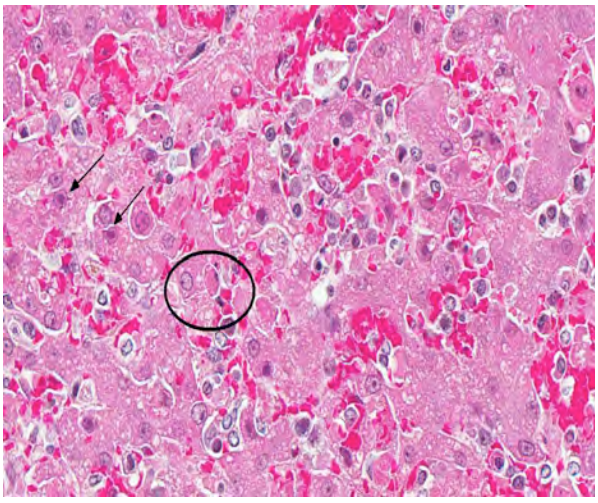

*3-3. Liver, dog: Within affected areas, hepatocytes are individualized and necrotic (circled), and often contain a 5-7 µm, rhomboidal, eosinophilic, intranuclear, adenoviral inclusion (arrows). (400X)*

Severe widespread hepatic and vascular damage, which may result in disseminated intravascular coagulation (DIC), often result in death in dogs that do not mount an adequate neutralizing antibody response. Dogs that respond with a high neutralizing antibody response by day 7 postinfection often recover from the disease. Dogs that demonstrate a partial neutralizing antibody response can develop chronic hepatitis. Dogs with a high neutralizing antibody titer before infection can develop mild or inapparent disease. In dogs that do recover from clinical illness with infectious canine hepatitis, the virus localizes in the kidney 10 to 14 days postinfection leading to secretion of the virus in the urine that can last 6 to 9 months.

The gross lesions of ICH are consistent with what one would expect considering the cellular tropism of CAV-1. The liver is slightly swollen with sharp edges, turgid, and friable with fine yellow mottling throughout the liver.[8] The gallbladder is often edematous with occasional intramural hemorrhages. There are serosal hemorrhages in the small intestine and stomach. The lymph nodes are enlarged and congested with hemorrhages. The lungs may contain hemorrhages with occasional hemorrhagic pneumonia in the caudal lung lobes. There may be hemorrhage infarcts in the cortices of the kidneys. The brain and the medullary cavity of the long bones may also contain hemorrhages.

The microscopic lesions of ICH also coincide with the cells CAV-1 infects. In fatal cases of ICH, the liver is the organ with the predominate lesions. The liver contains centrilobular to midzonal necrosis with dilated sinusoids filled with blood in the areas of necrosis.[8] There can be extension of the necrotic foci from one centrilobular area to another isolating the portal area. There is often a sharp distinction between the foci of necrosis and the normal liver in the periportal areas. The periportal hepatocytes are often normal, but can have increased apoptotic cells or be swollen and vacuolated. The leukocytic infiltrate is mild and surrounds the necrotic focus. The infiltrating leukocytes consist of neutrophils and mononuclear cells. Many of the Kupffer cells throughout the liver are necrotic. Intranuclear inclusion bodies can be seen in the intact hepatocytes, Kupffer cells, and macrophages. The microscopic lesions in the other affected organs consist of hemorrhage due to the widespread endothelial damage, which may lead to DIC. Intranuclear inclusion bodies can be seen in the endothelial cells, renal tubular epithelial cells, lymphoid follicles, red pulp of the spleen, and macrophages throughout the body.

**JPC Diagnosis**: Liver: Hepatits, necrotizing, centrilobular to midzonal, diffuse, acute, with intranuclear viral inclusions.

**Conference Comment**: The contributor did an excellent job of characterizing canine adenoviral infections. Conference participants discussed the classic distribution of this disease (centrilobular to midzonal) in comparison to the often random distribution of other viruses associated with hepatitis. Additionally, there was some discussion regarding the morphologic diagnosis, with some participants favoring "degeneration and necrosis" because of the presence of so few inflammatory cells; however, the majority of the group felt that "hepatitis" was more appropriate.

Historically, CAV-1 is synonymous with "fox encephalitis", described in 1933,[6] and "Rubarth's disease", described in 1947.[9] CAV-1 can affect dogs, foxes, wolves, coyotes, and bears.[5] Common lesions include hepatitis, anterior uveitis with corneal edema, and interstitial nephritis. Chronic changes seen in animals that survive the initial infection include hepatic fibrosis, interstitial fibrosis, glaucoma, and/or phthisis bulbi.[5]

**Contributing Institution:** New Mexico Department of Agriculture Veterinary Diagnostic Services
http://www.nmda.nmsu.edu/animal-and-plant-protection/veterinary-diagnostic-services

**References:**

1. Caudell D, Confer AW, Fulton RW, et al. Diagnosis of infectious canine hepatitis virus (CAV-1) infection in puppies with encephalopathy. *J Vet Diagn Invest.* 2005;17(1):58-61.
2. Decaro N, Campolo M, Elia G, et al. Infectious canine hepatitis: An "old" disease reemerging in Italy. *Res Vet Sci.* 2007;83(2):269-273.
3. Decaro N, Martella V, Buonavoglia C. Canine adenoviruses and herpesvirus. *Vet Clin North Am Small Anim Pract*. 2008;38(4):799-814.
4. Gese EM, Schultz RD, Johnson MR, et al. Serological survey for diseases in free-ranging coyotes (*Canis latrans*) in Yellowstone National Park. *J Wildl Dis*. 1997;33(1):47-56.
5. Greene CE. Infectious canine hepatitis and canine acidophil cell hepatitis. In: Greene CE, ed. *Infectious Diseases of the Dog and Cat.* 4th ed. St Louis, MO: Saunders Elsevier; 2012:42-47.
6. Green RG, Shillinger JE. Epizootic fox encephalitis. IV. The intranuclear inclusions. *Am J Hyg*. 1933;18:462–481.
7. Grinder M, Krausman PR. Morbidity-mortality factors and survival of an urban coyote population in Arizona. *J Wildl Dis*. 2001;37(2):312-317.
8. Pratelli A, Martella V, Elia G, et al. Severe enteric disease in an animal shelter associated with dual infections by canine adenovirus type 1 and canine coronavirus. *J Vet Med B*. 2001;48(5):385-392.
9. Rubarth S. An acute virus disease with liver lesion in dogs. (Hepatitis contagiosa canis). *Acta path. microbiol. Scand*. 1947;69 (Suppl).
10. Stalker MJ, Hayes MA. Liver and biliary system. In: Maxie MG, ed. *Jubb, Kennedy, and Palmer's Pathology of Domestic Animals*. 5th ed, vol 2. Philadelphia, PA: Elsevier Saunders; 2007:297-388.
11. Thompson H, O'Keeffe AM, Lewis JCJ, et al. Infectious canine hepatitis in red foxes (*Vulpes vulpes*) in the United Kingdom. *Vet Rec*. 2010;166(4):111-114 .

**CASE IV:** 1 (JPC 4019128).

**Signalment:** Adult female Holstein Friesian, bovine (*Bos taurus*).

**History:** This cow came from an intensive livestock farming facility of approximately 450 cows (200 lactating cows + 250 heifers, calf and dry cows). The farm had an 8 month history of several cows (approximately 15%) developing severe uncontrollable diarrhoea, including animals of 24 months of age. Cows affected were progressively slaughtered (30 animals / 230 lactating cows) with no additional investigations. The increasing disease severity and number of animals involved induced the breeder to ask for a full necropsy on one of his cows. The veterinarian sent multiple tissues for microscopical evaluation and a gross report indicating the presence of a severe and diffuse thickening of the intestine.

**Gross Pathology:** Severe and diffuse thickening of the jejunum, ileum and large intestine and multiple intestinal hemorrhages were reported by the referring veterinarian.

**Laboratory Results:** All cows were tested for paratuberculosis and bovine viral diarrhoea (ELISA). All livestock aged 24 months and older were tested for Paratuberculosis by ELISA. All animals including 2 month calving heifers (26 months old) were tested for BVD (PCR and serology for ns 2-3 proteins).

Approximately 30% of the cows of 24 months and older tested positive for paratuberculosis and only one heifer was BVD positive, persistently infected (viremic animal without antibodies). All the other tested animals were positive for BVD antibodies (according with a high viral environmental circulation). After these results, the BVD positive cow was slaughtered. Vaccination against BVD was performed in the farm.

Ziehl-Nielsen stain demonstrated numerous acid-fast bacilli in the cytoplasm of macrophages.

**Histopathologic Description:** Ileum: approximately 90% of intestinal villi are blunted, shortened and variably fused and lamina propria is severely expanded and obliterated by epithelioid macrophages, large foamy reactive macrophages and occasional multinucleated giant cells with up to six often horseshoe arranged nuclei (Langhans type cells). Occasionally, 1-2 micron rod shaped negative stained organisms (Mycobacteria) can be seen in the cytoplasm of giant cells. In the lamina propria, histiocytes are associated with moderate numbers of small mature lymphocytes and lesser numbers of plasma cells and occasional eosinophils. Mucosal lining is detached and multifocally missing (ulceration). Crypts are variably, multifocally dilated and lumens often contain homogeneous eosinophilic material associated with basophilic, granular debris and by karyorrhectic neutrophils (crypt necrosis and crypt abscesses). Crypt epithelium is multifocally ulcerated. Scattered

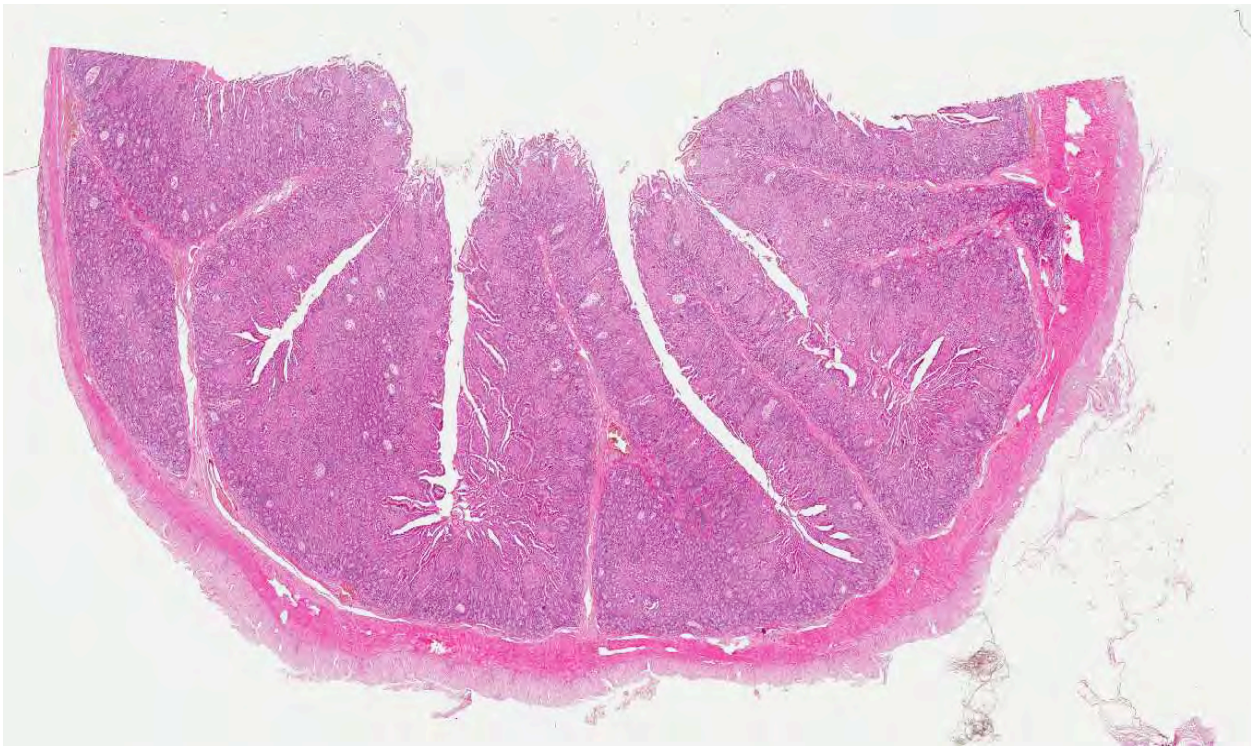

*4-1. Small intestine, ox: The mucosal epithelium is diffusely thickened by a marked cellular infiltrate which effaces both villi and crypts. (HE 70X)*

aggregates of epithelioid cells extend into the inner circular muscle cell layer. In the subserosal lining occasional granulomas composed of macrophages and lymphocytes are also present.

**Contributor's Morphologic Diagnosis:** Jejunum, severe chronic diffuse granulomatous enteritis with intralesional mycobacteria. Bovine.

**Contributor's Comment:** Microscopic findings were diagnostic for bovine paratuberculosis. In some sections occasional fungal hyphae with neither inflammation nor necrosis were also observed suggesting severe immune depression. Paratuberculosis or Johne's disease was first described in 1895 by Johne and Frothingham, who reported "a peculiar case of tuberculosis" in a cow with chronic enteritis characterized by diffuse thickening and corrugation of the intestinal mucosa and the presence of acid-fast bacilli in the lesions.[5] Paratuberculosis is caused by *Mycobacterium avium* subsp. *paratuberculosis*. This organism was originally named *Mycobacterium enteritidis chronicae pseudotuberculosae bovis john* and the name changed into *Mycobacterium johnei* followed by *Mycobacterium paratuberculosis* and, most recently, *Mycobacterium avium* subspecies *paratuberculosis* (MAPS).[4,5]

The etiologic agent of Johne's disease has been reduced to the subspecies status within *M. avium* on the basis of the high (>90%) DNA homology among typical paratuberculosis strains and type strains of M. *a. avium.* The Johne's disease agent, which in culture is slow-growing and dependent on mycobactin as a source of iron, possesses some unique cultural and biochemical traits. Genetically, a distinct difference from *M. a. avium* is the presence of the insertion sequence, IS900, of which *M. a. paratuberculosis* has 15-20 copies per organism.

Paratuberculosis is a chronic wasting enteritis that affects mainly domestic and wild ruminants worldwide but occurs also in camelids, lagomorphs, rodents, carnivores, birds and rarely in equids. Infection can also be experimentally reproduced in pigs, rabbits, mice, hamsters and primates.[2,4]

Mycobacteria are shed in feces, and the main route of infection is fecal-oral, but microorganisms are shed in milk, semen and urine and are able to cross the placental barrier. Infection occurs most commonly during the first days of life, when MAPS is ingested via colostrum or by contaminated foodstuff. Calves are especially prone to the infection due to the lack of a functional hematointestinal barrier. After ingestion MAPS binds to the luminal surface of M cells and

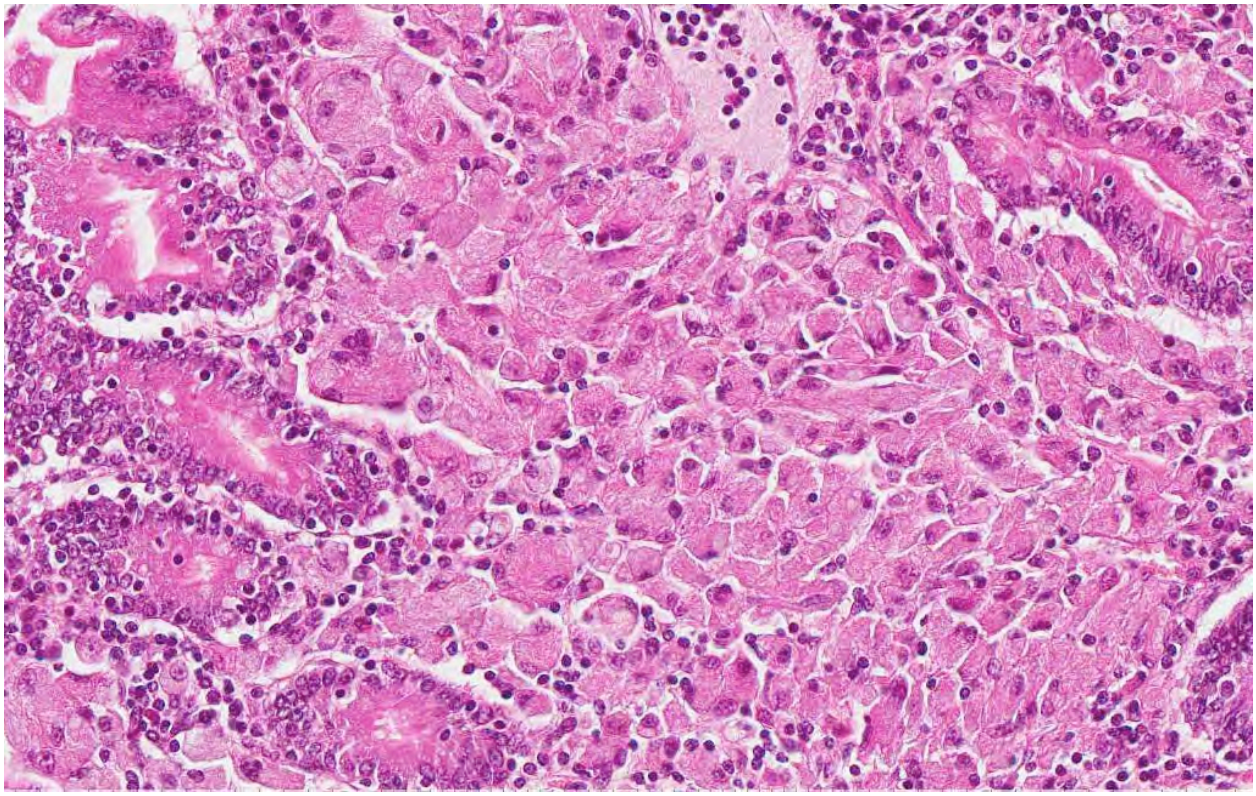

*4-2. Small intestine, ox: The lamina propria is expanded by numerous epithelioid macrophages and rare multinucleated giant cell macrophages. (HE 200X)*

reaches (through phagosomes) Peyer's patches where it can be phagocytosed by tissue macrophages. The virulence attributes of M. *a. paratuberculosis* are poorly understood, but presumably reside in *resistance to killing in macrophages,* through inhibition of the conversion of phagosomes to phagolysosomes. MAPS are highly adapted for survival within bovine mononuclear phagocytes.[15] The organisms proliferate in cytoplasmic vacuoles, and transmit to adjacent macrophages, expanding the population of infected cells and recruiting elements of the humoral and cell-mediated immune system to the lesional tissue. Both IL-14 dependent and IL-14 independent mechanisms appear to be involved in attenuation of phagosome acidification and phagolysosome fusion.[16] Mycobacteria acquire iron from ferritin stored in macrophages and, since the availability of iron is greatest in tissue macrophages of ileocecal junction, this is the site with initial and more severe lesions characterized by a diffuse granulomatous enteritis. Infected tissue macrophages spread via leukocyte trafficking in afferent lymphatic vessels to ileocecal lymph nodes leading also to a granulomatous lymphadenitis.[4,16]

Chronic, continuous or intermittent, often intractable, diarrhea, and emaciation are the most common and are associated with severe milk drop and reduced fertility.[16] Low total protein as a consequence of protein malabsorption and loss[2] is the most common clinical chemistry abnormality associated with low albumin serum while globulin values are usually unaffected.[14]

Specific gross lesions occur in the intestine and regional lymph nodes. The classical intestinal change is *diffuse thickening of the mucosa,* which is folded into transverse rugae, the crests of which may be congested. When well developed, the mucosal folds cannot be smoothed out by stretching. The intestinal serosa often has a slight granular and diffusely opaque appearance and foci of ulceration may be present. The *mesenteric nodes, particularly the ileocecocolic, are always enlarged,* pale, and edematous, especially in the medulla. Lymphangitis is the most frequent and common change and can be occasionally the only gross lesion granting a presumptive diagnosis of Johne's disease at necropsy. Advanced cases have signs of cachexia with loss of muscle mass, serous atrophy of fat deposits, intermandibular edema and effusions in body cavities. Plaques of intimal fibrosis and aortic mineralization have been reported. Focal granulomatous lesions can be occasionally found in liver, kidney and lungs.[4]

When gross lesions are well developed, the characteristic microscopic change, *transmural granulomatous enteritis,* is obvious. Characteristic histopathological finding in bovines is a transmural granulomatous enteritis, lymphadenitis and lymphangitis. *Masses of epithelioid macrophages may accumulate in the submucosa.* Foci of necrosis may occur within these aggregates of macrophages but in cattle, caseation and mineralization are extremely rare. Giant cells may be present. The inflammatory infiltrate may abnormally separate and displace crypts, which are elongate, with hyperplastic epithelium. Crypts may be distended with mucus and exfoliated cells. These lesions are characteristic of the multibacillary "lepromatous" phase of the disease as was in this case.[4,16] In cattle in which gross changes are minimal or absent, the microscopic abnormalities are more subtle. In these the lamina propria is diffusely infiltrated with lymphocytes and plasma cells, and a large number of eosinophils. There may be very few macrophages, and the most characteristic change is an infiltrate of lymphocytes and plasma cells in the submucosa, and associated with the submucosal and mesenteric lymphatics. *Lymphangitis* is one of the most consistent changes. Initially the lymphatics are surrounded by lymphocytes and plasma cells and many contain plugs of epithelioid cells in the lumen. Granulomas may form in the wall and project into the lumen. These nodules may undergo central necrosis. *Granulomatous lymphadenitis* occurs in mesenteric lymph nodes in advanced cases. In the early stages, there is histiocytosis of the subcapsular sinus. Ultimately, nodular or diffuse infiltrates of epithelioid macrophages and giant cells may replace much of the cortex, and infiltrate the medullary sinusoids.

In sheep and goats diarrhea is uncommon and the disease is characterized by chronic wasting. Enteric gross lesions are often mild, with little obvious thickening, and no transverse ridges; they are easily missed at necropsy. Gross lesions are similar but mineralized tubercle-like lesions have been reported.

*Mycobacterium avium* spp. *paratuberculosis* is an acid-fast, weakly Gram positive bacillus identifiable in the cytoplasm of macrophages as a rod shaped Ziehl-Neelsen positive organism. The organism is usually readily evidenced in macrophages and giant cells in the lesions when appropriately stained by acid-fast techniques. However, in some clinical cases, especially the ovine paucibacillary form, an extensive search may be needed for individual macrophages or giant cells bearing a few acid-fast bacilli. Johne's disease in sheep and especially in goats may resemble tuberculosis, on account of caseation and mineralization in granulomatous foci, and for such cases specific identification of the etiologic agent is necessary.

The antemortem diagnosis of Paratuberculosis in cattle is challenging and mirrors the evolution of immunopathological mechanisms elicited by MAPS.

Serological tests such as ELISA and PCR are available, but bacteriological assay is still considered the gold standard diagnostic technique ([1]; OIE http://www.oie.int/international-standard-setting/terrestrial-manual/access-online/). Vaccination has been reported as an effective strategy for Paratuberculosis control in several countries.[1]

Mycobacterium avium spp. Paratuberculosis has been identified in intestinal tissue from patients with Crohn's disease by culturing the organisms and by PCR.[16] Additionally, some patients with Crohn's disease respond to antimycobacterial therapy.[3] The detection of genome or the isolation of MAPS could be caused by ingestion of contaminated food, but the hypothesis that multiple exposure to MAPS via alimentary route could be involved in the pathogenesis of Crohn's patients has been taken into account.[16]

**JPC Diagnosis:** Small intestine: Enteritis, granulomatous, chronic, diffuse, severe, with crypt loss and abscessation, villar blunting and fusion, lymphangectasia and numerous intracytoplasmic acid-fast bacilli.

**Conference Comment:** The contributor provides an excellent description and characterization of *Mycobacterium avium* subsp *paratuberculosis* infection. Conference participants compared and contrasted the lepromatous (diffuse) and the tuberculoid forms of disease associated with *M. avium* subsp *paratuberculosis* in ruminants. Classically, clinical disease in cattle infected with *M. avium* subsp *paratuberculosis* is associated with a lepromatous reaction; however, in sheep and goats with subclinical to clinical paratuberculosis, a spectrum of lesions between lepromatous and tuberculoid inflammation can be observed.[6]

The type of granulomatous inflammation and clinical disease elicited by persistent, poorly degradable pathogens such as *Mycobacterium* species is dependent upon the host's immune response.[16] Lepromatous inflammation is characterized by macrophages and epitheloid macrophages arranged in sheets within tissue. In tuberculoid lesions, the macrophages are arranged in distinct nodules (granulomas) that generally have a central necrotic core surrounded by a layer of macrophages, epithleoid macrophages and multinucleated giant macrophages, further surrounded by a layer of lymphocytes and plasma cells and bounded by fibroblasts and collagen.[16] The lepromatous form is thought to be associated with a strong Th2 (humoral) immune response, whereas the tuberculoid form is associated with a strong Th1 (cellular) immune response.[6] With a strong Th1 response, fewer *Mycobacterium* organisms are present; therefore this form is also referred to as the "paucibacillary" form. On the contrary, with a strong Th2 response, less effective intracellular bacterial killing results in more numerous intralesional bacteria; hence the lepromatous form of disease is also referred to as the "multibacillary" form.[6,16]

Recent studies of cytokines in red deer infected with *M. avium* subsp *paratuberculosis* suggest that Th2 and Treg immune responses may not play a direct role in clinical disease; but rather, may control the immunopathology of the disease and that it is the loss of these responses that leads to the development of clinical disease.[13]

**Contributing Institution:** Dipartimento di Patologia Animale
Igiene e Sanita' Pubblica Veterinaria
Sezione di Anatomia Patologica e Patologia Aviare
Facolta' di Medicina Veterinaria
Milano - Italy
http://www.anapatvet.unimi.it/

**References:**

1. Bastida F, Juste RA. Paratuberculosis control: a review with a focus on vaccination. *J Immune Based Ther Vaccines*. 2011;9:8-25.
2. Begg DJ, Whittington RJ. Experimental animal infection models for Johne's disease, an infectious enteropathy caused by Mycobacterium avium subsp paratuberculosis. *Veterinary Journal*. 2008;176:129-145.
3. Borody TJ, Leis S, Warren EF, et al. Treatment of severe Crohn's disease using antimycobacterial triple therapy--approaching a cure? *Dig Liver Dis*. 2002;34:29-38.
4. Brown CC, Baker DC, Barker IK. Alimentary system. In: Maxie MG, ed. *Jubb, Kennedy & Palmer's Pathology of Domestic Animals*. 5th ed. Vol 2. Philadelphia, PA: Saunders Elsevier; 2007:69-128.
5. Clarke CJ. The pathology and pathogenesis of paratuberculosis in ruminants and other species. *J Comp Pathol*. 1997;116:217-261.
6. Corpa JM, Garrido J, Garcia Marin JF, et al. Classification of lesions observed in natural cases of paratuberculosis in goats. *J Comp Pathol*. 2000;122:255-265.
7. Coussens PM. Model for immune responses to Mycobacterium avium subspecies paratuberculosis in cattle. *Infect Immun*. 2004;72(6):3089-3096.
8. Dennis MM, Reddacliff LA, Whittington RJ. Longitudinal study of clinicopathological features of Johne's disease in sheep naturally exposed to Mycobacterium avium subspecies paratuberculosis. *Vet Pathol*. 2011;48:565-575.
9. González J, Geijo MV, García-Pariente C, et al. Histopathological classification of lesions associated with natural paratuberculosis infection in cattle. *J Comp Pathol*. 2005;133:184-196.

10. Greenstein RJ. Is Crohn's disease caused by a mycobacterium? Comparisons with leprosy, tuberculosis, and Johne's disease. *Lancet Infect Dis*. 2003;3:507-514.
11. Mann EA, Saeed SA. Gastrointestinal infection as a trigger for inflammatory bowel disease. *Curr Opin Gastroenterol*. 2012;28:24-29.
12. McKenna SL, Keefe GP, Tiwari A, et al. Johne's disease in Canada part II: disease impacts, risk factors, and control programs for dairy producers. *Can Vet J*. 2006;47(11):1089-1099.
13. Robinson MW, O'Brien R, Mackintosh CG, et al. Immunoregulatory cytokines are associated with protection from immunopathology following *Myocbacterium avium* subspecies *paratuberculosis* infection in red deer. *Infection and Immunity*. 2011;79 (5):2090-2097.
14. Scott PR, Clarke CJ, King TJ. Serum protein concentrations in clinical cases of ovine paratuberculosis (Johne's disease). *Vet Rec*. 1995;137:173.
15. Weiss DJ, Souza CD. Review paper: modulation of mononuclear phagocyte function by Mycobacterium avium subsp. paratuberculosis. *Vet Pathol*. 2008;45:829-841.
16. Zachary JF, McGavin DM. *Pathologic Basis of Veterinary Disease*. 5th ed. Philadelphia, PA: Elsevier Mosby; 2011;122-124, 172-173.

**Joint Pathology Center**
**Veterinary Pathology Services**

## WEDNESDAY SLIDE CONFERENCE 2012-2013

# Conference 2

**26 September 2012**

---

**CASE I:** 05-0560 7/ 05-0619 5 (JPC 3139510).

**Signalment:** 6-week-old male Swiss Webster mice (*Mus musculus*).

**History:** Multiple animals were euthanized due to visible swellings and masses around the head and mouth. Development of a head tilt was noted in some.

**Gross Pathologic Findings:** All mice were in good body condition at postmortem examination. Multiple, small white nodules (ranging from 2-10mm diameter) were present subcutaneously around the head, especially in the parotid and submandibular areas. On coronal sectioning of the head after fixation and decalcification, similar nodules effaced and expanded many tissues multifocally from the rostral to caudal aspect of the head. Nodules were firm and contained tan-brown fluid on cut section.

**Laboratory Results:** *Staphylococcus aureus* was cultured from the lesions.

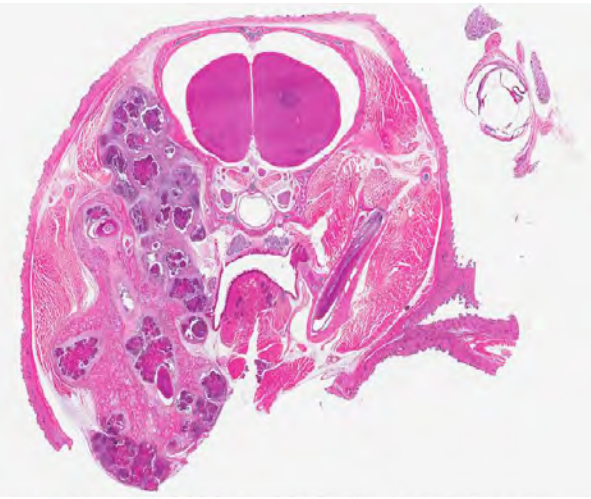

*1-1. Head at level of olfactory bulbs, mouse: Unilaterally, the dermis, subcutis, skeletal muscle and lamellar bone of the mandible are replaced by chronic suppurative inflammation centered on bacterial colonies (botryomycosis). (HE 40X)*

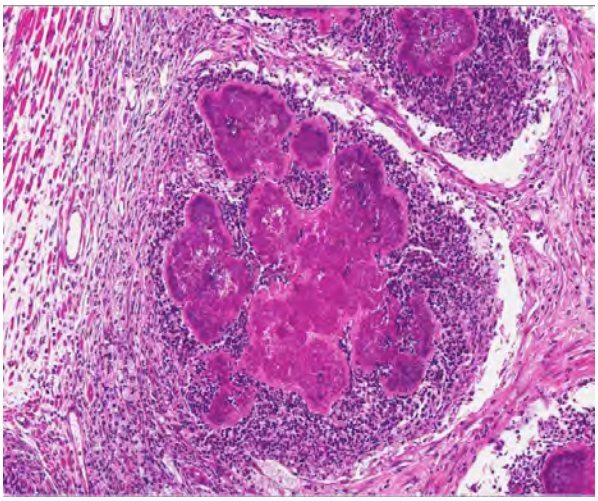

*1-2. Head, mouse: Bacterial colonies are embedded in aggregated brightly eosinophilic protein (Splendore-Hoeppli material) in turn surrounded by degenerate neutrophils, macrophages, and granulation tissue. (HE 120X)*

**Histopathologic Description:** Multiple coronal sections of the head are submitted. Lesions and anatomic structures captured subsequently vary on different sections. Multifocal to coalescing, large, discrete inflammatory cell aggregates bilaterally, efface and expand the ventrolateral aspects of the head, predominantly the mandibular bone, molar teeth, skeletal (masseter) muscle, adipose tissue and skin. Aggregates are composed of central foci of 2-3µm diameter cocci admixed with hyalinized, amorphous material that frequently forms peripheral, radiating, club-like projections (Splendore-Hoeppli material). Within and encircling these cores there are many neutrophils admixed with necrotic cell debris and basophilic mineralized foci. These foci are in turn encircled by epithelioid macrophages, lymphocytes, fibroblasts and collagen fibers. Additional associated microscopic changes include: thickening of mandibular bone by subperiosteal woven bone formation, bone lysis and increased numbers of osteoclasts, odontoclastic resorption of molar teeth, and skeletal myocyte loss/atrophy. Epidermal parakerototic hyperkeratosis and sub-epidermal pustule formation are additionally seen.

**Contributor's Morphologic Diagnosis:** Multifocal to coalescing, necrosuppurative osteomyelitis, myositis, panniculitis, dermatitis and cellulitis, with Splendore-Hoeppli material and intralesional bacterial cocci, bone lysis and subperiosteal woven bone formation.

**Contributor's Comment:** Splendore-Hoeppli material is the bright eosinophilic, club-shaped material that typically radiates around bacterial colonies in histologic sections.[1,4,5] Classically this phenomenon has been described in cases of chronic staphylococcal infection which is associated with formation of grossly visible bacterial colonies that resemble granules. The term botryomycosis is used to refer to such chronic infections where Splendore-Hoeppli material is seen. This condition usually affects the skin and subcutis and is typically initiated by a skin wound, resulting in lesions that present as local, firm nodules, ulcers or sinuses communicating with deep abscesses.[4,5] Ultimately these lesions may be walled off by fibrous connective tissue and can coalesce to form aggregates of granulomas within the subcutis and surrounding tissues.[4,5] Botryomycosis may also involve other organs such as the lung, and although it can affect immunocompetent animals, immunosuppression is considered to be a predisposing factor to its development.[1,2,4,5,8]

In addition to staphylococci (*S. aureus, S. hominus, S. xylosus*), other bacterial agents have also been isolated from cases of botryomycosis in rodents, including, *Streptococcus intermedius, Pseudomonas aeruginosa, Proteus* spp., *Escherichia coli and Nocardia asteroides.*[1,3,4,8,11] In other animals and in people however, Splendore-Hoeppli material has been reported to arise in association with infections due to fungi and other parasites, and has also been known to surround biologically inert substances such as suture material.[1,3,4,5,7,12]

Although the exact nature of this reaction is unknown, it is considered to be a localized immunological response to an antigen-antibody precipitate related to fungi, parasites, bacteria or inert materials.[5] The characteristic formation of the Splendore-Hoeppli reaction around infectious agents or biologically inert materials probably represents some attempt at containment of the agent on the part of the host. It likely prevents phagocytosis and intracellular killing of the injurious agent leading to chronicity of infection, so whether this degree of immune responsiveness is actually helpful or harmful remains to be determined.[5,6] Similarly the nature of the intense eosinophilic nature of this material remains poorly understood, but is thought to be due to its composition of antigen-antibody complexes (immunoglobulins and major basic proteins) combined with cell debris from inflammatory cells (lymphocytes, plasma cells, eosinophils and macrophages) and fibrin.[5] Composition of the reaction likely depends on the type of causative agent, and one hypothesis is that Splendore-Hoeppli material may be derived from host leukocytes that aggregate in response to the bacteria, parasites or inert foreign materials that can initiate the reaction.[5,6]

Morphological mimickers of the Splendore-Hoeppli reaction are said to include flame figures (as seen in conditions such as feline eosinophilic granuloma complex, insect bites and drug eruption), tophaceous lesions of gout, asteroid bodies (as may be rarely seen in some granulomatous lesions in animals) and actinomycotic sulfur granules (the radiating structures of Splendore-Hoeppli reaction resemble these sulfur granules). The absence of central branching filaments in Splendore-Hoeppli reaction helps to distinguish this from true actinomycotic sulfur granules.[5]

Flame figures represent degranulated eosinophils that form aggregates of granular necrotic material surrounded by collagen, and these foci are often basophilic with peripheral macrophages.[5] Gout tophi appear as variably sized deposits of amorphous, amphophilic material with parallel, acicular clefts; however, these crystals often have a brownish color and are doubly refractile with polarized light.[5] Asteroid bodies are stellate eosinophilic inclusions seen within giant cells of granulomas occasionally.[5] This reaction is histologically opposite to that which is seen in the Splendore-Hoeppli reaction, i.e., a central

stellate acellular region that is surrounded by inflammatory cells.[5]

**JPC Diagnosis:** Skin, subcutis and maxilla: Cellulitis, dermatitis, myositis and osteomyelitis, pyogranulomatous, multifocal to coalescing, severe, with large colonies of cocci and Splendore-Hoeppli material.

**Conference Comment:** There was considerable slide variation in this case, with the bone involvement totally absent in some slides. Also, bone marrow was visible in some slides, and it was noted that within the marrow there was myeloid hyperplasia, with the majority of cells being granulocytes. Conference participants discussed the various causes of botryomycosis as listed by the contributor, with the addition of a recent case of subcutaneous botryomycosis in a Texas Longhorn steer caused by *Bibersteinia trehalosi*.[10] Participants also noted that in addition to immunosuppressed mice, urokinase-type plasminogen activator-deficient mice are particularly susceptible to developing botryomycosis.[9] This is presumed to be due to their lack of urokinase-type plasminogen activator (uPA). Plasminogen activators are serine proteinases that cleave plasminogen to form plasmin in the fibrinolytic system. Plasmin is a serine proteinase that is involved in several physiological as well as pathological processes.[1] In this case, it is its impaired role in the proteolysis of fibrin and extracellular matrix (ECM) that contributes to the increased susceptibility of uPA deficient mice to developing botryomycosis.

**Contributing Institution:** Massachusetts Institute of Technology
Division of Comparative Medicine
77 Massachusetts Avenue
Cambridge, MA 02139
http://web.mit.edu/comp-med/

**References:**

1. Thompson ME. Proceedings: Department of Veterinary Pathology Wednesday Slide Conference 2006-2007, Conference 13, Case 1, AFIP #2812387.
2. Bridgeford EC, Fox JG, Nambiar PR, et al. Agammaglobulinemia and *Staphylococcus aureus* Botryomycosis in a Cohort of Related Sentinel Swiss Webster Mice. *J Clin Microbiol*. 2009;46(5): 1881-1884.
3. EL van den Berk G, Noorduyn LA, van Ketel RJ, et al. A fatal pseudo-tumour: disseminated basidiobolomycosis. *BMC Infectious Diseases*. 2006;6:140.
4. Ginn PE, Mansell JEKL, Rakich PM. Skin and appendages. In: Maxie MG, ed. *Jubb, Kennedy and Palmer's Pathology of Domestic Animals*. 5th ed. Philadelphia, PA: Elsevier; 2007:691.
5. Hussein MR. Mucocutaneous Splendore-Hoeppli phenomenon. *J Cutan Pathol*. 2008;35(11):979-988.
6. Mondino A, Blasi F. uPA and uPAR in fibrinolysis, immunity and pathology. *Trends Immunol.* 2004;25(8): 450-455.
7. Rodig SJ, Dorfman DM. Splendore-Hoeppli phenomenon. *Arch Pathol Lab Med*. 2001;125:1515-1516.
8. Schlossberg D, Pandey M, Reddy R. The Splendore-Hoeppli phenomenon in hepatic botryomycosis. *J Clin Pathol*. 1998;51:399-400.
9. Shapiro RL, et al. Urokinase-type plasminogen activator-deficient mice are predisposed to staphylococcal botryomycosis, pleuritis, and effacement of lymphoid follicles. *Am J Path.* 1997;2 (1):359-369.
10. Spagnoli S, Reilly TJ, Calcutt MJ, et al. Subcutaneous botryomycosis due to *Bibersteinia trehalosi* in a Texas longhorn steer. *Vet Pathol.* 2012;49 (5):775-778.
11. Weighardt H, Kaiser-Moore S, Vabulas RM, et al. Cutting edge: Myeloid differentiation factor 88 deficiency improves resistance against sepsis caused by polymicrobial infection. *J Immnunol*. 2002;169:2823–2827.
12. Zavasky D, Samowitz W, Loftus T, et al. Gastrointestinal zygomycotic infection caused by basidiobolus ranarum: Case report and review. *Clin Infec Dis.* 1999;28(6):1244-8.

**CASE II:** C6883 H0728 (JPC 4003092).

**Signalment:** Adult rabbit of unknown age and breed.

**Gross Pathology:** The rabbit showed severely swollen eyelids.

**Histopathologic Description:** Complete eyelid with epidermis and conjunctiva: The epidermis is generally hyperplastic and invades the dermis at the conjunctival-epidermal junction in a lobular pattern, extending into the lamina propria of the palpebral conjunctiva. The hyperplasia is predominantly acanthosis, but the non-invading epidermis exhibits orthokeratotic hyperkeratosis. Keratinocytes within the invading portion of the epidermis show widespread hydropic degeneration. Some keratinocytes contain a 10-15 µm long, eosinophilic cytoplasmic inclusion body surrounded by a clear halo (Splendore inclusions or bodies).

In the dermis, multiple large, stellate or polygonal cells with finely granular, basophilic cytoplasm and one or more large nuclei with finely granular to fragmented chromatin and one clear nucleolus are present. Mitoses are less than 1 per HPF. There is a slight infiltration of eosinophils, macrophages and some lymphocytes and plasma cells. The surrounding collagen fibers are loosely arranged and interspersed with a moderate amount of basophilic amorphous substance (proteoglycans).

Part of the conjunctival mucosa is desquamated due to autolysis.

**Contributor's Morphologic Diagnosis:** Proliferative dermatitis with myxomatous changes.

**Contributor's Comment:** Myxomatosis is a disease of wild and domestic rabbits or, rarely, hares caused by the myxoma virus, which belongs to the Leporipoxvirus genus of the family Poxviridae. Transmission of the virus occurs through direct contact or via vectors such as mosquitos or fleas.[1,4]

Three to five days after infection, affected animals first show signs of fever, depression and loss of appetite. Subsequently, edematous or firm skin nodules (mostly around the eye, mouth, nose, ear or genitalia), conjunctivitis and severe depression are seen. Death occurs within one to two weeks after the first symptoms appear.[5]

Histologically, one of the first apparent changes is an increase in number and size of the epidermal cells. After this, granular, pink cytoplasmic inclusions appear in these cells. The disease progresses until cell lysis occurs and epidermal vesicles develop. In the dermis, large stellate or polygonal cells with swollen nuclei and fragmented chromatin, polymorphonuclear leukocytes and multinucleated cells appear. Histological changes can also be seen in other organs. The lymph nodes, for example, first become activated,

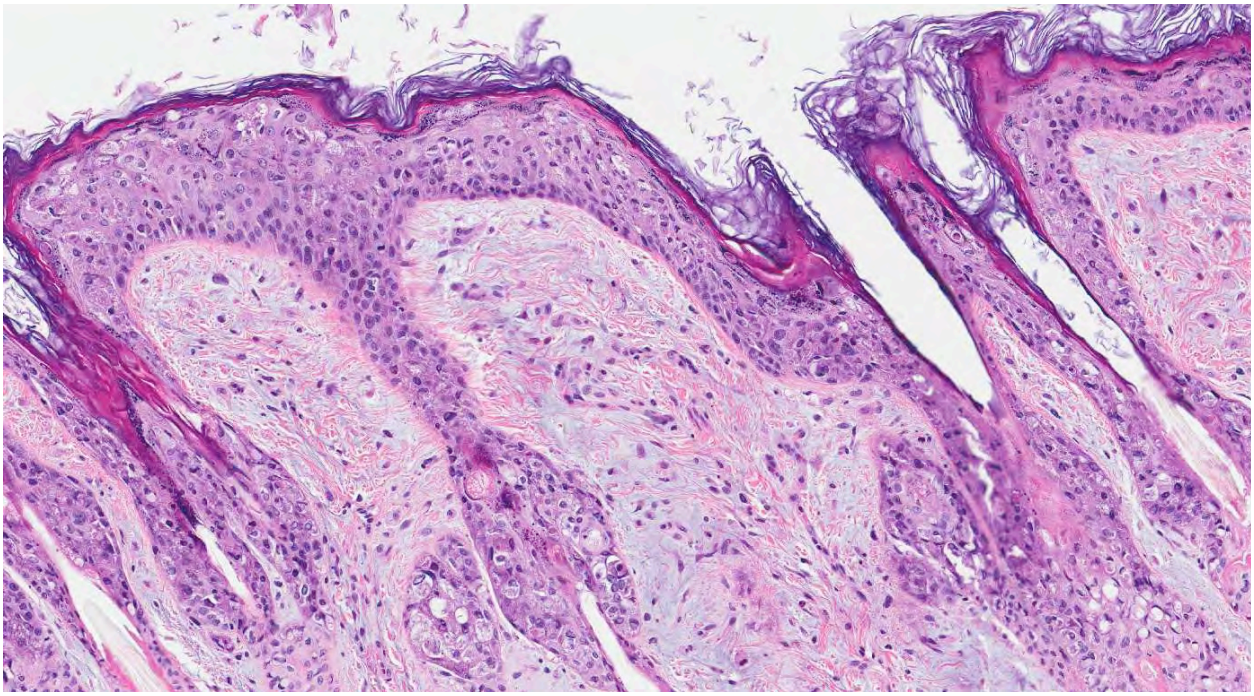

*2-1. Haired skin, eyelid, and rabbit: There is moderate hyperplasia of the epidermis (particularly surrounding follicles), with disorganization and lack of normal epidermal stratification. The superficial dermis is expanded by an accumulation of amphophilic ground substance which surrounds low numbers of plump stellate to spindle cells. (HE 180X)*

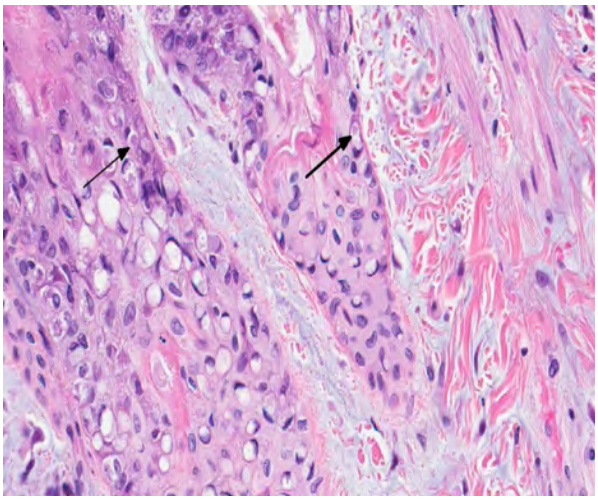

*2-2. Haired skin, eyelid, rabbit: Epithelial cells exhibit intracellular edema (ballooning degeneration) and occasionally contain a 10 µm, intracytoplasmic viral inclusion that peripheralizes the nucleus (arrows). (HE 360X)*

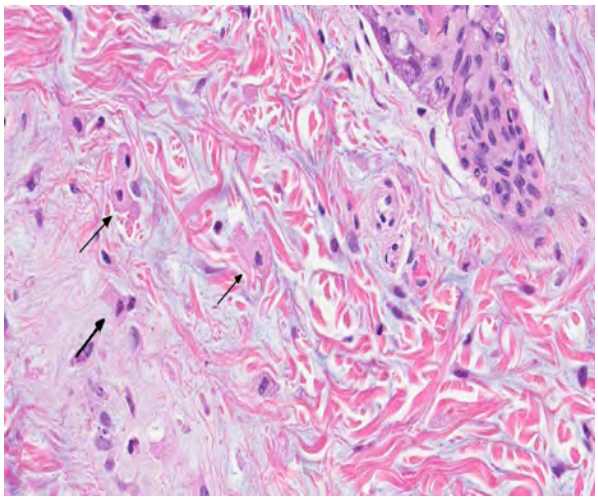

*2-3. Haired skin, eyelid, and rabbit: A population of plump, vacuolated mesenchymal cells populates the myxedematous areas of the dermis ("myxoma cells"). (HE 360X)*

while, as the disease progresses, lymphocytes are replaced with the large stellate or polygonal cells previously described. The same cellular infiltration can be seen in the spleen.[5]

**JPC Diagnosis:** Eyelid: Atypical mesenchymal proliferation, diffuse, moderate, with epithelial ballooning degeneration and necrosis, intraepithelial eosinophilic intracytoplasmic viral inclusions, and mild myxedema.

**Conference Comment**: Conference participants discussed the interesting history of myxomatosis, which was first recognized in European rabbits (*Oryctolagus cuniculus* ) in a South American laboratory in the late 1800's. Myxomatosis was first recognized in California in 1930, and remains enzootic in the western United States to this day. In the 1950s, the virus was implemented as a biological control in Australia, where it was introduced to cull the ballooning population of nonnative European rabbits. Mortality rates in the European rabbits at the time of introduction were as high as 99%; however, mortality dropped to around 25% in the years that followed, likely due to natural selection of resistant rabbits as well as the emergence of less virulent viral strains. In 1953, myxomatosis was introduced into the wild rabbit population in France, reportedly by a disgruntled individual; from there the virus spread to other parts of Western Europe, including England.[3]

Conference participants also discussed the pathogenesis of myxomatosis. As the contributor stated, myxoma virus is spread via arthropod vectors. The virus replicates in the host at the site of inoculation, resulting in a subcutaneous myxoid mass. In susceptible animals, the virus can then spread via cell-associated viremia (also known as leukocyte trafficking) and cause systemic disease. In less susceptible rabbit species, such as *Sylvilagus brasiliensis* and *S. bachmani*, viremia does not develop, and lesions are generally restricted to localized cutaneous fibromas.

A closely-related leporipoxvirus, rabbit fibroma virus (RFV, also known as Shope fibroma virus), occurs naturally in the eastern cottontail (*Sylvilagus floridanus*) and causes similar lesions, referred to as "Shope Fibromas", in both cottontails and European rabbits.[2] Shope fibromas appear grossly as flattened subcutaneous tumors on the legs, feet, and occasionally the face. Histologically, Shope fibromas are composed of a localized proliferation of reactive fibroblasts that may contain large intracytoplasmic eosinophilic inclusion bodies. The inclusion bodies can also be found in the cells of the overlying epidermis. These well-circumscribed fibrous masses are generally easily distinguishable from myxomatosis, which is characterized by proliferation of stellate mesenchymal cells on a mucinous matrix with epithelial hypertrophy. Participants noted that this case features a comparatively milder atypical mesenchymal spindle cell proliferation, and more severe epithelial proliferation and loss of normal epithelial stratification than is usually observed in this disease.

**Contributing Institution:** University of Ghent
Laboratory of Veterinary Pathology
Faculty of Veterinary Medicine
Salisburylaan 133
9820 Merelbeke
Belgium

**References:**

1. Day MF, Fenner F, Woodroofe GM. Further studies on the mechanism of mosquito transmission of Myxomatosis in the European rabbit. *J Hyg*. 1956;54:258-83.
2. Kerr PJ. Myxomatosis in Australia and Europe: a model for emerging infectious diseases. *Antiviral Res*. 2012;93(3):387-415.
3. Percy DH, Bathrold SW. Rabbit. In: *Pathology of Laboratory Rodents and Rabbits*. 3rd ed. Ames, Iowa: Blackwell; 2007:256-258.
4. Sobey WR, Conolly D. Myxomatosis: the introduction of the European rabbit flea Spilopsyllus cuniculi (Dale) into wild rabbit populations in Australia. *J Hyg*. 1971;69:331-346.
5. Rivers TM. Infectious myxomatosis of rabbits. *J Exp Med*. 1930;51:965-976.

**CASE III:** 07003965 (JPC 3125786).

**Signalment:** Adult female C57BL/6 mouse (*Mus musculus*).

**History:** This mouse was treated with six doses of 7,12-dimethylbenz[a]anthracene (DMBA) at 10mg/ml to induce mammary carcinomas.

**Gross Pathologic Findings:** On gross examination, there was an irregular, expansile, 13x18x18mm mass on the seventh and eighth mammary glands within the right axillary region. The mass was pale tan on cut surface with multifocal 2-4mm foci of hemorrhage and necrosis. Internally, the lungs were multifocally mottled pink to dark red, and there were two 1-2mm white foci on the right caudal lung lobe, and two 3-4mm white foci on the left lung lobe.

**Histopathologic Description:** Lung: In sections of lung, there were one to multiple, expansile, well-demarcated, unencapsulated proliferations of well-differentiated epithelial cells compressing the adjacent pulmonary architecture and collapsing subjacent alveolar spaces. The masses were composed of lobules, cords, and papillary projections of cuboidal to columnar epithelial cells with moderate faintly eosinophilic amorphous cytoplasm and a central round nucleus with coarsely clumped to condensed chromatin and an occasional nucleolus, supported by a fine fibrovascular stroma. Mitotic figures were not observed. Adjacent to and within the surrounding alveolar spaces were small to large numbers of large macrophages with moderate to abundant brightly eosinophilic cytoplasm containing refractile needle-shaped to acicular crystalline material. Occasional to frequent multinucleate giant cells were present, containing similar crystalline material. In some sections, large acicular crystals were present within small bronchioles, and there were multifocal inflammatory aggregates composed of small to moderate numbers of lymphocytes and plasma cells scattered randomly throughout the lung parenchyma.

**Contributor's Morphologic Diagnosis:** Lung: Pulmonary adenomas; Mild to moderate, chronic, multifocal to coalescing, accompanied by histiocytic to granulomatous interstitial pneumonia with intracytoplasmic eosinophilic crystalline material.

**Contributor's Comment:** Eosinophilic crystalline pneumonia is an idiopathic disease that occurs in several different strains of mice, most commonly in those of a C57BL/6 background.[4,8] This disease varies from mild and subclinical to severe, sometimes resulting in dyspnea and death. This disease may occur alone or in conjunction with other pulmonary lesions such as pulmonary adenomas (as in this case), lymphoproliferative disease, allergic lung disease, and parasitic or fungal infections.[1,3] The crystals that are found within the cytoplasm of macrophages and multinucleate giant cells, as well as often free within alveolar spaces and bronchioles, are reminiscent of Charcot-Leyden crystals morphologically, which are products of eosinophil breakdown and eosinophil-related diseases in humans.[3,8] However, crystals in ECP are composed primarily of Ym1 protein, a chitinase-like protein that is secreted by activated macrophages. The exact function of Ym1 protein is poorly understood, but is believed to play a role in host immune defense, eosinophil recruitment, and cell-cell and cell-matrix interactions consistent with tissue repair.[2,3]

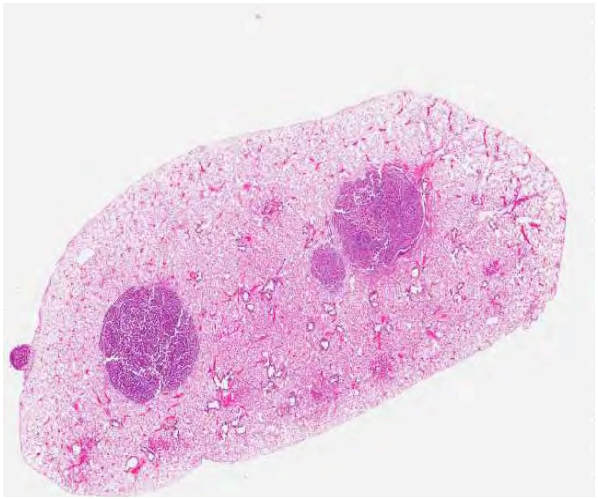

*3-1. Lung, mouse: There are several expansile proliferative lesions within this section of lung. (HE 50X)*

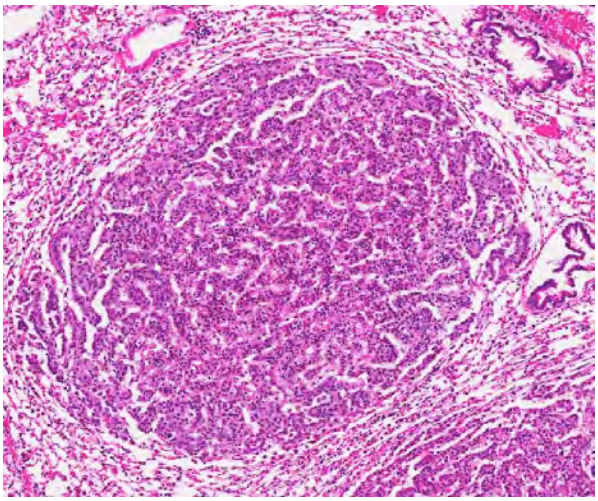

*3-2. Lung, mouse. Lesions often exhibit a combination of lepidic (growing in a "scale-like" fashion along preexisting alveolar septa – seen at bottom left) and expansile growth, compressing adjacent alveoli (at upper right). (HE 120X)*

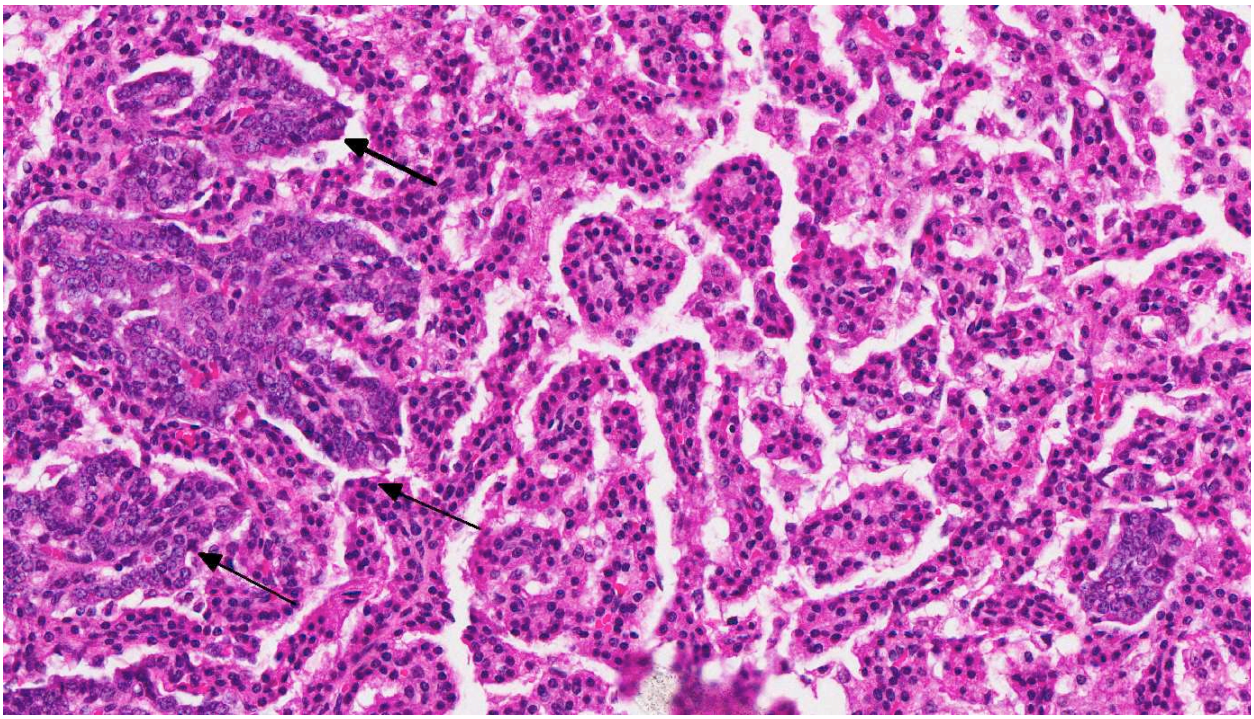

*3-3. Lung, mouse: In some neoplasms, neoplastic cells exhibit pleomorphism, a higher nuclear/cytoplasmic ration, and finely stippled chromatin (suggestive of malignant transformation) (arrows). (HE 400X)*

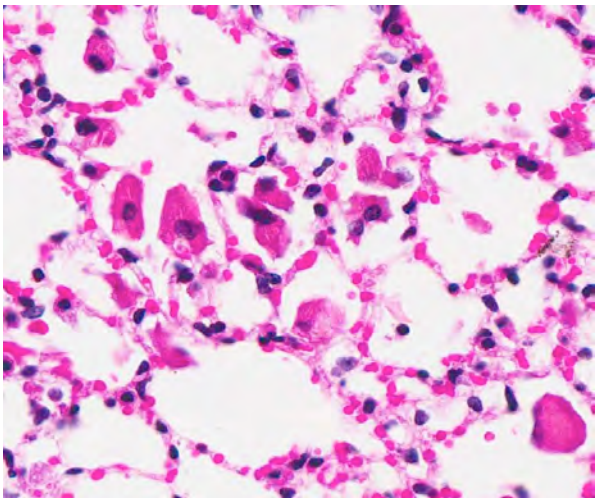

*3-4. Lung, mouse: Multifocally, alveoli contain variable numbers of macrophages which contain numerous brightly eosinophilic spicules ("acidophilic pneumonia"). (HE 400X)*

**JPC Diagnosis:** 1. Lung: Pulmonary (bronchioalveolar) carcinoma.
2. Lung: Pulmonary (bronchioalveolar) adenoma.
3. Lung: Bronchioalveolar hyperplasia, multifocal.
4. Lung: Pneumonia, interstitial, histiocytic, focally extensive, marked, with intracytoplasmic eosinophilic crystalline inclusions.

**Conference Comment:** The slide variation with this case initiated an excellent discussion amongst conference participants regarding the spectrum of lung lesions observed in various sections. The severity of eosinophilic crystalline pneumonia ranges from mild alveolar histiocytosis in some sections to granulomatous pneumonia in others. In some sections, eosinophilic crystals were visible within epithelial cells lining bronchi as well. Additionally, there are also several proliferative bronchoalveolar lesions comprising a continuum from what conference participants considered benign hyperplasia to adenoma to carcinoma. Within nodules of more quiescent hyperplastic/adenomatous cells, there are occasionally foci of cells with a more malignant appearance that were interpreted as representing malignant transformation.

Discussion also centered on the current variation in classification of and terminology for lung tumors in the mouse, arising from the lack of a consensus on histologic subtype.[6] In some instances, neoplasms showing lepidic growth along preexisting alveolar structures have been referred to as bronchioalveolar adenoma if < 3mm and bronchioalveolar carcinoma if > 3mm. However, Percy and Barthold, in the 3rd edition of *Pathology of Laboratory Rodents and Rabbits*, use the terminology "pulmonary" rather than "bronchioalveolar" when describing these neoplasms in mice.[5] Interestingly, in human pathology, the term "bronchioalveolar carcinoma" has recently been dropped from the terminology, and the new (2011) classification scheme uses the terms "atypical adenomatous hyperplasia" for preinvasive hyperplastic

lesions, “adenocarcinoma in situ” and “minimally invasive adenocarcinoma” for small (<3 cm) solitary adenocarcinomas with pure or predominant lepidic growth, respectively, and < 5 mm invasion, and “invasive adenocarcinoma” for tumors with > 5 mm invasion.[7]

**Contributing Institution**: National Institutes of Health
National Cancer Institute
Comparative Molecular Pathology Unit
Laboratory of Cancer Biology and Genetics
Center for Cancer Research
37 Convent Drive, Room 2002
Bethesda, MD 20892

**References:**

1. Guo L, Johnson RS, Schuh CL. Biochemical characterization of endogenously formed eosinophilic crystals in the lungs of mice. *J Biol Chem*. 2000;275:8032-8037.
2. Hoenerhoff MJ, Starost MF, Ward JE. Eosinophilic crystalline pneumonia as a major cause of death in 129S4/SvJae mice. *Vet Pathol*. 2006;43: 682-688.
3. Marchesi F, Monestiroli SV, Capillo M, et al. Eosinophilic crystals as a distinctive morphologic feature of a hyaline droplet nephropathy in a mouse model of acute myelogenous leukemia. *J Vet Med.* 2003;50:103-107.
4. Murray AB, Luz A. Acidophilic macrophage pneumonia in laboratory mice. *Vet Pathol*. 1990;27:274-281.
5. Percy DH, Bathrold SW. Rabbit. In: *Pathology of Laboratory Rodents and Rabbits*. 3rd ed. Ames, Iowa: Blackwell; 2007:117-118.
6. Rissoto KC, Lucas P, Fan TM. An update on diagnosing and treating primary lung tumors. *DVM 360*. 1 March 2008. http://veterinarymedicine.dvm360.com/vetmed/article/articleDetail.jsp?id=503048&sk=&date=&pageID=2
7. Travis WD, et al. International Association for the Study of Lung Cancer/American Thoracic Society/ European RespiratorySociety: International Multidisciplinary Classification of Lung Adenocarcinoma, An Executive Summary. *Proc Am Thorac Soc*. 2011;8:381–385.
8. Ward JM, Yoon M, Anver MR, et al. Hyalinosis and Ym1/Ym2 gene expression in the stomach and respiratory tract. *Am J Pathol.* 2001;158:323-332.

**CASE IV:** 09003277 (JPC 3165092).

**Signalment:** 1-year-old male Armenian hamster (*Cricetulus migratorius)*.

**History:** Over the course of a month, 8 male Armenian hamsters, ages 5 months to 1 year, presented to necropsy either moribund or dead from an illness of short duration. The hamsters were housed individually in an isolation cubicle and were manipulated only in a BSL-2 safety cabinet. The hamsters were used for monoclonal antibody production and were immunized with KLH-peptides (Keyhole Limpet Hemocyanin-conjugated peptides) emulsified in Titermax.

The hamsters routinely developed chronic dermatitis, most severe over the shoulders and dorsal neck. This is the injection location of the immunizations that were given 4-5 times over a 2-4 month period. All hamsters were purchased from the same vendor and often arrived with a history of receiving ivermectin treatment for demodicosis. Treatment for the chronic dermatitis over the cervical dorsal area consisted of triple antibiotic ointment (Vetropolycin®) applied three times per week topically.

**Gross Pathologic Findings:** At necropsy the hamsters were in good body condition, although all had varying degrees of chronic dermatitis localized to the dorsal cervical area, shoulders and extending to the base of the ears. Dermatitis was sometimes mild, with hyperemia and patchy hair loss or characterized by punctate excoriations with crust formation and associated alopecia. Approximately half of the hamsters had small, dermal pyogranuloma formation in these areas.

*4-1. Cecum, colon, and hamster: The ceca and colon are congested, with serosal erythema and petechiations. Photograph courtesy of Memorial Sloan-Kettering Cancer Center.*

All of the hamsters had formed fecal pellets in the rectum and stomachs distended with food. The cecum and large intestine contained pasty ingesta. Several hamsters presented with congested ceca and proximal colons, characterized by serosal erythema and petechia. No other gross abnormalities were detected.

**Laboratory Results:** *Clostridium difficile* toxins A/B identified by ELISA in the cecal contents.

**Histopathologic Description:** Cecum: Multifocally there is necrotizing fibrinopurulent mucosal inflammation, ranging from attenuation of surface enterocytes and patchy focal mucosal erosions which exude fibrin and neutrophils, to extension into the mildly hyperplastic glands, filling them with necrotic debris. The submucosa is multifocally infiltrated by macrophages, neutrophils, lymphocytes and scattered eosinophils, within an edematous stroma. Rarely inflammation is transmural and extends to the serosal surface. Lymphatics are dilated, and multifocally contain edema and viable and karyorrhectic inflammatory cells. Superficial mucosal vessels are multifocally congested and occasionally associated with fibrinoid necrosis. There is rare overlying pseudomembrane formation.

**Contributor's Morphologic Diagnosis:** Cecum: Typhlitis, fibrinopurulent, necrotizing, subacute, mucosal to transmural, multifocal, moderate to marked.

**Contributor's Comment:** *C. difficile* causes antibiotic-associated disease in a variety of laboratory animal species, but since the 1970s the hamster's renowned sensitivity has made it a model for human disease. A variety of antibiotics can initiate the clinical syndrome by rendering the hamster susceptible. Hamsters acquire *C. difficile* infection through direct contact, fomites contaminated with fecal material, and a recent report describes *C. difficile* present in the air surrounding human patients with the disease.[2]

Overgrowth of *C. difficile* occurs following the disturbance of the normal Bacteroides and *Lactobacillus* flora.[5] Clindamycin and ampicillin antibiotics are reported to directly enhance *C. difficile* colonization by increased expression of adherence factors beneficial for *C. difficile* colonization and adherence.[3] Typhlitis and enterotoxemia develop secondary to the elaboration of toxins A and B, responsible for the tissue damage and influence of the immune response, resulting in watery or hemorrhagic diarrhea, dehydration and death within 2-10 days.[5] Two A exotoxins, an enterotoxin, and the cytotoxin B are produced by *C. difficile*. Epithelial tissue damage from the toxins is likely following the glycosylation and inactivation of Ras GTPases, disabling signaling

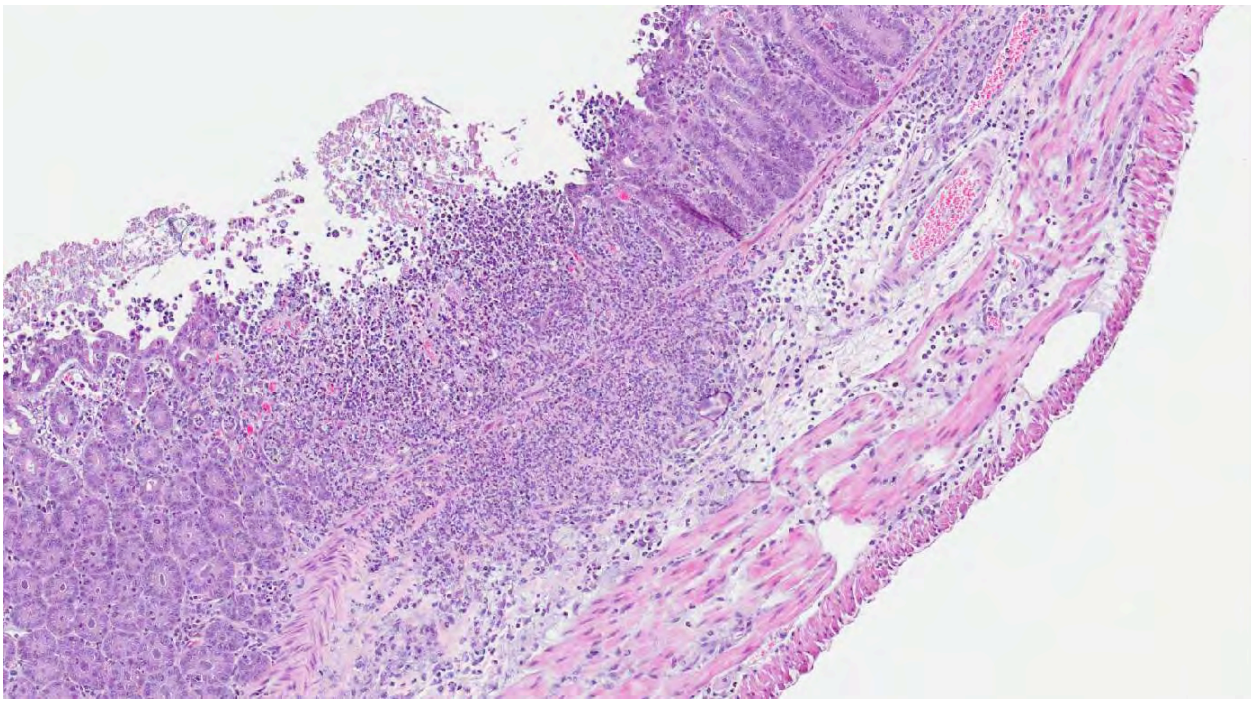

*4-2. Colon, hamster: The colonic mucosa is multifocally ulcerated with transmural infiltration of large numbers of neutrophils. (HE 35X)*

pathways.[4] Toxins also glycosylate Rho, which regulates the actin cytoskeleton, resulting in the opening of tight junctions, and eventual cell apoptosis.[4] The toxins also cause release of proinflammatory mediators, attracting neutrophils, and activate secretion stimulated by the enteric nervous system.[4] Demonstration of the toxins is necessary for interpretation of the diagnostic significance of *C. difficile*.

This case is similar to a recently reported fatal clostridial typhlitis of a Syrian hamster treated with topical antibiotic ointment, containing polymixin B, neomycin and bacitracin.[1] That case surmised that self-grooming may have resulted in unintentional oral exposure of the antibiotic, as well as possible absorption through the skin wound. Neomycin has been demonstrated to induce antibiotic-associated diarrhea in hamsters, and the other antibiotics are not known to induce diarrhea or colitis. Unlike the other antibiotics, neomycin can be absorbed through abraded skin or wounds. The Vetropolycin® applied repeatedly to the dorsal cervical region of the hamsters in this case contained the same mix of antibiotics: polymixin B, neomycin and bacitracin.

This case cautions against the topical clinical application of antibiotics to hamsters. Antibiotic therapy in hamsters is challenging, and trimethoprim sulfonamides, fluoroquinolones and chloramphenicol are generally safer antibiotic choices.

**JPC Diagnosis:** Cecum, colon: Typhlocolitis, necrotizing, multifocal, moderate.

**Conference Comment:** As stated by the contributor, demonstration of *Clostridium* toxin is necessary to evaluate the significance of observing *C. difficile*, as it is the toxins, rather than the mere presence of the bacteria that elicits disease. The primary toxins, TcdA and TcdB, belong to the family of large clostridial toxins (LCTs), along with lethal and hemorrhagic toxins from *C. sordelli,* α-toxin from *C. novyi*, and large cytotoxin from *C. perfringens*. LCTs inactivate host Rho and Ras GTPases, which are responsible for regulating many cellular processes, including maintenance of the cytoskeleton. More specifically, TcdA and TcdB intoxication results in loss of cytoskeketal structure and rounding of the affected cell, commonly referred to as the cytopathic effect. TcdB has more potent cytotoxic effects, and is therefore referred to as the "cytotoxin." TcdA also induces fluid accumulation in the intestinal tract, earning it the title "enterotoxin."[6] TcdA and TcdB cause cell death through a variety of mechanisms including both apoptosis (p-53 dependent, p-53 independent, caspase-dependent and caspase-independent) and necrosis. Other effects on cells exposed to these toxins include disruption of cell-cell junctions and increased secretion of cytokines TNF, IL-1, IL-6, and IL-8. Il-8 is an important factor in the recruitment of neutrophils, which play a major role in the host response to *C. difficile* infection.

Both TcdA and TcdB are composed of two subunits: A and B; subunit A is an N-terminal glucosyltransferase domain (GTD), and subunit B is responsible for the delivery of subunit A into the target cell. Repetitive oligopeptides on subunit B bind to sugar moieties on host cell surfaces; the toxins then enter the cell through clathrin-mediated endocytosis, and endosomal acidification induces structural changes that create a pore in the host membrane. Next subunit B is cleaved via proteolysis to release GTD into the cytosol, where it inactivates host cell GTPase by glucosylation, leading to the previously-described deleterious effects on the cell.[6]

**Contributing Institution:** Memorial Sloan-Kettering Cancer Center
Zuckerman Research Center
415 E. 68th St., ZRC-940
New York, NY 10021

**References:**

1. Alworth L, Simmons J, Franklin C, et al. Clostridial typhlitis associated with topical antibiotic therapy in a Syrian hamster. *Lab Animal.* 2009;43;304-309.
2. Best EL, Fawley WN, Parnell P, et al. The potential for airborne dispersal of *Clostridium difficile* from symptomatic patients. *Clin Infect Dis*. 2010;50:1450-1457.
3. Denève C, Deloménie C, Barc M-C, et al. Antibiotics involved in *Clostridium difficile*-associated disease increase colonization factor gene expression. *J Med Microbiol*. 2008;57:732-738.
4. Maxie MG, Robinson WF. Alimentary system. In: Maxie MG, ed. *Jubb, Kennedy, and Palmer's Pathology of Domestic Animals*. 5th ed. Vol. 2. Philadelphia, PA: Saunders Elsevier; 2007:214.
5. Percy DH, Barthold SW. Hamster. In: *Pathology of Laboratory Rodents and Rabbits*. 3rd ed. Ames, IA: Blackwell Publishing; 2007:186-187.
6. Pruitt RN, Lacy DB. Toward a structural understanding of *Clostridium difficile* toxins A and B. *Front Cell Infect Microbiol.* 2012:2:28.

**Joint Pathology Center**
**Veterinary Pathology Services**

## WEDNESDAY SLIDE CONFERENCE 2012-2013

# Conference 3

**3 October 2012**

**CASE I:** 096260 (JPC 3167342).

**Signalment:** 17-year-old, female, French trotter horse (*Equus caballus*).

**History:** A 17-year-old female horse was referred to the Veterinary School of Nantes for clinical signs of respiratory difficulty and persistent left sinus deformation.

Physical examination revealed a bilateral deformation of gums with multifocal ulceration. RMI showed maxillary bone and turbinate replacement by a material of fibrous density. The horse was euthanized for humane reasons and a complete necropsy examination was performed shortly after death.

**Gross Pathologic Findings:** At necropsy, a severe bilateral rostrocaudal osteolysis of maxillary bone was observed. Bone was replaced by a white, firm, fibrous tissue. Other macroscopic findings include a 6 cm diameter, white, firm, homogenous, and well-delimited nodule on the left kidney.

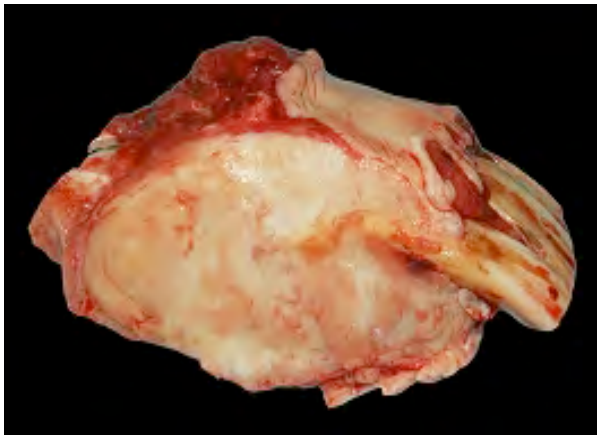

*1-1. Maxillary Bone; horse : Severe bilateral rostro-caudal osteolysis of maxillary bone replaced by a homogeneous white, firm fibrous tissue, multifocal ulceration of gums. (Photo courtesy of Department of Veterinary Pathology, ONIRIS (Nantes-Atlantic College of Veterinary Medicine, Food Science and Engineering), Nantes, France. http://www.oniris-nantes.fr)*

*1-2. Kidney; horse : 6 cm diameter, white, firm, homogeneous, well-delimited nodule. (Photo courtesy of Department of Veterinary Pathology, ONIRIS (Nantes-Atlantic College of Veterinary Medicine, Food Science and Engineering), Nantes, France. http://www.oniris-nantes.fr)*

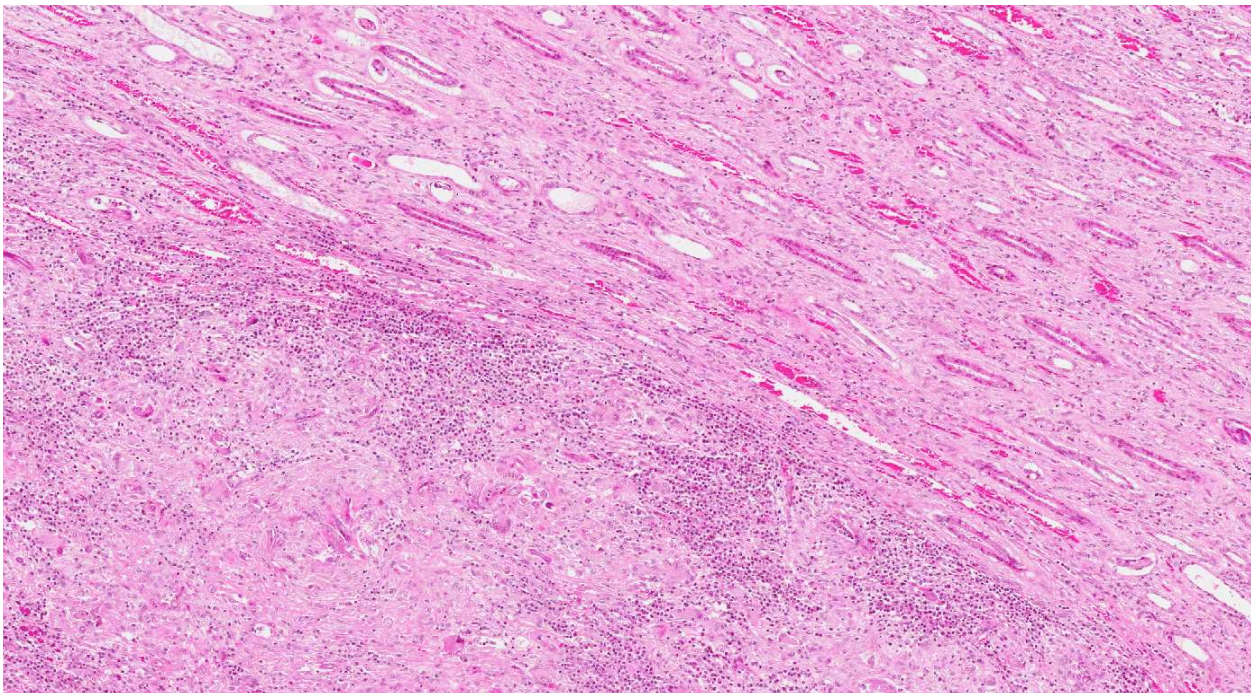

*1-3. Kidney, horse: Approximately 90% of the section is effaced by a well-demarcated area of granulomatous inflammation. (HE 40X)*

**Histopathologic Description:** The renal architecture was disrupted by multifocal coalescent granulomas cantered on numerous tangential and cross-sections of well-preserved round worms (nematodes). The inflammatory infiltrate mainly consisted of epithelioid cells, multinucleated giant cells, numerous plasma cells, eosinophils and few lymphocytes surrounded by abundant fibrous tissue. Multifocally, foci of dystrophic calcification were adjacent to degenerated nematodes. The nematodes were 250-300 µm length and 15-20 µm diameter, with a smooth thin cuticle, a tapered tail, a uterus containing a dorsoflexed ovary and a long characteristic rhabditiform esophagus with a corpus, an isthmus and a bulb. Smaller nematodes with a length of 150-180 µm and a diameter of 10-15 µm with a rhabditiform esophagus and granular internal basophilic structures were also detected. The nematodes were interpreted respectively as adult and larval stages of *Halicephalobus gingivalis* (formerly *H. deletrix*, *Micronema deletrix)*. Numerous eggs with a length of 35 µm and a diameter 20 µm were also observed.

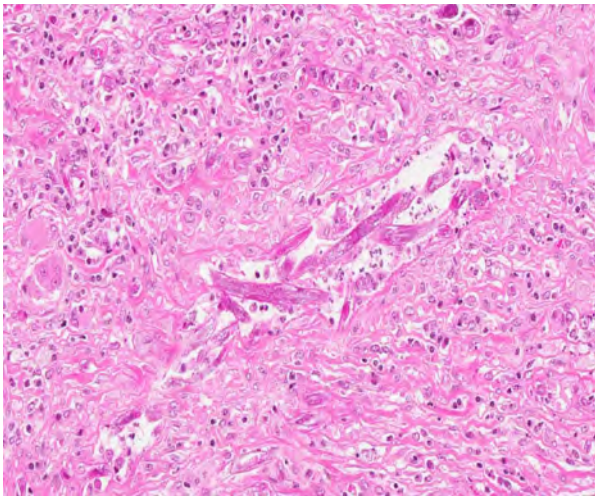

*1-4. Kidney, horse: Scattered throughout the affected area are poorly formed granulomas, often centered upon tangential and cross-sections of adult rhabditoid nematodes (center) as well as smaller larval forms with numerous somatic nuclei and developing internal structures. (HE 200X)*

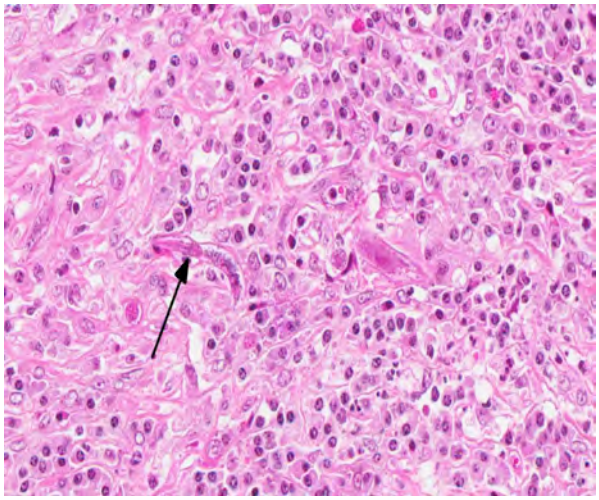

*1-5. Cross-section of Halicephalobus gingivalis larva with rhabitiform esophagus including corpus, isthmus, and bulb (arrow). (HE, 400X)*

**Contributor's Morphologic Diagnosis:** Kidney: nephritis, granulomatous, multifocal, coalescent, with intralesional *Halicephalobus gingivalis*.

**Contributor's Comment:** *H. gingivalis* (formerly *Micronema deletrix*) is a free-living, saprophytic and opportunistic small nematode of the order *Rhabditida*, family *Rhabditidae*. Most species inhabit decaying organic matter and are common in soil, foul water and manure. *H. gingivalis* infections occur sporadically. This parasitic infection is described at least in 60 cases in horses mainly in the USA, Canada, Japan, in few cases in ponies and humans.[1] One case in a horse was recently described in Switzerland but no case has been described in France before. The pathogenesis, life cycle and route of infection of *H. gingivalis* are poorly understood.[6] Free-living forms of the parasite in the soil are suspected to infect horses via skin or mucous membrane wounds in recumbent animals, and then disseminate hematogenously or to migrate along blood vessels or nerves to internal parenchymal tissues including the central nervous system.[3,6] Other routes of infection have been suggested, such as: infections from inhalation of the nematodes, possible colostral transfer to foals during nursing (as described in one report involving a Thoroughbred mare with mastitis and a nursing foal with encephalitis).[3,6] Additionally, the possibility of urogenital route has been considered, as viable organisms were noted in the sperm and urine of two stallions.[5] *H. gingivalis* life cycle is unknown. In tissues, only adult female, larvae and eggs are observed and asexual reproduction by parthenogenesis is suspected.[5] Free male and female worms are found in soil and a sexual reproduction is suspected. The classical granulomatous lesions of *Halicephalobus* in horses are mainly found in the brain, kidneys, oral and nasal cavities, lymph nodes, and spinal cord.[1,3,5] They are also frequently found in the adrenal gland and lung. Infrequent sites of granuloma formation include stomach, bone (mandible, femur, maxilla, nasal bones), ganglia, heart, liver, and eye, testicle and prepuce.[5,6] In human cases, granulomatous lesions are always found in brain and sometimes in the heart and liver.

The other rhabditid parasites infecting the horse are: *Pelodera strongyloides*, *Strongyloides westerii* and *Cephalobus sp*. *Pelodera strongyloides* causes a self-limiting dermatitis normally confined to the ventral abdomen. *Pelodera* is mostly observed in dogs and rarely in sheep. *S. westerii* larvae causes a cutaneous infection but adults and eggs are not found in the skin. In cutaneous and mucocutaneous lesions *Cephalobus* can be distinguished from *H. gingivalis* by its esophagus and stoma shape and blunt posterior end.[5,6]

**JPC Diagnosis: Kidney:** Nephritis, granulomatous and eosinophilic, focally extensive, severe with adult and larval rhabditoid nematodes.

**Conference Comment:** The contributor provided a very good description and discussion of the classic lesions caused by *Halicephalobus gingivalis* in horses. Conference participants, while discussing the pathogenesis of this disease, elaborated on the role of eosinophils in parasitic infections and reviewed several aspects of eosinophilic inflammation. Eosinophilia (defined as an increase in the number of eosinophils in tissue or blood) is generally observed in parasitic disease, hypersensitivity, and in some neoplasms. Eosinophils can be recruited in cases of both ectoparasitism and endoparasitism. Additionally, they play a role in the late phase of type I (immediate) hypersensitivity reactions (anaphylaxis, allergies, asthma etc.). Neoplastic diseases that often recruit eosinophils include eosinophilic leukemia, mast cell tumor, T-cell lymphoma, lymphomatoid granulomatosis, various carcinomas, fibrosarcoma, and thymoma.[4] Eosinophils are produced and mature in bone marrow. IL-5 is the most important cytokine involved in eosinophil production, influencing eosinophil proliferation, differentiation and maturation, as well as function. GM-CSF and IL-3 also play more minor roles in eosinophilic development.[4]

Eosinophils contain distinct granules, called secondary (aka specific) granules, which are lysosomes that contain several components, including major basic protein, acid hydrolases, eosinophilic cationic protein, and eosinophil-specific peroxidase.[2,4] Although eosinophils are also capable of phagocytizing and killing bacteria, they are not as adept at this as neutrophils, and generally cannot clear a bacterial infection independently. Their main function is against large organisms (such as helminths) that are too large to be phagocytized.[4] Under the influence of a Th2 biased immune response in a helminth-infected host, eosinophils are recruited predominantly by IL-5, as well as IL-2 and IL-16. These cytokines induce mature eosinophils to emigrate from the blood and respond to chemoattractants (such as eotaxin, aka CCL-11) to home in to the helminth-infected tissue. There eosinophils bind to immunoglobulins (particularly IgE) and complement components (C1q, C3b/C4b, iC3b, C5a) on the surface of their targets. They may also bind to ligands on the parasite surface (Lewis-related molecules and cell-adhesion molecules). Once activated by antigen-IgE complexes, eosinophils secrete cytokines and chemokines (IL-2, IL-4, IL-10, IL-12, IL-16, IL-3, IL-5, eotaxin, TGF-alpha, VEGF, TNG-alpha, among others) and proinflammatory mediators (substance P).[2] Additionally, they degranulate to release their cytotoxic substances with the following effects: Major basic protein is toxic to helminths, as well as tumor and host cells; it also activates platelets, neutrophils mast cells and basophils. Eosinophilic cationic protein is also toxic to helminths and host cells. Eosinophilic

specific peroxidases generate toxic oxygen radicals, providing a further weapon against helminths. Acid hydrolases have digestive functions. Once they degranulate, eosinophils die via apoptosis.[2] Although studies have shown that there may be species variability in the significance of the impact of IL-5 and eosinophils in helminth infections, generally it is accepted that IL-5-induced eosinophilia often plays an important role in the immune response to parasites.

**Contributing Institution:** Department of Veterinary Pathology, ONIRIS (Nantes-Atlantic College of Veterinary Medicine, Food Science and Engineering), Nantes, France
www.oniris-nantes.fr

**References:**

1. Akagami M, Shibahara T, Yoshiga T, et al. Granulomatous nephritis and meningoencephalomyeliis caused by *Halicephalobus gingivalis* in a Pony Gelding. *J Vet Med Sci***.** 2007;69 (11):1187-1190.
2. Behm CA, Ovington KS. The role of eosinophils in parasitic helminth infections: insights from genetically modified mice. *Parasitol Today.* 2000:16(5);202-209.
3. Bryant UK, Lyons ET, Fairfield TB, et al, *Halicephalobus gingivalis*-associated meningoencephalitis in Throroughbred foal. *J Vet Diagn Invest*. 2006;18:612-615.
4. Webb JL, Latimer KS. Leukocytes. In: Latimer KS, ed. *Duncan & Prasse's Veterinary Laboratory Medicine: Clinical Pathology.* 5th ed. Ames, Iowa: Wiley-Blackwell; 2011:54, 74-75.
5. Johnson JS, Hibler CP, Tillotson KM et al. Radiculomeningomyelitis due to *Halicephalobus gingivalis* in a horse. *Vet Pathol* 2001;38:559-561.
6. Muller S, Gryzbowskit M, Sager H, et al. A nodular granulomatous posthitis caused by *Halicephalobus sp*. in a horse. Journal compilation. ESVD and ACVD: 2007;19:44-48.

**CASE II:** V11-1130 (JPC 4001095).

**Signalment:** Eight-year, nine-month-old spayed female, domestic shorthair feline (*Felis catus*).

**History:** The cat presented with a lesion on its abdomen of unknown duration. The referring veterinarian initially suspected a possible spider bite that was too large to debride. The differential diagnosis included neoplasia and inflammation/ infection. Culture of the deep tissue tracts yielded growth of coagulase-positive *Staphylococcus aureus*. Convenia® (cefovecin sodium) and injectable corticosteroids were inconsistently administered by the owner. The cat initially appeared tolerant of the constantly growing and purulent lesion that involved over half of its abdomen. When the cat became lethargic, depressed, and inappetent, biopsies of the lesion were taken and submitted for histopathologic evaluation.

**Gross Pathologic Findings:** Extensive cutaneous fistulous tracts involving over half of the abdomen.

**Histopathologic Description:** Haired skin and subcutis, abdomen: Multifocally expanding the dermis and subcutis; separating, surrounding, and replacing adnexa; and elevating the mildly acanthotic and hyperkeratotic epidermis are multiple, densely cellular, up to 2 mm diameter nodules composed of numerous epithelioid macrophages, neutrophils, fewer lymphocytes and plasma cells, and rare mast cells and eosinophils surrounded by reactive fibroblasts and, in some areas, hemorrhage, fibrin, and edema. Multifocal nodules contain variably sized, up to 100 µm diameter extracellular lipid vacuoles (lipocysts) surrounded by a rim of neutrophils; these occasionally contain many 3-5 µm diameter filamentous bacilli. Occasionally, nodules contain a large central area of necrosis characterized by abundant amounts of eosinophilic cellular and karyorrhectic debris.

**Acid –fast stain (Ziehl-Neelsen):** Many intravacuolar and intrahistiocytic acid-fast, 3-5 µm, filamentous bacilli are present.

**Contributor's Morphologic Diagnosis:** Haired skin and subcutis, abdomen: Dermatitis and panniculitis, pyogranulomatous, nodular, multifocal to coalescing, marked, with many intravacuolar and intrahistiocytic, 3-5 µ m filamentous acid-fast bacilli, domestic shorthair (*Felis catus*) feline.

**Contributor's Comment:** Classically, three manifestations of feline mycobacteria-associated skin disease are recognized: (1) feline leprosy, (2) cutaneous tuberculosis, and (3) atypical mycobacteriosis (rapidly growing mycobacteria).[3,6]

The feline leprosy group is comprised of obligate pathogens and can be subdivided into lepromatous (multibacillary) and tuberculoid (paucibacillary) forms.[3,6] Affected cats are typically young adults (1-3 years old) and lesions typically occur on the head, limbs, and trunk.[3,4,6] Regional lymphadenopathy may be present, but affected cats are otherwise healthy.[3,4] The mode of transmission is thought to be by rodent or cat bites, biting insect vectors, or soil contamination of cutaneous wounds.[6] The causative agent is presumed to be *Mycobacterium lepraemurium*; however, other potentially causative mycobacteria (*M. visibilis*, *M. malmoense*) have been isolated from cutaneous lesions clinically consistent with feline leprosy by molecular techniques.[4,6] *M. lepraemurium* does not grow in culture using standard techniques, but has been isolated by PCR with DNA sequencing.[6] Feline leprosy has no

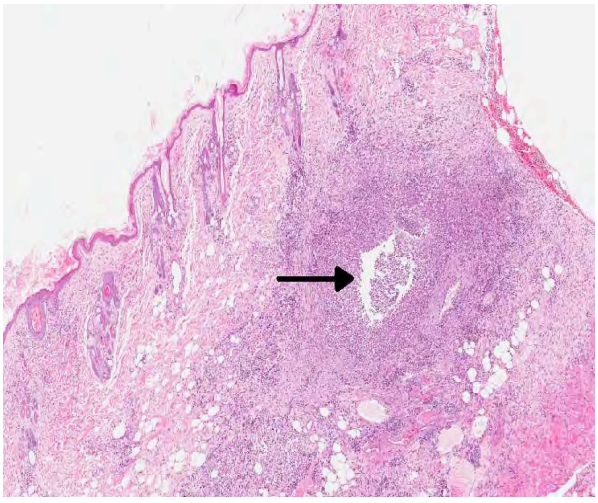

*2-1. Haired skin, cat: Extending from the dermis through the panniculus adiposus, there are dense areas of pyogranulomatous inflammation with scattered areas of lytic necrosis (arrow). (HE 20X)*

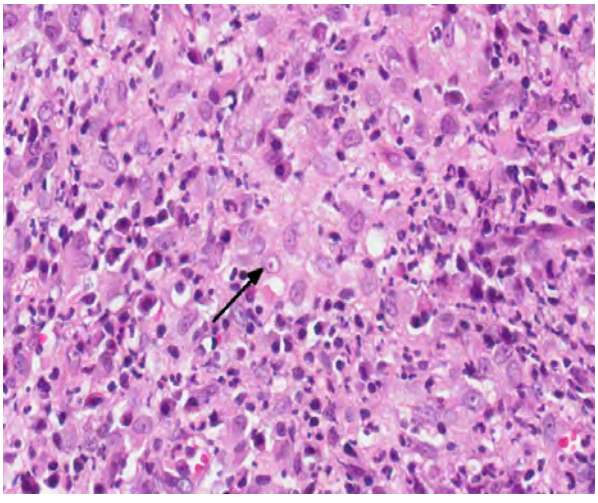

*2-2. Haired skin, cat: The inflammatory infiltrate is composed of sheets of epithelioid macrophages (arrow) admixed with viable neutrophils, lymphocytes, and plasma cells. (HE 400X)*

known zoonotic potential. Nerve involvement is not a characteristic feature of feline leprosy and is sporadic.[4]

The causative agents of cutaneous tuberculosis, *M. bovis* and *M. tuberculosis,* are also considered obligate pathogens. Cutaneous infections are rare. Feline cutaneous mycobacteriosis is most often caused by *M. bovis*.[3] Gastrointestinal and pulmonary infections are more common. Infections of the gastrointestinal tract and mesenteric lymph nodes usually occur following ingestion of milk or meat of infected cattle.[3] Cutaneous infections can occur alone (rare) or in combination with disseminated infection.[4,6] Lesions of feline cutaneous mycobacteriosis typically occur on the face, neck, shoulders, and forepaws. Less commonly the lesions occur on the ventral thorax and tail. Skin lesions can develop from bite wounds or as a result of dissemination from the gastrointestinal tract. Affected cats typically present with a local or generalized lymphadenopathy.[3] The causative agents of cutaneous tuberculosis are zoonotic.

Atypical mycobacteriosis (rapid growing Runyon Group IV mycobacteria) are considered opportunistic pathogens – saprophytes or facultative pathogens that are ubiquitous in soil, water, and decomposing vegetation.[3,4,6,8,10] Included in the atypical group are *M. fortuitum*, *M. phlei*, *M. smegmatis*, *M. chelonae*, *M. abscessus*, *M. flavescens*, *M. thermoresistible*, and *M. xenopi*. The Runyon Group IV mycobacteria have a predilection for lipid rich tissues. Consequently, lesions characteristically occur on the ventral abdomen in the subcutaneous fat of inguinal area in cats.[4,5,6] Female cats are overly represented possibly due to the propensity of spayed females to become obese.[3,7] Studies have shown that introduction of acid-fast bacilli into adipose tissue facilitates their pathogenicity, possibly by providing nutrients for growth or by protecting them from the host immune response.[1,4,8,10] Infections occur via wound contamination or traumatic implantation. Consequently, many cats with atypical mycobacteriosis have a history of previous trauma.[4,5] Animal-to-animal transmission is not thought to occur and affected cats are usually not immunocompromised.[4,8] Atypical mycobacteriosis is not considered zoonotic.

Cutaneous lesions with atypical mycobacteria have been reported primarily in cats.[4,6] The clinical course is prolonged and lesions present as single or multiple cutaneous and subcutaneous nodules, diffuse swellings, plaques, or purpuric macules.[4] Fistulous tracts discharge serous, serosanguinous, or purulent exudates that are not usually malodorous.[4,8] Lesions slowly enlarge and eventually may encompass the entire ventrum and extend up the lateral trunk. Undermining

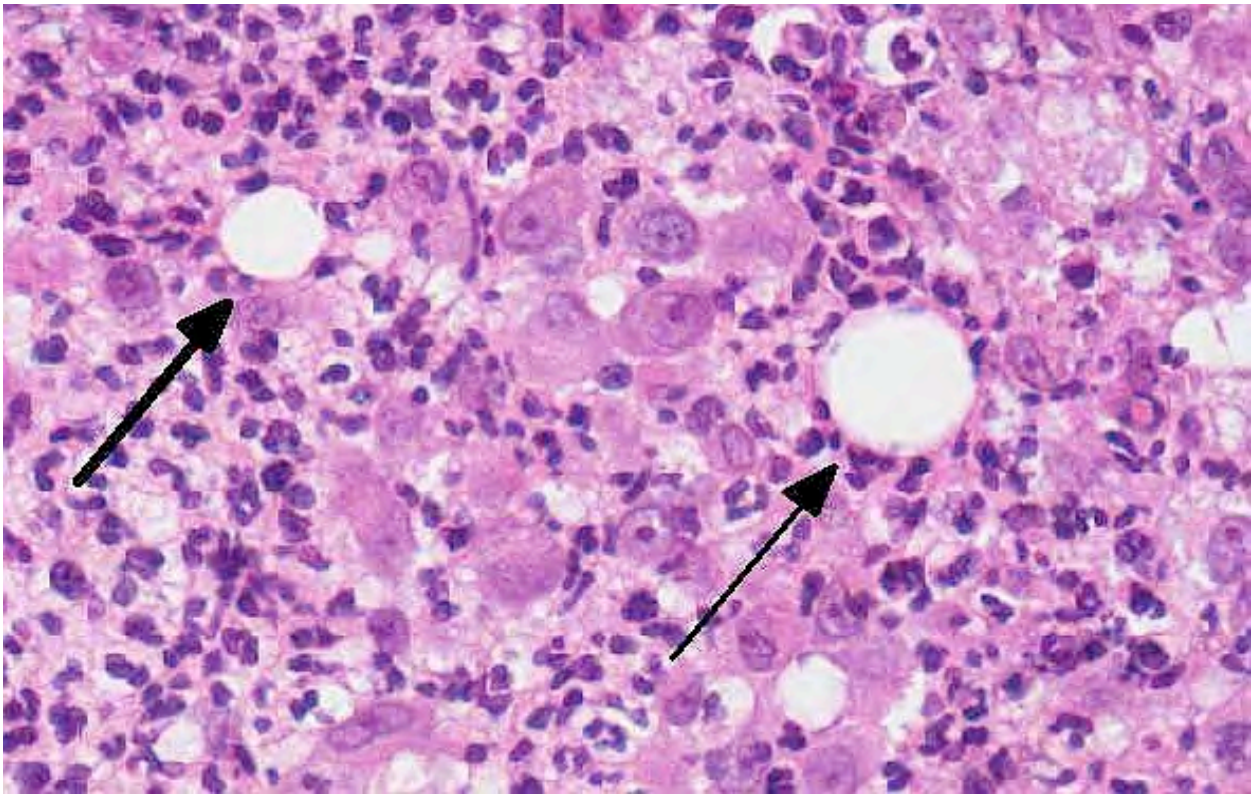

*2-3. Cleared spaces corresponding to residual lipid from degenerating adipocytes (lipocysts) are surrounded by neutrophils and epithelioid macrophages. (HE 360X)*

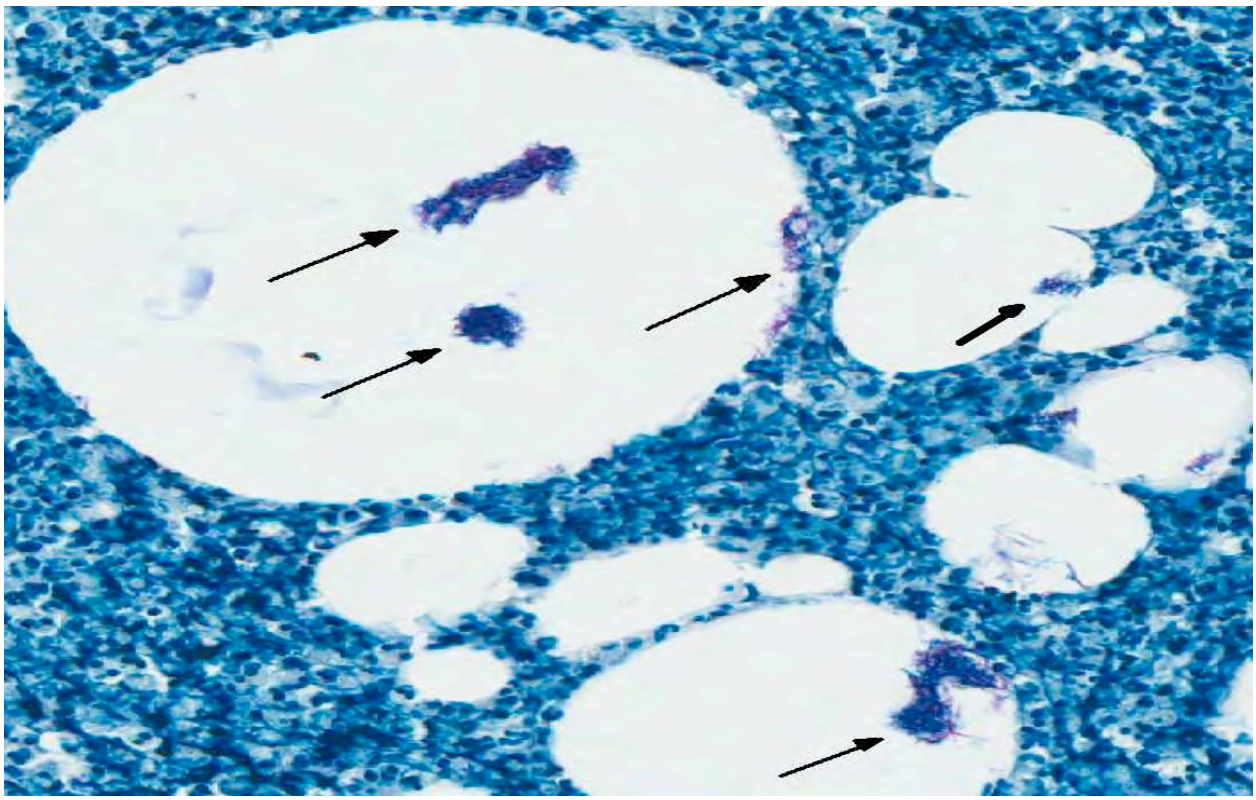

*2-4. Aggregates of partially acid-fast robust bacilli are present within lipocysts. (Fite-Faraco, 400X)*

of peripheral skin is characteristic with purple depressions (thin skin) overlying accumulations of pus.[5] Despite extensive cutaneous involvement, most animals remain active with no systemic signs of illness.[4,8]

Histologically, the epidermis is usually acanthotic or ulcerated with multinodular to diffuse pyogranulomatous dermatitis and panniculitis.[5] Thin rims of neutrophils with a wider zone of epithelioid macrophages usually surround varisized lipocysts (clear zones comprised of residual lipid from degenerating adipocytes).[5,6] Pyogranulomas without central spaces (lipocysts) may be seen as well. Pyogranulomas are often confluent and interspersed with diffuse inflammation composed primarily of macrophages and neutrophils. Chronic lesions may contain peripheral lymphoid nodules and/or fibrosis. Giant cells are usually absent.[5] Rapidly growing opportunistic mycobacteria may or may not be difficult to find in tissue section and have been described as rare to numerous.[4,8] When numerous, mycobacteria may be partially visible on hematoxylin and eosin (HE) stained tissue. Fite's stain (a Fite-Faraco modification of the acid-fast stain) is useful in accentuating difficult-to-see mycobacteria. Mycobacteria are most commonly found in lipocysts due to protective fat, but may also be present in macrophages.[5]

In summary, pyogranulomas surrounding clear central spaces are very suggestive of a rapidly growing mycobacterial infection with HE stain, but may also be seen in other deep infections (e.g., higher bacteria). Demonstration of acid-fast organisms in lipocysts is highly supportive of the diagnosis; however, this should be confirmed by culture or molecular techniques.[5]

The differential diagnosis for cutaneous infection with rapid growing mycobacteria includes bite wound abscesses, deep mycotic or bacterial infections, sterile nodular panniculitis, and foreign body reactions.[5] Deep wedge biopsies are preferred over punch biopsies for diagnosis since inflammation is most intense in the subcutaneous fat.[4,5]

Cases of feline atypical mycobacteriosis carry a guarded prognosis as treatment can be challenging, especially with chronic lesions.[5,10] Treatment involves radical surgical debridement followed by long-term (3-6 months) treatment with concurrent administration of multiple antimicrobial agents.[5,8,10] Identification by culture or molecular techniques is required so that appropriate therapy and zoonotic potential can be determined.[3,4] Infective mycobacterium can be difficult to culture and repeated cultures may be necessary to yield a positive response.[8]

**JPC Diagnosis:** 1. Haired skin: Dermatitis, cellulitis and panniculitis, pyogranulomatous, necrotizing, focally extensive, severe, with lipocysts and many intravacuolar and intrahistiocytic 3-5 µm filamentous acid-fast bacilli.
2. Haired skin: Dermatitis, eosinophilic and mastocytic, subacute, multifocal, mild with bacterial folliculitis and rare intracorneal pustules.

**Conference Comment:** The contributor provides an excellent overview of feline mycobacterial skin diseases. Mycobacterial cell walls are composed of mycolic acids, which not only provide physical protection for the mycobacteria, but also play important roles in the pathogenesis of the diseases they cause. Mycolic acids are glycolipids that regulate the intrahistiocytic growth rate of mycobacteria and influence the host immune response.[1] One important mycolic acid is trehalose 6,6-dimycolate (TDM, cord factor), which is found in large quantities in many species of *Mycobacterium*, including virulent strains of *M. tuberculosis* as well as saprophytic *M. fortuitum*.[1] TDM appears to regulate the intrahistiocytic growth of mycobacteria by inhibiting fusion between phospholipid vesicles, thus inhibiting phagosome-lysosome fusion during infection. TDM also induces macrophage production of proinflammatory cytokines (e.g., IL-1β, IL-6, TNF-α, IL-12), leading to the development of granulomas.[7] Mycolic acid-containing components of the cell wall also promote angiogenesis and interact with Toll-like receptors. Additionally, their presentation as antigens to CD1-restricted T cells further influence the host immune response. CD1-restricted T-cells are a group of T-cells that recognize lipid antigen (such as fatty acids, phospholipids, glycolipids, isoprenoids, mycolates and lipopeptides ) presented by the CD1 family of molecules independent of MHC.[2] CD1a, b and c-restricted T cells recognize several lipid antigens from *M. tuberculosis*. CD1 restricted T-cells are cytotoxic and secrete Th1 cytokines.[9] Hence, the presence of mycolic acids such as TDM in mycobacterial cell walls may partly determine the outcome of mycobacterial infections in host macrophages.

In addition to the prominent pyogranulomatous dermatitis, panniculitis and cellulitis, conference participants noted a second, more subtle lesion consisting of eosinophilic and mastocytic dermatitis; the relationship between the two lesions is uncertain. Additionally, conference participants debated the microscopic presence of fistulous tracts, which would correlate well with the usual gross findings in atypical cutaneous mycobacteriosis.

**Contributing Institution:** Air Force Research Laboratory, 2509 Kennedy Circle, Building 125, Brooks City Base, TX 78235

**References:**
1. Couto SS, Artacho CA. *Mycobacterium fortuitum* pneumonia in a cat and the role of lipid in the pathogenesis of atypical mycobacterial infections. *Vet Pathol*.2007;44:543-546.
2. Cohen NR, Garg S, Brenner M. Antigen Presentation by CD1 Lipids, T Cells, and NKT Cells in Microbial Immunity [abstract]. *Adv Immunol*. 2009;102:1-94. http://www.ncbi.nlm.nih.gov/pubmed. Accessed October 6, 2012. PMID: 19477319.
3. Davies JL, Sibley JA, Myers S, et al. Histological and genotypical characterization of feline cutaneous mycobacteriosis: a retrospective study of formalin-fixed paraffin-embedded tissues. *Vet Dermatol*. 2006;17:155-162.
4. Ginn PE, Mansell JEKL, Rakich PM. Skin and appendages. In: Maxie MG, ed. *Jubb, Kennedy, and Palmer's Pathology of Domestic Animals*. Vol. 1, 5th ed. New York, NY: Elsevier Saunders; 2007:687-690.
5. Gross TL, Ihrke PJ, Walder EJ, et al. *Skin Diseases of the Dog and Cat Clinical and Histopathological Diagnosis*. 2nd ed. Ames, Iowa: Blackwell Science Ltd; 2005:283-287.
6. Hargis AM, Ginn PE. The integument. In: McGavin MD, Zachary JF, eds. *Pathologic Basis of Veterinary Disease.* 4th ed. St. Louis, MO: Mosby Elsevier; 2007:1185-1187,
7. Indrigo J, Hunter RL, Actor JK. Cord factor trehalose 6,6'-dimycolate (TDM) mediates trafficking events during mycobacterial infection in murine macrophages. *Microbiology.* 2003;149(8):2049-2059.
8. Malik R, Wigney DI, Dawson D, et al. Infection of the subcutis and skin of cats with rapidly growing mycobacteria: a review of microbiological and clinical findings. *J Feline Med Surg.* 2000; 2(1):35-48.9.
9. Montamat-Sicotte DJ, et al. A mycolic acid-specific CD1-restricted T cell population contributes to acute and memory immune responses in human tuberculosis infection. *J Clin Invest.* 2011;121(6):2493-503.
10. Wilson VB, Rech RR, Austel MG, et al. Pathology in Practice. *J Am Vet Med Assoc.* 2011;238(2):171-173.

**CASE III:** 090031-35 (JPC 3141966).

**Signalment:** Seven-year-old, male Nubian-crossgoat, caprine *(Capra hircus)*.

**History:** This castrated adult male goat had lost approximately 35 lbs over two months and, at the time of necropsy, weighed approximately 175 lbs. Over the course of the last week, he exhibited labored, open-mouthed breathing, mucoid nasal discharge, and bruxism. On the day he was euthanized, he had blood and bloody froth coming from his nostrils. He had recently been treated with antibiotics, anthelmintics, and analgesics but continued his downward progression.

**Gross Pathologic Findings:** This approximately 175-pound male castrated goat was in good nutritional condition with adequate body fat stores. The nasal cavity contained mucoid to mucopurulent discharge and, on the right side of the nasal cavity, from the level of the upper 5th and 6th cheek teeth to the caudal termination of the nasopharynx, a space occupying mass. This mass was firm, measured approximately 5 cm long x 5 cm high x 1-2 cm wide, was partially covered in a mucopurulent, yellow exudate, and was partially adhered to the nasal respiratory mucosal epithelium.

The rumen was filled with brown fluid and watery hay ingesta; expanding the wall of a saccule, there was a 5 cm long x 3 cm wide x 3 cm thick mass with an ulcerated, crateriform center containing greenish-white pus. There were multiple 2-4 mm in diameter erosions around the central crater. On cut section, the crateriform ulcer extended into the rumen wall forming a pus-filled pocket which was surrounded by an approximately 1-2 cm thick band of white, firm, glistening tissue. Adhered to the adventitial surface of the caudal vena cava in the mid-abdomen was a 1.5 cm in diameter, fluid-filled translucent, sac-like structure. Multiple lymph nodes including the mediastinal, mesenteric, and axillary, as well as several subcutaneous lymph nodes, were bright green and enlarged up to three times normal size.

**Laboratory Results:** Immunohistochemistry was performed on sections of the rumen mass with the neoplastic cells showing the following results:

Positive: Vimentin; smooth muscle actin; S100 protein; desmin, multifocally positive.

Negative: Glial fibrillary acidic protein (GFAP); myoglobin; CD117a (c-kit); discovered on GIST-1 (DOG-1).

Microorganism stains:
Lilli Twort (Gram stain): Gram-positive coccobacilli in small colonies on the periphery of large colonies of Gram-negative filamentous bacteria within the necrotic exudate.

Periodic Acid-Schiff (PAS): Positive for long, filamentous bacterial rods forming club-shaped colonies; positive for fungal hyphae within the ulcer's necrotic core.

**Histopathologic Description:** Rumen: Expanding the muscularis externa and elevating the multifocally ulcerated and attenuated rumen papillae, there is a well-circumscribed, unencapsulated, highly cellular


*3-1. Rumen; goat: An ulcerated mass 5cm x 3cm x 3cm expands the rumen wall. Note the attenuated papillae overlaying the mass and the inspissated, purulent exudate in the center of the ulcer. (Photo courtesy of the U.S. Army Medical Research Institute of Infectious Diseases, (USAMRIID), Pathology Division, 1425 Porter Street, Fort Detrick, MD 21702-5011. http://www.usamriid.army.mil)*


*3-2. Rumen; goat: Cut surface of mass revealing a necrotic core surrounded by white, firm, glistening tissue and an adhered spleen. (Photo courtesy of the U.S. Army Medical Research Institute of Infectious Diseases, (USAMRIID), Pathology Division, 1425 Porter Street, Fort Detrick, MD 21702-5011. http://www.usamriid.army.mil)*

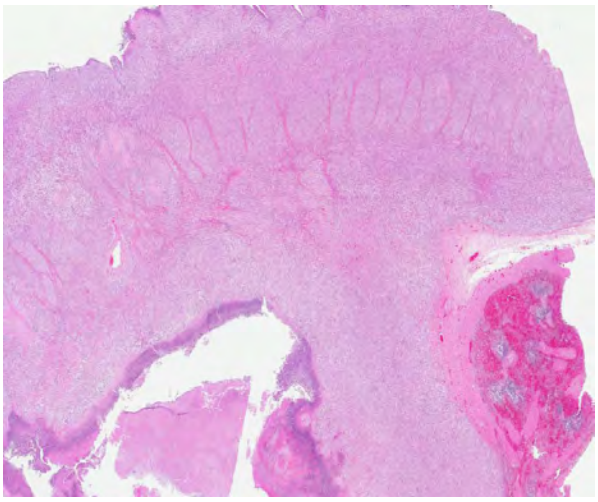

*3-3. Rumen, goat: The ulcerated rumen wall is transmurally effaced by a densely cellular mesenchymal neoplasm. (HE 4X)*

neoplasm composed of cells arranged in interlacing streams and bundles, often forming a herringbone pattern, and separated by interconnecting rays of fibrovascular matrix. Neoplastic cells range from tightly packed to loosely arranged spindle cells with indistinct cell borders and a moderate amount of eosinophilic and finely fibrillar cytoplasm. Nuclei are irregularly oval to elongate, with blunt ends, and are centrally located with finely stippled to vesiculate chromatin and indistinct nucleoli. Longitudinally arranged neoplastic cells are often rectangular, interlacing and surrounded by a thin rim of clear space. Mitotic figures average one per high power field, and there is mild anisocytosis and anisokaryosis. There are rare karyomegalic cells present. There is a large, 1 cm in diameter, necrotic core composed of a densely packed eosinophilic coagulum containing high numbers of viable and degenerate neutrophils and eosinophils mixed with necrotic cellular debris and large, dense club-shaped colonies of filamentous bacteria. Also present in scattered clusters throughout the coagulum are filamentous, 3-5 m wide, septate fungal hyphae which exhibit acute angle, dichotomous branching. In some sections there is mineralized debris with or without closely associated fungal hyphae. There are smaller foci of necrosis scattered throughout the neoplasm as well as lymphocytes and plasma cells frequently distributed along fibrovascular tissue. Multifocally, rumenal papillae are ulcerated or missing entirely and the exposed, subjacent neoplastic cells are covered by inflammatory cells and necrotic debris. Rumen papillae often have clusters of lymphocytes and plasma cells throughout the submucosa. The line of demarcation between the splenic capsule and serosa of the rumen is obscured by infiltrating neoplastic spindle cells, lymphocytes, plasma cells, hemorrhage, and fibrosis. There is mild lymphoid depletion within the white pulp of the spleen.

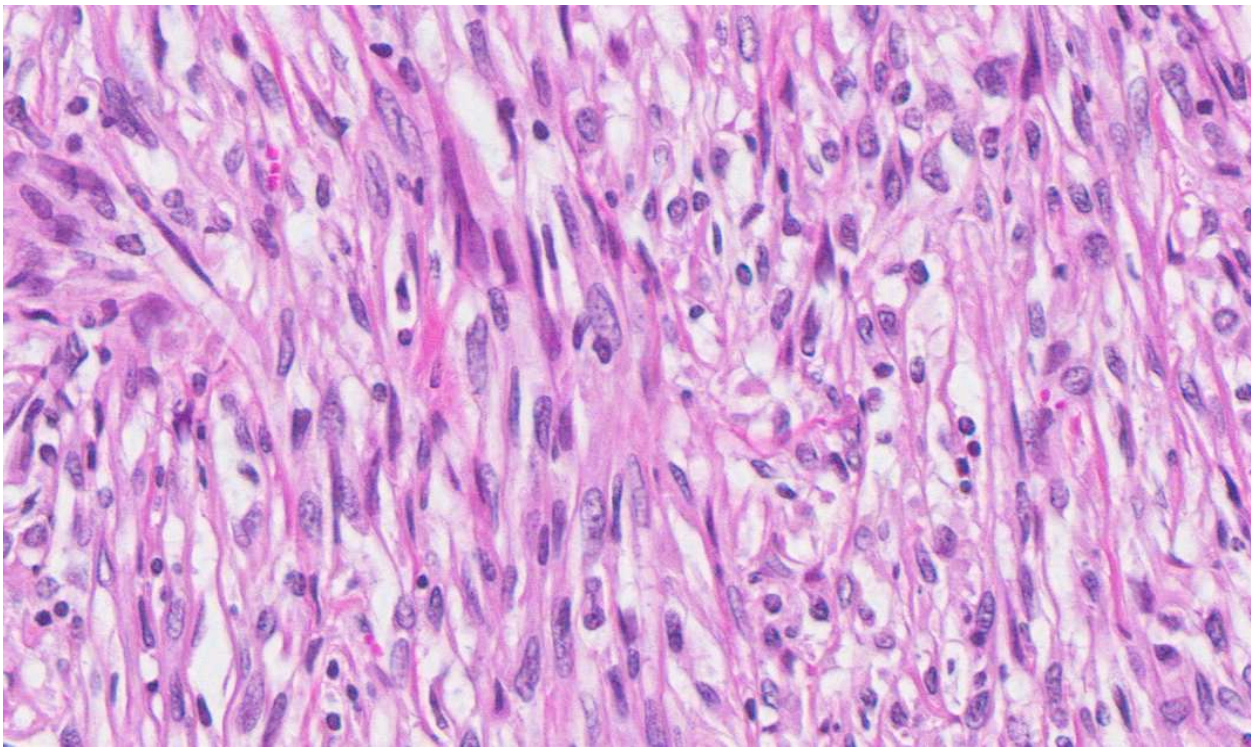

*3-4. Rumen, goat: Neoplastic cells are spindled and elongate, with indistinct cell borders and a moderate amount of a finely fibrillar eosinophilic cytoplasm. Nuclei are centrally placed, oval to elongate, with finely stippled chromatin and 1-3 small basophilic nucleoli. There is mild anisokaryosis, and mitotic figures are rare. (400X)*

**Contributor's Morphologic Diagnoses:**
1. Rumen: Leiomyosarcoma, goat, caprine.
2. Nasal mucosa: Rhinitis, granulomatous, focally extensive, severe, with fungal hyphae and granulation tissue (histoslides not submitted).
3. Vena cava: Pseudocyst with larval cestode (cysticercosis) (histoslides not submitted).
4. Lung: Pneumonia, interstitial, granulomatous, multifocal, mild, with intralesional nematode larvae, morphology consistent with *Muellerius capillaris* (histoslides not submitted).
5. Spleen, white pulp: Lymphoid depletion, diffuse, mild (histoslides not submitted).

**Contributor's Comment:** Leiomyomas and leiomyosarcomas are neoplasms of smooth muscle cell origin. Morphologic features of this neoplasm that support the diagnosis include the arrangement of interlacing fascicles or bundles of spindle-shaped cells occurring in both long and transverse section and often forming a herringbone pattern. Typical cytologic features include cells which resemble smooth muscle with a moderate amount of eosinophilic, fibrillar cytoplasm and elongate, oval nuclei with characteristic blunt ends.[3,4,5] Paranuclear cytoplasmic vesicles, a feature often described in soft-tissue leiomyomas in humans, were not a feature of the cells in this neoplasm.[7] In spite of a lack of either vascular or lymphatic invasion by neoplastic cells, the relatively brisk mitotic rate (one per high power field), cellular atypia, areas of necrosis, and mildly infiltrative neoplastic cells along the tumor's margins favor a diagnosis of leiomyosarcoma over leiomyoma. Metastases to regional lymph nodes were not identified.

Smooth muscle tumors (leiomyoma and leiomyosarcoma) of the alimentary system are the most common type of gastrointestinal stromal tumor reported in domestic animals.[3] In dogs, there are reports of leiomyomas arising from the wall of the gall bladder and outer muscle coats of the distal esophagus and stomach as well as reports of leiomyosarcomas arising throughout the digestive tract including the tongue, liver and spleen.[3,4,5] Likewise for cats, there are reports of leiomyomas and leiomyosarcomas throughout the gastrointestinal tract.[3] Additionally, there are rare reports of leiomyomas and/or leiomyosarcomas arising in the stomach, duodenum, jejunum, ileocecal junction, rectum and omentum of horses as well as reports of a leiomyoma in the spiral colon of a cow and the omasum of a goat.[2,3,10] In general, leiomyomas of the digestive tract are more likely to be located in the upper rather than the lower tract.[5] To the best of our knowledge, this is the first report of a primary leiomyosarcoma arising from the rumen of a goat.

In contrast to the alimentary system, leiomyomas and leiomyosarcomas are much more commonly reported in the urinary and reproductive tracts of laboratory and domestic animals. As such, there are reports in the veterinary literature of leiomyomas/leiomyosarcomas of the uterus in rats, rabbits, and guinea pigs; urinary bladder, vagina and uterus of cows; the scrotum, vagina, cervix, uterus, and urinary bladder of goats; the female genital tract, testis and urinary bladder of horses; and the urinary bladder, vagina, uterus, cervix and prostate gland of dogs and cats.[3,4,5,11]

Immunohistochemisty can be useful in differentiating and aiding in the diagnosis of neoplasms which have similar cellular morphology. In this case, gastrointestinal stromal tumor (GIST) and peripheral nerve sheath tumor were considered differential diagnoses.

Leiomyomas/leiomyosarcomas typically express vimentin, desmin, and smooth muscle actin (SMA).[4] GISTs are believed to arise from primitive mesenchymal cells and, as such, can express vimentin, smooth muscle actin (SMA), and S-100 protein to varying degrees.[3,7,9,4,8,10] Additionally, in humans, GISTs also commonly express both the tyrosine kinase receptor CD117 (c-kit), and/or the chloride channel protein, discovered on GIST-1 (DOG1).[9] Peripheral nerve sheath tumors are composed of spindloid cells with characteristics of Schwann cells and are typically vimentin, S-100 protein, and glial fibrillary acidic protein (GFAP) positive and SMA negative.[3] The neoplastic cells of the tumor described in this case expresses vimentin, desmin, SMA, and it does not express CD117, DOG1, or GFAP. These immunohistochemical findings support the diagnosis of a smooth muscle origin neoplasm; however, well-differentiated smooth muscle tumors do not typically express S100 protein as was seen in this neoplasm. There is a small percentage of human cases of leiomyosarcomas which do express immunoreactivity for S100 protein.[6]

Additional features of this lesion include large, up to 300 µm in diameter, radiating, club-shaped colonies of filamentous bacteria scattered throughout the necrotic exudate, often associated with mineralized debris ("sulfur granules"). Gram-negative and strong PAS staining of the large colonies of filamentous bacteria suggests infection by *Fusobacterium necrophorum,* a normal inhabitant of the alimentary tract and a common cause of necrobacillary rumenitis secondary to rumenal acidosis. Differentials for large colonies of filamentous bacteria include the higher forms of bacteria such as *Actinomyces* sp., *Nocardia* spp., or *Arcanobacterium pyogenes*; however, all three generally stain gram-positive. Additionally, with the aid of Gram stain, small colonies of gram-positive

coccobacilli, suggestive of *Corynebacterium pseudotuberculosis*, are also identified within the necrotic exudate.

Multifocally concentrated along the deep margin of the exudate are clusters and individually scattered fungal hyphae. These hyphae have a width of approximately 3-5m with regularly septate parallel walls and dichotomous acute angle or Y-shaped branching consistent with *Aspergillus* sp. Based on microscopic morphology, differential diagnoses for *Aspergillus* sp. include *Fusarium* spp., *Pseudoallescheria boydii* and *Candida* sp.

The yellow, firm, tissue-like mass partially adhered to the nasal respiratory mucosal epithelium was several centimeters long and partially occluded the respiratory passages on the right side of the head. This mass was composed of necrotic debris and a thick mat of fungal hyphae also consistent with *Aspergillus* sp. infection. Additionally, several lymph nodes were greatly enlarged and contained bright green pus suggestive of infection by *Corynebacterium pseudotuberculosis*, a known pathogen of this herd.

**JPC Diagnosis:** Rumen: Leiomyosarcoma.

**Conference Comment:** The contributor provided an excellent summary of both the primary lesion (leiomyosarcoma ) as well as the additional findings of bacteria, fungi, inflammation, and mucosal ulceration in this specimen.

Conference participants began their discussion with a review of the histological morphology of ruminant forestomachs:

Forestomach
Papillar structure
Presence/Absence of muscularis mucosae
Rumen
Long, finger or paddle-like papillae covered by stratified squamous epithelium
Muscularis mucosae is absent; no muscle is observed microscopically within ruminal papillae
Reticulum
Conical papillae project from crests of the honeycomb like folds, as well as from the bottom of the wells
Muscularis mucosae is present in the tips of the folds, but is discontinuous down the rest of the fold
Omasum
Papillae project from long folds
Muscularis mucosae is continuous projecting into omasal fold[1]

Conference participants went on to discuss the criteria for malignancy, asking the following questions:

*1. Is there evidence of metastasis?*
*2. Is there evidence of local vascular or lymphatic invasion?*
*3. Is the neoplasm infiltrative?*
*4. Are there necrotic foci within the neoplasm?*
*5. Do neoplastic cells display cellular features of malignancy --Are the cells anaplastic?*
*6. Are the cells pleomorphic?*
*7. Is the chromatin clumped? Are the nucleoli large and/or irregular?*
*8. Is there a high mitotic rate? Are there bizarre mitoses?*
*9. Is there loss of cellular polarity or orientation?*
*10. Are the cells forming multinucleated cells?*

These questions must be addressed whenever evaluating a neoplasm to differentiate benign from malignant tumors. The most important features of malignancy are the ability to metastasize systemically and/or the ability to invade local tissue. Malignant tumors owe their invasive nature to enhanced cell motility, increased protease production, and alterations in cell adhesions. Furthermore, malignant tumors tend to grow independent of exogenous growth factors and are resistant to environmental growth inhibitory signals; thus they have virtually unlimited growth potential. Malignant cells are also more adept at avoiding apoptosis and escaping the cytotoxic immune response and inducing angiogenesis than benign tumors, further enhancing their proliferative abilities.[8] In this case, the infiltrative nature of the tumor, as well as necrotic foci and cellular features of malignancy such as karyomegaly prompted a diagnosis of leiomyosarcoma rather than leiomyoma.

**Contributor:** U.S. Army Medical Research Institute of Infectious Diseases (USAMRIID), Pathology Division, 1425 Porter Street, Fort Detrick, MD 21702-5011 http://www.usamriid.army.mil/

**References:**

1. BachaWJ, Bacha LM. Digestive System. In: *Color Atlas of Veterinary Histology.* 3rd ed. Ames, Iowa: Wiley-Blackwell; 2012:155-157.
2. Collier MA, Trent AM. Jejunal intussusceptions associated with leiomyoma in an aged horse. *J Am Vet Med Assoc*. 1983;182:819-821.
3. Cooper BJ, Valentine BA. Tumors of muscle. In: Meuten DJ, ed. *Tumors in Domestic Animals*. 4th ed. Ames, Iowa; Iowa State Press: 2002:319-341.
4. Head KW, Cullen JM, Dubielzig RR, et al. Histological classification of tumors of the alimentary system of domestic animals. In: Schulman FY, ed. *World Health Organization Histological Classification of Tumors of Domestic Animals*. Second Series. Vol.

10. Washington, DC: Armed Forces Institute of Pathology, American Registry of Pathology; 2003:35-36, 38, 79-81, 102-104.
5. Hulland TJ. Tumors of muscle. In: Moulton JE, ed. *Tumors of Domestic Animals*. 3rd ed. Los Angeles, CA: University of California Press; 1990:88-92.
6. Kempson RL, Fletcher CDM, Evans HL, et al. Tumors of the soft tissues. In: Rosai J, Sobin LH, eds. *Atlas of Tumor Pathology*. Third Series. Fascicle 30. Washington, DC: Armed Forces Institute of Pathology, American Registry of Pathology; 2001:239-256.
7. Lewin KJ, Appelman HD. Tumors of the esophagus and stomach. In: Rosai J, Sobin LH, eds. *Atlas of Tumor Pathology*. Third Series. Fascicle 18. Washington, DC: Armed Forces Institute of Pathology, American Registry of Pathology; 1996:145-150.
8. Kusewitt DF. Benign versus malignant tumors. In: Zachary JF, McGavin D, eds. *Pathologic Basis of Veterinary Disease.* 5th ed. St. Louis MO: Elsevier Mosby; 2011:291.
9. Miettinen M, Wang ZF, Lasota J. DOG1 antibody in the differential diagnosis of gastrointestinal stromal tumors. *Am J Surg Pathol*. 2009;33:1401-1408.
10. Schaudien D, Muller JMV, Baumgartner W. Omental Leiomyoma in a Male Adult Horse. *Vet Pathol.* 2007;44:722-726.
11. Whitney KM, Valentine BA, Schlafer DH. Caprine genital leiomyosarcoma. *Vet Pathol.* 2000;37:89-94.

*Research was conducted in compliance with the Animal Welfare Act and other Federal statutes and regulations relating to animals and experiments involving animals and adheres to principles stated in the Guide for the Care and Use of Laboratory Animals, National Research Council, 1996. The facility where this research was conducted is fully accredited by the Association for Assessment and Accreditation of Laboratory Animal Care International.

**Opinions, interpretations, conclusions, and recommendations above are those of the author and are not necessarily endorsed by the U.S. Army or Department of Defense.

**CASE IV:** 7-16-12 (JPC 4019384).

**Signalment:** Adult female wild turkey (*Meleagris gallopavo*).

**History:** Several individuals within a single flock of turkeys reported to be exhibiting clinical signs, including falling out of the trees where they roost and circling on the ground. An unspecified number were found dead.

**Gross Pathology:** Within the oral cavity of affected animals, and largely effacing the normal mucosal surfaces, are numerous variably sized and irregularly shaped, multifocal to coalescing, proliferative, yellow-tan to pale yellow-green, caseous, nodular masses, which are variably covered in necrotic debris and fibrin.

**Histopathologic Description:** Oral cavity and tongue (sections vary): Within the sections examined are several areas of moderate to severe, locally to regionally extensive epithelial hyperplasia with occasional formation of variably sized and shaped papillary and frond-like projections. Many affected regions are characterized by variable degrees of erosion and superficial, adherent mats and masses of abundant amorphous eosinophilic necrotic material, cellular debris, blood, and occasional colonies of mixed bacteria. Individual epithelial cells in affected regions frequently have swollen, pale cytoplasm and there are many prominent, large, round to frequently ring-shaped, eosinophilic cytoplasmic inclusion bodies (Bollinger bodies). Affected cells also contain variably sized clear cytoplasmic vacuoles. Scattered individual cell necrosis is present. Similar hyperplastic and cytoplasmic changes occasionally extend into the epithelium of the underlying glandular tissue (not present in all slides). Within the underlying submucosal tissue is an inflammatory response composed predominantly of heterophils and macrophages, with smaller numbers of lymphocytes. Some sections contain deeper skeletal muscle, which contains rare, round to oval, intra-sarcoplasmic protozoal cysts characterized by a thin outer wall and abundant, central, crescent-shaped, basophilic bradyzoites (*Sarcocystis*).

**Contributor's Morphologic Diagnosis:** Oral cavity: Severe, multifocal to locally extensive, hyperplastic, necrotizing and erosive stomatitis, heterophilic and histiocytic, with epithelial ballooning degeneration and intracytoplasmic inclusion bodies, etiology consistent with avian poxvirus.

**Contributor's Comment:** The gross and histologic appearances of the lesions in the affected animals are typical of avian pox. This is a viral disease of birds

*4-1, 4-2. The oral cavity of affected animals contain numerous multifocal to coalescing proliferative yellow-tan nodular masses, which are covered in necrotic debris and fibrin. (Photos courtesy of the Montana Veterinary Diagnostic Laboratory, PO Box 997, Bozeman, MT 59771. http://liv.mt.gov/lab)*

that occurs nearly worldwide, with the exception of the polar regions. The avipoxviruses consist of a large, incompletely described group of viruses that affect both domestic and wild birds, and exhibit significant variability in host-specificity.[1,5,8] Poxviral disease has been reported in up to 278 species of birds and across at least 20 orders, and tends to be more prevalent in warmer and temperate regions of the globe.[8] At this time, the International Committee on Taxonomy of Viruses only recognizes 10 distinct avipoxviruses, but 3 other viruses are tentatively recognized, and there are many additional viruses that have not yet been fully characterized.[9] The primary source of infection is infected birds, and transmission occurs both by means of biting insects serving as mechanical vectors, and through direct contact.[8]

Clinical disease in all affected birds occurs in two main forms: the cutaneous form, in which multiple nodular and proliferative lesions develop on the skin, and the

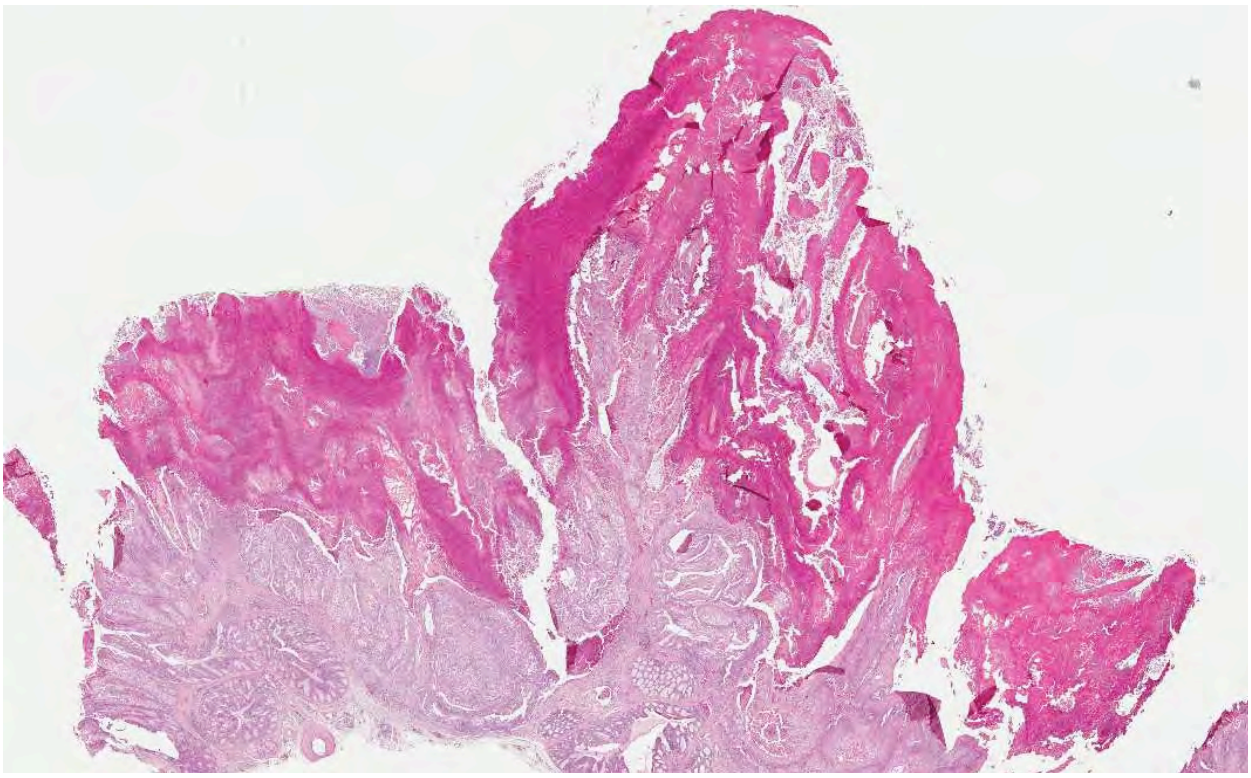

*4-3. Oral cavity, turkey: The glandular submucosa of the oral cavity is covered by markedly hyperplastic epithelium as well as a brightly eosinophilic necrotic coagulum. (HE 110X)*

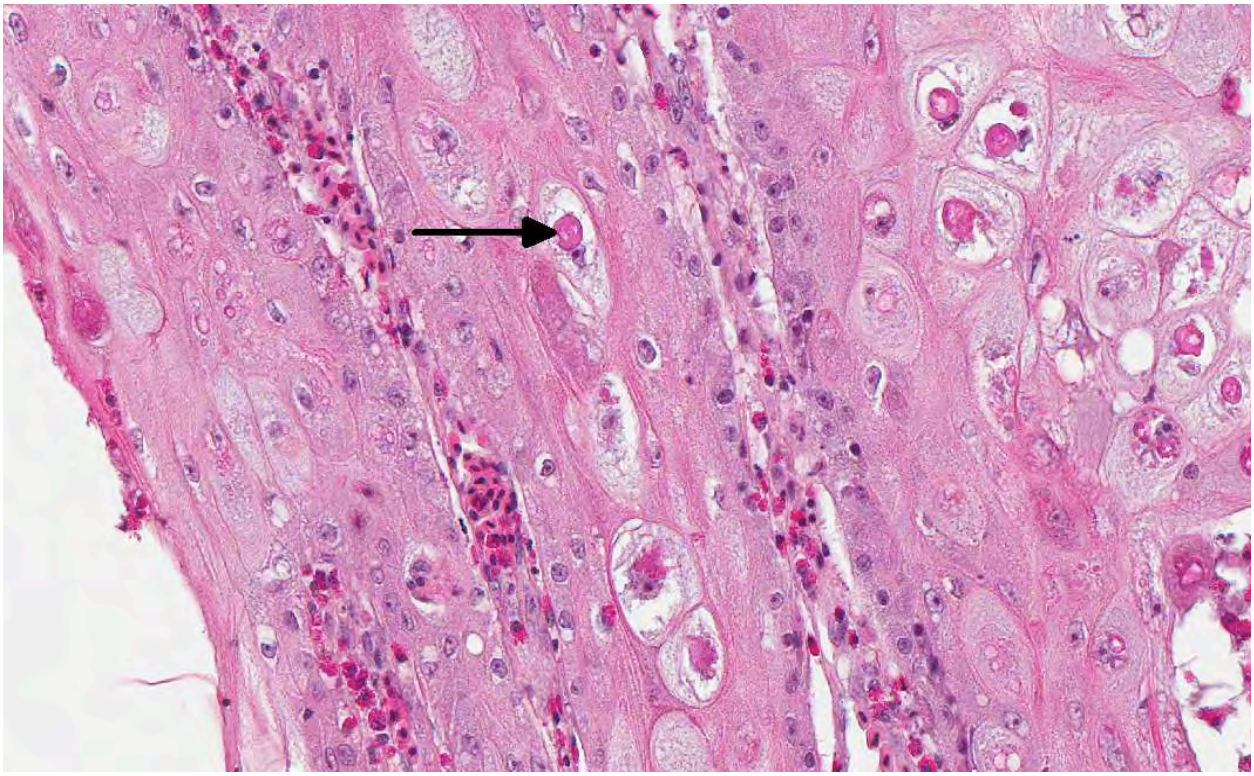

*4-4. Oral cavity, turkey: Epithelial cells within the hyperplastic mucosa often undergo ballooning degeneration and contain a 15-30 m, eosinophilic, intracytoplasmic inclusion (Bollinger body). (Arrow) (HE 260X)*

diphtheritic form, which is characterized by extensive necrotizing foci in the oral cavity and upper respiratory tract.[8] The diphtheritic form is less commonly observed, especially in wild birds, but frequently results in increased morbidity and mortality. This particular case represents an example of the diphtheritic form.

Avipoxviruses are large, oval-shaped viruses with a double stranded DNA genome. Due to their large size (up to 250 by 350 nm), and unlike other DNA viruses, poxviruses replicate in the cytoplasm of infected cells where they induce a cytopathic effect and form characteristic eosinophilic inclusion bodies (Bollinger bodies).[9] Avipoxviruses have classically been viewed as highly species-specific, but there is great variability in this, with some isolates inducing severe disease in non-host species, and other isolates causing little to no clinical disease.[6,9]

In North American wild turkeys, poxviral infection has been observed, and is the most commonly diagnosed viral disease in several states, but is geographically centered on the southeastern portion of the United States.[2,3] One report describes a localized outbreak within a single flock in Oregon, but in general this disease is not frequently observed in western or northern states.[7] This particular outbreak is unusual in that it occurred in the northwestern region of the continent, during mid-winter, when insect vectors are at their lowest numbers. Given these considerations, there may have been some other point source of infection, potentially including contact with infected domestic poultry.

Further diagnostics to specifically identify the virus within these affected animals were not performed. As previously mentioned, avipoxviruses have traditionally been regarded as highly species specific, and clinical disease in turkeys (wild or domestic) would be expected to be caused by infection with turkeypox virus. However, a recent report describes infection of turkeys with the closely related fowlpox virus, calling the extent of species-specificity into question and raising the possibility that this particular outbreak may also have been caused by fowlpox virus or even another closely related virus.[5,6]

**JPC Diagnosis:** Oral cavity: Stomatitis, necrotizing and proliferative, multifocal, marked, with ballooning degeneration and eosinophilic intracytoplasmic viral inclusion bodies.

**Conference Comment:** The contributor provided a very good summary of avian poxviruses. Viruses in the family *Poxviridae* are epitheliotropic DNA viruses that cause cutaneous or systemic disease in many species of animals, including wild and domestic mammals, birds, and humans. Poxviruses induce their characteristic lesions of epidermal hyperplasia, ballooning degeneration and vesicular lesions through several mechanisms. Many poxviruses encode a gene whose product is analogous to epidermal growth factor, and whose stimulation of host cell DNA results in epidermal hyperplasia. Vascular damage (due to viral multiplication in endothelial cells) and epidermal hyperplasia can result in ischemic necrosis and subsequent degenerative lesions in dermal and submucosal tissues.[7] Another characteristic feature of poxvirus-infected cells is the presence of one or more, variably-sized, intracytoplasmic eosinophilic viral inclusions that are composed predominantly of proteins. In addition to the previously-described genes, poxviruses also contain genes that encode proteins to circumvent the host's defense systems. One such protein is closely related to the superfamily of proteins known as SERPINS, which act as regulators of serine protease enzymes that mediate kinin, complement, fibrinolytic and coagulation pathways, thus allowing the poxviruses to inhibit host defenses. Additional poxvirus genes encode proteins that have anti-interferon activities, further rendering the host defenses inadequate against the virus. Pox lesions generally develop in a typical sequence, beginning as erythematous macules, which become papules, then progress to vesicles, which further develop into pustules which ultimately rupture and become umbilicated with a characteristic depressed center and raised, erythematous border (the "pock"). Once the pustules rupture, a crust forms and healed lesions often leave scars. Mucosal lesions often develop into ulcers rather than pustules. In addition to these cutaneous lesions, some poxviruses (such as Sheeppox virus, Ectromelia virus, Monkeypox virus, and Variola virus) also cause severe systemic disease. Following is a list of important poxviruses in veterinary medicine:[7]

**Genus**
**Poxvirus**
Orthopoxvirus
Camelpox virus, Cowpox virus, Ectromelia virus (mousepox), Monkeypox virus, Vaccinia virus (buffalopox virus, rabbitpox virus), Uasin Gishu disease virus*
Parapoxvirus
Bovine popular stomatitis virus, Contagious ecthyma virus (Orf virus), Parapox virus of red deer, Pseudocowpox virus, Auzduk disease virus* (Camel contagious ecthyma virus), Chamois contagious ecthyma virus*, Sealpox virus*
Avipoxvirus
Fowlpox virus, Pigeonpox virus, many other avian poxviruses
Capripoxvirus
Goatpox virus, Lumpy skin disease virus, Sheepox virus
Leporipoxvirus

Myxoma virus, Rabbit fibroma virus (Shope fibroma virus)
Suispoxvirus
Swinepox virus
Molluscipoxvirus
Molluscum contagiosum virus
Yatapoxvirus
Tanapox virus, Yaba monkey tumor virus
*Unassigned members of the genus[7]

**Contributing Institution**: Montana Veterinary Diagnostic Laboratory, PO Box 997,
Bozeman, MT 59771
http://liv.mt.gov/lab

**References:**

1. Bolte AL, Meurer J, Kaleta EF. Avian host spectrum of avipoxviruses. *Avian Pathol*. 1999;28:415-432.
2. Davidson WR, Nettles VF, Couvillion E, et al. Diseases diagnosed in wild turkeys (Meleagris gallopavo) of the southeastern United States. *J Wildl Dis*. 1985;21(4):386-390.
3. Forrester DJ. The ecology and epizootiology of avian pox and aalaria in wild turkeys. *Bull Soc Vector Ecol*. 1991;16(1):127-148.
4. Ginn PE, Mansell JEKL, Rakich PM. Skin and appendages. In: Maxie MG, ed. *Jubb, Kennedy and Palmer's Pathology of Domestic Animals.* 5th ed. New York, NY: Saunders Elsevier; 2007:664-665.
5. Hess C, Maegdefrau-Pollan B, Bilic I, Liebhart D, et al. Outbreak of cutaneous form of poxvirus on a commercial turkey farm caused by the species fowlpox. *Avian Dis*. 2011;55:714-718.
6. Jarmin S, Manvell R, Gough RE, et al. Avipoxvirus phylogenetics: identification of a PCR length polymorphism that discriminates between the two major clades. *J Gen Virol*. 2006;87:2191-2201.
7. Lutz RS, Crawford JA. Prevalence of poxvirus in a population of Merriam's Wild Turkeys in Oregon. *J Wildl Dis*. 1987;23(2):306-307.
8. Van Riper III C, Forrester DJ. Avian pox. In: Thomas NJ, Hunter DB, Atkinson CT, eds. *Infectious Diseases of Wild Birds*. Ames, IA: Blackwell Publishing; 2007:131-176.
9. Weli SC, Tryland M. Avipoxviruses: infection biology and their use as vaccine vectors. *Virology Journal*. 2011;8(49):1-15

**Joint Pathology Center**
**Veterinary Pathology Services**

# WEDNESDAY SLIDE CONFERENCE 2012-2013

## Conference 4

**10 October 2012**

---

**CASE I:** 10-122 (JPC 4004524)

**Signalment:** Juvenile, female, spayed ferret (*Mustela putorius furo*).

**History:** Approximately six months after arrival from a commercial vendor, this ferret became progressively anorexic with weight loss, diarrhea, and had palpable intra-abdominal masses. There was poor response to IBD-type treatments and the ferret was euthanized.

**Gross Pathology:** An approximately 3 x 3 x 5 cm multi-lobular white-tan mass was present in the area of the mesenteric lymph nodes and surrounding mesenteric fat.

**Histopathologic Description:** Mesenteric lymph node and mesentery: The lymph node and mesenteric fat are effaced by multifocal to coalescing pyogranulomatous infiltrates. There are large central regions of necrosis with admixed degenerate neutrophils and fibrin surrounded concentrically by epithelioid macrophages

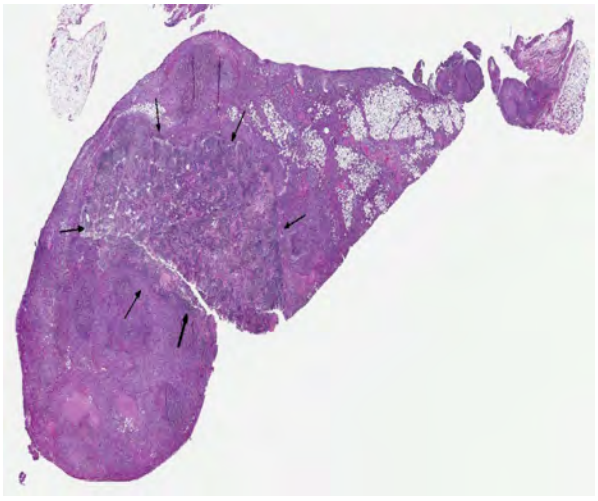

*1-1. Mesenteric lymph node and adjacent mesentery, ferret: Marked necrotizing and pyogranulomatous inflammation affecting the mesenteric lymph node (arrows) and extending into and effacing the surrounding mesenteric fat. (HE 10X)*

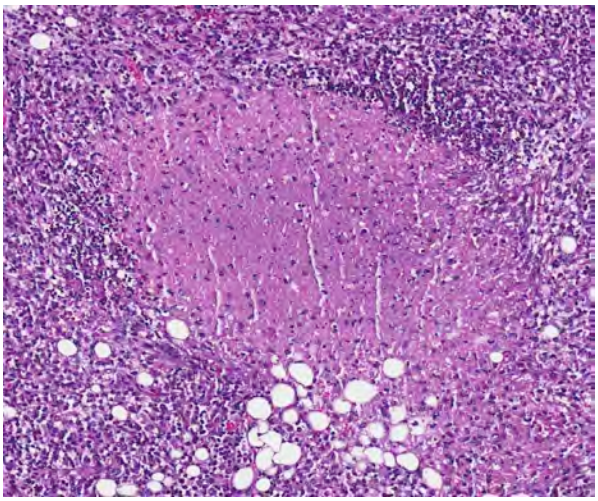

*1-2. Mesenteric lymph node and adjacent mesentery, ferret: Foci of necrosis within both the mesenteric lymph node and the adjacent mesentery (as shown here) are surrounded by pyogranulomatous inflammation. (HE 10X)*

and fibroblasts with fewer peripheral lymphocytes, plasma cells, and rare multinucleated giant cells. Several large arteries are partially or completely occluded by fibrin thrombi and portions of the wall are replaced by inflammatory cells and debris.

Coronavirus immunohistochemistry performed at Michigan State University using a monoclonal antibody against group 1c coronavirus antigen reveals strong positive intracytoplasmic staining of macrophages within the center of pyogranulomas.

**Contributor's Morphologic Diagnosis:** Mesenteric lymph node and mesenteric fat: Severe multifocal to coalescing pyogranulomatous and necrotizing lymphadenitis, peritonitis, and vasculitis.

**Contributor's Comment:** The primary differential etiology for this animal from gross and microscopic lesions was ferret systemic coronavirus infection which was subsequently confirmed by immunohistochemistry. Both the ferret enteric coronavirus (FRECV) and the ferret systemic coronavirus (FRSCV) were recently identified as group 1 coronaviruses.[3,4] Ferret enteric coronavirus causes an enteric disease called epizootic catarrhal enteritis (ECE).[4] More recently, a new systemic coronavirus-associated disease closely resembling the granulomatous or dry form of feline infectious peritonitis (FIP) has been reported.[1] Although the similarities in clinical disease and histologic lesions between FRSCV and FIP virus suggest a similar pathogenesis for FRSCV-associated disease and FIP, this has yet to be proven experimentally.

**JPC Diagnosis:** Lymph node: Lymphadenitis, necrotizing and pyogranulomatous, multifocal to coalescing, severe, with mild fibrinoid vasculitis and necrotizing mesenteric steatitis.

**Conference Comment:** Viruses in the family *Coronaviridae*, genus *Coronavirus,* are 80-220 nm, enveloped and often spherical (although they can be pleomorphic), with large club-shaped viral spike peplomers (S protein) surrounding an icosahedral core that contains a helical nucleocapsid (N protein). These viruses consist of a single molecule of positive single-stranded RNA.[2] Coronavirus infections have been

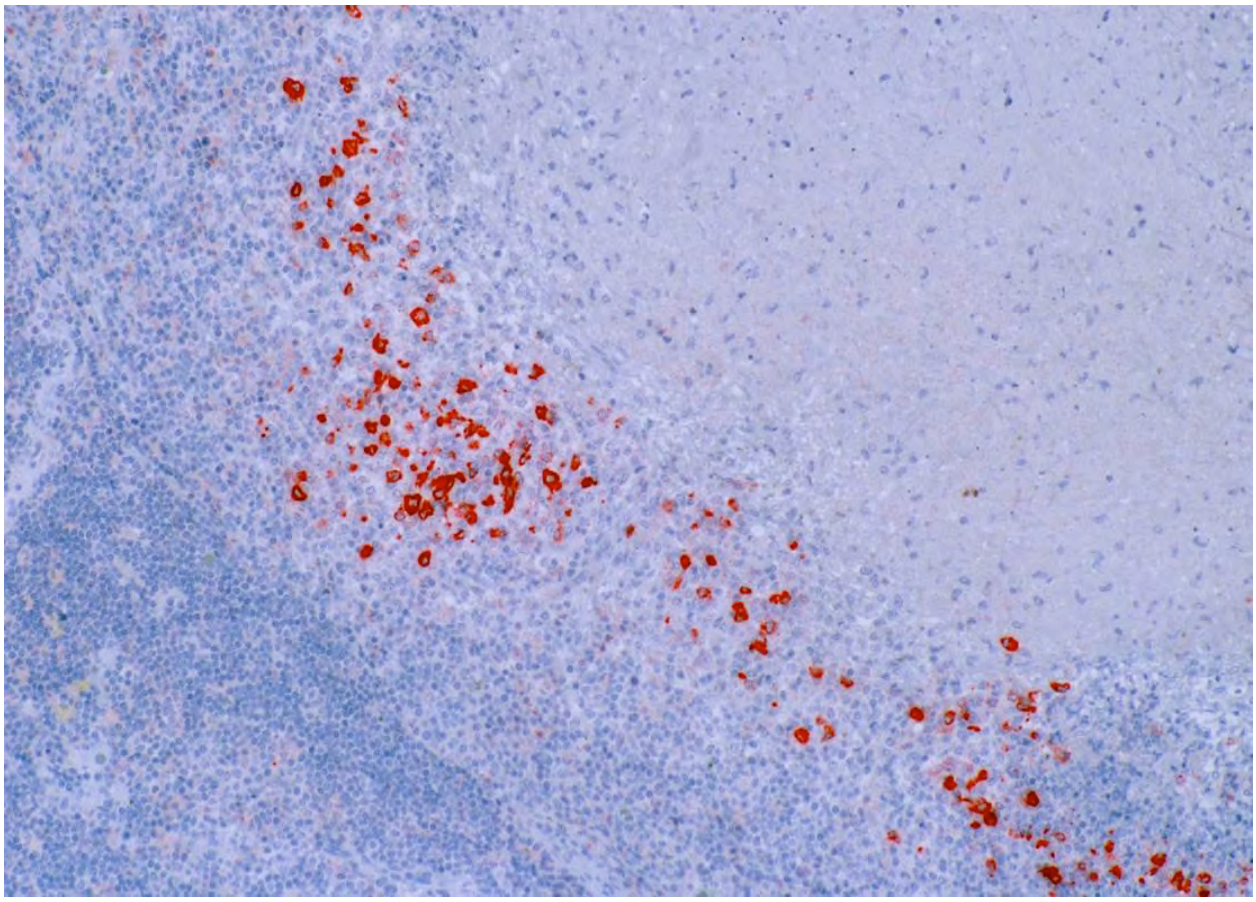

*1-3. Mesenteric lymph node and adjacent mesentery, ferret: Coronavirus immunohistochemistry performed at Michigan State University using a monoclonal antibody against group 1c coronavirusantigen reveals strong positive intracytoplasmic staining of macrophages within the center of pyogranulomas. (Photo courtesy of the Division of Laboratory Animal Resources, University of Pittsburgh, http://www.dlar.pitt.edu/)*

reported in many species, including pigs, cattle, horses, cats, frogs, rats, birds, rabbits, ferrets, mink, and mice. The host spectrum of each coronavirus depends on the S protein, which mediates receptor binding and fusion of the virus with the host cell. Coronaviruses use different receptors, including aminopeptidase N, used by several group 1 coronaviruses; carcinoembryonic antigen-related cell adhesion molecule 1 (CEACAM-1), used by mouse hepatitis virus; and N-acetyl-9-*O*-acetyl neuraminic acid, used by other group 2 coronaviruses. Group 3 coronavirus receptors are unknown at this time; however, heparan sulfate and sialic acid residues may play a role as non-specific attachment factors.[2] Coronviruses of veterinary importance include:

**Group 1a:**
Transmissible gastroenteritis virus of swine
Porcine respiratory coronavirus
Canine coronavirus
Feline enteric coronavirus (formerly feline infectious peritonitis virus)
Ferret and mink coronaviruses
**Group 1b:**
Porcine epidemic diarrhea virus
Bat coronavirus
**Group 2a:**
Mouse hepatitis virus
Bovine coronavirus
Sialodacryoadenitis virus of rats
Porcine hemagglutinating encephalomyelitis virus
Canine respiratory coronavirus
**Group 3:**
Avian infectious bronchitis virus
Turkey coronavirus[2]

In carnivores infected by coronaviruses, disease manifests in one of two ways: infection can be self-limiting enteritis (such as in canine coronavirus, feline coronaviral enteritis, ferret epizootic catarrhal enteritis), or severe systemic disease can occur (such as in feline infectious peritonitis [FIP] or ferret systemic coronavirus infection [FRSCV].)[1] As the contributor noted, pathogenesis for FRSCV is suspected to be similar to that of FIP, based on gross, histologic and immunohistochemical features of the disease.[1] The key feature in FIP is the ability of genetic variants of feline enteric coronavirus to infect macrophages, due to mutations of the S protein and possibly other proteins which alters the tropism of the virus. Strong antibody response (often evidenced clinically as a polyclonal gammopathy) is ineffective at eliminating the virus and cellular immune responses are unable to prevent virus replication in macrophages. The lesions in FIP are often centered on small blood vessels, with vascular injury (necrosis) and leakage of a viscous, protein-rich transudate playing a major role in the wet form of the disease.[2] In this case of ferret systemic coronavirus infection, conference participants noted that, although there was significant slide variation, in some specimens, variable amounts of necrotizing vasculitis are visible. Despite this finding, ferrets generally do not develop the effusive ("wet") form of the disease, as they more often present with lesions consistent with the non-effusive ("dry") end of the disease spectrum.[1]

**Contributing Institution:** Division of Laboratory Animal Resources, University of Pittsburgh
http://www.dlar.pitt.edu/

**References:**
1. Garner MM, Ramsell K, Morera N, et al. Clinicopathologic features of a systemic coronavirus-associated disease resembling feline infectious peritonitis in the domestic ferret (Mustela putorius). *Vet Pathol*. 2008;45:236–46.
2. Maclachlan NJ, Dubovi EJ, eds. Coronaviridae. In: *Fenner's Veterinary Virology*. London UK: Elsevier Science; 2010:394-413.
3. Wise A, Kiupel M, Garner MM, et al. Comparative sequence analysis of the distal one-third of the genomes of a systemic and an enteric ferret coronavirus. *Virus Res.* 2010;149:42–50.
4. Wise AG, Kiupel M, Maes RK. Molecular characterization of a novel coronavirus associated with epizootic catarrhal enteritis (ECE) in ferrets. *Virology*. 2006;349:164–74.

**CASE II:** UFSM-1 (JPC 4003260).

**Signalment:** 3- to 4-year-old, female, Murrah water buffalo (*Bubalus bubalis*).

**History:** Fifty 3- to 4-year-old water buffalo of both sexes were purchased from a farm (farm 1) in southern Brazil and shipped by truck to another farm (farm 2) 300 km away. The buffalo were kept in a holding pen on farm 1 for 12 hours without food or water, immediately prior to being transported for 8 hours to farm 2. As a result, the animals had no food or water for a total of 20 hours. Upon arrival at farm 2, the animals were released into a 200-hectare pasture that already held 200 cattle (*Bos taurus*) that had been there for several months. Ten buffalo died within 24-48 hours of being placed in the pasture. Most of the affected buffalo were found dead, but the owner was able to observe one moribund buffalo that had serous ocular discharge, incoordination, mild bloat, and muscle trembling. The pasture on farm 2 where the 10 water buffalo died had several spots of marshy land where large amounts of a plant later identified as *Baccharis megapotamica* var. *weirii* was found. There was evidence that livestock had been consuming these plants. *Baccharis megapotamica* var. *weirii* was absent from farm 1. A diagnosis of *Baccharis megapotamica* var. *weirii* was made and, to confirm the diagnosis, a susceptible calf (*Bos taurus*) was fed a single dose of 5g/kg/body weight of *B. megapotamica* var. *weirii* harvested from the same site where the buffalo died. Twenty hours after the administration of the plant this calf died with clinical signs and lesions similar to those observed in the naturally poisoned.

**Gross Pathology:** Necropsy was performed two hours after death. Gross findings in the necropsied buffalo included dehydration and markedly distended rumen with abundant liquid content. There was mild to moderate edema of the wall of the rumen, particularly in the pillars, and diffuse reddening of the mucosa of the forestomachs, abomasum, and intestine.

**Histopathologic Description:** Epithelial cells lining the forestomachs displayed coagulative necrosis, the severity of which varied, so that in some segments the more superficial cells of the stratified epithelium were affected, sparing deeper cells. In some instances, these deeper cells had hydropic degeneration. In some other segments, coagulative necrosis affected the entire thickness of the stratified epithelium. Myriads of bacterial aggregates could be observed attached to segments of necrotic epithelial lining. Thrombi were occasionally observed in the submucosal vessels, and neutrophilic infiltrate was evident in some segments of degenerate/necrotic epithelium. Necrosis of the intestinal mucosa was also observed (slides not included). Lymph nodes, spleen, lymphoid aggregates,

*2-1. Rumen, Murrah water buffalo: Diffuse reddening of the mucosa of the rumen of a water buffalo (Bubalus bubalis) naturally poisoned by Baccharis megapotamica var. weirii. (Photo courtesy of: Departamento de Patologia, Universidade Federal de Santa Maria, 97105-900 Santa Maria, RS, Brazil. http://www.ufsm.br/lpv) 2-2. Reticulum, Murrah water buffalo: Diffuse reddening of the reticulum in a water buffalo (Bubalus bubalis) naturally poisoned by Baccharis megapotamica var. weirii. (Photo courtesy of: Departamento de Patologia, Universidade Federal de Santa Maria, 97105-900 Santa Maria, RS, Brazil. http://www.ufsm.br/lpv) 2-3. Abomasum, Murrah watter buffalo: Diffuse reddening of the abomasum in a water buffalo (Bubalus bubalis) naturally poisoned by Baccharis megapotamica var. weirii. (Photo courtesy of: Departamento de Patologia, Universidade Federal de Santa Maria, 97105-900 Santa Maria, RS, Brazil. http://www.ufsm.br/lpv)*

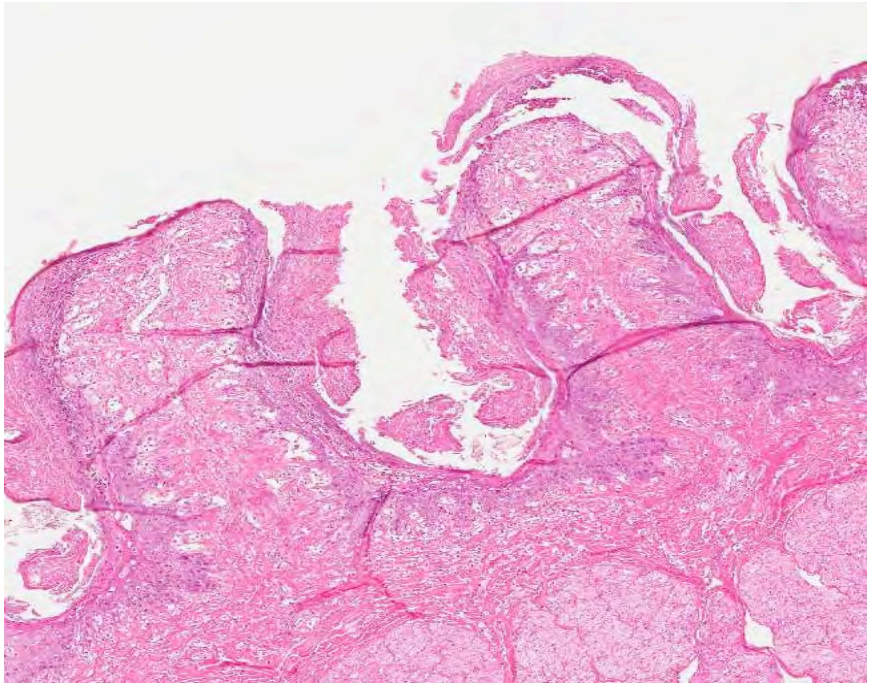

*2-4. Rumen, Murrah water buffalo: Rumenal papilla exhibit partial to full-thickness mucosal necrosis and are covered by a brightly eosinophilic necrotic coagulum. (HE 40X)*

and liver were also affected (slides not included). Mesenteric lymph nodes had necrosis of lymphocytes in secondary germinal centers. The subcapsular, trabecular, and medullary sinuses were filled with macrophages, and erythrophagocytosis was conspicuous. Lymphoid necrosis was also observed in the white pulp of the spleen. Gut associated lymphoid tissue and other lymphoid aggregates were not available for histology. Hepatic lesions consisted of intense hepatocellular vacuolization with eosinophilic globules, and marked dilatation of lymphatics in portal triads. The lumina of these lymphatics were filled by faint eosinophilic homogenous material.

**Contributor's Morphologic Diagnosis:** Rumen, epithelial lining, degeneration and coagulative necrosis, marked, acute, associated with neutrophilic infiltration, bacterial aggregates and submucosal thrombi, water buffalo, female.

**Contributor's Comment:** The *Baccharis* genus (Asteraceae: tribe Asteraceae) includes nearly 500 species. All are found in the New World with the exception of *Baccharis halimifolia*, which was introduced into Australia from the United States.[10] This species is suspected of poisoning cattle in both countries[8] and proved toxic when administered experimentally to chicks.[7] *Baccharis glomerulifolia*, another North American species, was toxic to mice and chicks under experimental conditions, and *Baccharis pteronioides* has been associated with cattle poisoning in the southwestern United States.[7,12,18] *Baccharis pteronioides* toxicosis was also experimentally produced in hamsters.[18] *Baccharis artemisioides* causes disease in cattle in a restricted zone of Argentina northwest of Buenos Aires and southeast of Cordoba.[13]

Nearly 120 species of *Baccharis* have been recorded in Brazil; of those, only *Baccharis coridifolia* and *Baccharis megapotamica* have been proven to be toxic to livestock.[3,6,14,19,20] Both *B. megapotamica* and *B. coridifolia* are found in southern Brazil, but they occupy different habitats; *B. megapotamica* is found in marshy areas whereas *B. coridifolia* grows in pastureland.[3,20] Two varieties of *B. megapotamica* with essentially the same distribution and toxic effects on livestock are known, namely *B. megapotamica* var. *megapotamica* and *B. megapotamica* var. *weirii*.[20]

The two varieties of *B. megapotamica* and *Baccharis coridifolia* cause a severe acute poisoning in livestock characterized by degeneration and necrosis of the epithelial lining of the gastrointestinal tract and necrosis of lymphocytes in lymph nodes, spleen, tonsils, and several lymphoid aggregates.[3,20,22] *Baccharis megapotamica*, *B. coridifolia* and *B. artemisioides* contain a series of potent cytotoxic

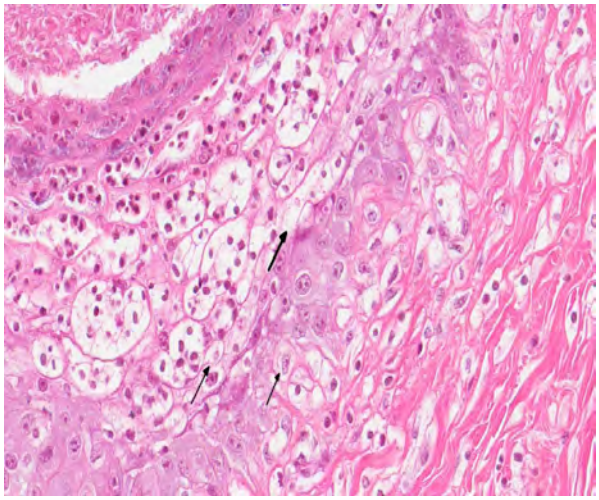

*2-5. Ruman, Murrah water buffalo: Epithelial cells between rumenal papilla exhibit ballooning degeneration (arrows), and in more superficial layers undergo necrosis, and pustule formation as a result on infiltration of neutrophils. Numerous bacteria (of little significance in the pathogenesis of this lesion) are present in the overlying crust. (HE 360X).*

agents belonging to the macrocyclic trichothecene complex of antibiotics previously believed to be produced only by fungi.[5,9] These cytotoxic substances were demonstrated to be the toxic principles in these plants.[10,22] In the case of *B. megapotamica*, the macrocyclic trichothecenes accumulate in the plant as baccharinoids, which are named B1, B2, B3, B4, etc. The B4 baccharinoid is most abundant, but there are also large concentrations of B1-B8. To date, no macrocyclic trichothecenes have been demonstrated in *B. halimifolia*, *B. pteronioides*, or *B. glomerulifolia*.

Spontaneous poisoning by *B. coridifolia* occurs frequently in cattle, occasionally in sheep and rarely in horses.[2,15,17] Spontaneous outbreaks involving *B. megapotamica var. weirii* have been reported in cattle, sheep and buffalo.[6,13,14] Typically, the toxicosis in livestock occurs when naïve animals raised in areas free of *Baccharis* spp. are transferred to pastures infested by the plant. The risk of toxicosis increases considerably if the animals are subjected to such stress factors as fatigue, hunger, or thirst; cattle that are raised in pastures where *Baccharis* spp. exist will graze it very rarely, if ever.[3]

Livestock will not usually ingest either variety of *B. megapotamica*, but a combination of hunger, dehydration, and lack of familiarity with the plant most likely led the buffalo of this report to the lethal ingestion of *B. megapotamica* var. *weirii*.[20] In the southern region of Brazil there are reports of spontaneous poisoning by four plants that induce similar disturbances in the gastrointestinal tract and should be included in the differential diagnosis, namely *B. coridifolia*, *B. megapotamica* var. *weirii*, *Baccharidastrum triplinervium*, and *Eupatorium tremulum*. The toxic principle of the latter two plants is as yet undetermined. Poisoning caused by the first two plants is virtually clinically and pathologically indistinguishable; however, the habitats of *B. megapotamica* var. *weirii* (marshy areas) and *B. coridifolia* (dry pastureland) differ, and this helps in differentiating between the two intoxications.[3,20]

Additionally, lymphoid necrosis is reportedly less severe in cases of *B. coridifolia* and *E. tremuluman* poisoning and does not occur in the poisoning caused by *B. triplinervium*. Lesions in the forestomachs are much less severe in *B. triplinervium* poisoning than in the poisonings caused by the other three plants. Larger amounts (20-30 g/kg/bw) of *E. tremulum* and *B. triplinervium* must be consumed to induce disease and death in cattle; this translates to much lower mortality ratios for these two plants when compared to *Baccharis* spp. toxicosis. To confirm the diagnosis of poisoning by any of these plants it is important to find evidence of plant consumption.[13] From the standpoint of the morphological aspects of the lesions in the forestomachs, *B. megapotamica* var. *weirii* poisoning closely resembles ruminal acidosis. However, ruminal acidosis usually follows the ingestion of excess carbohydrate in the form of grain or other fermentable foodstuffs, and is associated mainly with intensive beef and dairy production and not with cattle at pasture.[4]
The cause of death in cases of *B. megapotamica* poisoning is unknown. However, since the disease is virtually identical to *B. coridifolia* poisoning, comparisons can be made. *Baccharis*-induced death is believed to be caused by dehydration and acid-base imbalance resulting from fluid loss into the ruminal compartment in a similar manner to what happens in ruminal acidosis.[15] The finding of myriads of bacteria attached to the necrotic ruminal mucosa in cases of *B. coridifolia* and *B. megapotamica* poisoning, even in animals freshly dead, suggests the possibility that bacteremia could play a role in the mechanism of death.[15]

Trichothecenes are terpenoids, which can be divided into two groups: the simple trichothecenes (e.g., deoxynivalenol [DON], diacetoxyscirpenol [DAS], and T-2 toxin) and the macrocyclic trichothecenes (e.g., baccharinoids, roridins, and verrucarins). They exhibit a wide range of biological activity, which includes dermatonecrosis, gastroenteritis, feed refusal, coagulopathy, and immunosuppression.[1,16,21] Trichothecenes are also potent phytotoxins, and the macrocyclics are particularly toxic to plants.[9,10] The T-2 toxin and DAS are highly toxic, causing necrosis of mucous membranes (mouth, pharynx, esophagus, rumen, stomach) on contact similar to lesions produced by plant-associated macrocyclic trichothecene poisoning.[11] In this regard, the lymphoid necrosis associated with baccharinoid-induced poisoning has a close morphological resemblance with the lymphoid necrosis induced by T-2 toxin, and extracts of *B. megapotamica* were used in treatment trials of B-cell leukemia in rats.[9] The cytotoxicity of trichothecenes is attributed to ribosomal binding and subsequent inhibition of protein synthesis in actively dividing cells of lymph nodes, spleen, bone marrow, and thymus.[16] Induction of apoptosis in these cells by the trichothecenes is likely to contribute to lesion expression.[21] Changes in cell membrane structure, with resultant lipid peroxidation due to amphophilic trichothecene molecules, inhibition of RNA and DNA synthesis, and inhibition of mitosis are additionally recognized deleterious effects of T-2 toxin on cells.[16] Although the mode of action of macrocyclic trichothecenes in *B. megapotamica* on subcellular levels is not completely determined, macrocyclic trichothecenes are believed to act by compromising protein synthesis by inhibiting the peptide bond formation step, and it is fair to assume that mechanisms associated with all types of trichothecene toxicoses are similar.[1] Interesting results that could

shed some light on the pathogenesis of *Baccharis*-induced toxicosis stemmed from experimental *B. pteronioides* poisoning in hamsters.[18] Hamsters in the highest dosed group (200 mg) developed multiple hemorrhagic infarcts in the liver and kidney, with severe hemorrhagic enteritis and severe necrotizing vasculitis with vascular thrombosis of hepatic and renal vessels associated with fibrin thrombi in glomerular capillaries. The authors of the hamster study compared their findings to those of bacterial endotoxin–produced vasculitis and infarction.[18]

The diagnosis of *B. megapotamica toxicosis* in the buffalo of this report was made based on the characteristic acute clinical disease, the presence of the plant in large amounts in its characteristic habitat, and the experimental reproduction of the disease by feeding the plant present in the pasture to a calf. *Baccharis megapotamica* var. *megapotamica* and var. *weirii* had been previously experimentally fed to calves and lethal doses were determined to be between 3 and 4 g/kg/bw for var. *megapotamica* and 1 g/kg/bw for var. *weirii*.[20] Fatal poisoning was acute with both varieties. The most important postmortem findings were edema of the ruminal wall along with congestion of the rumen, abomasum, small intestine, cecum, and colon. Histologically, the rumen showed necrosis characterized by pyknosis and karyorrhexis of epithelial cells, mainly of the stratum spinosum. Lymphoid tissue (spleen, lymph nodes, Peyer's patches) showed necrosis characterized by pyknosis and karyorrhexis of the lymphoid cells. Thus, the disease observed in the spontaneous outbreak in buffalo was essentially the same as described previously in cattle and sheep.[6,14,20]

**JPC Diagnosis:** Rumen, mucosa: Necrosis and hydropic degeneration, diffuse, acute, severe.

**Conference Comment:** The contributor provided an excellent and thorough discussion of *Baccharis*-induced toxicosis. Conference participants noted moderate slide variation, with several sections exhibiting neutrophilic inflammation and pustule formation in the mucosal epithelium, and few slides containing occasional submucosal fibrin thrombi. Participants debated whether the lesions in the ruminal mucosa represent a necrotizing rumenitis; however, participants ultimately agreed that inflammation was not the primary feature, and thus favored the morphologic diagnosis of "necrosis" over "necrotizing rumenitis."

**Contributing Institution:** Departamento de Patologia, Universidade Federal de Santa Maria, 97105-900 Santa Maria, RS, Brazil
http://www.ufsm.br/lpv

**References:**

1. Abbas HK, Johnson BB, Shier WT, et al. Phytotoxicity and mammalian cytotoxicity of macrocyclic trichothecenemycotoxins from *Myrothecium verrucaria*. *Phytochemistry*. 2002;59:309-313.
2. Alda JL, Sallis ESV, Nogueira CEW et al. Intoxicação espontânea por *Baccharis coridifolia* (Compositae) em eqüinos no Rio Grande do Sul. *Pesq Vet* Bras. 2009;29:409-414.
3. Barros CSL. Livestock poisoning by *Baccharis coridifolia*. In: Garland T, Barr AC, eds. *Toxic Plants and Other Natural Toxicants* Wallingford, Oxfordshire, UK: CAB International; 1998:569–572.
4. Brown CC, Baker DC, Barker IK. Rumenitis and acidosis caused by carbohydrate overload. In: Maxie MG, ed. *Jubb, Kennedy, and Palmer's Pathology of Domestic Animals*. 5th ed. Vol. 2. Philadelphia, PA: Saunders; 2007:46-48.
5. Busam L, Habermehl GG. Accumulation of mycotoxins by *Baccharis coridifolia*: a reason for livestock poisoning. *Naturwissenschaften*. 1982;69:392-393.
6. Driemeier D, Cruz CEF, Loretti AP. *Baccharis megapotamica* var. *weirii* poisoning in Brazilian cattle. *Vet Hum Toxicol*. 2000;2:220-221.
7. Duncan WH, Piercy PL, Feurt SD, et al. Toxicological aspects of southeastern plants. II. Compositae. *Econ Bot*. 1957;11:75–85.
8. Everist SL. *Poisonous Plants of Australia*. Sidney, Australia: Angus and Robertson; 1981:160-161.
9. Jarvis BJ, Midiwo JO, Bean GA, et al. The mystery of trichothecene antibiotics in *Baccharis* species. *J Nat Prod.* 1988;51:736-744.
10. Jarvis BJ, Mokhtari-Rejali N, Schenkel EP, et al. Trichothecene mycotoxins from Brazilian *Baccharis* species. *Phytochemistry*. 1991;30:789-797.
11. Jones TC, Hunt RD, King NW. *Veterinary Pathology*. 5th ed. Baltimore, MD: William & Wilkins; 1997.
12. Marsh CD, Clawson AB, Eggleston WW. *Baccharis pteronioides* as a poisonous plant of the southwest. *J Am Vet Med Assoc*. 1920;57:430-434.
13. Oliveira-Filho JC, Carmo PMS, Lucena RB, et al. *Baccharis megapotamica* var. *weirii* poisoning in water buffalo (*Bubalus bubalis*). *J Vet Diagn Invest*. 2011;23:610-614.
14. Pedroso PMO, Bandarra PM, Feltrin C, et al. Intoxicação por *Baccharis megapotamica* var. *weirii* em ovinos. *Pesq Vet Bras*. 2010;30:403-405.
15. Rissi DR, Rech RR, Fighera RA, et al. Intoxicação espontânea por *Baccharis coridifolia* em bovinos. *Pesq Vet Bras*. 2005;25:111-114.
16. Rocha O, Ansari K, Doohan FM. Effects of trichothecene mycotoxins on eukaryotic cells: a review. *Food Addit Contam*. 2005;22:369-378.
17. Rozza DB, Raymundo DL, Corrêa AMR, et al. Intoxicação espontânea por *Baccharis coridifolia*

(Compositae) em ovinos. *Pesq Vet Bras*. 2006;26:21-25.
18. Stegelmeier BL, Sani Y, Pfister JA. *Baccharis pteronioides* toxicity in livestock and hamsters. *J Vet Diagn Invest.* 2009;21:208-213.
19. Tokarnia CH, Döbereiner J. Intoxicação experimental em bovinos por "mio-mio" *Baccharis coridifolia*. *Pesq Agropec Bras Ser Vet*. 1975;10:79-97.
20. Tokarnia CH, Peixoto PV, Gava A, et al. Intoxicação experimental por *Baccharis megapotamica* var. *megapotamica* e var. *weirii* (Compositae) em bovinos Pesq Vet Bras 1992;12:19-31.
21. Uzarski RL, Islam Z, Pestka JJ. Potentiation of trichothecene-induced leukocyte cytotoxicity and apoptosis by TNF alpha and Fas activation 2. *Chem Biol Interact*. 2003;146:105-119.
22. Varaschin MS, Barros CSL, Jarvis BB. Intoxicação experimental por *Baccharis coridifolia* (Compositae) em bovinos. *Pesq Vet Bras*. 1998;18:69-75.

**CASE III:** 05-1595 (JPC 3031293).

**Signalment:** Nine-year-old owl monkey (*Aotus* sp.).

**History:** Acute onset of weakness and depression with hypothermia, weight loss and anemia (PCV =18%). The animal responded slightly to palliative therapy but then was found dead.

**Laboratory Results:** PCV= 18%.

**Gross Pathologic Findings:** At necropsy the animal was in poor body condition. The scent gland was enlarged and both kidneys were pale, firm and pitted.

**Histopathologic Description:** Small and medium sized arteries of the pancreas and duodenum are infiltrated and disrupted by low numbers of neutrophils, macrophage, and lymphocytes. Vessel walls are often necrotic and expanded by abundant fibrin and hemorrhage. Occasionally the entire vessel is replaced by fibrin and necrotic debris that completely occludes the vessel lumen (thrombus). Often the tunica intima is proliferative. The tunica adventitia and perivascular connective tissue contain moderate numbers of macrophages, fewer lymphocytes and fibroblasts. Both in the duodenum and more extensively in the pancreas there is coagulative necrosis. Multifocally pancreatic lobules contain tubules and ducts that are surrounded by a loosely arranged, proliferative, edematous stroma. Other tissues affected in this case with a necrotizing arteritis include the heart, gallbladder, jejunum, and adrenal gland.

**Contributor's Morphologic Diagnoses:**
1. Pancreas; duodenum: Arteritis, fibrinonecrotic, multifocal, marked, with coagulative necrosis.
2. Pancreas: Mesenchyme proliferation, peritubular and periductal, multifocal, moderate.

**Contributor's Comment:** In humans polyarteritis nodosa (PAN) is a systemic vasculitis of small and medium-sized arteries, most often affecting young adults. It typically involves renal and gastrointestinal vessels with a predilection for branching points but spares the lungs.[5] It has been reported in rats, mice, dogs, cats, pigs, and non-human primates, specifically cynomolgus macaque.[4] In rats it typically involves the mesentery, pancreas, and testis of aged Sprague-Dawley rats, with a higher incidence in males.[3] In dogs it is most often reported in beagles, referred to as beagle pain syndrome, affecting vessels of the mediastinum, cervical spinal cord, and heart.[2] To our knowledge, this is the first case involving an Aotus monkey. The tissues affected and histologic characteristics of the lesion make it similar to the case previously reported in a cynomolgus.[4] The lesion typically involves a necrotizing vasculitis with transmural infiltration by neutrophils, eosinophils and fewer macrophages often with fibrinoid necrosis of the vessel wall. Eventually the vessel wall is replaced by a fibrous thickening. In humans renal involvement is often the cause of death. Interestingly approximately 30% of humans with PAN have hepatitis B antigen in the serum. Characteristically various stages of chronicity exist simultaneously, even within the same vessel.[5] The pathogenesis of PAN is unknown but is suspected to be immunological. Patients with PAN have elevations of serum interferon- gamma and interleukin-2. Immunohistochemistry showed inflammatory cell infiltrates are mainly macrophages

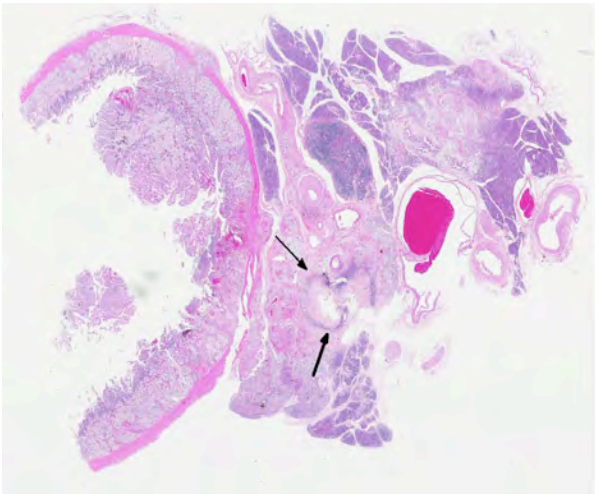

*3-1. Pancreas and duodenum, aotus monkey: The section is comprised of a multifocally ulcerated duodenum at left, mesentery and mesenteric lymph node center, and atrophic pancreas at right. Centrally, the common bile duct (arrows) exhibits autolytic change not associated with the vascular lesions. (HE 4X)*

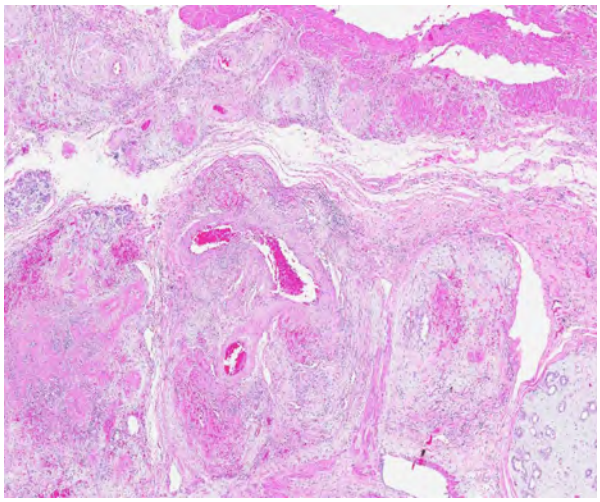

*3-2. Pancreas and duodenum, aotus monkey: Throughout the section, arterioles are tortuous, with marked mural thickening by hemorrhage, abundant protein, and infiltrating inflammatory cells (fibrinoid necrosis); they are often surrounded by proliferating fibroblasts and collagen. (HE 50X)*

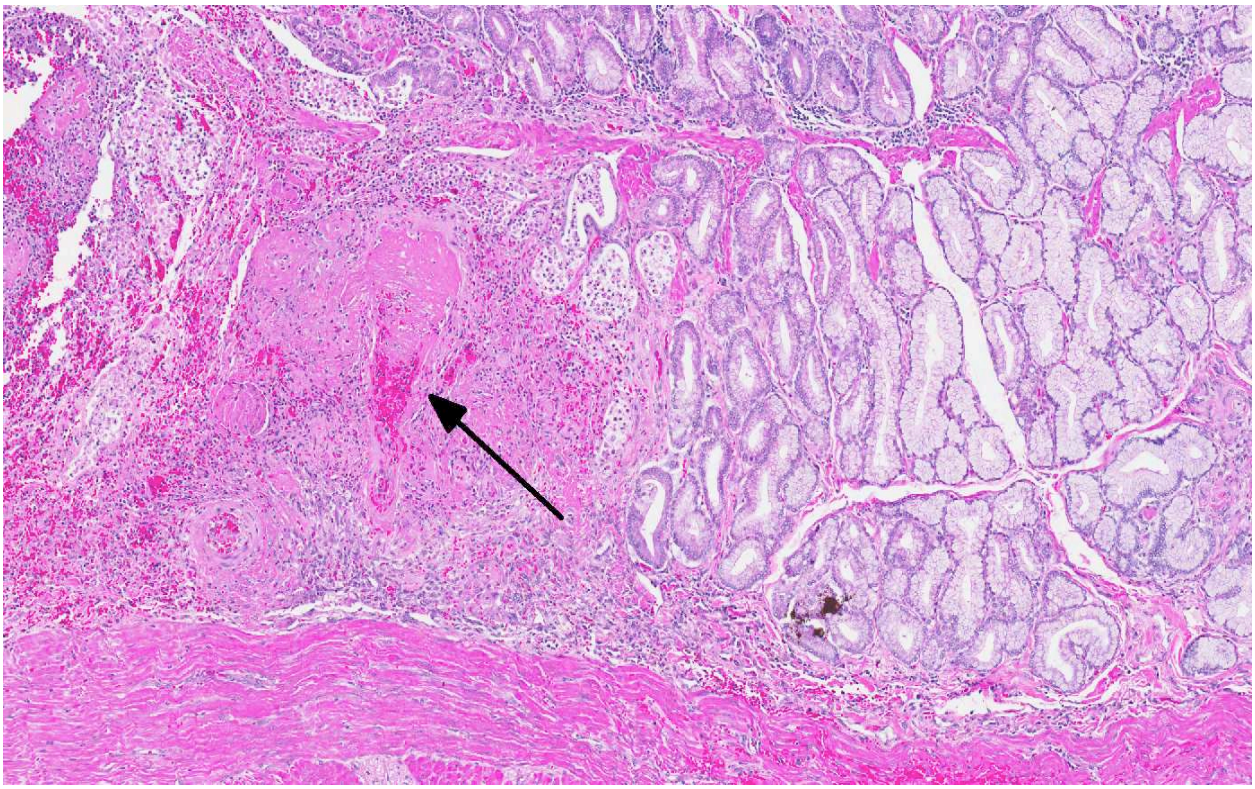

*3-3. Duodenum, aotus monkey: Areas of necrosis and ulceration in the duodenal mucosa are in association with fibrinoid necrosis and thrombosis of submucosal vessels (arrows). (HE 67X)*

and CD4+ T cells.[4] Clinical response to immunosuppressive therapy further supports an immunologic-based pathogenesis. In this case the histologic lesions in the pancreas and duodenum are typical of PAN. Within the pancreas, however, there are lobules that contain tubules, and to a greater extent ducts, that are surrounded by a loosely arranged, edematous stroma. In more severely affected areas this stroma appears proliferative. To our knowledge this change has not been reported in association with PAN. We speculate that these areas are proliferative due to the many cytokines and growth factors being released in the local area from the extensive necrosis and inflammation. Why only peritubular and periductal areas are affected is not known and other possible explanations for this morphologic characteristic cannot be excluded.

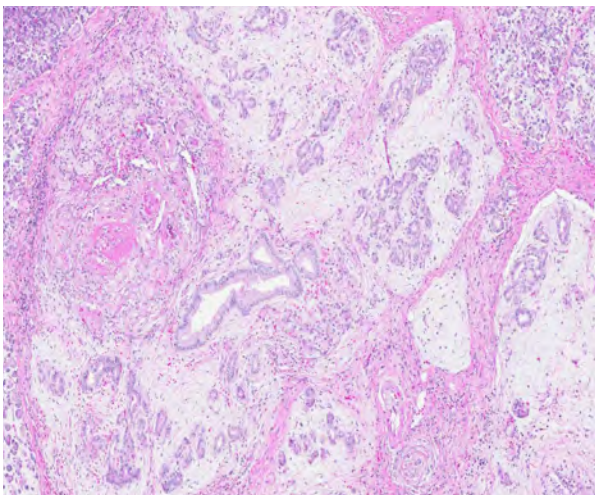

*3-4. Pancreas, aotus monkey: Areas of lobular atrophy with ductal proliferation are associated with fibrinoid necrosis and thrombosis of small pancreatic arterioles (at left center). (HE 50X)*

**JPC Diagnosis:** 1. Duodenum: Arteritis, proliferative and necrotizing, chronic, multifocal, severe, with mucosal necrosis.
2. Pancreas: Arteritis, proliferative and necrotizing, chronic, multifocal, severe, with acinar necrosis, atrophy and loss and ductal hyperplasia.

**Conference Comment:** The contributor provided an excellent review of polyarteritis nodosa. The conference moderator noted the presence of autolysis of the common bile duct, and cautioned students not to mistake this for a focus of lytic necrosis. Participants noted the areas of necrosis within the duodenum and pancreas correspond to areas of arteritis. The occurrence of abundant stroma within the pancreas that the contributor described and speculated to be due to cytokines and growth factors in areas of inflammation and necrosis led to discussion of the induction of mesenchymal tissue due to acinar loss. This phenomenon that occurs during acute and chronic

pancreatitis is thought to be due to the release of TGF-β (which acts as the main stimulator), TNF-α, IL-1 and IL-6, and PDGF (which acts as the main mitogen), from acinar cells, inflammatory cells and platelets. These factors induce the activation and proliferation of periacinar myofibroblasts (aka pancreatic stellate cells) by inducing them to transform from their fat-storing phenotype to their matrix-producing phenotype, which plays a role in tissue repair and result in pancreatic fibrosis.[1]

**Contributing Institution:** Walter Reed Institute of Research/Naval Medical Research Center
http://wrair-www.army.mil
http://www.nmrc.navy.mil

**References:**

1. Bachem MG, Xhou Z, Zhou S, et al. Role of stellate cells in pancreatic fibrinogensis associated with ace and chronic pancreatitis. *J Gastroenterol and Hepatol.* 2006; 21(s3):s92-s96.
2. Catharine J, Scott-Moncrieff R, Snyder PW, et al. Systemic necrotizing vasculitis in nine young Beagles. *JAVMA*. 1992;201:1553-1557.
3. Percy DH, Barthold SW. In: *Pathology of Laboratory Rodents and Rabbits*. 2nd ed. Ames, IA: lowa State Press;2001:153.
4. Porter BF, Frost P, Hubbard Gf. Polyarteritis nodosa in a cynomolgus macaque (Macaca fascicularis). *Vet Pathol.* 2003;40:570-573.
5. Schoen FJ. Blood vessels. In: Kumar V, Abbas AK, Fausto N, eds. *Robbins Pathologic Basis of Disease*. 7th ed. Philadelphia, PA: Elsevier Inc; 2005:539.

**CASE IV:** S11-686-v11 (JPC 4019872).

**Signalment:** 12-year-old mixed breed female spayed cat.

**History:** This cat had a lumpectomy in November of 2010. One month later, regrowth was found, and the mass had grown fast since. Mastectomy was recommended and performed on July 7, 2011. At operation, pyometra was detected and an OHE was also performed. The uterus was submitted for examination along with the ovaries.

**Gross Pathology:** The uterine horns and body were submitted in formalin. The uterus was bilaterally swollen and the uterine horns multifocally enlarged. Bilaterally, ovaries were shrunken and interpreted to be atrophic. Upon sectioning, the uterus was diffusely and bilaterally thickened, had a cystic nature, and the lumen was filled with inspissated chocolate-colored material.

**Histopathologic Description:** Uterus: Expanding the endometrium and encroaching upon the lumen is a well-demarcated, unencapsulated, poorly circumscribed, infiltrative, moderately cellular neoplasm. Neoplastic cells form florid papillary and micropapillary projections into the lumen; neoplastic cells are supported by a moderate fibrous stroma. Neoplastic cells are cuboidal to columnar with indistinct cell borders and a moderate amount of finely granular eosinophilic cytoplasm. Nuclei are round to oval with finely stippled chromatin and 1-2 basophilic nucleoli and there is mild anisocytosis. Mitotic figures are rare. Throughout the neoplasm, there are multinucleated neoplastic cells with dense, hyperchromatic nuclei. These giant cells range up to 250 µm in diameter. The uterine lumen and spaces between papillary projections are filled with brightly eosinophilic cellular and basophilic nuclear debris, admixed with small amounts of hemorrhage and mineral. Within the underlying endometrium, there are numerous mildly ectatic glands containing bright red secretory material.

**Contributor's Morphologic Diagnosis:** Uterus: Endometrial adenocarcinoma, giant cell variety.

**Contributor's Comment:** Epithelial malignancies of the uterus are considered to be rare in domestic species. In domestic species, uterine adenocarcinoma is most commonly seen in the cow, but has also been reported in the mare, ewe, bitch, and queen.[2,8] In the bitch and queen, uterine malignancies constitute less than 1% of all neoplasms. In the ox, uterine carcinomas are solitary, often scirrhous neoplasms which invade the endometrium and myometrium, and often metastasize to the iliac and sublumbar lymph nodes, and ultimately to the lung and liver. Endometrial adenocarcinoma has been reported rarely in the queen.[3] In the largest review 8 of 13 uterine neoplasms arose in the endometrium; one of these was a mixed Mullerian neoplasm.[3] Myometrial invasion was variable in these cases, and carcinomatosis was noted in three, and pulmonary metastasis in one. Only two of the cats with endometrial adenocarcinoma had disease-free intervals longer than five months. Neoplastic cells are immunopositive for cytokeratin, vimentin, smooth muscle actin, COX-2, beta catenins, progesterone and estrogen receptors and caveolin-1.[3,7] In laboratory species uterine adenocarcinomas are most commonly reported in the rabbit and mouse. In the mouse, endometrial carcinomas are infiltrative neoplasms which invade the endometrium and myometrium, may occlude the uterine lumen, and may metastasize to distant sites. Squamous differentiation is seen with endometrial adenocarcinoma in the B6C3F1 mouse, usually in association with chemical administration. Uterine adenocarcinomas are considered to be the most common spontaneous neoplasm in the rabbit, usually seen in animals four years or older. In this species, multiple neoplasms may arise in both horns of the uterus and metastasize readily to the peritoneal cavity and ultimately to lungs and viscera. In humans, a variety of endometrial carcinomas have been diagnosed, based on the predominant cell-type (serous, clear cell, and poorly-differentiated endometrial carcinoma).[4] One of the many variants of poorly-differentiated endometrial

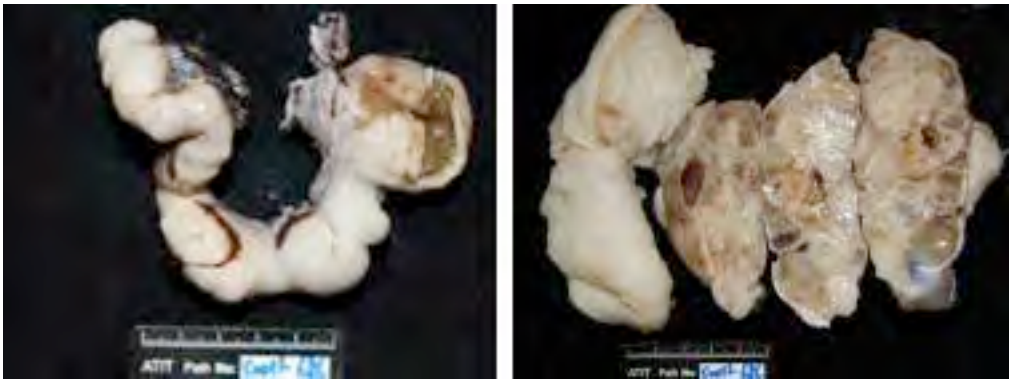

*4-1. Formalin fixed uterus, cat: Uterine horns are multifocally swollen and upon cut section, the lining was cystic, with a chocolate-colored material filling the lumen. (Photo courtesy of the Animal Technology Institute of Taiwan, Division of Animal Medicine, P.O. Box 23, Chunan, Miaoli, 350 Taiwan)*

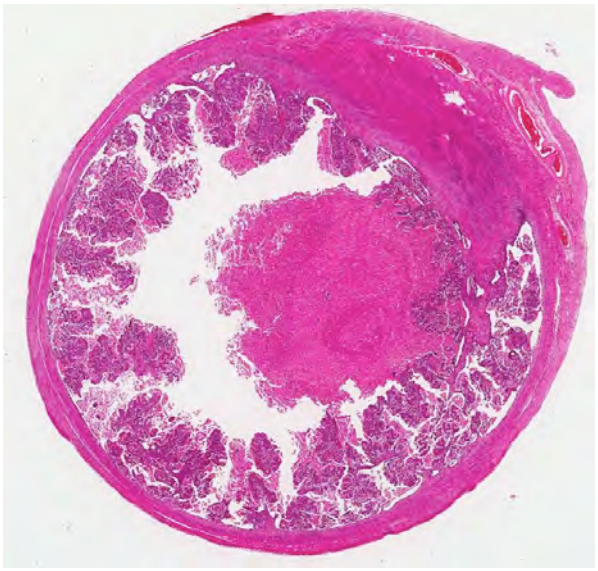

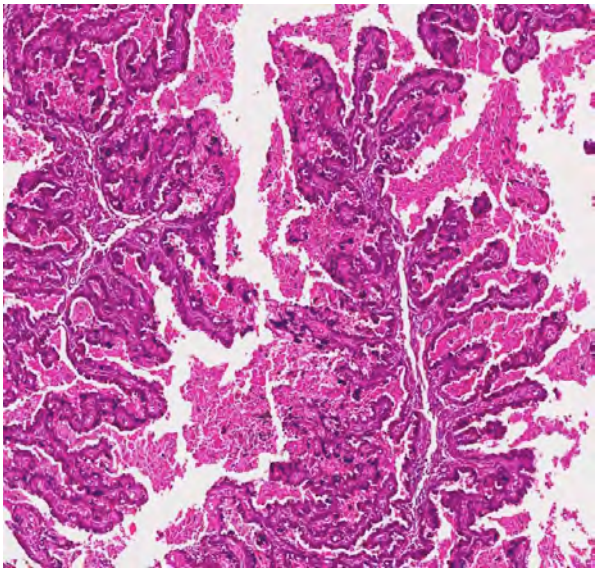

*4-2, 4-3. Uterus, cat: Neoplastic endometrium forms large papillary and micropapillary projections into the dilated lumen. Necrotic debris separates papillary projections as well as forms a large coagulum in the uterine lumen. (HE 4X, 60X)*

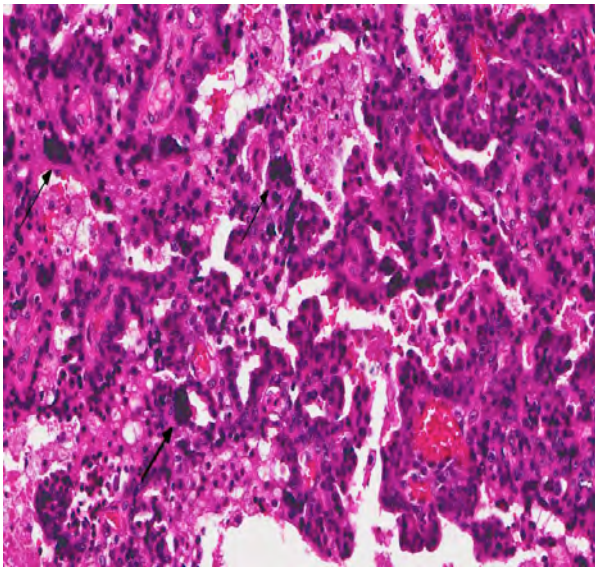

*4-4. Uterus, cat: Neoplastic endometrium forms large papillary and micropapillary projections into the dilated lumen. Necrotic debris separates papillary projections as well as forms a large coagulum in the uterine lumen. (HE 400X)*

carcinoma in the human is the endometrial giant cell carcinoma which morphologically resembles the neoplasm of this case. In a limited number of cases in one study, visceral metastasis was seen in one of five individuals. The presence of giant cells is of special interest in this case. In addition to the human cases listed above, giant cells have been rarely reported in endometrial carcinoma in domestic species, with one reported in the bitch.

**JPC Diagnosis:** Uterus: Endometrial carcinoma.

**Conference Comment:** The contributor provided a very good summary of endometrial carcinoma in various species. Interestingly, in women, post-menopausal hormone replacement (estrogen) is understood to be a risk factor for developing endometrial adenocarcinoma. Other species in which endometrial adenocarcinomas have been reported (i.e. rabbits, cats) are induced ovulators, which can result in extended periods of estrogen stimulation similar to post-menopausal women receiving estrogen replacement therapy . Rabbits have a high incidence of uterine adenocarcinoma, with 79% of females affected after 5 years of age.[3] The lower prevalence of uterine adenocarcinoma in cats may be attributable to the common practices of either neutering females, or breeding intact queens, thus reducing the number of individuals that experience the prolonged increases in estrogen. In women, there are estrogen-dependent and estrogen-independent adenocarcinomas, of low and high grade, respectively. In one study, feline tumors with marked nuclear atypia and metastasis usually did not express estrogen receptors, suggesting that estrogen independence may indicate a worse prognosis.[3]

**Contributing Institution:** Animal Technology Institute of Taiwan, Division of Animal Medicine, P.O. Box 23, Chunan, Miaoli, 350 Taiwan
path@mail.atit.orq.tw

**References:**

1. Gil da Costa RM, Santos M, Amorim L, et al. An Immunohistochemical Study of Feline Endometrial Adenocarcinoma. *J Com Path*. 140:254-259, 254-259.
2. Maclachlan NJ, Kennedy PC. Tumors of the genital systems, teratoma. In: Meuten DJ, ed. *Tumors in*

*Domestic Animals*. 4th ed. Ames, IA: Iowa State University Press; 2002:554.
3. Miller MA, Ramos-Vara JA, Dickerson MF, et al. Uterine neoplasia in 13 cats. *J Vet Diagn Invest*. 2003;15:51 5-522.
4. Mulligan AM, Plotkin A, Rouzhahman M, et al. Endometrial giant cell carcinoma: a case series and review of the spectrum of endometrial neoplasms containing giant cells. *Am J Surg Pathol*. 2010;34:1132-1138.
5. Davis BJ, Dixon D, Herbert H. Ovary, oviduct, uterus, cervix and vagina. In: Maronpot RR, ed. *Pathology of the Mouse, Reference and Atlas*. 1st ed. St. Louis, MO: Cache River Press, Inc.; 1999:433-434.
6. Pena FJ, Gines JA, Duque J, et al. Endometrial adenocarcinoma and mucometra in a 6-year-old Alaska malamute dog. *Reprod Dom Anim*. 2006;41:189-190.
7. Pires MA, Seixas F, Palmeira C, et al. Histopathologic and immunohistochemical exam in one case of canine endometrial adenocarcinoma. *Reprod Dom Anim*. 2010;45:545-549.
8. Schlafer DH, Miller RB. Female genital system. In: Maxie MG, ed. *Jubb, Kennedy, and Palmer's Pathology of Domestic Animals*. 5th ed. Vol. 3. St. Louis, MO: Saunders Elsevier; 2007:453454.

**Joint Pathology Center**
**Veterinary Pathology Services**

## WEDNESDAY SLIDE CONFERENCE 2012-2013

# Conference 5

**24 October 2012**

**CASE I:** N12-35 (JPC 4018122).

**Signalment:** 6- to 8-month old, female feral pig, *Sus scrofa,* porcine.

**History:** This pig was trapped and killed as part of a feral swine monitoring project.

**Gross Pathology:** A female, black, wild hog in good body condition (BCS 6/9) was presented for necropsy. Numerous live ticks were present on the surface of the body. A 2 cm bullet hole was present caudal to the right eye. Coagulated blood was in the oral cavity. Pink froth was in the lumen of the trachea and extended to the larynx (pulmonary edema). The lungs were diffusely reddened with only approximately 5 cm x 2 cm areas of normal pink lung tissue at the distal poles of the caudal lung lobes. The lung contained large coalescing areas of depressions. The bronchioles of both caudal lung lobes contained numerous white nematodes that were 4-6 cm in length (*Metastrongylus* sp.). The brain contained multifocal areas of hemorrhage (status post brain trauma induced by euthanasia).

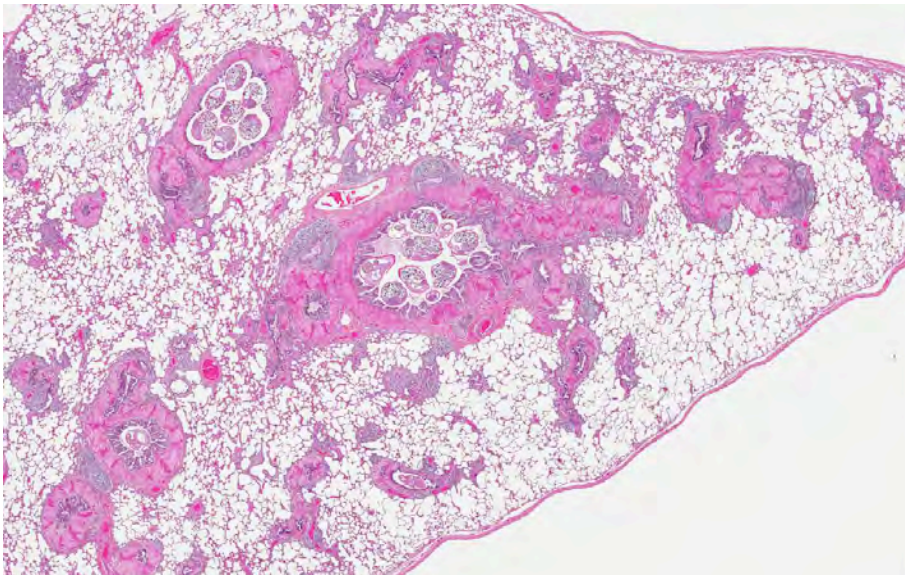

*1-1. Lung, pig: Throughout the section, bronchioles are tortuous, exhibit marked smooth muscle and BALT hyperplasia, and contain adult nematodes within lumens. (HE 4X)*

**Histopathologic Description:** Lung. Bronchi and bronchioles contain intraluminal nematodes that are 500-700 micrometers in diameter, with a thin cuticle surrounding a body cavity with coelomyarian musculature, an intestinal tract lined by few multinucleated cells, ovaries, and uteri filled with oocytes

*1-2. Lung, pig: Bronchioles contain numerous cross-sections of male (smaller) and female (larger) adult metastrongyle nematodes. (HE 36X)*

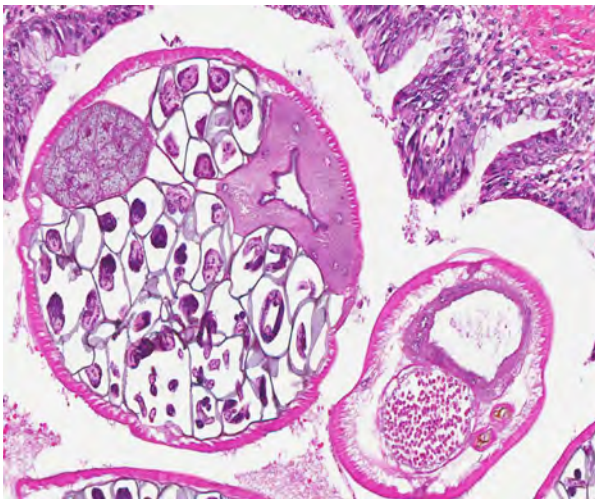

*1-3. Lung, pig: The larger adult females have polymyarian-coelomyarian musculature, a multinucleated intestine (right) and a large uterus filled with larvated eggs. (HE 90X)*

and developing larva. The eggs are occasionally free in the lumen of bronchi. There are small to moderate amounts of intraluminal edema, fibrin and mucus admixed with eosinophils and few macrophages, lymphocytes, plasma cells and neutrophils. The bronchial and bronchiolar epithelium is hyperplastic with goblet cell metaplasia and occasionally forms outpouchings. There is marked peribronchial and peribronchiolar smooth muscle hypertrophy. Bronchi and bronchioles are surrounded by moderate to numerous eosinophils with lesser numbers of lymphocytes and plasma cells. There is bronchial associated lymphoid tissue (BALT) hyperplasia. There are multifocal to coalescing areas of alveolar capillary congestion with associated intra-alveolar edema.

**Contributor's Morphologic Diagnosis:** Lung: Moderate multifocal eosinophilic pneumonia with smooth muscle hypertrophy, goblet cell metaplasia, BALT hyperplasia and numerous intrabronchial and intrabronchiolar nematodes, consistent with *Metastrongylus* sp.

**Contributor's Comment:** *Metastrongylus* sp. is the common lung nematode that is parasitic in the bronchi and bronchioles of the pig. *M. apri* is the most common, but other species include *M. pudendotectus*, and *M. salmi*.[1] They are nematodes of the superfamily *Metastrongyloidea* and the family *Protostrongylidae*. The intermediate host is the earthworm, and the infective third stage larvae may survive in the earthworm for as long as 18 months. Once the intermediate host is ingested, the larvae migrate through the lymphatics from the intestine to the lungs. Some larvae pass through the liver, producing focal hepatitis, as seen with *Ascaris suum* larval migration. The prepatant period for *Mestastrongylus* sp. is approximately 25 days after which there is a rapid rate of egg production, which eventually subsides to a low level.

Clinical signs include persistent cough, which may be paroxysmal, and growth retardation of the host—which can have a significant negative economic impact in domestic swine.[2] When noticeable, gross lesions typically consist of gray nodules on the pleural surface of the lung, and adult nematodes which can be visualized in bronchi and bronchioles. Heavy pulmonary infections are usually in younger pigs, where worms may be found in all lung lobes. Whereas in older animals, there are typically fewer worms that are often restricted to airways along the caudoventral borders of the caudal lung lobes. Because the earthworm is the intermediate host, pulmonary metastrongylosis is common in wild pigs, but is rare in housed domestic swine. Lungworms are considered to play a role in the transmission of swine influenza.

**JPC Diagnosis:** Bronchiolitis, eosinophilic and lymphohistiocytic, diffuse, mild, with marked smooth muscle hyperplasia, BALT hyperplasia and numerous cross sections of adult metastrongyles.

**Conference Comment:** The contributor provided a good summary of metastrongylosis in swine, as well as excellent specimens that allow easy visualization of many of the characteristics of *Metastrongylus* species. In addition to the genus *Metastrongylus*, phylum *Nematoda* contains numerous parasitic species that are of concern in veterinary medicine. When evaluating nematodes in tissue section, it is important to note and describe several key characteristics in a consistent and organized format, paying particular attention to any diagnostically salient features, some of which allow for the diagnosis of a nematode and some of which allow further identification to genus and perhaps even

species. A description of important features of nematodes, and specifically metastrongyles, follows. Nematodes have a cuticle that can vary in thickness from barely discernible to very thick and may be smooth or adorned with bumps, ridges, or wing-like structures. Internal to the cuticle is the hypodermis. In phasmid nematodes such as metastrongyles, lateral extensions of the hypodermis (lateral chords), and dorsal and ventral nerve chords protrude into the pseudocoelom (body cavity), dividing it into quadrants. Additionally, metastrongyles also have accessory hypodermal chords that further subdivide the quadrants. Lateral chords may protrude deeply into the pseudocoelom, or may be low and flat. The hypodermis of phasmid nematodes contains very few nuclei except in the lateral chords. Internal to the hypodermis, nematodes have somatic musculature which either projects into the pseudocoelom in a cylinder-like manner (coelomyarian), or lies low and flat on the hypodermis (platymyarian). Coelomyarian muscle arrangement is such that numerous muscle cells can be present in a single cross section (polymyarian). Conversely, platymyarian muscles are generally larger and fewer (meromyarian). Metastronglyes differ from other members of the strongyle group (i.e. true strongyles and trichostrongyles) by having coelomyarian musculature. Another important feature of nematodes is their digestive tract, which is composed of a mouth, buccal cavity, esophagus, intestine and anus. Esophagus and intestine shape and composition can be useful in identification. Intestines are large, medium or small (described relative to the size of the nematode), and are lined by either many cuboidal to columnar cells, or few multinucleate cells. A brush border of microvilli may be present. Metastrongyles, like other strongyles, have a large intestine lined by few multinucleate cells. Lastly, adult nematodes also have reproductive tracts. In phasmid nematodes, the female has two or more reproductive tracts composed of ovaries, oviducts and uteri. Uteri contain developing eggs or embryos, the presence of which is another identifying feature, as eggs vary among and within groups. Eggs can contain zygotes or larvae; they can be thin- or thick -shelled, or, as in the case of metastrongyle larvae, the shell can be so thin it is not discernible. Metastrongyle larvae have more structure than other nematode larva, which often appear as a sac of nuclei; metastrongyle larvae have a primitive alimentary tract, as well as eccentric tail tips and, in some genera, caudal spines. Adult male nematodes have only one reproductive tract. The testis produces sperm which can be seen in the vas deferens. Sperm can also be found in the female, as the distal part of the uteri (seminal receptacle) stores sperm from previous copulations.[3]

**Contributing Institution**: Tuskegee University School of Veterinary Medicine
1200 Old Montgomery Road
Tuskegee, AL 36088
http://www.tuskegee.edu/academics/colleges/cvmnah/school_of_veterinary_medicine.aspx

**References:**

1. Pence DB, Warren RJ, Ford CR. Visceral helminth communities of an insular population of feral swine. *J Wildl Dis.* 1988;24(1): 105-112.
2. Kahn, CM., ed. *The Merck Veterinary Manual.* 9th ed. Whitehouse Station, NJ: Merck & Co., Inc.; 2005:1181-1184.
3. Gardiner CH, Poynton SL. *An Atlas of Metazoan Parasites in Animal Tissues.* Washington, DC: Armed Forces Institute of Pathology/ American Registry of Pathology; 2006:2-29.

**CASE II:** N12-70 RM (JPC 4019377).

**Signalment:** 11-year-old Thoroughbred mare, *Equus caballus,* equine.

**History**: The horse was presented with history of coughing, bilateral epistaxis and severe respiratory distress, and later developed colic signs. Thoracic ultrasound examination revealed decreased lung sounds, marked consolidation and pleural effusion on the left side. About 1 liter of thick proteinaceous yellow fluid was removed after placing a chest tube. Cytology of pleural fluid showed few lymphocytes and macrophages. Heart auscultation was within normal limits. Serum chemistry was unremarkable. However, the mare failed to improve despite treatment with broad-spectrum antibiotics and other medications to relieve respiratory discomfort, and was humanely euthanized.

**Gross Pathology**: The entire left lung is consolidated, firm, and on cut section the architecture is effaced by a multilobulated (0.5-5 cm diameter) tan-pink, firm mass mixed with green-yellow, mucous material. There are 2 liters of serosanguinous pleural effusion in the left hemithorax.

**Histological Description**: The pulmonary architecture is effaced by a well-demarcated, unencapsulated, expansile, highly cellular mass that surround bronchioles and bronchial glands and compresses the adjacent parenchyma. The mass is composed of sheets of densely packed round to polygonal cells supported by a fine fibrovascular stroma. Neoplastic cells have distinct borders, eccentrically placed nuclei and abundant eosinophilic granular cytoplasm. Nuclei are round to oval and contain finely stippled chromatin and one distinct nucleolus. There are five mitotic figures in ten 400x fields.

In the adjacent parenchyma, the interstitial septa are expanded (up to 10 times normal) by abundant fibrous connective tissue containing plump fibroblasts mixed with a moderate number of neutrophils, lymphocytes, plasma cells, and macrophages containing intracytoplasmic golden- yellow pigment (hemosiderophages). The bronchoalveolar spaces are filled with a moderate number of degenerate and intact neutrophils, lymphocytes, plasma cells, foamy macrophages, hemosiderophages, necrotic debris, and in few sections they contain granular to fibrillar amphophilic material (mucin). Epithelium lining the bronchioles and alveolar ducts is infiltrated by few neutrophils (exocytosis), and is degenerate (intracytoplasmic vacuolation). Most of the alveolar spaces are compressed by interstitial fibrosis and those remaining are lined by a single layer of low cuboidal epithelium (type II pneumocyte hyperplasia).

**Contributor's Morphological Diagnosis**: 1. Left lung: Granular cell tumor.
2. Left lung: Marked, diffuse, chronic-active, neutrophilic and lymphohistiocytic bronchointerstitial pneumonia with fibrosis.

**Contributor's Comment**: Granular cell tumors (GCT) have been reported in a variety of species such as dogs, cats, rats, horses and humans. They occur on the tongue in dogs; the digits, tongue, and vulva in cats; central nervous system in rats and in a wide variety of sites including subcutaneous tissue in humans.[4,5,7,8] In horses, GCTs arise as primary lung tumors and are more prevalent in aging horses.[4,5] There is no reported sex or breed predisposition. They occur as multiple, peribronchial, white to tan, lobular, well circumscribed, expansile nodules that frequently compress adjacent tissue. They are histologically benign but locally invasive tumors, and are often

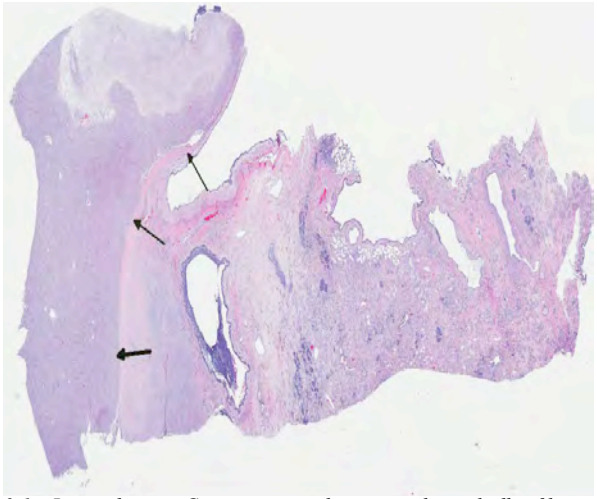

*2-1. Lung, horse: Compressing adjacent and markedly fibrotic pulmonary parenchyma is an encapsulated, well-demarcated, moderately cellular neoplasm. (arrows ) (HE 5X)*

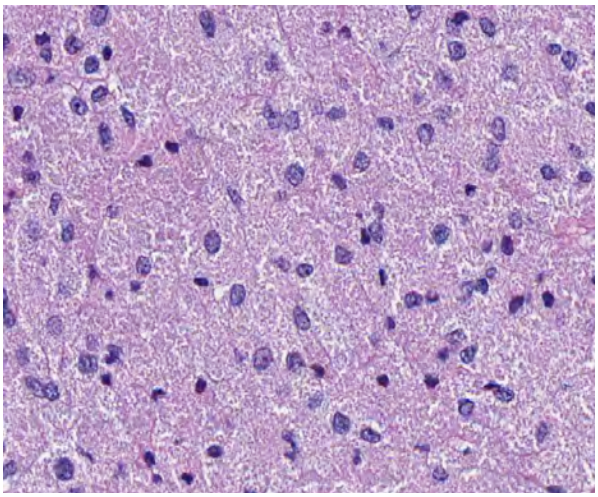

*2-2. Lung, horse: The neoplasm is composed of densely packed polygonal cells containing numerous, distinct eosinophilic granules. (HE 400X)*

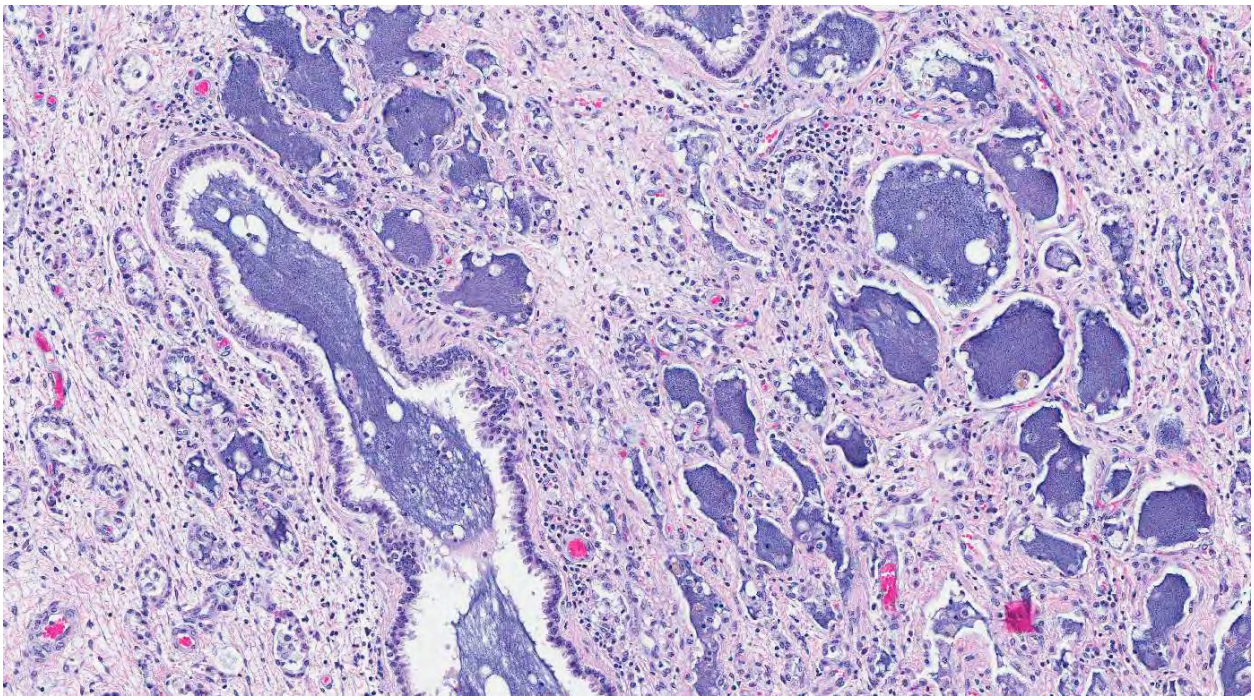

*2-3. Lung, horse: The adjacent lung is fibrotic with loss of alveolar architecture; remaining airways are often dilated and filled with mucin, and there is mild chronic inflammation. (HE 108X)*

recognized as an incidental finding. Ultrastructurally, the neoplastic cells have indented or convoluted nuclei and intracytoplasmic granules that are thought to be accumulations of lysosomes.[6,8]

Although previous reports in humans and in horses strongly support a Schwann cell or neural origin, the histogenesis of GCTs is still controversial.[2,4] While the light and electron microscopic appearance of GCTs in most species is similar, histochemical and immunohistochemical staining varies between the tumor site(s) and species, suggesting multiple cell origins.[2,4] GCTs are vimentin positive and inconsistently positive for S-100, neuron-specific enolase (NSE) and cytokeratin; however, they consistently stain PAS-positive and are diastase resistant. GCTs should be differentiated from other tumors with granular cytoplasm such as oncocytoma (PAS- positive, but sensitive to diastase digestion), rhabdomyoma (desmin- and myoglobin-immunopositive), chemodectoma/carcinoids (packets and nests of cells immunopositive for neuroendocrine markers) and large granular lymphocyte tumors.

In the present case, there was significant involvement of the left lung. Chronic-active pneumonia and fibrosis are secondary to obstruction of the major airways by the neoplasm and the consequential blockage/reduction of normal mucociliary clearance (a critical innate immune response) of pathogens.

**JPC Diagnosis:** Lung: Granular cell tumor.

**Conference Comment:** Conference participants discussed several aspects of granular cell tumors (GCTs) adeptly summarized by the contributor, including the occurrence of GCTs in other species, and the controversy regarding their histiogenesis. Human GCTs were once thought to be derived from myoblasts, histiocytes, smooth muscle cells, fibroblasts, or Schwann cells. Immunohistochemical studies suggest that human endobronchial GCTs, the human counterpart of equine pulmonary GCTs, are derived from Schwann cells; as in their human counterparts, the microscopic and immunohistochemical properties of equine pulmonary GCTs indicate that they are of neural crest origin and are most consistent with Schwann cells of the nervous system in the peribronchial/peribronchiolar tissues.[1,3]

In a study of four horses with pulmonary GCTs, all tumors showed uniformly strong positive labeling with antibodies to vimentin, S100 protein, and glial fibrillary acidic protein (GFAP).[3] Vimentin expression is common in cells of mesenchymal origin, and S100 is commonly found in cells of neural crest origin. GFAP is expressed by non-myelin forming Schwann cells in mice and humans. Although myelin-forming Schwann cells express both S100 protein and vimentin, this expression is not specific, as S100 and vimentin antibodies also react with some tumors of non-neural origin. Virtually all tumor cells in all four horses in this study showed positive immunoreactivity to myelin basic protein (MBP) and protein gene product 9·5 (PGP9·5). MBP antibodies react with components of

Schwann cell-derived myelin. PGP9·5 is a major component of neuronal cytoplasm; it is a reliable marker for neurons, and is used in the diagnosis of intraoral granular cell tumors in humans. A few tumor cells from all horses in this study also showed positive immunoreactivity with Leu7. Leu7 reacts with myelin-associated glycoprotein in human neuroectodermal tissue, and some human GCTs have been labeled with antibodies against specific neural markers such as MBP and Leu7. All four tumors lacked expression of neurofilament protein (NF), cytokeratin (CK), chromogranin, α1 antichymotrypsin (AACT), myoglobin, desmin, α-actin and α-SMA, ruling out neuroendocrine or myogenic cell origin. This study, along with others, supports the hypothesis that equine pulmonary GCTs are composed of myelinating and nonmyelinating Schwann cells.[3]

Conference participants uniformly agreed with the contributor's conclusion that the chronic pulmonary pathology in the adjacent lung tissue is secondary to the neoplasm.

**Contributing Institution:** Tufts University
Cummings School of Veterinary Medicine
Section of Pathology, Department of Biomedical Science
http://vet.tufts.edu/dbs/pathology.html

**References**

1. Kagawa Y, et al. Immunohistochemical analysis of equine pulmonary granular cell tumours. *J Comp Path.* 2001;124:122-127.
2. Kelley LC, Hill JE, Hafner S, Wortham KJ. Spontaneous equine pulmonary granular cell tumors: morphologic, histochemical, and immunohistochemical characterization. *Vet Pathol.* 1995:32:101-106.
3. Lopez A. Respiratory system, mediastinum, and pleura. In: McGavin MD, Zachary JF, eds. *Pathologic Basis of Veterinary Disease.* 5th ed. St Louis MO: Elsevier Mosby; 2012:533.
4. Mittal KR, True LD. Origin of granules in granular cell tumor. *Arch Pathol Lab Med*. 1986;112:302-303.
5. Patnaik AK. Histologic and immunohistochemical studies of granular cell tumors in seven dogs, three cats, one horse, and one bird. *Vet Pathol*. 1993;30:176-185.
6. Troncoso P, Ordonez NG, Raymond AK, Mackay B. Malignant granular cell tumor: immunocytochemical and ultrastructural observations. *Ultrastruct Pathol.* 1988;12:137-144.
7. Van der Gaag I, Walvoort HC. Granular cell myoblastoma in the tongue of a dog: a case report. *Vet Quart.* 1983;5:89-93.
8. Wright JA, Goonetilleke URP, Waghe M, Stewart M, Carlile A. Comparison of a human granular cell tumour (myoblastoma) with granular cell tumours (meningiomas) of the rat meninges - an immunohistological and ultrastructural study. *J Comp Pathol*. 1990;103:191-198.

**CASE III:** S1107769 (JPC 4019380).

**Signalment:** 25-year-old Quarter Horse gelding, *Equus caballus,* equine.

**History:** One of three horses on a ranch in Southern California was found within a week circling and walking aimlessly. According to the submitting veterinarian this horse had "elevated liver enzymes" (specific enzymes and their values were not provided) and it was treated for a week for "hepatic encephalopathy" (no further details provided), after which it was euthanized due to lack of response to treatment.

**Gross Pathology:** The carcass was in poor nutritional condition, with no fat reserves, sunken eyes and mild generalized muscle atrophy. The cardiac and bone marrow (femur) fat showed severe and diffuse serous atrophy. There was a moderate amount (occupying approximately 1/5 of the lumen) of coarse sand, mixed with digesta in all four sections of the large colon. The cecum contained a large amount of reddish, translucent fluid, although no significant gross abnormalities were observed on the mucosa of this organ. The liver was reduced in size (approximately 1/3 to 1/2 of its normal size) and thickness; the consistency was, however, unremarkable. No other significant gross abnormalities were observed in the rest of the carcass.

**Laboratory Results:** Salmonella culture of liver: negative; Aerobic culture of liver: no growth in 48 hours; Anaerobic culture of colon content: no growth in 48 hours; *C. difficile* culture (colon content): negative; Fecal float: no parasite eggs seen; *C. perfringens* toxins (alpha, beta, epsilon) ELISA in small intestine and colon content: negative; *C. difficile* toxins A/B ELISA in small intestine and colon content: negative; Brain cholinesterase activity: within normal range; Heavy metal screen in liver (including selenium): within normal range. Examination of a bale of alfalfa hay from a batch that this horse and his companions had been eating for the past several months identified the following plants: common groundsel, cheeseweed, wild lettuce, shepherd's purse and green foxtail.

**Histopathologic Description:** Diffusely, there is severe megalocytosis consisting of enlargement of the nuclei and cytoplasm of a high percentage of hepatocytes. The volume of affected cells is increased as much as to 5 to 10 times. The nuclear membrane is basophilic and sharply delimited. Most hepatocytes have one nucleolus, although up to four nucleoli are present in some cells. The chromatin is fragmented. The peripheral part of the cytoplasm is usually pale and presents multiple coalescing vacuoles. Acidophilic, more or less spherical bodies (cytosegresomes), are occasionally seen in the cytoplasm of some hepatocytes. Because the enlarged hepatocytes are closely apposed, the sinusoids are rarely evident and the general architecture of the organ is distorted. Small to medium size pools of bile (bile stasis) are present in canaliculi and in the cytoplasm of hepatocytes. Multifocally, individual cell necrosis is observed. Diffusely, the liver presents moderate fibrosis, which is mostly restricted to the portal areas, although some fibrosis can be seen attempting to dissect lobules and separate individual cells. Multifocally, there is bile duct proliferation with hypertrophic epithelium. Multifocally there is hemorrhage, and infiltration of neutrophils, lymphocytes, plasma cells and macrophages. Blood

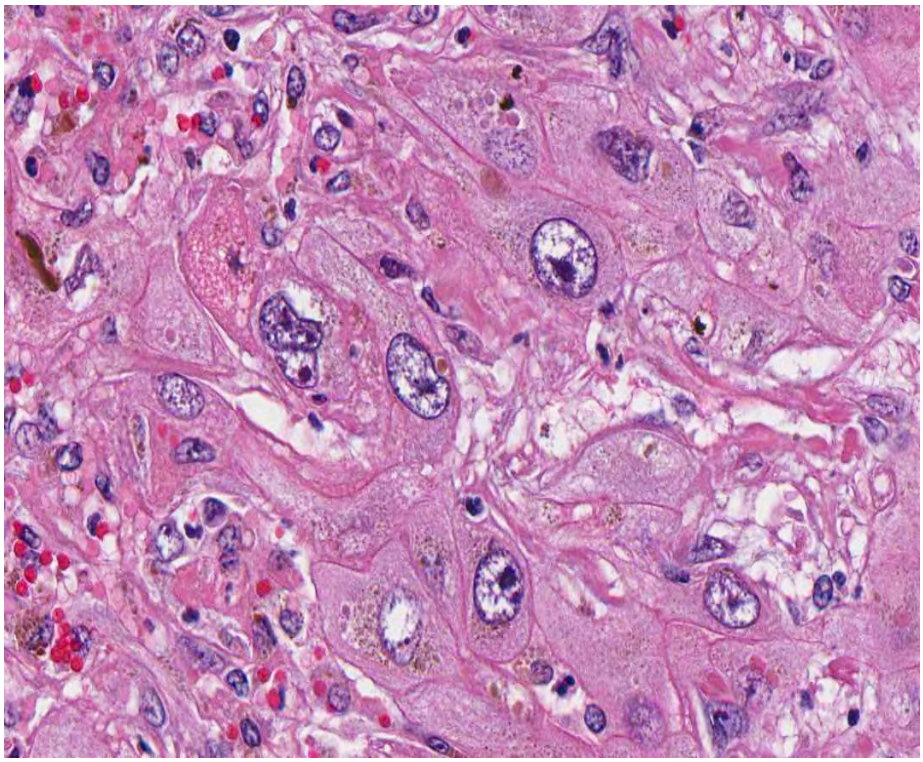

*3-1. Liver, horse: There is diffuse distortion of the hepatocellular lobular and plate architecture. Remaining hepatocytes are enlarged up to 2-3X normal and have large, often multiple nuclei and a prominent nucleolus (megalocytosis). (HE 400X)*

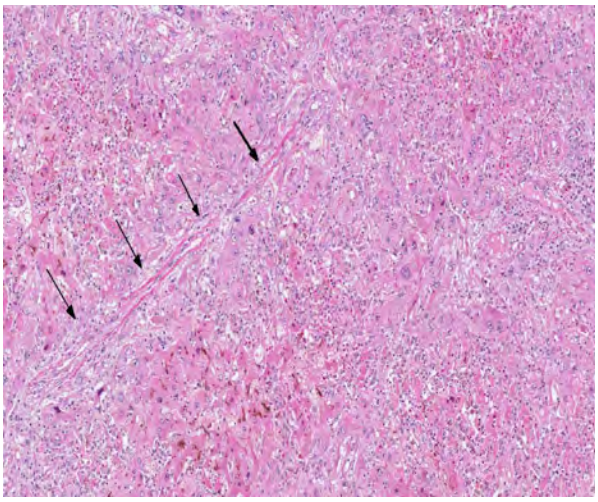

*3-2. Liver, horse: There is marked fibrosis which bridges portal areas (arrows) and occasionally replaces portal hepatocytes. (HE 60X)*

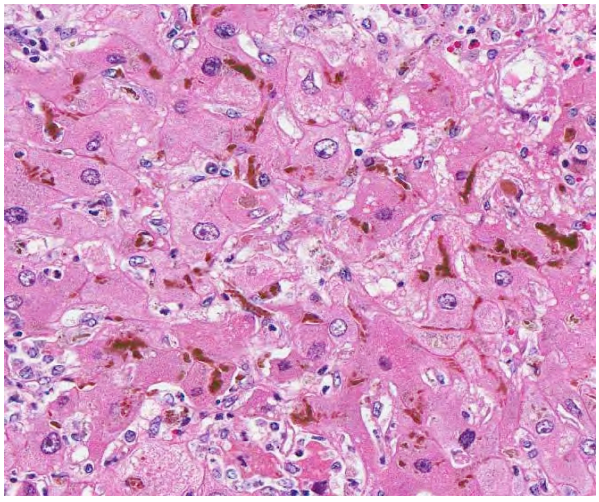

*3-3. Liver, horse: Distortion of hepatic architecture and fibrosis of portal area has resulted in marked cholestasis and numerous bile plugs. (HE 80X)*

vessels in portal areas show plump, hypertrophic epithelium. These changes tend to affect all the cells of all the lobules with no special predilection for any part of the lobule.

In the brain (not submitted) there are single or small groups of astrocytes with clear, vesicular nuclei (Alzheimer type II cells), with scant cytoplasm, mostly restricted to basal nuclei, cerebellar peduncles and hippocampus.

**Contributor's Morphologic Diagnosis:** Hepatopathy, with megalocytosis, portal fibrosis, bile duct proliferation and bile stasis, diffuse, chronic.

**Contributor's Comment:** The changes described in the liver are classic of pyrrolizidine alkaloids (PA) intoxication, which is consistent with the presence of common groundsel (*Senecio vulgaris*), a plant known to contain PAs, in the hay that this animal was eating.[4] PAs are hepatotoxic, causing irreversible liver damage. Horses and cattle are the major livestock species affected by PAs. Clinical signs of chronic PA poisoning may often not appear for 2-8 months after the first ingestion of PA-containing plants. Affected animals lose condition, and develop liver failure. Neurological signs are commonly seen in horses, and the condition is called "walking disease".[2] After the onset of clinical signs, the prognosis is poor. The most characteristic effect of PA on the liver is the induction of megalocytosis, due to an antimitotic effect. Megalocytosis is not due to inhibition of DNA synthesis, as continued nucleoprotein synthesis, combined with mitotic inhibition, accounts for the increase in size of the nuclei. Although megalocytosis is a hallmark of PA intoxication, this change is not specific for this intoxication, as it can be seen in intoxication by aflatoxins and nitrosamines as well. In this case, however, the hepatic lesions (including megalocytosis, fibrosis and bile duct proliferation) coupled with the detection of *Senecio vulgaris* in the hay that this horse was consuming, is compelling evidence that this horse suffered from PA intoxication.[4] Although PAs can be tested for gastrointestinal contents, the fact that the lesions were so chronic makes testing of doubtful value as it was likely that any PA would have been metabolized long before this animal died. This horse also had neurological clinical signs and presence of Alzheimer type II cells in the brain. These clinical signs and lesions are characteristic of hepatic encephalopathy, a frequent complication of liver failure due to PA intoxication in horses and other animal species. While hepatic encephalopathy in several animal species is characterized by the presence of Alzheimer type II cells and spongiform change of white matter, in the horse, changes are limited to the development of type II cells, which was the case with this animal.[2]

Several toxic plants were identified in the bale of hay belonging to the batch that this animal was eating. Amongst those, the most significant is *Senecio vulgaris* (common groundsel), which was most likely responsible for the hepatic lesions and related clinical signs observed in this animal. *Senecio vulgaris* is a common weed in hayfields in California and is also widely distributed along the East Coast and Canada. Identification of PA-containing weeds in alfalfa and detection of PAs in forage are important to establish an accurate diagnosis.[1] Other plants found in the hay bale are also considered to be toxic, although they probably did not play a role in the disease of this horse. Amongst these, cheeseweed (*Malva parviflora*) is suspected to cause tremors (i.e. shivers or staggers), which may be intensified by exercise, followed by prostration and death. The causative agent is thought

to be malvalic and sterculic acid. Wild Lettuce (*Lactuca virosa*) is reported to cause "opium-like" symptoms. It possesses mild sedative and hypnotic properties. Shepherd's purse (*Capsella bursa-pastoris*) belongs to the mustard family and is reported to cause congenital hypothyroid dysmaturity syndrome in foals. Green foxtail (*Setaria spp.*) is among many species of grass with long, stiff awns or bristles that can cause physical injury to animals. The bristles can puncture sensitive tissue in the mouth and around the nose or eyes. The minutely barbed awns or bristles can work further into a wound by the movement of the animal.[1]

**JPC Diagnosis**: Liver: Hepatocellular degeneration, necrosis and loss, diffuse, severe, with megalocytosis, bridging portal fibrosis and cholestasis.

**Conference Comment**: The contributor provides a very good description of clinical and histologic manifestations of pyrrolizidine alkaloid intoxication. There are many PA-containing plants, including species in the *Senecio*, *Crotalaria*, *Cynoglossum*, *Echium, Heliotropium, Amsinckia, Symhytum, Borago, and Trichodesma* genera.[3]

Pyrrolizidine alkaloids are composed of free base and *N*-oxides. Although not directly toxic, once these alkaloids are bioactivated by mixed function oxidases, primarily in centrilobular regions of the liver, the resulting pyrroles are potent electrophiles that bind to and cross-link DNA, proteins, amino acids and glutathione. This results in both cytotoxic and antimitotic effects on hepatocytes. Plant species vary in the amount and variety of PAs they contain; hence the resulting pyrroles vary as well, with some being significantly more hepatotoxic than others. For example, the metabolites of seneciphylline and retrorsine are primarily hepatotoxic, whereas less reactive PAs such as trichodesmine and monocrotaline result in fewer hepatic changes and more extensive extrahepatic lesions. Animal species vary significantly in their susceptibility to toxic effects, likely due to variation in metabolism. For example, the toxic dose of some PA containing plants is 20 times higher for sheep than that for cattle. Relative susceptibility to PA poisoning in domestic animals are: pigs=1 (most sensitive); chickens =5; cattle and horses =14; rats = 50; mice =150; sheep and goats=200 (least sensitive). Additionally, the age, nutrition status and gender of the animal are also important factors in determining the severity of disease. Young animals and animals with suboptimal nutrition are at higher risk, and studies have found male rats are more susceptible than females.[3]

Early cellular changes in PA intoxication are dose-dependent hepatocyte swelling which progresses to degeneration and necrosis. Quickly-ingested high doses result in acute intoxication, characterized by panlobular hepatocellular necrosis, hemorrhage and minimal inflammation. Serum clinicopathologic abnormalities in acute toxicity include elevations in aspartate aminotransferase (AST), sorbitol dehydrogenase (SDH), alkaline phosphatase (ALK), and gamma-glutamyl transpeptidase (GGT) as well as increased bilirubin and bile acids. When lower doses are ingested over a longer period of time, chronic poisoning results. Early chronic lesions include piecemeal hepatic necrosis, minimal peribiliary fibrosis and mild bile duct regeneration. With time, megalocytosis and fibrosis occurs, as in this case, and animals eventually develop clinical liver failure and sequalae such as photosensitization, icterus, and increased susceptibility to hepatic lipidosis and ketosis. In chronic cases, animals may develop transient elevations of serum enzymes, bilirubin and bile acids; however, these may remain within normal limits for months after the PA ingestion.[3]

**Contributing Institution:** California Animal Health and Food Safety Laboratory
School of Veterinary Medicine
University of California, Davis
105 W. Central Ave.
San Bernardino, CA 92408
www.cahfs.ucdavis.edu

**References:**

1. Burrows GE, Tyrl RJ. *Toxic plants of North America*. Ames, Iowa: Iowa State University Press; 2001.
2. Kelly WR. The liver and biliary system. In: Jubb KVF, Kennedy PC, Palmer N. *Pathology of Domestic Animals*. Vol. 2. London, UK: Academic Press; 1993:319-406.
3. Stegelmeier BL. Pyrrolizidine Alkaloid–containing toxic plants (Senecio, Crotalaria, Cynoglossum, Amsinckia, Heliotropium, and Echium spp.). *Vet Clin Food Anim*. 2011;27:419–428.
4. Summers BA, Cummings JF, de Lahunta A. Degenerative diseases of the central nervous system. In: *Veterinary Neuropathology*. St. Louis, Missouri: Mosby; 1995:208-350.

**CASE IV:** 110592-22 (JPC 4019408).

**Signalment:** Aged male common marmoset, *Callithrix jacchus,* non-human primate.

**History:** This colony marmoset was housed at the U.S. Army Medical Research Institute of Infectious Diseases. The marmoset was euthanized because of chronic weight loss and lethargy.

**Gross Pathology:** The wall of the proximal jejunum was circumferentially thickened and firm for a length of approximately 0.5 cm with marked narrowing of the lumen ("napkin-ring" appearance/stricture). Other necropsy findings included: minimal subcutaneous and visceral adipose tissue; several missing and worn incisor teeth; mild splenomegaly; a moderately enlarged, pale tan liver with patchy white to pale yellow coalescing areas that bulged on cut surface; and few, approximately 0.5 mm diameter, white, slightly raised foci on the capsular surface of the right liver lobe.

**Histopathologic Description:** Jejunum: Expanding and infiltrating the mucosa, submucosa, and tunica muscularis is an unencapsulated, poorly circumscribed, moderately cellular neoplasm composed of polygonal cells (epithelial origin) arranged in disorganized acini and nests often separated and surrounded by an abundant amphophilic finely fibrillar material (mucin). Neoplastic cells have generally distinct cell borders, small to moderate amount of eosinophilic cytoplasm, round nuclei with finely stippled chromatin, and 1-2 distinct, occasionally prominent, nucleoli. A subpopulation of neoplastic cells is rounded with amphophilic cytoplasm that peripheralizes the nucleus (signet-ring appearance). There is moderate anisokaryosis with occasional multinucleate neoplastic cells. Mitotic figures are not observed. The tunica muscularis is markedly expanded (up to 5x normal) by fibrosis and reactive fibrous tissue (desmoplasia). There are moderate numbers of lymphocytes and plasma cells with fewer macrophages, neutrophils, and eosinophils scattered within the neoplasm. Multifocally, moderately expanding the basement membrane of vessels and adjacent connective tissue within the lamina propria is a pale eosinophilic amorphous material (consistent with amyloid). Other findings in some sections include: villous fusion and blunting (atrophy); erosion/ulceration; crypt abscesses; serositis with reactive mesothelium; and lymphoid follicular aggregates in the deep tunica muscularis.

**Contributor's Morphologic Diagnosis:** 1. Jejunum: Adenocarcinoma, mucinous. 2. Jejunum, lamina propria: Amyloidosis, multifocal, mild.

**Contributor's Comment:** Small intestinal adenocarcinomas are generally uncommon in human and nonhuman primates. The most commonly reported intestinal carcinomas in nonhuman primates are ileocecal adenocarcinomas in aged rhesus macaques (*Macaca mulatta*) and colorectal adenocarcinoma in cotton-top tamarins (*Saguinus oedipus*).[5] In humans, most small intestinal malignant tumors are metastases from tumors arising in other locations with colorectal adenocarcinomas much more commonly reported.[1] The association of chronic-active colitis with development of colorectal adenocarcinomas in cotton-top tamarins and humans is also generally well-accepted.[3,5,6,8]

A recent report suggests that small intestinal adenocarcinoma may be a relatively common neoplasm in aged common marmosets (*Callithrix jacchus*).[5] In this report, tumors were usually located

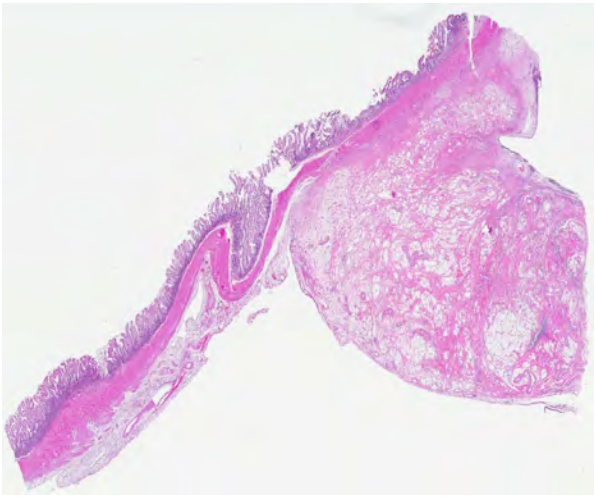

*4-1. Small intestine, marmoset: There is transmural infiltration and marked expansion, especially of the serosa, by an unencapsulated, poorly demarcated neoplasm. (HE 5X)*

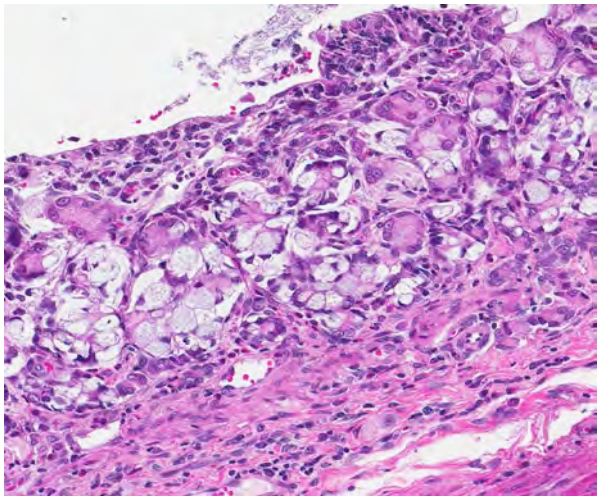

*4-2. Small intestine, marmoset: Neoplastic cells infiltrate the mucosa resulting in architectural distortion as well as marked blunting of overlying villi. (HE 80X)*

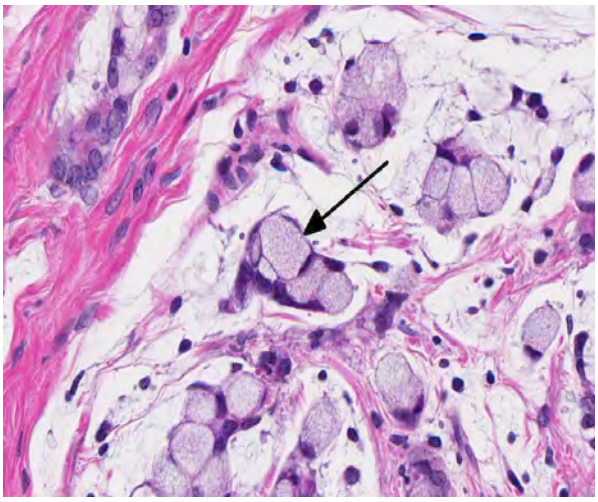

*4-3. Small intestine marmoset: The large "lakes" of mucin surrounding neoplastic cells is a characteristic feature of the mucinous type of intestinal adenocarcinoma. (HE 92X)*

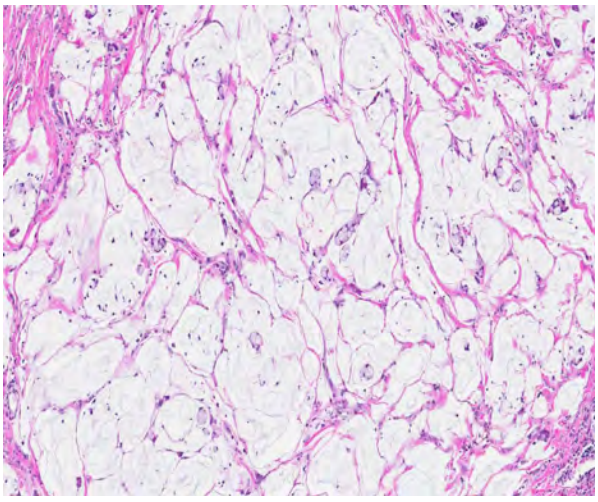

*4-4. Small intestine, marmoset: Nests of neoplastic cells are often surrounded by lakes of clear to amphophilic mucinous matrix. In some neoplastic cells, large vacuoles of amphophilic mucin peripheralize the nucleus (signet ring cells)(arrow). (HE 400X)*

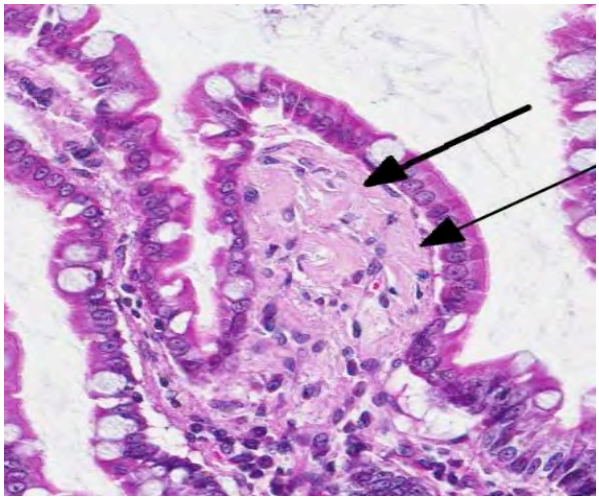

*4-5. Small intestine, marmoset: Multifocally, the adjacent lamina propria is multifocally expanded by a waxy, eosinophilic homogeneous material (amyloid). (HE 200X)*

within the proximal small intestine, immediately distal to the duodenum, with grossly observed thickening and stricture at the tumor site often present. Signet-ring cell differentiation, lymphatic infiltration, and metastatic spread to the regional lymph nodes were other common findings. Carcinomatosis was not observed. An association between presence of callitrichine herpesvirus 3 (marmoset lymphocryptovirus) or *Helicobacter* sp. and tumor development was not found.[5] This case shares similar features to those reported; however, evidence of metastasis was not observed in histologically examined tissues.

The reason for the predisposition of development of small intestinal adenocarcinoma at the duodenal-jejunal interface is unknown; however, there is a belief among some pathologists that components of biliary or pancreatic secretions that enter the intestine at this location may result in cell damage and subsequent tumorigenesis.[1] Even though the small intestine has a high cell turnover and large epithelial surface, adenocarcinomas develop much less frequently than in the large intestine. Several hypotheses have been postulated to explain this disparity in occurrence and these include: dilution of potential carcinogens due to the more liquid nature of small intestinal contents allows decreased mucosal contact; rapid transit time in the small intestine allows decreased mucosal contact of potential luminal carcinogens; presence of Paneth cells in the small intestine aids in antibacterial activity; lack of anaerobic bacteria in the small intestine that are able to convert bile salts to potential carcinogens; large amounts of lymphoid tissue (lamina propria and Peyer's patches) that provide increased immunosurveillance against tumor cells; large amounts of mucosal enzymes that can detoxify luminal contents; less mechanical trauma to the mucosa due to more liquid luminal contents; and crypt stem cells are further away from contact with potential luminal carcinogens.[1]

Intestinal adenocarcinomas can often be further described based on their predominant morphologic appearance into acinar, papillary, mucinous, signet-ring cell, undifferentiated, or adenosquamous subtypes. In general, small intestinal adenocarcinomas are uncommon in domestic animals. However, in some countries, small intestinal adenocarcinoma can be common in cattle and is associated with ingestion of bracken fern and bovine papillomavirus type 4 infection.[2] Tumors are usually multiple and vary from adenoma to carcinoma affecting all levels of the small intestine. In sheep, there has also been an association

with bracken fern ingestion and herbicide use.[2] Unlike in cattle, these tumors are usually mid-jejunal and solitary.

An additional finding in this marmoset was the presence of a pale eosinophilic amorphous material in widespread tissues (gastrointestinal tract, spleen, liver, kidney, adrenal gland, and thyroid gland). Congo red stain of a replicate section of kidney from this marmoset confirmed that the eosinophilic material is amyloid. Systemic AA or reactive secondary amyloidosis has been reported in common marmosets, usually related to a chronic inflammatory process that results in elevated serum amyloid A (SAA) protein levels. A genetic factor may also play a role in the common marmoset.[4] In addition to the small intestinal adenocarcinoma, this marmoset exhibited marked to severe granulomatous and eosinophilic cholangitis with intralesional degenerate parasitic remnants suggesting that this chronic inflammatory process likely contributed to elevated SAA levels with resulting widespread amyloid deposition.

**Note:** Opinions, interpretations, conclusions, and recommendations are those of the author and are not necessarily endorsed by the U.S. Army.

Research involving this marmoset was conducted in compliance with the Animal Welfare Act and other federal statutes and regulations relating to animals and experiments involving animals and adheres to principles stated in the Guide for the Care and Use of Laboratory Animals, National Research Council, 2011. This research was conducted under an Institutional Animal Care and Use Committee (IACUC) approved protocol. The facility where this research was conducted is fully accredited by the Association for Assessment and Accreditation of Laboratory Animal Care International.

**JPC Diagnosis:** 1. Jejunum: Adenocarcinoma, mucinous type.
2. Jejunum, lamina propria: Amyloidosis, multifocal, moderate.
3. Jejunum: Ulcer, focal.

**Conference Comment:** The contributor provides an excellent discussion of intestinal adenocarcinomas in non-human primates, as well as the association between inflammation, cell damage and tumorigenesis. Conference participants discussed the pathogenesis of colorectal cancer in humans and nonhuman primates, noting that similar pathogeneses are proposed for both colorectal and small intestinal adenocarcinomas.[5] Colorectal adenocarcinomas account for 15% of all human cancer-related deaths in the United States, making it the second leading cause of cancer-related deaths, behind lung cancer.[7] While numerous infectious, genetic and environmental factors contribute to the development of gastrointestinal tumors, two distinct genetic pathways have been implicated with playing major roles in the development of intestinal adenocarcinomas: the Wnt signaling pathway (involving APC and β-catenin ) and the microsatellite instability pathway.[5,7] Wnt is a signaling pathway that regulates β-catenin. The APC (adenomatous polyposis coli gene) is a potent tumor suppressor that, under normal conditions, complexes with and phosphorylates β-catenin, marking it for ubiquitination and ultimately destruction. When Wnt is activated, the destruction complex between APC and β-catenin is deactivated, resulting in increased cytoplasmic β-catenin levels. As levels rise, β-catenin translocates into the nucleus, where it binds to TCF, a transcription factor that activates genes such as MYC and cyclin D1 that promote proliferation and increase cell cycle progression. Loss or mutation of APC can likewise lead to increased levels of β-catenin and cell cycle promotion and growth. This is followed by other mutations, such as activating mutations in KRAS, SMAD2 and SMAD4, which further promote cell proliferation and inhibit apoptosis. SMAD2 and SMAD4 are effectors of TGF-β signaling. TGF-β normally inhibits the cell cycle; hence, loss of these genes can allow unregulated cell proliferation. Additionally, mutations (chromosome deletions) in the tumor suppressor gene p53 also occur in later stages of tumor progression. Mutations such as these are due to chromosomal instability, which is a hallmark of APC/β-catenin pathway.[7] Another pathway implicated in the development of intestinal adenocarcinomas is microsatellite instability, which occurs when DNA mismatch repair is deficient, allowing mutations to accumulate in microsatellite repeats. Generally, microsatellites are in noncoding regions, but some microsatellite sequences are located in coding or promoter regions in genes that regulate cell growth (i.e. genes encoding type II TGF-β receptor and the proapoptotic protein Bax). Type II TGF-β mutations can contribute to uncontrolled cell growth, whereas loss of Bax may enhance the survival of neoplastic cells.[5,7]

In addition to playing a role in the Wnt signaling pathway, β-catenin activity also has effects on cell-cell organization. β -catenin normally binds to the cytoplasmic domain of type I cadherins, facilitating linkage to the actin cytoskeleton and contributing to normal cellular structure and organization. Perturbed interactions between β-catenin and type I cadherins destabilize cell-cell interactions and thus promote the loss of cell cohesion which may contribute to metastatic spread of neoplastic cells.[7]

**Contributing Institution**: U.S. Army Medical Research Institute of Infectious Diseases
Pathology Division
Fort Detrick, MD
http://www.usamriid.army.mil/

**References:**

1. Fenoglio-Preiser CM, Noffsinger AE, Stemmermann GN, Latz PE, Isaacson PG. *Gastrointestinal Pathology: An Atlas and Text*. 3rd ed. Philadelphia, PA: Lippincott Williams & Wilkins; 2008:471-494.
2. Head KW, Cullen JM, Dubielzig RR, Else RW, Misdorp W, Patnaik AK, et al. In: Schulman Y, ed. Histological Classification of Tumors of the Alimentary System of Domestic Animals, 2nd series, Vol. X. Washington, DC: Armed Forces Institute of Pathology/ American Registry of Pathology; 2003:89-94.
3. Johnson LD, Ausman LM, Sehgal PK, King, Jr. NW. A prospective study of the epidemiology of colitis and colon cancer in cotton-top tamarins (*Saguinus oedipus*). *Gastroenterology*. 1996:110:102-115.
4. Ludlage E, Murphy CL, Davern SM, Solomon A, Weiss DT, Glenn-Smith D, et al. Systemic AA amyloidosis in the common marmoset. *Vet Pathol*. 2005;42(2):117-124.
5. Miller AD, Kramer JA, Lin KC, Knight H, Martinot A, Mansfield KG. Small intestinal adenocarcinoma in common marmosets (*Callithrix jacchus*). *Vet Pathol.* 2010;47(5):969-976.
6. Riddell RH, Petras RE, Williams GT, Sobin LH. In: Rosai J, ed. Atlas of Tumor Pathology: Tumors of the Intestines, 3rd series, Fascicle 32. Washington, DC. Armed Forces Institute of Pathology/ American Registry of Pathology. 2002:189-194.
7. Turner JR. The gastrointestinal tract. In: Kumar V, Abbas AK, Fausto N, Aster JC, eds. *Robbins and Cotran Pathologic Basis of Disease*. 8th ed. Philadelphia, PA: Elsevier/Saunders; 2010:822-825.
8. Valverde CR, Tarara RP, Griffey SM, Roberts JA. Spontaneous intestinal adenocarcinoma in geriatric macaques (*Macaca* sp.). *Comp Med*. 2000;50(5): 540-544.

**Joint Pathology Center**
**Veterinary Pathology Services**

# WEDNESDAY SLIDE CONFERENCE 2012-2013

## Conference 6

**17 October 2012**

---

**CASE I:** Stanford 1 (JPC 4019361).

**Signalment:** 4-month-old, female, C57BL/6 mouse (*Mus muculus*).

**History:** This mouse received a single 400 mg/kg dose of acetaminophen (suspension in PBS) by oral gavage. The mouse was sacrificed 24 hours after.

**Gross Pathology:** This mouse is presented alive in good body condition. There is mild, diffuse, red and tan mottling of the liver. All other organs and tissues are within normal gross limits.

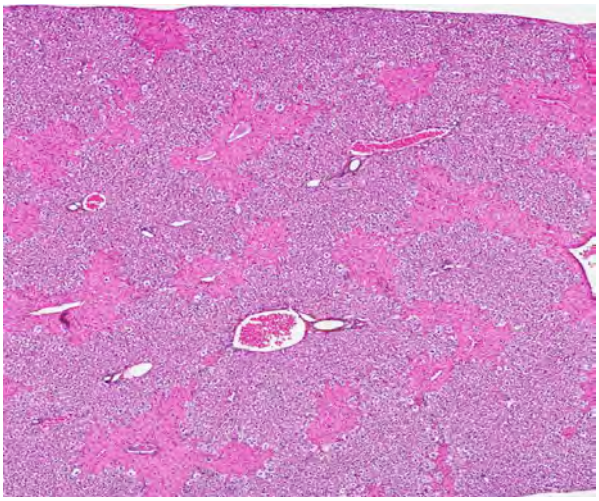

*1-1. Liver, mouse: A reticular pattern of eosinophilic coagulative necrosis surrounds centrilobular veins diffusely throughout the section. (HE 33X)*

**Histopathologic Description:** Multiple sections of liver are examined, revealing moderate acute hepatocellular necrosis of hepatocytes around central veins (centrilobular necrosis; zone III necrosis). The necrosis is coagulative in nature, characterized by hypereosinophilia and swelling of affected hepatocytes with karyolysis and rarely pyknosis and/or karyorrhexis. Rare scattered individual hepatocytes throughout the liver are condensed, hypereosinophilic, round with absent nuclei (interpreted as apoptosis; Councilman bodies). Diffusely, remaining hepatocytes in other areas/zones are mildly swollen due to intracellular accumulation of small to moderate amounts of small- to medium-sized, clear, round vacuoles (interpreted as microvesicular lipid droplets).

**Contributor's Morphologic Diagnosis:** 1. Liver, centrilobular necrosis, diffuse, moderate, acute.
2. Liver, microvesicular hepatic lipidosis, diffuse, mild.

**Contributor's Comment:** Acetaminophen (APAP; paracetamol) is a nonprescription drug used in humans. APAP is an aniline analgesic, and at therapeutic doses (500-1000 mg per human tid/qid), it has similar analgesic and antipyretic effects as ibuprofen and aspirin.[2,3] However, it is not classified as a NSAID anti-inflammatory agent because it is a weak COX inhibitor.[2,3]

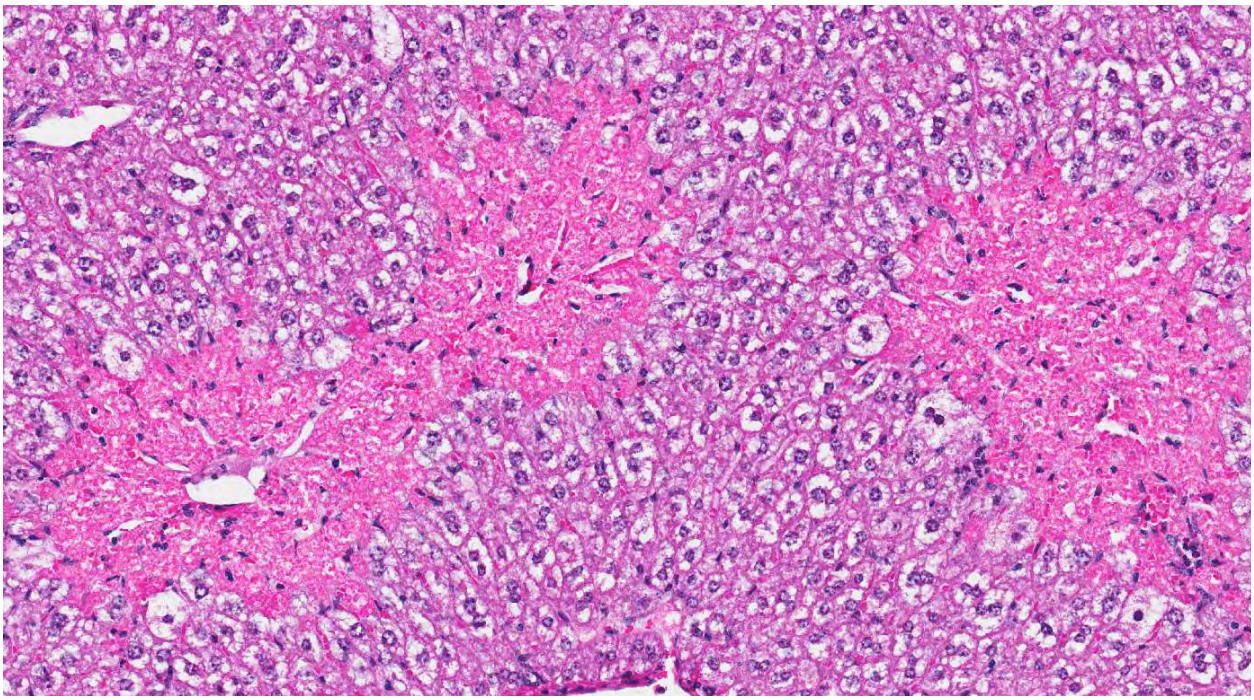

*1-2. Liver, mouse: Higher magnification of a focus of centrilobular necrosis characterized by maintenance of hepatic architecture granular eosinophilic cytoplasm, and hypertrophy of Kupffer and endothelial cell nuclei. (HE 164X)*

In most mammalian species (including humans, mice and dogs), the biotransformation of APAP involves conjugation with glucuronic acid or sulfate in the liver, which are subsequently excreted by urinary system.[1,2,3,4,7] A small amount of APAP is metabolized by the P-450 (CYP) system to the reactive metabolite N-acetyl –*p*-benzoquinone imine (NAPQI) in centrilobular zone hepatocytes, which is subsequently scavenged by glutathione.[2,3,4,5,6]

APAP toxicity manifests primarily as centrilobular hepatic necrosis that can lead to acute liver failure. In humans, a single or accumulative daily toxic dose is usually >15-25 g.[2,3,4] The mechanism of APAP hepatotoxicity is as follows:[2,3,5,6]

1. At toxic doses, increased metabolism of APAP by the P-450 (CYP) system leads to higher concentrations of NAPQI formation in centrilobular zone hepatocytes.
2. Higher concentrations of NAPQI deplete glutathione concentrations in centrilobular zone hepatocytes, leading to increased formation of reactive oxygen and nitrogen species.
3. Increased oxidative stress in centrilobular zone hepatocytes results in alterations in calcium homeostasis and initiation of mitochondrial permeability transition.
4. Loss of mitochondrial membrane potential in mitochondria of centrilobular zone hepatocytes leads to loss of ATP synthesis subsequent necrosis.

Antidotes that can prevent or ameliorate APAP toxicity aim to prevent the loss/promote the synthesis of glutathione, such as with cysteine and methionine administration.[2,3,4]

Cats are more sensitive to APAP toxicity and have a different pattern of APAP toxicity due to a species deficiency in glucuronyl transferase, resulting in relatively higher conversion rates of APAP to the reactive NAPQI metabolite.[1,7] In addition to depleting glutathione in centrilobular hepatocytes, NAPQI can also deplete glutathione in erythrocytes, leading to methemoglobinemia, Heinz body hemolytic anemia, and methemoglobinuria.[1,7]

Currently, APAP toxicity is the leading cause of liver failure in humans in the US and UK. Since APAP biotransformation and toxicity is similar between humans and mice, this makes mice an attractive and clinically relevant animal model for research into acetaminophen hepatotoxicity and other toxicities leading to centrilobular necrosis of the liver via the P-450 (CYP) system.[2,4]

**JPC Diagnosis:** Liver, centrilobular hepatocytes: Necrosis, coagulative, diffuse.

**Conference Comment:** The contributor provided a very good summary of acetominophen (APAP;

paracetamol) toxicity. During the discussion of this case, the moderator stressed the importance of phase 1 and phase 2 drug metabolism. Xenobiotics (chemicals not normally found or expected to be in the body) can undergo metabolism via various pathways. with the ultimate endpoint being excretion of water soluable metabolites through urine or bile. Many xenobiotic drugs are lipid-soluble and therefore pose a challenge to such excretion. Thus, a critical step in xenobiotic metabolism is the formation of water-soluble metabolites. Phase 1 drug metabolism includes oxidation, reduction and hydrolysis by various enzyme systems. If the resulting compound is sufficiently water soluble, then it is excreted via the kidneys or bile; however, if phase 1 does not render the drug excretable, it undergoes phase 2 metabolism. Phase 2 metabolism involves conjugation with ionized groups to significantly increase its water solubility and thus further enhance its excretion. Examples of phase 2 conjugation reactions include glucuronidation, sulphation, acetylation ad methylation.[8]

Drug metabolism occurs at several sites, including liver, intestines, lung, kidney, and plasma with the liver being the primary site. The liver contains a realtively large percentage of the body's metabolizing enzymes, most importantly a group of proteins known as cytochrome P450 mixed function oxidases. These enzymes are found within microsomes in the smooth endoplasmic reticulum of centrilobular hepatocytes. The most common reaction catalyzed by the cytochrome P450 enzymes is a mono-oxygenase reaction in which a molecule of oxygen ($O_2$) is split, with one oxygen atom oxidizing the xenobiotic and reduction of the other oxygen atom to produce a molecule of water. This oxidation-reduction reaction is responsible for the metabolism of a variety of drugs, to include paracetamol. Cytochrome P450 enzymes also catalyze reduction reactions to metabolize drugs such as prednisone, warfarin, and halothane. The third type of phase 1 metabolism reaction is hydrolysis, which is catalyzed by esterases and amidases (which also occur in hepatocytes and other extrahepatic sites, including plasma).[8]

Of the phase 2 reactions, glucuronidation and sulphation play a major role in the metabolism of paracetamol, with approximately 40% of the drug undergoing each reaction. As the contributor states, a small amount of paracetamol undergoes phase 1 N-hydroxylation which results in the toxic product N-acetyl-p-amino-benzoquinoneimine which is normally further metabolized (conjugated) by glutathione.[8]

Further discussion on this case centered on the use of severity modifiers ("mild," "moderate," "severe") to quantify the extent of necrosis, which can be important in a case such as this in which there is a dose-dependent response. Toxicologic pathologists often use such modifiers for quantification; however, this terminology is not traditionally used in diagnostic pathology at the AFIP/JPC, with the reasoning that necrosis in itself cannot be "mild" nor "severe".

**Contributing Institution:** Veterinary Services Center, Department of Comparative Medicine, Stanford School of Medicine (http://med.stanford.edu/compmed/)

**References:**

1. Court MH, Greenblatt DJ. Molecular basis for deficient acetaminophen glucuronidation in cats. *Biochem Pharmacol*. 1997;53:1041-1047.
2. Hinson JA, Roberts DW, James LP. Mechanisms of acetaminophen-induced liver necrosis. *Handb Exp Pharmacol*. 2010;196:369-405.
3. James LP, Mayeux PR, Hinson JA. Acetaminophen hepatotoxicity. *Drug Metab Disposition*. 2003;31:1499-1506.
4. Jaschke H, McGill MR, Williams CD, et al. Current issues with acetaminophen hepatotoxicity – a clinically relevant model to test the efficacy of natural products. *Life Sciences*. 2011;88:737-745.
5. Kumar V, Abbas AK, Fausto N. Cellular adaption, cell injury, and cell death. In: Kumar V, Abbas AK, Fausto N, eds. *Robbins and Coltran Pathologic Basis of Disease*. 7th ed. Philadelphia, PA: Elsevier Saunders; 2005:25-26.
6. Maitra A, Kumar V. Environmental and nutritional pathology. In: Kumar V, Abbas AK, Fausto N, eds. *Robbins and Coltran Pathologic Basis of Disease*. 7th ed. Philadelphia, PA: Elsevier Saunders; 2005:424.
7. Savides MC, Oehme FW, Nash SL, et al. The toxicity and biotransformation of single doses of acetaminophen in dogs and cats. *Toxicol Appl Pharmacol.* 1984;74:26-34.
8. Schonborn JL, Gwinnutt C. The role of the liver in drug metabolism. Anesthesia tutorial of the week 179. *ATOTW.* 2010(179):1-6. http://www.aagbi.org/sites/default/files/179-The-role-of-the-liver-in-drug-metabolism.pdf. Accessed 18 October 2012.

**CASE II:** 12-661 3 9 (JPC 4019358).

**Signalment:** 8-month-old, intact female, mouse, *Mus musculus*, B6.Cg-Tg (APPSwFlLon,PSEN1*M146L*L286V)6799Vas/Mmjax.

**History:** The goal of this experiment was to test the efficacy of a novel compound. This mouse was in the control group and was administered the vehicle without the compound by subcutaneous injection. Mice were sacrificed at the end of the study and tissues were collected to assess the effect of the compound by histopathology and other methods.

**Gross Pathology:** Complete necropsies were performed and no gross lesions were observed.

**Histopathologic Description:** Coronal sections of the head are provided, and include sections of the brain at the level of the cerebral cortex, hippocampus, thalamus, midbrain, and pituitary gland, and at the level of the cerebellum and brainstem. Multifocally in the neuropil of the cerebral cortex, hippocampus, thalamus, and midbrain, there are numerous aggregates of a basophilic, amorphous to finely fibrillar material, which is often surrounded by a rim of decreased staining intensity of the neuropil. On Congo Red stain, this material is congophilic and shows green birefringence when observed with polarized light.

**Contributor's Morphologic Diagnosis:** Brain, cerebral cortex, hippocampus, thalamus, and midbrain: Abundant neuritic plaques with amyloid core, multifocal.

**Contributor's Comment:** The mouse strain B6.Cg-Tg(APPSwFlLon,PSEN1*M146L*L286V)6799Vas/Mmjax is also known by the common names 5XFAD and Tg6799. This strain overexpresses two mutant human genes on a C57BL/6 and SJL background. The first gene, APP695, contains four mutations associated with familial Alzheimer's disease (FAD): the Swedish (K670N, M671L), Florida (I716V), and London (V717I) mutations. The second gene, PS1, contains two mutations also associated with FAD: M146L and L286V. Expression of both transgenes is regulated by neural-specific elements of the mouse Thy1 promoter

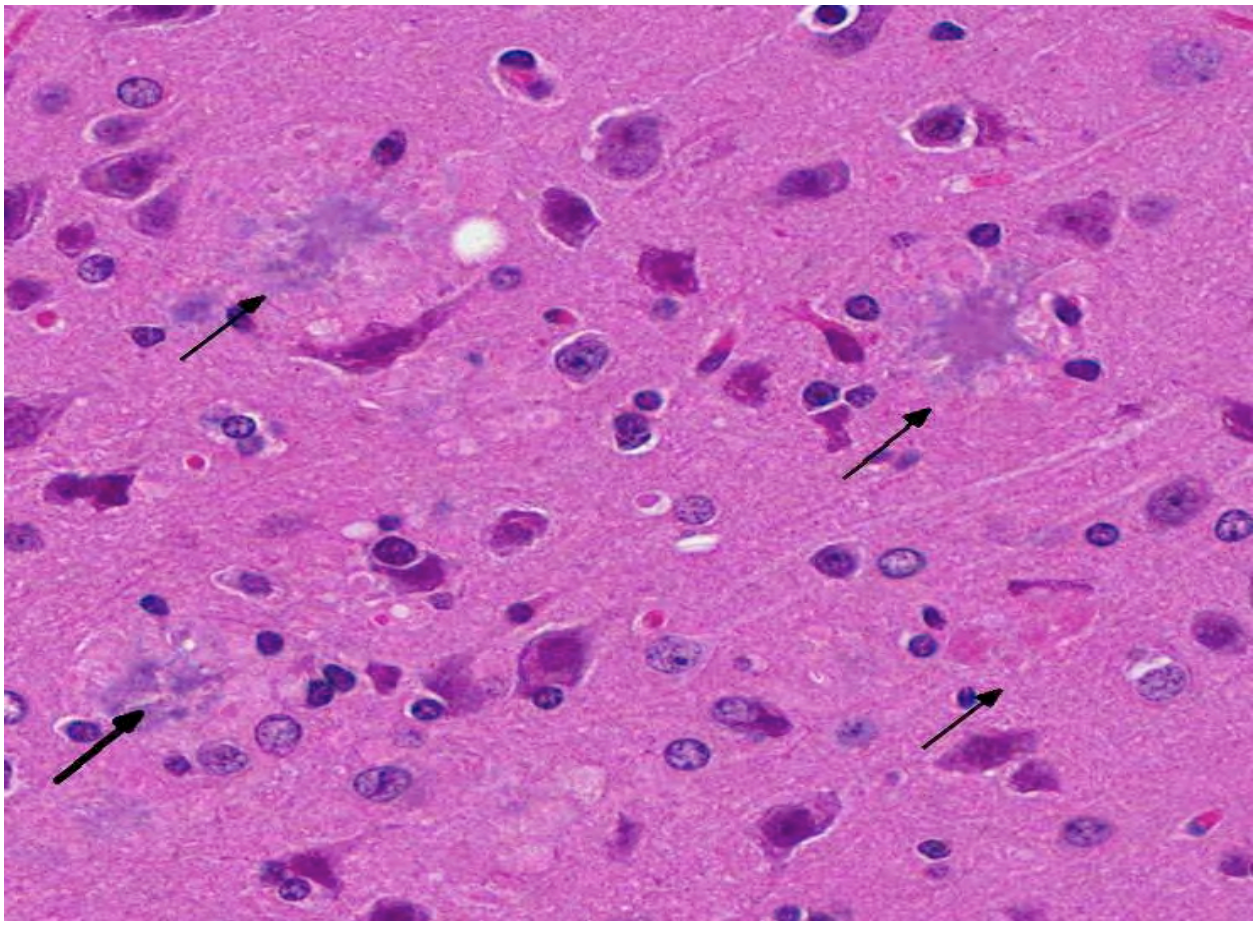

*2-1. Brain, cerebrum, superficial cortex, B6.Cg-Tg(APPSwFlLon,PSEN1*M146L*L286V)6799Vas/Mmjax mouse: There are numerous well-formed neuritic plaques (arrows) composed of beta-amyloid. (HE 230X)*

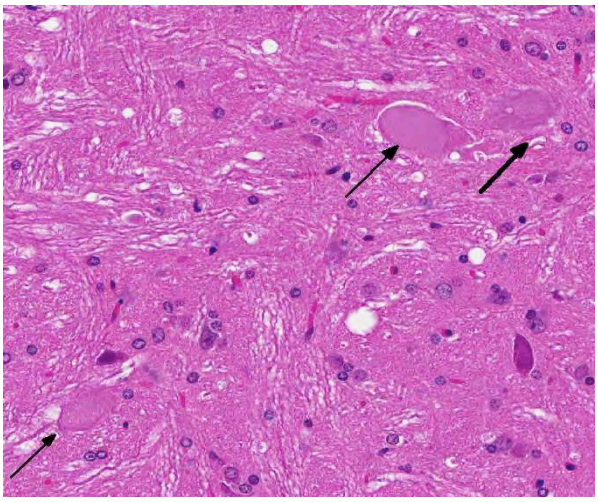

*2-2. Brain, cerebrum, superficial cortex, B6.Cg-Tg (APPSwFlLon,PSEN1*M146L*L286V)6799Vas/Mmjax mouse: Multifocally, neurons within the brainstem nuclei exhibit central chromatolysis (arrows), neuronal cell body swelling, and axonal dilation (spheroid formation). (HE 320X)*

to drive overexpression in the brain. This strain rapidly recapitulates the amyloid pathology of Alzheimer's disease (AD), beginning at 2 months of age and characterized by the formation of a heavy burden of neuritic plaques.[1] Neuritic plaques (also called senile plaques) are focal round collections of dilated and tortuous neurites that surround an amyloid core that can be stained with Congo Red.[2] Neuritic plaques are often surrounded by a clear halo and by reactive astrocytes and microglial cells. In humans, these plaques range in size from 20 to 200 µm and are predominantly observed in the hippocampus, amygdala, and neocortex, with relative sparing of primary motor and sensitive cortices.

The main component of the amyloid core is A, a peptide derived from cleavage of the larger protein Amyloid Precursor Protein (APP), a cell surface protein that may function as a receptor.[2] The A peptides readily aggregate and can be directly neurotoxic and can result in synaptic dysfunction and an inflammatory response. Other proteins that present in plaques in smaller amounts include complement proteins, pro-inflammatory cytokines, 1-antichymotrypsin, and apolipoproteins. Findings in individuals affected by the familiar form of AD have supported the hypothesis that the generation of A is a critical step in the initiation of the disease. Some patients with familial AD have point mutations of the APP gene. Two other commonly affected loci are in the Presenilin 1 and 2 (PS1, PS2), which lead to a gain of function of the -secretase complex, which is involved in the cleavage of APP into A.

The other main morphologic change in AD is the formation of neurofibrillary tangles, which are composed of bundles of filaments in the cytoplasm of neurons.[2] These are seen as basophilic structures by H&E staining, and can be demonstrated by silver stain methods such as Bielschowsky. A major component of these filaments is a hyperphosphorylated form of the protein tau. Tangles are not specific to AD, as they can be found in other diseases. There was no evidence of neurofibrillary tangles in the brain of these mice on H&E and Bielschowsky stains.

**JPC Diagnosis:** 1. Cerebrum, hippocampus, amygdaloid nucleus and brainstem: Neuritic plaques, numerous, diffuse, with gliosis and neuronal loss.
2. Brainstem nuclei and neurons: Chromatolysis, multifocal, marked, with spheroid formation.

**Conference Comment:** The contributor provided a thorough description of the components of the senile (neuritic) plaques and neurofibrillary tangles (NFT), the two microscopic hallmarks of Alzheimer's disease first described by Alois Alzheimer in 1906.[3] Senile plaques and NFTs represent two manifestations of abnormally folded A proteins.[1] Normally the body prevents such misfolded proteins from depositing in tissues and interfering with normal functions via several mechanisms collectively known as the "unfolded protein response" (UPR). The UPR activates signaling pathways that: 1) increase chaperone production in an attempt to repair, refold, and return proteins to normal; 2) slow protein translation; and 3) enhance the ubiquitination and proteolysis of misfolded proteins via the ubiquitin-proteasome pathway.[1,4,5] If the UPR is insufficient, abnormal proteins may be removed by autophagy, the major degradative pathway for intracellular components. Failure of autophagy has been implicated in the pathogenesis of several neurodegenerative diseases, including Alzheimer's disease.[5]

Three autophagic mechanisms are described in mammalian cells: chaperone-mediated autophagy, microautophagy, and macroautophagy, all which result in the lysosomal degradation of targeted cellular components. In chaperone-mediated autophagy, cytoplasmic proteins exposing a KFERQ-like motif are targeted directly to the lysosomes for degradation. Microautophagy involves the invagination of the lysosomal membrane to nonselectively engulf and degrade small portions of the cytoplasm. Macroautophagy is the best characterized mechanism of autophagy; thus, it is often referred to as simply "autophagy."

Unlike chaperone-mediated autophagy and microautophagy, macroautophagy relies on the *de novo* synthesis of double membrane-bound autophagosomes. The major upstream inhibitor of macroautophagy initiation is the mammalian target of rapamycin complex 1 (mTORC1), which regulates several cellular

processes, to include autophagy, cell growth and proliferation, and protein synthesis. Various cell signaling pathways converge upon mTORC1; for instance, in response to insulin and growth factors, the class I phosphatidylinositol-3-kinase (PI3K)/Akt signaling pathway activates mTORC1 and thus suppresses autophagy. Conversely, energy depletion signals through the liver kinase B1 (LKB1)/AMP-activated protein kinase (AMPK) pathway to inhibit mTORC1, and thereby activate autophagy.

When mTORC1 is inhibited, autophagy-related (Atg) proteins coordinate a series of events that results in the formation of an autophagosome (i.e., vesicle nucleation, vesicle elongation, docking and fusion, and vesicle maturation). This series begins with the formation of a phagophore (i.e., pre-autophagosomal structure) and progresses to the formation of a double membrane enclosed autophagosome, the outer membrane of which fuses with a lysosome or a late endosome to form an autolysosome or an amphisome, respectively. Acidic hydrolases digest material within the autolysosome or amphisome, after which the lysosome is restored.[5]

Current research strongly suggests the disruption of proteolysis within autolysosomes is the principle mechanism underlying autophagy failure in Alzheimer's disease. Various forms of autophagic vacuoles representing intermediate stages in autophagy (including autophagosomes, amphisomes, and autolysosomes) have been observed to accumulate in the brains of patients with Alzheimer's disease and other neurodegenerative diseases.[4,5] Interestingly, attempts to restore lysosomal proteolysis and enhance autophagy in mouse models of Alzheimer's disease have shown positive effects on neuronal function and cognitive performance.[5]

**Contributing Institution:** Tri-Institutional Laboratory of Comparative Pathology, Memorial Sloan-Kettering Cancer Center, Weill Cornell Medical College, and The Rockefeller University, New York, NY 10065.

**References:**

1. Frosch MP, Anthony DC, De Girolami U. The central nervous system. In: Kumar V, Abbas AK, Fausto N, Aster JC, eds. *Robbins and Cotran Pathologic Basis of Disease*. 8th ed. Philadelphia, PA: Saunders Elsevier; 2010:1279-1344.
2. Oakley H, Cole SL, Logan S, et al. Intraneuronal amyloid aggregates, neurodegeneration, and neuron loss in transgenic mice with five familial Alzheimer's disease mutations: potential factors in amyloid plaque formation. *J Neurosci*. 2006;26:10129-10140.
3. Gibbs G. Alois Alzheimer: The Man. http://www.unmc.edu/intmed/geriatrics/docs/alois_alzheimer.pdf Accessed 19 October 2012.
4. Levine B, Kroemer G. Autophagy in the pathogenesis of disease. *Cell.* 2008;132(1):27-42.
5. Nixon RA, Yang DS. Autophagy failure in Alzheimer's disease—Locating the Primary Defect. *Neurobiol Dis.* 2011; 43(1):38-45.

**CASE III:** C-16154-08 (JPC 3134053).

**Signalment:** 5-year-old, male/castrated, American Pit Bull Terrier, dog, *Canis familiaris*.

**History:** The dog had a two week history of listlessness and decreased appetite. When examined at the clinic, the animal was dehydrated, lethargic, showing neurological signs (standing in the corner staring at the wall) and had anisocoria. Pain was elicited on flexion and extension of the neck. An intracranial mass was suspected and the owners opted to euthanize the dog.

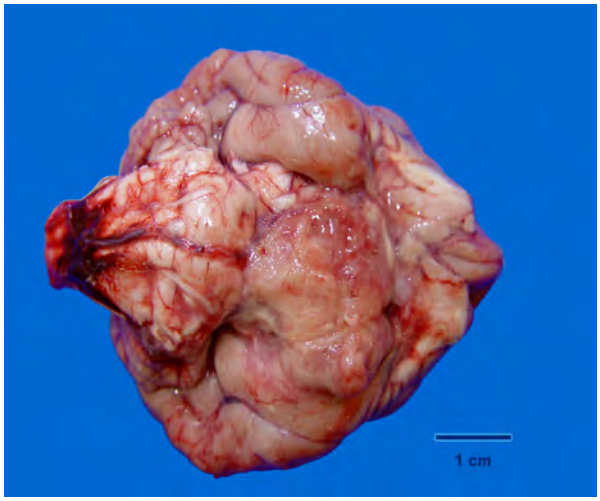


*3-1. Cerebrum, hypothalamus: A soft, pink, irregular mass measuring approximately 1 x 2 x 2 cm is present on the ventral surface of the brain, centered over the diencephalon slightly to the left of midline (image 1). (Photo courtesy of: Department of Pathology and Microbiology, Atlantic Veterinary College, University of Prince Edward Island, 550 University Avenue, Charlottetown, PE C1A 4P3, http://www.upei.ca/~avc/index.html)*

**Gross Pathologic Findings:** The carcass is in good body condition; significant changes are restricted to the brain/skull base. A soft, pink, irregular mass measuring approximately 1 x 2 x 2 cm is present on the ventral surface of the brain, centered over the diencephalon slightly to the left of midline. The mass extends caudally from the olfactory tract to the rostral margin of the pons. Laterally the mass abuts the piriform lobe on the right and covers half of the piriform lobe on the left. On cut section, the mass infiltrates and compresses the hypothalamus, thalamus, piriform lobe and the hippocampus. The underlying floor of the skull appears irregular, thickened, and slightly yellow; the pituitary gland could not be identified.

**Laboratory Results:** Paraffin embedded tissue sections were sent to the Diagnostic Center for Population and Animal Health (Michigan State University). Sections were evaluated for Alpha-fetoprotein immunohistochemical markers. Approximately 60-70 % of the atypical cell population had strong positive cytoplasmic labeling with Alpha-fetoprotein.

**Histopathologic Description:** A well-delineated, nonencapsulated, moderately cellular, multilobulated mass compresses and invades the neuropil of the thalamus, hypothalamus, hippocampus, piriform lobe, optic tract, and the pituitary gland (depending on the section). Three cell types comprise the mass. Nests and solid lobules of loosely packed neoplastic cells separated by fine collagenous septa predominate; these

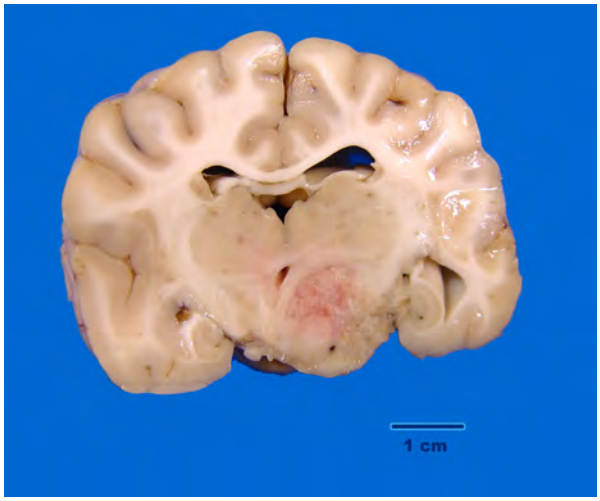


*3-2. On cut section, the mass infiltrates and compresses the hypothalamus, thalamus, piriform lobe and the hippocampus. (Photo courtesy of: Department of Pathology and Microbiology, Atlantic Veterinary College, University of Prince Edward Island, 550 University Avenue, Charlottetown, PE C1A 4P3, http://www.upei.ca/~avc/index.html)*

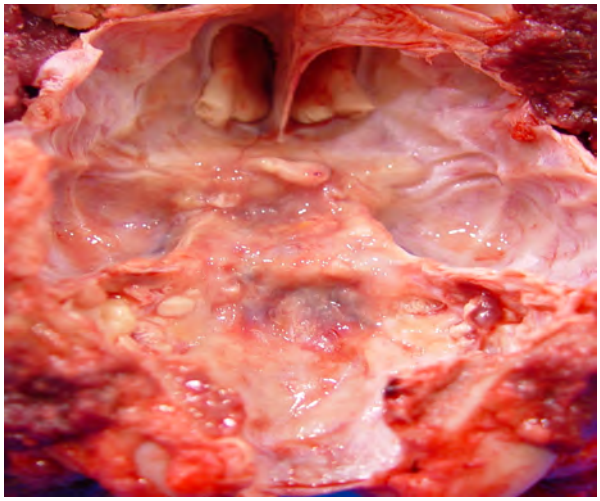

*3-3. The underlying floor of the skull appears irregular, thickened, and slightly yellow; the pituitary gland could not be identified. (Photo courtesy of: Department of Pathology and Microbiology, Atlantic Veterinary College, University of Prince Edward Island, 550 University Avenue, Charlottetown, PE C1A 4P3, http://www.upei.ca/~avc/index.html)*

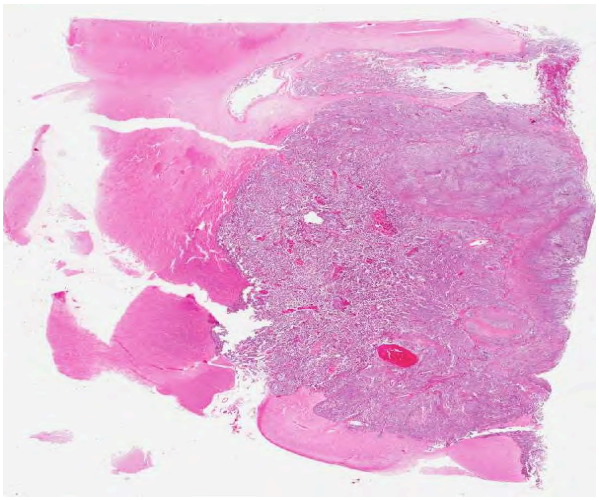

*3-4. Cerebrum, thalamus: A large well-demarcated densely cellular neoplasms compresses the thalamus and overlying cerebrum. (HE 20X)*

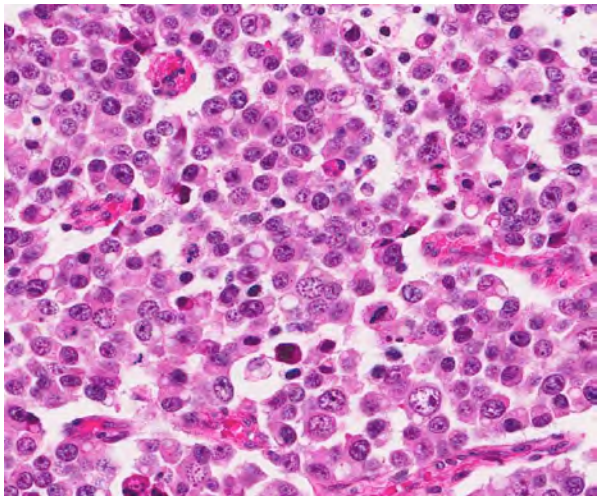

*3-5. Cerebrum, thalamus: The majority of the neoplasm is composed of round germ cells and are arranged in sheets and nests on a fine fibrovascular stroma. (HE 224X)*

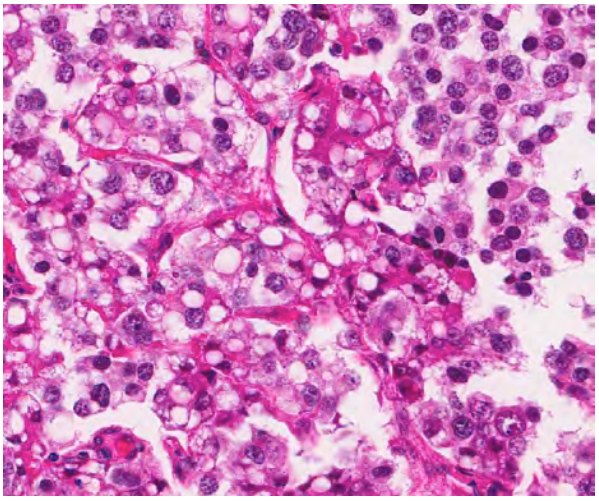

*3-6. Cerebrum, thalamus: A second, less common cell type, is similar to the neoplastic germ cells, but contains a single large clear vacuole. Rarely, these cells may exhibit squamous differentiation. (HE 260X)*

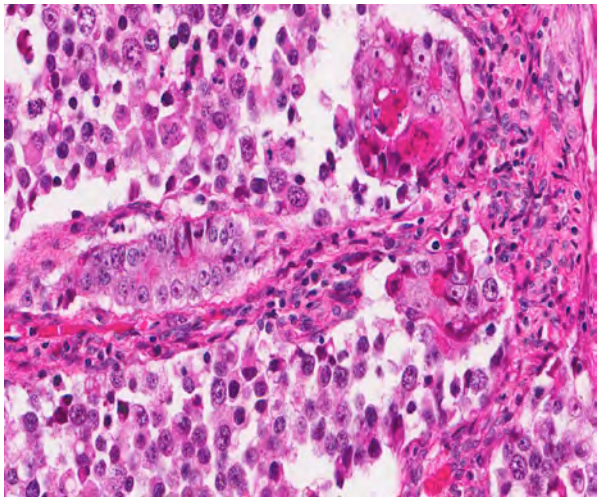

*3-7. Cerebrum, thalamus: Rare trabeculae of neoplastic cuboidal to columnar cells are scattered throughout the neoplasm, rarely forming acinar-like structures. (HE 260X)*

cells are round to polygonal with distinct cell margins, a scant to moderate amount of flocculent amphophilic cytoplasm and a central round nucleus with granular to coarsely clumped, often hyperchromatic, chromatin and an indistinct nucleolus. Scattered amongst these cells are discrete islands and trabeculae of large polygonal cells with moderate amounts of eosinophilic cytoplasm and a large oval vesicular nucleus with a single distinct nucleolus; these cells often contain discrete cytoplasmic vacuoles which displace the nucleus to the periphery or, less often, exhibit squamous differentiation. Rare aggregates of tubule-like structure lined by one to multiple layers of cuboidal to columnar epithelial cells with basal nuclei, granular chromatin and single to multiple nucleoli comprise the third population (not present in all slides). There is moderate anisocytosis and anisokaryosis. Mitoses, which are largely restricted to the round cells, average between 2 and 3 per HPF (40X). Small to moderate numbers of lymphocytes form multifocal aggregates within the supporting stroma, often surrounding blood vessels. Variably sized foci of necrosis and/or hemorrhage are scattered throughout the mass and rare mineral deposits and intravascular fibrin thrombi are noted.

**Contributor's Morphologic Diagnosis:** Malignant mixed germ cell tumor, brain (Canine suprasellar germ cell tumor).

**Contributor's Comment:** Tumors in the sellar region of the canine brain include pituitary tumors, craniopharyngioma, and suprasellar germ cell tumor.[8] Histological features in this case were not compatible with a pituitary tumor. Suprasellar germ cell tumors

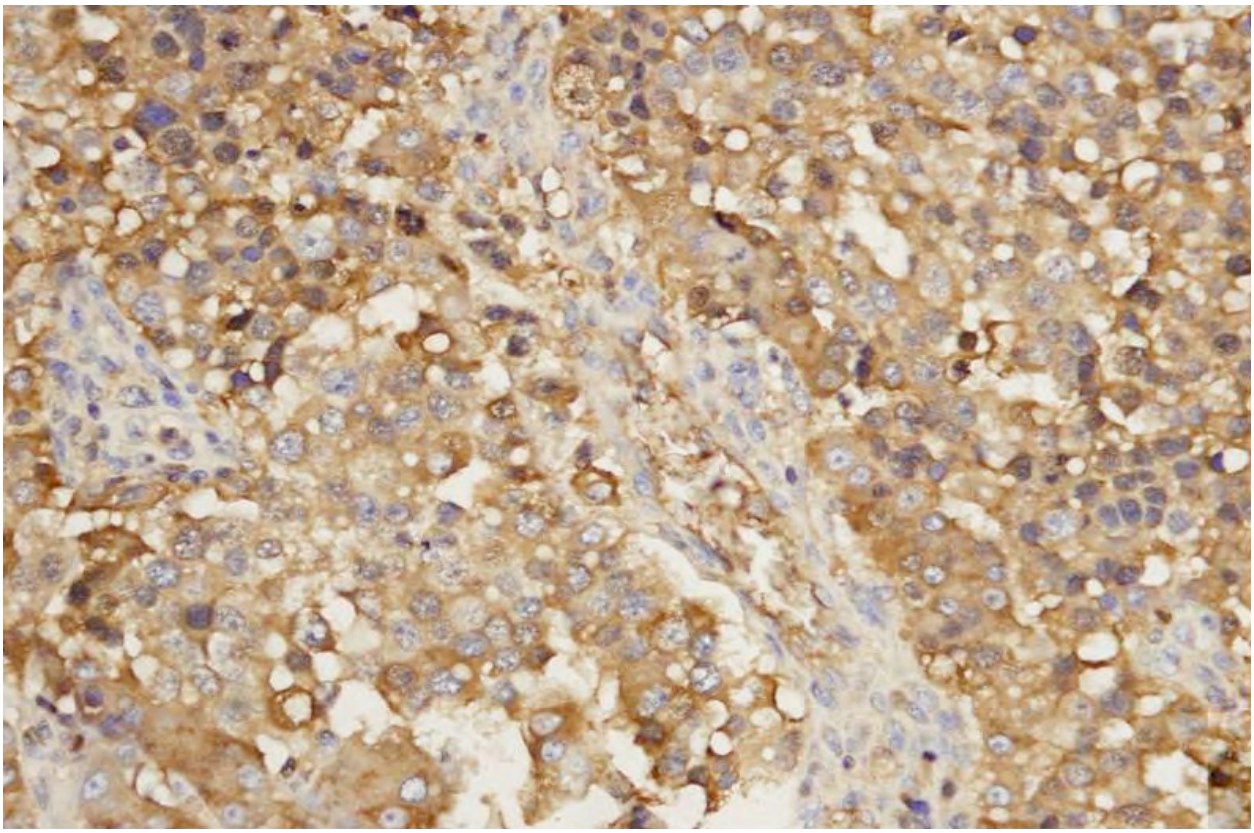

*3-8. Cerebrum, thalamus: Neoplastic cells show multifocal moderate to strong cytoplasmic positivity for alpha-fetoglobulin. (AFG 400X) (Photo courtesy of: Department of Pathology and Microbiology, Atlantic Veterinary College, University of Prince Edward Island, 550 University Avenue, Charlottetown, PE C1A 4P3, http://www.upei.ca/~avc/index.html)*

may be misclassified as craniopharyngioma, and this diagnosis was considered in this case.[6,14] A diagnostic feature of craniopharyngioma in humans is an epithelial component consisting of outer palisading columnar cells with central stellate cells resembling ameloblastoma; this characteristic was not observed in this mass.[10,14]

A diagnosis of suprasellar germ cell tumor was made based on three criteria: (1) midline suprasellar location, (2) presence within the tumor of several distinct cell types; one population resembling seminoma or dysgerminoma and others suggesting teratomatous differentiation into secretory glandular and squamous elements, and (3) positive staining for alpha-fetoprotein.[14] Alpha-fetoprotein is a commonly used marker for germ cells in human and has been shown to be a useful marker for canine intracranial germ cell tumors.[14]

Germ cell tumors most commonly occur in the ovaries and testes (dysgerminomas and seminomas respectively). Extragonadal germ cell tumors, with similar histology, are reported less commonly and typically occur on midline, affecting the mediastinum, brain, and coccyx in humans.[13] In dogs, these rare tumors have been reported in the brain, the eye, and the spinal cord.[5,10,11,12,14] Intracranial germ cell tumors tend to localize in the pineal and suprasellar regions in humans, while the suprasellar region is preferentially affected in dogs.[14] Suprasellar germ cell tumors have also been described in three lake whitefish (*Coregonus clupeaformis*).[9]

Presenting clinical signs in affected dogs include visual disturbance, pupil abnormality, lethargy, anorexia, and less often, signs of pituitary dysfunction.[10,12,14] Typically young adult dogs are affected and there is a possible breed predilection for the Doberman Pinscher.[14]

The pathogenesis of these tumors remains poorly understood, with the main question being the origin of the germ cells in the brain.[6] During embryonic development, progenitor germ cells originate in the epiblast. These germ cells then migrate to the caudal yolk sac endoderm and reach the gonadal ridge via the dorsal mesentery of the hindgut. Extragonadal germ cell tumors are presumed to arise from ectopic embryonic germ cells which may become displaced during development, survive physiologic dissolution, and undergo neoplastic transformation.[3,6]

**JPC Diagnosis:** Cerebrum: Suprasellar germ cell tumor.

**Conference Comment:** The contributor provided a very good summary of suprasellar germ cell tumors. In describing the key features of this tumor, the contributor noted the midline suprasellar location as one of three criteria used for diagnosis. "Suprasellar" refers to the location above the sella turcica, a bony complex in the basisphenoid formed by the tuberculae sellae, the hypophyseal fossa, and the dorsum sellae with its two clinoid processes.[3] The sella turcica houses the hypophysis. In dogs, this shallow fossa is lined by the endosteal layer of dura mater. The meningeal layer of the dura mater forms the diaphragm sellae, which extends partially over the dorsal aspect of the fossa to form an incomplete septum.[5]

Recently, a supracellar germ cell tumor was described in a 16-month-old Wagyu heifer calf adding to the list of species affected.[1] In the human literature, intracranial germ cell tumors have been divided into germinoma, teratoma, yolk sac tumor, embryonal carcinoma, and choriocarcinoma. Mixed germ cell tumors contain elements from more than one of these types.[2]

Conference participants noted there was significant slide variation, with some slides having polygonal neoplastic cells forming tubular structures, while others lacked these features. In addition, due to slide variation, the participants chose the generic location "cerebrum" for the morphologic diagnosis, as specimens varied in their anatomic location.

**Contributing Institution:** Department of Pathology and Microbiology, Atlantic Veterinary College, University of Prince Edward Island, 550 University Avenue, Charlottetown, PE C1A 4P3, http://www.upei.ca/~avc/index.html.

**References:**

1. Brooks AN, Brooks KN, Oglesbee MJ. A suprasellar germ cell tumor in a 16-month-old Wagyu heifer calf. *J Vet Diag Invest.* 2012;24:587-590.
2. Burger PC, Scheithauer BW. *Tumors of the Central Nervous System.*Third series, Fascicle 10. Washington, DC: Armed Forces Institute of Pathology/ American Registry of Pathology. 1993:251-257.
3. Echevarria ME, Fangusaro J, Goldman S. Pediatric central nervous system germ cell tumors: a review. *The Oncologist*. 13: 690 -699, 2008.
4. Evans HE. The skull. In: Evans HE, ed. *Miller's Anatomy of the Dog.* Philadelphia, PA: WB Saunders Company; 1993:139.
5. Ferreira AJA, Peleteiro MC, Carvalho T, et al. Mixed germ cell tumor of the spinal cord in a young dog. *J Small Anim Pract*. 2003;44:81-84.
6. Hoei-Hansen CE, Sehested A, Juhler M, et al. New evidence for the origin of intracranial germ cell tumors from primordial germ cells: expression of pluripotency and cell differentiation markers. *J Pathol*. 2006;209:25–33.
7. Hullinger RL. The endocrine system. In: Evans HE, ed. *Miller's Anatomy of the Dog.* Philadelphia, PA: WB Saunders Company; 1993:139, 561.
8. Maxie MG, Youseff S. Neoplastic diseases of the nervous system. In: Maxie MG, ed. *Jubb, Kennedy and Palmer's Pathology of Domestic Animals.* Vol. 1. 5th ed. Philadelphia, PA: Saunders Elsevier Limited; 2007:446-457.
9. Mikaelian I, Lapointe J-M , de Lafontaine Y, et al. Suprasellar germinoma in three lake whitefish (*Coregonus clupeaformis*). *Acta Neuropathol*. 2000;100: 228-232.
10. Nyska A, Harmelin A, Baneth G, et al. Suprasellar differentiated germ cell tumor in a male dog. *J Vet Diagn Invest*. 1993;5:462-467.
11. Patterson-Kane JC, Schulman FY, Santiago N, et al. Mixed germ cell tumor in the eye of a dog. *Vet Pathol.* 2001;38:712-714.
12. Rech RR, de Souza SF, da Silva MC, et al. Suprasellar germ cell tumor in a dog. *Ciencia Rural.* 2008;38:830-832.
13. Schneider DT, Schuster AE, Fritsch MK, et al. Multipoint imprinting analysis indicates a common precursor cell for gonadal and nongonadal pediatric germ cell tumors. *Cancer Research*. 2001;61:7268–7276.
14. Valentine BA, Summers BA, de Lahunta A, et al. Suprasellar germ cell tumors in the dog: a report of five cases and review of the literature. *Acta Neuropathol.* 1988;76:94-100.

**CASE IV:** K09-038255 (JPC 3167327).

**Signalment:** 4.5-year-old spayed female domestic ferret, *Mustela putorius furo.*

**History:** The ferret was presented as an emergency to a local veterinary clinic for dyspnea. The ferret was treated with intravenous fluids, Baytril, Cefazolin, Amoxicillin and oxygen, then euthanized after review of thoracic radiographs.

**Gross Pathologic Findings:** All lung lobes were similarly affected: pale, mottled, with a firm texture, and patchy red areas on cut section. Mediastinal lymph nodes were enlarged.

**Laboratory Results**: PCR for influenza virus was negative.

**Histopathologic Description:** Pulmonary architecture is distorted by locally extensive, alveolar infiltrates of eosinophilic foamy material, which on higher power examination is composed of myriad approximately 4-10 micron diameter discrete round or oval structures with thin eosinophilic outlines (which stain with Gomori's methenamine silver) and unstained content except for one or more tiny 0.5 micron central basophilic bodies. These infiltrates are located predominantly in subpleural, peribronchiolar, perivascular and intramural vascular locations. Surrounding these areas is a more generalized alveolar infiltrate of large foamy macrophages, many of which contain similar organisms, admixed with moderate numbers of multinucleated giant cells, and lesser numbers of lymphocytes, plasma cells, neutrophils, with alveolar edema and focal fibrin exudation.

Similar infiltrates were present in the enlarged mediastinal lymph nodes and spleen (sections not provided).

**Contributor's Morphologic Diagnosis:** Severe, subacute granulomatous interstitial pneumonia with infiltrates of organisms morphologically consistent with *Pneumocystis.*

**Contributor's Comment:** *Pneumocystis* spp. are inhabitants of the lung of various domestic and laboratory animal species including ferrets, pigs, foals, dogs, rats, mice, non-human primates as well as humans.[1,2] Originally thought to be a protozoan, *Pneumocystis* is now classified as a fungus, likely an

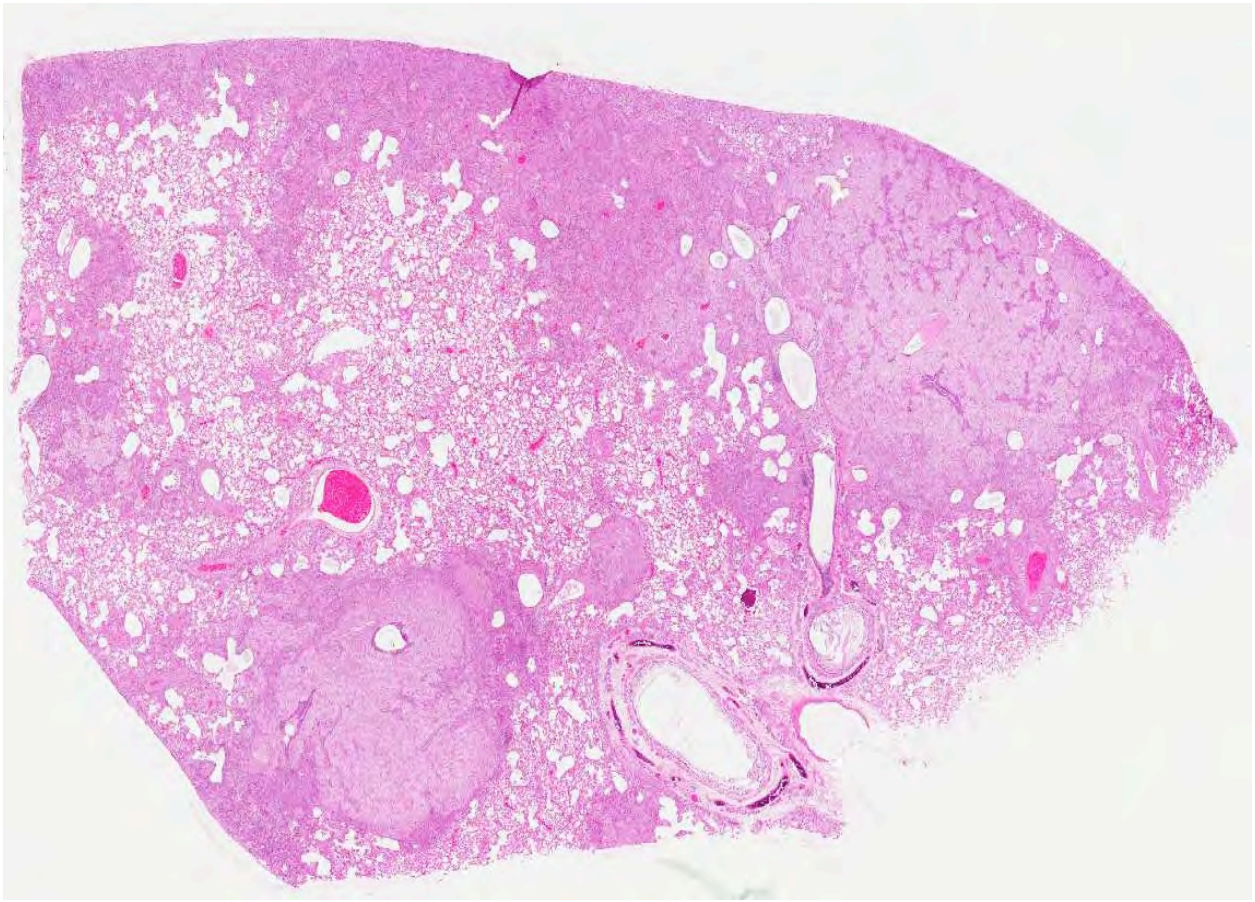

*4-1. Lung, ferret: Approximately 50% of the alveoli, especially in subpleural areas, are filled with exudate. (HE 4X)*

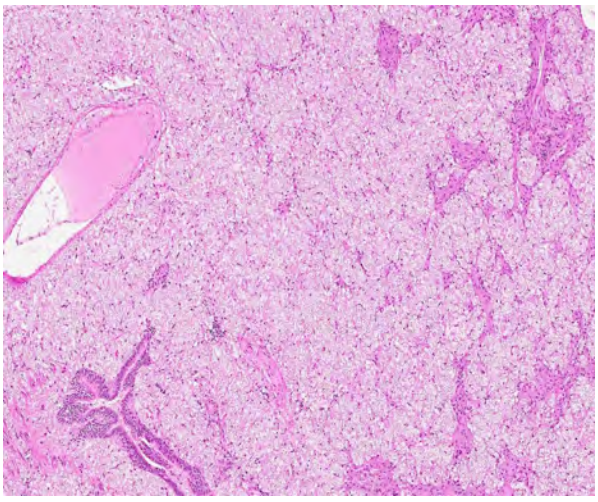

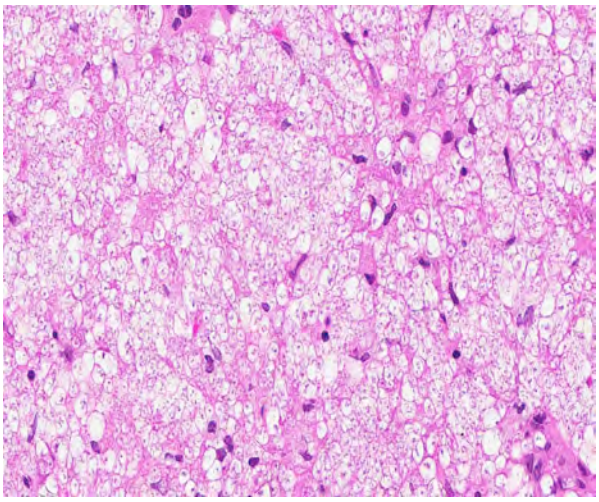

*4-2, 4-3. Lung, ferret: Alveoli are filled with a flocculent exudate comprised of low numbers of macrophages and neutrophils and numerous intra- and extracellular fungal organisms consistent with Pneumocystis carinii. (HE 60X, 300X)*

early divergent lineage of the genus *Ascomycetes*.[1] The organism is considered an opportunistic pathogen, and development of clinical disease usually requires immunosuppression, either by concurrent disease or the use of immunosuppressive drug therapy.

There are significant genomic, karyotypic, isoenzymatic and antigenic differences among the *Pneumocystis* species isolated from different animal hosts, and there appears to be close hostspecificity.[1] The taxonomy of these organisms has undergone significant changes in the last decade, and the organisms originally classified as *Pneumocystis carinii* include various divergent strains now recognized as unique species, including *Pneumocystis jirovecii* which colonizes humans, *P. wakefieldiae* which together with the original *P. carinii* has been found in the Norway rat, *P. murina* in laboratory mice and *P. oryctolagi* in Old World rabbits. Genetically distinct populations of *Pneumocystis* have been also been recognized in the ferret, and may represent multiple separate species, although these have not yet been completely characterized.[6]

*Pneumocystis* infection is thought to be maintained in host populations by airborne circulation, as the organism is capable of at least transiently colonizing and replicating in the lung of immunocompetent hosts, and can be spread between healthy hosts as well as to immunocompromised susceptible hosts.[1] In the lung, life cycle stages recognized include a 1-4 micron diameter, thin-walled vegetative or trophic form, which attaches to type 1 alveolar epithelial cells and appears to develop through three consecutive sporocyte stages to produce a 3-8 micron diameter, thick-walled cyst form, in which multiple nuclear divisions lead to the formation of eight intracystic spores.[1] These intracystic bodies are released and presumably develop into trophic forms. (Note that the names of these stages still reflect the original classification of these organisms as protozoa; appropriate renaming of these stages as fungal developmental stages awaits further elucidation of the sexual stages of the cycle). Binding to type I pneumocytes as well as to macrophages is mediated by the cell wall major surface glycoprotein A. Both macrophages and cell-mediated immunity are important for control of infection, and development of clinical disease implies impairment of either macrophage function or cell-mediated immunity.[2]

The ferret has been used as an animal model of *Pneumocystis* pneumonia induced by corticosteroid administration, while development of disease in pet ferrets is recognized as a potential complication of long-term corticosteroid therapy or hyperadrenocorticism.[3] In this case, no predisposing condition was identified. Both adrenal glands were histologically unremarkable (although the right adrenal had a small intracortical cyst). Extrapulmonary localization of the organisms was apparent in this case, and has been reported in liver and kidney from 10% of experimentally immunosuppressed ferrets.[6]

**JPC Diagnosis:** Lung: Pneumonia, interstitial, histiocytic and necrotizing, diffuse, marked, with numerous intra-alveolar fungal cysts consistent with *Pneumocystis carinii.*

**Conference Comment:** The contributor provided a good summary of disease associated with *Pneumocystis* species. As stated, *Pneumocystis* can affect several species of animals, usually causing disease only in immunocompromised hosts. Interestingly, however, studies have linked *Pneumocystis carinii* to infectious interstitial pneumonia (IIP), a common, transient, usually mild

disease of immunocompetent laboratory rats that has been, until recently, attributed to an alleged virus referred to as rat respiratory virus (RRV). The distinctive lung lesions (lymphohistiocytic interstitial pneumonia with perivascular lymphocytic cuffs) associated with IIP, first described in the mid-1990s, led researchers to suspect a viral cause. Subsequent studies showed the presence of a virus that could be propagated in cell culture; this virus was referred to as RRV. However, the RRV antibody assays did not correspond to the IIP status of colonies as determined by histopathology, leaving histopathology as the only reliable diagnostic method for rat colony surveillance. Since then, several investigations have demonstrated a cause and effect relationship between *Pneumocystis carinii* and IIP in immunocompetent rat colonies using PCR and IFA, as well as histopathology. These studies also found that the concentration of *Pneumocystis carinii* in the lung corresponded with the histologic severity of IIP. Furthermore, clearance of *Pneumocystis carinii* lung infection via a humoral response corresponded with resolution of pneumonia. *Pneumocystis carinii* is the most common *Pneumocystis* species found in rats, occurring much more frequently than *Pneumocystis wakefieldiae*. *Pneumocystis wakefieldiae* was not found to be associated with IIP.[4]

**Contributing Institution:** Animal Health Laboratory, University of Guelph, Guelph, Ontario, Canada
http://ahl.uoguelph.ca

**References:**

1. Aliouat-Denis C-M, Chabe M, Demanche C, et al. *Pneumocystis* species, co-evolution and pathogenic power. *Infect Genet Evol*. 2008;8:708-726.
2. Caswell JL, Williams KJ. Respiratory system. In: Maxie MG, ed. *Jubb, Kennedy, and Palmer's Pathology of Domestic Animals*.5th ed. Philadelphia, PA: Saunders Elsevier; 2007:593.
3. Dei-Cas E, Brun-Pascaud M, Bille-Hansen V, et al. Animal models of pneumocystosis. *FEMS Immunol Med Microbiol*. 1998;22:163-168.
4. Henderson KS, et al. *Pneumocystis carinii* causes a distinctive interstitial pneumonia in immunocompetent laboratory rats that had been attributed to "rat respiratory virus." *Vet Pathol*. 2012;49: 440-452.
5. Oz HS, Hughes WT, Vargas SL. Search for extrapulmonary *Pneumocystis carinii* in an animal model. *J Parasitol*. 1996;82:357-359.
6. Wakefield AE. Genetic heterogeneity in Pneumocystis carinii: an introduction. FEMS *Immunol Med Microbiol*. 1998;22:5-13.

**Joint Pathology Center**
**Veterinary Pathology Services**

# WEDNESDAY SLIDE CONFERENCE 2012-2013

## Conference 7

**7 November 2012**

---

**CASE I:** 12-670 (JPC 4019866).

**Signalment:** Young adult, intact female New Zealand White rabbit (*Oryctolagus cuniculus*).

**History:** Found dead in the morning 3 days after arrival at facility. Feces and urine were present in the cage pan; food provided the day before had not been eaten. A jugular catheter had been placed by the vendor 1 week prior to arrival. There had been no subsequent experimental manipulation.

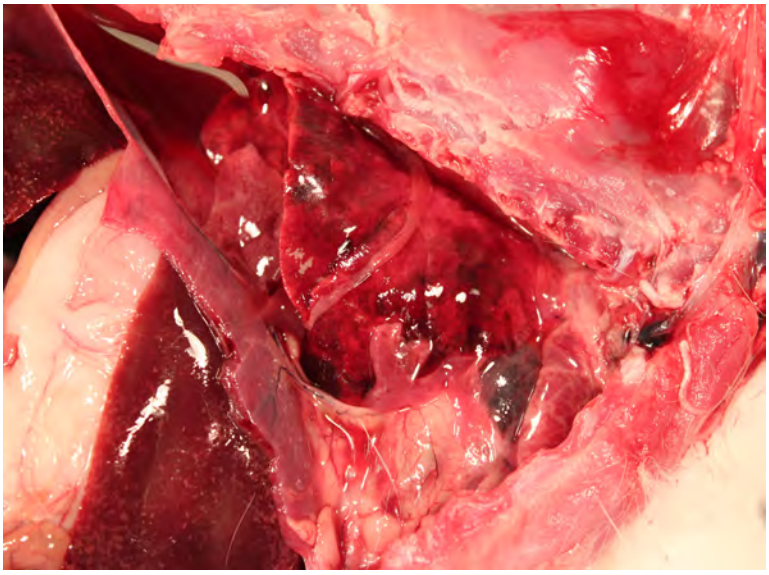

*1-1. Thoracic cavity, rabbit: The pleural cavity contains approximately 10mL of cloudy red-orange fluid. Dozens of 1-3mm thick strands and large coalescing mats of fibrin bilaterally cover the cranial lung lobes. Bilaterally, the cranioventral 15% of the lungs is dark red and consolidated. The remainder of the lung is mottled dark red. (Photograph courtesy of Memorial Sloan-Kettering Cancer Center, 1275 York Ave, New York, NY 10065)*

**Gross Pathology:** The fur around the neck and cranial thorax is shaved. Within the right jugular vein is an indwelling catheter that tunnels subcutaneously to be secured to the overlying skin of the dorsal right neck. Adjacent to the catheter, midway along the neck, the wall of the right jugular vein is thickened with a yellow/white 2 x 2 x 3 mm, firm focal swelling.

The pericardium of the heart is diffusely thick (up to 3mm wide), discolored red-tan, and rough. Approximately 1mL of yellow-red, opaque pericardial fluid is present. The epicardial surface of the heart is rough and covered with multifocal strands of gelatinous to stringy, tan material (fibrin). The endocardial surface of the heart and heart valves are grossly within normal limits.

The pleural cavity contains approximately 10mL of cloudy red-orange fluid. Dozens of 1-3mm thick strands and large coalescing mats of fibrin bilaterally cover the cranial lung lobes. Bilaterally, the cranioventral 15% of the lungs is dark red and consolidated. The remainder of the lung is mottled dark red.

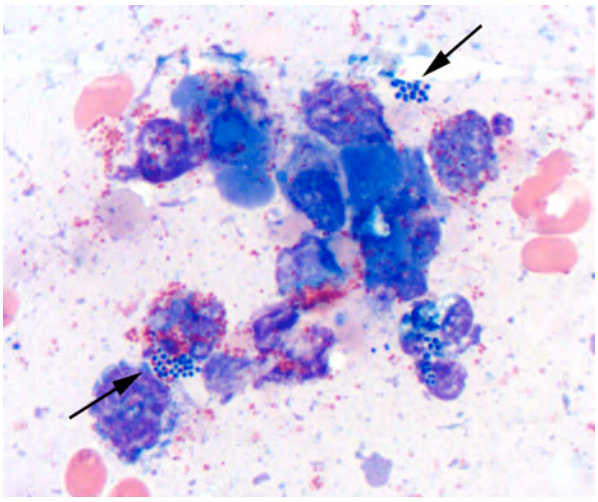

*1-2. Pericardial fluid: Cytology of pericardial fluid revealed abundant degenerate heterophils with myriad intra- and extra-cellular Gram positive cocci in clusters. (Photograph courtesy of Memorial Sloan-Kettering Cancer Center, 1275 York Ave, New York, NY 10065)*

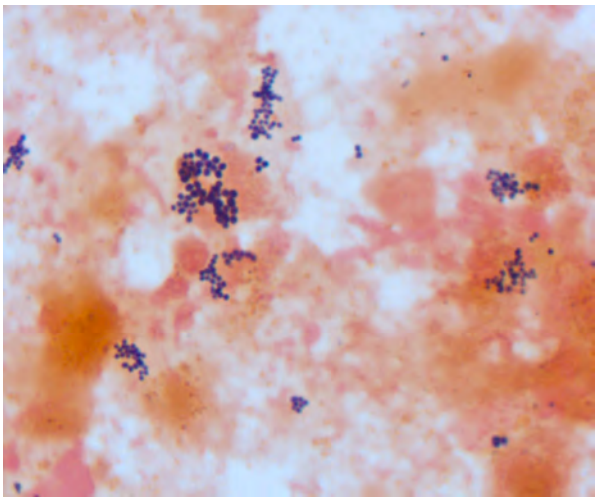

*1-3. Pericardial fluid, Gram stain: Heterophils contain numerous intracellular, gram positive cocci (arrow). (Photograph courtesy of Memorial Sloan-Kettering Cancer Center, 1275 York Ave, New New York, NY 10065)*

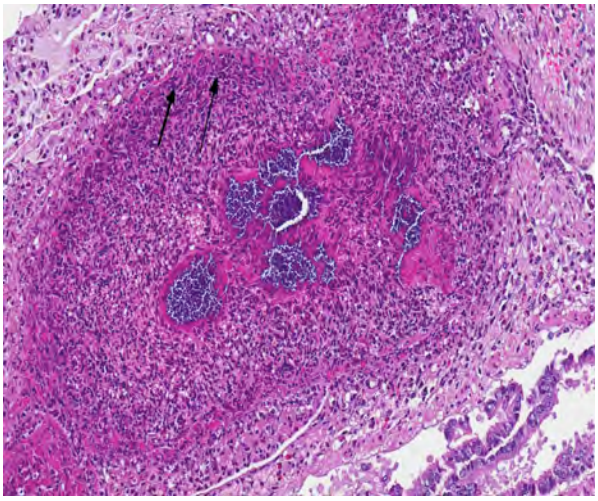

*1-4. Lung, rabbit: Multifocally, arteriolar walls are necrotic and contain large numbers of heterophils admixed with fibrin, hemorrhage, and cellular debris (fibrinoid necrosis) (arrows). Occlusive thrombi within the arteriolar lumen is composed of fibrin, degenerate heterophils, and abundant cellular debris and are centered upon large colonies of cocci. (HE 210X) (Photograph courtesy of Memorial Sloan-Kettering Cancer Center, 1275 York Ave, New York, NY 10065)*

Multifocally throughout the liver are hundreds of coalescing 1-2mm pale tan foci.

**Laboratory Results:** Cytology of pericardial fluid revealed abundant degenerate heterophils with myriad intra- and extra-cellular Gram-positive cocci in clusters. Microbial culture of the pericardial fluid, pleural fluid, lung, and liver grew *Staphylococcus aureus*.

**Histopathologic Description:** Multifocally within the lungs, many small, medium and large pulmonary vessels have a lumen that is occluded by large numbers of degenerate heterophils and moderate amounts of fibrin and cell debris, often with centrally located colonies of large coccoid bacteria. Transmurally, the vascular wall is hypereosinophilic with loss of cellular detail (fibrinoid necrosis), and moderate numbers of heterophils extend into the perivascular tissue and adjacent alveolar spaces. Within some sections of lung there are locally extensive areas of coagulative necrosis and hemorrhage that are often adjacent to a thrombosed vessel. Degenerate heterophils are often present at the margin of necrotic and viable tissue with proliferation of coccoid bacterial colonies within areas of necrosis. Moderate numbers of heterophils and few megakaryocytes are present multifocally within the interstitium. Alveolar spaces multifocally contain large amounts of eosinophilic foamy material and mild hemorrhage, and the alveolar capillaries are markedly congested. Multifocally (not present on every slide), the pleural surface of the lung is necrotic and expanded by moderate amounts of fibrin and degenerate heterophilic cellular debris.

**Contributor's Morphologic Diagnosis:** Lung: Marked, acute, multifocal, heterophilic and necrotizing pulmonary thrombosis, vascular fibrinoid necrosis and heterophilic, necrotizing bronchointerstitial pleuropneumonia with intralesional coccoid bacteria and marked, multifocal pulmonary congestion and edema.

**Contributor's Comment:** This rabbit had an intravenous catheter inserted into the right jugular vein by the vendor, approximately one-week prior to arrival at the research facility. The unexpected death of this otherwise unmanipulated rabbit was attributed to catheter-related septicemia. *Staphylococcus aureus* was isolated from the lung, liver, pericardial fluid, and pleural fluid. Large coccoid bacteria were also

visualized histologically within the large fibrinosuppurative thrombus in the right jugular vein, near the point of catheter entry. It is hypothesized that infection was initiated at either the catheter exit point in the skin or from an infection of the catheter hub, which tracked down the catheter to the lumen of the vein. Embolism of the thrombus within the jugular vein would result in lodgment of the emboli in the next vascular bed, in this case, the lungs. This is consistent with the vasculocentric distribution of the fibrinosuppurative and necrotizing embolic lesions in lungs of this rabbit.

Vascular catheters are commonly used indwelling medical devices in both animals and humans. In a research setting, they are frequently used in laboratory animals to provide convenient vascular access for repeated injections with less restraint and handling stress on the animal. However, catheterization can be associated with many complications, the most serious being catheter-related septicemia.[1] Although catheter-related complications in humans are widely reported, there are very few reports of cases in animals.

Microbes that colonize catheter hubs and the skin surrounding the insertion site are the most common source of catheter-related infections.[2] Migration of skin organisms into the cutaneous catheter tract with subsequent colonization of the catheter tip is the most common route in humans.[2] Infection of the catheter hub, hematogenous seeding from a distant site of infection, or contaminated infusate are other sources of catheter-related infection.[1,2,3] Bacteria, including *Staphylococcus epidermidis*, *S. aureus*, *Pseudomonas aeruginosa*, *Klebsiella pneumoniae* and *Enterococcus faecalis*, and the *Candida* spp. of fungi are commonly involved in human catheter-related infections.[1,2]

Studies have shown that virtually all indwelling central venous catheters in people are colonized by microorganisms embedded within a biofilm matrix.[2] The biofilm consists of both host and microbe-associated components. As the host reacts to the catheter, a thrombin sleeve rich in fibrin and fibronectin coats the catheter. Microbes may also produce an extracellular polysaccharide 'slime'. Together, these form the biofilm which enhances adherence of organisms and also protects organisms from phagocytosis, antibiotics and antibodies.[1,2]

The presence of a catheter within a vessel lumen can result in endothelial injury as well as alterations in normal blood flow around the catheter, both of which predispose to thrombosis.[4] There are four possible sequelae to thrombus formation – propagation, embolization, dissolution, or organization and recanalization.[4] In this rabbit, multiple emboli showered the pulmonary vessels of the lungs resulting in acute death.

**JPC Diagnosis:** Lung: Pneumonia, heterophilic and necrotizing, diffuse, severe, with necrotizing vasculitis, thrombosis, and large colonies of intraalveolar and intravascular cocci.

**Conference Comment:** Conference participants discussed the aspects of intravenous catheters that contribute to thrombosis, as accurately described by the contributor. Three primary abnormalities, referred to as "Virchow's triad", lead to thrombus formation: 1) endothelial injury, 2) alterations in blood flow (stasis or turbulence), and 3) hypercoagulability of blood.[4] Of these, endothelial injury is the most important factor, and damaged endothelium can affect the other aspects of the triad; specifically, it can lead to abnormal blood flow and increased coagulability. Under normal conditions, intact endothelial cells prevent thrombosis by a combination of antiplatelet, anticoagulant and profibrinolytic effects. Antiplatelet properties of endothelial cells include the production of prostacyclin and nitric oxide, which inhibit platelet adhesion and promote vasodilation. Endothelial cells also produce adenosine diphosphatase which degrades ADP, an effective activator of platelet aggregation. Membrane-associated heparin-like molecules, thrombomodulin, and tissue factor pathway inhibitor mediate the anticoagulant properties of normal endothelium. Heparin-like molecules are cofactors in the activation of antithrombin III, which in turn enhances the inactivation of thrombin and other serine protease coagulation factors (factors IXa, Xa, Xia, and XIIa). Thrombomodulin converts thrombin to an anticoagulant which activates protein C, resulting in the inactivation of clotting factors Va and VIIIa. Tissue factor pathway inhibitor further impedes the coagulation cascade by inhibiting tissue factor-VIIa and factor Xa. Additionally, normal endothelial cells produce tissue type plasminogen activator (t-PA). t-PA cleaves plasminogen to form plasmin; plasmin then cleaves fibrin to degrade thrombi.

In contrast to these antithrombotic properties of normal endothelium, injured or activated endothelium induces thrombosis by inducing platelet binding and aggregation, activating the extrinsic coagulation cascade and enhancing the activation of clotting factors IX and Xa. Endothelial cells can by activated by trauma, infectious agents, hemodynamic forces, circulating plasma mediators, and cytokines. Endothelial injury results in exposure of the underlying extracullular matrix and subsequent adhesion of platelets to it via interactions with von Willebrand factor (vWF). vWF, which is secreted by endothelial cells, acts as a bridge between the ECM and the glycoprotein Ib receptor on platelets, allowing the

formation of the primary hemostatic plug. Endothelial cells also produce tissue factor (factor III, thromboplastin), the primary activator of the extrinsic pathway of the coagulation cascade that results in secondary hemostasis. Finally, endothelial cells secrete antifibrinolytic substances such as inhibitors of plasminogen activator s (PAIs) which restrict fibrinolysis.[4]

The second factor in Virchow's triad, abnormal blood flow (turbulence or stasis), is characterized by a disruption in the normal laminar flow of blood in which cellular elements flow centrally in the vessel, separated from the endothelium by a layer of plasma. Disturbance in this laminar flow promotes endothelial activation, enhances coagulation, brings platelets into contact with the endothelium, and prevents washout and dilution of activated clotting factors, all of which contributes to thrombosis.[4]

The third component of Virchow's triad, hypercoagulability, can be heightened by inflammation, stress, surgery, neoplasia, pregnancy and renal disease (i.e. the loss of antithrombin III in the nephrotic syndrome). Inflammation is the most common cause of hypercoagulability, resulting in a prothrombotic state due to increased amounts of tissue factor, increased platelet reactivity, increased fibrinogen, and decreased thrombomodulin.[4,5] Stress and tissue necrosis (trauma, surgery) can cause transient increases in fibrinognen. Lastly, conditions that increase platelet activation (e.g. heartworm disease, nephrotic syndrome, and neoplasia) can also contribute to increased blood hypercoagulability and thus predispose an individual to thrombus formation.[5]

**Virchow's Triad in Thrombosis*:**

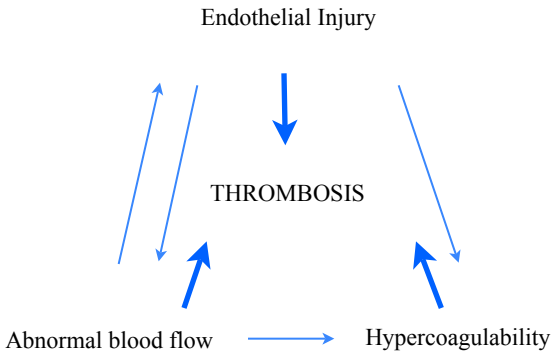


**adapted from Robbins and Cotran Pathologic Basis of Disease, 8th ed.*

**Contributing Institution:** Memorial Sloan-Kettering Cancer Center
1275 York Ave
New York, NY 10065

**References:**

1. Isaam I, Bodey GP. Infectious complications of indwelling vascular catheters. *Clin Infect Dis*. 1992;15:197-208.
2. Leonidou L, Gogos CA. Catheter-related blood stream infections: catheter management according to pathogen. *Int J Antimicrob Agents*. 2010;36S:S26-S32.
3. O'Grady NP, Alexander M, Burns LA, et al. 2011 Guidelines for the prevention of intravascular catheter-related infections. Healthcare Infection Control Practices Advisory Committee, Publication of the Centers for Disease Control and Prevention, 2011. http://www.cdc.gov/hicpac/BSI/BSI-guidelines-2011.html Accessed June 5, 2012.
4. Mitchell RN. Hemodynamic disorders, thromboembolic disease, and shock. In: Kumar V, Abbas A, Aster JC, eds. *Robbins and Cotran Pathologic Basis of Disease* 8th ed. Philadelphia, PA: Saunders Elsevier; 2010:121-127.
5. Mosier DA. Vascular disorders and thrombosis. In: Zachary JF, McGavin MD, eds. *Pathologic Basis of Veterinary Disease*. 5th ed. St Louis, Missouri: Elsevier Mosby; 2012:78-82.

**CASE II:** 51529 (JPC 3164931).

**Signalment:** Adult, male, naked mole rat (*Heterocephalus glaber*).

**History:** This naked mole rat was one of several that developed a slow-growing subcutaneous mass at a rabies vaccine injection site. Rabies vaccines were given as part of international pre-shipment requirements. Due to the size of the masses and the presence of more diffuse, crusted skin lesions over much of the body, two of the naked mole rats were euthanized. Other affected mole rats with only subcutaneous masses were treated with surgical excision of the masses. All tissues were submitted for histologic examination.

**Gross Pathologic Findings:** Gross and histologic findings are similar in both euthanized animals. At the base of the neck, within the right, dorsal cervical subcutis is a 2.0 x 1.5 x 1.5 cm, soft mass filled with thick white fluid. On a Wright-Giemsa stained smear, the fluid consists of acellular colorless to pale blue, refractile granular material that is birefringent when viewed with polarized light. The skin over approximately 90% of the ventral thoracic and abdominal body wall is diffusely dark yellow, thickened and rough. Body condition is good with moderate adipose stores and adequate skeletal muscling.

**Histopathologic Description:** Within multiple sections of haired skin, the integument contains moderate to large amounts of deeply basophilic, fragmented material that stains positive for mineral with a von Kossa stain. In the deep dermis, there are large lakes of mineral surrounded by a variably thick rim of macrophages and multinucleated giant cells (granuloma). In the surrounding dermis there are small numbers of neutrophils and peripheral follicular accumulations of lymphocytes. In the superficial dermis, mineral and granulomatous inflammation is more diffuse and there is mineralization of individual collagen fibers. The overlying epidermis is multifocally mineralized, necrotic, and/or ulcerated. There is mild orthokeratotic hyperkeratosis. A Ziehl-Neelsen acid-fast stain is negative for bacteria.

In each of the excisional biopsy samples there is a large dermal granuloma with central mineral as described in the preceding paragraph.

**Contributor's Morphologic Diagnoses:** Haired skin, neck: Multiple dermal granulomas with intralesional mineral (calcinosis circumscripta).

Haired skin, ventral body wall: Moderate to severe, multifocal dermal mineralization (calcinosis cutis) with granulomatous dermatitis, epidermal necrosis, ulceration, mild orthokeratotic hyperkeratosis and serocellular surface crusts.

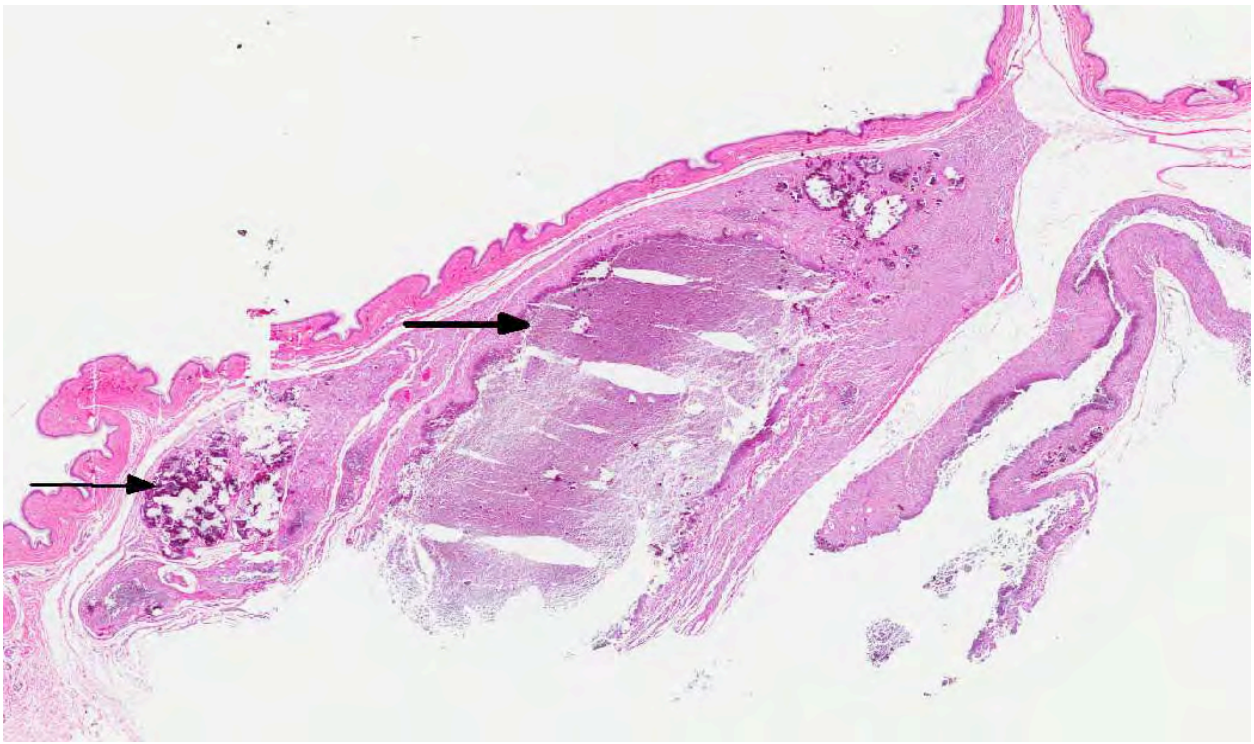

*2-1. Skin, naked mole rat: Multifocally, the deep dermis and subcutis are expanded by multiple granulomas centered on granular and crystalline mineral (arrows). (HE 11X)*

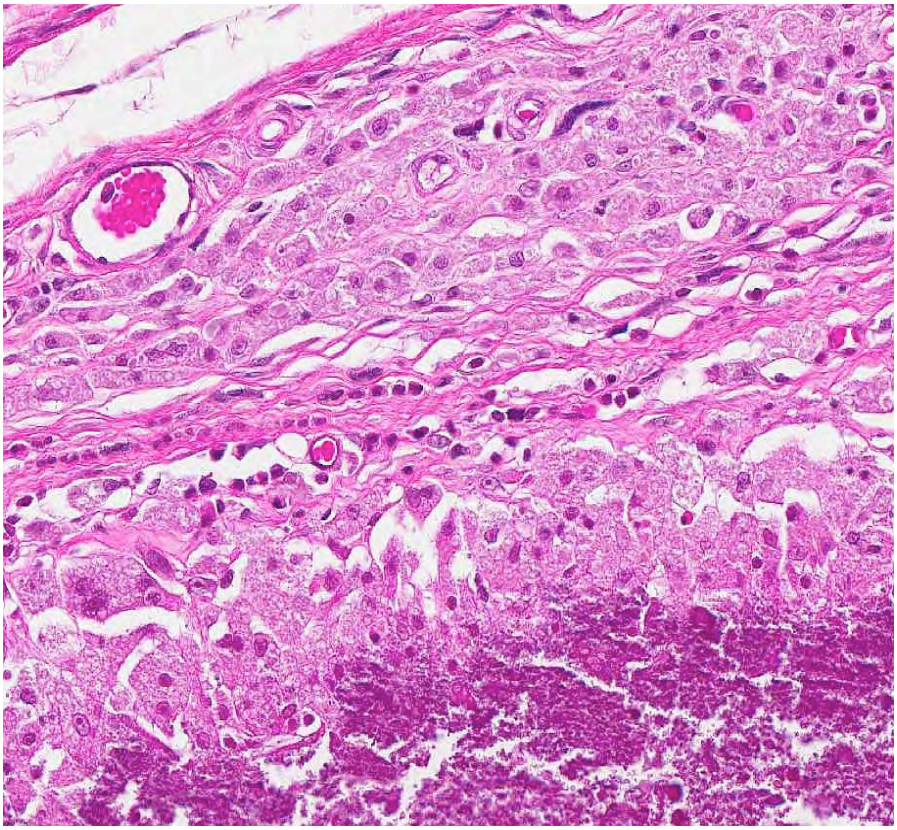

*2-2. Skin, naked mole rat: Within the granulomas, large numbers of polygonal epithelioid macrophages border lakes of granular mineral. (HE 228X)*

**Contributor's Comment:** Deposition of calcium salts in soft tissues has a variety of underlying causes which are broadly classified as dystrophic or metastatic based on the mechanism. Dystrophic mineralization is the result of local tissue damage. Causes may include trauma, infection and neoplastic disease. The mechanism of dystrophic mineralization involves increased intracellular calcium secondary to release of calcium from damaged mitochondria and accumulation of extracellular calcium through vesicular phospholipid-binding of calcium and phosphate. Metastatic calcification, in contrast, is a response to hypercalcemia. Underlying causes include parathyroid hormone release (associated with renal disease or parathyroid tumors), parathyroid-like hormone, damage to bone, vitamin D toxicity and increased calcium intake. All of these mechanisms ultimately raise serum calcium levels leading to precipitation of mineral into otherwise normal soft tissue. Mineralization tends to occur in tissues that lose acid such as the lung, kidney and stomach.[7]

Calcinosis cutis and calcinosis circumscripta are characterized by ectopic cutaneous and subcutaneous deposition of calcium salts and may be part of a metastatic or dystrophic process, though in domestic mammals the lesions are often idiopathic.[10] Calcinosis cutis refers to lesions in which there is more diffuse involvement of collagen and adnexa while the diagnosis of calcinosis circumscripta is reserved for circumscribed mass-like lesions (also called tumoral calcinosis).[5] Interestingly, the lesions in these naked mole rats appear to have features of both. The larger mass at the neck and shoulder is a nodular accumulation of mineral with secondary granulomatous inflammation, consistent with calcinosis circumscripta. Dermal lesions along the body wall are more diffuse and characteristic of calcinosis cutis.

In domestic animals, calcinosis cutis is most often associated with either iatrogenic or Cushing's disease-related hyperglucocorticoidism. In domestic dogs, calcinosis circumscripta has been reported in the footpads in association with renal failure. Lesions also occur in the tongue, possibly secondary to local trauma. Additionally there is an uncommon form of idiopathic cutaneous calcinosis circumscripta that seems to occur mainly in large breed dogs, particularly of the German Shepherd dogs. In these cases, dogs often have normal serum calcium and phosphorus levels, a lack of identifiable nutritional deficiency or excess and lack of known pre-existing trauma to the affected areas.[10]

As is frequently the case in domestic mammals, the cause of the lesions in these naked mole rats is poorly understood. There is a strong temporal and spatial association between rabies vaccination and the tumoral calcinosis, but this may not explain the calcinosis cutis–like lesions along the body wall. Skin trauma in naked mole rats does not typically lead to calcinosis; perhaps mineral deposition in these cases was exacerbated by the injection. The vaccine given (IMRAB® 3, Merial) makes use of an aluminum hydroxide adjuvant to promote macrophage antigen presentation and contains gentamicin as a preservative. Naked mole rats are not typically vaccinated for rabies at this institution so it is unknown if the type of vaccine and/or adjuvant had anything to do with the development of the lesions. In those animals treated via surgical excision, tumoral lesions did not recur.

There did not appear to be calcinosis cutis-like lesions in the biopsied animals, though sampling of skin in places other than at tumoral lesions was not attempted. Injection site calcinosis circumscripta has been previously reported in a dog that had received medroxyprogesterone acetate contraception.[4] No reports were found in which calcinosis circumscripta was associated with vaccination.

Given that multiple members of the colony were affected, a review of commonalities among these animals (such as diet, genetics and clinical history) and possibly serum chemistry analyses may be helpful. Adrenal and pituitary glands in the necropsied cases were grossly and histologically within normal limits, so hyperadrenocorticism was considered less likely. Given their subterranean lifestyle and lack of normal exposure to vitamin D, differences in calcium/phosphorus metabolism could make this animal more susceptible to cutaneous calcinosis. Abnormal skin calcification has been reported previously in naked mole rats. In this study, despite massive dietary vitamin D overload, mineralization was only evident in the skin and in increased tooth density. It was speculated that in naked mole rats, skin and teeth may be used for deposition and subsequent sloughing of excess calcium, perhaps to help prevent metastatic calcification in other organs.[3]

Naked mole rats are a fascinating rodent species of relatively recent interest as research animals. Naked mole rats are native to Africa where they live deep underground in a complex system of burrows. They are a eusocial species, meaning they have a complex social structure whereby many non-reproductive 'workers' care for a single dominant 'queen' and a few other reproductively active individuals.[8] They are extraordinarily long-lived for a rodent species (in excess of 20 years). Naked mole rats appear to lack pain response to certain irritants (ammonia, capsaicin and acids) and have a high tolerance for hypoxic conditions, adaptations that are likely courtesy of the extreme environment in which they live. Neoplastic disease has yet to be reported in this species.[1,2,6] For these reasons, naked mole rats are being utilized in aging, pain and cancer studies.

**JPC Diagnosis:** 1. Haired skin, neck: Dermal granulomas, calcareous, multiple, coalescing (calcinosis circumscripta), with mild epidermal pigmentary incontinence.
2. Haired skin, ventral body wall: Dermatitis, granulomatous, diffuse, marked, with multifocal dermal mineralization (calcinosis cutis) and fibrosis, moderate acanthosis, orthokeratotic hyperkeratosis and serocellular surface crusts.

**Conference Comment:** The contributor provided an excellent review of cutaneous calcium deposits. Calcinosis circumscripta occurs in both humans and animals. In humans, calcinosis circumscripta has been associated with pressure points, tendon sheaths, and distal digits.[9] It is more commonly reported in females than males and may be associated with connective tissue disorders such as Reynaud's phenomenon, scleroderma, systemic lupus erythromatosis, telangiectasia, and dermatomyositis. Trauma, insect bites, renal failure, and inherited disorders such as pseudoxanthoma elasticum, Werner's syndrome, and Ehlers-Danlos syndrome are suspected causes of calcinosis circumscripta in humans. A recently described autosomal recessive disorder termed normophosphatemic familial tumoral calcinosis (NFTC) has also been implicated in the formation of calcinosis circumscripta lesions in people. NFTC is associated with an absence of functional SAMD9, a tumor suppressor and anti-inflammatory protein, and histologically appears similar to dystrophic calcinosis.[9]

In addition to the naked mole rats described by the contributor, other animals affected by calcinosis circumscripta include dogs, cats, horses, cows, buffalo, rabbits, turtles, nonhuman primates and a captive antelope. Reports of calcinosis circumscripta in nonhuman primates include two female rhesus macaques and a male common marmoset, in which the lesion was associated with microchip implantation. Additionally, idiopathic calcinosis circumscripta has been reported in two cynamologus macaques and a case of bilateral dystrophic calcinosis circumscripta was recently reported in a six-year-old female cynomolgus macaque with a history of bilateral foot trauma.[9]

There was moderate slide variation; the slide used for the JPC morphologic diagnosis did not exhibit the necrosis and ulceration associated with the calcinosis cutis as described by the contributor.

**Contributing Institution**: Wildlife Disease Labs
San Diego Zoo Institute for Conservation Research
http://www.sandiegozoo.org/conservation/

**References:**
1. Austad SN. Methusaleh's zoo: how nature provides us with clues for extending human health span. *J Comp Path*. 2010;142: S10-S21.
2. Borges RM. Of pungency, pain, and naked mole rats: chili peppers revisited. *J Biosci*. 2009;34:349-351.
3. Buffenstein R, Laundy MT, Pitcher T, Pettifor JM. Vitamin $D_3$ intoxication in naked mole-rats (*Heterocephalus glaber*) leads to hypercalcaemia and increased calcium deposition in teeth with evidence of abnormal skin calcification. *Gen Comp Endocrinol*. 1995;99:35-40.

4. Ginel PJ, Lopez R, Rivas R, Perez J, Mozos E. A further case of medroxyprogesterone acetate associated with calcinosis circumscripta in the dog. *Vet Rec*. 1995;136:44-45.
5. Gross TL, Ihrke PJ, Walder EJ, Affolter VK. Degenerative, dysplastic and depositional diseases of dermal connective tissue. In: *Skin Diseases of the Dog and Cat*. 2nd ed. Ames, IA; 2005:373-380.
6. Larson J, Park TJ. Extreme hypoxia tolerance of naked mole rat brain. *Neuroreport*. 2009:20;1634-1637.
7. Kumar V, Abbas AK, Fausto N. Cellular adaptations, cell injury and cell death. In: *Pathologic Basis of Disease*. 7th ed. Philadelphia, PA: Elsevier Saunders; 2005:41-42.
8. Nowak RM, Paradiso JL. Rodentia; Bathyergidae; genus *Heterocephalus*. In*: Walker's Mammals of the World*. 4th ed. Baltimore, MD: Johns Hopkins University Press; 1983:855-857.
9. Radi ZA, Sato K. Bilateral dystrophic calcinosis crcumscripta in a cynomolgus macaque (*Macaca fascicularis*). *Toxicol Pathol*. 2010;38:637.
10. Scott DW, Buerger RG. Idiopathic calcinosis circumscripta in the dog: a retrospective analysis of 130 cases. *J Am Anim Hosp Assoc*. 1988;24:651-658.

**CASE III:** 12/253 (JPC 4020024).

**Signalment:** 4-year-old female, Norwegian red, *Bos taurus*.

**History:** The cow was submitted to the large animal clinic at the Norwegian School of Veterinary Science due to a large (walnut-sized) tumor-like growth in the cornea of the right eye. A squamous cell carcinoma or a granuloma due to trauma was suspected, and the eye was enucleated and submitted for histopathologic examination.

**Gross Pathology:** Slightly off the center in the cornea there is a 3x2x2 cm large exophytic pedunculated nodule with a stalk that measures 1.5 cm in diameter. The surface of the lesion is rugged with a grey to yellow discoloration. There is opacity of the surrounding corneal tissue. On the cut surface the lesion appears to be composed of an outward bulging of the cornea with a central core of gelatinous material. Black pigmented tissue (iris) is adhered to the internal surface of the cornea and also protrudes into the stalk of the lesion.

**Laboratory Results:** The intraocular pressure was decreased in the eye.

**Histopathologic Description:** In the eye there is a focally extensive anterior bulging of a fibrous membrane, and the bulging area consists of connective tissue with collagen fibers parallel with the surface and vessels that are perpendicular to the surface (granulation tissue). The granulation tissue is continuous with cornea on each side. The outer surface of the bulging area is severely inflamed and infiltrated by numerous leukocytes, mainly necrotic neutrophils.

Descemet's membrane is ruptured, and the ends are located at each side of the stalk area, thus the inner surface of the granulation tissue is not lined by Descemet's membrane. The center of the nodule (macroscopic gelatinous area) consists of scattered vessels and spindle shaped cells or round cells with dark brown pigment, and very few lymphocytes and plasma cells. Towards the anterior chamber, the lesion is lined by iridal pigmented tissue that is adhered to the cornea (anterior synechia) and bulging into the defect in the cornea. The pigment in the adhered iris and the central area was Prussian blue negative, and it was bleached by potassium permanganate (melanin).

**Contributor's Morphologic Diagnosis:** Eye: keratitis, ulcerative and purulent, focally extensive, chronic, severe with anterior synechia and corneal staphyloma.

**Contributor's Comment:** The lesion in this eye was interpreted to have been caused by a traumatic injury to the eye, most likely perforating the cornea, although there was no known history of trauma. Transcorneal gaps may be initially plugged with fibrin and sometimes by prolapsed iris.[3] The outward bulging of the cornea in this specimen has the morphology of granulation tissue, indicating the severity and chronicity of the condition. Although severely inflamed, the inflammation is mainly present in the superficial layer of the granulation tissue that was continuous with the cornea. Infectious ulcerative keratitis, e.g. mycotic of bacterial, may also cause severe corneal lesions. Proteases from microbes or leukocytes may cause stromal liquefaction (keratomalacia) that may reach Descemet's membrane and result in its forward

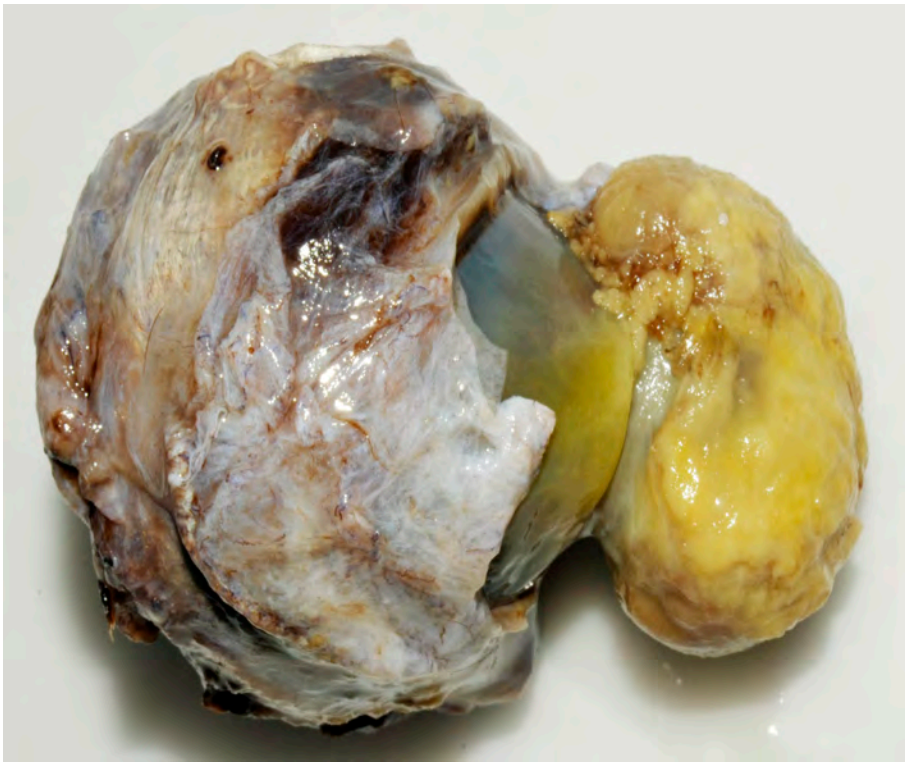

*3-1. Eye, ox: Arising near the central cornea is a 3x2x2 cm, exophytic, pedunculated nodule. (Photograph courtesy of Norwegian School of Veterinary Science, P.O. Box 8146 Dep, 0033 Oslo, Norway. www.nvh.no)*

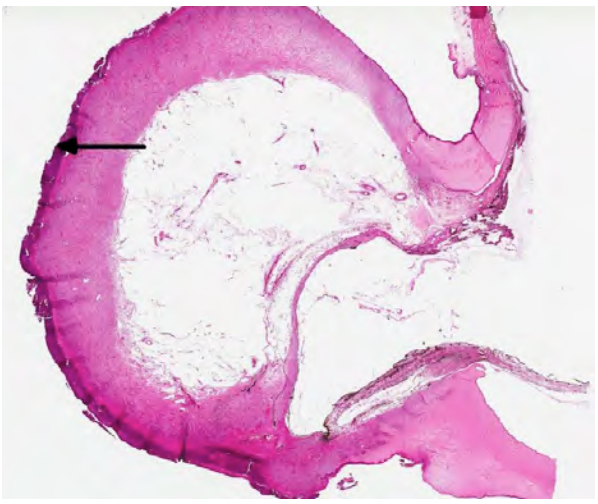

*3-2. Eye, cornea, ox: Diffusely, the cornea is markedly thickened and the anterior edge is extensively ulcerated (arrow). (HE 3X)*

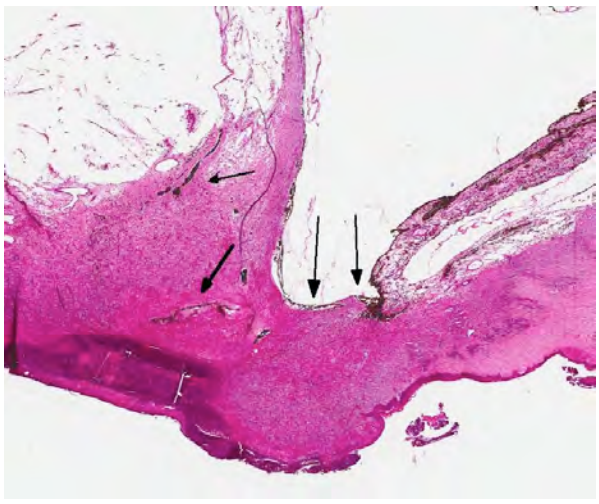

*3-3. Eye, cornea, ox: Portions of the iris and ciliary body are entrapped within the granulation tissue replacing the cornea (staphyloma/anterior synechia). (HE 80X)*

bulging as a descemetocele.[3] In this case, the Descemet's membrane was ruptured with its ends located at each side of the protruding iridal tissue. Staphyloma is defined as a protrusion of the sclera or cornea, usually lined by uveal tissue. The lesion can be anterior or posterior and affect both sclera and cornea. Corneal staphyloma is defined as a bulging of the cornea with adherent uveal tissue, as was present in this case.[1] Between the granulation tissue and the protruding iridal tissue there was a large area with scattered blood vessels and pigmented cells. The pigment was negative in Prussian blue staining, however it was bleached in potassium permanganate treated slides, indicating that these cells contain melanin pigment.

**JPC Diagnosis:** Cornea: Keratitis, ulcerative, chronic, focally extensive severe with staphyloma.

**Conference Comment:** Corneal injury, such as was suspected in this case, often results in alterations of normal healing that disrupt the normal structure and interfere with the function of corneal tissue.[2] The cornea, which covers the anterior portion of the globe, serves to both protect the intraocular structures and to refract light for vision. Therefore its most important feature is its transparency, which is achieved by its architecture. The cornea is composed of three layers (epithelial, stromal and endothelial layers) and two acellular layers (Bowman's layer and Descemet's membrane, which separate the epithelium from the stroma and the stroma from the endothelium, respectively). These layers have a uniform, consistent arrangement that allows light transmission and refraction. The corneal epithelium is the outermost layer; it is made up of five to seven layers of nonkeratinized, stratified epithelia. The basal epithelial cells of this layer have a prominent nucleus and are mitotically active, as epithelial cells turn over every five to seven days. The basal cells adhere to the basement membrane via a complex t hat also anchors the epithelium to Bowman's layer. Subjacent to the epithelium lies the stroma, which is the thickest layer, accounting for approximately 90% of the cornea. It is composed of highly organized connective tissue (predominantly collagen type I fibrils) arranged in orderly sheets that form lamellae, admixed with proteoglycans that maintain the regular spacing between the lamellae. A meshwork of flat cells (called "keratocytes") is also found between the collagenous lamellae. Keratocytes slowly secrete collagen and ECM components that are needed to maintain the stroma. The endothelium is the innermost layer of the cornea, formed by a single layer of polygonal cells which secrete Descemet's membrane and regulate water content in the stroma via Na+/K+-ATPase pumps. Descemet's membrane is composed mostly of collagen type IV, glycoproteins and fibrin. Dysfunction of the endothelium causes stromal edema and corneal opacity. In addition to these components, the cornea also contains numerous nerve endings (300-400 times more than similarly-sized sections of skin). Most of these nerves are sensory, derived from the ciliary nerves of the trigeminal ganglion ophthalmic branch.[2]

Once the cornea is damaged, the outcome depends on the degree of injury. If only the outer epithelium is damaged, adjacent epithelial cells will quickly migrate to cover the injury. This initial response is immediately followed by a proliferation to regain normal epithelial thickness. Concurrently, upon receiving signals from the damaged epithelium (via cytokines, neuropeptides, growth factors, lipid mediators and chemokines) underlying keratocytes undergo apoptosis and activate adjacent keratocytes. If

the stroma is damaged as well, there is a stronger activation of keratocytes, resulting in their transformation into fibroblasts and myofibroblasts, leading to scar tissue formation and loss of transparency.[2]

Corneal injury will also result in an inflammatory response, generally characterized by infiltration of the stroma by neutrophils and proinflammatory lipid mediators. If this inflammation is not resolved, then corneal fibrosis, pigmentation, and neovascularization occur, ultimately resulting in scarring and disruption of the blood-ocular barrier.[2]

**Contributing Institution**: Norwegian School of Veterinary Science
www.nvh.no

**References:**

1. Blood DC, Studdert V. Baillière's comprehensive veterinary dictionary. London, UK: 1, Ballière Tindall; 1990.
2. Kenchegowda S, Bazan HEP. Significance of lipid mediators in corneal injury and repair. *J Lipid Res.* 2010;51(5):879-891.
3. Wilcock BP. Eye and ear. In: Maxie MG, ed. *Jubb, Kenndey, and Palmer's pathology of domestic animals*. 5th ed. Vol. 1. Philadelphia, PA: Elsevier Saunders; 2007:459-552.

**CASE IV:** 11A-259 (JPC 4019137).

**Signalment:** 15-year-old female cynomolgus macaque (*Macaca fascicularis)*.

**History:** This animal was acquired in 2005 from a domestic source. In-house assays for *Macacine herpesvirus 1* and SRV-2 were negative during quarantine examination. Lethargy was reported on 4-19-11. Gingival erosion and hepatomegaly were noted on physical examination. Pertinent laboratory data appears below. A lingual vesicle was noted on 4-20-11. Microscopic examination of a hepatic biopsy collected via ultrasound guidance on 4-20-11 revealed a necrotizing hepatitis. Despite supportive care, the animal was found expired on 4-23-11.


*4-1. Gingiva, cynomolgus monkey: At initial presentation, gingival erosions and hepatomegaly were noted. At necropsy, an additional 4cm ulcer was noted over the left maxillary canine tooth. (Photograph courtesy of Oregon National Primate Research Center. http://onprc.ohsu.edu)*

**Gross Pathology:** Multiple cutaneous crusting to weeping ulcers and erosions were present over the dorsal thorax, the inguinal region, the left upper lip and the posterior aspect of the left crus. There was an ulcer over the left maxillary canine tooth that measured approximately 4 cm in diameter. The tonsils protruded from the crypts and were mildly enlarged and soft with multifocal hemorrhage.

A large gelatinous blood clot was present within the thoracic cavity on the right side. The lung lobes were soft, edematous, and congested. The right side was mildly to moderately affected. The left was mildly affected.

Approximately 150 cc of hemorrhagic fluid was present within the peritoneal cavity. The liver was pale, friable and moderately enlarged with rounded margins. The hepatic capsule was dull and irregular with random, multifocal to coalescing areas of necrosis interspersed among beaded yellow-brown foci arranged in a reticulate fashion. The necrotic foci were either miliary or exhibited target-like lesions with distinct, raised white rims and depressed red centers that measured up to 0.4 cm in greatest dimension. The spleen was pale, enlarged and pulpy with multiple, irregular foci of necrosis. The splenic margins were rounded and the capsule was smooth and taut. The kidneys were streaked and pale and bulge on sectioned surface. There were multifocal hemorrhages throughout the adrenal glands. Multiple cervical hemorrhages were present and the mucosa was overlain by a fibrinopurulent exudate.


*4-2. Multiple cutaneous, crusting to weeping ulcers and erosions were present over the dorsal thorax, the inguinal region, the left upper lip and the posterior aspect of the left crus. (Photograph courtesy of Oregon National Primate Research Center. http://onprc.ohsu.edu)*

*4-3. Liver, cynomolgus monkey: The liver was pale, friable and moderately enlarged with rounded margins. The hepatic capsule was dull and irregular with random, multifocal to coalescing areas of necrosis interspersed among beaded yellow-brown foci arranged in a reticulate fashion. (Photograph courtesy of Oregon National Primate Research Center. http://onprc.ohsu.edu)*

**Laboratory Results**:

***Macacine herpesvirus* 1 Testing**

| Sample | Test | Result |
|---|---|---|
| Vaginal mucosal swab | Cell culture, PCR* | Positive |
| Oral mucosal swab | Cell culture, PCR* | Positive |
| Liver | Cell culture, PCR* | Positive |
| Spleen | Cell culture, PCR* | Negative |
| Serum, 6 years prior to death | IgG Antibody ELISA** | Negative |
| Serum, 5 weeks prior to death | IgG Antibody ELISA & Western blot* | Negative |
| Serum, 2 days prior to death | IgG Antibody ELISA | Positive |
| Serum, 2 days prior to death | IgG Antibody Western blot | Negative |
| Serum, 2 days prior to death | IgM Antibody Western blot | Positive |

*National B Virus Resource Laboratory, Georgia State University
**In-house laboratory

| Analyte (unit) | Value | Reference interval |
|---|---|---|
| ALT (IU/L) | 202 | 0 – 37 |
| ALP (IU/L) | 1887 | 30 – 120 |
| Total protein (g/dl) | 4.8 | 6.0 – 8.0 |
| Albumin (g/dl) | 1.3 | 3.0 – 4.1 |
| RBC ($x10^6/\mu L$) | 3.9 | 5.0 – 6.5 |
| PCV (%) | 21.1 | 35 – 45 |
| Platelets ($x10^3/\mu L$) | 112 | 330 – 650 |
| Leukocytes ($x10^3/\mu L$) | 5.0 | 6.00 – 14.00 |
| Neutrophils ($x10^3/\mu L$) | 2.45 | 2.40 – 11.20 |
| Bands ($x10^3/\mu L$) | 0.50 | 0 |
| Lymphocytes ($x10^3/\mu L$) | 2.35 | 1.50 – 7.00 |
| Monocytes ($x10^3/\mu L$) | 0.15 | 0 – 1.12 |
| Eosinophils ($x10^3/\mu L$) | 0 | 0 – 0.70 |
| Basophils ($x10^3/\mu L$) | 0 | 0 – 0.28 |

**Histopathologic Description:** Randomly distributed throughout the pancreatic parenchyma are mild to moderately extensive foci of lytic necrosis characterized by central accumulation of eosinophilic material and cellular and karyorrhectic debris surrounded by degenerate neutrophils and moderate numbers of cells containing amphophilic to eosinophilic intranuclear inclusions with marginated chromatin and occasionally a clear halo. There are numerous syncytia with 3-7 nuclei bearing intranuclear inclusions. Multifocally, the interlobular septa and perivascular spaces are mildly expanded by clear space (edema) and an inflammatory infiltrate composed of neutrophils, lymphocytes, plasma cells, and eosinophils.

**Contributor's Morphologic Diagnosis:** Pancreas: Pancreatitis, fibrinonecrotic, neutrophilic, with fewer lymphocytes, histiocytes and eosinophils, multifocal, moderate with moderate numbers of amphophilic to eosinophilic intranuclear inclusions and syncytia with intranuclear inclusions.

**Microscopic findings of tissues not submitted:** Neutrophilic fibrinonecrotizing inflammation affected the spleen, adrenal gland, liver, tonsil, cervix, esophagus, haired skin, gingiva, and lip. Most tissues contained intranuclear inclusion bodies and syncytia as described in the pancreas.

**Contributor's Comment:** This was a laboratory-confirmed case of a fatal, disseminated infection by *Macacine herpesvirus* 1 (McHV1; formerly *Cercopithecine herpesvirus* 1). Primary findings in this case included moderate to severe fibrinonecrotic inflammation of the gingiva, haired skin of the lip, inguinal region, dorsal thorax, left leg, liver, pancreas, adrenal gland, palatine tonsil, and cervix. Rare to high numbers of viral intranuclear inclusions and syncytia were present in most of the affected tissues. Multifocally, necrotizing vasculitis was present and rarely viral inclusions were noted within endothelial cells. The viral infection is thought to have induced disseminated intravascular coagulation.

Swabs of the vaginal and oral mucous membranes and hepatic and splenic tissue samples were submitted to the National B Virus Resource Laboratory at Georgia State University for virus isolation. All samples were positive for McHV1. Serum collected five weeks prior to death was McHV1 IgG antibody negative and a second sample collected two days prior to death had detectable levels of IgG antibody on recombinant ELISA and IgM antibody on western blot. Seroconversion during experimental primary infection results in detectable levels of IgM six days post-infection and IgG 12 days post-infection.[9] IgM levels peak at 12 days, followed by rapid decline. In this case, prior negative tests, positive serum IgM and IgG antibodies, and the acute disease course suggest this was a primary infection.

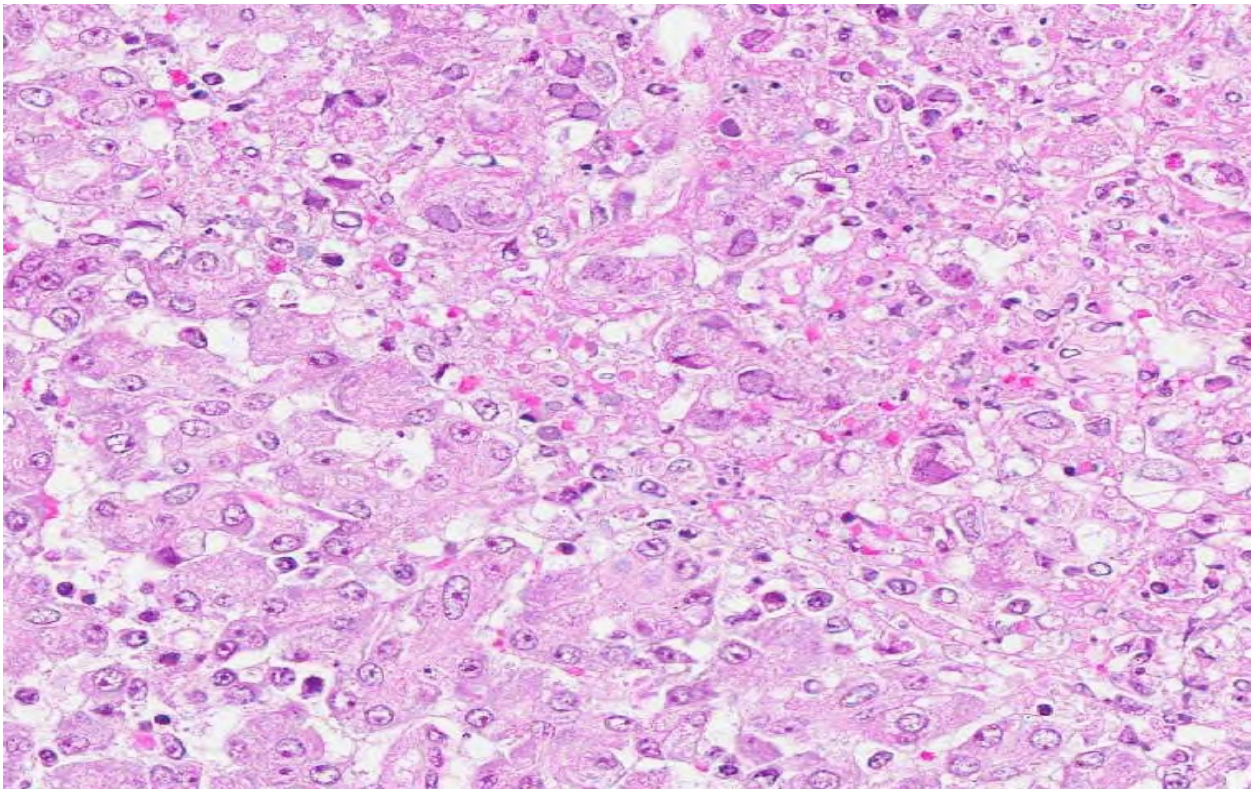

*4-4. Pancreas, cynomolgus monkey: Poorly demarcated areas of necrosis (top left) are scattered throughout the pancreas. Normal acini at bottom left. (HE 228X)*

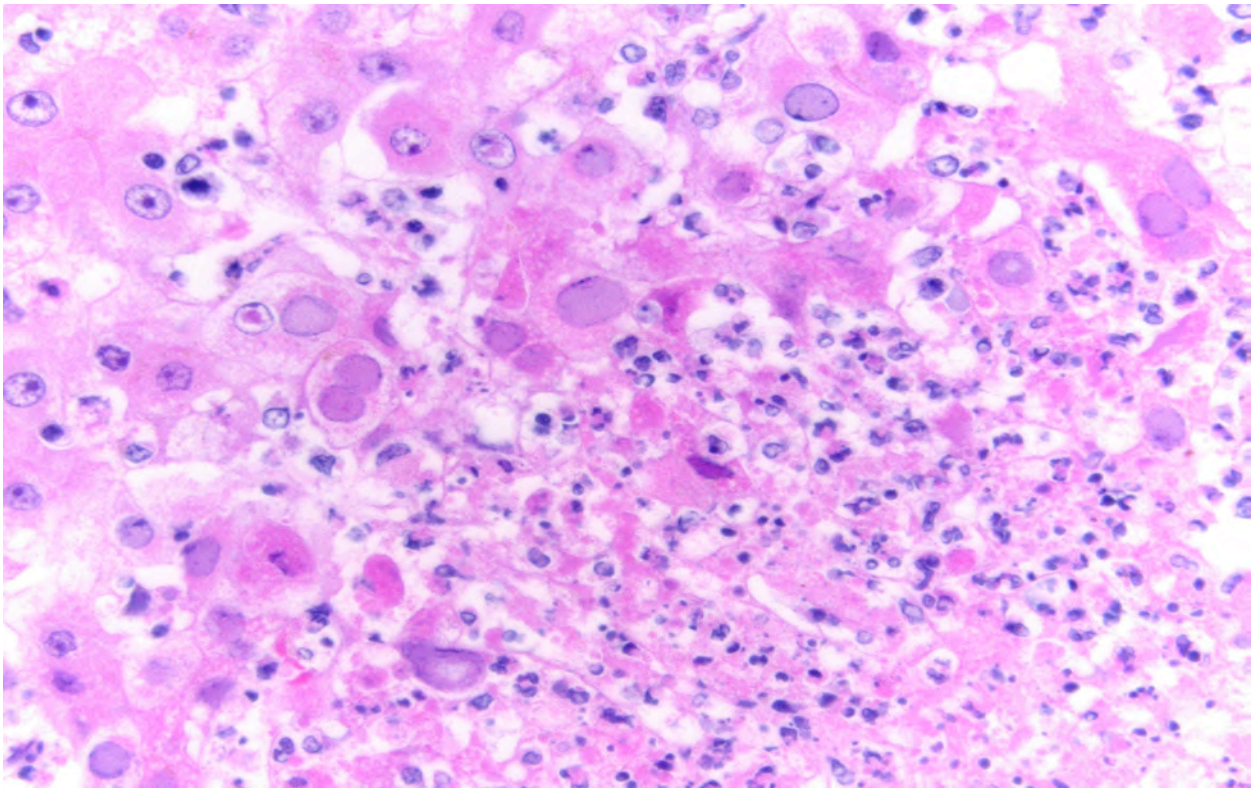

*4-5. Liver, cynomolgus monkey: Hepatocytes frequently contain large, amphophilic intranuclear inclusion bodies that peripheralize nuclear chromatin. (Photograph courtesy of Oregon National Primate Research Center. http://onprc.ohsu.edu)*

McHV1 is an enveloped double stranded DNA virus, member of the family *Herpesviridae*, subfamily *Alphaherpesvirinae*, genus *Simplexvirus.* It is endemic in Asian macaques and has been isolated from rhesus (*M. mulatta*), cynomolgus (*M. fascicularis*), stump-tailed (*M. arctoides*), pigtail (*M. nemestrina*), Japanese (*M. fuscata*), bonnet (*M. radiata*), and Taiwanese (*M. cyclopis*) macaques.[8] It is genetically similar to *Human herpesvirus* 1 and 2, though phylogenetic analysis indicates it is more closely related to non-human primate α -herpesviruses *Cercopithecine herpesvirus* 2 (simian agent 8), and *Papiine herpesvirus* 2 (Herpesvirus papio 2).[6]

Transmission occurs horizontally with increasing seroprevalance coinciding with sexual maturity and typically approaching 80% in captive and wild adult cohorts.[6] Primary infection occurs when orogenital mucosa or open wounds are inoculated with virus-contaminated oral or genital fluid, blood, urine, or feces. McHV1 initially replicates in the epithelium at the site of inoculation and may result in vesicular lesions in the mucosae and skin of the mucocutaneous junctions of the oral cavity, genitals, and conjunctiva, though infection is typically asymptomatic. Virus is transported along axons of sensory neurons to ganglia, and subsequent cessation of replication results in latent infection. Virus reactivation and anterograde axonal transport to epithelium with recrudescence and viral particle shedding can occur in the absence of clinical disease or with similar vesicular lesions. Virus shedding is reportedly more prevalent during the breeding season.

Similar to other members of the *Alphaherpesvirinae*, fatal cross-species transmission can occur. As such, McHV1 is an important zoonotic disease for humans interacting with macaque species. Exposure to infected bodily fluids via mucosa membranes, open skin, and penetrating wounds can result in infection. Infection may produce vesicular lesions at the site of exposure, flu-like symptoms of fatigue, body aches, and fever, and fatal encephalitis has occurred in greater than 70% of documented cases. Excellent reviews detailing prevention and post-exposure treatment are available.[4,6,7]

Spontaneous disseminated McHV1 infection in macaque species that results in death or euthanasia is infrequent, and animals that develop any McHV1 lesions are typically culled rather than treated clinically due to the zoonotic risk to personnel. Primary and latent reactivation resulting in systemic infection has been described in rhesus (*M. mulatta*), cynomolgus (*M. fascicularis*), bonnet (*M. radiata*), and pigtail (*M. nemestrina*) macaques and virus has been isolated from brain, oral cavity, esophagus, liver, adrenal gland, pancreas, and skin.[1,2,3,5,11,12] Latent reactivation is typically associated with immunosuppression by comorbid disease, including dystocia and simian retrovirus type D infection, social stress, and with chronic administration of immunosuppressive drugs.[1,2,3,11,12] In this case, serologic testing suggests this was a naïve animal that contracted McHV1 from another animal in the cohort. Review of the clinical history and experimental treatments did not reveal a potential source of immunosuppression. Testing for simian type D retrovirus was done multiple times over a six-year period with consistently negative results (blood, cell culture; serum, IF membrane antibody).

**JPC Diagnosis:** Pancreas: Pancreatitis, necrotizing, acute, multifocal and random, with syncytia, eosinophilic intranuclear viral inclusion bodies, mild interstitial edema, and diffuse exocrine atrophy, cynomolgus macaque, (*Macaca fascicularis*), primate.

**Conference Comment:** The contributor provides an excellent review of *Macacine herpesvirus 1.* Herpesviruses are a large, diverse group of viruses that have been found in almost every species of birds and mammals, as well as in insects, fish, reptiles, amphibians, and mollusks. The order *Herpesvirales* consists of three families: *Herpesviridae* (herpesviruses of mammals, birds, and reptiles), *Alloherpesviridae* (herpesviruses of fish and frogs), and *Malacoherpesvirida* (a single virus found in oysters). The family *Herpesviridae* are further divided into three subfamilies: *Alphaherpesvirinae*, *Betaherpesvirinae*, and *Gammaherpesvirinae*. Generally herpesviruses are adapted to their individual hosts, often causing disease only in young, immunocompromised individuals or in alternate host species. Persistent infection with periodic or continuous shedding of virus and recurrence of disease brought on by stress occurs in many herpesviral infections. In addition to McHV1, there are numerous members of *Herpesviridae* that are of importance in veterinary medicine (summarized in the included tables).[10]

*Alphaherpesvirinae* is subdivided into four genera: *Simplexvirus, Varicelovirus, Mardivirus,* and *Iltovirus*.[10] Most alphaherpesviruses grow rapidly, lyse infected cells and establish latent infections in sensory ganglia.

Members of subfamily *Betaherpesvirinae* are also divided into four genera: *Cytomegalovirus*, *Muromegalovirus*, *Proboscivirus* and *Roseolovirus*. Betaherpesviruses are generally characterized by a slow replication cycle and delayed cell lysis; they often remain latent in secretory glands, the kidneys, and lymphoreticular tissue.[10]

Gammaherpesviruses are generally lymphotropic and reside latent in lymphocytes. Some

gammaherpesviruses have been linked to oncogenic transformation of lymphocytes such as Epstein-Barr virus resulting in Burkitt's lymphoma. Although gammaherpesviruses of ruminants and nonhuman primates generally do not cause significant disease in their immunocompetent natural hosts, some may cause severe lymphproliferative disease in alternate hosts.[10]

**Alphaherpesviruses of importance in veterinary medicine[10]:**

| | |
|---|---|
| Bovine Herpesvirus 1 | Infectious Bovine Rhinotracheitis and Infectious Pustular Vulvovaginitis Viruses |
| Bovine Herpesvirus 2 | Mammillitis/ Psuedo-Lumpy Skin Disease Virus |
| Bovine Herpesvirus 5 | Bovine Encephalitis Virus |
| Canid Herpesvirus | Systemic hemorrhagic disease in pups <4 weeks old |
| Caprine Herpesvirus | Abortion; Infectious pustular vulvovaginitis |
| Macacine Herpesvirus 1 | B Virus disease of macaques (formerly Cercopithecine Herpesvirus 1) |
| Herpes simplex 1 | Severe generalized disease with high mortality in New World primates |
| Cercopithecine Herpesvirus 9 | Simian Varicella Virus |
| Equid Herpesvirus 1 | Equine Abortion Virus |
| Equid Herpesvirus 3 | Equine Coital Exanthema Virus |
| Equid Herpesvirus 4 | Equine Rhinopneumonitis Virus |
| Felid Herpesvirus 1 | Feline Rhinotracheitis Virus |
| Gallid Herpesvirus 1 | Avian Infectious Laryngotracheitis Virus |
| Gallid Herpesvirus 2 | Marek's Disease Virus |
| Suid Herpesvirus 1 | Pseudorabies or Aujeszky's Disease Virus |

**Betaherpesviruses of importance in veterinary medicine[10]:**

| | |
|---|---|
| Murid Herpesvirus 1 | Mouse Cytomegalovirus |
| Murid Herpesvirus 2 | Rat Cytomegalovirus |
| Caviid Herpesvirus 2 | Guinea Pig Cytomegalovirus |
| Rhesus Cytomegalovirus | *Many Old and New World non-human primates have their own cytomegaloviruses |
| Elephantid Herpesvirus | Endotheliotropic Elephant Herpesvirus |
| Suid Herpesvirus 2 | Porcine Cytomegalovirus |

**Gammaherpesviruses of importance in veterinary medicine[10]:**

| | |
|---|---|
| Alcelaphine Herpesvirus 1 | Malignant Catarrhal Fever |
| Ovine Herpesvirus 2 | Malignant Catarrhal Fever |
| Equid Herpesvirus 5 | Multinodular Pulmonary Fibrosis |
| Saimiriine Herpesvirus 2 (Herpesvirus saimiri) and Herpesvirus ateles | T lymphocytotropic virus that causes subclinical latent infections in squirrel monkeys (*H. saimiri*) and spider monkeys (*H. ateles*), but rapid and fatal lymphoproliferative disease in New World monkeys (marmosets, tamarins, owl monkeys) |
| Retroperitoneal Fibromatosis Herpesvirus and Rhesus Rhadinovirus | Retroperitoneal fibromatosis and B-cell lymphomas in retroviral-infected Rhesus macaques |

**Unassigned members of Herpesviridae of importance in veterinary medicine[10]:**

| | |
|---|---|
| Anatid Herpesvirus 1 | Duck Viral Enteritis Virus; Duck Plague Virus |

**Contributing Institution:** Oregon National Primate Research Center
http://onprc.ohsu.edu

## References

1. Anderson DC, Swenson RB, Orkin JL, Kalter SS, McClure HM. Primary *Herpesvirus simiae* (B-virus) infection in infant macaques. *Lab Anim Sci*. 1994;44 (5):536-530.
2. Carlson CS, O'Sullivan MG, Jayo MJ et al. Fatal disseminated Cercopithecine herpesvirus 1 (Herpes B) infection in cynomolgus monkeys (*Macaca fascicularis*). *Vet Pathol.* 1997;34:405-414.
3. Chellman GJ, Lukas VS, Eugui EM, Altera KP, Almquist SJ, Hilliard JK. Activation of B virus (*Herpesvirus simiae*) in chronically immunosuppressed cynomolgus monkeys. *Lab Anim Sci*. 1992;42(2): 146-151.
4. Cohen JI, Davenport DS, Stewart JA, Deitchman S, Hilliard JK, Chapman LE. Recommendations for prevention and therapy for exposure to B virus (*Cercopithecine herpesvirus* 1). *Clin Infect Dis*. 2002;35:1101-1203.
5. Daniel MD, Garcia FG, Melendez LV, Hunt RD, O'Connor J, Silva D. Multiple *Herpesvirus simiae* isolation from a rhesus monkey which died of cerebral infarction. *Lab Anim Sci*. 1975;25(3):303-308.
6. Elmore D, Eberle R. Monkey B virus (*Cercopithecine herpesvirus* 1). *Comp Med*. 2008;58 (1):11-22.

7. Estep RD, Messaoudi I, Wong SW. Simian herpesviruses and their risk to humans. *Vaccine*. 2010;28S:B78-B84.
8. Huff JL, Barry PA. B-virus (*Cercopithecine herpesvirus* 1) infection in humans and macaques: potential for zoonotic disease. *Emerg Infect Dis*. 2003;9(2):246-250.
9. Lees DN, Baskerville A, Cropper LM, Brown DW. *Herpesvirus simiae* (B virus) antibody response and virus shedding in experimental primary infection of cynomolgus monkeys. *Lab Anim Sci*. 1991;41:360-364.
10. Maclachlan NJ, Dubovi EJ, Herpesvirales. In: *Fenner's Veterinary Virology*. 4th ed. London, UK: Elsevier; 2011:179-201.
11. Scharf BA, Wan CH, Bluth M, et al. Lethargy, ulcers, bronchopneumonia and death in two aged female bonnet macaques presumed to be caused by Cercopithecine herpes virus 1. *J Med Primatol*. 2008;37(Suppl1):60-64.
12. Simon MA, Daniel MD, Lee-Parritz D, King NW, Ringler DJ. Disseminated B virus infection in a cynomolgus monkey. *Lab Anim Sci*. 1993;43(6): 545-550.

**Joint Pathology Center**
**Veterinary Pathology Services**

# WEDNESDAY SLIDE CONFERENCE 2012-2013

## Conference 8

**14 November 2012**

**CASE I:** A2010-02 (JPC 3164123).

**Signalment:** 7-year-old female Golden Retriever, canine (*Canis lupus familiaris*).

**History:** An incisional biopsy of a right mandibular mass is submitted by the referring veterinarian for histopathology.

**Gross Pathologic Findings:** Several fixed sections of a bony oral mass are submitted.

**Histopathologic Description:** Infiltrating the submucosa and extending to tissue borders is a non-encapsulated, poorly delineated epithelial neoplasia. There are coalescing islands and cords of epithelial cells supported by a variably dense collagenous stroma with few foci of osseous metaplasia. The epithelial cells have prominent intercellular junctions and often display palisading around the periphery with polarization of nuclei away from the associated

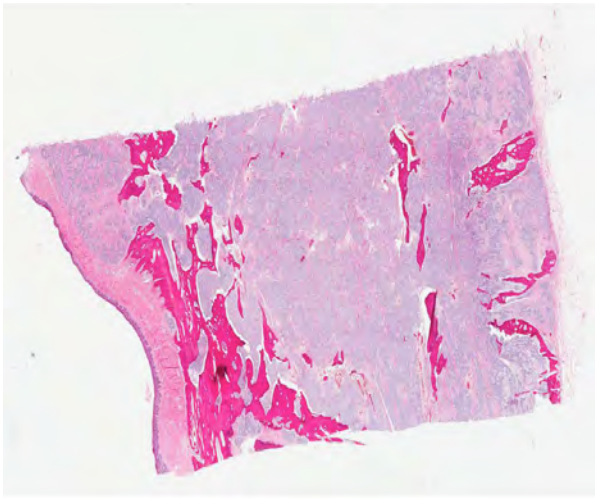

*1-1. Dog, mandible: The mandible is effaced by an infiltrative unencapsulated neoplasm, which focally extends into the overlying mucosa. Acanthomatous ameloblastomas such as this are often referred to as "central", as opposed to "peripheral" tumors, which arise in the submucosa and invade downward into the bone. (HE 0.63X)*

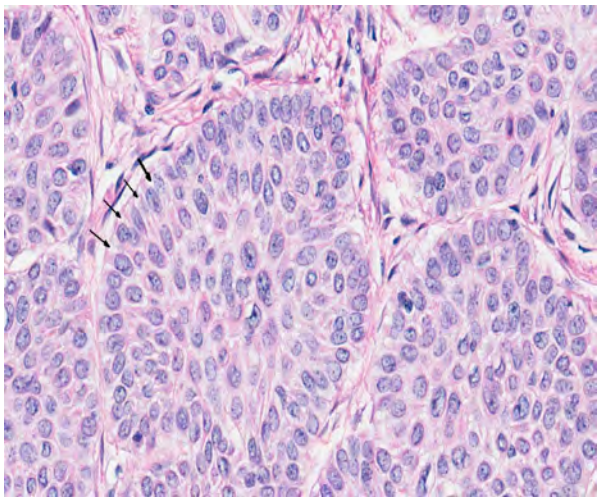

*1-2. Columnar neoplastic cells palisade along the periphery of islands, and characteristically exhibit antibasilar nuclei basilar cytoplasmic clearing (arrows). (HE 210X)*

basement membrane. There is moderate anisocytosis and anisokaryosis.

**Contributor's Morphologic Diagnosis:** Acanthomatous ameloblastoma.

**Contributor's Comment:** The mass is consistent with an acanthomatous ameloblastoma (acanthomatous epulis, peripheral ameloblastoma). This is a common tumor in dogs of odontogenic epithelial origin.[2] These gingival tumors arise in the oral cavity on the mandible or maxilla and seem to exhibit a predilection for the mandibular incisor-premolar region (adjacent to the canines).[7] The masses present as exophytic, verrucous lesions and histologically the coalescing cords of neoplastic odontogenic epithelium have peripheral palisading with reverse polarity of the nuclei (away from basement membrane) and prominent intercellular bridges centrally typical of stellate reticulum.[2,4,5] Clinically, these tumors are characterized by rapid growth, invasive infiltration and repeated recurrences following incomplete removal (91% recurrence with marginal excision). Bone invasion is routinely described although metastasis is not considered to be a feature of this neoplasia.[2,4,5,6,7] Complete removal, hemimandibulectomy, and chemotherapy with bleomycin appear to be effective treatment options for acanthomatous ameloblastomas.[7]

Another common name for this tumor is acanthomatous epulis although acanthomatous ameloblastoma correctly identifies this tumor as a neoplasia of odontogenic epithelial origin. Epulis is a non-specific, clinical designation used to describe localized, exophytic, non-neoplastic and neoplastic gingival growths.[4,6,7] Epulides are generally classified as fibromatous, ossifying and giant cell types with fibromatous epulides occurring most frequently. Fibromatous, ossifying, and giant cell epulides are thought to be developmental, inflammatory and/or hyperplastic in origin and often develop in association with chronic inflammation (periodontal disease) whereas acanthomatous ameloblastomas are invasive, recurrent and generally occur in animals with milder dental plaque and inflammation. Shetland sheepdogs and mixed breed dogs appear to develop all types of epulides and acanthomatous ameloblastomas. Fibromatous, ossifying and giant cell epulides most commonly develop from the gingiva around the maxillary and mandibular premolars whereas acanthomatous epulides (71%) arise from the gingiva around the maxillary and mandibular canines. Marginal excision is generally curative for fibromatous, ossifying and giant cell epulides (90%) although acanthomatous ameloblastomas persistently exhibit invasive growth, bone infiltration and recurrence following marginal excision.[7]

**JPC Diagnosis:** Gingiva: Acanthomatous ameloblastoma.

**Conference Comment:** Ameloblastomas are tumors of odontogenic origin that arise from dental lamina rests, the developing enamel organ, the epithelial lining of an odontogenic cyst, or the basilar epithelial cells of the gingival surface epithelium. Microscopically, ameloblastomas resemble the enamel organ of a developing tooth, mimicking its inner enamel epithelium and central stellate reticulum.[1]

Conference participants discussed the variation in odontogenic tumor naming and classification schemes in veterinary and human medicine. In humans, ameloblastomas are classified into several clinicopathologic subtypes: conventional solid or multicystic, unicystic and peripheral.[1] The vast majority of human ameloblastomas are of the conventional solid or multicystic type, which appear grossly as intraosseous growths with both solid and cystic areas. Microscopically the growth pattern of these tumors are divided into the more common follicular and plexiform patterns and the less common acanthomatous, granular cell, desmoplastic, and basal cell patterns. The follicular variants appear as islands of odontogenic epithelium within a mature fibrous stroma, often with cyst formation. The plexiform variant is composed of long anastomosing cords and sheets of odontogenic epithelium, on a more loosely arranged, vascular stroma, with cysts formation much less common. Other, less common variants include the acanthomatous variant, in which squamous differentiation with keratinization or keratin pearl formation occurs within the central regions of the tumor islands, and the granular cell variant, which is composed of cells with abundant eosinophilic, granular cytoplasm within the center of the tumor islands. In the desmoplastic variant the stroma is composed of dense collagen, and the epithelial component is relatively sparse. The basal cell variant closely resembles basal cell carcinomas of the skin; they exhibit nests or islands of basaloid epithelial cells, with less evident peripheral nuclear palisading and reverse polarization and no stellate reticulum. It is possible to have multiple types within the same tumor, and the microscopic diagnosis is made based on the dominant growth pattern. All subtypes of conventional ameloblastomas tend to be locally aggressive and tend to recur with conservative treatment. A second subtype of ameloblastoma in humans is the unicystic ameloblastoma; these tend to occur in younger patients and exhibit less aggressive biological behavior than their conventional counterparts. Microscopically these tumors appear as a single cystic sac. The third subtype, peripheral ameloblastoma, arises within soft tissue, as opposed to the other intraosseous forms. Clinically these tumors may look like a fibroma,

granuloma or papilloma. Microscopically, they are similar to conventional ameloblastomas and follicular, plexiform, acanthomatous and basal cells patterns are possible. Odontogenic epithelium is often exhibited but stellate reticulum-like differentiation may not be evident. Neoplastic epithelium may be continuous with overlying surface mucosal epithelium. Peripheral ameloblastomas exhibit a less aggressive behavior and have a lower recurrence rate than their intraosseous counterparts.[1]

Tumors of odontogenic epithelium without odontogenic mesenchyme in animals are classified as peripheral or central ameloblastomas, amyloid-producing odontogenic tumors, or acanthomatous ameloblastomas.[3] Peripheral and central ameloblastomas are defined as tumors occurring from gingival soft tissue or deeper tissue within the bone of the jaw, respectively. Acanthomatous ameloblastomas are more aggressive and can be differentiated from peripheral ameloblastomas by an increased amount of stroma that resembles periodontal ligament connective tissue (characterized by abundant fibrillar collagen, regularly-positioned stellate mesenchymal cells, and regularly dispersed empty blood vessels) and a plexiform pattern consisting of interconnecting cords and sheets of epithelium. Cysts often form in acanthomatous ameloblastomas, but keratinization or keratin pearl formation is rare. Keratinization is more common in ameloblastomas, and heavily keratinized ameloblastomas may be difficult to differentiate from squamous cell carcinoma.[3]

**Contributing Institution**: TVMDL
PO Box 3200
Amarillo, TX 79116-3200
http://www.tvmdl.tamu.edu

**References:**

1. Chi AC, Neville BW. Odontogenic cysts and tumors. *Surgical Pathology Clinics*. 2011;4(4):1027-1091.
2. Head KW, Else RW, Dubielzig RR. Tumors of the alimentary tract. "Canine Acanthomatous Ameloblastoma". In: *Tumors in Domestic Animals*. 4th ed. Ames, Iowa: Iowa State Press; 2002:405-406.
3. Head KW, et al. Tumors of odontogenic epithelium without odontogenic mesenchyme. In: *Tumors of the Alimentary System of Domestic Animals.* Washington DC: AFIP and CL Davis DVM Foundation and WHO Collaborating Center for Worldwide Reference on Comparative Oncology; 2003: 49-51.
4. Gardner DG. Epulides in the dog: a review. *J Oral Path Med*. 1996;25:32-37.
5. Gardner DG, Baker DC. The relationship of the canine acanthomatous epulis to ameloblastoma. *J Comp Path*. 1993;108:47-55.
6. Verstraets FJM, Ligthelm AJ, Weber A. The histological nature of epulides in dogs. *J Comp Path*. 1992;106:169-182.
7. Yoshida K, Yanai T, Iwasaki T, Sakai H, Ohta J, Kati S, et al. Clinicopathological study of canine oral epulides. *J Vet Med Sci*. 1999;61(8):897-902.

**CASE II:** T12-13569 (JPC 4019453).

**Signalment:** Unknown age, male neutered domestic shorthair, feline (*Felis catus*).

**History:** The cat had a clinical history of drooling for about two months. An oral examination was made to determine the cause and a 1 x 2 x 2 cm growth was present on the upper gingiva near the left incisor. Neoplasia or gingival hyperplasia was suspected. The mass was surgically removed and submitted to the lab in 10% buffered formalin solution for histopathological evaluation.

**Gross Pathology:** Grossly, the tissue contained a multilobulated mass.

**Histopathologic Description:** The gingival submucosa is expanded by a poorly demarcated, unencapsulated, multilobulated neoplasm. The neoplasm is composed of trabeculae, cords, islands and nests of basaloid to cuboidal/columnar and polygonal cells supported on ample fibrovascular stroma. The neoplastic cells occasionally exhibit a palisading pattern on the periphery, often surround light eosinophilic amorphous to fibrillar material and centrally located fragments of laminated keratin. The neoplastic cells have distinct cell borders, scant to ample eosinophilic cytoplasm, and round to oval nuclei with finely stippled nuclear chromatin. The nucleoli are variably distinct. Scattered mitotic cells (0-2/HPF) are observed. Multifocally, the polygonal cells exhibit squamous differentiation. Multifocal areas of osteoid formation and mineralization are evident in the mass. The light eosinophilic material stains positive for Congo red dye, remains congophilic after treatment with potassium permanganate and exhibits apple-green birefringence under polarized light.

**Contributor's Morphologic Diagnosis:** Amyloid-producing odontogenic tumor (APOT).

**Contributor's Comment:** Two broad groups of epithelial odontogenic tumors are recognized: tumors lacking inductive properties on connective tissue and those having inductive properties on connective tissue. Ameloblastoma and calcifying epithelial odontogenic tumors (amyloid- producing odontogenic tumors) are considered non-inductive. In contrast, ameloblastic fibroma, dentinoma, ameloblastic odontoma, complex odontoma, and compound odontoma have inductive influence on the oral mesenchyme.[7] Amyloid-producing odontogenic tumor (APOT) is a rare oral neoplasm reported in dogs and cats and contains variable amounts of amyloid deposition in the neoplastic mass.[2] Amyloid is comprised of a heterogeneous group of proteins derived from any of at least 25 different precursor molecules, and is considered a pathologic substance that appears histologically as an extracellular, amorphous, congophilic protein with green birefringence under polarized light.[5]

In humans, a neoplasm similar to amyloid producing odontogenic tumor in animals is named a calcifying epithelial odontogenic tumor (CEOT). Amyloid-producing odontogenic tumor was originally referred to as the counterpart of human CEOT. However, it was later described that APOT in dogs and cats is not a counterpart of CEOT in humans. Human CEOTs consist of sheets of eosinophilic epithelial cells showing considerable nuclear pleomorphism and invasive growth, whereas APOTs in animals mostly show basal cells with hyperchromatic nuclei, are arranged in palisades, and are benign masses that grow by expansion.[5] Due to such differences, amyloid-

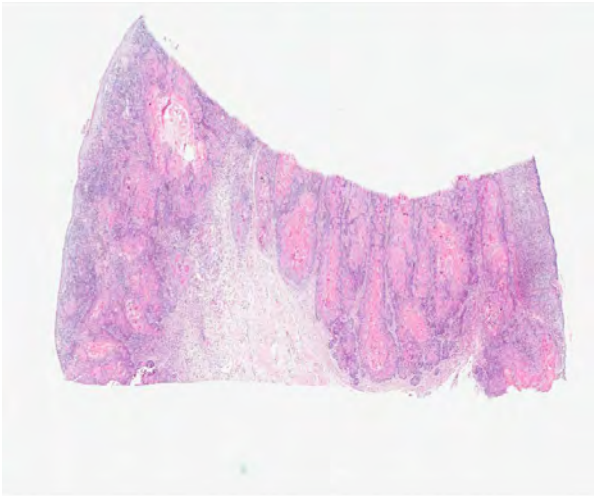

*2-1. Dog, mandible: The ulcerated oral mucosa contains a well-demarcated infiltrating odontogenic neoplasm. (HE 4X)*

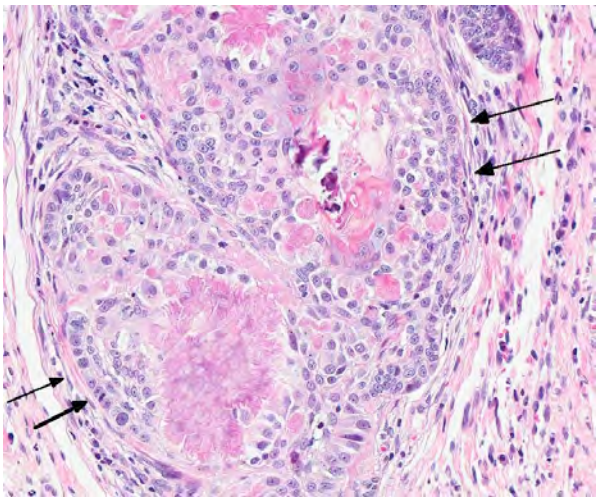

*2-2. Cat, gingiva: Neoplastic cells are cuboidal to columnar, palisade along the periphery, and are separated by abundant waxy eosinophilic material (amyloid) which is occasionally mineralized. (HE 192X)*

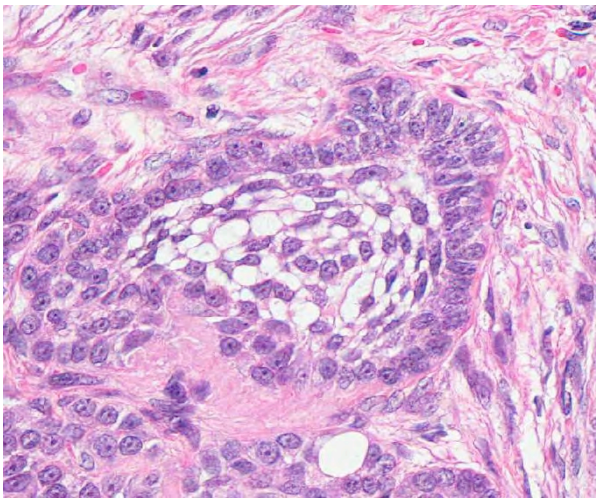

*2-3. Cat, gingiva: Occasionally, neoplastic cells surround a central focus of loosely arranged small spindle to stellate cells on a pale myxomatous matrix (stellate reticulum). (HE 356X)*

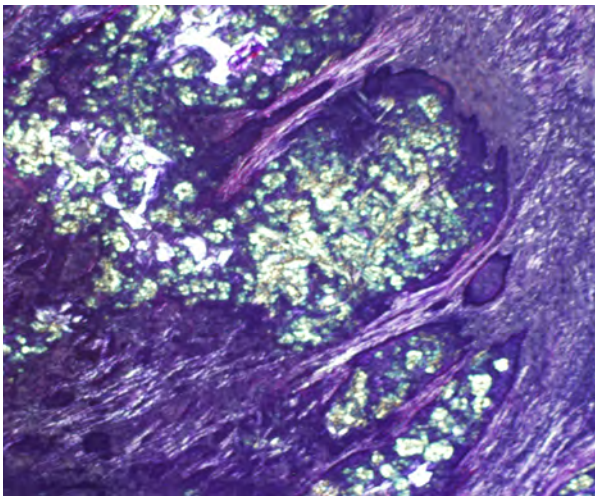

*2-4. Cat, gingiva: Amyloid within the neoplasm exhibits strong apple-green birefringence under polarized light. (Congo red, 100X) (Photo courtesy of the Tifton Veterinary Diagnostic and Investigational Laboratory, Tifton, GA 31793, http://www.vet.uga.edu/dlab/tifton/index.php)*

producing odontogenic tumor (APOT) was proposed as an appropriate alternative term for CEOTs in animals.[4]

Amyloid-producing odontogenic tumor is characterized by dental epithelium, with deposits of amyloid and sometimes prominent trabeculae of osteoid (dentinoid). The epithelium may be arranged in strands, nests or masses. Occasionally, there may be areas of mineralization of the epithelium or stroma in the form of small nodules or amorphous masses.[2] The distinctive features of calcifying epithelial odontogenic tumors in cats and dogs are the spherical amyloid-like deposits, which may undergo concentrically laminated calcification within the epithelial islands and stroma.[7]

It is believed that APOT passes through various developmental stages in which the neoplastic epithelium degenerates, forming amyloid globules which coalesce and calcify. However, the amyloid component seen in animal odontogenic tumors has not been thoroughly examined. Whether it is a secreted substance or a degenerative product remains controversial.[8] The neoplasm is suggested to originate from oral gingival epithelium or odontogenic epithelium within the connective tissue of the gingiva or within bone.[4] The amyloid in these tumors is suggested to be a secretory product of the neoplastic cells and possibly reflects an attempt to produce enamel by neoplastic ameloblasts.[1] Hirayama and co-workers examined the immunohistochemical profile of the amyloid protein from canine APOT using antibodies to ameloblastin, sheathlin, and amelogenin.[4] The neoplastic epithelial cells of APOT were focally reactive with antibodies to ameloblastin, sheathlin, amelogenin, and canine APOT amyloid. The similarity in amino acid sequence of the amyloid protein of canine APOT to that of enamel proteins, such as ameloblastin, sheathlin, and amelogenin, and the expression of these antigens in both APOT amyloid and in the neoplastic cells suggest that the amyloid of canine APOT is derived from enamel proteins secreted by ameloblasts. Based on these findings, the authors concluded that the precursor protein of amyloid fibrils in canine APOT may be derived from enamel proteins produced by ameloblasts and proposed that canine amyloid-producing odontogenic tumor (APOT) would more properly be named as canine amyloid-producing ameloblastoma (APA).[5] If this would apply to feline amyloid-producing odontogenic tumor remains to be determined.

In animals, almost all epithelial odontogenic tumors warrant a good prognosis. None has ever been reported to metastasize. They remain localized in the mandible or the maxilla, where they cause swelling and distortion. Complete surgical excision is usually curative. There is one exception to this rule: the calcifying epithelial odontogenic tumor (amyloid-producing odontogenic tumor) in cats and dogs, which although histologically benign is usually a locally invasive neoplasm and can cause destruction of bone and displacement of teeth.[7,8] Some cases were described to recur after excision.[4] In most cases, the neoplasms are considered as low grade malignancy and rarely metastasize.[8]

**JPC Diagnosis:** Amyloid-producing odontogenic tumor.

**Conference Comment:** As the contributor discussed in an excellent overview of amyloid-producing odontogenic tumors, recent studies have suggested the

protein in canine APOTs is derived from an ameoblastin-like peptide (AAmel), in contrast to the odontogenic amyloid ameloblastic-associated protein (ODAM) found in human CEOTs.[3] In an even more recent study, Delaney and co-workers analyzed the amyloid of three feline APOTs, and found the amyloid from all three feline APOTs to contain an ameloblastin peptide identical to the AAmel that had previously been identified in APOTs from a cat, a dog, and a tiger. Furthermore, the presence of ameloblastin is consistent with the findings of a similar enamel protein in the amyloid of APOTs from a Shih Tzu and eight other dogs, all of which were immunoreactive to rat ameloblastin, porcine amelogenin and sheathlin; however, unlike their canine counterparts, neither the feline amyloid nor the feline neoplastic epithelium exhibited positive immunoreactivity for amelogenin. Ameloblastin (formerly called sheathlin) is an enamel matrix protein that maintains the differentiation state of the ameloblast and is essential for enamel formation. Ameloblastin and amelogenin (another enamel protein) are both produced by ameloblasts during amelogenesis. In addition to ameloblastin, the feline APOTs in this study also showed positive immunoreactivity with laminin antibodies. Laminins are found in dental basement membrane during early tooth development; hence its presence in the amyloid of APOTs further suggests APOTs are ameloblastic in origin.[3]

Additionally, in Hirayama and co-workers' study of canine APOTs, the neoplastic cells exhibited positive immunoreactivity for cytokeratins (CK) AE1/AE3, CK9 and CK14. In the feline study, neoplastic cells were positive for CK AE1/AE3, CK14 and CK19. CK14 and CK19 are type I intermediate filaments of odontogenic epithelium; however, they are not specific, as they are also expressed in inner and outer enamel epithelium, cells from the stellate reticulum, stratum intermedium, dental lamina and Serres rests of the developing tooth.[3]

Overall, these results suggest that ameloblasts are the cell of origin of canine and feline APOTs, and ameloblasts produce the amyloid found in APOTs. Furthermore, feline and canine APOTs both apparently produce a similar type of amyloid which is distinct from the ODAM found in human CEOTs.[3]

**Contributing Institution:** The University of Georgia
College of Veterinary Medicine
Department of Pathology
Tifton Veterinary Diagnostic and Investigational Laboratory
Tifton, GA 31793
http://www.vet.uga.edu/dlab/tifton/index.php

**References**

1. Abbott DP, Walsh K, Diters RW. Calcifying epithelial odontogenic tumor in three cats and a dog. *J Comp Pathol.* 1986;96:131-136.
2. Brown CC, Baker DC, Barker IK. Alimentary tract, oral cavity, amyloid producing odontogenic tumor. In: Grant M Ed. *Jubb, Kennedy and Palmer's Pathology of Domestic Animals*. Vol. II, 5th ed. Philadelphia, PA: Saunders Elsevier; 2007:25.
3. Delaney MA, Singh K, Murphy CL, Solomon A, Nel S, Boy SC. Immunohistochemical and biochemical evidence of ameloblastic origin of feline amyloid-producing odontogenic tumors in cats. *Vet Pathol.* Published online 25 June 2012. http://vet.sagepub.com/content/early/2012/06/25/0300985812452583 Accessed 23 November 2012.
4. Gardner DG, Dubielzig RR, McGee EV. The so-called calcifying epithelial odontogenic tumour in dogs and cats (amyloid-producing odontogenic tumour). *J Comp Pathol.* 1994;111:221–230.
5. Hirayama K, Miyasho T, Ohmachi T, Watanabe T, Yokota H, Taniyama H. Biochemical and immunohistochemical characterization of the amyloid in canine amyloid-producing odontogenic tumor. *Vet Pathol*. 2010;47(5)915-922.
6. Kuwamura M, Kanehara T, Yamate J, Shimada T, Kotani T. Amyloid-producing odontogenic tumor in a Shih-Tzu dog. *J Vet Med Sci.* 2000;62(6):655–657.
7. Poulet FM, Valentine BA, Summers BA. A survey of epithelial odontogenic tumors and cysts in dogs and cats. *Vet Pathol*. 1992;29:369–380.
8. Tsai YC, CR. Jeng, YX Zhuo, YC. Tsai, CH. Liu, VF Pang. Amyloid-producing odontogenic tumor and its immunohistochemical characterization in a Shih Tzu dog. *Vet Pathol*. 2007;44:233–236.

**CASE III:** 11-1832 (JPC 4019823).

**Signalment:** 5-month-old male Great Dane, canine *(Canis lupus familiaris)*.

**History and Gross Pathology:** A 5-month-old male Great Dane was euthanized for multiple congenital heart defects. Necropsy confirmed a clinical suspicion of a ventricular septal defect, pulmonic stenosis, tricuspid dysplasia and severe right ventricular dilation. In addition, both mandibles were uniformly expanded by marked, diffuse bony proliferation that preserved mandibular anatomy. Multiple axial and appendicular bones including the radius, ulna, humerus and femur were sectioned and were normal.

**Histopathologic Description:** Bone, mandible: Diffusely filling and expanding the mandible by 4 to 5 times the normal size, is a well-organized subperiosteal proliferation of bone that extends from the periosteum into the medullary cavity and to the lamina dura of teeth. The cortex is not evident. This bone proliferation is composed of approximately 90% woven bone and 10% lamellar bone, with a concentration of lamellar bone at the periphery. Haversian canals can be seen on cross sections of the trabeculae. Trabeculae are frequently lined by a single layer of well-differentiated osteoblasts that are occasionally interrupted by osteoclasts within Howship's lacunae. Trabeculae are densely packed with small areas separated by moderate amounts of loose fibrous connective tissue mixed with many plump fibroblasts that are punctuated by rare aggregates of degenerative neutrophils and eosinophils, mixed with small amounts of necrotic cellular debris. There is an absence of hematopoietic elements. Multifocally, the cambium is irregularly expanded up to 3 times normal by dense granulation tissue that merges with the bony trabeculae. There is a moderate increase in osteoclastic activity along this junction. Centrally, a single tooth is present and surrounded by periodontal ligament that merges with dentin, with an absence of cementum.

*3-1,2. Dog, mandible: Diffuse thickening of the mandible and tympanic bullae by dense bone. (Photo courtesy of The Department of Anatomic Pathology, PHP Department, College of Veterinary Medicine, N. C. State University, 1060 William Moore Drive, Raleigh, NC 27607.)*

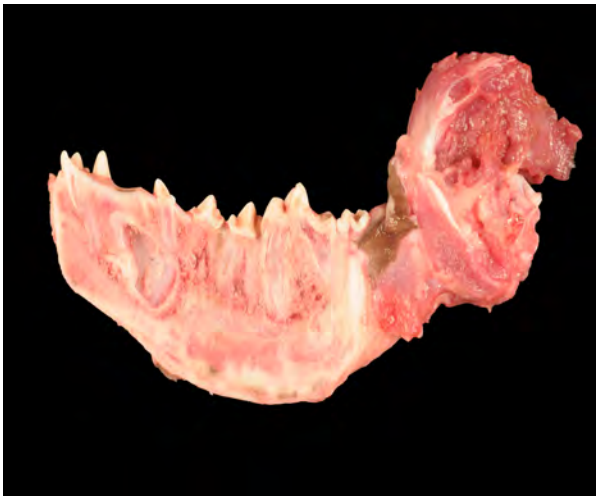

**Contributor's Morphologic Diagnosis:** Bone, mandible: Hyperostosis, diffuse, marked.

**Condition:** Craniomandibular osteopathy.

**Contributor's Comment:** This is a classic case of craniomandibular osteopathy, with bony expansion of the jaw characterized by filling of the medullary spaces with woven bone. Craniomandibular osteopathy (CMO) or "lion jaw" is a nonneoplastic, proliferative bony disease of the dog affecting primarily the mandible, tympanic bullae, and occasionally other bones of the head, and rarely long bones of unknown etiology.[1] The disease predominates in Scottish terriers, West Highland White Terriers, and Cairn Terriers; however, other dog breeds such as boxers, Shetland sheepdog, Great Danes, Doberman pinschers and Labrador retrievers have also been reported in the literature.[1,2,4,5,8,9] The disease is seldom recognized until signs of discomfort due to chewing and eating are observed. This usually occurs when the dogs are 4 to 7 months old. It is likely that this dog was euthanized before clinical signs developed. In addition, the peripheral replacement of woven bone by lamellar bone in this case is suggestive of resolution of the disease. The pathogenesis of CMO is unknown but is likely multifactorial. Some cases resolve spontaneously and in others the pain is so great that owners request euthanasia. This animal has multifocal areas of subperiosteal bone resorption with granulation tissue. This is interpreted to be secondary to trauma or inflammation, rather than as part of the primary disease process.

*3-3. Dog, mandible: Cross section through mandible with a subperiosteal proliferation of trabecular bone up to 1.2 cm thick. The trabeculae are arranged perpendicular to the periosteum and are composed primarily of woven bone with some lamellar bone in closer proximity to the medullary cavity. (HE 4X)*

*3-4. Dog, mandible: The pre-existent cortex with heavily remodeled and largely resorbed. (HE 9X)*

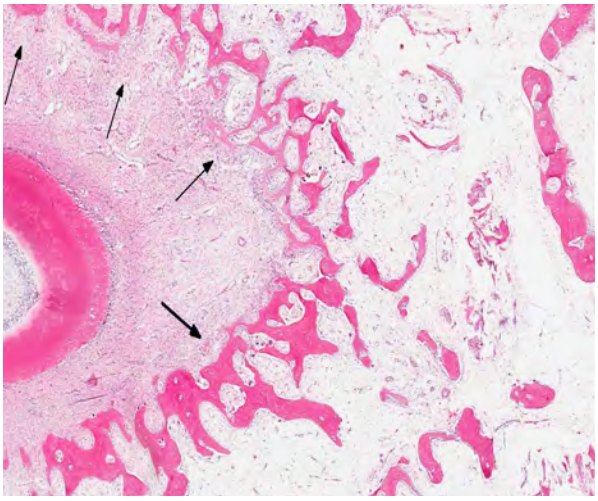

*3-5. Dog, mandible: There is marked resorption of alveolar bone surrounding the tooth (arrows). (HE 11X)*

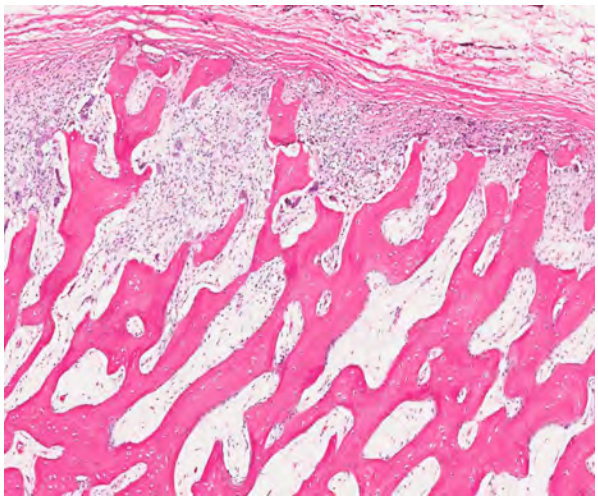

*3-6. Dog, mandible: There is marked remodeling of bone subjacent to the active periosteum. (HE 90X)*

Long-bone involvement has been reported mainly in West Highland White Terriers. In a 1995 retrospective study of 10 terriers, 2 terriers had long-bone involvement.[7] Our dog was a Great Dane and did not have long bone involvement.

**JPC Diagnosis:** Mandible: Subperiosteal new bone growth, diffuse, marked, with medullary fibrosis.

**Conference Comment:** CMO is characterized by intermittent and concurrent bone resorption and production involving the endosteum, periosteum, and trabecular bone of the skull (most often the mandible).[6] As the contributor states, the pathogenesis of CMO is unknown. The occurrence of this condition in multiple breeds may suggest more than one cause.[6] In West Highland White and Scottish Terriers there is some evidence that CMO is an autosomal recessive inherited trait. Alternatively, the presence of inflammation in many cases has raised the suspicion of an infectious etiology, although none has yet been identified. It is also possible that both an inherited predisposition followed by an additional factor or agent is necessary to initiate disease.[6]

Conference participants compared and contrasted CMO and hypertrophic osteopathy (HOD), another syndrome that is characterized by periosteal new bone formation. HOD is often associated with thoracic cavity chronic inflammation or neoplasia, as well as with botryoid rhabdomyosarcoma of the urinary bladder in dogs and ovarian tumors in horses.[6] In

contrast to the distribution of CMO, which is usually confined to the bones of the skull, the periosteal hyperostotic lesions associated with HOD generally occur along the diaphyses and metaphyses of certain bones (predominantly the radius, ulna, tibia, metacarpals, metatarsals); however, HOD bony proliferation can occasionally occur in the mandible as well. Like CMO, the pathogenesis of HOD is poorly understood, and although several mechanisms have been proposed to explain the increased blood flow to the limbs that appears to consistently occur early in HOD, the exact cause remains unknown.[6]

**Contributing Institution**: N.C. State University
Anatomic Pathology PHP Department
College of Veterinary Medicine
1060 William Moore Drive
Raleigh, NC 27607

**References:**

1. Burk RL, Broadhurst JJ. Craniomandibular osteopathy in a Great Dane. *J Am Vet Med Assoc*. 1976;169(6):635-6.
2. LaFond E, Breur GJ, Austin CC. Breed susceptibility for developmental orthopedic diseases in dogs. *J Am Anim Hosp Assoc*. 2002;38:467–477.
3. WH Riser, CD Newton. International Veterinary Information Service, www.ivis.org. Document No. B0055.0685.
4. Schulz S. A case of craniomandibular osteopathy in a Boxer. *J. smd Anim. Pract*. 1978;19:749-757.
5. Taylor SM, Remedios A, Myers S. Craniomandibular osteopathy in a Shetland sheepdog. *Can Vet J*. 36(7): 437–439, 1995.
6. Thompson K. Bones and joints. In: Maxie MG, ed. *Jubb, Kennedy and Palmer's Pathology of Domestic Animal*. Vol. II, 5th ed. Philadelphia, PA: Saunders Elsevier; 2007:106-108.
7. Watson ADJ, Adams WM, Thomas CB. Cranomandibular osteopathy in dogs. *Compendium on Continuing Education for the Practicing Veterinarian*. 1995:17:911.
8. Watson ADJ, Huxtable CRR, Farrow BRH. Craniomandibular osteopathy in Doberman Pinschers. *J. small Anim. Pract.* 1975;16:11-19.
9. Watkins JD, Bradley RR. Craniomandibular osteopathy in a Labrador puppy. *Vet Rec*. 1966;79:262.

**CASE IV:** 11-233 (JPC 4015808).

**Signalment:** 16-year-old, neutered male, mixed breed horse (*Equus caballus*).

**History:** The horse was donated and become part of a research study. The horse received a commercially available *Escherichia coli* O55:B5 lipopolysaccharide (LPS) solution infused via intravenous catheter at a dose of 5 ng/kg/hr for 8 hours. Twenty-four hours later the horse was given 5g/kg of oligofructose (OF) via a nasogastric tube and was euthanized 27 hours later with an Obel laminitis score of 2+.

**Gross Pathology:** Grossly all tissues were within normal limits. Laminar tissue was obtained by sectioning with a bandsaw as previously described.[1] Mid-dorsal laminar sections were trimmed into 2 cm × 1 cm × 0.5 cm strips using a scalpel, formalin-fixed and then processed routinely.

**Histopathologic Description:** Slides were stained with periodic acid-Schiff preparation to highlight the basement membranes. Histologically, there is tapering and retraction of the secondary epidermal lamina leaving empty sleeves of basement membrane trailing off the tips of the secondary epidermal lamina. There is also some retraction of the basement membrane and secondary dermal lamina from between the secondary epidermal lamina, which creates the appearance of a thicker primary epidermal lamina.

**Contributor's Morphologic Diagnosis:** Multifocal degeneration and loss of epidermal lamina.

**Contributor's Comment:** In horses, the hoof is attached to the underlying distal (third) phalanx (P3) by the interdigitation of epidermal and dermal lamina. Laminitis refers to separation of the epidermal and dermal lamina in the hoof, which results in lameness and in chronic cases, rotation of P3. Laminitis can be caused by a variety of insults, including, but not limited to: obesity, endocrinopathies, colic, sepsis, toxemia, diarrhea, shock, lush pastures, excess carbohydrates, drug therapy, intense training, and black walnut shavings.[3,4] Laminitis is typically induced experimentally with oligofructose. This horse was involved in a research project investigating the 'two-hit' hypothesis, which proposes that sequential exposure to inflammatory stimuli (LPS and OF) can exacerbate the laminitic response. Clinically the degree of laminitis (Obel score) has been correlated to the degree of histologic lesions using Politt's grading scheme.[3]

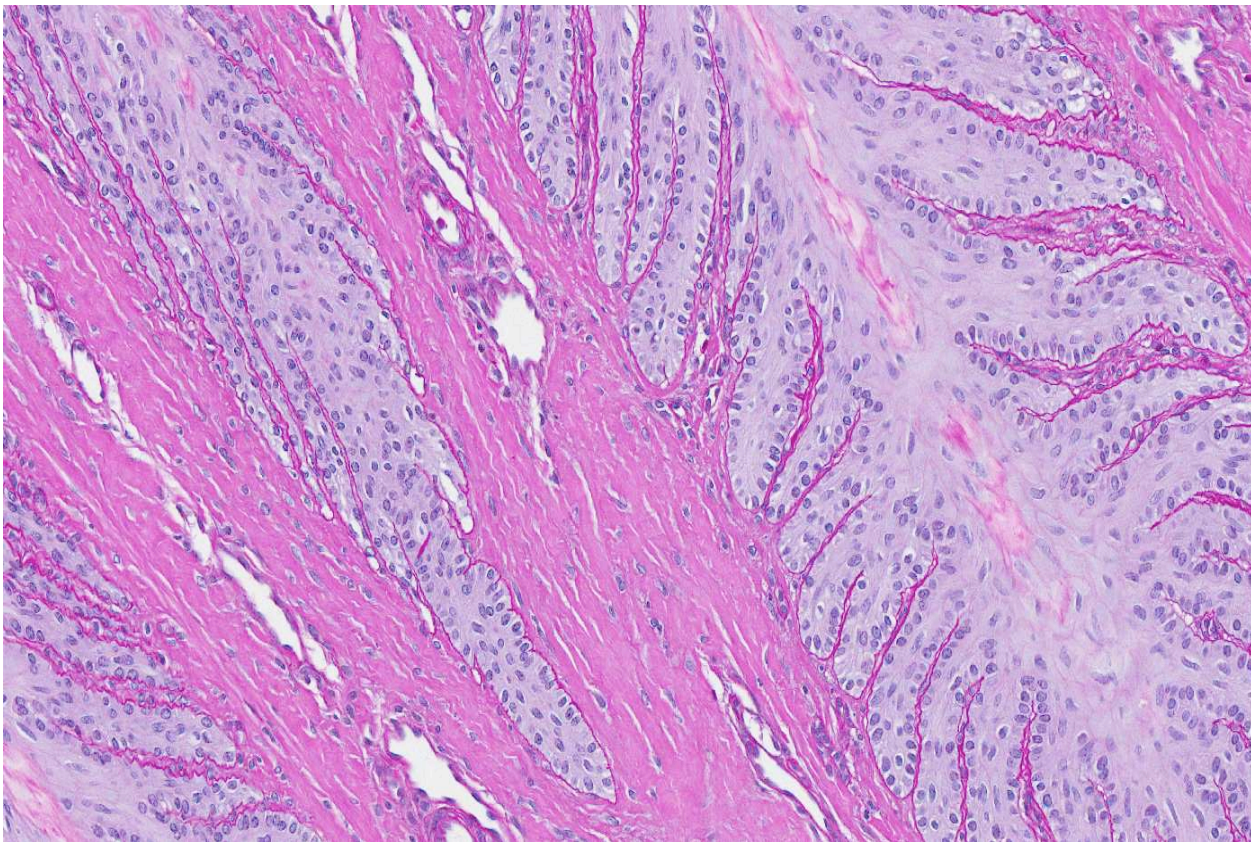

*4-1. Hoof, horse: The epidermal laminae at left demonstrate early lesions of laminitis, with elongation, attenuation and collapse of the normally club-shaped ends of the secondary epidermal lamina (seen at right). (Periodic acid-Schiff, 120X).*

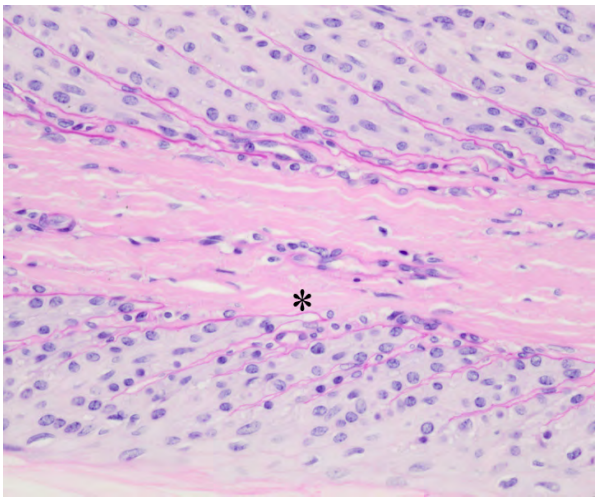

*4-2. Hoof, horse: In early lesions, when epidermal cells detach from the basement membrane, small teat-shaped bubbles may form (asterisk). (PAS, 200X) (Photograph courtesy of the University of Tennessee http://www.vet.utk.edu/departments/path/index.php)*

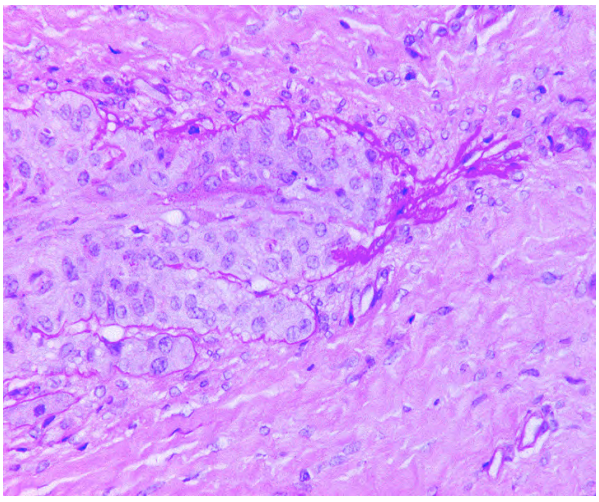

*4-3. Hoof, horse: Retraction of the tip of the primary epidermal lamina may result in fingers of collapsed basement membrane which are well-demonstrated with use of a PAS stain. (PAS 600X) (Photograph courtesy of the University of Tennessee http://www.vet.utk.edu/departments/path/index.php)*

The pathogenesis of laminitis remains complex and poorly understood, but matrix metalloproteinases are present at increased levels in laminitic tissues and are thought to mediate the dissolution of cell-cell and cell-basement membrane adhesion.

The earliest changes involve transformation of the normally club-shaped ends of the secondary epidermal lamina with elongation and attenuation of the tips of the secondary epidermal lamina and detachment from the underlying basement membrane (Grade I). Where the epidermal cells detach from the basement membrane, small teat-shaped bubbles may form. In Grade II lesions, these changes progress and there is retraction of the basement membrane and secondary dermal lamina from between the bases of the secondary epidermal lamina.[4] As the dermal lamina are retracted, the epidermal cells become further from their blood supply, predisposing to subsequent ischemia.[2] Retraction of the capillaries also results in increased resistance to blood flow, which is noticed clinically as 'bounding pulses'. These changes in blood flow can also result in arteriovenous anastomoses or shunts.[3,4] In grade III lesions there is almost complete separation of the epidermal lamina from the basement membrane with loss of distinction between primary and secondary epidermal lamina. Ultimately there is retraction of the tip of the primary epidermal lamina as well.[4] The lesions in this case are most consistent with grade II laminitis.

**JPC Diagnosis:** Hoof lamina: Epidermal laminar degeneration and necrosis with multifocal basement membrane retraction and edema.

**Conference Comment:** As the contributor states, the pathogenesis of equine laminitis is complex and not fully understood. Historically, laminitis has been thought to be due to an ischemic event caused by a vascular condition that constricted blood flow to the hoof.[2] Recent research suggests that degeneration of the primary epidermal lamellae and basement membrane loss may be the initial lesion, with vascular events and subsequent ischemia being an important consequence of the initial laminar degeneration. This "enzymatic theory" of laminitis is based on the findings of significantly increased amounts of matrix metalloproteinase-2 (MMP-2 aka gelatinase A) and matrix metalloproteinase-9 (MMP-9 aka gelatinase B) in lamellar tissues affected by laminitis, as well as the finding that in the developmental phase of laminitis, vessels in the feet are actually dilated rather than constricted. MMPs are found in normal lamellar tissues and are thought to play a role in the required remodeling of the epidermal lamellae that occurs as a normal part of hoof growth. MMPs are produced locally, and function to release epidermal cell-to-cell and cell-to-basement membrane adhesions, maintaining the correct shape and orientation of the hoof lamellae as the hoof grows. The increase of MMP-2 and MMP-9 and the subsequent destruction of the lamellar attachment apparatus has been shown to be a key feature in acute laminitis, although the trigger factors have yet to be elucidated. Interestingly, epidermal cells of some non-equine species, including humans, readily increase their production of MMPs when exposed to cytokines such as TNF, IL-1, and TGH-1; however, in-vitro studies have shown that equine MMPs are not activated on exposure to these cytokines. Additionally, laminitic changes in equine lamellae have not been triggered experimentally by the

administration of endotoxin, prostaglandins, black walnut extract, or anaerobic conditions. The one exception is a factor present in the supernatant from cultures of *Streptococcus bovis* isolated from the horse cecum; this factor has been found to activate equine hoof MMP-2 and has experimentally resulted in lamellar separation. Thus the *S. bovis* MMP activator may play a role in naturally-occurring carbohydrate-overload laminitis.[2] Perhaps with continued research, the complete pathogenesis of equine laminitis will finally be revealed.

**Contributing Institution:** University of Tennessee
http://www.vet.utk.edu/departments/path/index.php

**References:**

1. Pollitt CC. Basement membrane pathology: a feature of acute equine laminitis. *Equine Vet J.* 1996;28:38-46.
2. Pollitt CC. Laminitis pathophysiology. In: Floyd AE, Mansmann RA, eds. *Equine Podiatry.* St. Louis, MO: Saunders Elsevier; 2007.
3. Ginn PE, Mansell JEKL, Rakich PM. Skin and appendages. In: Maxie MG, ed. *Jubb, Kennedy, and Palmer's Pathology of Domestic Animals*. 5th ed. Toronto, CA: Saunders Elsevier; 2007:553-781.
4. Polit CC. Equine laminitis. *Clinical Techniques in Equine Practice.* 2004;3:34-44.

**Joint Pathology Center**
**Veterinary Pathology Services**

# WEDNESDAY SLIDE CONFERENCE 2012-2013

## Conference 9

**28 November 2012**

**CASE I:** 09-1-481 (JPC 3167630).

**Signalment:** 4-year-old female rhesus macaque, *Macaca mulatta*, nonhuman primate.

**History:** A week before necropsy, the animal received intravenous antibiotic therapy (Cefazolin) following surgical placement of hormonal implants as part of a research protocol. A day before necropsy, the animal was lethargic and was reported to be sitting with head tucked under hind limbs and with loss of appetite. On the day of necropsy, abdominal bloating was noted.

The animal was azotemic and hypoglycemic with marked leukopenia and metabolic alkalosis. The animal had not responded to fluid therapy and was euthanized. *Candida albicans* was isolated from the stomach contents at necropsy.

**Laboratory Results:**

| | | Reference Range |
|---|---|---|
| RBC | 6.37 X$10^6$/$mm^3$ | 5.0 - 6.5 X $10^6$/$mm^3$ |
| WBC | 2.8 X$10^3$/$mm^3$ | 6.0 - 15.0 X$10^3$/$mm^3$ |
| Lymphocytes | 19% | 25.0 - 60 % |
| Monocytes | 1% | 0 – 8 % |
| Eosinophils | 0% | 0.0 - 5.0 % |
| pH | 7.304 | >7.40 |
| Sodium | 150 mmol/L | 141-153 mmol/L |
| Potassium | 3.0mmol/L | 2.9-4.1 mmol/L |
| Blood Urea Nitrogen | 82mg/dl | 16-27 mg/dl |
| Glucose | 34 mg/dl | 39-82 mg/dl |


*1-1. Esophagus, rhesus macaque: The mucosa of the esophagus and gastric cardia are multifocally ulcerated, necrotic, hemorrhagic, and edematous. (Photo courtesy of Oregon National Primate Research Center. http://onprc.ohsu.edu)*

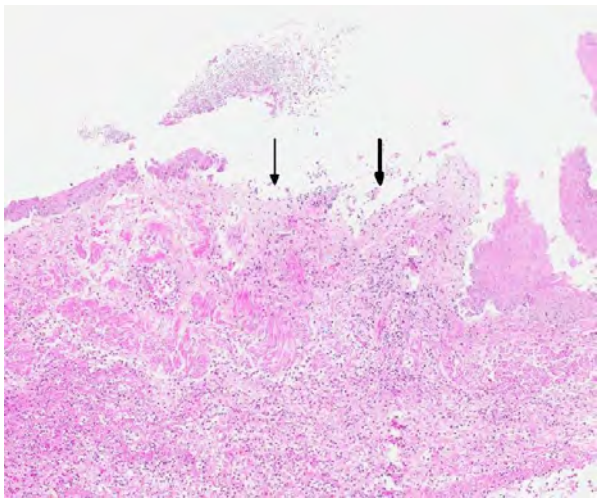

*1-2. Esophagus, rhesus macaque: The mucosal epithelium is multifocally lost (arrows) with infiltration and expansion of the subepithelial connective tissue and submucosa by a large numbers of neutrophils and lesser numbers of macrophages. (HE 60X)*

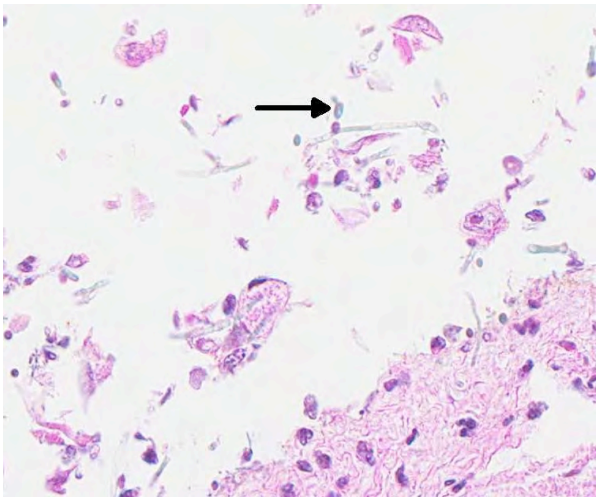

*1-3. Esophagus, rhesus macaque: Within the lumen, mucosa, and rarely the submucosa there are numerous oblong yeasts (arrow) and hyphae, characteristic of Candida species. (HE 400X)*

**Gross Pathologic Findings:** The abdomen was distended and doughy. On opening the abdominal cavity, severe bloating and distension of stomach was noted. The stomach contained about 200 g of partially digested feed material admixed with blood. The mucosa of the esophagus was multifocally ulcerated, thickened with multifocal areas of hemorrhage. The mucosa of the stomach was multifocally ulcerated and hemorrhagic.

**Histopathologic Description:** The stratified squamous epithelium of the esophagus is multifocally necrotic and ulcerated. There is a focally extensive suppurative focus characterized by the presence of large numbers of viable and degenerate neutrophils disrupting the mucosa, submucosa and extending into muscular tunics and serosal layer. Overlaying and infiltrating the necrotic mucosa are aggregates of numerous oval to round, 3-6 µm diameter, pale staining, thin-walled yeast; blastoconidia arranged in short chains (pseudohyphae); and slender, 3-4 µm wide, septate, parallel-walled, hyphae that often show acute angle branching. Multifocally, the collagen fibers in the submucosa are disrupted by edema and the walls of medium and small sized blood vessels are necrotic and infiltrated by neutrophils.

**Contributor's Morphologic Diagnosis:** Esophagus: Esophagitis, necrosuppurative, ulcerative, transmural with vasculitis, intralesional mycelia and yeasts consistent with *Candida albicans.*

**Contributor's Comment:** *Candida albicans* is a normal inhabitant of the nasopharynx, GI tract, and reproductive tract of many species of animals and is opportunistic in causing disease.[2] Predisposing factors include disruption of mucosal integrity, indwelling intravenous or urinary catheters, administration of antibiotics or immunosuppressive drugs and diseases. Activation of virulence factors play a major role in dissemination and colonization in systemic *Candida* infections.[1]

This animal received multiple intravenous antibiotics following surgical implantation of hormonal depots. The gastritis lesions were chronic and the esophageal lesions are attributed to acid reflux and subsequent colonization by *Candida albicans*. In rhesus monkeys infected with simian immunodeficiency virus (SIV), candidiasis is a common opportunistic infection; however, this animal has not been infected with SIV. Also, nonhuman primates are an excellent animal model for studying oral candidiasis.[8,9]

Systemic and cutaneous candidiasis has also been described in cattle, calves, sheep, and foals secondary to prolonged antibiotic or corticosteroid therapy.[4] In cats, candidiasis is rare but has been associated with oral and upper respiratory disease, pyothorax, ocular lesions, intestinal disease, and urocystitis. In dogs, *C. albicans* is reported to cause stomatitis, spondylitis, endophthalmitis and purulent pericarditis.[3,5,6,7] *Candida* spp. has been considered a cause of arthritis in horses and mastitis and abortion in cattle. In birds, the infection causes stomatitis, esophagitis and ingluvitis. In piglets, the infection causes stomatitis, esophagitis and gastritis.[1] In horses, *C. albicans* causes ulcerative gastritis adjacent to margo plicatus.[1]

*Candida* spp. are pleomorphic, with both yeast and mycelia phases present in tissue. The differential diagnoses include: *Aspergillus* species., which form septate hyphae with dichotomous branching and bears conidiospores; *Zycomycetes* species, which form nonseptate, branching hyphae with bulbous enlargement; *Histoplasma capsulatum*, which are intrahistiocytic yeast; and *Blastomyces dermatitidis,* which are 7-17 µm large yeast with broad- based budding.

**JPC Diagnosis**: Esophagus: Esophagitis, ulcerative and neutrophilic, with moderate numbers of extracellular yeast and pseudohyphae.

**Conference Comment**: Conference participants discussed the distinguishing morphologic features of *Candida albicans*, a trimorphic fungus that is one of only three species of *Candida,* along with *C. tropicalis* and *C. dubliniensis,* that occur in three vegetative morphologies: yeast, pseudohyphae, and hyphae. The yeast form, also called blastoconidia or blastospores, are oval, single-celled structures; hyphae and pseudohyphae are filamentous multicellular structures in which elongated cells are attached end-to-end. Psuedohyphae can be differentiated from true hyphae by the following characteristics: Pseudohyphal cell walls are not parallel; rather, they are wider at their center and narrower at their ends, with constrictions at cell junctions. Hyphal cells, on the other hand, have parallel walls, and are more uniform in width, with true septa (internal cross walls that divide the cells). Additionally, true hyphal cells have pores in their septa, allowing for cell-to-cell communication. Although pseudohyphae appear more similar to hyphae microscopically, they are actually more closely related to the yeast form, and thus can be thought of as an intermediate between yeast and true hyphae composed of strings of attached, elongated yeast cells.[10]

Pathogenicity of fungal organisms is related to their morphology. In *Candida albicans,* the single-cell yeast form is thought to be evolutionarily adapted for colonization of mucosal cell surfaces and allows for rapid dissemination via the bloodstream in systemic infections; pseudohyphae are associated with increased virulence properties and enhanced nutrient scavenging; and the formation of hyphae is an important virulence factor which allows the fungus to invade epithelial and endothelial cells and lyse macrophages and neutrophils. The necessity of hyphal formation for pathogenicity is demonstrated by the significant attenuation of virulence in *C. albicans* cells lacking the filament-induced gene HGC1, which drives hyphal development. In addition, several other hyphal-specific genes are also important for pathogenicity. ALS3 and HWP1 encode adhesins, which allow *C. albicans* to leave the circulation, colonize tissue, and form a biofilm. Degredative enzymes such as aspartyl proteinase (SAP) contribute to tissue invasion. SOD5, which encodes a superoxide dismutase that protects against oxidative stress, is also induced during hyphal growth. HYR, another hypha-specific gene, plays a role in neutrophil killing. Thus, the ability of *C. albicans* to form hyphae contributes to their increased virulence compared to other *Candida* species that only form yeast and pseudohyphae.[10]

**Contributing Institution**: Pathology Services Unit
Department of Animal Resources
Oregon National Primate Research Center
505 NW 185th Avenue
Beaverton, OR 97006

**References:**

1. Brown CC, Baker DC, Barker LK. Alimentary system. In: Jubb KVF, Kennedy PC, Palmer N, eds. *Pathology of Domestic Animals*, 5th ed. Edinburgh, Scotland: Saunders Elsevier; 2007:1-106.

2. Brown MR, Thompson CA, Mohamed F. Systemic candidiasis in an apparently immunocompetent dog. *J. Vet. Invest*. 2005;17:272-276.

3. Jadahav VJ, Pal M. Canine mycotic stomatitis due to *Candida albicans*. *Rev Iberoam Micol*. 2006;23: 233-234.

4. Jones T, Hunt R, King N. *Veterinary Pathology*. 6th ed. Baltimore, MD: Williams and Wilkins; 1997:528-529.

5. Kuwamura M, Ide M, Yamate J, Shiraishi Y, Kotani T. Systemic candidiasis in a dog, developing spondylitis. *J. Vet. Med. Sci*. 2006;68(10):1117-1119.

6. Linek J. Mycotic endophthalmitis in a dog caused by *Candida albicans*. *Vet. Ophthal*. 2004;7:159-162.

7. Mohri T, Takashima K, Yamane T, Sato H, Yamane Y. Purulent pericarditis in a dog administered immune-suppressing drugs. *J. Vet. Med. Sci*. 2009;71:669-672.

8. Osborn KG, Prahalada S, Lowenstein LJ, Gardner MB, Maul, DH, Henrickson RV. The pathology of an epizootic of acquired immunodeficiency in rhesus

macaques. *American Journal of Pathology*. 1984;114 (1):94-103.
9. Samaranayake Y, Samaranayake LP. Experimental oral candidiasis in animal models. *Clini. Microbio. Rev*. 2001;14:398-429.
10. Thompson DS, Carlisle PL, Kadosh D. Coevolution of morphology and virulence in Candida species. *Eukaryotic Cell*. 2011;10(9):1173-1182.

**CASE II**: Yn12-31 (JPC 4019363).

**Signalment:** 4-year-old male rhesus macaque (*Macaca mulatta*).

**History:** An adult male rhesus macaque was transferred from CRO to YNPRC and assigned to a renal transplantation study protocol. Post-transplant day 38, the monkey showed signs of failure to thrive after immunosuppression was induced by T-cell depletion and steroids, and maintained on anti-rejection drugs. Animal continued to lose weight despite treatment with low dose steroids and antibiotics. Anemia was diagnosed and treatment with iron and B12, and a transfusion of irradiated whole blood (100mL) were given. Anorexia and weight loss continued. Due to poor prognosis the monkey was euthanized.

**Gross Pathology:** This adult male rhesus macaque weighed 5.20 kilograms. The animal was in a very thin body condition with prominent bony structures. Omental adhesions to the transplanted kidney were present. There were no other gross findings.

**Laboratory Results:**

| Hematology Parameters | Pre-study | Post renal transplant<br>Day 28 | Post whole blood transfusion and<br>Prior to necropsy |
|---|---|---|---|
| **RBC - µl** | 5.31 | 2.31 | 2.93 |
| **Hemoglobin - gm%** | 12.8 | 5.1 | 6.9 |
| **Hematocrit (HCT) - %** | 37.6 | 14.9 | 19.0 |
| **Reticulocyte count (RETIC) - % RBC** | 0.0 | 0.3 | 2.7 |
| **Mean corpuscular volume (MCV) - fl** | 70.8 | 64.5 | 64.8 |
| **Mean corpuscular hemoglobin (MCH) - pg** | 24.1 | 22.1 | 23.5 |
| **Mean corpuscular hemoglobin concentration (MCHC) - g/dL** | 34.0 | 34.2 | 36.3 |
| **Platelets** | 377000 | 373000 | 619000 |
| **WBC** | 8700 | 2860 | 1420 |
| **Neutrophils** | 2436 (28%) | 1801 (63%) | 908 (64%) |
| **Lymphocytes** | 6003 (69%) | 858 (30%) | 454 (32%) |
| **Monocytes** | 87 (1%) | 143 (5%) | 56 (4%) |
| **Eosinophils** | 174 ( 2%) | 57 (2%) | 0 (0%) |

**Histopathologic Description:** Microscopic examination of femoral bone marrow revealed hypercellular marrow with abnormal erythroid cells with bizarre nuclear forms and intranuclear inclusions. These cells have a glassy intranuclear eosinophilic inclusion body, stained pink or lilac, that displaces the chromatin to the periphery. Ultrastructural examination revealed intranuclear viral particles and an occasional viral array characteristic of parvoviruses.

**Contributor's Morphologic Diagnosis:** Hypercellularity of femoral bone marrow with numerous intra-nuclear viral inclusion of Simian Parvovirus.

**Contributor's Comment:** *Simian parvovirus* (SPV) is a erythrovirus within the *Parvoviridae* family, related antigenically to human B19 virus.[1,2,4] All of the primate erythroviruses have a predilection for erythroid precursors. The epizoology of SPV is poorly understood, but infection has been recognized in cynomolgus and rhesus macaques.

In humans, B19 can persist at low levels in the bone marrow of infected humans for extended periods, establishing latency, and a similar situation can be anticipated to occur in macaques with the related SPV. Both viruses target rapidly dividing cells and demonstrate a tropism for cells within the erythrocytic lineage. In immunologically normal animals, infection has not been associated with clinical disease, but with immunosuppression or immunodeficiency; infection may cause anemia and widespread infection of erythroid cells. In bone marrow, poorly-defined eosinophilic intranuclear inclusions may be observed, in association with dyserythropoiesis.[4] Ultrastructural examination and *in situ* hybridization can be used to confirm the diagnosis.[4] Such infections and pathology have been observed in both SIV- and SRV-infected rhesus macaques, as well as in immunosuppressed

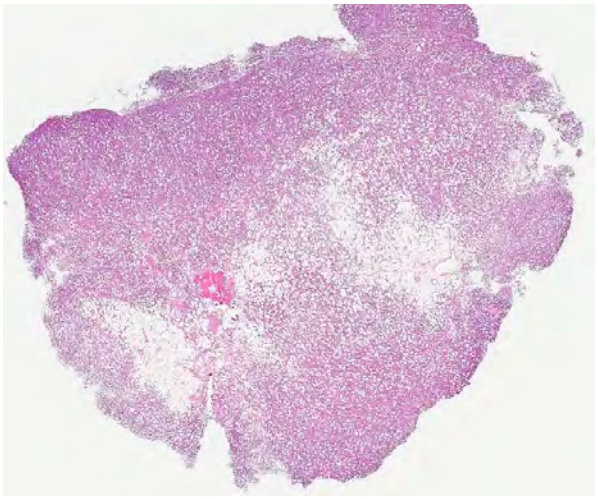

*2-1. Bone marrow, rhesus macaque: The bone marrow is diffusely hypercellular, as evidenced by a subjective decrease in adipose tissue. (HE 20X)*

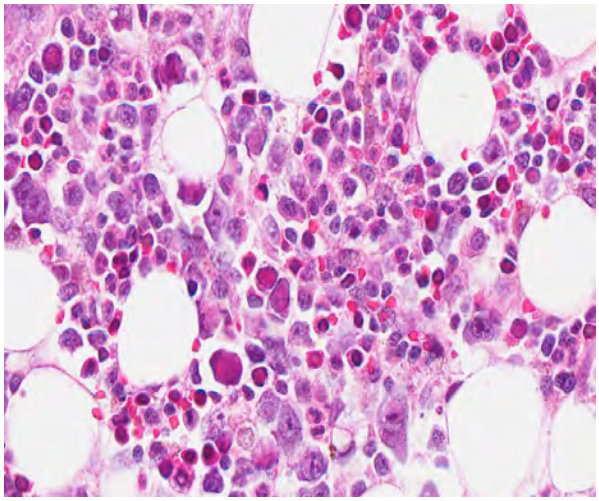

*2-2. Bone marrow, rhesus macaque: Erythroid cells outnumber myeloid cells by a 3:1 margin and often contain large intranuclear viral inclusions. (HE 400X)*

cynomolgus macaques, in which severe clinical anemia has been diagnosed.[1,4]

A SPV infection can be particularly problematic in transplantation studies in which NHPs received some form of immunosuppressive therapy to prevent transplant rejection. Using a combination of molecular detection techniques such as PCR and serologic testing, monkeys can be screened prior to initiation of studies and the selection of viral-negative animals will help prevent transmission from donor to recipient. However, immunosuppression allows latent infection to manifest itself, as in this case.

**JPC Diagnosis**: 1. Bone marrow: Erythrocytic hyperplasia, mild to moderate.
2. Bone marrow, erythrocytic precursors: Intranuclear viral inclusions, numerous.

**Conference Comment:** In addition to discussing simian parvovirus, for which the contributor provided a good review, conference participants also discussed other parvoviruses of importance in veterinary medicine. Viruses in the family *Parvoviridae* are non-enveloped, single-stranded DNA viruses that lack enzymes for DNA replication and thus require host cell DNA polymerase;[3] hence, they replicate in host cell nuclei during the S phase of the cell division cycle. Their need to replicate in cells undergoing cell division determines the pathogenicity of the virus. Infections in fetuses or newborns during organogenesis can lead to serious defects, as the virus destroys developing tissues such as the cerebellum (such as in feline panleukopenia) and the myocardium (such as in canine parvovirus). In older animals, only rapidly dividing cells (hematopoietic precursors, lymphocytes and mucosal cells lining the gut) are affected.[3]

The family *Parvoviridae* is divided into two subfamilies, *Parvovirinae* and *Densovirinae*. *Parvovirinae* contains viruses of vertebrates, and *Densovirinae* viruses affect insects. The *Parvovirinae* subfamily is further divided into five genera: *Parvovirus, Erythrovirus, Dependovirus, Amdovirus, and Bocavirus*.[3] The following tables list parvoviruses of veterinary importance and the diseases associated with them:[3]

**Genus *Parvovirus***

| **Virus** | **Disease** |
|---|---|
| Feline Panleukopenia Virus | Generalized disease in kittens; panleukopenia; enteritis; in-utero or neonatal infection can cause cerebellar hypoplasia; raccoon, mink and coatimundi are also susceptible |
| Mink Enteritis Virus | Leukopenia; enteritis |
| Canine Parvovirus 2 (3 major variants: subtypes 2a, 2b, 2c) | Generalized disease in puppies; enteritis; myocarditis; lymphopenia |
| Porcine Parvovirus | Stillbirth, mummification, embryonic death, infertility (SMEDI); rare respiratory disease, vesicular disease and systemic disease of neonates |
| Rodent Parvoviruses (Mouse parvoviruses, minute virus of mice, Kilham's rat virus, Toolans's H-1 virus of rats) | Subclinical or persistent infection; fetal malformations; hemorrhagic syndrome in rats; Confounding effects on research; hamsters with hamster parvovirus develop periodontal and craniofacial deformities |
| Rabbit Parvoviruses (Lapine Parvovirus) | Usually no clinical signs; may produce disseminated infection, mild enteritis in young kits |

**Genus *Erythrovirus***

| Virus | Disease |
|---|---|
| Non-Human Primate Parvoviruses (Simian Parvovirus, Rhesus Parvovirus, Cynomolgus Parvovirus) | Anemia; fetal abnormalities; related to human B19 virus |

**Genus *Amdovirus***

| Virus | Disease |
|---|---|
| Aleutian Mink Disease Virus | Adults (primarily mink that are homozygous for Aleutian coat color, which is associated with a Chediak-Higashi type abnormality): Chronic immune complex disease; encephalopathy; Neonates: interstitial pneumonia |

**Genus *Dependovirus***

| Virus | Disease |
|---|---|
| Goose Parvovirus | Hepatitis; myocarditis; myositis; lethal disease in 8-30 day old goslings |
| Duck Parvovirus | Hepatitis; myocarditis; myositis in Muscovy ducks |

**Genus *Bocavirus***

| Virus | Disease |
|---|---|
| Bovine Parvovirus | Rarely associated with clinical disease; mild diarrhea in neonates |
| Canine Parvovirus 1 (Canine Minute Parvovirus) | Subclinical; rarely causes diarrhea or sudden death in neonates |

Tables adapted from *Fenner's Veterinary Virology,* 4th ed. 2011.[3]

**Contributing Institution:** Yerkes National Primate Research Center

Emory University
954 Gatewood Road
Atlanta, GA 30329
http://www.yerkes.emory.edu/

**References:**

1. O'Sullivan MG, Anderson DC, Fikes JD, Bain FT, Carlson CS, Green SW, et al. Identification of a novel simian parvovirus in cynomolgus monkeys with severe anemia. *J Clin Invest*. 1994;93:1571–1576.
2. O'Sullivan MG, Anderson DK, Goodrich JA, Tulli H, Green SW, Young NS, et al. Experimental infection of cynomolgus monkeys with simian parvovirus. *J Virol*. 1997;71:4517–4521.
3. Parris CR. Parvoviridae. In: Maclachlan JN, Dubovi EJ, eds. *Fenner's Veterinary Virology.* 4th ed. New York, NY: Academic Press; 2011:225-235.
4. Simon MA. Simian parvoviruses: biology and implications for research. *Comp Med***.** 2008;58:47-50.

**CASE III**: 07221 (JPC 4017799-00).

**Signalment:** 6-week-old Holstein-cross bull calf (*Bos taurus*).

**History:** The calf had chronic ear infections since two weeks of age. No improvement was seen with multiple antibiotics or bilateral myringotomy. Intermittent purulent discharge was seen bilaterally. Persistent worsening neurologic signs include severe ataxia, obtundation, and absence of hind limb reflexes, withdrawal, and deep pain sensation. CT exam of the skull revealed expansion of both tympanic bullae with multifocal areas of marked lysis and soft tissue or caseous material filling the bullae. Similar material was seen in both external ear canals.

**Gross Pathology:** Within the external ear canals, tympanic bullae and inner ears is a severe bilateral white purulent to caseous exudate, with osseous thickening of the tympanic bulla. No gross changes to the meninges are seen.

**Histopathologic Description:** Inner ear: Examined is a cross-section of inner ear consisting primarily of the cochlea within the petrous temporal bone, the adjacent vestibule lined by ciliated epithelium containing abundant mucus cells, and associated vestibulocochlear nerve. In the center of the cochlea is a central core of spongy bone which contains the spiral sensory ganglion. The pseudostratified lining epithelium and associated hair cells of the cochlea are necrotic and replaced by abundant granulation tissue. Filling the vestibule and the cochlea, and abutting portions of the cochlear nerve, is a marked inflammatory exudate comprised of neutrophils, lymphocytes, plasma cells, macrophages associated with severe necrosis, which is evidenced by eosinophilic amorphous cellular debris, basophilic karyorrhectic nuclear debris, and multifocal dystrophic mineralization. Similar necrosis, inflammation and granulation tissue fill the middle ear, which is lined by ciliated pseudostratified epithelium displaying squamous metaplasia. No etiologic agents are seen.

**Contributor's Morphologic Diagnosis:** Severe, chronic, necrosuppurative otitis interna and media.

**Contributor's Comments:** Differentials for otitis interna and media in calves includes: *Histophilus somnus, Mannheimia haemolytica, Pasteurella multiocida, Streptococcus* spp., *Actinomyces* spp., *Arcanobacterium pyogenes,* and *Mycoplasma bovis*.[2,5] A heavy growth of *Mycoplasma* was cultured from an ear swab collected at necropsy, with a light growth of both *E. coli* and non-haemolytic *Streptococcus*. Bacteria were not speciated.

*Mycoplasma* are extracellular bacteria that lack a cell wall and may be transmitted via infected secretions of the respiratory tract, genital tract, or mammary gland from infected cows or other calves.[1] *Mycoplasma* evades the host immune system by suppressing neutrophil and lymphocyte activation, as well as inducing lymphocyte apoptosis.[1] *Mycoplasma* otitis typically affects male dairy calves less than 2 months of age.[3] The pathogenesis of otitis interna and media due to *Mycoplasma* in calves is not completely understood but is thought to involve one or more of the following mechanisms: (1) ingestion of infected milk causing nasopharyngeal infection, with extension through the Eustachian tube to the middle ear, (2)

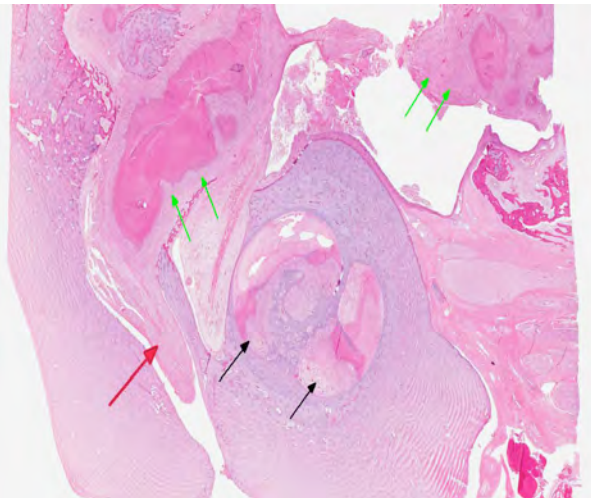

*3-1. Middle and inner ear, calf: The tympanic cavity (green arrows) and vestibular system (black arrows) is lined by a thick layer of granulation tissue with multiple cores of homogenous lytic necrosis. The granulation tissue forms a polypoid mass which occludes the vertical ear canal (red arrows). (HE 4X)*

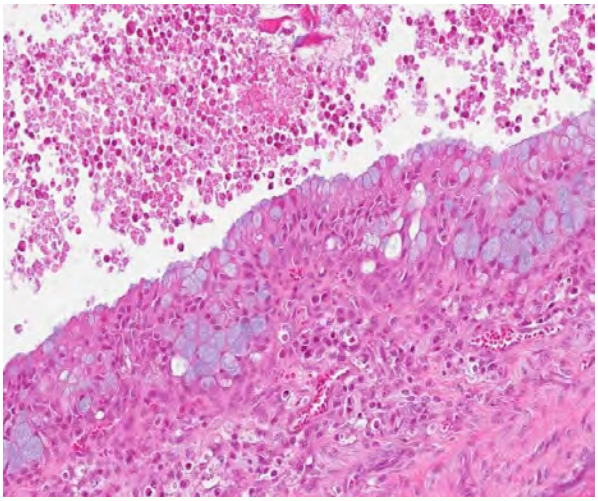

*3-2. Middle and inner ear, calf: The normal squamous epithelial lining of the tympanic cavity is lined by pseudostratified ciliated epithelium with numerous goblet cells (metaplastic change). (HE 200X)*

immunosuppression or a primary viral infection (BVDV, IBRV) allowing overgrowth of resident flora, (3) direct extension from the external ear canal through the tympanic membrane to the middle and inner ear, or (4) hematogenous spread, which is more commonly seen in rodents, lambs, and swine.[3,5] Infection may then ascend via the vestibulocochlear and facial nerves to the brainstem to cause meningitis. Spleen, liver, kidney, and thymus from this case were tested for bovine viral diarrhea virus via a fluorescent antibody test. Testing for herpesvirus (IBRV) was not performed.

*Mycoplasma bovis* infections are of economic importance, causing widespread systemic disease, including pneumonia, arthritis, and mastitis.[1,3] Antigenic variation of the surface lipoproteins is thought to contribute to a poor response to antibiotic therapy and evasion of the host immune response.[1,2] Therefore, the cellular and humoral immune responses offer no protection, despite the development of antibody titers.[1] Ingestion of infected milk is thought to be the most likely route of infection, therefore, control measures include pasteurization of colostrum and milk being fed to calves, preventing direct contact between calves, and culling infected cows.[2]

**JPC Diagnosis**: Middle and inner ear: Otitis media and labrynthitis, necrosuppurative, severe, with osteonecrosis and osteolysis.

**Conference Comment:** *Mycoplasma* are small, fastidious, pleomorphic, facultative anaeroic bacteria that generally do not replicate outside the host.[4] Although many species are non-pathogenic, several species cause diseases in both humans and animals. *Mycoplasma* species are generally found on the mucosal epithelium of the conjunctiva, nasal cavity, oropharynx, intestinal and genital tracts.

Recently some species have been reclassified from the rickettsial group into the genus *Mycoplasma;* these bacteria are referred to as "hemoplasms," as they have a tropism for red blood cells rather than epithelium.[4]

In addition to the diseases associated with *Mycoplasma bovis* that were adeptly described by the contributor, conference participants also discussed a variety of other *Mycoplasma* species of importance in veterinary medicine[4]:

Conference participants noted the presence of an inflamed mucosal lining, interpreted as a polyp, that

| ***Mycoplasma* species** | **Hosts** | **Disease** |
|---|---|---|
| *M. mycoides* subsp. *mycoides* (small colony type) | Bovine | Contagious bovine pleuropneumonia |
| *M. bovis* | Bovine | Mastitis, pneumonia, arthritis, otitis |
| *M. agalactiae* | Ovine, Caprine | Contagious agalactia (mastitis) |
| *M. capricolum* subsp. *capripneumoniae* | Caprine | Contagious caprine pleuropneumonia |
| *M. capricolum* subsp. *capricolum* | Ovine, Caprine | Septicemia, mastitis, polyarthritis, pneumonia |
| *M. mycoides* subsp. *capri* (includes strains previously classified as *M. mycoides mycoides* large colony type) | Ovine, Caprine | Septicemia, pleuropneumonia, mastitis, arthritis |
| *M. ovioneumoniae* | Ovine, Caprine | Pneumonia |
| M. pulmonis | Rodents--rat and mouse | Colonize nasopharynx and middle ear; affect respiratory and reproductive tracts and joints |
| *M. hyopneumoniae* | Swine | Enzootic pneumonia |
| *M. hyosynoviae* | Swine (10-30 weeks of age) | Polyarthritis |
| *M. hyorhinis* | Swine (3-10 weeks of age) | Polyserositis |
| *M. suis* | Swine | Mild anemia, poor growth rates |
| *M. ovipneumoniae* | | mild pneumonia |
| *M. haemofelis* | Feline | Feline infectious anemia |
| *M. cynos* | Canine | Implicated in kennel cough complex |
| *M. haemocanis* | Canine | Mild or subclinical anema; more severe signs in splenectomized animals |
| *M. gallisepticum* | Turkeys and Chickens | Chronic respiratory disease; infectious sinusitis |
| *M. synoviae* | Turkeys and Chickens | Infectious synovitis |
| *M. meleagridis* | Turkeys | Air sacculitis, skeletal abnormalities, reduced hatchability and decreased growth rates |
| *M. felis* | Feline, Equine | Conjunctivitis in cats, pleuritis in horses |
| *M. equigenitalium* | Equine | Abortion |

Table adapted from *Veterinary Microbiology and Microbial Disease.* 2nd ed., 2011[4]

did not appear to be attached to the rest of the tissue. The relationship between the polyp and the other structures was difficult to ascertain in the sections examined. Also, participants noted there is osteolysis of the petrous portion of the temporal bone.

**Contributing Institution:** Department of Microbiology
Immunology and Pathology
CSU Veterinary Diagnostic Lab
200 West Lake Street
1644 Campus Delivery
Fort Collins, CO 80523-1644
http://www.dlab.colostate.edu/index.htm

**References**:

1. Caswell JL, Williams KJ. Respiratory system. In: Maxie MG, ed. *Jubb, Kennedy, and Palmer's Pathology of Domestic Animals.* 5th ed. New York, NY: Elsevier; 2007:611-613.
2. Foster AP, Naylor RD, Howie NM, Nicholas RAJ, Ayling RD. *Mycoplasma bovis* and otitis in dairy calves in the United Kingdom. *The Veterinary Journal*. 2009;179:455-457.
3. Lamm CG, Munson L, Thurmond MC, Barr BC, George LW. *Mycoplasma* otitis in California calves. *J Vet Diagn Invest*. 2004;16:397-402.
4. Quinn PJ, Markey BK, Leonard FC, FitzPatrick ES, Fanning S, Hartigan PJ. Mycoplasmas. In: *Veterinary Microbiology and Microbial Disease.* 2nd ed. Ames, Iowa: Wiley-Blackwell; 2011; Kindle edition.
5. Wilcock BP. Eye and ear. In: Maxie MG, ed. *Jubb, Kennedy, and Palmer's Pathology of Domestic Animals*. 5th ed. New York, NY: Elsevier; 2007:548-549.

**CASE IV**: M07-1049 (JPC 3069496).

**Signalment:** Three six-month-old female SCID-Beige mice, *Mus musculus*.

**History:** More than six Scid/Beige mice (C.B-lgh-Gbms Tac-Prkdcscid-Ly) from the same colony died during the course of one month. These mice had not been experimentally manipulated and presented weak, lethargic, hunched and losing weight before death. Three sick animals were submitted to the Laboratory of Comparative Pathology for diagnosis. They presented similarly to those that had died previously, except for one animal that had a head tilt to the left.

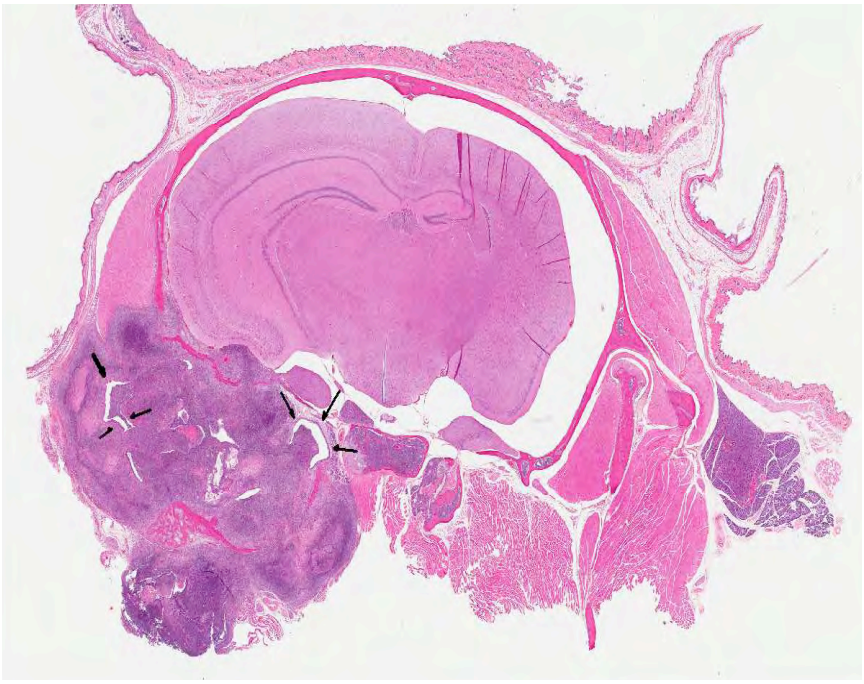

*4-1. Cranium, mouse: The external ear canal (arrows), middle and inner ear is effaced by a focally extensive area of pyogranulomatous inflammation which has resulted in resorption of the cranium and extension, into the cerebrum. (HE 6.0X)*

**Laboratory Results**: Microbiological culture results of the purulent exudate from the abscesses, as well as from blood and spleen indicated *Burkholderia cepacia*. Cultures were sent to the Research Animal Diagnostic Laboratory at the University of Missouri for PCR to differentiate *B. cepacia* from *B. gladioli*. PCR results confirmed *B. cepacia*.

**Gross Pathologic Findings:** On necropsy, the skin covering the head and neck was removed and one to three, small, rounded, tan to yellow, firm but slightly fluctuant nodules measuring up to 0.5 cm in diameter (abscesses) were found at the base of the ear canal in two out of three mice. The left ear was affected by the largest of these abscesses on the mouse that presented with left head tilt, and the right ear was affected on another mouse. The third mouse did not have gross lesions but all three mice had similar microscopic changes. Purulent material from these abscesses, as well as blood and spleen, were collected for culture. No other gross lesions were detected in the three mice.

**Histopathologic Description:** Coronal sections of head containing tympanic bulla, surrounding soft tissues and brain are submitted to conference participants. Microscopic appearance varies slightly from slide to slide, according to the depth of the section. In all slides the tympanic bulla is filled and obliterated by a cellular exudate composed of neutrophils, fibrin, proteinaceous and cellular debris, and colonies of small gram negative rods. There is extensive osteolysis of the bulla, with involvement of the surrounding soft tissue and abscess formation within the mandibular musculature locally. A rim of early fibroplasia and large number of rods, free or within macrophages, are noted at the periphery of these abscesses. The inflammation extends into the internal ear in some slides. There is focal lysis of the skull bone adjacent to the tympanic bulla with involvement of the meninges and cerebral parenchyma. The extent of cerebral involvement varies from slide to slide. In areas of cerebral abscess formation the surrounding parenchyma is compressed and a thick band of Gitter cells packed with bacterial rods is noted at the border between necrotic and healthy tissue. There is fibrinoid necrosis of small vessels in the affected cerebral parenchyma. The lesions in all three cases were unilateral. Other changes included miliary histiocytic inflammation of the liver in one of the mice, likely due to septicemia as indicated by the recovery of *B. cepacia* from cultures of blood and spleen.

**Contributor's Morphologic Diagnosis:**

1. Middle ear: Severe, chronic, suppurative, unilateral otitis media with extensive bulla osteolysis and intralesional gram negative rods.
2. Inner ear (depending on slide): Severe, chronic, suppurative, unilateral otitis interna.
3. Brain and meninges: Severe, chronic, focal, suppurative meningoencephalitis with focal cerebral abscess and intralesional gram negative rods (secondary to otitis).

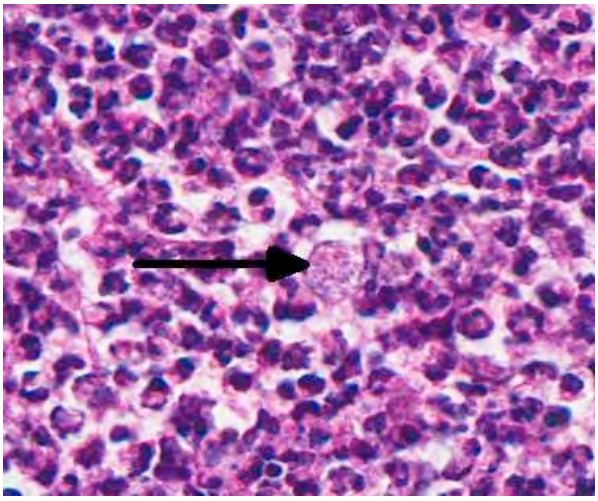

*4-2. Cranium, mouse: The inflammatory infiltrate is composed of numerous degenerate neutrophils and fewer macrophages which occasionally contain 2-3µm bacilli within their cytoplasm (arrow). (HE 400X)*

**Contributor's Comment**: Spontaneous otitis media in immunocompetent mice has been frequently associated with *Mycoplasma pulmonis*, *Pasteurella pneumotropica*, *Pseudomonas aeruginosa*, *Streptococcus* sp., and viral agents such as reovirus.[1] The inflammatory infiltrate can vary from neutrophilic (in most of the bacterial infections) to lymphoplasmacytic and serous and is usually unilateral. When bilateral, the inflammatory infiltrate can differ, i.e. suppurative in one side and serous on the other. Proliferative and papillary lesions, as well as fibrosis of the tympanic cavity are common findings in chronic cases. Causative agents such as bacterial rods or cocci are rarely seen histologically, despite the use of special stains. The incidence of otitis media in mice varies according to strain and age. It is very common in aging 129:B6 mice with a 79 -84% incidence, independent of gender. cBA/J mice are also susceptible to otitis media with a 90% incidence in animals older than one year.[2] However, otitis was found to be more common in aging 129S6 mice than in another CBA strain studied (CBA/Caj).[3]

The most common clinical presentation is head tilt, but neurologic signs such as circling and rolling have been reported in C3H mice and likely depend on the extent and severity of the lesion.[4] A history of previous chemically-induced otitis with ear damage has been found to predispose Rb/3 mice (non-susceptible strain) to audiogenic seizures.[5] In the ICR strain, otitis is manifested as mutilation of the external ear canal due to self-trauma.[6] In addition, Jeff (Jf) mutant mice are also predisposed to otitis, likely due to craniofacial abnormalities in the strain.[7]

In athymic Balb/C-derived nude mice, naturally-occurring Sendai virus infection can cause a chronic respiratory disease characterized by rhinitis, laryngotracheitis, bronchitis/ bronchopneumonia and otitis media (usually suppurative).[8]

The pathogenesis of otitis media in the mouse is uncertain but since it is commonly found without associated otitis externa it may be a sequel of previous viral or bacterial infection of the nasopharynx with ascending infection via the Eustachian tube.[1] Acidification of the drinking water is an effective preventive measure. Tetracycline is recommended for treatment of affected animals.

Otitis media can be experimentally induced in mice by direct injection of the middle ear (often transtympanic) with human pathogenic organisms such as *Streptococcus pneumonia*, *Haemophilus influenzae* or *Moraxella catharralis*.[9] Interleukin-8, as well as *Salmonella typhimurium* endotoxins can also be used to induce otitis media experimentally in mice.[10,11]

In 2004, an outbreak of otitis media associated with *Burkholderia gladioli* was reported in immunosuppressed mice. After an athymic nude mouse presented with head tilt and otitis, several other immunosuppressed mice in the facility presented with similar clinical and pathological findings. Culture of the middle ear of the affected mice initially yielded the phytopathogen *Burkholderia cepacia*, however the isolate was later identified as *Burkholderia gladioli* based on 16S rDNA PCR.[12]

SCID-beige mice are severely immunosuppressed because they lack mature T- and B- lymphocytes (prkdc$^{scid}$ mutation) and have a series of other defects affecting granulocytes, such as the lack of NK cells, reduced bacteriocidal activity of granulocytes, and decreased lysosomal enzymes in neutrophils (Beige or Bg mutation), as noted in the Jackson Laboratory Database. In light of the findings in these mice and the previously reported otitis outbreak in immunosuppressed mice caused by *B.gladioli*, we sent a subculture of the organism to a referral lab at the University of Missouri for PCR. *B. cepacia* was confirmed as the causative agent of otitis in the sick and dying Scid-Beige mice from our colony.

The genus Burkholderia was initially divided in four species: *B. mallei*, *B. pseudomallei*, *B. gladioli* and *B.cepacia*. *B. mallei* is the causative agent of glanders in horses, mules and donkeys; *B. pseudomallei* is the cause of melioidosis, a disease prevalent in Southeast Asia and Australia; *B.gladioli* is a primary plant pathogen but has also been isolated from the sputum of human patients with cystic fibrosis (CF); and *B. cepacia* causes respiratory failure in at least 20% of patients with cystic fibrosis (CF). Currently, the so-called *Burkholderia cepacia*-complex consists of nine

genetically distinct species, all important to humans due to their ability to cause CF-related infections. *B. cepacia* is a small, gram negative, non-motile rod that can be transmitted from individual to individual. When patients with a mild form of cystic fibrosis are infected by *B. cepacia* there is a rapid decline of lung function and resulting respiratory failure with a poor outcome. Immunosuppressed CF patients that received a lung transplant are at high risk of infection with subsequent bacteremia that may result in death (cepacia syndrome).[12,14] In domestic animals, *B. cepacia* has only been reported as a cause of subclinical mastitis in sheep, but may have been reported in the past under the name *Pseudomonas aeruginosa* associated with reptile diseases and infections.[15] In the present cases, large numbers of gram-negative rods can be seen in the histologic sections submitted to conference participants. The culture of *B. cepacia* from blood and spleen confirms a bacteremia and explains the death of the many affected animals. Antibiotic sensitivity results indicated that the *B. cepacia* strain affecting these mice was resistant to some of the most common antibiotics, such as amoxicillin/clavulanic acid, ampicillin, penicillin, tetracycline, oxacillin, and erythromycin. The strain was susceptible to chloramphenicol, ciprofloxacin/ enrofloxacin, gentamicin, trimethoprim/sulfa and amikacin. The remaining colony was treated with Sulfatrim (sulfamethoxazole and trimethoprim) in the feed and recovered from the outbreak.

**JPC Diagnosis**: Head, sagittal section: Otitis externa, otitis media, labrynthitis, neuritis, myositis, osteomyelitis and meningoencephalitis, necrosuppurative, with intrahistiocytic bacilli.

**Conference Comment**: The contributor provides a thorough summary of otitis in mice as well a review of *Burkholderia gladioli* and *B.cepacia* infections in both humans and animals. The significant slide variation noted by the contributor was discussed by participants, and the moderator cautioned participants to always evaluate multiple sections when examining the structures of the ear, as a full visualization of the structures of the middle and inner ear requires multiple serial sections to visualize *in toto*. Additionally, in keeping with terminology used in human medicine, the morphologic diagnosis of "labrynthitis" was favored over otitis interna.

**Contributing Institution**: Memorial Sloan-Kettering Cancer Center
Weill Medical College of Cornell University
Rockefeller University
1275 York Ave.
Box 270; RARC, ZRC-933
New York, NY 10021
http://www.mskcc.orq/ms kcc/html/14131.cfm
http://www.med.cornell.edu/research/reasup/mousephenotvp.html
http://www.med.cornell.edu/research/reasup/labcompat.html
http://www.rockefeller.edu

**References**:

1. Haines DC, Chattopadhyay S, Ward JM. Pathology of aging B6;129
mice. *Toxicol Pathol*. 2001;29(6):653-6.
2. McGinn MD, Bean-Knudsen D, Ermel RW. Incidence of otitis media in CBA/J and CBA/CaJ mice. *Hear Res*. 1992;59(1):1-6.
3. Rosowski JJ, et al. The aging of the middle ear in l29S6/SvEvTac and CBA/CaJ mice: measurements of umbo velocity, hearing function, and the incidence of pathology. *J Assoc Res Otolaryngol*. 2003;4(3):371-83.
4. Kohn DF, MacKenzie WF. Inner ear disease characterized by rolling in C3H mice. *J Am Vet Med Assoc*. 1980;177(9):815-7.
5. Niaussat MM. Experimentally induced otitis and audiogenic seizure in the mouse. *Experientia*. 1977;33:4734.
6. Harkness JE, Wagner JE. Self-mutilation in mice associated with otitis media. *Lab Anim Sci*. 1975;25(3): 315-8.
7. Hardisty RE, et al. The deaf mouse mutant Jeff (Jf) is a single gene model of otitis media. *J Assoc Res Otolaryngol*. 2003;130-8.
8. Ward JM, et al. Naturally-occurring Sendai virus infection of athymic nude mice. *Vet Pathol*. 1976;13 (1):36-46.
9. Ryan AF, et al. Mouse models of induced otitis media. *Brain Res*. 2006;1091(1):3-8.
10. Krekorian TD, et al. Endotoxin-induced otitis media with effusion in the mouse Immunohistochemical analysis. *Acta Otolaryngol*. 1990;109(3-4):288-99.
11. Johnson M, Leonard G, Kreutzer DL. Murine model of interleukin-8 induced otitis media. *Laryngoscope*. 1997;107(10):1405-8.
12. Foley PL, Lipuma JJ, Feldman SH. Outbreak of otitis media caused by Burkholderia gladioli infection in immunocompromised mice. *Comp Med*. 2004-53(1): 93-9.
13. McDowell A, et al. Epidemiology of Burkholderia cepacia complex species recovered from cystic fibrosis patients: tissues related to patient segregation. *J Med Microbiol.* 2004;53(7):663-8.
14. Coenye T, LiPuma JJ. Molecular epidemiology of Burkholderia species. *Front Biosci*. 2003;8:55-67.
15. Berriatua E, et al. Outbreak of subclinical mastitis in a flock of dairy sheep associated with Burkholderia cepacia complex infection. *J Clin Microbiol*. 2001;39 (3):990-4.

**Joint Pathology Center**
**Veterinary Pathology Services**

# WEDNESDAY SLIDE CONFERENCE 2012-2013

## Conference 10

**2 January 2013**

---

**CASE I:** S08-0943 (JPC 3136037).

**Signalment:** 3.5-year-old, neutered male, Shar Pei *(Canis lupus familiaris)*.

**History:** The animal was sent to the Institute of Veterinary Pathology from the small animal clinic of the University of Zurich without any anamnesis but with the question of liver amyloidosis and proteinuria.

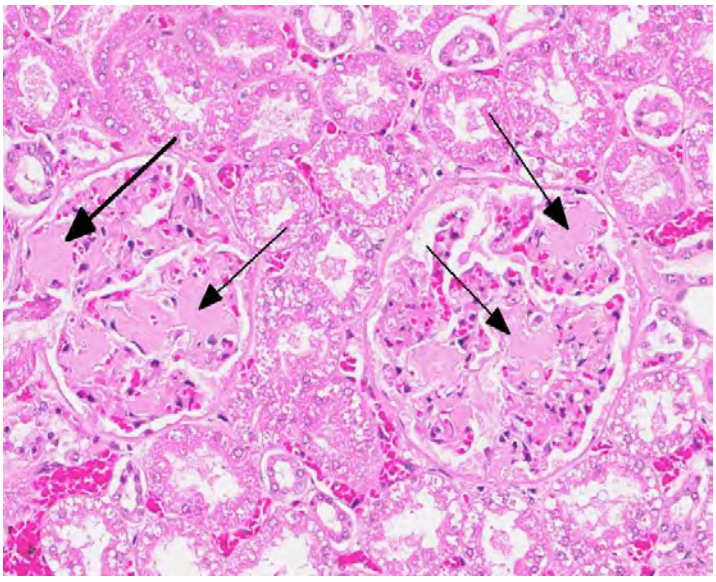

*1-1. Kidney, dog: Diffusely, glomerular tufts are segmentally to globally expanded by variable amounts of amorphous, finely fibrillar to waxy, lightly eosinophilic material (amyloid) (arrows). (HE 172X)*

**Gross Pathologic Findings:** Liver was moderately enlarged, friable and soft. Kidneys were slightly enlarged, pale, increased in consistency and had a finely granular cortical cut surface.

**Histopathologic Description:** Liver: An abundant amount of amorphous, eosinophilic, homogeneous, extracellular material interpreted as amyloid is deposited diffusely in the space of Disse and encroaches on adjacent hepatic parenchymal cells and sinusoids. There is multifocal deformity, pressure atrophy and disappearance of hepatocytes, causing total replacement of large areas of liver parenchyma. There is a small amount of the same material in the vessel walls of few portal areas.

Kidney: In all glomeruli, there is a segmental to diffuse, moderate to abundant amount of amorphous, eosinophilic, homogeneous, extracellular material in the mesangial area and in the subendothelium of glomerular capillaries. The depositions gradually develop until the glomeruli, when entirely involved, are enlarged and appear as hypocellular, eosinophilic, homogeneous spheres in which the capillaries are obliterated. With Congo red, amyloid is stained a light orange-red. In the medulla, not visible on the slide, the tubules are dilated and contain a striking amount of homogeneous, pink, hyaline casts interpreted as protein (proteinuria).

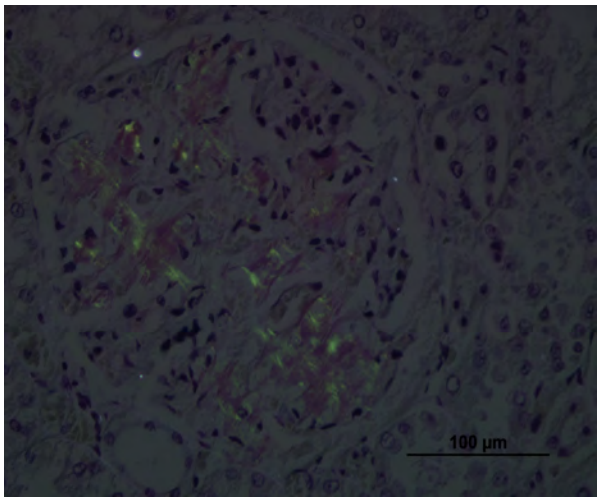


*1-2. Kidney, dog: Glomerular amyloid shows apple-green birefringence when transilluminated with polarized light. (Congo Red 400X)*

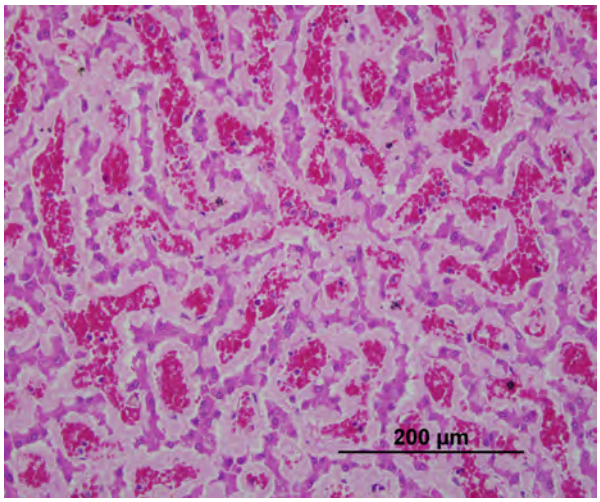


*1-3. Liver, dog: Diffusely, sinusoids are expanded by abundant amyloid within the subendothelial space, which compresses hepatocytes and distorts hepatic plate architecture. (HE 360X)*

**Contributor's Morphologic Diagnosis:** 1. Liver: Amyloidosis, diffuse, severe.
2. Kidney, glomeruli: Amyloidosis, severe.

**Contributor's Comment:** Amyloidosis of Shar-Pei dogs, also known as Shar-Pei fever, hock fever, swollen hock syndrome, and familial renal amyloidosis of Chinese Shar-Pei dogs, is a well-recognized syndrome of unknown etiology. Clinical signs include lethargy, anorexia, recurrent fever, joint swelling and pain, and/or cellulitis over affected joints.[1] Renal and hepatic involvement are described in 3 reports from the early 1990s documenting amyloidosis in a total of 17 Chinese Shar-Pei dogs having common ancestry.[2-4] The disorder is postulated to have autosomal recessive inheritance, and affected dogs typically manifest recurrent bouts of fever before developing renal amyloidosis.[1] Histopathologic findings of amyloidosis in this case were similar to those in previous reports. In Shar-Pei dogs, hepatic amyloid deposition is commonly observed within the space of Disse, vessel walls, and perivascular areas. In the kidney, both glomerular and interstitial medullary deposition have been reported.[1] Additionally, the dog in this case had a small amount of amyloid deposition in the spleen.

Amyloidosis is a group of disorders in which amyloid is deposited in the walls of small blood vessels and extracellularly in a variety of sites, particularly in renal glomeruli. All amyloid fibrils have a β-pleated sheet structure.[5] By light microscopy and standard hematoxylin and eosin staining, amyloid appears as an amorphous, eosinophilic, hyaline, extracellular substance.[6] The histologic diagnosis is usually confirmed with special stains. Amyloid is stained a light orange-red with Congo red, and then exhibits green birefringence in polarized light.[5]

Amyloidosis is seen in a number of presentations:
1. Immunoglobulin-derived (primary, or AL) amyloidosis is the most common form in humans, but it is uncommon in domestic animals. AL amyloid is produced from immunoglobulin light chains in plasma cell dyscrasias as a product of monoclonal B-cell proliferation.[5]
2. Reactive systemic (secondary or AA) amyloidosis is the most common form in domestic animals. AA amyloid is derived from serum protein AA, an acute-phase reactant apoprotein product of hepatocytes predominantly. Serum protein AA is produced in excess as a result of chronic antigenic stimulation, such as occurs in persistent infectious, inflammatory or neoplastic (nonimmunocyte dyscrasias) conditions.[5,7]
3. Familial amyloidosis is a systemic form of AA amyloidosis that is hereditary in some breeds of dogs and cats.[7] AA amyloidosis occurs in Beagles, Shar-Pei dogs, gray Collies, English Foxhounds, Abyssinian cats and Siamese and Oriental cats.
4. Apolipoprotein AI-derived amyloidosis affects the pulmonary vessels of old dogs.
5. Islet amyloid polypeptide-derived amyloidosis is common in the pancreatic islets of cats with non-insulin-dependent diabetes mellitus.[5]

Both AA and AL amyloidosis can occur in either systemic or localized forms. The cause of amyloid fibril formation and deposition is obscure, but the nidus theory postulates that amyloid fibrils serve as templates for fibril growth and as scaffolding for fibril polymerization. Amyloid-enhancing factor may be involved.[5]

**JPC Diagnosis:** 1. Liver, space of Disse: Amyloidosis, diffuse, severe, with cholestasis and hepatocyte atrophy and loss.

2. Kidney, glomeruli: Amyloidosis, segmental to global, diffuse, marked, with scattered tubular degeneration and necrosis.

**Conference Comment**: In addition to the points discussed by the contributor in their excellent summary, conference participants discussed several properties of amyloid, including anatomic locations of deposition in various species, clinicopathologic findings in amyloidosis and characteristics of amyloid on electron microscopy.

The location of amyloid deposits varies based on the pathogenesis and the species affected. Overall, the kidney is the most common site for amyloid deposition in many domestic species, with the glomeruli being most frequently affected in most domestic species, except the cat where medullary interstitial deposition of amyloid is more common. The space of Disse in the liver is also a common site for amyloid deposition in birds, cattle, horses, dogs and cats. The spleen is a frequent site in reactive systemic amyloidosis, with amyloid deposits occurring in the periarteriolar lymphoid sheaths and red pulp. Organs affected in localized amyloidosis include the skin and nasal septum and turbinates in horses and pancreatic islets of Langerhans in cats.[6]

Clinocopathologic consequences of renal amyloidosis include the nephrotic syndrome, which is characterized by the tetrad of hypercholesterolemia, proteinuria, hypoproteinemia, and generalized edema. Additionally, a urine-protein-to-urine-creatinine ratio (UP/UC) greater than 18 is associated with renal amyloidosis. Ultrastructually, amyloid fibrils are non-branching, 7.5 to 10 nm in diameter, and lack the periodicity which is characteristic of fibrin and collagen diameter tubules by electron microscopy.[7]

There was some slide variation, with some slides having only the section of kidney.

**Contributing Institution:** Institute of Veterinary Pathology
University of Zurich
Winterthurerstrasse 268, CH-8057
Zürich, Switzerland
www.vetpathology.uzh.ch

**References:**

1. Flatland B, Moore RR, Wolf CM, Yeomans SM, Donnell RL, Lane IF, et al. Liver aspirate from a Shar Pei dog. *Vet Clin Pathol*. 2007;36(1):105-8.
2. DiBartola SP, Tarr MJ, Webb DM, Giger U. Familial renal amyloidosis in Chinese Shar Pei dogs. *J Am Vet Med Assoc*. 1990;197(4):483-7.
3. Loeven KO. Hepatic amyloidosis in two Chinese Shar Pei dogs. *J Am Vet Med Assoc*. 1994;8:1212-16.
4. Loeven KO. Spontaneous hepatic rupture secondary to amyloidosis in a Chinese Shar Pei. *J Am Anim Hosp Assoc.* 1994;30:577-79.
5. Maxie MG, Newman SJ. Glomerular disease: Amyloidosis. In: Maxie MG, ed. *Jubb, Kennedy, and Palmer's Pathology of Domestic Animals*. 5th ed. Philadelphia, PA: Saunders Elsevier; 2007:463-65.
6. Myers RK, McGavin MD, Zachary JF. Cellular adaptations, injury and death: morphologic biochemical and genetic bases. In: McGavin MD, Zachary JF, eds. *Pathologic Basis of Veterianry Disease.* 5th ed. St Louis, MO: Elsevier Mosby; 2012:36-38.
7. Snyder PW. Diseases of immunity: Amyloidosis. In: McGavin MD, Zachary JF, eds. *Pathologic Basis of Veterinary Disease.* 4th ed. St. Louis, MO; Mosby Elsevier; 2007:246-51.
8. Tripathi NK, Gregory CR, Latimer KS. Urinalysis. In: Latimer KS, ed. *Duncan & Prasse's Veterinary Laboratory Medicine Clinical Pathology.* 5th ed. Ames, Iowa: Wiley-Blackwell; 2011:253-282.

**CASE II:** 48646 (JPC 4019427).

**Signalment:** 7-year-old, male castrated, Russian Blue cat *(Felis catus)*.

**History:** The cat had a history of weight loss for approximately one year, and left tarsal arthrodesis surgery five months prior. Clinical workup at the time of surgery revealed sternal lymphadenopathy, thick-walled intestines, mild anemia, thrombocytopenia and neutropenia. FIV/FeLV tests were negative.

More recent clinical presentation was for an ulcerated lip mass which had been noted for eight weeks. The owners also described that the cat had been wandering around the house, stuck in small spaces, was incoordinated, stumbling and vocalizing, with a decreased appetite. On physical exam, there were multifocal neurologic signs including decreased menace bilaterally, positional nystagmus and inappropriate mentation. Additional findings included left retinal detachment, heart murmur and thickened intestines with palpation.

**Gross Pathology:** On the lower left lip, there is a 1.0 x 0.5 x 0.5 cm ulcerated, firm red nodule. The left tarsal joint is fused (tarsal arthrodesis). Internally, subcutaneous and visceral fat stores are markedly reduced, with mild yellow discoloration of the adipose tissue (icterus).

The vermis of the cerebellum is focally compressed and flattened against the underlying brainstem at the foramen magnum (herniation). The leptomeninges of the rostral and dorsal cerebrum are thickened by granular, irregular, yellow to tan material (meningitis). When the fixed brain is sectioned, there is marked leptomeningeal expansion by similar granular material, with adherence of the right and left hemispheres of the rostral cerebrum at the longitudinal cerebral fissure.

**Laboratory Results:** Normocytic, normochromic, nonregenerative anemia, mildly elevated ALT and AST, mild hypoalbuminemia and hyperglobulinemia.

Cytology: Aspirate of mass from the right lower lip region: All slides are examined and are found to be similar; the specimen is of moderate cellularity and contains moderate numbers of red blood cells with low to moderate numbers of nondegenerate neutrophils and activated macrophages. Rare tissue cells are identified and these are uniform fibrocytes showing no evidence of dysplasia or atypia. On several of the slides there are extremely low numbers of intracellular yeast structures; these are 1-3 microns in diameter, round to oval with a variably thick capsule and are primarily found within the cytoplasm of very few of the macrophages. The yeast organisms most resemble *Histoplasma* sp.

Microscopic interpretation: Mild to moderate mixed (neutrophilic and histiocytic) inflammatory infiltrate associated with intracellular yeast organisms.

Comment: Although the numbers of yeast structures are quite low, they provide unequivocal evidence of a primary fungal etiology and are most characteristic of *Histoplasma capsulatum*.

**Histopathologic Description:** One section of rostral cerebrum is examined. The leptomeninges, including those along the longitudinal cerebral fissure, are markedly expanded up to 3 mm by large populations of inflammatory cells which extend into the brain

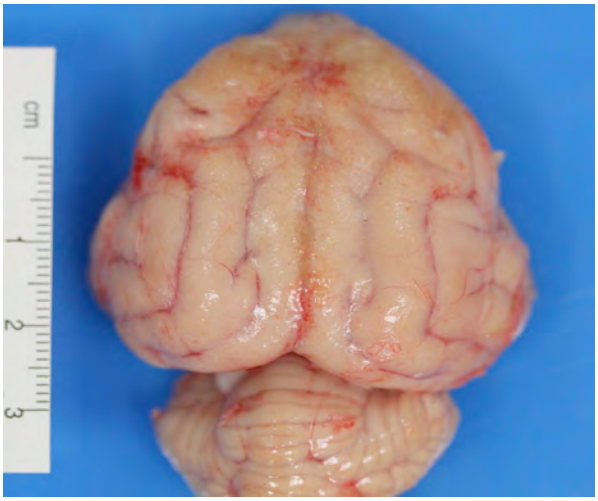


*2-1. Cerebral cortex, telencephalon, cat: The leptomeninges of the rostral and dorsal cerebrum are thickened by granular, irregular, yellow to tan material. (Photograph courtesy of Animal Medical Center, http://www.amcny.org)*

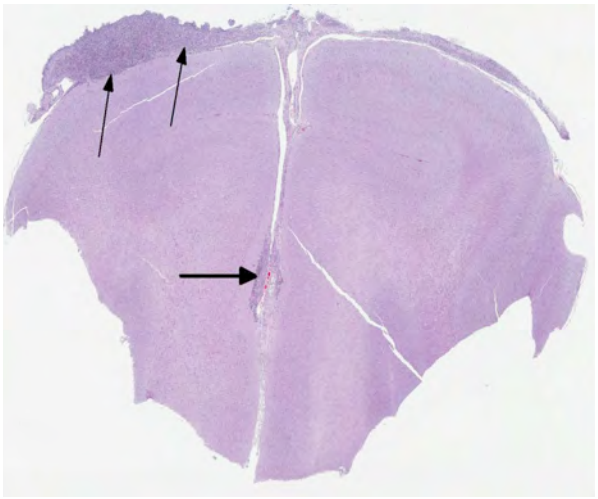

*2-2. Cerebral cortex, telencephalon, cat: Diffusely, the meninges are markedly expanded by a dense cellular infiltrate. (HE 5X)*

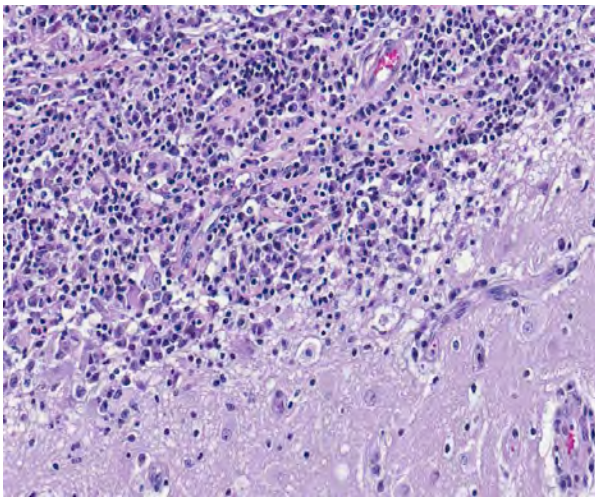

*2-3. Cerebral cortex, telencephalon, cat: The meningeal infiltrate is composed of numerous macrophages and neutrophils with fewer numbers of lymphocytes and plasma cells. The inflammatory infiltrate occasionally extends into and replaces the superficial cerebral cortex. (HE 400X)*

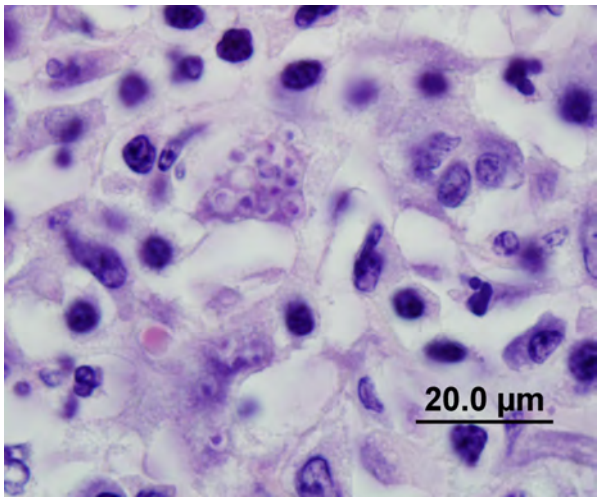


*2-4. Cerebral cortex, telencephalon, cat: Macrophages and multinucleated macrophage giant cells contain one or numerous (up to 20) 2-4 m diameter, round to oval intracytoplasmic yeast. These intracytoplasmic structures are characterized by a central, 1-2 m, eosinophilic nucleus which is surrounded by clear space. (HE 1000X)*

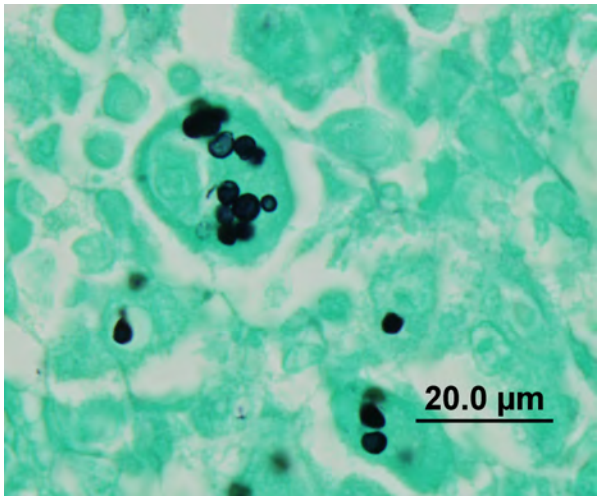


*2-5. The somewhat irregular shape of Histoplasma capsulatum is well demonstrated by silver stains.*

parenchyma. Inflammatory populations consist of macrophages, neutrophils, lymphocytes and plasma cells. Multinucleate cells and occasional Mott cells are present. Multifocally, macrophages and multinucleate cells contain one or numerous (up to 20) 2-4 µm diameter, round to oval intracytoplasmic yeast characterized by a central, 1-2 µm, eosinophilic nucleus which is surrounded by clear space. Inflammatory cells similar to those described above are observed within Virchow-Robin spaces and infiltrate the adjacent neural parenchyma. Macrophages commonly contain enlarged nuclei with marginated chromatin and eosinophilic material (presumed reactive change). Small vessels in the regions of infiltration exhibit endothelial hypertrophy and there is regional rarefaction of the neuropil (edema). Gliosis is abundant, consisting of astrogliosis and numerous gemistocytic astrocytes. Fewer microglial cells are present, which exhibit rod cell morphology. Round, eosinophilic structures (spheroids) are also dispersed throughout the infiltrated brain parenchyma.

*Histoplasma* immunohistochemistry (provided by the University of Connecticut Veterinary Medical Diagnostic Laboratory): Brain: Multifocally throughout the meninges, within macrophages, there are numerous positive staining, intracellular, spherical, 3-4 µm diameter organisms (*Histoplasma capsulatum*). Similar, positive staining organisms are identified in the previous bone biopsy, lungs, adrenal glands and eye.

**Contributor's Morphologic Diagnosis:** Brain (rostral cerebrum): Severe, chronic, pyogranulomatous, lymphoplasmacytic meningoencephalitis with intralesional, intracytoplasmic fungal yeast (consistent with *Histoplasma capsulatum*), regional edema, spheroids and gliosis with gemistocytic astrocytosis.

**Contributor's Comment:** *Histoplasma capsulatum* is a dimorphic, soil-borne fungus, existing in the environment as a mycelial form, and in the host as a yeast.[2,3] Infections with this fungus are prevalent in the Midwest and southern United States, and regions along the Ohio, Missouri and Mississippi Rivers.[2,7,9] The organism grows best in soil containing nitrogen-rich organic matter, including bird and bat excrement.[3] Infection typically develops via inhalation or ingestion, and most animals clear the infection without developing clinical signs of disease.[1,2,6] In dogs and cats, macrophages phagocytize the organisms and can distribute them to other organ systems. Clinical signs

are typically nonspecific and include weight loss, lymphadenopathy, lethargy, fever, and respiratory signs as well as cutaneous nodules, ocular disease, diarrhea, and lameness.[1-3,6] Histoplasmosis is the second most common fungal disease reported in cats after cryptococcosis.[1,3]

A retrospective study of 22 cases of feline histoplasmosis found that amongst three categories (disseminated, pulmonary and gastrointestinal), disseminated was the most common manifestation, occurring in 68% of cases. The most frequent sites of infection were listed as the lungs, lymph nodes, liver, spleen, kidney, adrenal glands, eyes, bone marrow and the gastrointestinal tract.[1] Disseminated infection with involvement of the brain is rarely reported in cats and dogs.[4,7,9] In this case, the brain was the most severely affected organ, and the cat re-presented for its neurologic signs. Immunohistochemistry for *Histoplasma* was performed at the University of Connecticut Veterinary Medical Diagnostic Laboratory. The combination of H&E, silver stains and IHC confirmed *Histoplasma* organisms in the brain, eye, lungs, adrenal glands, bone marrow at site of previous surgery (taken at the time of surgery) and the ulcerated lip lesion. Demonstrable organisms in the ulcerated lip lesion correlated with the cytologic results. In one report, a review of cases from the authors' institution revealed that several cats with oral histoplasmosis presented with focal or multifocal exophytic or ulcerative lesions within the oral cavity, with no apparent systemic involvement.[6] Osseous lesions with associated soft tissue swelling or joint effusion and lameness have been described with feline histoplasmosis.[3] *Histoplasma* organisms were immunohistochemically identified in the bone marrow biopsy obtained 5 months before euthanasia, indicating a long time frame of infection. Although the intestines were palpably thickened, neither granulomatous enteritis nor intralesional organisms were identified at postmortem examination; however, the intestines displayed mucosal fibrosis, which may indicate previous infection.

The cat in this case had a history of being indoor-only for 3 years, and prior to this had intermittent access to the outdoors in rural Pennsylvania. Other reports of histoplasmosis in indoor only cats without travel to endemic regions suggest that household dust or potting soil are possible sources of infection.[3] Some studies found a high prevalence of FeLV in cats with the disseminated form of histoplasmosis, whereas others found a low prevalence.[1,4] In our case, the cat was negative for both FIV and FeLV. Typical clinicopathologic changes in cats with disseminated histoplasmosis include normochromic, normocytic, nonregenerative anemia, hypoalbuminemia, and thrombocytopenia, with variable leukocyte counts.[3,4] Nonregenerative anemia is suspected to result from chronic inflammatory disease, *Histoplasma* infection of the bone marrow, and intestinal blood loss in gastrointestinal disease. Some cats have been reported to have hyperproteinemia, hyperglobulinemia, mild hyperglycemia or hyperbilirubinemia, and elevations of alanine aminotransferase activities. Hypercalcemia has been reported in several cats and is likely due to granulomatous disease.[3] In our case, mild elevations of ALT and AST may be explained by concurrent chronic cholangiohepatitis.

**JPC Diagnosis:** Cerebrum: Meningoencephalitis, pyogranulomatous, multifocal, moderate with intrahistiocytic yeast.

**Conference Comment:** The contributor provided a very good summary of histoplasmosis caused by *Histoplasma capsulatum* var. *capsulatum* in dogs and cats. Conference participants reviewed two other variants of *H. capsulatum*: *H. capsulatum* var. *farciminosum* (also referred to as *H. farciminosum*) and *H. capsulatum* var. *duboisii*. *H. farciminosum* causes equine epizootic lymphangitis in horses and mules, characterized by ulcerated discharging cutaneous nodules located along thickened lymphatic vessels, and regional lymphadenopathy, resembling farcy. *H. capsulatum* var. *duboisii* causes African histoplasmosis in humans and nonhuman primates.[5,8]

**Contributing Institution:** Animal Medical Center
510 East 62nd St.
New York, NY 10065
www.amcny.org

**References:**

1. Aulakh HK, Aulakh KS, Troy GC. Feline histoplasmosis: a retrospective study of 22 cases (1986-2009). *J Am Anim Hosp Assoc*. 2012;48(3): 182-187.
2. Brömel C, Greene CE: Histoplasmosis. In: Greene CE, ed. *Infectious Diseases of the Dog and Cat*. 4th ed. St Louis, MO: Elsevier Saunders; 2012:614-621.
3. Brömel C, Sykes JE. Histoplasmosis in dogs and cats. *Clin Tech Small Anim Pract*. 2005;20(4):227-32. Review.
4. Clinkenbeard KD, Cowell RL, Tyler RD. Disseminated histoplasmosis in cats: 12 cases (1981-1986). *J Am Vet Med Assoc*. 1987;190(11): 1445-1448.
5. Gades NM, Marler RJ. Pathology in practice. *J Am Vet Med Assoc.* 2009;234(12):1535-1537.
6. Lamm CG, Rizzi TE, Campbell GA, Brunker JD. Pathology in practice. Histoplasma capsulatum infections. *J Am Vet Med Assoc*. 2009;235(2):155-7.
7. Lavely J, Lipsitz D. Fungal infections in the central nervous system in the dog and cat. *Clin Tech Sm Anim Prac.* 2005;20:212-219.

8. Quinn PJ, Markey BK, Leonard FC, FitzPatrick ES, Fanning S, Hartigan PJ. Dimorphic fungi. In: *Veterinary Microbiology and Microbial Disease.* 2nd ed. Ames, Iowa: Blackwell Science Ltd; 2011: Kindle edition.
9. Schaer M, Johnson KE, Nicholson AC. Central nervous system disease due to histoplasmosis in a dog: a case report. *J Am Anim Hosp Assoc*. 1983;19:311-315.

**CASE III:** 12-9677 (JPC 4019858).

**Signalment:** 9-year-old, male, neutered, Golden Retriever mix dog (*Canis familiaris*).

**History:** One year prior to presentation, the dog had developed epistaxis and a right nasal mass that was diagnosed as nasal adenocarcinoma following biopsy and histopathologic examination. The epistaxis responded well to treatment with tramadol, firocoxib, and Chinese herbs. In March of 2012, the dog presented for a 3-day history of progressive anorexia, diarrhea, vomiting, and lethargy. The dog was salmon fishing 10 days prior to admission and was found with a fish carcass. The owners elected empirical therapy and additional medications prescribed were meropitant and metronidazole. The dog re-presented two days later due to lack of improvement and development of dark colored diarrhea. On physical exam he was dull and panting, with a temperature of 99.8 degrees Celsius and a heart rate of 150 bpm. The right mandibular lymph node was moderately enlarged and there was dark brown fecal staining on fur around perineum. Due to the lack of response to the medications and continuing anorexia, the owner's elected euthanasia and necropsy.

**Gross Pathology:** Mucous membranes and abdominal fat were pale with a yellow tinge. There was an irregular, thin, undulating mass in the right ethmoid concha measuring 2 x 3 x 2 cm. On impression smear of the mass there were clusters of epithelial cells with anisokaryosis and prominent nucleoli and also macrophages with Neorickettsial organisms found intracytoplasmically. There was lymphadenopathy characterized by an enlarged right mandibular lymph node (2 x 1 x 2 cm), enlarged tracheobronchial lymph nodes (0.5 x .05 x 0.5 cm to 1 x 2 x 1 cm) with multifocal hemorrhages, and enlarged mesenteric lymph nodes (1 x 1 x 1 cm to 2.5 x 1 x 1.5 cm) also with multifocal hemorrhages. On impression smears of the mesenteric and tracheobronchial lymph nodes there were large numbers of organisms consistent with *Neorickettsia* within macrophages. The spleen was moderately enlarged with a vaguely cobblestone surface and was meaty on cut section.

**Laboratory Results:** Mildly increased ALP 298 U/L (RI: 10-84); CBC: Normal; U/A: Unremarkable; PCR: Lymph node and feces, positive for Neorickettsial spp real time PCR assay (still in validation process).

**Histopathologic Description:** The lymph node is hyperplastic and hemorrhagic. The medulla is edematous often with large foamy macrophages filled with red blood cells (erythrophagocytosis). Macrophages are also often characterized by large, swollen, pale basophilic cytoplasm with numerous fine blue organisms. There are multifocal areas of necrosis characterized by leukocytes with pyknotic and karyorrhectic nuclei, cellular debris, occasional neutrophils and flocculent amphophilic debris. There are multifocal areas of hemorrhage. The cortex is packed with large histiocytes and fewer lymphocytes and plasma cells. Sinuses often contain macrophages displaying erythrophagocytosis. Subcapsular sinuses are congested often with erythrophagocytic macrophages and deposition of fibrillar to amorphous eosinophilic material deposits consistent with fibrin.

**Contributor's Morphologic Diagnosis:** Lymph node: granulomatous lymphadenitis with hemorrhage and intralesional rickettsial organisms (salmon poisoning-*Neorickettsia helminthoeca*).

**Contributor's Comment:** Salmon poisoning disease (SPD) was first described in 1814 and occurs in northwest coastal regions including California,

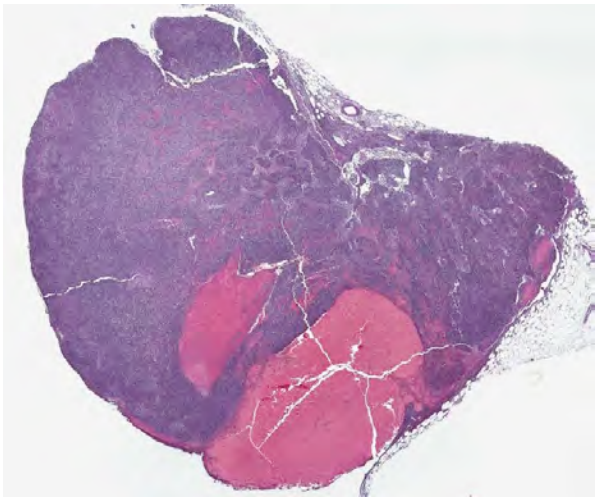

*3-1. Lymph node, dog: Marked hyperplasia largely effaces normal lymph node architecture. (HE 7X)*

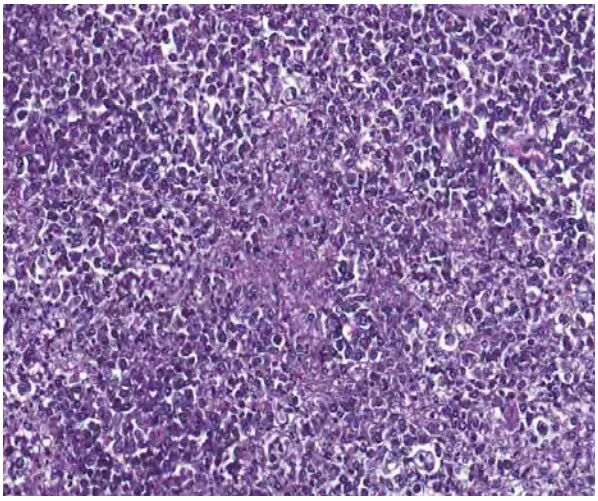

*3-2. Lymph node, dog: Cortical lymphoid follicles are often replaced by necrotic debris. (HE 200X)*

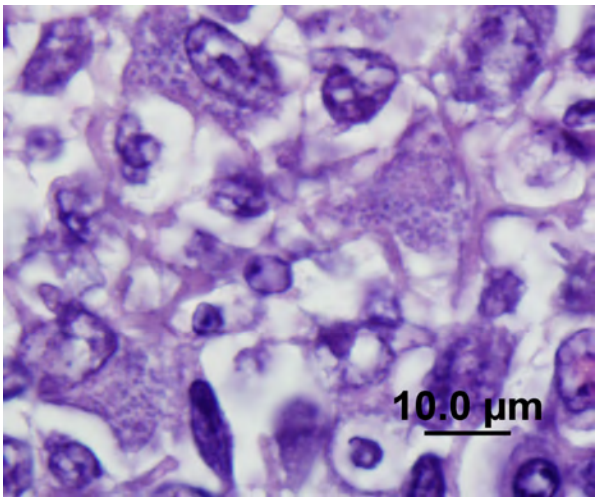


*3-3. Lymph node, dog: Throughout the lymph node, macrophages occasionally contain numerous small intracytoplasmic coccobacilli (rickettsia). (HE 1000X)*

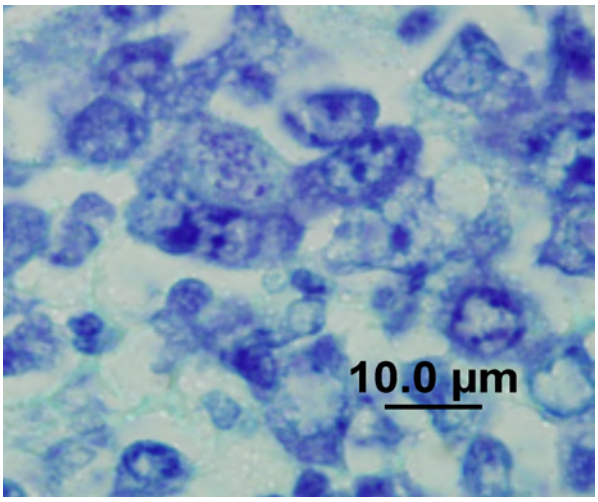


*3-4. Lymph node, dog: Coccobacilli can also be demonstrated with Giemsa stains. (HE 1000X)*

Oregon, Washington, and southern British Columbia.[10] Recently, SPD has been reported in Brazilian dogs confirmed with IHC and PCR for *N. helminthoeca*.[5,6] The disease is caused by *Neorickettsia helminthoeca* and the definitive host includes foxes, coyotes, and dogs; captive bears have also been reported to be highly susceptible to clinical disease after ingestion of trematode infected fish.[2,3,7] *N. helminthoeca* require three hosts for life cycle completion.[6] The life cycle includes a trematode vector, *Oxytrema silicula,* considered important in the geographic distribution of the disease, and a fish.[6] Miracidia of *Nanophyetus salmincola* penetrate the fresh water snail, *Oyxtrema silicula,* the cercariae then infect the second intermediate host by skin penetration or ingestion of infected snails or free cercariae.[1,4] The second intermediate host is most often salmon or trout.[1] The cercariae develop into metacercariae and become encysted in tissue of the salmon including eyes, kidneys, liver, intestine, fins and musculature.[1] Salmon in enzootic area are often heavily infected with the metacercariae.[1] Infection in dogs occur when uncooked fish is ingested and the metacercariae mature into flukes in the intestine.[1] The fluke does not cause the clinical signs but eggs appear in the feces of dogs five to ten days after infection and are a method of diagnosis.[1] The neorickettsial organisms, present in all stages of the fluke life cycle, spread via macrophages to visceral tissues of the dog causing disease.[1,8] The pathogenesis is still unclear in some ways, but the fluke attaches deep in the intestinal mucosa causing an inflammatory response and release of *N. helminthoeca* by an unknown mechanism.[6] The *N. helminthoeca* are taken up by intestinal macrophages and are disseminated through the lymph systems to lymph nodes where they proliferate with subsequent hypertrophy of the lymph nodes due to influx of macrophages and edema.[6] Enteritis is caused by the inflammation of the Peyer's patches and intestinal lymphoid tissue.[6] The organism is found in circulation of infected dogs 8-12 days after infection.[3] Mortality rate is about 90% in untreated cases and death occurs at least 18 days after ingestion of metacercariae.[1,6] Dogs are immune to reinfection but only with the same strain. Subsequent infection of recovered dogs has been reported with alternate strains resulting in disease.[8,10] A similar but sometimes less severe disease has been described in the Elokomin River of Washington called Elokomin fluke fever.[6] This disease has a wider host range and the causative agent is thought to be another strain of *N. helminothoeca*.[6,10]

Pathologic findings include enlarged mesenteric lymph nodes. Other nodes are usually less affected. Peyer's patches are hypertrophic and the entire intestinal tract may be hemorrhagic.[6] Histopathologic findings are usually in the intestine and mesenteric lymph nodes with lymphoid tissue depletion and proliferation of lympho-histiocytic cells with neorickettsial bodies.[6] Giemsa or Machiavello's stains demonstrate organisms within macrophages.[6] Non-suppurative leptomeningitis and centrilobular fatty degeneration in the liver have also been described.[6] In this case there was a non-suppurative leptomeningitis and multifocal areas of hepatocellular vacuolation suggestive of lipid in the liver. The lymph nodes examined, including tracheobronchial and mesenteric, had obscured architecture with high cellularity and multifocal areas of necrosis with infiltration by large foamy macrophages containing neorickettsial organisms. There were similar findings in the spleen.

Diagnosis is based on a combination of fecal sedimentation and flotation, abdominal ultrasound, lymph node aspirate and PCR.[10] Identification of operculated trematode eggs via direct smear or

washing-sedimentation in feces of infected dogs 5-8 days post infection or identification of the adult fluke within the intestine are methods of diagnosis.[6] Trematode infection may also occur in dogs recovered from salmon poisoning disease and during recovery.[6] Microscopic identification of neorickettsial bodies within macrophages may be performed on lymph node aspirates.[6] Definitive diagnosis includes isolation and culture of *N. helminthoeca,* serology, and PCR.[6] In this case, PCR was performed on lymph node impression smears, serum, and feces and was positive in both lymph node aspirate and fecal sample but the serum was negative. Giemsa and Rickettsia-Pierce VanderKamp staining identified organisms in the macrophages in several tissues including the adenocarcinoma, multiple lymph nodes, spleen, intestine, and liver. In endemic areas this disease should be considered in dogs with clinical gastrointestinal signs such as anorexia, vomiting, and diarrhea as recognition of the disease and prompt treatment with a tetracycline type antibiotic is important for patient survival. Although it was known that the dog had been near salmon prior to development of clinical signs the owners were certain that the dog did not ingest any salmon. This case illustrates the importance of treatment with a tetracycline family antibiotic in dogs developing clinical signs of gastroenteritis when salmon exposure is known or suspected.

**JPC Diagnosis:** Lymph node, mesenteric: Lymphadenitis, necrotizing, diffuse, moderate to severe with hemorrhage and intrahistiocytic coccobacilli.

**Conference Comment:** The contributor provides a thorough and current review of salmon poisoning disease in dogs. Conference participants discussed the pathogenesis and temporal qualities of the histopathologic lesions in the submitted lymph node. The multifocal preponderance of plasma cells and the expanded paracortex are evidence of a reactive lymph node; however, the most significant feature is the marked necrosis, characterized by the loss of normal follicular architecture and replacement by necrotic debris admixed with fibrin, hemorrhage, numerous macrophages and fewer neutrophils, as well as multifocal, widespread lymphocytolysis. Participants hypothesized that this sample represents a necrotizing lymphadenitis due to *N. helminthoeca* infection in a lymph node with pre-existing reactive hyperplasia. Additionally, the large amount of subcapsular and sinus hemorrhage was speculated to be due to draining from hemorrhagic enteritis, a feature commonly seen in this disease.

The genus *Neorickettsia,* along with three other genera (*Anaplasma, Ehrlichia,* and *Aegyptianella*) comprise the family *Anaplasmatacea,* within the order *Rickettsiales*. *Anaplasmatacea* organisms are minute, non-motile Gram-negative obligate intracellular bacteria that lack cell walls and infect cells of hemopoietic origin. Generally, they cause arthropod-borne systemic disease in animals as well as humans. *Anaplasmatacea* species of importance in veterinary medicine are summarized in the included table.[9]

**Contributing Institution:** Oregon State University Veterinary Diagnostic Laboratory
http://vetmed.oregonstate.edu/diagnostic

| Pathogen | Host | Vector | Target cells | Disease |
|---|---|---|---|---|
| *Aegyptianella pullorum* | Poultry | Ticks | Erythrocytes | Aegyptianellosis |
| *Anaplasma bovis* | Cattle | Ticks | Monocytes, macrophages | Bovine anaplasmosis |
| *Anaplasma marginale* | Ruminants | Ticks | Erythrocytes | Anaplasmosis |
| *Anaplasma ovis* | Sheep, goats | Ticks | Erythrocytes | Anaplasmosis |
| *Anaplasma phagocytophilum* *Formerly Ehrlichia equi and Ehrlichia phagocytophila* | Ruminants, horses, humans | Ticks | Granulocytes | Tick-borne fever, equine and human granulocytic ehrlichiosis |
| *Anaplasma platys* | Dogs | Ticks? | Platelets | Canine cyclic thrombocytopenia |
| *Ehrlichia canis* | Dgos | Ticks | Monocytes, macrophages | Canine monocytic ehrlichiosis |
| *Ehrlichia ewingii* | Dogs | Ticks | Granulocytes | Canine granulocytic ehrlichiosis |
| *Ehrlicia* (formerly Cowdria) ruminantium | Ruminants | Ticks | Granulocytes | Heartwater |
| *Ehrlichia ondiri* | Cattle | Ticks? | Granulocytes, monocytes | Bovine petechial fever |
| *Ehrlichia ovina* | Sheep | Ticks | Monocytes, macrophages | Ovine ehrlichiosis |
| *Neorickettsia elokominica* | Dogs, bears, raccoons | Flukes | Monocytes, macrophages, lymphoid cells | Elokomin fluke fever |
| *Neorickettsia helminthoeca* | Dogs, bears | Flukes | Monocytes, macrophages, lymphoid cells | Salmon poisoning disease |
| *Nerickettsia risticii* | Horses | Flukes | Monocytes, ntestinal epithelial cells, mast cells | Potomac horse fever |

Table adapted from *Veterinary Microbiology and Microbial Disease,* 2nd ed, 2011.

**References:**

1. Booth AJ, Stogdale L, Grigor JA. Salmon poisoning disease in dogs on Southern Vancouver Island. *Can Vet J*. 1984;25:2-6.

2. Foreyt WJ, Thorson S. Experimental salmon poisoning disease in juvenile coyotes (*Canis Latrans)*. *Journal of Wildlife Diseases*. 1982;18(2):159-162.

3. Gai JJ, Marks SL. Salmon poisoning disease in two Malayan sun bears. *Journal of the American Veterinary Medical Association.* 2008;232(4):586-588.

4. Gebhardt GA, Millemann RE, Knapp SE, Nyber PA. "Salmon poisoning" disease. II. Second intermediate host susceptibility studies. *The Journal of Parasitology*. 1966;52(1):54-59.

5. Headly SA, Kano RS, Scorpio, DG, Tamekuni K, Barat NC, Bracarense AP, et al. *Neorickettsia helminthoeca* in Brazilian dogs: a cytopathological, histopathological and immunohistochemical study. *Clinical Microbiology and Infection*. 2009;15:21-23.

6. Headley SA, Scorpio DG, Vidotto O, Dumler JS. *Neorickettsia helminthoeca* and Salmon Poisoning disease: A review. *The Veterinary Journal*. 2011;187:165-173.

7. Johns JL. Salmon poisoning disease in dogs: A satisfying diagnosis. *The Veterinary Journal*. 2011;187:149-150.

8. Nyberg PA, Knapp SE, Millemann RE. "Salmon poisoning" disease. IV. Transmission of the disease to dogs by Nanophyetus salminocola eggs. *The Journal of Parasitology*. 1967;53(4):694-699.

9. Quinn PJ, Markey BK, Leonard FC, FitzPatrick ES, Fanning S, Hartigan PJ. Rickettsiales and Coxiella burnetii. In: *Veterinary Microbiology and Microbial Disease.* 2nd ed. Ames, Iowa: Blackwell Science Ltd; 2011: Kindle edition.

10. Sykes JE, Marks SL, Mapes S, Schultz RM, Pollard RE, Tokarz D, et al. JE. Salmon poisoning disease in dogs: 29 cases. *J Vet Intern Med*. 2010;24:504-513.

**CASE IV:** N335/11 (JPC 4007441).

**Signalment:** 1-year-old male rabbit, *Oryctolagus cuniculus*.

**History:** Found dead without premonitory signs.

**Gross Pathology:** Poor body condition score (2/5). Bilateral diffuse lung congestion. Diffusely pale, enlarged liver containing multiple randomly distributed < 1mm diameter, ovoid pale yellow lesions.

**Histopathologic Description:** Liver: Diffuse hepatocyte necrosis with the cells exhibiting hyper-eosinophilic, frequently shrunken and fragmented cytoplasmic outline and karyopyknosis/lysis. Entire hepatic acini are involved including cells of the limiting plates (massive necrosis), with associated light scatterings of heterophils (peracute event). Bile ducts are severely distended with florid papillomatous hyperplasia of the lining epithelium and in some cases by infiltrates of macrophages, multinucleate macrophage giant cells with surrounding mantles of admixed lymphocytes and plasma cells in the fibrotic portal stroma. Eosinophilic refractile debris along with myriad ovoid to oblong structures with well-defined cytoplasmic boundaries and contained crescent-shaped structures with eosinophilic cytoplasm and a single nucleus (unsporulated coccidial oocysts) and smaller, ovoid structures with basophilic granular content (macrogametes) noted in duct lumens.

**Contributor's Morphologic Diagnosis:** Liver: 1. Hepatocyte necrosis, peracute, diffuse (massive), severe, consistent with a diagnosis of viral haemorrhagic disease of rabbits.
2. Bile duct hyperplasia and granulomatous cholangitis, chronic, severe with intra-luminal oocysts/ macrogametes consistent with a diagnosis of hepatic coccidiosis.

**Contributor's Comment:** This case was unusual in that the rabbit presented with a severe, peracute necrotising hepatitis, consistent with a diagnosis of viral haemorrhagic disease of rabbits (VHD), superimposed on more longstanding lesions of hepatic coccidiosis. The most consistent pathological findings in VHD are severe necrotising hepatitis and

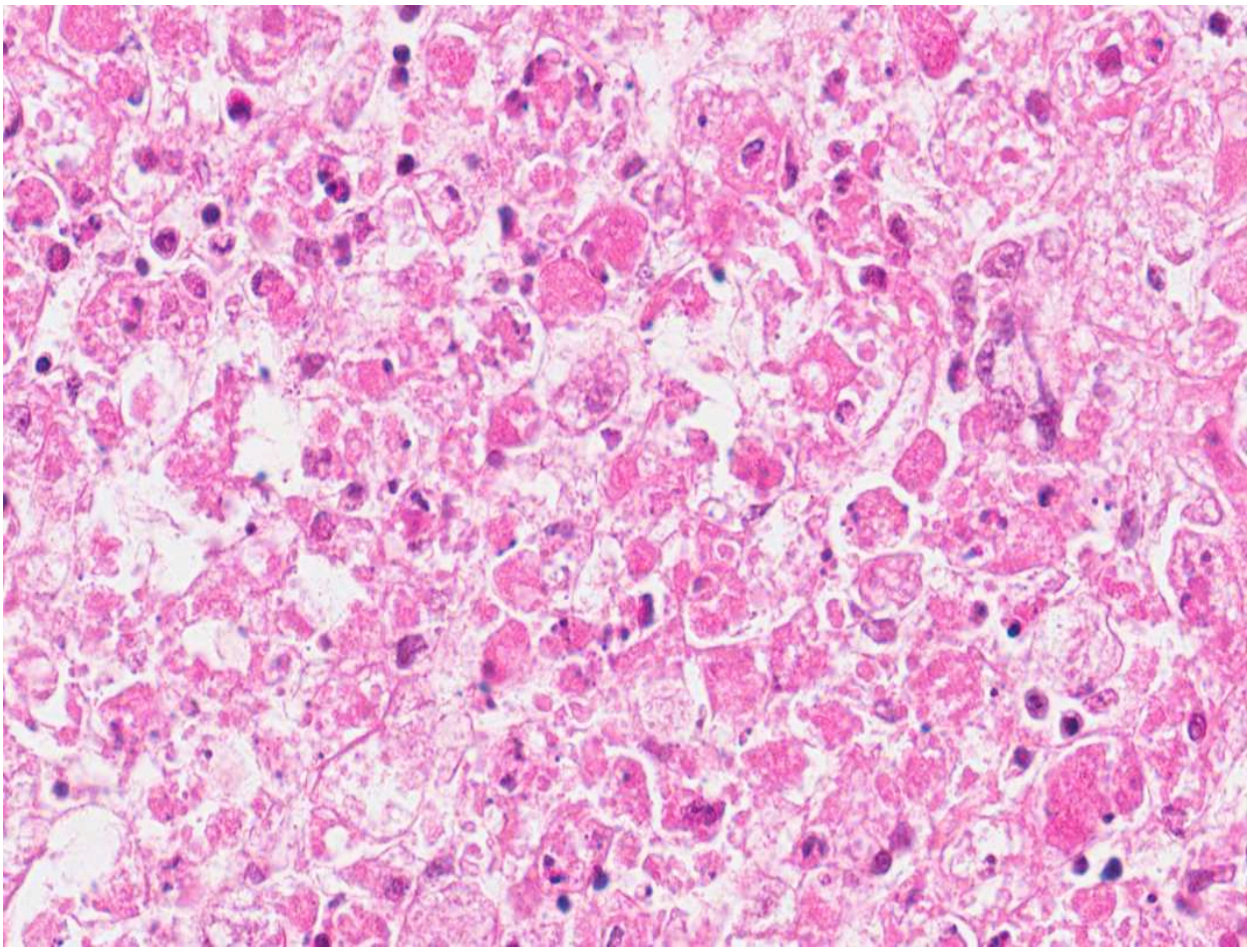

*4-1. Liver, rabbit: There is diffuse massive necrosis (necrosis in all areas of the hepatic lobule) with loss of hepatic plate architecture. (HE 400X)*

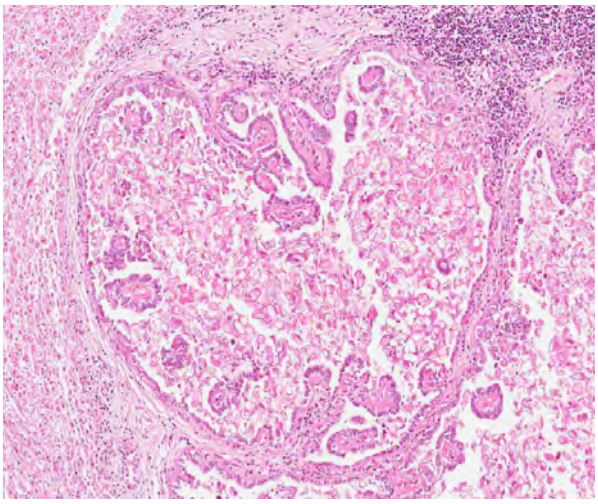

*4-2. Liver, rabbit: Liver, rabbit: Multifocally, bile ducts are markedly ectatic, and filled with numerous coccidial oocysts and fronds of proliferating epithelium. (HE 16X)*

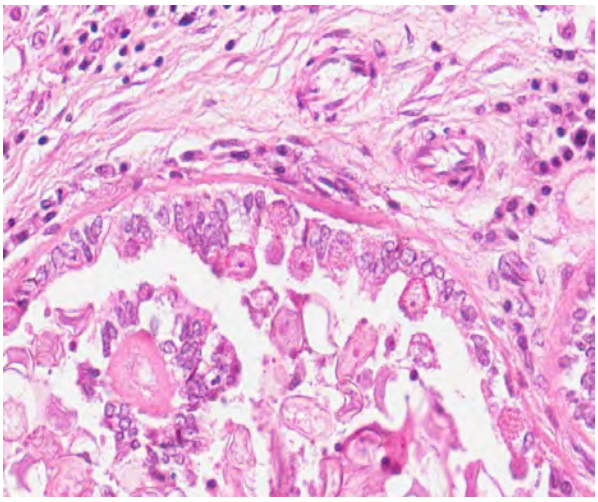

*4-3. Liver, rabbit: Biliary epithelial cells often contain macro- and microgametes of Eimeria steidae. (HE 400X)*

disseminated intravascular coagulation (DIC).[2,5,13,14,17] Complete hepatic acini including the hepatocytes of the limiting plates are frequently affected in this case justifying the designation massive necrosis. In previous reports hepatocyte necrosis is described as confined to the peripheral zones of lobules.[5] Such extensive peracute hepatic necrosis in rabbits found dead without premonitory signs is considered pathognomonic for VHD.

VHD is an acute, highly fatal disease of European wild and domestic rabbits, first reported from the People's Republic of China in 1984.[5,10] The causative agent is a calicivirus.[10,13] The virus spreads via oral, nasal or parenteral transmission and rapidly replicates in the liver of adult rabbits resulting in death within 48 - 72 hours.[9,13] Virus-induced hepatocyte death is due to apoptosis and in experimentally induced disease, in-situ hybridization identified viral replication in both hepatocytes and macrophages, suggesting infected macrophages contribute to viral dissemination.[2,7,14] Naturally occurring VHD is rarely seen in rabbits less than two months of age, possibly due to differences in the leucocyte response to hepatocyte infection between adults and juveniles. The lymphocytic rather than heterophilic response observed in the more resistant younger rabbits possibly reflects a protective host response to viral antigens on the hepatocyte surface.[4]

Hepatic coccidiosis in rabbits occurs worldwide and is caused by infection with *Eimeria stiedae*.[6,16] The coccidial oocysts are highly resistant and remain viable in soil and on fomites for long periods. Rabbits become infected by ingesting sporulated oocysts which are broken down in the duodenum, releasing sporozoites that penetrate the intestinal mucosa and travel to the liver either via the blood stream or within macrophages in the lymphatic system. In the liver the sporozoites invade the bile duct epithelium. Following developmental and reproductive phases oocysts are produced and are passed via the bile ducts into the intestines. Oocysts become infective one to four days after they are shed in the faeces.[6,16] The environment can become heavily contaminated in intensive conditions and wild rabbits can be a potential source of infection to domestic rabbits allowed access to grass grazed by wild rabbits.[6]

Infection of bile duct epithelial cells results in hyperplasia and inflammation with large numbers of ellipsoid oocysts in the walls and lumen of the bile ducts.[12] Destruction and regeneration of the bile duct epithelium results in significant cystic enlargement, papillomatous hyperplasia and duct reduplication. There is usually accompanying infiltration of plasma cells, lymphocytes, and occasional epithelioid cells.[12,15] Some enlarged bile ducts rupture initiating a granulomatous response and accompanying portal fibrosis is often prominent.[12] The oocysts may obstruct biliary outflow resulting in a distended bile duct and ischaemic necrosis can occur in the surrounding liver parenchyma due to compression of adjacent blood vessels by the bile duct enlargement.[12] In rabbits which survive such infection, fibrous tissue can replace much of the normal liver parenchyma.[16]

While there may be no clinical signs in mild infections, heavy infections can result in abdominal enlargement and ascites, with jaundice occurring in advanced stages of the disease. These signs reflect blockage of the bile ducts and interference with hepatic function.[12] Serum biochemistry may reveal elevated alkaline phosphatase, ALT and total bilirubin.[6]

**JPC Diagnosis:** 1. Liver: Necrosis, massive, diffuse.

2. Liver: Cholangiohepatitis, proliferative and lymphoplasmacytic, diffuse, moderate, with coccidial oocysts and gametocytes.

**Conference Comment:** Viral hemorrhagic disease virus (also referred to as rabbit hemorrhagic disease virus, RHDV) along with the closely-related and highly pathogenic European brown hair syndrome virus (EBHSV) make up the *Lagovirus* genus of the family *Caliciviridae*.[8] RHDV causes severe acute periportal to mid-zonal hepatic necrosis resulting in disseminated intravascular coagulopathy in rabbits in the *Oryctolagus* genus; whereas EBHSV causes similar disease in members of the *Lepus* genus. Recently there has been a report of an outbreak of a novel virus, designated Michigan rabbit calicivirus (MRCV), in a privately-owned New Zealand White rabbitry in Michigan. This outbreak was associated with a case fatality rate of 32.5%, with clinical signs including vulvar hemorrhage, epistaxis, ataxia, diarrhea, opisthotonos, ocular discharge, vocalization, hepatic necrosis and death. Experimental infection resulted in subclinical disease, and viral RNA sequencing and capsid amino acid sequencing indicated this calicivirus is distinct from other know lagoviruses.[3] It was suggested that MRCV represents a new variant of the nonpathogenic RCV-like group that includes RCV, Ashington and Lambay.[1] Further research is needed to fully elucidate the phylogenetic relationships of these viruses.[3]

Caliciviruses are non-enveloped, icosahedral, single stranded RNA viruses with characteristic 32 cup-shaped depressions on their surface. Other caliciviruses of veterinary importance include: vesicular exanthema of swine virus, San Miguel sea lion virus, feline calicivirus, and murine norovirus. Other caliciviruses in the genera *Norovirus* and *Sapovirus* have been reported to cause disease in cattle, pigs, wildlife, and non-human primates.[8]

**Contributing Institution**: Veterinary Sciences Centre
School of Veterinary Medicine
University College Dublin
Belfield, Dublin 4, Ireland
http://www.ucd.ie/vetmed/

**References:**

1. Abrantes J, Esteves PJ. Not-so-novel Michigan rabbit calicivirus. *Emerg Infect Dis.* 2010;16(8): 1331-1332.
2. Alonso C, Oviedo JM, Martín-Alonso JM, Díaz E, Boga JA, Parra F. Programmed cell death in the pathogenesis of rabbit hemorrhagic disease. *Arch Virol*. 1998;143:321–332.
3. Bergin IL, Wise AG, Bolin SR, Mullaney TP, Kiupel M, Maes RK. Novel Calicivirus identified in rabbits, Michigan USA. *Emerg Infect Dis.* 2009;15(12): 1955-1962.
4. Ferreira PG, Costa-E-Silva A, Oliveira MJR, Monteiro E, Aguas AP. Leukocyte–hepatocyte interaction in calicivirus infection: Differences between rabbits that are resistant or susceptible to rabbit haemorrhagic disease (RHD). *Vet Immunol Immunopath*. 2005;103:217–221.
5. Fuchs A, Weissenbock H. Comparative histopathological study of rabbit haemorrhagic disease (RHD) and European brown hare syndrome. *J Comp Path*. 1992;107:103-113.
6. Harcourt-Brown F. *Textbook of Rabbit Medicine*. Oxford, UK: Reed Educational and Professional Publishing Ltd; 2002.
7. Kimura T, Mitsui I, Okada Y, Furuya T, Ochiai K, Umemura T, et al. Distribution of rabbit haemorrhagic disease virus RNA in experimentally infected rabbits. *J Comp Path*. 2001;124:134-141.
8. MacLachlan NJ, Dubovi EJ. Caliciviridae. In: MacLachlan NJ, Dubovi EJ, eds. *Fenners Veterinary Virology*. 4th ed. San Diego, CA: Elsevier; 2011:443-450.
9. Mitro S, Krauss H. Rabbit hemorrhagic disease: A review with special reference to its epizootiology. *Eur J Epid*. 1993;9:70–78.
10. Moussa A, Chasey D, Lavazza A, Capucci L, Šmid B, Meyers G, et al. Haemorrhagic disease of lagomorphs: Evidence for a calicivirus. *Vet Microbiol*. 1992;33:375-381.
11. Ohlinger VF, Haas B, Meyers G, Weiland F, Thiel HJ. Identification of the virus causing rabbit hemorrhagic disease. *J Virol*. 1990;64:3331–3336.
12. Pakes SP, Gerrity LW. Protozoal diseases. In: Manning PJ, Ringler DH, Newcomer CE, eds. *The Biology of the Laboratory Rabbit*. 2nd ed. London, UK: Academic Press Limited; 1994;205-230.
13. Parra F, Prieto M. Purification and characterization of a calicivirus as the causative agent of a lethal hemorrhagic disease in rabbits. *J Virol*. 1990;64:4013–4015.
14. Prieto JM, Fernandez F, Alvarez V, Espi A, Garcia-Marin JF, Alvarez M, et al. Immunohistochemical localisation of rabbit haemorrhagic disease virus vp-60 antigen in early infection of young and adult rabbits. *Res Vet Sci*. 2000;68:181–187.
15. Schoeb TR, Cartner SC, Baker RA, Gerrity LW. Parasites of rabbits. In: Baker DG, ed. *Flynn's Parasites of Laboratory Animals*. 2nd ed. Ames, Iowa: Blackwell Publishing; 2007:451-499.
16. Soulsby EJL. *Helminths, Arthropods and Protozoa of Domesticated Animals*. 7th ed. London, UK: Bailliere Tyndall; 1982.
17. Ueda K, Park JH, Ochiae K, Itakura C. Disseminated intravascular coagulation (DIC) in rabbit haemorrhagic disease. *Jap J Vet Res*. 1992;40:133–141.

**Joint Pathology Center**
**Veterinary Pathology Services**

## WEDNESDAY SLIDE CONFERENCE 2012-2013

# Conference 11

**9 January 2013**

**CASE I:** 508A (JPC 4017936).

**Signalment:** 1-year-old male Montezuma quail (*Cyrtonyx montezumae*).

**History:** This animal was found dead with no premonitory signs. It was the second Montezuma quail death from this enclosure in a three-day period.

**Gross Pathology:** At necropsy, the quail was in good body condition with appropriate muscling and adipose tissue stores. The lungs were diffusely wet, dark red and slightly heavy. On section, they exuded a moderate amount of yellow-tinged, watery fluid.

**Histopathologic Description:** Lungs: Cellularity is increased throughout the lungs, resulting in marked thickening of air capillary walls and mild thickening of air atria septa. Increased cellularity is the result of numerous infiltrating macrophages with fewer lymphocytes and rare plasma cells. Dense accumulations of leukocytes are occasionally present

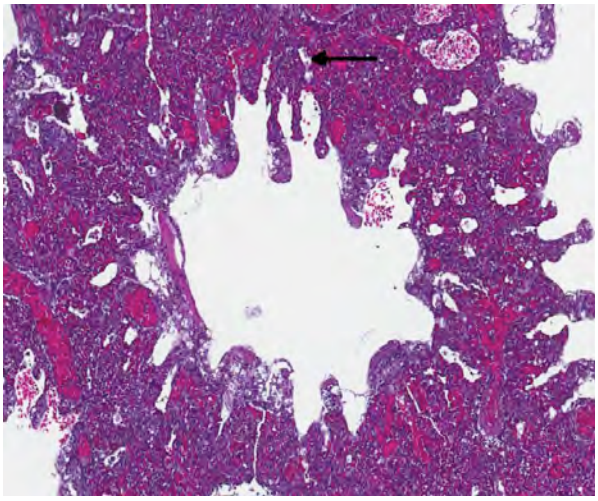

*1-1. Lung, Montezuma quail: Diffusely, the lungs are hypercellular, with loss of air capillary architecture and compression of respiratory atria (arrow). (HE 80X)*

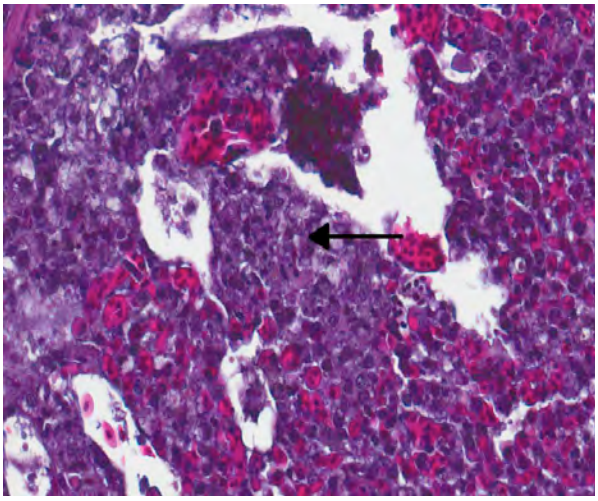

*1-2. Lung, Montezuma quail: Multifocally, there are numerous foci of necrosis (arrow) composed of cellular debris and necrotic histiocytes. (HE 400X)*

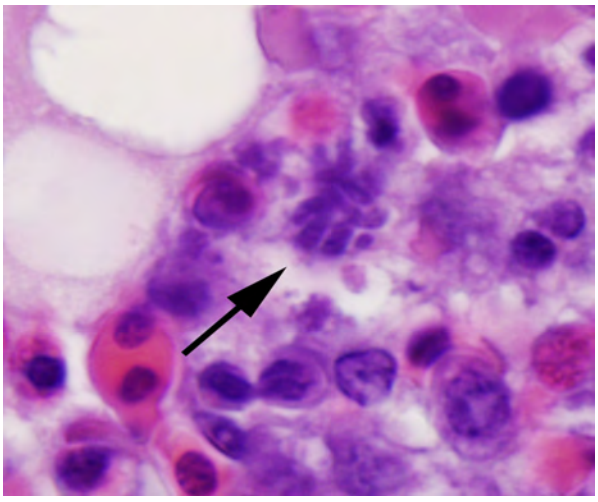

*1-3. Lung, Montezuma quail: Multifocally, endothelial cells contain protozoal meronts. (HE 1000X)*

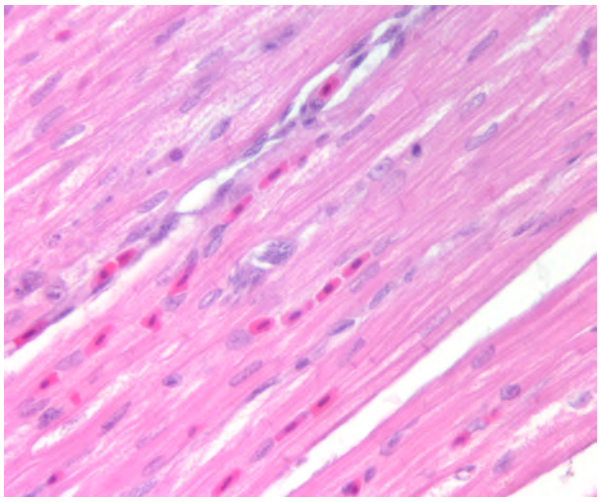

*1-4. Heart, Montezuma quail: A focal mature meront containing numerous elongate merozoites is focally present. The affected cell type is not discernible, but is presumed to be an endothelial cell. H&E. (Photo courtesy of the Wildlife Conservation Society, Zoological Health, 2300 Southern Blvd., Bronx, NY 10460, www.wcs.org)*

in perivascular spaces. Pale eosinophilic foci with loss of architecture and containing karyorrhectic debris are scattered randomly throughout the parenchyma (necrosis). Numerous protozoa-laden cells are scattered amongst the inflammatory population. Affected cells' cytoplasm contains large, immature, uninucleate meronts as well as mature meronts with numerous merozoites that are approximately 2µ x 4µ. Occasionally, meronts filling capillary lumens have a serpentine appearance. Foamy macrophages are present within airways, along with free erythrocytes and a small amount of pale eosinophilic wispy to homogenous material. There is frequent expansion of perivascular tissue by clear space (edema). The pulmonary vasculature is diffusely congested.

**Contributor's Morphologic Diagnosis:** Lungs: Pneumonia, interstitial, histiocytic to lymphoplasmacytic, subacute, diffuse, marked, with intracellular protozoa, scattered necrosis and pulmonary edema.

**Contributor's Comment:** This was one of two Montezuma quail to die within a three-day span at an urban zoological park in the spring of 2010. Both birds had similar gross and microscopic findings, the most significant of which was marked interstitial pneumonia with intralesional protozoa. Fatal pulmonary sarcocystosis was presumed to be due to a *Sarcocystis falcatula*-like infection which has been responsible for multiple mortalities in thick-billed parrots (*Rhynchopsitta pachyrhyncha*) at the zoo. Affected parrots had identical pulmonary lesions as these quail and were housed in the same enclosure.

*Sarcocystis falcatula* (and *S. falcatula*-like organisms) is typical of the genus in that it utilizes a two-host life cycle. The only known definitive host in North America is the opossum (*Didelphis virginiana*) but unlike most *Sarcocystis* species it can utilize a number of avian species as intermediate hosts.[3,5,6,7,8] Susceptible birds ingest sporocysts shed in the feces of opossum, which release sporozoites once in the intestinal tract. Tissue invasion and local asexual reproduction ensues, followed by additional cycles of merogony in capillaries and venules throughout the body.[6] In the lungs, where merogony is often most pronounced, endothelial cells become swollen with cytoplasmic meronts. The presence of protozoa can lead to vascular obstruction, perivasculitis and vasculitis, and significant interstitial and airway edema.[2,3,6] Pulmonary lesions can be fatal in birds with heavy protozoal burdens, such as the quail in this case. In addition to the lungs, merogony has been noted to occur in the liver, spleen, pancreas, adrenal glands and heart.[6] Other than the liver, the protozoal presence is typically insignificant with mild or no inflammation.[6] In these quail, endothelial cells of the heart were the only extrapulmonary site of merogony and low numbers of organisms were occasionally associated with mild lymphohistiocytic myocarditis. In birds that survive the initial reproductive cycles, sarcocysts typically develop in skeletal and cardiac muscle, where they remain until ingestion by the definitive host.[2,3,6,7] Sarcocysts were not identified in the case presented here, presumably an effect of how quickly the quail succumbed to pulmonary disease.

Multiple opossum were trapped on zoo grounds following initial diagnosis of this disease. In addition to direct infection via opossum feces, paratenic hosts

| *Sarcocystis* sp. | Intermediate host | Definitive host | Comments |
|---|---|---|---|
| *S. cruzi* | Cattle | Domestic and wild canids | Eosinophilic myositis; Hemolysis, abortion, lymphadenitis, tail tip sloughing, death |
| *S. gigantea* | Sheep | Cat | Only species of domestic animals visible to naked eye |
| *S. tenella (S. ovicanis)* | Sheep | Dog | Encephalomyelitis; severe disease in lambs |
| *S. miescheriana* | Swine | Domesitc and wild canids | Diarrhea, myositis, lameness |
| *S. neurona* | Birds/horses* | Opossum | Equine protozoal myeloencephalitis |

*Horses are assumed to be dead end hosts, but may act as intermediate hosts.

or mechanical vectors, such as cockroaches and other insects, can cause infection indirectly.[2]

Confirmation of *S. falcatula*-like organisms in avian patients requires diagnostic evaluation beyond light microscopy. Individual merozoites can be mistaken for *Toxoplasma* or *Neospora* tachyzoites, and light microscopic morphology alone (of any stage) is not sufficient to differentiate individual *Sarcocystis* species.[3] Immunohistochemistry is available for *S. falcatula*, and organisms in previous thick-billed parrot sarcocystosis cases at our institution reacted positively to *S. falcatula* antisera. As *S. neurona* can also reactive positively to this antisera, *S. neurona*-specific immunohistochemistry was also performed and was negative. [3] Ultrastructural evaluation of *Sarcocystis* spp. reveals typical apicomplexan features, such as a conoid and micronemes; unlike *Toxoplasma*, however, *Sarcocystis* spp. are intracytoplasmic rather than within a parasitophorous vacuole. Rhoptries are likely absent in *S. falcatula* -like organisms, but this observation differs between authors.[2,5,8]

Recent molecular investigations into the genus have revealed differences between organisms previously grouped together as *S. falcatula*.[3] Such research suggests the presence of multiple species, thus prompting the use of "*S. falcatula*-like" rather than definitive identification.

**JPC Diagnosis:** Lung: Pneumonia, interstitial, histiocytic and necrotizing, diffuse, with numerous protozoal schizonts.

**JPC Comment:** The contributor provides a very good summary of *Sarcocystis falcatula*-like organisms. *Sarcocystis* species, like other protozoal parasites in the phylum Apicomplexa, have a two-host life cycle; however, they differ from other genera in that asexual reproduction (schizogony and cyst formation) occur exclusively in the intermediate (herbivorous) host, and sexual reproduction (gametogony, fertilization, and sporulation) occur only in the definitive (carnivorous) host. *Sarcocystis* spp. usually do not cause illness in the definitive host, but schizogony in the endothelium of the intermediate host can result in serious and often fatal disease.[1] Clinical disease in the intermediate host may include fever, mucous membrane petechiation, edema, icterus, and macrocytic hypochromic anemia during the schizogonous phase or myositis during the encystment phase.[9] There are over 90 *Sarcocystis* species identified in mammals, birds and reptiles; some are associated with disease and others are considered nonpathogenic. The included chart details species which are pathogens of importance in domestic animals.[4,9]

**Contributing Institution**: Wildlife Conservation Society
Zoological Health
2300 Southern Blvd.
Bronx, NY 10460
www.wcs.org

**References:**

1. Bowman DD. Protozoans. In: *Georgis' Parasitology for Veterinarians*. St Louis, MO: Saunders Elsevier; 2009:104-106.
2. Clubb SL, Frenkel JK. *Sarcocystis falcatula* of opossums: transmission by cockroaches with fatal pulmonary disease in psittacine birds. *J. Parasitol*. 1992;78(1):116-124.
3. Dubey JP, Garner MM, Stetter MD, Marsh AE, Barr BC. Acute *Sarcocystis falcatula*-like infection in a carmine bee-eater (*Merops nubicus*) and immunohistochemical cross reactivity between *Sarcocystis falcatula* and *Sarcocystis neurona*. *J. Parasitol*. 2001;87(4):824-832.
4. Maxie MG, Youssef S. Nervous system. In: Maxie MG, ed. *Jubb, Kennedy and Palmer's Pathology of Domestic Animals.* 5th ed. Vol 1. New York, NY: Elsevier Saunders; 2007:435.
5. Smith JH, Meier JL, Neill JG, Bos ED. Pathogenesis of *Sarcocystis falcatula* in the budgerigar. I. Early pulmonary schizogony. *Lab Invest.* 1987;56(1):60-71.
6. Smith JH, Neill PJG, Box ED. Pathogenesis of *Sarcocystis falcatula* in the budgerigar. III. Pathologic and quantitative parasitologic analysis of extrapulmonary disease. *J. Parasitol*. 1989;75(2): 270-287.
7. Smith JH, Neill PJG, Dillard EA III, Box ED. Pathology of experimental *Sarcocystis falcatula* infections of canaries (*Serinus canarius*) and pigeons (*Columba livia*). *J. Parasitol*. 1990;76(1):59-68.
8. Speer CA, Dubey JP. Ultrastructure of schizonts and merozoites of *Sarcocystis falcatula* in the lungs of budgerigars (*Melopsittacus undulatus*). *J. Parasitol*. 1999;85(4):630-637.

9. Van Vleet JF, Valentine BA. Muscle and tendon. Maxie MG, ed. *Jubb, Kennedy and Palmer's Pathology of Domestic Animals.* 5th ed. Vol. 1. New York, NY: Elsevier Saunders; 2007:266-268.

**CASE II**: TVMDL 2012-01 (JPC 4018765).

**Signalment:** Four-year-old, male red-tailed boa constrictor.

**History:** A four-year-old, male, 10-pound boa constrictor from a local zoo was submitted for necropsy following a 12-month duration respiratory tract disease. The illness was non-responsive to multiple antibiotics and, as the disease progressed, the animal exhibited increased respiratory effort, intermittent lethargy, and anorexia.

**Gross Pathology:** The animal was in thin body condition. There was extensive replacement of up to 80% of the normal pulmonary parenchyma by coalescing granulomas.

**Histopathologic Description:** The normal pulmonary architecture is predominately effaced by coalescing granulomas. The parabronchial submucosa and air capillary interstitium are moderately to markedly expanded by granulomas, which extend into and variably occlude air spaces and faveoli. The granulomas are composed of central necrotic debris surrounded by large numbers of epithelioid macrophages admixed with low numbers of heterophils and few lymphocytes and rare giant cells. Moderate numbers of macrophages, lymphocytes, and heterophils infiltrate the interstitium between granulomas with mild fibrosis. Ziehl-Neelsen staining revealed large numbers of acid-fast bacilli within macrophages consistent with *Mycobacterium* spp.

**Contributor's Morphologic Diagnosis:** Pneumonia, granulomatous, chronic, severe.

**Contributor's Comment:** Spontaneous mycobacterial infections have been reported in a wide variety of reptiles, including snakes, turtles, lizards, and crocodiles and descriptions of mycobacterial infections in reptiles have been reported since the early 1900s.[2,3,4] *Mycobacterium marinum* is a ubiquitous opportunistic pathogen and is the predominant mycobacterial pathogen reported in snakes. The original source of infection in captive reptiles is likely the environment, whether its introduction into the exhibit is via plant matter or other inanimate objects, or via a previously infected animal.[2] Infection is believed to be acquired by ingestion of infected material or via defects in the integumentary or respiratory systems.[1,4] Mycobacterial infections in reptiles can cause systemic illness accompanied by nonspecific signs such as anorexia, lethargy, and wasting.[3] Gross lesions present as grayish-white nodules present in the affected tissue. Histopathologic examination illustrates classic

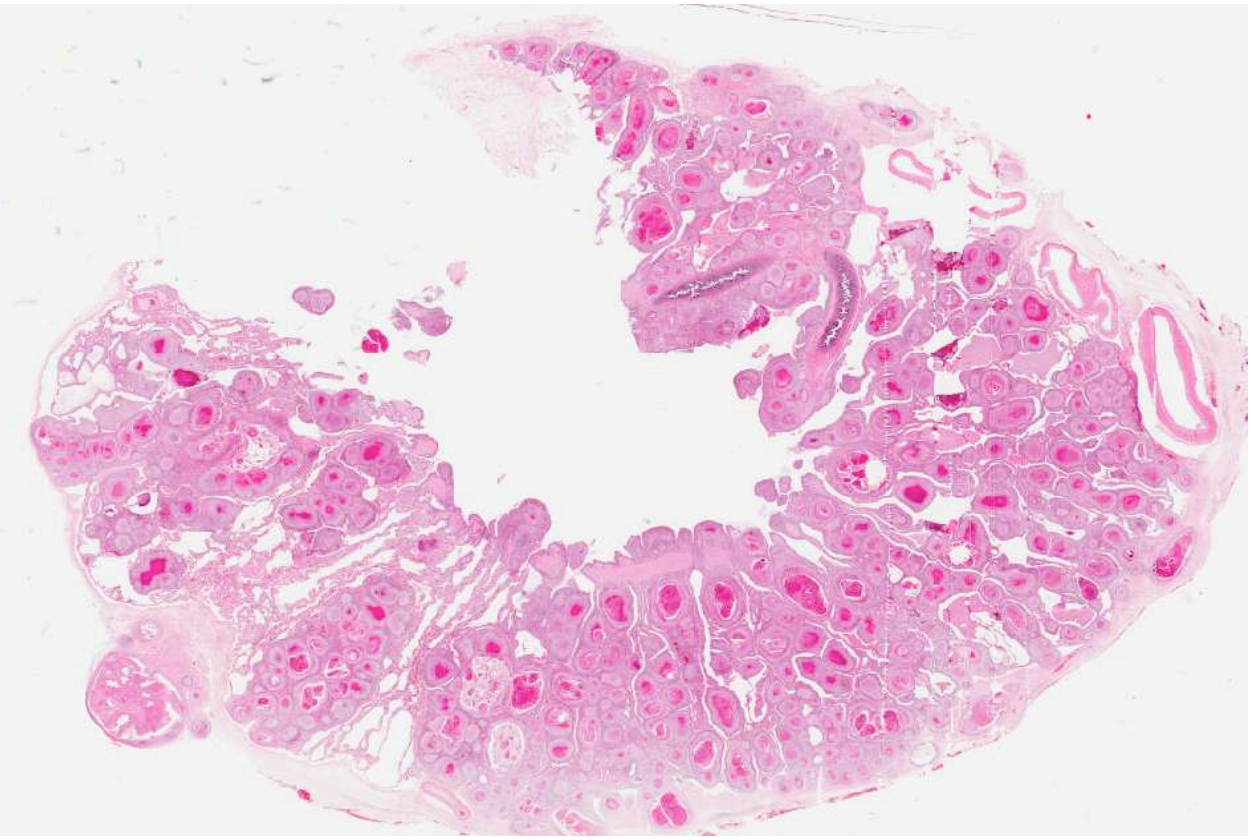

*2-1. Lung, snake: Diffusely, the faveolar interstitium is expanded by numerous granulomas. (HE 3.0X)*

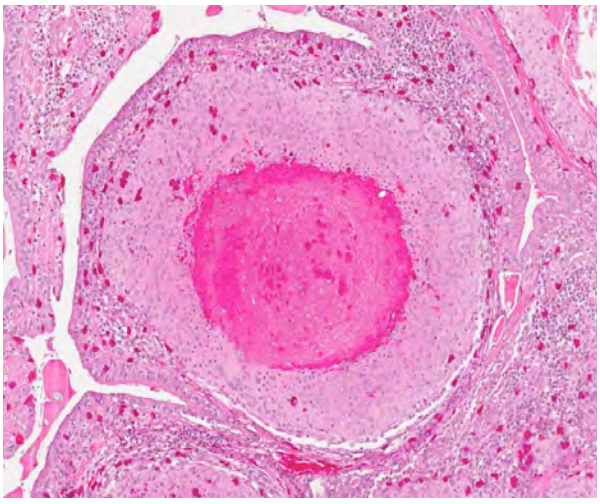

*2-2. Lung, snake: Granulomas are up to 700 µm in diameter and are centered on areas of cellular debris and degenerate heterophils. (HE 100X)*

granulomas with a central core of necrotic debris surrounded by epithelioid macrophages.

Early diagnosis of mycobacterial diseases in captive reptiles is crucial to limiting the extent of disease transmission. The detection of mycobacteria among captive animals in zoos is concerning and treatment is often not advised considering the chronic and often advanced state of the disease, risk of infection to animals within the same and other exhibits, transfer of animals with unrecognized infection, and spread of infection to animal handlers.[1,2] Additionally, no successful treatment of infection with *Mycobacterium* spp. has been reported in reptiles.[3]

**JPC Diagnosis:** Lung: Pneumonia, interstitial, granulomatous, diffuse, severe.

**Conference Comment:** The contributor provides a concise review of mycobacterial diseases in snakes. Conference participants discussed the differential diagnosis for granulomatous inflammation in snakes. Reptiles typically respond to infectious agents with a granulomatous inflammatory response, which is predominantly heterophilic or histiocytic, depending on both the etiologic agent and the host response.[4] Histiocytic granulomas are usually associated with intracellular pathogens, whereas heterophilic granulomas are generally associated with extracellular pathogens. In heterophilic granulomas, heterophil degranulation and central necrosis induce a strong histiocytic response; thus, both types of granulomas can progress to chronic granulomas.
*Mycobacterium* species including *M. avium*, *M. chelonae*, *M. fortuitum*, *M. intracellulare*, *M. marinum*, *M. phlei*, *M. smegmatis*, and *M. ulcerans* have frequently been reported to cause histiocytic granulomas in reptiles. Additionally, other intracellular bacteria from the family Chlamydiaceae, which sporadically infect reptiles, can also incite histiocytic granulomas. A retrospective study of ninety reptiles with granulomas (i.e., 48 snakes, 27 chelonians, and 15 lizards) showed that, although *Mycobacterium* species other than *Mycobacterium tuberculosis* (MOTT) are the most important infectious agents causing granulomatous inflammation in reptiles, *Chlamodyphila pneumoniae* and "Chlamydia-like" microorganisms (e.g., *Parachlamydia acanthamoebae* and *Simikania negevensis*) can also induce well-formed granulomas, and therefore should be considered in the differential diagnosis for granulomatous lesions in reptiles. Mycobacteria and chlamydia can be identified microscopically by Ziehl-Neelsen acid fact stain and immunohistochemistry for cLPS antigen, respectively; however, both of these methods are less sensitive than PCR.[4]

**Contributing Institution**: Texas Veterinary Medical Diagnostic Laboratory
6610 Amarillo Blvd West
Amarillo, TX 79106
tvmdl.tamu.edu

**References**

1. Hernandez-Divers SJ, Shearer, D. Pulmonary mycobacteriosis caused by *Mycobacterium haemophilum* and *M marinum* in a royal python. *JAVMA*. 2002;220(11):1661-1663.
2. Maslow JN, Wallace R, Michaels M, Foskett H, Maslow E, Kiehlbauch JA. Outbreak of *Mycobacterium marinum* infection among captive snakes and bullfrogs. *Zoo Biology*. 2002;21:233-241.
3. Slany M, Knotec Z, Skoric M, Knotkova Z, Svobodova J, Mrlik V, et al. Systemic mixed infection in a brown caiman (*Caiman crocodiles fuscus*) caused by *Mycobacterium szulgai* and *M. chelonae:* A case report. *Veterinarini Medicina*. 2010;55(2):91-96.
4. Soldati G, Lu ZH, Vaughan L, Polkinghorne A, Zimmermann DR, Huder JB, et al. Detection of mycobacterial and chlamydiae in granulomatous inflammation of reptiles: A retrospective study. *Vet Path*. 2004;41:388-397.

**CASE III:** 08-72416 (JPC 3134858).

**Signalment:** A five-month-old male white-tailed deer (*Odocoileus virginianus*).

**History:** The fourth fawn to die from the herd.

**Gross Pathologic Findings:** The cornea of the right eye was partially cloudy. There was a 1.5 cm area of hemorrhage in the skin of the right ear. There was subcutaneous yellow edema fluid in the ventral neck, surrounding the trachea and esophagus. The right half of the thorax contained a large blood clot. Dorsal to the lungs and heart there was a blood clot approximately 20 cm long that surrounded the aorta and was attached to the musculature ventral to the spinal column. There was acute hemorrhage in one of the adrenal glands and the left testicle. There were small multifocal hemorrhages in the right testicle.

**Laboratory Results:** No anaerobic bacterial growth from lung, liver, or brain. Negative for epizootic hemorrhagic disease virus by PCR. PCR positive for Caprine Herpesvirus-2.

**Histopathologic Description:** Cerebrum: Surrounding numerous meningeal and parenchymal vessels is an infiltrate composed of low to medium numbers of lymphocytes and neutrophils. The inflammatory cells often are equally present in the tunica media and tunica adventitia. There are variable numbers of macrophages, lymphocytes, and occasional plasma cells in the meninges. There are scattered glial cell infiltrates within the neuropil.

In most of the sections, there are several vessels in the leptomeninges that have fibrinoid necrosis of the vessel wall. Affected vessels often have adventitial to subintimal accumulation of neutrophils, lymphocytes, and macrophages.

In some sections, choroid plexus is present; it is heavily infiltrated by lymphocytes, plasma cells, macrophages, and neutrophils.

**Contributor's Morphologic Diagnosis:** 1. Cerebrum: Vasculitis and perivasculitis, necrotizing, lymphocytic, multifocal, moderate.
2. Cerebrum: Meningoencephalitis, lymphocytic, diffuse.

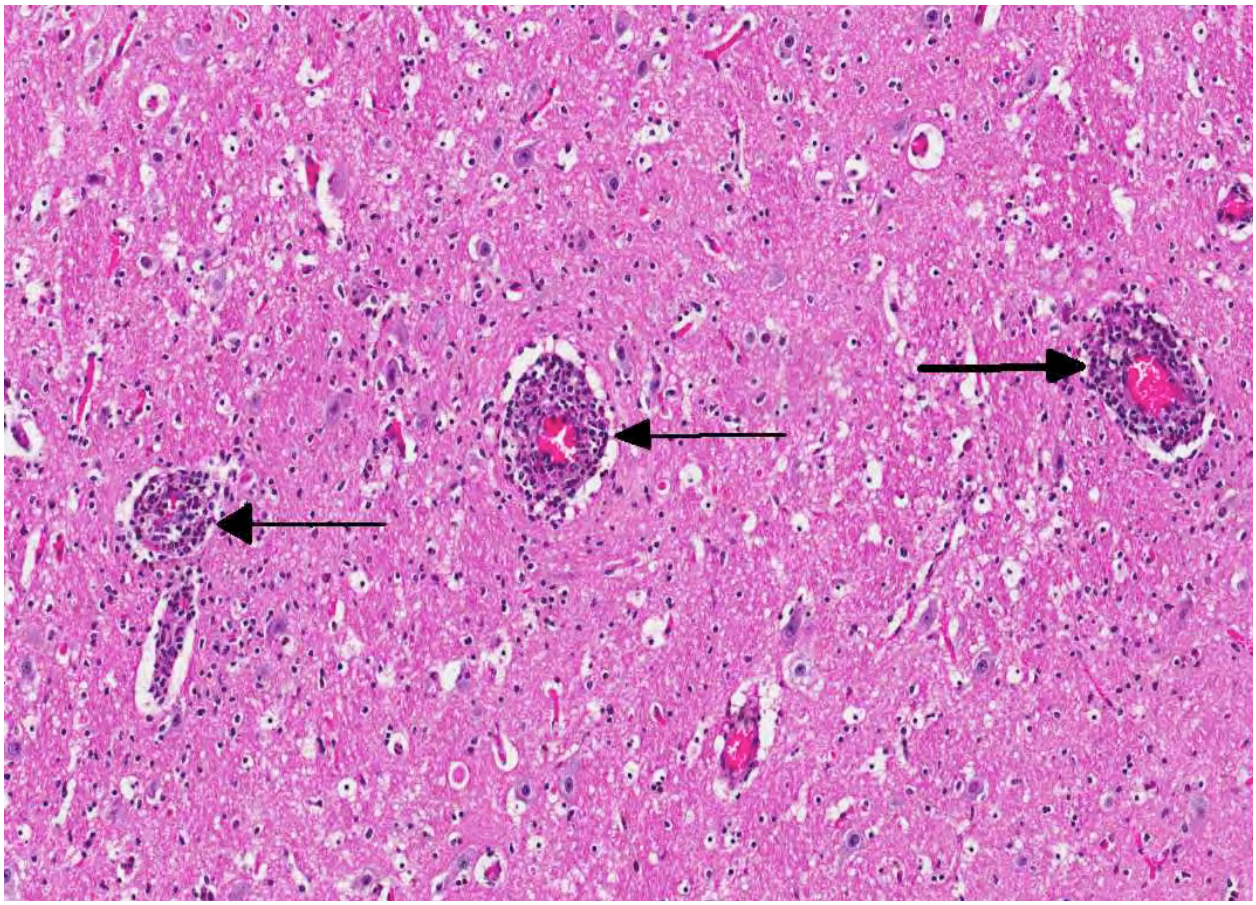

*3-1. Cerebrum at level of lateral ventricles, deer: Within the neuropil, vessels are often surrounded by prominent cuffs of lymphocytes and plasma cells (arrows). (HE 100X)*

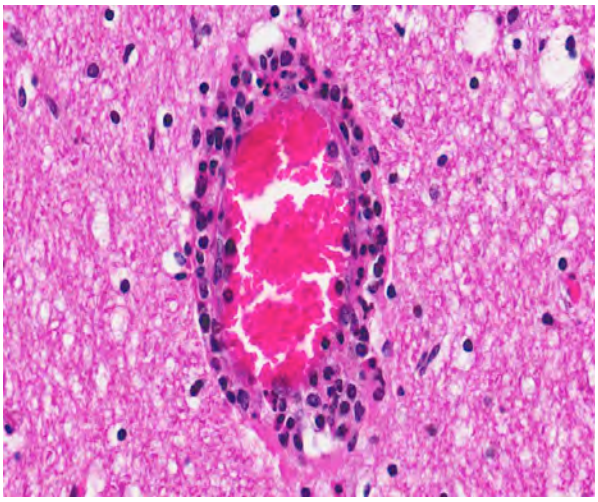

*3-2. Cerebrum at level of lateral ventricles, deer: Occasionally, inflammatory cells are present within vessel walls, along with small amounts of necrotic debris and fibrin (vasculitis). (HE 400X)*

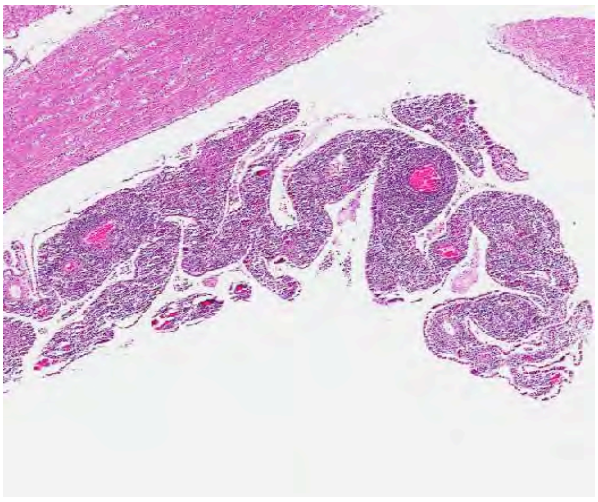

*3-3. Cerebrum at level of lateral ventricles, deer: Diffusely, the choroid plexus is markedly expanded by a large numbers of lymphocytes and plasma cells. (HE 20X)*

**Contributor's Comment:** Gross and histologic lesions were consistent with malignant catarrhal fever (MCF), and infection with caprine herpesvirus 2 was confirmed by PCR testing. MCF occurs in ruminant species and is caused by several herpesviruses, an enveloped, linear, doubled-stranded DNA virus. These viruses are in the *Rhadinovirus* genus of the subfamily *Gammaherpesvirinae*. There are currently four known members of the MCF virus group: alcelaphine herpesvirus 1 (AlHV-1), ovine herpesvirus 2 (OvHV-2), caprine herpesvirus 2 (CpHV-2), and a gammaherpes virus found in white-tailed deer with no known reservoir (MCFV-WTD).[3,4] Infection of white-tailed deer with CpHV-2 has been previously reported.[3]

Typical gross changes associated with MCF include conjunctivitis, cutaneous exanthema, crusting, and alopecia, nasal discharge, oral and esophageal ulcerations, urinary mucosal hemorrhages, and lymphoid enlargement.[2] Mortality in susceptible species approaches 100%; however, in the natural host, infection is latent or inapparent with intermittent virus shedding. These viruses are difficult or impossible to isolate in cell culture.

The common histologic changes associated with MCF are lymphocytic perivasculitis and vasculitis with fibrinoid necrosis of medium sized arteries, and lymphoid hyperplasia.[2] Lesions are characterized by a proliferation of CD8+ T lymphocytes and tissue necrosis.[5,7] The mechanism of proliferation and vasculitis is unknown.[5]

MCF has been documented in white-tailed deer, along with other wild cervids, pigs, and cattle.[1,2,8] Raising bovids and deer around other small ruminants (sheep, goats) can be risky due to transmission of the MCF viruses from the host species that is not clinically ill. The incubation period is usually 2-10 weeks, but may on occasion be very much longer than this. Epizootic hemorrhagic disease (orbivirus) is a differential diagnosis for MCF in deer with acute hemorrhage.

**JPC Diagnosis:** Cerebrum: Arteritis and phlebitis, lymphoblastic and necrotizing, diffuse, moderate, with meningitis and choroid plexitis.

**Conference Comment:** The contributor provides an excellent summary of the gamma herpesviruses associated with malignant catarrhal fever in various species. In addition to the four members of the MCF virus group, there are several viruses that have been reported to cause MCF or MCF-like diseases in various species of hoofstock within zoological collections.[6] Recently, one such novel virus (MCFV-ibex) was identified as the etiologic agent for MCF observed in bongo antelope. In this outbreak, a Nubian ibex was found to be the source of the virus. The presentation of MCF in bongos differs from the classic presentation in domestic ruminants and deer in the following ways: The bongos developed necrotizing cholangiohepatitis, neutrophilic necrotizing myocarditis, and they lacked the typical erosive or ulcerative oronasal lesions and enteritis often seen in other ruminants with MCF.[6]

**Contributing Institution**: Kansas State University
College of Veterinary Medicine
Dept. Diagnostic Medicine/Pathobiology
1800 Denison Ave
Manhattan, KS 66506
www.vet.k-state.edu/depts/dmp/

**References:**

1. Alcaraz A, Warren A, Jackson C, Gold J, McCoy M, Cheong SH, et al. Naturally occurring sheep-associated

malignant catarrhal fever in North American pigs. *J Vet Diagn Invest*. 2009;21:250-253.
2. Brown CC, Baker DC, Barker IK. The Alimentary system. In: Maxie MG, ed. *Jubb, Kennedy and Palmer's Pathology of Domestic Animals*, 5th ed. Vol 2. Philadelphia, PA: Elsevier Saunders; 2007:152-158.
3. Li H, Wunschmann A, Keller J, Hall DG, Crawford TB. Caprine herpesvirus-2–associated malignant catarrhal fever in white-tailed deer (*Odocoileus* virginianus). *J Vet Diagn Invest.* 2003;15:46–49.
4. Li H, Dyer N, Keller J, Crawford TB. Newly recognized herpesvirus causing malignant catarrhal fever in white-tailed deer (*Odocoileus* virginianus). *J Clin Micro*. 2000;38(4):1313–1318.
5. Dewals B, Boudry C, Farnir F, Drion PV, Vanderplasschen A. Malignant catarrhal fever induced by alcelaphine herpesvirus 1 is associated with proliferation of CD8+ T cells supporting a latent infection. *PLoS ONE*. 2008;3(2):e1627.
6. Gasper D, Barr B, Li H, Taus N, Peterson R, Benjamin G, et al. Ibex-associated malignant catarrhal fever−like disease in a group of bongo antelope (Tragelaphus eurycerus ). *Vet Pathol*. 2012:49;492.
7. Russell GC, Stewart JP, Haig DM. Malignant catarrhal fever: A review. *Vet J*. 2009;179(3):324-35.
8. Vikøren T, Li H, Lillehaug A, Jonassen CM, Böckerman I, Handeland K. Malignant catarrhal fever in free-ranging cervids associated with OvHV-2 and CpHV-2 DNA. *J Wildl Dis*. 2006;42(4):797-807.

**CASE IV:** 1016743 (JPC 4020067).

**Signalment:** Adult (unknown age) female common northern boa constrictor (*Boa constrictor imperator*).

**History:** The patient was presented to the West Esplanade Veterinary Clinic (Metairie, LA) for a four-month history of anorexia and weight loss. Two other boa constrictors that were housed in close proximity to the patient had recently died after a period of anorexia of unknown duration. Also, there was a history of mite infestation in the household one year prior to presentation. Upon physical examination, the patient was thin with a body condition score of 2/5 and excess gas was noted on abdominal palpation. Heparinized blood was collected via cardiocentesis and submitted to the Louisiana State University Clinical Pathology Laboratory for a complete blood count. A blood smear from the patient is submitted for review. The patient died one week after initial presentation.

**Gross Pathology:** No gross lesions were noted.

**Laboratory Results:**

Complete Blood Count:

| **Parameter** | | **Reference[3]** |
|---|---|---|
| WBC (x103/µL) | **40 H** | 4 – 10 |
| Heterophils (x103/µL) | 4 | 0.8 – 6.5 |
| Lymphocytes (x103/µL) | **34.8 H** | 0.4 – 6 |
| Azurophils (x103/µL) | **1.2 H** | 0 – 0.58 |
| Eosinophils (x103/µL) | 0 | 0 – 0.3 |
| Basophils (x103/µL) | 0 | 0 – 2 |
| Thrombocytes | Adequate | N/A |
| PCV (%) | 37 | 24 – 40 |
| Total Protein (g/dL) | **9.7 H** | 4.6 – 8.0 |

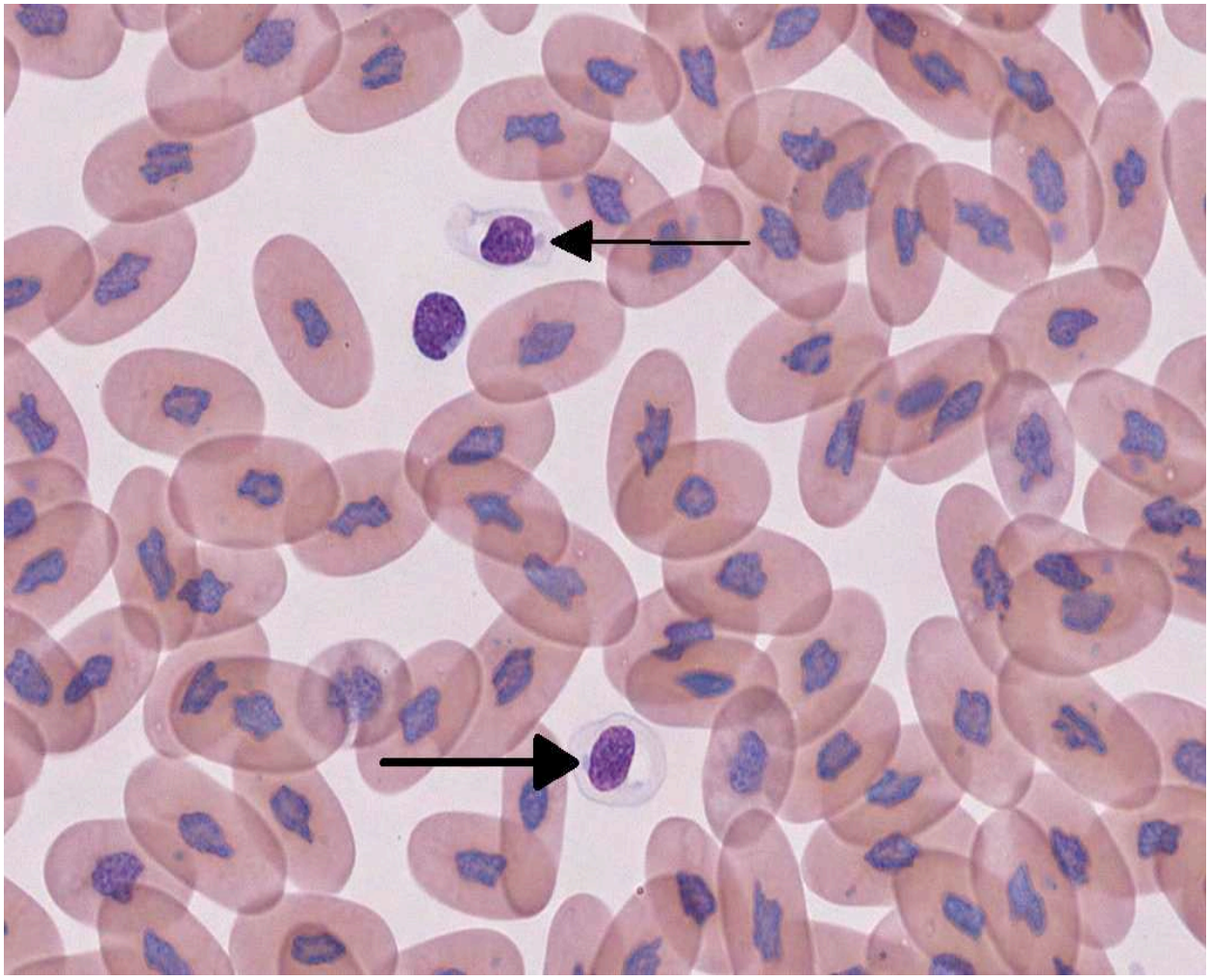

*4-1. Blood smear, boa constrictor: Lymphocytes often contain a 2µm in diameter, round, cytoplasmic inclusion body (arrows). (Wright-Giemsa 1000X)*

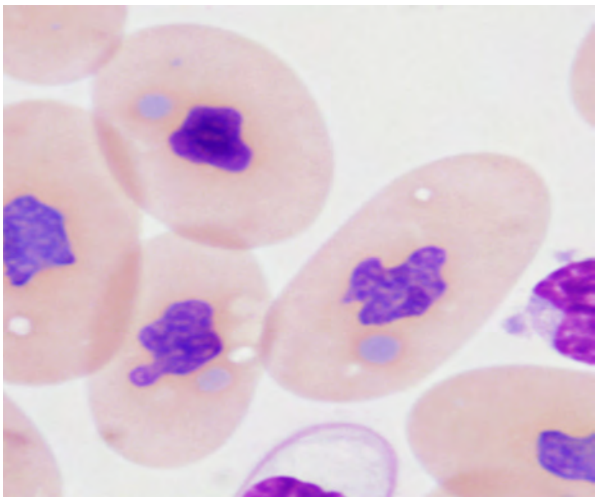

*4-2. Blood smear, boa constrictor. Three erythrocytes (center) each contain a small (1-2 µm in diameter) round light blue inclusion similar in color to those found in the lymphocytes. (Wright-Giemsa 1000x) (Photograph courtesy of Louisiana State University School of Veterinary Medicine. www.vetmed.lsu.edu/pbs/)*

**Histopathologic Description:** A blood smear is submitted for review. The smear contains a marked increase in the number of leukocytes. The leukocytes consist of predominantly small lymphocytes with rare lymphocytes that are intermediate in size. Many lymphocytes contain a single lightly basophilic intracytoplasmic inclusion of homogeneous texture that displaces the nucleus to the periphery of the cell. These inclusions vary in shape from round to oval to elongate with a diameter of 2-6 µm. Smaller (~1-3 µm in diameter) round inclusions of similar color are noted in moderate numbers of erythrocytes and rarely in heterophils. The erythrocytic inclusions were distinct from incidental basophilic punctate structures that are found frequently in erythrocytes from reptiles, believed to be degenerate organelles.[1] The erythrocyte density appears to be within normal limits. Mild polychromasia and rare earlier erythroid precursors are noted. Thrombocytes are adequate in number with normal morphology.

**Contributor's Morphologic Diagnosis:** Blood smear: Marked lymphocytosis with numerous basophilic intracytoplasmic inclusions consistent with boid inclusion body disease.

**Contributor's Comment:** Inclusion body disease (IBD) is a common and highly contagious disease seen worldwide in snakes of the families *Boidae* and *Pythonidae*.[3,9,11] The causative agent is unknown. Viral-like particles were observed with transmission electron microscopy in boid snakes with IBD.[6,9,11,12] Also, retroviruses have been isolated from boids with IBD.[6] However, a cause and effect relationship has yet to be proven. Clinical signs are variable and include neurologic deficits and regurgitation.[3,9,11] Snakes may die within weeks; while others may remain asymptomatic for long periods of time.[3] The results of CBCs from boids with IBD vary depending on the stage of infection.[9] Lymphocytosis is more commonly seen in acutely infected boids, whereas chronically infected boids may have normal to low lymphocyte concentration.[9] The lymphocytosis is presumably secondary to antigenic stimulation. Chronic lymphoid leukemia or disseminated small cell lymphoma is considered less likely in the current case, since a neoplastic focus was not found on necropsy. However, bone marrow evaluation was not performed.

The diagnosis of IBD relies on identifying the characteristic intracytoplasmic inclusions. These inclusions can be found antemortem in blood films or buffy coat preparations.[3,5,8,11] In blood films, inclusions can be found in lymphocytes, erythrocytes, or heterophils.[3] IBD inclusions stained with Wright-Giemsa are intracytoplasmic and lightly basophilic with variable size and shape.[3,8] The diagnosis of IBD can be confirmed with H&E staining, in which case, these inclusions stain eosinophilic to amphophilic.[3,5] However, not all histologically confirmed IBD cases have easily identifiable inclusions in the circulating blood.[5] On postmortem examination, the inclusions can be found in glial cells and neurons of the central nervous system, lymphocytes in lymphoid organs, and epithelial cells of internal organs (gastrointestinal tract, liver, pancreas, etc).[3,7,11] In the current case, histopathology revealed inclusions in lymphocytes in the spleen, in hepatocytes, and pancreatic epithelium.

There are several reports of C-type retrovirus-like budding particles in IBD inclusions with TEM.[6,7,9,11,12] However, a recent report suggests that the inclusions are instead composed of aggregates of a unique, non-viral 68 kD IBD protein.[3] To the author's knowledge, there are no TEM descriptions of inclusions in circulating lymphocytes. The inclusions described here consisted of large aggregates of non-membrane bound amorphous granular electron dense material without viral-like particles.

When snakes demonstrating clinical signs are diagnosed with IBD the prognosis is grave, as the disease is always fatal.[11] However, the long term survival of asymptomatic animals with IBD has not been evaluated. This case highlights the importance of evaluating blood films of susceptible snakes for IBD inclusions. Although there may be poor sensitivity, a blood film or buffy coat evaluation is a cheap, non-invasive test that can be used to detect this disease, especially if there is a lymphocytosis.

****Note**: Portions of this case have been published – Banajee KH, Chang L, Jacobson ER, Rich GA, Royal AB. What's your diagnosis? blood film from a boa constrictor. *Vet Clin Path.* 2012;41(1):158-159.

**JPC Diagnosis:** Peripheral blood: marked lymphocytosis with numerous intralymphocytic and intraerythrocytic intracytoplasmic inclusions.

**Conference Comment:** The contributor provides an excellent review of IBD. Participants discussed recent findings that suggest IBD may be caused by novel viruses that appear to be related to both arenaviruses and filoviruses.[10] In this study, viral nucleoprotein from three viruses with a typical but divergent arenavirus genome was localized within large cytoplasmic inclusions in infected cells. Interestingly, envelope glycoproteins from the viruses are more similar to those of filoviruses than to other arenaviruses. The presence of these viral proteins in 6/8 confirmed IBD cases and 0/10 controls indicates that these newly discovered viruses are possible etiologic agents of IBD.[10]

Additionally, participants discussed characteristics of reptilian blood cells and reptilian hemoparasites that can be found on blood films. In reptiles, mature erythrocytes are larger than their mammalian or avian counterparts, and, as in birds, reptile erythrocytes are ellipsoidal with centrally-placed, oval to round nuclei with dense purple chromatin and irregular margins.[2] Often, small (0.5 µm to 2.0 µm) round to irregular, basophilic intracytoplasmic inclusions are found in the cytoplasm of reptile erythrocytes and are suspected to be degenerate organelles, likely due to slide preparation artifact. Likewise, the basophilic stippling associated with a regenerative response or lead poisoning should not be confused with pathogen associated intracytoplasmic inclusions. Reptilian lymphocytes are similar in appearance and function to mammalian and avian lymphocytes. Circulating monocytes (azurophils) are usually found in small numbers; however, increased numbers are seen with granulomatous inflammation. Granulocytes in reptiles are classified as acidophils (heterophils and eosinophils) and basophils. Heterophils have bright orange fusiform cytoplasmic granule, and function similarly to avian heterophils (i.e. they rely heavily on oxygen-independent mechanisms to destroy phagocytized microbes.) Eosinophils contain eosinophilic spherical granules, and function much like their mammalian counterparts. Basophils appear and function similarly to those found in mammals and birds; however, their relative number can be higher and in some species comprise up to 40% of the leukocyte differential. Reptilian thrombocytes are elliptical to fusiform with a centrally-positioned nucleus, dense chromatin and colorless cytoplasm with few azurophilic granules.[2]

Hemoparasites and microfilaria are common in reptiles and are often encountered on blood films. Although usually considered incidental, some can cause disease (i.e. hemolytic anemia).[2] Common hemoprotozoa in reptiles include hemogregarines (*Hemogregarina, Hepatozoon, Karyolysus*), trypanosomes and *Plasmodium* spp. Less common hemoprotozoans of reptiles include *Leishmania, Saurocytozoon, Haemoproteus, Schellackia,* and the *piroplasmids.* Hemogregarines are identified in erythrocytes by the presence of intracytoplasmic gametocytes that lack refractile pigment granules. Trypanosomes are large extracellular flagellate protozoa. *Plasmodium* trophozoites are small, signet-ring structures found in erythrocyte cytoplasm and have gametocytes with refractile granules; whereas *Sauroleishmania* appear as round to oval 2-4 µm blue organisms with an oval, red nucleus in the cytoplasm of thrombocytes or mononuclear leukocytes. *Saurocytozoon* can be identified by their round gametocytes that lack pigment granules in the cytoplasm of lizard leukocytes. *Haemoproteus* gametocytes have refractile pigment granules and, similar to *Haemoproteus* in birds, can cause dehemoglobinization of the infected erythrocyte.[2] *Lainsonia* and *Schellackia* are coccidian parasites whose sporozoites appear as intracytoplsasmic inclusions in erythrocytes and lymphocytes of lizards and snakes. The sporozoites are round to oval, pale staining, nonpigmented inclusions that deform the host cell nucleus into a crescent shape. Piroplasmids such as *Babesia, Aegyptianella, Sauroplamsa* or *Serpentoplasma* appear as small nonpigmented, round to piriform and signet ring-like inclusions in erythrocyte cytoplasm.

**Contributing Institution:** Louisiana State University
School of Veterinary Medicine
Department of Pathobiological Sciences
Skip Bertman Drive
Baton Rouge, LA 70803
www.vetmed.lsu.edu/pbs/

**References:**

1. Alleman AR, Jacobson ER, Raskin RE. Morphologic and cytochemical characteristics of blood cells from the desert tortoise (Gopherus agassizii). *Am J Vet Res.* 1992;53(9):1645-1651.
2. Campbell TW. Hematology of reptiles. In: Thrall MA, Weiser G, Allison RW, Campbell TW, eds. *Veterinary Hematology and Clinical Chemistry*. 2nd ed. Ames, Iowa: Wiley-Blackwell; 2012:Kindle edition, retrieved from *Amazon.com;* location 34%).
3. Chang L, Jacobson ER. Inclusion body disease, a worldwide infectious disease of boid snakes: a review. *J Exotic Pet Med*. 2010;19(3):216-225.
4. Diethelm G, Stein G. Hematologic and blood chemistry values in reptiles. In: Mader DR, ed. *Reptile Medicine and Surgery*. 2nd ed. St. Louis, MO: Saunders Elsevier; 2006:1103-1118.

5. Garner MM. Methods for diagnosing inclusion body disease in snakes. *Proc North Am Vet Conf*. 2005;19:1283-1284.
6. Jacobson ER, Oros J, Tucker S, et al. Partial characterization of retroviruses from boid snakes with inclusion body disease. *Am J Vet Res*. 2001;62(2): 217-224.
7. Orós J, Tucker S, Jacobson ER. Inclusion body disease in two captive boas in the Canary Islands. *Vet Rec*. 1998;143(10):283-285.
8. Pees M, Schmidt V, Marschang RE, Heckers KO, Krautwald-Junghanns M-E. Prevalence of viral infections in captive collections of boid snakes in Germany. *Vet Rec*. 2010;166(14):422-425.
9. Schumacher J, Jacobson ER, Homer BL, Gaskin JM. Inclusion body disease in boid snakes. *J Zoo Wildl Med*. 1994;25(4):511-524.
10. Stenglein MD, Sanders C, Kistler AL, et al. Identification, characterization, and *In Vitro* culture of highly divergent arenaviruses from boa constrictors and annulated tree boas: candidate etiological agents for snake inclusion body disease. *mBIO*. 2012;3(4): 1-12.
11. Vancraeynest D, Pasmans F, Martel A, et al. Inclusion body disease in snakes: a review and description of three cases in boa constrictors in Belgium. *Vet Rec*. 2006;158(22): 757-761
12. Wozniak E, McBride J, DeNardo D, Tarara R, Wong V, Osburn B. Isolation and characterization of an antigenically distinct 68-kd protein from nonviral intracytoplasmic inclusions in boa constrictors chronically infected with the inclusion body disease virus (IBDV: Retroviridae). *Vet Path*. 2000;37(5): 449-459.

**Joint Pathology Center**
**Veterinary Pathology Services**

# WEDNESDAY SLIDE CONFERENCE 2012-2013

## Conference 12

**23 January 2013**

**CASE I:** A10-5331 (JPC 3167830).

**Signalment:** Female, age unknown, spotted eagle ray (*Aetobatus narinari*).

**History:** This 11.6 kg, 90.8 cm disc width female had been collected 5 months earlier off the Florida coast and had completed an uneventful 45-day quarantine period prior to display in a public aquarium. Acute onset of an intermittent rolling swimming pattern and "flashing," typically a sign of external parasitism, was followed by progressive lethargy. Supportive treatment was initiated and a gill clip performed. Wet mount preparations of the clip revealed large numbers of large amorphous spherical bodies free and within gill lamellae. Despite treatment with oxytetracycline and chloramphenicol, the animal's condition continued to deteriorate and euthanasia was elected.

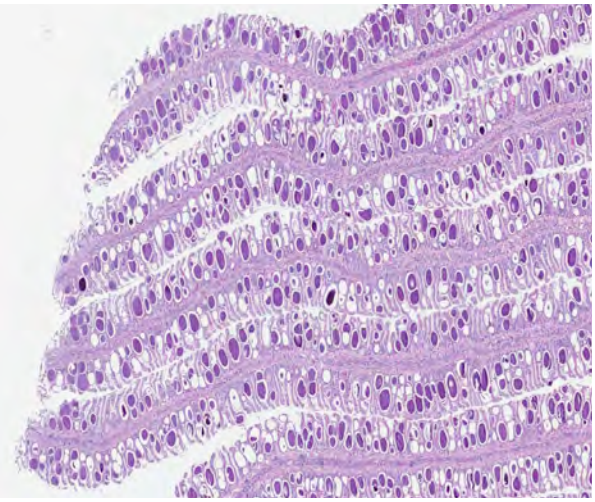

*1-1. Gill, spotted eagle ray: Multifocally, numerous lamellar epithelial cells are expanded by granular basophilic intracytoplasmic inclusions. (HE 24X)*

**Gross Pathologic Findings:** Gross necropsy findings were minimal. External changes were limited to mild pallor and mottling of the gills. Internally, the gastrointestinal tract was devoid of contents. The liver was unusually small, firm and tan for an elasmobranch species and failed to float in formalin.

**Laboratory Results:** Aerobic cultures of liver, spleen and kidney were negative. PCR using pan-chlamydial primers for the 16S rRNA gene sequence produced a 276 bp product with 84% identity to *Candiditus Piscichlamydia salmonis*.

**Histopathologic Description:** Approximately 60-80% of lamellar troughs were occluded by one or more well delineated, 50-200 µm, amorphous, pale basophilic inclusions that markedly distended lamellar epithelial cells. Additional changes included widespread mild to occasionally moderate epithelial cell hypertrophy and hyperplasia, with patchy multifocal lamellar fusion. Multifocal infiltrates of small to moderate numbers of mixed inflammatory cells, predominated by lymphocytes and granulocytes, were located primarily in gill filaments and at the bases of lamellar toughs.

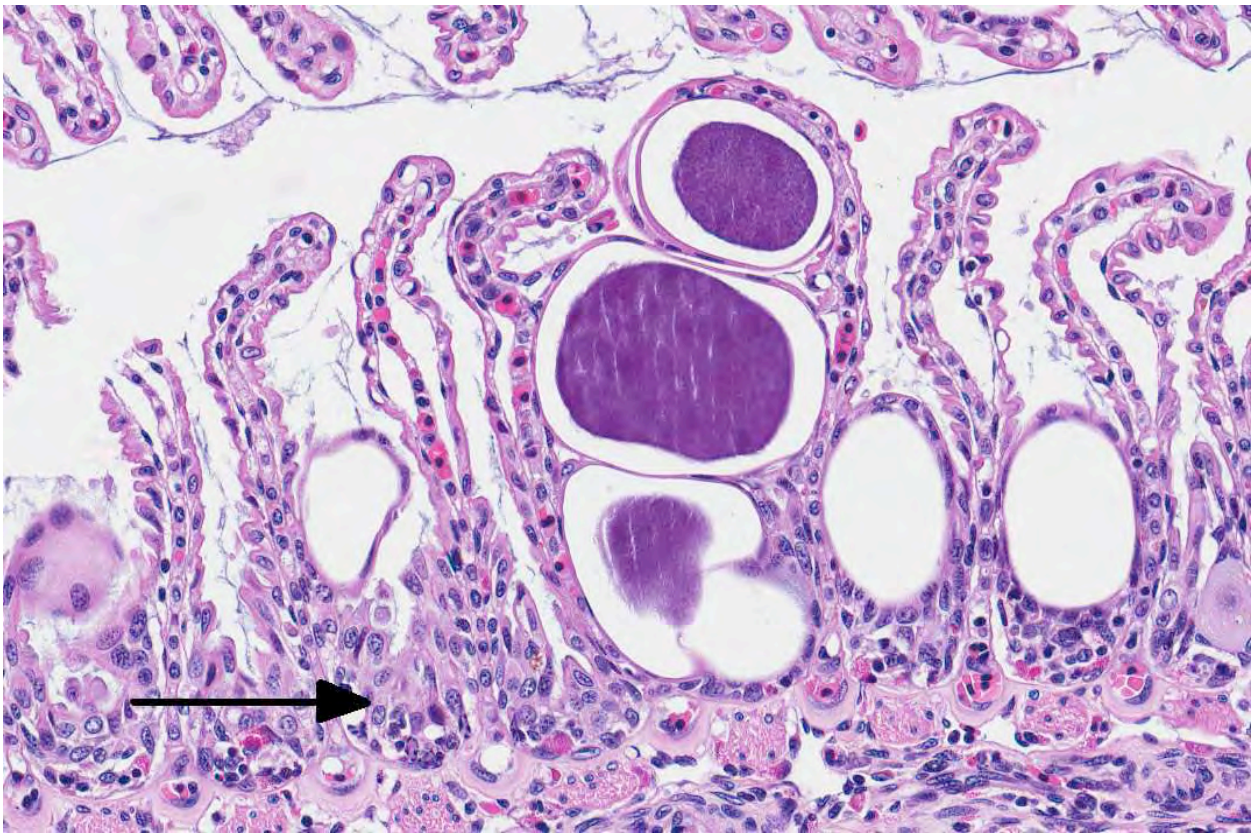

*1-2. Gill, spotted eagle ray: Multifocally lamellar epithelial cells are expanded up to 150 µm by granular intracytoplasmic inclusions composed of myriad bacteria, and multifocally, there is hyperplasia of lamellar epithelium with bridging and fusion of lamellae (arrow). (HE 200X)*

**Contributor's Morphologic Diagnosis:** Gill: Multifocal, mild, epithelial hypertrophy and lamellar fusion, with widespread intraepithelial amorphous basophilic inclusions and subacute, mild to moderate, filamental bronchitis.

**Contributor's Comment:** Microscopic findings were consistent with epitheliocystis disease and supported by PCR results indicating 16s rDNA homology with other piscine chlamydia-like agents associated with the condition. *Epitheliocystis* was first observed by Plehn in 1920 and the first connection made with a chlamydial or rickettsial-like agent by Hoffman in 1969. The disease is now known to affect the skin and gills of over 50 freshwater and marine teleosts, but is unusual in elasmobranch species. Although lesions are not uncommon in wild fish, they are rarely associated with mortalities and the condition is considered primarily a disease of aquaculture. Under intensive culture conditions mortalities can reach 100%, probably due to respiratory compromise, but are generally age dependent, with young fingerlings showing the greatest susceptibility. Losses are also influenced by stress factors typical of aquaculture, such as high stocking densities and suboptimal water quality conditions.[3,7]

Lesions are characterized by hypertrophied epithelial cells containing intracellular, spherical, membrane bound inclusions. Localization in the gill, as well as proliferative and inflammatory responses to the bacteria are highly variable. By electron microscopy two distinct developmental cycles exhibiting different histochemical and immunohistochemical staining properties have been identified in fish, but their significance is unclear. Cycle I is typical of chlamydia, involving reticulate, intermediate, and infectious elementary bodies that all possess distinct compact nucleoid regions. Microscopically, this cycle has been associated with granular inclusions in young fish during epizootics. Cycle II involves elongate forms lacking nucleoids and is reported to be more common in older animals.[3]

Growing molecular evidence indicates wider genetic biodiversity and host range among the *Chlamydiales* than previously recognized. This is reflected in the recent expansion of the order to include a number of new families (*Simkaniaceae*, *Parachlamydiaceae*, *Waddliaceae*) and reorganization of the family *Chlamydiaceae*.[2] Concomitant with this, several specific agents have been described for the first time in association with epitheliocystis, including *Candiditus Piscichlamydia salmonis* in Atlantic salmon,

*Candiditus Clavochlamydia salmonicola* in multiple salmonid species, and a *Neochlamydia* sp. in Arctic char.[4,5,6] To date, however, no piscine chlamydial agents have been isolated in culture and Koch's postulates remain unfulfilled. Diagnosis is based largely on histopathology.

**JPC Diagnosis:** 1. Gill: Lamellar epithelial hyperplasia and hypertrophy with multifocal lamellar fusion, numerous intraepithelial intracytoplasmic bacilli, and subacute branchitis.
2. Gill: Lamellar telangiectasia with multifocal thrombosis.

**Conference Comment:** The contributor provides a very good summary of epitheliocystis disease in fish. In addition to the characteristics and causes of this disease, conference participants discussed the presence and role of alarm cells in the sections examined. Alarm cells (aka alarm substance cells) in fishes in the superorder *Ostariophysi* (minnows, characins, catfishes etc) and the similar club cells in non-ostariophysans (perch, walleye, saugers and darters) are specialized cells found in superficial epidermis. When damaged by predatory attack or other traumatic insult, their contents are released and serve as a chemical alarm to warn neighboring fishes of danger. The pheromone released from alarm cells is referred to as "Schreckstoff" which means "fear substance" in German. Recent studies have suggested that in addition to acting as a warning system, alarm cells may also provide protection against pathogens, parasites and UV radiation that compromise the integrity of the epidermis.[1] In the sections of gill from this spotted eagle ray there were numerous cells that appeared similar to alarm cells (large, round to oval cells with centrally placed nuclei with one to two prominent nucleoli). Due to the lack of a control, participants were unable to determine if these alarm cells were present in normal numbers, or were increased in numbers as a response to chronic gill pathology. Interestingly, the chlamydial colonies appear to be infecting the alarm cells as well as the lamellar epithelium.

**Contributing Institution:** Department of Pathology
University of Georgia College of Veterinary Medicine
Department of Pathology
University of Georgia
501 DW Brooks Drive
Athens, GA 30602
www.vet.uga.edu/VPP

**References:**
1. Chivers DP, Wisenden BD, Hindman CJ, et al. Epidermal "alarm substance" cells of fishes maintained by non-alarm functions: possible defense against pathogens, parasites and UVB radiation. *Proc. R. Soc. B*. Accessed online on 26 January 2013 http://people.oregonstate.edu/~blaustea/pdfs/PRSB%20-%20Chivers%20et%20al.pdf
2. Corsaro D,Greub G. Pathogenic potential of novel chlamydiae and diagnostic approaches to infections due to these obligate intracellular bacteria. *Clinical Microbiology Reviews*. 2006;283-297.
3. Crespo S, Zarza C, Padros F, Marin de Mateo M. Epitheliocystis agents in sea bream Sparus aurata: morphological evidence for two distinct chlamydia-like developmental cycles. *Diseases of Aquatic Organisms*. 1999;37:61-72.
4. Draghi A, Popov VL, Kahl MM, Stanton JB, Brown CC, Tsongalis GJ, et al. Characterization of *Candidatus* Piscichlamydia salmonis (Order *Chlamydiales*), a chlamydia-like bacterium associated with epitheliocystis in farmed Atlantic Salmon (Salmo salar). *Journal of Clinical Microbiology*. 2004;42:5286-5297.
5. Draghi A, Bebak J, Popov VL, Noble AC, Geary SJ, West AB, et al. Characterization of a *Neochlamydia*-like bacterium associated with epitheliocystis in cultured Arctic char *Salvelinus alpinus*. *Diseases of Aquatic Organisms*. 2007;76:27-38.
6. Karlsen M, Nylund A, Watanabe K, Helvik JV, Nylund S, Plarre H. Characterization of *Candidatus* Clavochlamydia salmonicola: an intracellular bacterium affecting salmonid fish. *Environmental Microbiology*. 2008;10:208-218.
7. Nowak BF, LaPatra SE. Epitheliocystis in fish. *Journal of Fish Diseases*. 2006;29:573-588.

**CASE II:** F-09-044 (JPC 3149419).

**Signalment**: Approximately six months old, no gender noted, green grouper (*Epinephelus coioides*).

**History:** Eleven thousand green grouper (*Epinephelus coioides*) were imported from Taiwan in October 2008 and delivered to nine cages in Hong Kong SAR for culture. In mid-June 2009, gradual mortalities began to occur. Up to 70% of the fish displayed clinical signs of lethargy and whirling swimming movement. There were no external lesions noted. Microscopic examination in the field revealed gill parasites. Seven fish were submitted for pathological examination.

**Gross Pathologic Findings:** Moderate levels of parasitic infestation of the gills identified as dactylogyrid flukes. No other significant findings.

**Laboratory Results**:

Red sea bream Iridovirus detection by gel PCR:

| | Gel PCR on **Tissue homogenate** | Gel PCR on **Tissue homogenate** |
|---|---|---|
| Sample ID | RSIV1 set primers | RSIV4 set primers |
| Spleen | **Pos** | Neg |
| Kidney | **Pos** | Neg |
| Brain | **Pos** | Neg |
| Eye | **Pos** | Neg |

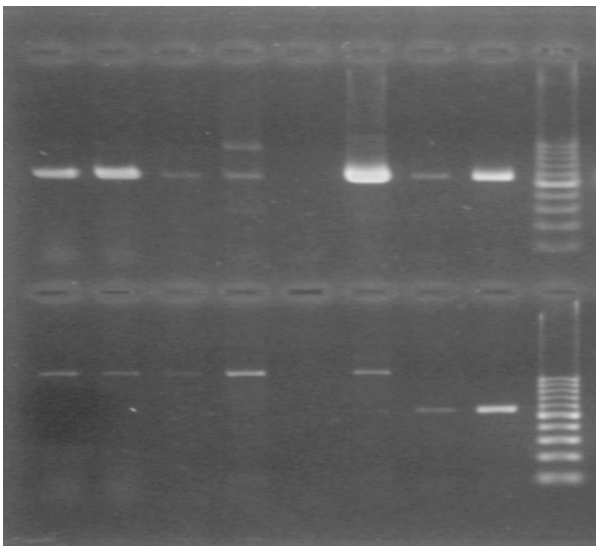

**Histopathologic Description:** Spleen: Diffusely, normal splenic architecture is disrupted by the presence of hypertrophic cells that have enlarged nuclei with stippled, faintly basophilic cytoplasm. Small numbers are contracted and densely amphophilic. Some cells measure up to 25 µm in diameter.

**Contributor's Morphologic Diagnosis:** Spleen: Splenitis, severe, diffuse, subacute, cellular hypertrophy consistent with Red sea bream iridovirus disease.

**Cause:** Infectious spleen and kidney necrosis virus.

**Contributor's Comment:** Red sea bream iridovirus disease (RSIVD) is caused by a particular strain of Red sea bream Iridovirus (Ehime-1) as well as by other genotypes of Red sea bream Iridovirus (RSIV). Infectious spleen and kidney necrosis Virus (ISKNV) has also been proven to cause RSIVD.[3]

*Iridoviridae* gets its name from Tipula iridescent virus, which grows in the haemocele of the crane fly (*Tipula* sp.) and makes the fly iridescent. The iridoviruses may have an envelope derived from the host plasma membrane. This membrane may not be critical for infectivity but enhances it. The iridoviruses are large isometric viruses with icosahedral symmetry, 130-133 nm in diameter, and comprise a spherical nucleoprotein core surrounded by a membrane consisting of lipid modified by protein subunits. The genome consists of a single linear molecule of double stranded DNA. Transcription and DNA synthesis are nuclear. Virion assembly is cytoplasmic.[4] Replication occurs in two stages: the first stage is in the nucleus and second stage is in the cytoplasm.[1]

Piscine iridoviruses belong to the genera *Ranavirus, Lymphocystivirus* and *Megalocytivirus*. In recent years, the genotypical variation between newly found iridovirus strains included in the genus *Ranavirus* has been studied in this viral family. However, the properties of and variation between iridovirus species have not been well characterized except for a few iridoviruses isolated from amphibians. Members of the *Megalocytivirus* genus produce characteristic basophilic inclusion bodies in the enlarged cells of host fish organs, which have been collected from mass mortalities occurring in wild and cultured fish species. Many other piscine iridoviruses have been reported in Asian countries from more than 100 different species, including freshwater and marine fish.[4]

In this case, gel PCR was performed on tissue homogenate by using two sets of primers according to the recommended World Organization for Animal Health (OIE) protocol. RSIV1 primers revealed virus in all tissues tested (i.e., spleen, kidney, brain, and eye). RSIV1 (Forward & Reverse) primers are used for the amplification of the gene sequence (570 bp) of

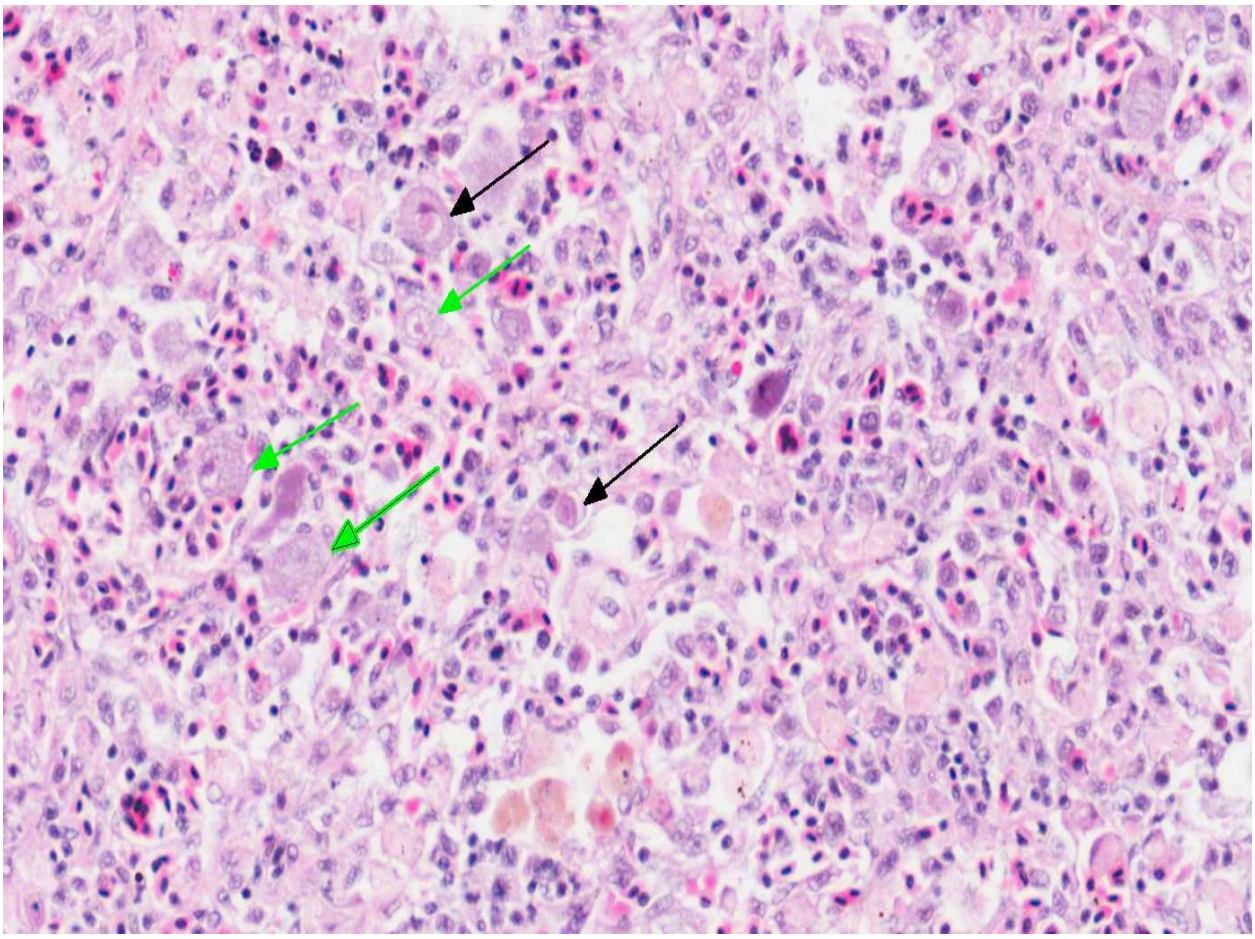

*2-1. Spleen, green grouper: Myeloid precursors are enlarged up to 40 µm with a large nucleus and a prominent nucleolus (green arrows) and variably distinct, basophilic, irregular intracytoplasmic viral inclusion bodies (black arrows). (HE 400X)*

both RSIV DNA and ISKNV DNA. RSIV4 primers were used for amplification of DNA gene sequence (open reading frame, ORF) (563 bp); however, all results were negative.[3] RSIV4 primers (Forward & Reverse) amplify RSIV, but not ISKNV DNA. These results indicated that the virus detected in these tissues is ISKNV, one of the causative agents of Red sea bream Iridovirus Disease.

The first outbreak of RSIVD was recorded in 1990 on Shikoku Island, Japan. Since that time, the disease has also been found widely in East and Southeast Asian countries, including Chinese Taipei, People's Republic of China, Hong Kong, Republic of Korea, Malaysia, Philippines, Singapore and Thailand. Transmission is horizontal via the water. Vertical transmission of RSIVD has not yet been investigated. Carrier states of the agents have also not yet been investigated.[3]

As in this case (which occurred in July 2009), disease outbreaks seem to occur most often during the summer months when water temperatures are 25ºC or above.[3] Diseased fish are typically lethargic, show severe anemia, petechiae of the gills and hypertrophic spleens.[6] The susceptibility of juveniles is generally higher than adults.[3] The only clinical sign seen in this case was lethargy. Histological preparations characteristically show enlarged cells of the spleen, kidney, liver and gill.[4] Hematopoietic tissue is located in the stroma of the spleen and the interstitium of the kidney in teleosts. Therefore, histopathological observations are consistent with the anemia and splenomegaly observed in fish with RSIVD.[6] Not all of the fish in this group had histopathological changes and many had no lesions in any organ examined.

We found some inconsistencies in the terminology from the literature regarding the enlarged cells seen in RSIVD. Some texts and journals refer to the hypertrophied cells as having inclusion bodies, while others distinctly refrain from using that term.

**JPC Diagnosis:** 1. Spleen, leukocytes: Cytomegaly, diffuse, marked, with intracytoplasmic viral inclusions. 2. Mesentery: Peritonitis, subacute, mild.

**Conference Comment:** Participants noted that, although cells displaying advanced cytoplasmic effects

(i.e., degeneration and necrosis) are seen in the tissues examined, the more prominent feature in these sections is cytomegaly, which is typical of *Megalocytivirus* infections.

In addition to RSIVD, proficiently described by the contributor, participants discussed other viruses in the family *Iridoviridae* that affect commercial fish production. Specifically, *Lymphocystivirus* spp., including lymphocystis disease virus 1 (LCDV-1) and LCDV-2, cause lymphocystis disease in many species of freshwater and marine fish.[2] These viruses infect fibroblasts in the skin, gills, and internal connective tissue and arrest cell division but not cell growth, resulting in markedly hypertrophied cells (i.e., "lymphocysts") that can reach up to 100,000 times their normal size.[2] Microscopically, lymphocysts have the following distinct features: a large nucleus, a hyaline-like capsule, and bizarre and segmented cytoplasmic inclusions. Grossly they appear as raised, pearl-like lesions. Lymphocystis is generally a self-limiting disease and is rarely fatal, as fish usually slough the external lymphocysts; however, the virus does impact the fish industry due to the cosmetic effects in fish sold for food or as ornamental fish. Additionally, the lesions may provide portals of entry for secondary pathogens.[2]

Conference participants briefly discussed the nomenclature for green grouper. In addition to green grouper, *Epinephelus coioides* is known by several common names, including orange spotted grouper, estuary cod, and estuary rock cod.[7]

**Contributing Institution:** Agriculture, Fisheries and Conservation Department
Tai Lung Veterinary Laboratory
Sheung Shui, New Territories, Hong Kong SAR
http://www.afcd.gov.hk

**References:**

1. Jacobson ER. *Infectious Diseases and Pathology of Reptiles*. Boca Raton, FL: CRC Press; 2007:404.
2. Knowles DP. Asfarviridae and Iridoviridae. In: MacLachlan NJ, Dubovi EJ, eds. *Fenner's Veterinary Virology.* 4th ed. London, UK: Elsevier Academic Press; 2011:172-176.
3. Office International des Epizooties Aquatic Animal Health Standards Commission: Red sea bream Iridoviral Disease. OIE Manual of Diagnostic Tests for Aquatic Animals. Chapters 2, 3, 7. World Organization for Animal Health. 2009:251-261.
4. Roberts RJ. *Fish Pathology*. 3rd ed. London, UK: WB Saunders; 2001:182-191.
5. Shinmoto H, Taniguchi K, Ikawa T, Kawai K, Oshima S. Phenotypic diversity of infectious Red sea bream iridovirus isolates from cultured fish in Japan. *Applied and Environmental Microbiology*. 2009;75:3535-3541.
6. Wang CS, Shih HH, Ku CC, Chen SN. Studies on epizootic iridovirus infection among Red sea bream, *Pagrus major* (Temminick & Schlegel), cultured in Taiwan. *Journal of Fish Diseases.* 2003;26:127-133.
7. www.arkive.org

**CASE III:** 11-8273184 (JPC 4004721).

**Signalment:** Adult blacklip abalone (*Haliotus rubra*).

**History:** Approximately twenty sick and dying abalone were found off Tyringa, near Baird's Bay on the west coast of South Australia. Post-mortem changes were significant and the cause of death was unclear. Due to an outbreak of abalone viral ganglioneuritis (AVG), a notifiable disease of abalone in South Australia occurring in Tasmania, the case was regarded as urgent and treated as a possible emergency disease.

Samples of mouthparts and a part of the foot and surrounding mantle from 3 affected blacklip abalone, 1, 2, and 3 were submitted in 10% buffered formalin for microscopic examination as well as a part of the foot with pedal nerves in alcohol for referral to Australian Animal Health Laboratory for PCR for abalone ganglioneuritis (ABG).

**Gross Pathology:** Multiple randomly scattered, firm, yellow, raised or centrally cystic nodules, ranging from 2 mm to 8 mm were seen within and along the edges of the foot of all three abalone. The cystic nodules contained flocculent yellow or yellow-brown watery fluid. Lesions were most numerous in abalone 2 (from which these sections have been prepared).

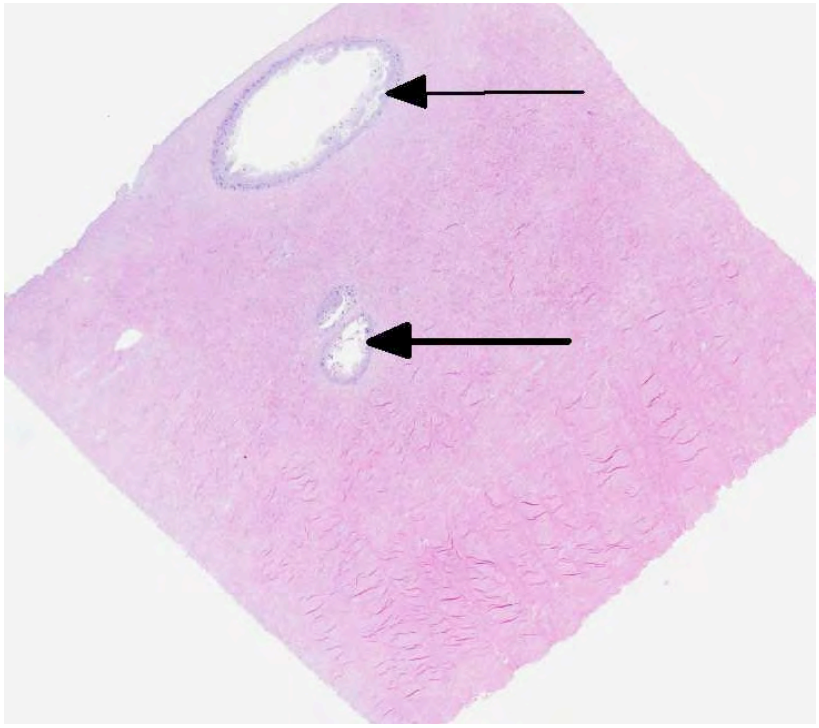

*3-1. Foot, abalone: Within the skeletal muscle of the foot, there are multifocal areas of necrosis measuring up to 5 mm in diameter (arrows). (HE 40X)*

**Laboratory Results:** PCR was negative for ABG.

**Histopathologic Description:** Pedal tissue: Moderate post mortem changes are present. There are single (in some sections) or multiple rounded cystic lesions containing large numbers of ovoid vacuolated or dark-staining unicellular organisms 10-17 µm in diameter and multicellular rounded organisms 12-30 µm in diameter amongst moderate numbers of infiltrating haemocytes. The lesions are well delineated but non-encapsulated. In occasional sections, similar lesions are seen abutting onto, but not infiltrating into, pedal nerves.

There were no histopathological lesions of ABG in the mouthparts (sections not presented).

**Contributor's Morphologic Diagnosis:** Multifocal necrosis and cavitation with numerous intralesional protistal organisms consistent with *Perkinsus* spp. and haemocyte infiltration, pedal tissue.

**Contributor's Comment:** *Perkinsus* spp. is a group of protists in the phylum *Perkinsozoa*, in the infra-kingdom *Alveolata*, but there remains uncertainty about the status of the genus and there are divergent views regarding its taxonomy. Susceptible hosts include abalone: *Haliotis rubra*, *Haliotis laevigata*, *Haliotis cyclobates* and *Haliotis scalaris,* but a wide range of other molluscs are also susceptible. The known range of *P. olseni* includes Australia, Europe and eastern Asia.

O'Donoghue et al linked *P. olseni* to widespread kills of abalone in the Gulf of St. Vincent side of the Yorke Peninsula, South Australia, and abalone stocks in this area have not recovered (S. Mayfield personal communication).[5] In the early 1990's, a significant proportion of *H. rubra* along approximately 500 km of the NSW coastline between Port Stephens and Jervis Bay died in association with *P. olseni* infections.

The route of entry of *Perkinsus olseni* is unknown. It proliferates in tissues but is eventually sequestered by the host and killed or ejected. During sequestration the parasite becomes surrounded by abalone pigment, causing the yellow/brown appearance of the nodules. These reduce market value, causing losses in fishery value. In some severe infections, death occurs

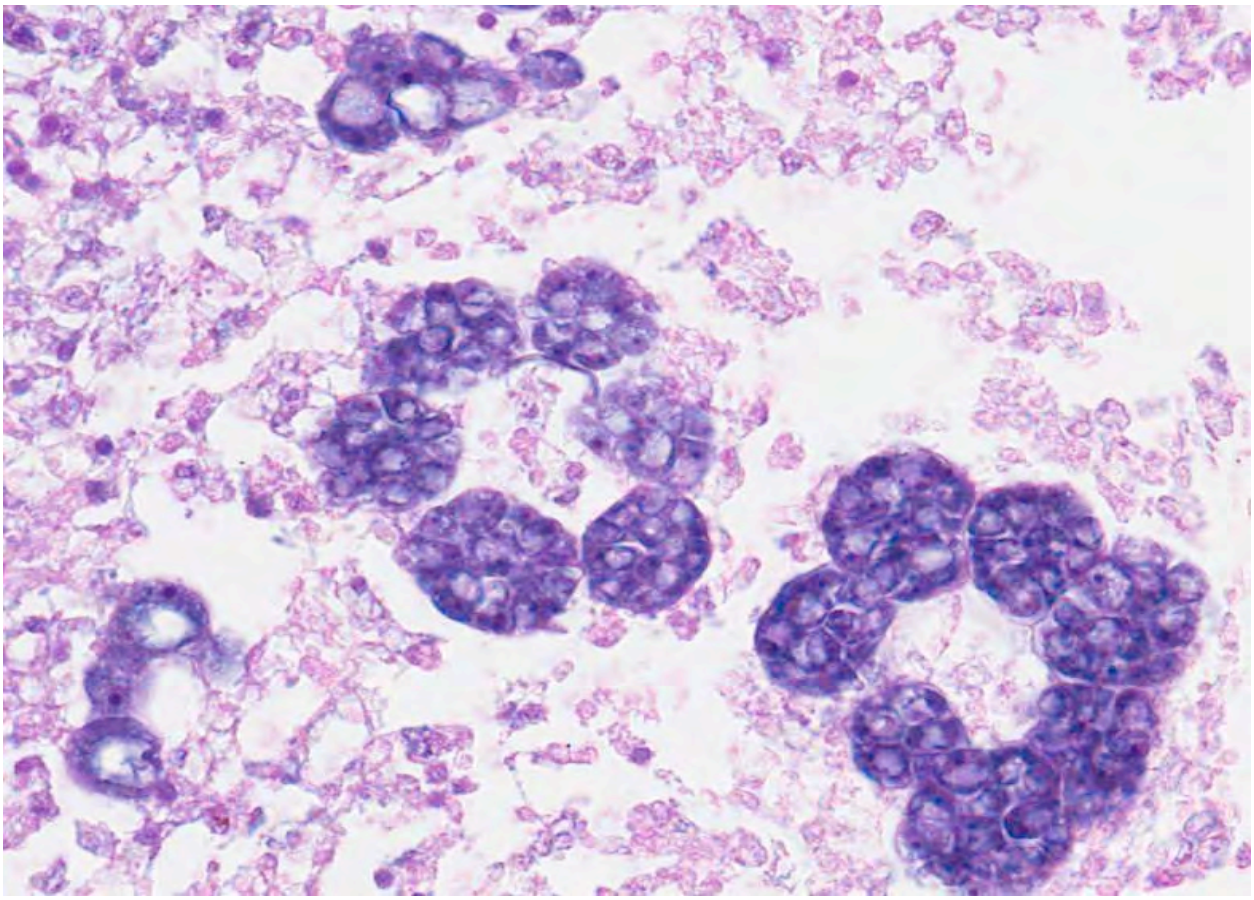

*3-2. Foot, abalone: Areas of necrosis contain numerous protozoal trophozoites and multinucleated hypnospores. (HE 400X)*

without nodule formation, suggesting that the host is unable to mount an effective immune response in some cases. Infection is not always lethal to *H. rubra* and expression of disease is widely associated with environmental variables, primarily temperature, with infections becoming more severe at higher temperatures or when food availability diminishes.[4] Transmission occurs directly; prezoosporangia develop into zoosporangia in seawater which then release hundreds of motile, biflagellated zoospores (about 3 by 5 µm) which are infective to abalone and other molluscs.[3]

**JPC Diagnosis:** Pedal tissue: Rhabdomyositis, necrotizing, focally extensive with numerous protistal trophozoites and schizonts.

**Conference Comment:** The contributor provides a good summary of *Perkinsus olseni* infections in mollusks. Conference participants discussed terminology for the life stages of these protists. The life cycle of *Perkinsus olseni* consists of trophozoite, hypnospore and zoospore stages.[1,6] Hypnospores (prezoosporangia) are dormant, thick-walled cells that develop into motile, flagellated zoospores in aerated seawater. Once ingested by the host, the zoospore develops into a non-motile, multi-nucleated single cell trophozoite. Under anaerobic conditions, such as occurs in necrotic tissue, the trophozoites develop the vegetative hypnospores.[1,6] Participants also discussed another *Perkinsus* species, *P. marinus*, which causes Dermo disease in oysters. Dermo is a significant cause of mortality in the Eastern oyster, *Crassostrea virginica*.[6]

Although this animal did not have abalone viral ganglioneuritis (AVG), participants discussed this disease as well. AVG is caused by a herpesvirus that affects only abalone; other mollusks appear to not be affected. Mortality rates in farmed abalone are up to 100%. The disease has been found to be slowly spreading in wild abalone along the Victorian (Australia) coast as well; however, the exact mortality rate in wild populations is uncertain.[2]

There was moderate slide variation, with some sections exhibiting more significant necrosis, and others showing cavitation of the pedal tissue.

**Contributing Institution**: Gribbles Vet Lab
33 Flemington Street
Glenside, SA 5065
Australia

**References:**

1. Choi KS, Park KI. Review on the protozoan parasite *Perkinsus olseni* (Lester and Davis 1981) Infection in Asian Waters. In: Ishimatsu A, Lie HJ, eds. *Coastal Environmental and Ecosystem Issues of the East China Sea.* Terrapub and Nagasaki University; 2010. *http://www.terrapub.co.jp/onlineproceedings/fs/nu/pdf/nu2010269.pdf.* Accessed online 26 January 2013.
2. Corbeil S, McColl KA, Williams LM, et al. Abalone viral ganglioneuritis: establishment and use of an experimental immersion challenge system for the study of abalone herpes virus infections in Australian abalone. *Virus Res.* 2012;65(2):207-13.
3. Goggin, CL, Sewell KB, Lester RGJ. Cross-infection experiments with Australian Perkinsus species. *Diseases of Aquatic Organisms*. 1989:T:55-59.
4. Lester RJG, Hayward CJ. Control of *Perkinsus* Disease in Abalone. Final Report for FRDC Project no. 2005;2000/151.
5. O'Donoghue PJ, Phillips PH, Shepherd SA. *Perkinsus* (Protozoa: Apicomplexa) infections in abalone from South Australian waters. *Transactions of the Royal Society of South Australia*. 1991;115:77-82.
6. Petty D. Perkinsus infections in bivalve mollusks. University of Florida IFAS Extension. http://shellfish.ifas.ufl.edu/PDFs/Publications/Perkinsus%20Infections%20of%20Bivalve%20Molluscs.pdf. Accessed online 26 January 2013.

**CASE IV:** 116910 (JPC 4020017).

**Signalment:** Adult female African clawed frog (*Xenopus (Silurana) tropicalis)*.

**History:** Chronic mortality in the colony, severe weight loss, and in some animals, cutaneous nodular, lesions.

**Gross Pathology:** Splenomegaly, hepatomegaly and nephromegaly with multiple round, whitish, 1 to 2 mm in diameter nodules. Three cutaneous, whitish and firm, round, ulcerated, 2 to 5 mm in diameter lesions, associated to loss of a claw.

**Laboratory Results:** Culture and sequencing 500pbb rADN16S: *Mycobacterium gordonae*.

**Histopathologic Description:** Liver: Over 80% of the parenchyma is affected by multifocal to coalescent lesions replacing normal hepatic parenchyma. These foci are characterized by aggregates of round to polygonal cells, up to 100 µm in diameter, with abundant pale staining or often foamy cytoplasm and an eccentric ovoid nucleus (epithelioid macrophages) admixed with small numbers of lymphocytes and granulocytes. Numerous acid-fast staining intracellular bacilli are often present within the cytoplasm of epithelioid macrophages.

**Contributor's Morphologic Diagnosis:** Liver: hepatitis, granulomatous, multifocal to coalescing, chronic, severe, with acid-fast staining intracellular bacilli, etiology consistent with *Mycobacterium gordonae*.

**Contributor's Comment:** The African tropical clawed frog, *Xenopus tropicalis*, is an increasingly used vertebrate model system for biological studies. Mycobacteria are acid-fast organisms that are commonly found in aquatic environments.[2] Amphibian mycobacteriosis has been described as a disease of the integument and/or as a systemic disease with multiple nodules in different organs. Several species of mycobacteria have been isolated in the past from frogs: *M.marinum*, *M.chelonae*, *M.szulgai*, *M. xenopi*, *M.gordonae*, and *M.liflandii*.[3,4,5,6,10,11,13]

In *Xenopus tropicalis*, *M. szulgai* and *M.liflandii* have been described as a systemic disease and *M.gordonae* as a disease of the integument until now.[3,11,5,13] *M.gordonae* is considered as an occasional human pathogen, especially in immunocompromised patients.[1,9] It has been associated with granulomatous skin lesions or with disseminated lesions.[1,9]

In our case, *Mycobacterium gordonae* has been isolated from internal organs (spleen and liver) and therefore associated with a systemic disease.
The source of the infection has not yet been identified.

**JPC Diagnosis:** Liver: Hepatitis, granulomatous, diffuse, severe, with moderate hepatocellular atrophy.

**Conference Comment:** Conference participants discussed several aspects of amphibian immune responses, including the tendency for granuloma formation in non-mammalian vertebrates. In this case, there was discussion on the appropriate terminology to describe the immune response, with some participants favoring "granulomatous" and others favoring "histiocytic." Although the macrophages in this case do not have the expected morphology that typically accompanies a mammalian granulomatous response (i.e., epitheloid and multinucleated macrophages) they

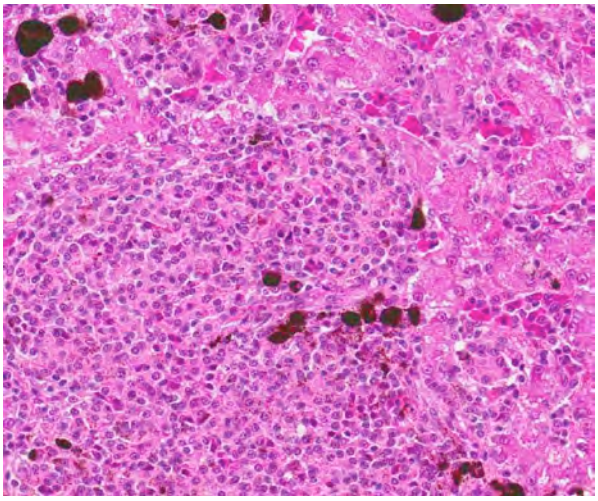

*4-1. Liver, African clawed frog: Multifocally, hepatic sinusoids are expanded by a dense, nodular aggregates of histiocytes which results in hepatocyte compression and atrophy. (HE 260X)*

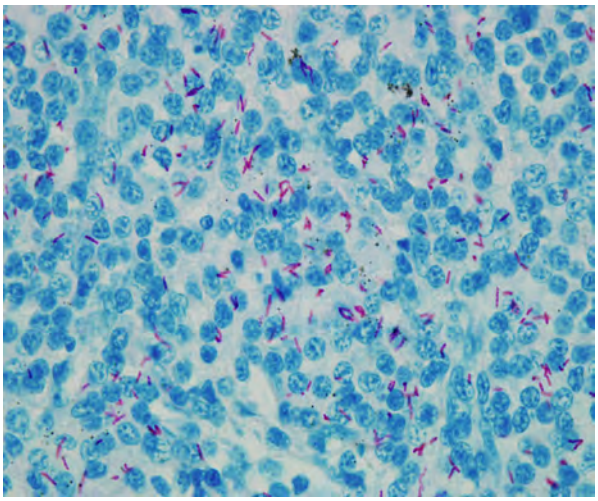

*4-2. Liver, frog: Multifocally, within granulomas are numerous 1x4 µm acid-fast bacilli. (Fite-Faraco 1000X)*

do have characteristics of activated macrophages, thus the participants agreed on "granulomatous."

Participants also discussed the role of melanomacrophages in amphibians. Amphibians, like reptiles and fish, have aggregates of phagocytic macrophages within several organs (liver, spleen, and kidney of fish; liver and spleen of amphibians and reptiles).[7] Systemic inflammation can cause these macrophages to proliferate and develop aggregates in other organs as well, such as the atrium of fish. Macrophages within these aggregates often contain melanin granules, as well as hemosiderin and lipofuscin. While melanomacrophage aggregates are sometimes considered metabolic dumps, the melanin granules are thought to play a role in the production of free radicals and microbial killing.[8,14] In fish, melanomacrophage aggregates have been shown to function as primitive analogues to lymphoid germinal centers, trapping antigens and immune complexes. In higher fish, amphibians and reptiles, melanomacrophage aggregates may have a capsule.[14]

Lastly, participants noted the presence of few hepatocytes with eosinophilic intracytoplasmic vacuoles. These were likened to the postmortem vacuoles described in mice that result from plasma influx into the cytoplasm, as such, they were considered clinically insignificant to this case.[7]

**Contributing Institution:** Department of Pathology
Nantes-Atlantic National College of Veterinary Medicine
Food Science and Engineering – ONIRIS
44 307 Nantes Cedex 03
France
www.oniris-nantes.fr

**References:**

1. Bagarrazi ML, Watson B, Kim IK, Hogarty M, McGowan Kl. Pulmonary *Mycobacterium gordonae* infection in a two-year-old child: case report. *Clin Infect Dis*. 1996;22:1124-5.
2. Beran V, Matlova L, Dvorska L, Svastova P, Pavlik I. Distribution of mycobacteria in clinically healthy ornamental fish and their aquarium environment. *J Fish Dis*. 2006;29:383-93.
3. Chai N, Deforges L, Sougakoff W, Truffot-Pernot C, De Luze A, Demeneix B. *Mycobacterium sulzgai* infection in a captive population of African clawed frogs (*Xenopus tropicalis*). *J Zoo Wildl Med*. 2006;37:55-58.
4. Ferreira R, Fonseca L, Alfonso A, Da Silva M, Saad M, Lilenbaum W. A report of mycobacteriosis caused by *Mycobacterium marinum* in bullfrogs (Rana catasbeiana). *Vet J*. 2004;171:177-180.
5. Fremont-Rahl JJ, Ek C, Williamson HR, Small PLC, Fox JG, Muthupalani S. Mycobacterium liflandii outbreak in a research colony of *Xenopus (Silurana) tropicalis* frogs. *Vet Pathol.* 2011;48:856-867.
6. Green S, Lifland B, Bouley D, Brown B, Wallace R, Ferrel J. Disease attributed to *Mycobacterium chelonae* in South African clawed frogs (Xenopus laevis). *Comp Med.* 2000;50:675-679.
7. Li X, Elwell MR, Ryan AM, Ochoa R. Morphogenesis of postmortem hepatocyte vacuolation and liver weight increases in Sprague-Dawley rats. *Toxicologic Pathology*. 2003;31:682–688.
8. Roberts RJ. Fish Pathology. 3rd ed. New York: WB Saunders; 2001:30-31.
9. Rusconi S, Gori A, Vago L, Marchetti G, Franzetti F. Cutaneous infection caused by Mycobacterium gordonae in a human immunodeficiency virus-infected patient receiving antimycobacterial treatment. *Clin Infect Dis*. 1997;25:1490-1.
10. Schwabacher H. A strain of mycobacterium isolated from skin lesions of a cold-blooded animal, *Xenopus laevis*, and its relation to atypical acid-fast bacilli occurring in man. *J Hyg* (Lond). 1959;57:57-67.
11. Sanchez-Morgado J, Gallagher A, Johnson L. *Mycobacterium gordonae* in a colony of African clawed frogs (*Xenopus tropicalis). Lab Anim*. 2009;43:300-303.
12. Schwabacher H. A strain of mycobacterium isolated from skin lesions of a cold-blooded animal, *Xenopus laevis*, and its relation to atypical acid-fast bacilli occurring in man. *J Hyg* (Lond). 1959;57:57-67.
13. Suykerbuyk P, Vleminckx K, Pasmans F, Stragier P, Ablordey A, Tran H, et al. *Mycobacterium liflandii* infection in European colony of *Silurana tropicalis*. *Emerg Infect Dis*. 2007;13:743-746.
14. Terio KA. Comparative Inflammatory Responses of Non-Mammalian Vertebrates: Robbins and Cotran for the Birds. In: ACVP and ASVCP, eds. 55th Annual Meeting of the American College of Veterinary Pathologists (ACVP) & 39th Annual Meeting of the American Society of Clinical Pathology (ASVCP). Middleton WI: American College of Veterinary Pathologists & American Society for Veterinary Clinical Pathology. Internet Publisher: Ithaca, New York: International Veterinary Information Service. http://www.ivis.org/proceedings/ACVP/2004/Terio/IVIS.pdf Accessed online 1 February 2013.

**Joint Pathology Center**
**Veterinary Pathology Services**

# WEDNESDAY SLIDE CONFERENCE 2012-2013

## Conference 13

**30 January 2013**

---

**CASE I:** Case 1 AVD-SV2 (JPC 3174956).

**Signalment:** Nine-month-old, male mouse/C57BL\6/ TRAMP.

**History:** Breeding animal for TRAMP mouse colony. Did not receive any treatments.

**Gross Pathologic Findings:** Seminal vesicle – enlarged, lobulated, firm, white, and pink.

**Histopathologic Description:** Focally, approximately 45% of the lining glandular epithelium of the seminal vesicle projects into the lumen as a neoplastic mass characterized by extensive arborizing, multiple, often coalescing, long and short, papillary projections overlying a sparsely cellular neoplastic mesenchymal stroma, supported by compact, dense smooth muscle matrix. The lining glandular epithelium is comprised of cuboidal to columnar epithelium often with piling of layers. Individual cells of the lining epithelium reveal basal,

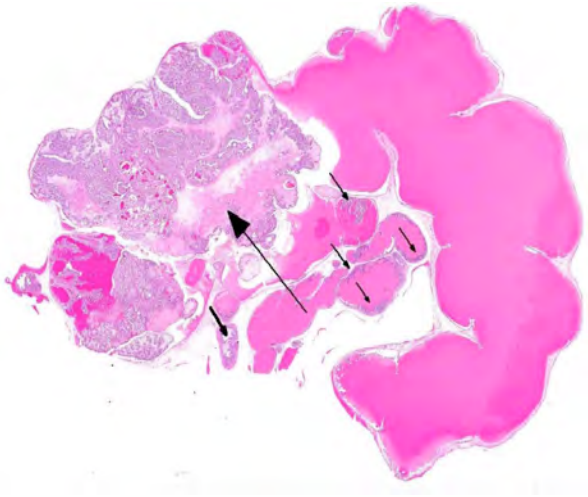

*1-1. Seminal vesicle, TRAMP mouse: The mucosa of the seminal vesicle contains multiple proliferative lesions including a large biphasic tumor (large arrow) and multiple foci of epithelial hyperplasia (small arrows). (HE 6.3X)*

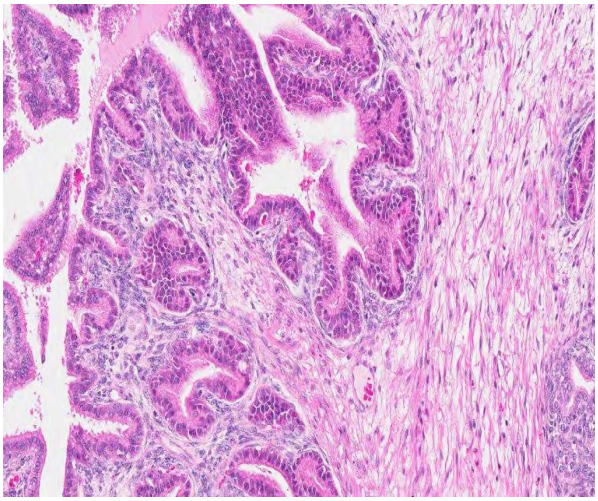

*1-2. Seminal vesicle, TRAMP mouse: The large biphasic neoplasm is composed of two populations of neoplastic cells, proliferative spindled cells which with the overlying covering of epithelial cells (which occasionally form glands deeper inside the neoplasm, for papillary fronds supported by dense fibrous connective tissue. (HE 175X)*

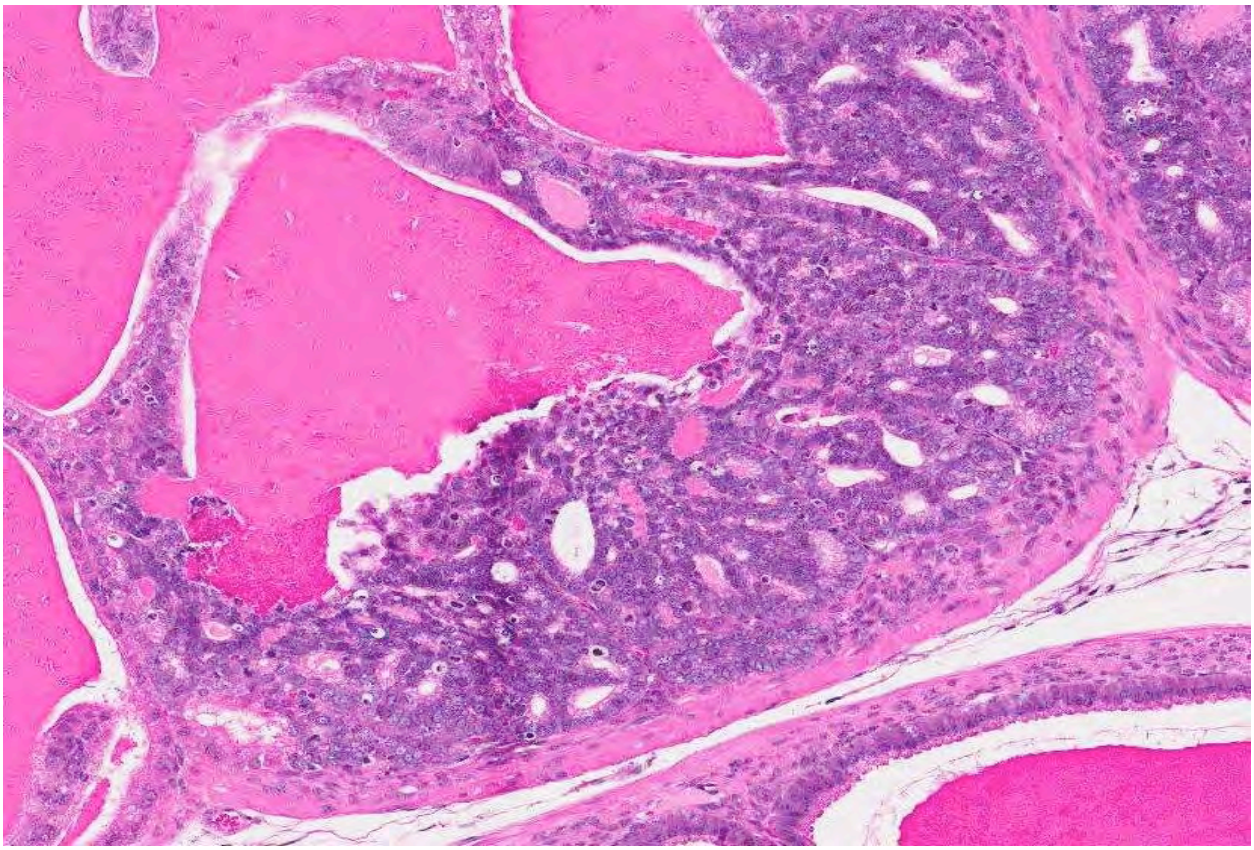

*1-3. Seminal vesicle, TRAMP mouse: Multifocally, the remainder of the mucosal epithelium lining the seminal vesicle is markedly hyperplastic, often forming a cribriform pattern. (HE 175X)*

round to oval nuclei with coarsely stippled chromatin, indistinct nucleoli, and abundant eosinophilic cytoplasm. The mitotic index is ~ 0-1 PHF (400x). There is mild anisocytosis and anisokaryosis. The underlying mesenchymal stroma is often myxomatous, sparsely cellular and comprised of loosely arranged cells with indistinct borders; loose, wispy, eosinophilic vacuolated cytoplasm; spindle-shaped to angular and stellate nuclei with stippled chromatin, and indistinct nucleoli. Mitotic figures are numerous in the mesenchymal stromal cell population ranging between ~ 4-12 PHF (400x). There is moderate to marked anisokaryosis of the mesenchymal stroma. No unequivocal evidence of malignancy, such as invasion or metastases was noted.

The lumen and ducts are often variably ectatic, lined by attenuated epithelium, and contain homogeneous, brightly eosinophilic, proteinaceous material/colloid with occasional hemorrhage. Multifocally, occasional foci of necrotic debris are noted within the stroma associated with breaching of the lining epithelium into the lumen admixed with eosinophilic debris and hemosiderin-laden macrophages.

Multifocally, other areas of the lining epithelium of the seminal vesicle extend as nodular, papillary proliferations into the lumen and have piling of the epithelial cells, and mildly expanded supporting stroma with increased mitoses.

**Contributor's Morphologic Diagnosis:** Seminal vesicle: Focal papillary adenoma with epithelial stromal differentiation.

**Contributor's Comment:** **TR**ansgenic **A**denocarcinoma **M**ouse **P**rostate (TRAMP) mice are a well-studied animal model for human prostate cancer.[3,5,8] TRAMP mice are genetically engineered to harbor a transgene composed of SV 40 Large T/small-t antigen promoted by the rat probasin gene.

Typically, lesions noted in TRAMP mice include the prostate, for which lesions may be assessed using a well-characterized grading scheme.[6] In addition to prostate neoplasms, tumors are also noted in the seminal vesicles.[7]

The normal luminal surface of seminal vesicles in mice is lined by an anastomosing glandular epithelium lined by cuboidal to tall columnar cells forming an intricate arrangement of primary, secondary and tertiary folds. These folds are normally present and should not be confused with hyperplastic changes. Brightly eosinophilic luminal secretions expand the seminal vesicles, resulting in an extended vesicular wall lined by

| Species | Seminal Vesicles | Prostate | | Bulbourethral (Cowper's) |
|---|---|---|---|---|
| | | Body | Disseminate | |
| Bull | ++ | + | + | + |
| Ram | + | - | + | ++ |
| Boar | +++ | + | + | +++ |
| Stallion | +++ | ++ | -(+) | + |
| Dog | - | ++ | - | - |
| Cat | - | ++ | - | ++ |
| Rodent | +++ | ++ | - | ++ |
| Human | + | ++ | - | + |

short epithelial papillae, a scanty submucosal layer, and a thin smooth muscle layer.

As in the present case, seminal vesicle tumors in TRAMP mice typically exhibit features of biphasic organization. Although stromal cells proliferate rapidly, they are always lined by a single-layered epithelial component and do not form solid stromal masses such as those seen in uterine stromal tumors. Also, compared to prostatic tumors in TRAMP mice, seminal vesicle tumors display prominent proliferation of stromal cells with frequent mitotic figures lined by bland epithelium, whereas prostatic tumors display epithelial tumor cell proliferation with scant stromal components.[7]

Although the tumors of TRAMP seminal vesicles resemble epithelial–stromal tumors found in the breast, prostate, and seminal vesicles in humans, no reports of this type of tumor in any other rodents exist, and these tumors are considered to be TRAMP mouse-specific lesions.

**JPC Diagnosis:** Seminal vesicle: Papillary adenoma.

**Conference Comment:** The contributor provides a very good description of both normal and neoplastic changes in TRAMP mouse seminal vesicles. When the moderator emphasized the importance of describing the biphasic population of cells when characterizing this tumor, a question arose as to the cell of origin in the spindle cell population, specifically whether these cells are myoepithelial or mesenchymal. In an attempt to answer this question, immunohistochemistry was performed. The stromal cells showed multifocal positive cytoplasmic immunoreactivity to desmin; however, other stains (calponin, vimentin, pancytokeratin, p63 and CD10) were noncontributory, precluding a definitive determination as to the cell of origin of the spindle cell population.

Accessory genital glands, found along the length of the pelvic urethra in males, have two purposes: providing nutrition and a transport medium for spermatoazoa.[1] There are four main male accessory genital glands: the ampullae, seminal vesicles (vesicular glands), prostate and bulbourethral glands (Cowper's glands). Their presence, size, type and number vary among species. The ampullae are paired glands located on the dorsal neck of the bladder. They are composed of secretory alveoli lined by cuboidal to columnar pseudostratified epithelial cells with few basal cells. The seminal vesicles are paired saccular glands that are located between the prostate gland and the ampulla.[1,4] Seminal vesicles consist of lobules of tubuloalveolar glands with pseudostratified epithelium with sparse basal cells, divided by interlobular septa that contains either abundant smooth muscle (in ruminants) or connective tissue with little smooth muscle (stallions and boars).[1] The prostate, which has a higher proportion of connective tissue than the seminal vesicles, originates at the urinary bladder and surrounds the urethra.[4] The prostate is composed of either the corpus (body) of compact prostatic tissue located external to the urethra, and/or the disseminated prostate, characterized by diffuse prostatic tissue found along the length of the pelvic urthera.[4] Prostatic glands are classified as compound tubuloacinar glands, and are lined predominantly by pseudostratified and occasionally low cuboidal or squamous epithelium. Bulbourethral glands are paired, dense glands containing abundant fibrous connective tissue located below the prostate and are composed of compound tubuloalveolar glands.[4]

The moderator provides the included chart summarizing the presence and relative size of accessory genital glands in various species.

**Contributing Institution:** National Institute of Environmental Health Sciences
Cellular and Molecular Pathology Branch
P.O. Box 12233
Research Triangle Park, NC 27709
http://ntp-server.niehs.nih.gov/

**References:**

1. Bacha WJ, Bacha LM. Male reproductive system. In: *Color Atlas of Veterinary Histology.* 2nd ed. Philadelphia, PA: Lippincott Williams and Wilkins. 2000:04-220.
2. Foster RA. Male reproductive system. In: McGavin MD, Zachary JF, eds. *Pathologic Basis of Veterinary Disease*. 5th ed. St Louis, MO: Elsevier Mosby; 2012:1128.
3. Gupta S, Hastak K, Ahmad N, et al. Inhibition of prostate carcinogenesis in TRAMP mice by oral infusion of green tea polyphenols. *Proc Natl Acad Sci USA*. 2001;98:10350-10355.
4. Johnson L, Welsh Jr TH, Curley Jr KO, Johnston CE. Anatomy and physiology of the male reproductive system and potential targets of toxicants. In: McQueen CA, ed. *Comprehensive Toxicology*. Oxford, UK: Elsevier. 2010:5-59. Accessed online at http://www.sciencedirect.com/science/article/pii/B9780080468846011027 on 3 February 2013.
5. Nyska A, Suttie A, Bakshi S, et al. Slowing tumorigenic progression in TRAMP mice and prostatic

carcinoma cell lines using natural anti-oxidant from spinach, NAO--a comparative study of three anti-oxidants. *Toxicol Pathol*. 2003;31:39-51.
6. Suttie A, Nyska A, Haseman JK, et al. A grading scheme for the assessment of proliferative lesions of the mouse prostate in the TRAMP model. *Toxicol Pathol*. 2003;31:31-38.
7. Tani Y, Suttie A, Flake GP, et al. Epithelial-stromal tumor of the seminal vesicles in the transgenic adenocarcinoma mouse prostate model. *Vet Pathol*. 2005;42:306-314.
8. Wechter WJ, Leipold DD, Murray ED, Jr., et al. E-7869 (R-flurbiprofen) inhibits progression of prostate cancer in the TRAMP mouse. *Cancer Res*. 2000;60:2203-2208.

**CASE II:** 2009913311 (JPC 3165094).

**Signalment:** 11-year-old, female, mixed breed, dog (*Canis familiaris*).

**History:** The dog showed clinical signs suggestive of endometritis or pyometra and underwent ovariohysterectomy.

**Gross Pathologic Findings:** An approximately 4 cm diameter mass of the right ovary was surgically resected and sent to our laboratory for histopathologic examination with the uterine tissue. The mass was soft with a milky-white, smooth surface. The cut surface was solid and homogeneous. No abnormal change was detected in the left ovary.

**Histopathologic Description:** The tumor mass is formed in the ovary, so stretched ovarian tissue is detected on the surface of the mass. The tumor mass consists of solid or trabecular cellular nests surrounded by thin connective tissue stroma. Irregularly-sized cysts filled with eosinophilic homogeneous fluid are sometimes formed in the nests. The tumor mass has an appearance similar to granulosa-theca cell tumor, but nuclear size varies among the cells. The tumor cells are irregular to spindle shaped, having an elongated or oval nucleus of medium to smaller size, and resembling neoplastic cells of granulosa-theca cell tumor. However, large round to polygonal cells similar to germ cells are mingled with smaller cells at various rates in the nest. The granulosa-theca cell-like tumor cells have a hyperchromatic nucleus and prominent nucleolus. The cytoplasm of these cells is relatively scanty and eosinophilic. In contrast, large tumor cells similar to germ cells have large round nuclei with scattered chromatin, and one or a few large nucleoli with abundant pale eosinophilic or clear cytoplasm. Mitotic figures are seen more frequently among the large cells similar to germ cells than other tumor cells. Structures resembling to Call-Exner bodies with or without central calcification are not observed.

Immunohistochemically, the large round cells are positive for one of the germ cell markers, PLAP (placental alkaline phosphatase) and are negative for granulosa cell markers such as WT-1 and vimentin. In contrast, small spindle cells are positive for WT-1 and vimentin, and are negative for PLAP. Some tumor cells of middle-sized nuclei are positive for all three markers.

**Contributor's Morphologic Diagnosis:** Ovary: Ovarian mixed germ cell sex cord-stromal tumor, canine.

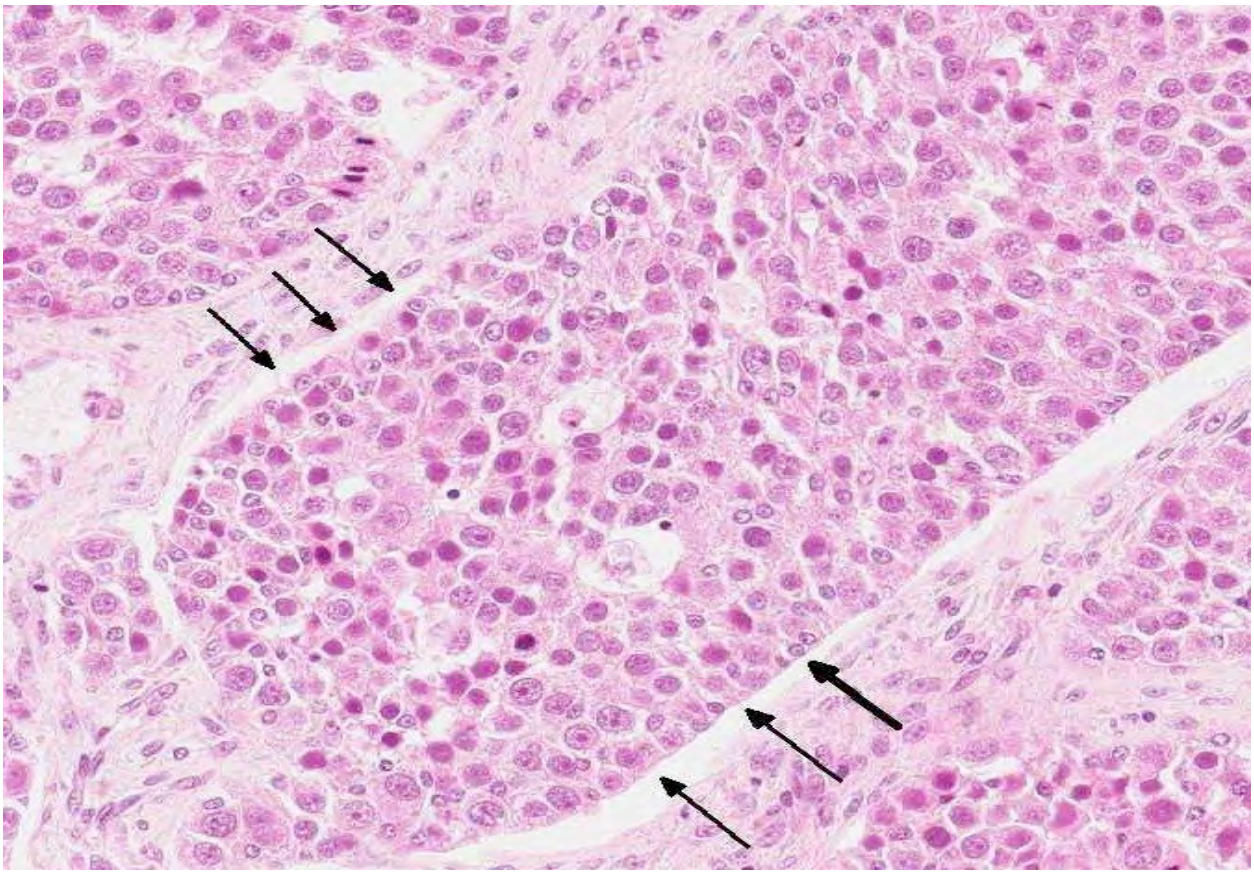

*2-1. Ovary: The ovary is effaced by a multilobular neoplasm composed of tubules containing two populations of cells – columnar stromal cells palisading along the basement membranes (small arrows), and centrally, round, mildly anisokaryotic germ cells.*

**Contributor's Comment:** Mixed germ cell sex cord-stromal tumors have been rarely reported in human ovaries and testes and in canine testes;[4,5] however, this tumor is extremely rare in female dogs and was not included as an ovarian tumor in the second series of WHO classification in domestic animals.[3] Among the ovarian tumors in dogs, granulosa cell tumors and epithelial tumors are the most common.

The histological appearance of canine ovarian granulosa cell tumors is variable; testicular Sertoli cell tumor-like appearance is observed along with the follicular (i.e., micro- and macro- follicular), insular, diffuse, and trabecular growth patterns.[1,3] Granulosa cell tumors in the human ovary are further classified into adult and juvenile types. Juvenile granulosa cell tumors have solid and follicular growth patterns of tumor cells with abundant (luteinized) cytoplasm. Solid or follicular growth pattern of tumor cells with immature nuclei and abundant cytoplasm are thought to be important characteristics distinguishing juvenile from adult granulosa cell tumors.[8] The histological characteristic of the ovarian tumor in the present case is similar to the micro follicular pattern of canine granulosa cell tumors, but nuclear size varies among tumor cells and there are very large cells that appear similar to germ cells. According to the criteria for classification of human ovarian granular cell tumors, variation of nuclear size and the presence of very large nuclei, which may represent immature nuclei, suggest the diagnosis of juvenile granulosa cell. However, tumor cells characterized by large round nuclei and abundant cytoplasm in the present case are positive for PLAP (one of the germ cell markers), suggesting that these tumor cells are characteristic of germ cells rather than malignant neoplastic granulosa cells with immature nuclei. Although a majority of canine ovarian granulosa cell tumors are composed of multiple growth patterns in a single mass, the present tumor is composed of a single pattern throughout.[1,3] This growth pattern may be further evidence to rule out the diagnosis of granulosa cell tumor.

Patnaik and Mostofi first reported mixed germ cell-stromal tumors that were different from collision tumors of seminoma and Sertoli cell tumors in the testis of 16 dogs, whereas cellular components are identical in both tumors.[5] In their mixed germ cell-stromal tumors, the tumor is composed of uniform and close intermixing of two type cells: germ cells with a large round nucleus and Sertoli cells with a smaller elongated nucleus.[4] It is unlikely that the present tumor is a collision tumor of dysgerminoma and granulosa-theca cell tumor that originated in different sites of the ovary, because the histopathological features of the tumor were almost uniform throughout the mass.

Mixed germ cell sex cord-stromal tumors are further subdivided into two types: gonadoblastoma and mixed germ cell sex cord-stromal tumor. These two types of tumors are distinct clinicopathological and histopathological entities. In human cases, approximately 80 percent of gonadoblastomas occur in phenotypic female patients who have a Y chromosome (almost all have karyotypes of 46XY or 46XY/XO and dysgenetic gonads).[2,5,7] In contrast, mixed germ cell sex cord-stromal tumors develop in phenotypically and karyotypically normal females and males. Mixed germ cell sex cord-stromal tumors have been reported in male dogs with recognizable gonads.[2,4,5,7] Judging from normal development of the left ovary and other genital organs, the present dog was probably a genotypically normal female; however, an examination was not done on gene abnormality.

**JPC Diagnosis:** Ovary: Mixed germ cell sex cord-stromal tumor.

**Conference Comment:** This interesting case stimulated a great deal of discussion among conference participants, with some favoring the diagnosis of mixed germ cell sex-cord stromal tumor (MGCSCST) and others questioning the diagnosis, since, as the contributor noted, MGCSCSTs are not well-documented in canine ovaries. Like the contributor, conference participants considered a differential diagnosis that included juvenile granulosa cell tumor, gonadoblastoma and collision tumor. We reviewed this case in consultation with physician reproductive pathologists at the Joint Pathology Center, who favored a diagnosis of dysgerminoma; however, the majority of conference participants agreed that the stromal component is a significant part of the neoplastic process, and therefore concurred with the contributor's diagnosis of MGCSCST. Participants agreed that a karyotype would be useful to rule out gonadoblastoma.

The conference moderator led a practical discussion of immunohistochemical markers in human ovarian germ cell and sex cord-stromal tumors based on a recent report in *Histopathology*. The authors describe the use of SALL4 (Sal-like protein 4) and PLAP (placental alkaline phosphatase) to mark germ cell differentiation; OCT4 (octamer-binding transcription factor 4), CD117 and D2-40 to mark dysgerminoma; α-fetoprotein and glypican-3 to mark yolk sac tumors; OCT4, CD30 and SOX2 (sex determining region Y-box 2) to mark embryonal carcinoma; calretinin, inhibin, SF-1 (splicing factor 1) and FOXL2 (forkhead box L2) to mark sex cord–stromal differentiation; and melan-A to mark steroid cell tumors.[6] The following is a summary of immunohistochemical stains used to differentiate human ovarian tumors as discussed in this article:

- PLAP is expressed in dysgerminomas, gonadoblastomas, embryonal carcoinomas, yolk sac tumors and choriocarcinomas.
- SALL4, a transcription factor required for development and maintenance of embryonic

stem cell pluripotency, is more sensitive and specific than PLAP in identifying ovarian germ cell tumors; however, PLAP is more sensitive for choriocarcinomas.

- OCT4, a transcription factor required for maintaining embryonic stem cell pluripotency, is expressed in dysgerminomas, gonadoblastomas and embryonal carcinomas, whereas other germ cell tumors lack OCT4.
- CD-117 is a transmembrane tyrosine kinase growth factor receptor for stem cell factor (SCF) that shows strong membranous immunohistochemical staining in over 85% of dysgerminomas, and half of solid pattern yolk sac tumors. CD-117 is also overexpressed in other tumors, such as gastrointestinal stromal tumors and mast cell tumors; expression in these tumors is often cytoplasmic.
- D2-40, which marks the protein podoplanin, expressed in fetal germ cells, shows cytoplasmic and membranous expression in most dysgerminomas.
- NANOG is expressed in up to 83% of dysgerminomas and in the germ cell population of gonadoblastoma.
- SOX2 and CD30 expression is present in many embryonal carcinomas.
- Alpha-fetoprotein and glypican-3 is expressed in many yolk sac tumors.
- Glypican-3, a surface heparan sulphate proteoglycan that regulates cell growth during fetal development, is very specific for yolk sac tumors. Choriocarcinomas are also positive for glypican-3 but are usually easily differentiated from yolk sac tumors by histomorphology.
- HCG (human chorionic gonadotropin) is expressed by the syncytiotrophoblastic cells but not the mononuclear trophoblasts of an ovarian choriocarcinoma. Keratin, inhibin and glypican-3 are also expressed in choriocarcinomas.
- Inhibin is sensitive and specific for sex cord-stromal cell tumors.
- Calretinin, a maker of mesothelial differentiation, is more sensitive but less specific than inhibin for sex cord-stromal differentiation.
- SF-1, a transcription factor that regulates steroidogenesis, sexual differentiation and gonadal and adrenal gland development, is expressed in 100% of granulosa cell tumors.
- FOXL2, which encodes a transcription factor that is required for granulosa cell function and ovarian follicle development, is expressed in almost all granulosa cell tumors; it also appears to mark all types of sex cord-stromal tumors except for steroid cell tumors.
- WT-1 (Wilms tumor 1) is sensitive for sex cord-stromal differentiation.
- Steroid cell tumors express calretinin, inhibin, and SF-1and melan-A (also known as MART-1, or melanoma antigen recognized by T-cells 1).
- EMA (epithelial membrane antigen) is the best marker to exclude epithelial ovarian cancer.[6]

These markers have proven to be quite helpful in diagnosing ovarian germ cell tumors and sex cord-stromal tumors in humans; however, their efficacy in canine tumors has not been determined.

**Contributing Institution**: Department of Pathology
Faculty of Pharmaceutical Science
Setsunan University
45-1 Nagaotohge-cho
Hirakata, Osaka, 5730 101
Japan

**References**

1. Akihara Y, Shimoyama Y, Kawasako K, Komine M, Hirayama K, Kagawa Y, et al. Immunohistochemical evaluation of canine ovarian tumors. *J Vet Med Sci*. 2007;69:703-708.
2. Bolen JW. Mixed germ cell-sex cord stromal tumor. A gonadal tumor distinct from gonadoblastoma. *Am J Clin Pathol*. 1981;75:565-573.
3. Kennedy PC, Edwards JF, Goldschmidt MH, Larsen S, Munson L, Nielsen S. Histological classification of tumor of genital system of domestic animals. In: *World Health Organization International Histological Classification of Tumors of Domestic Animals*. Second Series. IV. Washington, DC: Armed Forces Institute of Pathology/ American Registry of Pathology; 1998.
4. Owston MA, Ramos-Vara JA. Histologic and immunohistochemical characterization of a testicular mixed germ cell sex cord-stromal tumor and a Leydig cell tumor in a dog. *Vet Pathol*. 2007;44:936-943.
5. Patnaik AK, Mostofi FK. A clinicopathologic, histologic, and immunohistochemical study of mixed germ cell-stromal tumors of the testis in 16 dogs. *Vet Pathol*. 1993;30:287-295.
6. Rabban JT, Zaloudek CJ. A practical approach to immunohistochemical diagnosis of ovarian germ cell tumours and sex cord–stromal tumours. *Histopathology*. 2013;62: 71–88.
7. Talerman A, Roth LM. Recent advances in the pathology and classification of gonadal neoplasms composed of germ cells and sex cord derivatives. *Int J Gynecol Pathol*. 2007;26:313-321.
8. Young RH. Sex cord-stromal tumors of the ovary and testis: their similarities and differences with consideration of selected problems. *Mod Pathol*. 2005;18 Suppl 2:S81-98.

**CASE III:** N1012728 (JPC 4006582).

**Signalment:** 20-year-old, female, intact, nonhuman primate (NHP) *(Macaca mulatta).*

**History:** In February 2010, the NHP presented with heavy menstruation and a depressed attitude. A mid-abdominal mass, approximately 5 cm in diameter, was found on palpation, and confirmed by radiography. The NHP was used in psychotropic drug studies. Her past medical history included kyphosis and irritable bowel syndrome. The latter currently managed with bi-weekly injections of 1.2 mg dexamethasone. Past gynecological exams detected an enlarged uterus and cervix. Laboratory results (see below) included neutrophilia, hypoproteinemia and mild azotemia. A working diagnosis of endometriosis led to monthly administration of medroxyprogesterone injections (40 mg, IM). The NHP presented three months later with a dark, red mass protruding from the vulva. At the first surgery, three masses were removed. The vaginal mass was determined to be a hemangioma. The uterus was firm and enlarged with multiple red foci over the ovaries that were confirmed as endometriosis. The dorsal aspect of the cervix had a 2 cm, firm, whitish-pink mass confirmed as a leiomyoma. Post surgery, the uterus was opened and found to contain a firm, white, lobulated mass. A second surgery was performed to remove a large 6.5 cm omental mass and smaller 2-3 cm omental mass (not shown) similar in appearance to the large omental mass.

**Gross Pathology:** 1. Vaginal mass: 4.8 x 3.2 x 2 cm multilobular dark red/black mass. 2. Uterus and ovaries: serosa: multiple dark red/black foci. 3. Uterus Lumen. 1.9 x 2.8 x 1.9 white, firm polyploid intrauterine mass. 4. Omentum: 6.5 x 5.5 x 3 cm round mass with numerous fingerlike projections covered by a smooth surface found in the omentum. 5. Omentum: 2 cm smaller mass.

**Laboratory Results:**

| Parameter | Normal range | Feb 2010 | April 2010 |
|---|---|---|---|
| WBC | 5.5-19.0 x $10^3$/mL | 21.9 | 4.0 |
| Total protein | 7.8-9.6 g/dl | 5.1 | 6.1 |
| BUN | 8-20 mg/dl | 25 | 24 |
| Albumin | 3.1-5.3 g/dl | 3.0 | 3.8 |
| AST | 14-30 U/L | 22 | 40 |

**Histopathologic Description:** The intrauterine mass was endometrial in origin and extended into the lumen. It was comprised of disorganized, predominantly spindle-shaped cells with one to two large, ovoid nuclei per cell. The cytoplasm was amphophilic to eosinophilic, with varied volume. There were frequent foci of glandular cells. Neoplastic stromal cells were frequently whorled around arterioles. Mitotic figures ranged from 0-3 per 40 power field. Tumor cells were variably positive for collagen (not shown) by Masson's trichrome and displayed variably positive immunohistochemistry (IHC) against CD10, and were uniformly negative against CD34 (not shown). The large omental mass had small foci of endometriosis, as well as neoplastic cells similar to the intrauterine mass. Scattered foci of necrosis, increased cellular atypia and frequent mitotic figures were present.

**Contributor's Morphologic Diagnosis:** 1. Intra-uterine mass, endometrial stromal sarcoma (ESS), high grade.
2. Omental masses, metastatic ESS.

**Contributor's Comment:** In humans, common uterine tumors include leiomyosarcoma, endometrial stromal tumors (ESS) and carcinosarcoma.[10] Uterine sarcomas may be from 3-7% of all uterine cancers.[8] In the NHP, endometrial stromal tumors are rare, while tumors of the uterine musculature are common.[4,5,20] Poorly differentiated, high-grade endometrial stromal tumors have not been reported in the NHP.[5] Endometrial stromal tumors have been reported in a chimpanzee, rats, mice, African hedgehogs and in a cat.[1,10,3,11,15,17,19,13] The frequency of ESS has been reported as less than 1% in B6C3F1 mice.[13] ESS has also been reported in the Donryu and F344 rat strains, though at a much lower incidence compared to other uterine tumors.[17] Two studies of the F344 rat found a 0.9 % and 0.11 % occurrence of ESS.[11,13-15]

A uterine tumor in a 25-year-old chimpanzee, presented to necropsy for tuberculosis, was comprised of cells similar to proliferating endometrial stroma, and contained medium sized muscular arteries, as well as a fibrillar lattice around the cells.[20] The cells, arranged in cords, clumps and swirls, had lightly basophilic, ovoid to spindle-shaped nuclei with an indistinct nucleolus, and a moderate amount of eosinophilic cytoplasm.[20]

In the mouse, ESS is not uncommon. It is found within the wall or protruding into the lumen of the uterus. Murine ESS may arise within benign, endometrial stromal polyps.[13,15] These polyps may contain foci of greater malignancy, characterized by mitosis, cellular atypia, vascular deformation with hematoma or hemorrhage, and necrosis.[13] As in other species, ESS is arranged in sheets with whorls or fascicles of intersecting, spindle-shaped cells with indistinct borders and marked cellular pleomorphism.[15] Giant cells may be seen, though most cells are oval, fusiform cells with scanty basophilic

cytoplasm and spherical nuclei with dispersed clumps of chromatin.[13] The neoplastic cells may be surrounded by a fibrillar and collagenous matrix.[3] Metastases may occur in the myometrium, cervix, and other abdominal structures.[15] ESS can be modeled *in vivo* using mice with mutations in p53 genes, which are treated with mutagens such as N-ethyl-N-nitrosurea (ENU).[9]

ESS has been reported in a 12-year-old, domestic shorthair queen presenting with depression, anorexia, panting, vomiting and a purulent vaginal discharge. A 3 x 10 cm solid mass was palpated in the abdomen, and radiographs demonstrated different sized masses less than 1.5 cm in the lungs.[19] The intra-abdominal mass showed both endometrial stromal and smooth muscle cells with focal tumor cell necrosis. The stromal cells had small, ovoid and spindle-shaped cells with scant cytoplasm, arranged in a diffuse pattern, with prominent vasculature.[19] The cells showed moderate nuclear pleomorphism and no mitotic figures. Neoplastic cells were also seen within blood and lymphatic vessels. Endometrial stromal cells stained positive with Vimentin.[19]

In captive African hedgehogs, *Atelerix albiventris*, submitted to IDEXX and Zoo/Pathology services for routine pathology, ESS was the second most commonly diagnosed uterine tumor, and was often found during hysterectomies.[16] Vaginal bleeding (13/15 animals), hematuria for two days to six months (11/15), as well as weight loss (5/12), were reported.[16] The ESS tumors were similar to adenosarcomas (the most common tumor), except they did not contain a tubular epithelial component. ESS tumors were dense, polyploid nodules of 1-15 mm in diameter, and often were locally invasive. The stromal cells contained mitotic figures, formed fascicles and whorls, and were supported by fibrovascular stroma.[16]

In summary, ESS are formed from the glandular epithelium or connective tissue stroma.[5] The tumors are tan to grey, and extend by polyploid growth into the endometrial cavity, the myometrium and myometrial vessels.[1,8,12] The cells are small, resembling the proliferative phase of endometrial stroma.[1,5] They often encircle small and medium size muscular arteries.[5] ESS is usually aggressive, with local recurrence and metastases.[10] The current classification system states tumors previously called high-grade ESS are now called poorly differentiated or undifferentiated uterine sarcomas.[1] The undifferentiated tumors invade the myometrium, have severe nuclear pleomorphism, high mitotic activity and/or tumor cell necrosis.[8] Immunohistochemical staining has shown endometrial stromal sarcomas to be positive for CD 10 and uniformly negative for CD 34.[2,8] The tumors lack estrogen and progesterone receptors.[18]

The human literature reports early diagnosis is often a challenge, as no imaging modality is reliable

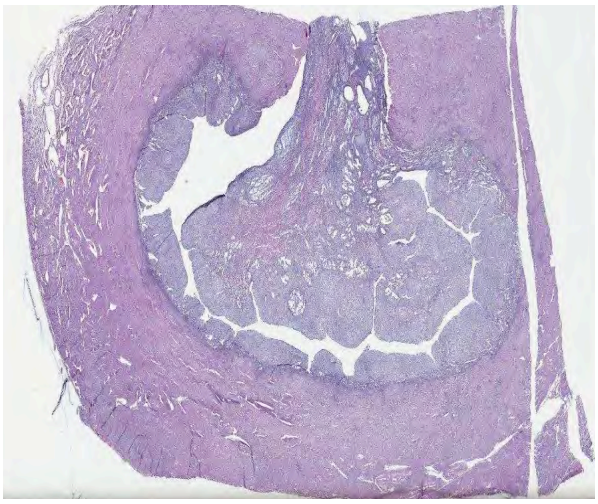

*3-1. Uterus, macaque: A neoplasm circumferentially expands the endometrium and forms a polypoid mass that protrudes into the lumen. (HE 4X)*

preoperatively, although ultrasound and MRI may be more useful than CT.[1] After preoperative imaging for metastasis, bilateral salpingo-oorphorectomy and total hysterectomy are usually performed.[1,18] Lymphadenectomy is controversial as it may not produce a survival benefit.[1,18] Radiotherapy may decrease local recurrence.[10] Chemotherapy, as well as endocrine therapy options are also used.[10,18] JAZF1/JJAZ1, JAZF1/PHF1 and EPC1/PHF1 are cancer –specific fusion genes that are being studied as diagnostic and treatment targets.[1,12] Genetic testing of the tissues is planned at a future date.

Survival times vary from months to years, depending on the extent and classification of the tumor. Median recurrence time is usually less than two years.[7,10] In one retrospective study, the median survival time in humans for high grade sarcomas was one year, while the median survival time for lower grades ESS was 11 years.[8] The hedgehogs reported had a mean survival time of 303 days post-surgery.[16]

**JPC Diagnosis:** Uterine mass: Endometrial stromal cell sarcoma.

**Conference Comment:** The contributor provides an excellent review of ESS. In addition to the special stains and immunohistochemistry performed by the contributor, JPC performed AE1/AE3, desmin and smooth muscle actin (SMA) with the following results: Epithelial cells showed strong cytoplasmic immunoreactivity with AE1/AE3; desmin was negative; and there was moderate to strong positive cytoplasmic immunoreactivity with smooth muscle actin within the stromal component.

A recent study of gene expression signatures in uterine endometrial stromal sarcoma (ESS) and leiomyosarcoma (LMS) in humans found that genes overexpressed in ESS included *SLC7A10*, *EFNB3*, *CCND2*, *ECEL1*, *ITM2A*,

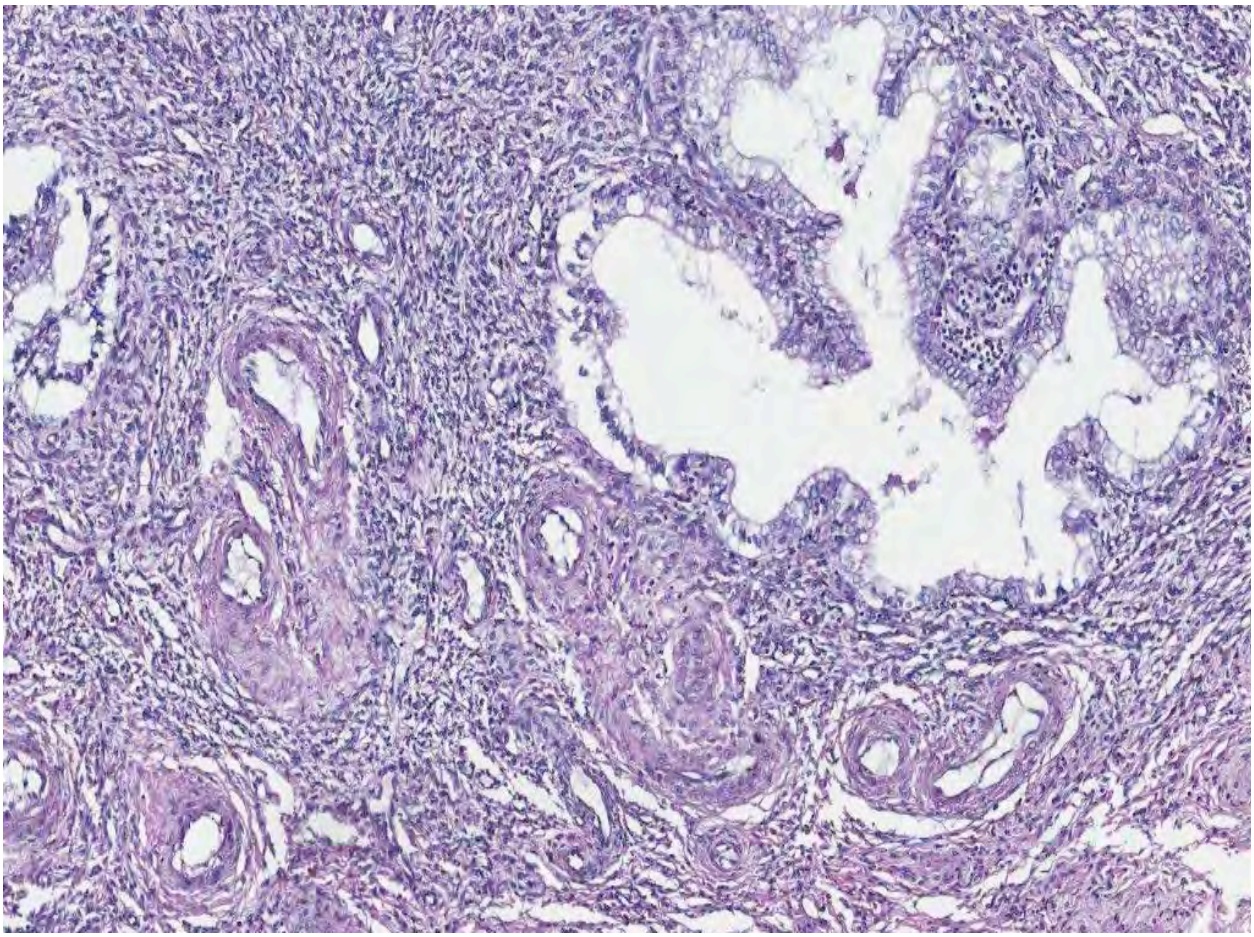

*3-2. Uterus, macaque: Neoplastic spindle cells, which recapitulate endometrial stroma, surround and separate tortuous cystic endometrial glands and blood vessels. (HE 144X)*

*NPW*, *PLAG1* and *GCGR*; whereas, genes overexpressed in LMS included *CDKN2A*, *FABP3*, *TAGLN*, *JPH2*, *GEM*, *NAV2* and *RAB23*.[6] Many genes overexpressed in LMS included those that code for myosin light chain and caldesmon, but not the genes coding for desmin or actin. *CD10* was not overexpressed in ESS. Interestingly, although CD10 was once considered specific for ESS, it has been shown to be expressed in many adenosarcomas as well as LMS and 33% of undifferentiated endometrial or uterine sarcoma. Approximately a quarter of all ESS in this study were CD10 negative, thus raising the question of the usefulness of this marker in human uterine sarcomas.[6]

**Contributing Institution:** Section of Comparative Medicine
Yale University School of Medicine
New Haven, CT 06520-8016
http://medicine.yale.edu/compmed/index.aspx

**References:**

1. Amant F, Coosemans A, Debiec-Rychter M, Timmerman D, Vergote I. Clinical management of uterine sarcomas. *Lancet Oncol.* 2009;10:1188-1198.
2. Bhargava R, Shia J, Hummer AJ, Thaler HT, Tornos C, Soslow RA. Distinction of endometrial stromal sarcomas from 'hemangiopericytomatous' tumors using a panel of immunohistochemical stains. *Mod Pathol*. 2005;18:40-47.
3. Brayton C. Spontaneous disease in commonly used mouse strains. In: *The Mouse in Biomedical Research*. 2nd edition. Anonymous 2nd ed. 2007: Ch 25.
4. Cline JM, Wood CE, Vidal JD, Tarara RP, Buse E, Weinbauer GF, et al. Selected background findings and interpretation of common lesions in the female reproductive system in macaques. *Toxicologic Pathology*. 2008;36:142S-163S.
5. Cooper TK, Gabrielson KL. Spontaneous lesions in the reproductive tract and mammary gland of female non-human primates. *Birth Defects Res B Dev Reprod Toxicol*. 2007;80:149-170.
6. Davidson B, Abeler VM, Hellesylt E, et al. Gene expression signatures differentiate uterine endometrial stromal sarcoma from leiomyosarcoma. *Gynecol Oncol*. 2013;128(2):349-55.
7. D'Angelo E, Prat J. Uterine sarcomas: a review. *Gynecol Oncol*. 2010;116:131-139.

8. D'Angelo E, Spagnoli LG, Prat J. Comparative clinicopathologic and immunohistochemical analysis of uterine sarcomas diagnosed using the World Health Organization classification system. *Hum Pathol*. 2009;40:1571-1585.
9. Friel AM, Growdon WB, McCann CK, Olawaiye AB, Munro EG, Schorge JO, et al. Mouse models of uterine corpus tumors: clinical significance and utility. *Front Biosci* (Elite Ed). 2010;2:882-905.
10. Gadducci A, Cosio S, Romanini A, Genazzani AR. The management of patients with uterine sarcoma: a debated clinical challenge. *Crit Rev Oncol Hematol*. 2008;65:129-142.
11. Goodman D. Neoplastic and nonneoplastic lesions in aging F344 rats. *Toxicol Appl Pharmacol*. 1979;48:237-248.
12. Kurihara S, Oda Y, Ohishi Y, Iwasa A, Takahira T, Kaneki E, et al. Endometrial stromal sarcomas and related high-grade sarcomas: immunohistochemical and molecular genetic study of 31 cases. *Am J Surg Pathol*. 2008;32:1228-1238.
13. Maekawa A, Maita, K. Changes in the ovary. In: Uea M, ed. *Pathobiology of the Aging Mouse*. 1996.
14. Maita K, Hirano M, Harada T, Mitsumori K, Yoshida A, Takahashi K, et al. Spontaneous tumors in F344/DuCrj rats from 12 control groups of chronic and oncogenicity studies. *J Toxicol Sci*. 1987;12:111-126.
15. Maronpot RR, Boorman GA, Gaul BW. *Pathology of the Mouse, Reference and Atlas*. 1st ed. Vienna, IL: Cache River Press;1999.
16. Mikaelian I, Reavill DR, Practice A. Spontaneous proliferative lesions and tumors of the uterus of captive African hedgehogs (Atelerix albiventris). *J Zoo Wildl Med*. 2004;35:216-220.
17. Nagaoka T. Spontaneous uterine adenocarcinomas in aged rats and their relation to endocrine imbalance. *J Cancer Res Clin Oncol*. 1990;116:623.
18. Reich O, Regauer S. Hormonal therapy of endometrial stromal sarcoma. *Curr Opin Oncol*. 2007;19:347-352.
19. Sato T, Maeda H, Suzuki A, Shibuya H, Sakata A, Shirai W. Endometrial stromal sarcoma with smooth muscle and glandular differentiation of the feline uterus. *Vet Pathol*. 2007;44:379-382.
20. Toft JD. Endometrial stromal tumor in a chimpanzee. *Vet Pathol.* 1975;12:32-36.

**CASE IV:** CRL-1 (JPC 4019837).

**Signalment:** Female mouse (*Mus musculus*), age and strain not given.

**History:** Incidental finding at sentinel health monitoring.

**Gross Pathology:** The left ovary was enlarged and hemorrhagic.

**Histopathologic Description:** The enlarged ovary contains a mass, characterized by sheets of large pleomorphic cells with abundant eosinophilic cytoplasm, in a large focus of hemorrhage within the ovarian bursa. The cells have a large round to oval, sometimes irregular, nucleus, with vesicular chromatin and multiple nucleoli, with occasional dark staining nuclei, and rare binucleate cells. Mitoses are rare.

**Contributor's Morphologic Diagnosis:** Ovary: choriocarcinoma.

**Contributor's Comment:** Tumors of the ovary are divided into three groups based on the presumed tissue of origin: tumors of surface epithelium, including adenomas and carcinomas; germ cell tumors including teratomas, dysgerminomas, choriocarcinomas; and sex cord–stromal tumors including granulosa cell tumors, thecomas, fibromas.[1]

The choriocarcinoma is a malignant neoplasm of trophoblastic cells, which in women often has widespread metastases. Choriocarcinoma is one of the rarest ovarian tumors in women, estimated to occur in only 1 in 369,000 women.[3] Most choriocarcinomas in women occur in the uterus, post pregnancy. These tumors are also rare in animals, although they have been reported in rhesus and cynomolgus macaques, rabbits, a cow, dogs, mice and rats.[1,2,3,4,6,7] Choriocarcinomas may arise in the uterus, ovary or testis.

The incidence of ovarian tumors in mice varies with the strain.[2,4] Ovarian tumors are also more common in older mice (> 18 months of age). In mice, ovarian neoplasms are more common in the B6C3Fl mouse, but ovarian choriocarcinoma is only 1% of ovarian tumors.[4] The most common ovarian tumors in B6C3F1 mice are epithelial, granulosa cell tumors and teratomas.[1] In our laboratory, we have identified six ovarian choriocarcinomas in the last 10 years, all in sentinel mice as an incidental finding during health monitoring.

**JPC Diagnosis:** Ovary: Choriocarcinoma.

**Conference Comment:** Malignant trophoblastic tumor variants are classified as choriocarcinomas (CC), epithelioid trophoblastic tumors (ETT), or placental site trophoblastic tumors (PSTT). Trophoblastic tumors usually develop either during or following gestation, but

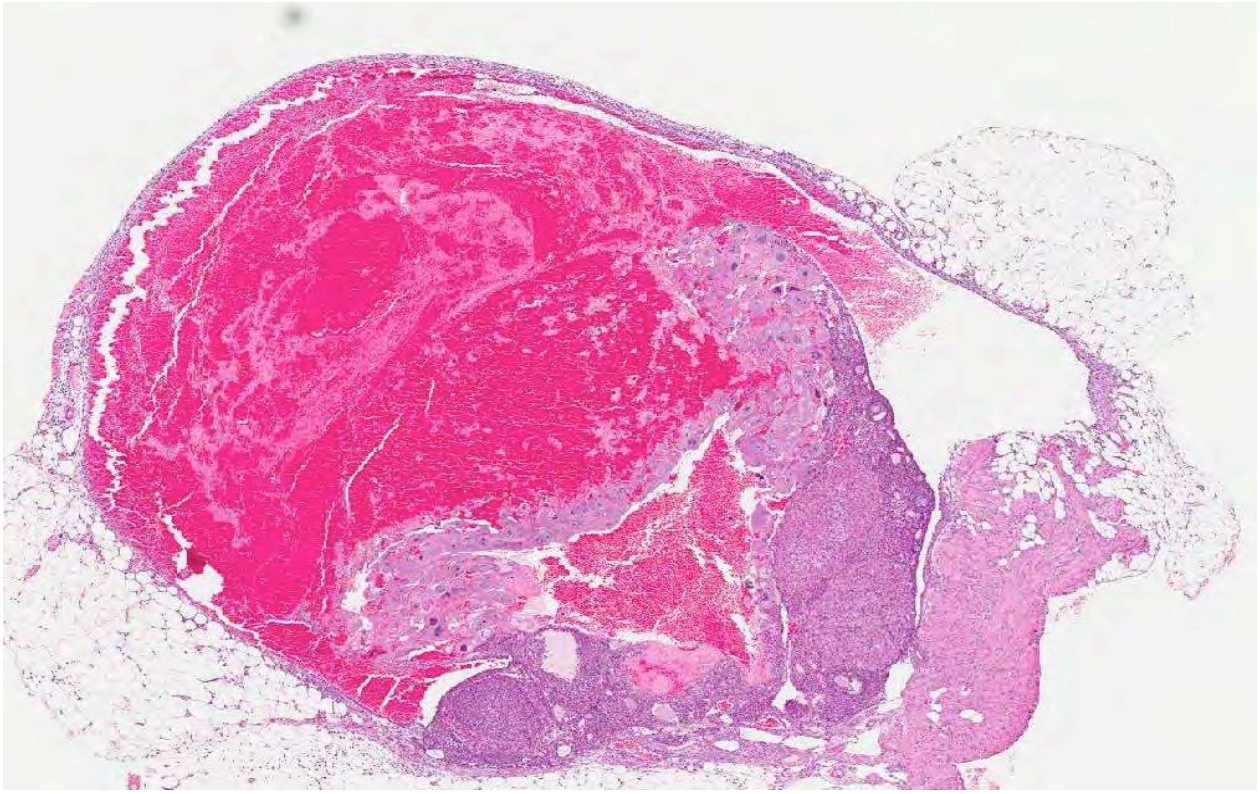

*4-1. Ovary, mouse: The ovary is expanded and largely effaced by a neoplasm. Hemorrhage within the neoplasm extends into the ovarian bursa. (HE 40X)*

have rarely been reported to develop from germ cells in the absence of pregnancy.[7] Choriocarcinomas, as seen in this case, are characterized by a bilaminar pattern composed of cytotrophoblasts and syncytiotrophoblasts often associated with prominent hemorrhage.[5] Although pure nongestational choriocarcinomas are extremely rare in humans, CC can be a component of a mixed germ cell tumor of the ovary.[7] ETTs are composed of a relatively uniform population of mononucleate trophoblastic cells with eosinophilic or clear cytoplasm; these cells are intermediate trophoblastic cells that resemble chorion laeve.[5] PSTTs originate from large, polygonal intermediate trophoblastic cells of the placental bed. Although nongestational trophoblastic tumors are rare in humans, several have been described in captive non-human primates, including CC and ETT. Additionally, a pure nongestational malignant PSTT of the ovary was recently reported in a young rhesus monkey.[7]

**Contributing Institution:** Research Animal Diagnostic Services
Charles River
Wilmington, MA 01887
www.criver.com

**References:**

1. Alison RH, Morgan KT. Ovarian neoplasms in F344 rats and B6C3F1 mice. *Environ Health Perspect*. 1987;73:91-106.
2. Alison RH, Lewis DJ, Montgomery CA. Ovarian choriocarcinoma in the mouse. *Vet Pathol*. 1987;24:226-230.
3. Farman CA, Benirschke K, Horner M, Lappin P. Ovarian choriocarcinoma in a rhesus monkey associated with elevated serum chorionic gonadotropin levels. *Vet Pathol*. 2005;42:226-229.
4. Frith CH, Evans MG. Spontaneous ovarian choriocarcinoma, yolk sac carcinoma, and teratoma in B6C3F1 mice: a case report. *Toxicol Pathol*. 1993;21:91-98.
5. Horn LC. Intermediate Trophoblastic Tumors and Tumor-like Lesions-the Clinicopathologic Aspects. IAP 2006 Annual Congress. Symposium #41, section 3. Accessed online at http://www.uscap.org/index.htm?iap2006/symp41-3.htm on 3 February 2013.
6. Kaufmann-Bart M, Fischer I. Choriocarcinoma with metastasis in a rabbit (Oryctolagus cuniculi). *Vet Pathol*. 2008;45:77-79.
7. Marbaix E, Defre're S, Ho Minh Duc K, Lousse JC, Dehoux JP. Nongestational malignant placental site trophoblastic tumor of the ovary in a 4-year-old Rhesus Monkey. *Vet Pathol.* 2008;45:375-378.
8. Pirak M, Waner T, Abramovici A, Scolnik M, Nyska A. Histologic and immunohistochemical study of a spontaneous choriocarcinoma in a male Sprague Dawley rat. *Vet Pathol*. 1991;28:93-95.

**Joint Pathology Center**
**Veterinary Pathology Services**

## WEDNESDAY SLIDE CONFERENCE 2012-2013

# Conference 14

**6 February 2013**

---

**CASE I:** RP18165 (JPC 4018046).

**Signalment:** Young adult female American white pelican, *(Pelecanus erythrorhynchos)*.

**History:** This native bird was found dead on the grounds of a zoological institution.

**Gross Pathology:** The liver and spleen were enlarged and dark red with approximately 60-75% of the capsular surface and parenchyma replaced by multifocal to coalescing, 1-3 mm, irregular, slightly bulging, yellow, dry, soft to firm foci. Myriad endoparasites were present: pouch lice in the oral cavity, trematodes in the trachea, and nematodes in the esophagus and proventriculus.

**Laboratory Results:** PCR (fresh frozen liver): PCR targeting a portion of the eukaryote 18S rRNA and subsequent sequencing identified a 126 bp fragment of DNA that was 96% identical with *Tetratrichomonas gallinarum* partial 18S rRNA gene when compared to known sequences using the Basic Local Alignment Tool (BLAST).

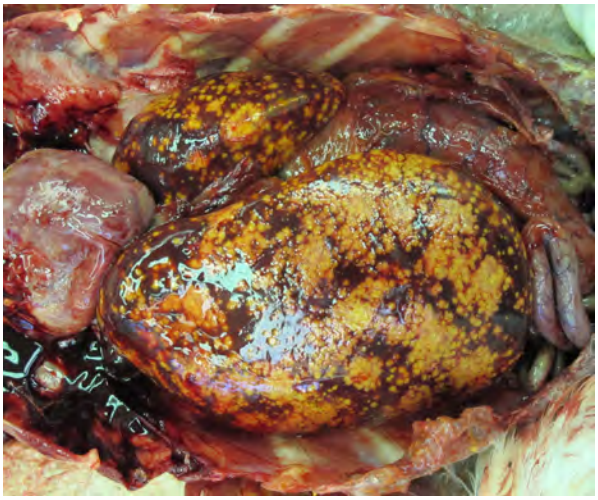

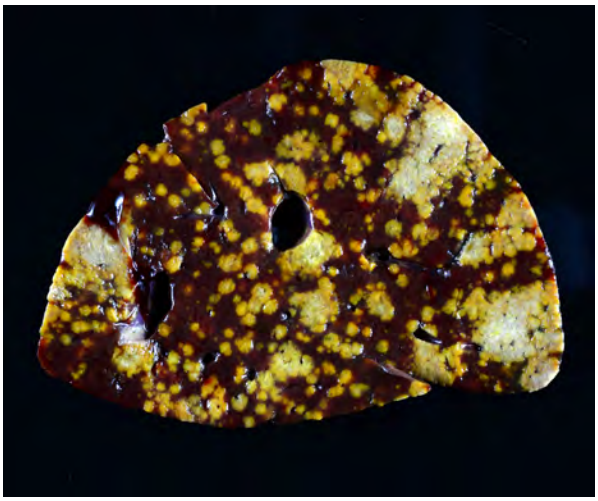

*1-1, 1-2. Liver, pelican: There are multifocal to coalescing well-delineated areas of coagulative necrosis throughout all lobes of the liver. (Photo courtesy of: Wildlife Disease Laboratories, San Diego Zoo Institute for Conservation Research, San Diego Zoo Global, PO Box 120551, San Diego, CA 92112-0551, http://www.sandiegozoo.org/conservation/)*

Electron microscopy (formalin-fixed liver): Flagellated protozoal organisms consistent with a trichomonad were seen. On transmission EM within areas of necrosis there were numerous 10.3 X 6.3 µm single-celled microorganisms with 4 anterior flagella, one recurrent flagellum, basal bodies, pelta, axostyle, costa, hydrogenosomes, and glycogen granules. With scanning EM, round to oval spherules were mixed with cell debris. Occasionally these organisms had four anterior flagella and a single recurrent flagellum, but most lacked flagella and an undulating membrane.

**Histopathologic Description:** Liver: The parenchyma is severely disrupted by multifocal to coalescing, areas of necrosis characterized by loss of cellular and architectural detail and accumulation of hypereosinophilic cellular debris and hyaline eosinophilic material (fibrin). Within these necrotic foci are myriad round to pleomorphic organisms that are amphophilic to basophilic, approximately 5-20 µm wide, and have one to multiple round nuclei. The adjacent hepatic parenchyma is multifocally infiltrated by variable numbers of lymphocytes and plasma cells, and diffusely there are perivascular infiltrates of hematopoietic cells (extramedullary hematopoiesis).

**Contributor's Morphologic Diagnosis:** 1. Liver: severe, acute to subacute, multifocal to coalescing, necrotizing hepatitis with intralesional protozoal trophozoites (*Tetratrichomonas gallinarum*).
2. Liver: moderate extramedullary hematopoiesis.

**Contributor's Comment:** The organisms in the hepatic lesions in this case were identified as trichomonad flagellates by electron microscopy and were a close match (96%) to *Tetratrichomonas gallinarum* by PCR of the 16s rRNA gene. This organism is most commonly isolated from the intestinal tract (cecum) of galliform and anseriform birds, where its role as a pathogen remains unclear. In turkeys and some species of ducks, it has been described as a cause of typhlohepatitis similar to histomoniasis.[9] However, other experimental infections in turkeys and have shown no clinical significance and only mild to absent changes in the cecum.[1,7] Disease in chickens infected with *T. gallinarum* also appears to be rare.[1,4,6] Recent comparison of *T. gallinarum* isolates from multiple species of galliform and anseriform birds by PCR detected differences in nucleotide sequences of up to 8.9%, which exceeded differences between some species of trichomonads.[3] This marked heterogeneity among *T. gallinarum* isolates could account for some of the differences in pathogenicity between studies.

The appearance of the hepatic lesions on gross and histopathologic examination was similar to those of histomoniasis caused by the trichomonad *Histomonas meleagridis*. The pleomorphic size and shape of the organisms was comparable to that of *H. meleagridis* in its amoeboid phase, the form that occurs in tissues.[6] Therefore, a similar change in morphology between organisms in the intestinal lumen or culture and those in tissue might occur with *T. gallinarum*. The presence of basal bodies and the variable presence of flagella of the organisms in the liver lesions were seen with electron microscopy and consistent with the PCR results. The presence of apparently multinucleated forms on routine histopathology in this case was unusual and was not appreciated on EM. Replication by binary fission and dense crowding of the organisms could possibly account for this appearance.

To our knowledge, there are no reports of *Tetratrichomonas* sp. infections in pelicans, and the reason for disease in this bird is unknown. The liver and spleen were most severely affected with necrotizing lesions effacing large areas of the parenchyma, but smaller foci of necrosis with intralesional organisms were also occasionally seen in the lung, heart, skeletal muscle, bone marrow, proventriculus and intestine, consistent with hematogenous dissemination of the infection. The likely origin of these trichomonads was the intestinal

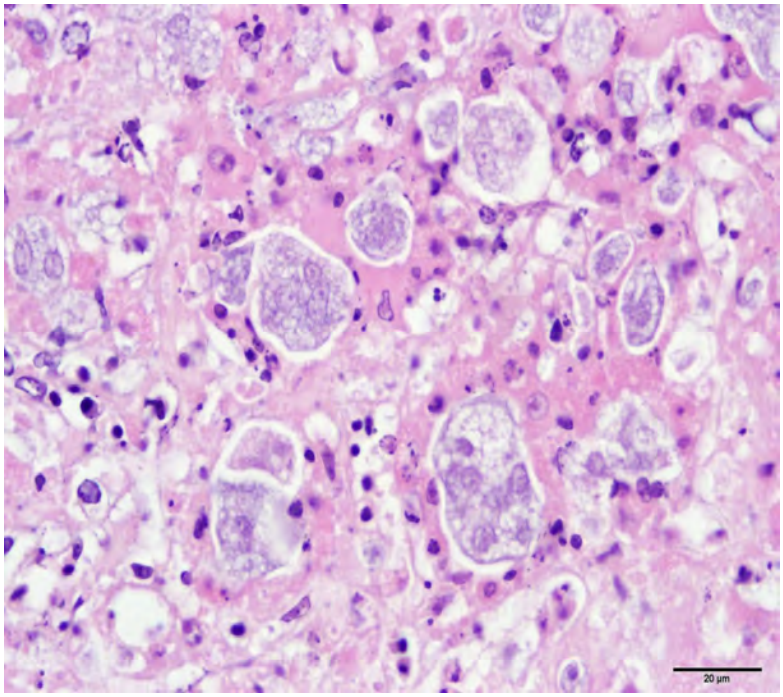


*1-3. Liver, pelican: Areas of coagulative necrosis contain numerous 25 µm amoebic trophozoites. (Photo courtesy of: Wildlife Disease Laboratories, San Diego Zoo Institute for Conservation Research, San Diego Zoo Global, PO Box 120551, San Diego, CA 92112-0551, http://www.sandiegozoo.org/conservation/)*

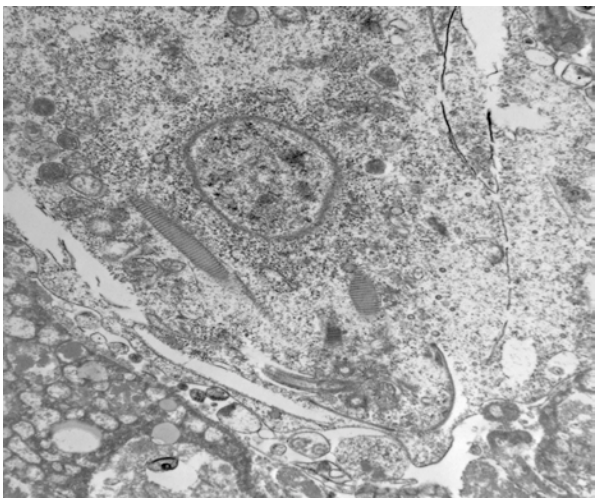

*1-4. Liver, pelican: Amoebic trophozoites have 4 anterior flagella, one flagellum, basal bodies, pelta, axostyle, costa, hydrogenosomes, and glycogen granules. (Photo courtesy of: Wildlife Disease Laboratories, San Diego Zoo Institute for Conservation Research, San Diego Zoo Global, PO Box 120551, San Diego, CA 92112-0551, http://www.sandiegozoo.org/conservation/)*

tract, although no areas of colonization of the lumen or crypts were seen. However, in addition to the variety of endoparasites noted grossly, myriad small trematodes invaded and multifocally disrupted the small intestinal, colonic and cecal mucosa. Secondary bacterial infections were also present in the ceca, and it is possible that this damage to the intestinal mucosa allowed invasion and dissemination of the flagellates. Poor immune function could also have been a contributing factor, as this pelican was young, heavily parasitized and in poor nutritional condition. In a previous report of this infection in ducks, all affected ducks were juveniles or subadults.[9]

Finally, as previously noted, isolates of *T. gallinarum* have a high degree of molecular polymorphism which could indicate the presence of multiple species or subspecies within this group, many of which could be host-adapted.[3] Infection of a non-galliform or anseriform bird (such as a pelican) or cross-infections between galliforms and anseriforms, might be more likely to result in disease. A previous report of encephalitis due to *T. gallinarum* was in a mockingbird, a passerine bird, and in the previous outbreak in ducks, a turkey was a possible source of the parasite.[8,9] The pelican in this report could have been exposed to a variety of native and exotic anseriform and possibly galliform birds at our zoological institution, none of which to date have been found to have a disseminated form of this infection.

**JPC Diagnosis**: Liver: Hepatitis, necrotizing, multifocal to coalescing, random, severe, with numerous trichomonads.

**Conference Comment**: See the contributor's comment ror an excellent review of infection by the trichomonad *Tetratrichomonas gallinarum*. Trichomonads are protozoa in the phylum *Parabasalia*; they are flagellated, pear-shaped organisms with a single nucleus and an axostyle that protrudes from the posterior end. Trichomonads include the pathogens *Tritrichomonas foetus, Trichomonas gallinae,* and *Histomonas meleagridis,* as well as several nonpathogenic (commensal) species.

As the contributor notes, the pathogenicity of *Tetratrichomonas gallinarum* is unclear, as it is often identified in the cecum and colon of domestic species without causing disease.[2] However, recently a case of fatal hepatic tetratrichomoniasis was reported in a captive-raised juvenile Waldrapp ibis (*Geronticus eremita).*[5] Similar to the pelican in this case, the Waldrapp ibis had necrotizing hepatitis associated with numerous protozoa. The protozoa showed positive immunoreactivity to antibodies against *Tritrichomonas foetus*. RNA sequence analysis (of the first ribosomal internal transcribed spacer region (ITS1), 5.8S ribosomal RNA, and ITS2 regions) revealed 96-97% genetic similarity to members of the *Tetratrichomonas gallinarum* complex. Cross-species transmission is suspected as the source of infection in this case as well. Further studies are needed to fully elucidate the pathogenicity of members of the *T. gallinarium* complex and their role in disease in wild and captive birds.

**Contributing Institution**: Wildlife Disease Laboratories
San Diego Zoo Institute for Conservation Research
San Diego Zoo Global, PO Box 120551
San Diego, CA 92112-0551
http://www.sandiegozoo.org/conservation/

**References:**

1. Amin A, Liebhart D, Weissenbock H, Hess M. Experimental infection of turkeys and chickens with a clonal strain of *Tetratrichomonas gallinarum* induces a latent infection in the absence of clinical signs and lesions. *J Comp Path*. 2011;144:55-62.
2. Bowman DD. Protozoans. In: *Georgis' Parasitology for Veterinarians.* 9th ed. St. Louis, MO: Saunders Elsevier; 2009:87-89.
3. Cepicka I, Kutisova K, Tachezy J, Kulda J, Flegr J. Cryptic species within the *Tetratrichomonas gallinarum* species complex revealed by molecular polymorphism. *Vet Parasitol*. 2005;128:11-21.
4. Friedhoff KT, Kuhnigk C, Muller I. Experimental infection in chickens with *Chilomastix gallinarum*, *Tetratrichomonas gallinarum*, and *Tritrichomonas eberthi*. *Parasitol Res*. 1991;77:329-334.
5. Laing ST, Weber ES 3rd, Yabsley MJ, Shock BC, Grosset C, Petritz OA, et al. Fatal hepatic tetratrichomoniasis in a juvenile Waldrapp ibis (Geronticus eremita) [abstract]. *J Vet Diagn Invest.;* 2013: Feb 12. [Epub ahead of print]. Accessed online at http://www.ncbi.nlm.nih.gov/pubmed/23404476 on 17 February 2013.

6. McDougald LR. Other protozoan diseases of the intestinal tract. In: Calnek BW, ed. *Diseases of Poultry*. 10th ed. Ames, IA: Iowa State University Press; 1997:890-899.
7. Norton RA. Pathogenicity of a strain of *Trichomonas gallinarum* in turkeys and its possible interaction with cecal coccidia. *Avian Dis*. 1997;41:670-675.
8. Patton CS, Patton S. *Tetratrichomonas gallinarum* encephalitis in a mockingbird (*Mimus polyglottos*). *J Vet Diagn Invest*. 1996;8:133-137.
9. Richter B, Schulze C, Kammerling J, Mostegl M, Weissenbock H. First report of typhlitis/typhlohepatitis caused by *Tetratrichomonas gallinarum* in three duck species. *Avian Pathol*. 2010;39(6):499-503.

**CASE II:** N2012-0372 (JPC 4017930).

**Signalment:** 5.5-year-old, male Muscovy duck (*Cairina moschata*).

**History:** This duck was found dead with no premonitory signs.

**Gross Pathology:** There was moderate, diffuse enlargement of the liver with multifocal to coalescing tan foci. These foci were not raised, extended into the parenchyma and bulged minimally on section. Red-tinged, dark brown fluid filled the duodenum, the distal small intestine, ceca and colon. There were multiple raised tan foci on the ileal and cecal mucosa. Pinpoint to 1.0 mm diameter red to dark brown foci were present on the esophageal mucosa. Red streaking and mottling was present on the epicardial surface and the endocardium of the left ventricle, and pinpoint red foci were identified in the pancreas and coelomic adipose tissue.

**Laboratory Results:** PCR was performed using primers targeting the herpesvirus DNA polymerase gene, and an appropriately-sized PCR product of 180 base pairs was amplified. The product was sequenced and found to be 100% identical to Anatid herpesvirus 1 (Genbank accession No. JQ647509).

A Gram stain performed on the liver identified intravascular and intrasinusoidal Gram negative bacilli.

**Histopathologic Description:** Liver: There is extensive disruption of hepatic architecture with moderate to large numbers of free erythrocytes (hemorrhage) interrupting hepatic cords. Individualized hepatocytes with eosinophilic and shrunken cytoplasm, and karyorrhectic or karyolytic nuclei are scattered throughout the section (individual cell necrosis). Additionally, there are multifocal, random areas of necrosis characterized by diffuse eosinophilia and variable retention of architecture. Hepatocytes in less affected portions of the liver frequently contain large, clear cytoplasmic vacuoles or have a lacy cytoplasmic appearance. Throughout the liver, in areas of necrosis, hemorrhage and architectural disruption, as well as in less affected areas, moderate numbers of hepatocytes contain eosinophilic intranuclear inclusion bodies. These are often centrally located with peripheral chromatin clearing. They occasionally fill the nucleus, leaving only a thin clear halo within the nuclear envelope. Similar intranuclear inclusion bodies are rarely found within biliary epithelial cells and affected cells are often sloughed into the ductular lumen. Necrotizing vasculitis, predominantly affecting central veins, is uncommon. There are multifocal, small, dense accumulations of bacteria (predominantly short bacilli) in sinusoidal and intravascular spaces and, occasionally, in foci of hepatocellular necrosis.

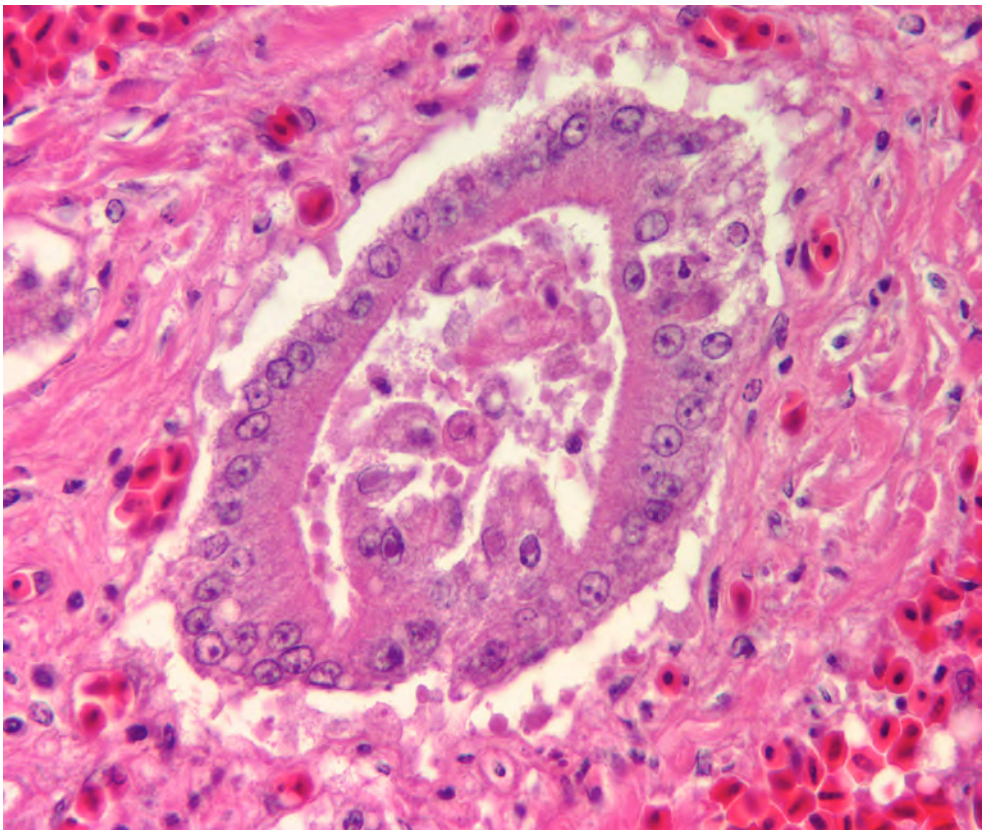

*2-1. Liver, Muscovy duck: Multiple biliary epithelial cells contain eosinophilic intranuclear viral inclusions consistent with herpesvirus infection. There is sloughing of most of these cells. (HE 600X) (Photo courtesy of: The Wildlife Conservation Society, Zoological Health, 2300 Southern Blvd., Bronx, NY 10460, http://www.wcs.org)*

Esophagus: The mucosal epithelium contains multifocal ulcers and erosions and exhibits scattered necrosis of epithelial cells. There is disruption of normal layering, accumulation of kary orrhectic debris, few transmigrating leukocytes and variable intracellular edema (ballooning degeneration) in affected areas. Epithelial cells in these areas also occasionally contain intranuclear inclusion bodies similar to those described in the liver. Rare, variably sized, eosinophilic

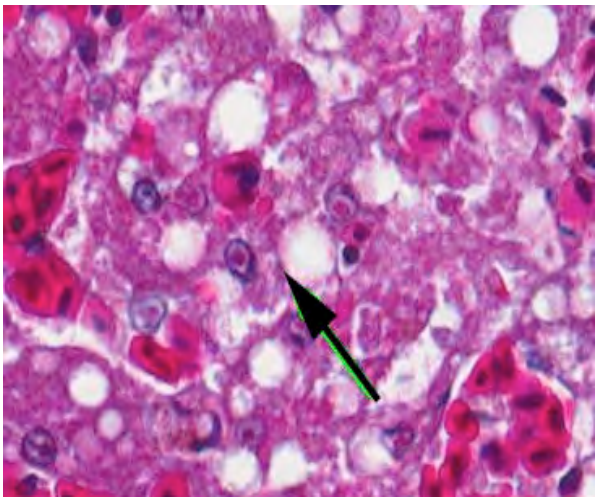

*2-2. Liver, Muscovy duck: Intranuclear inclusions are also seen in hepatocytes. (HE 400X)*

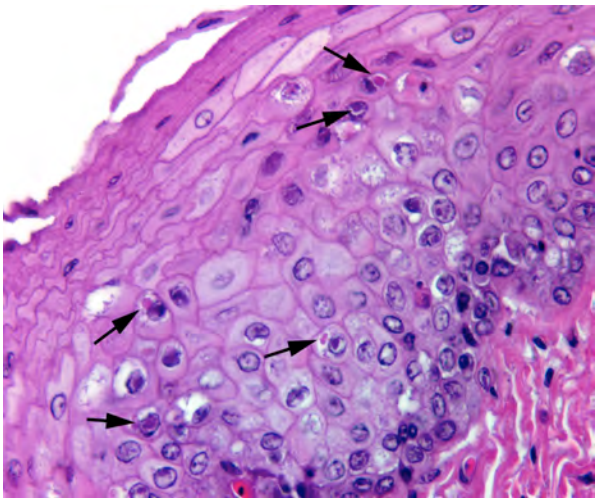

*2-3. Esophagus, Muscovy duck: Scattered squamous epithelial cells contain variably sized, eosinophilic, intracytoplasmic inclusion bodies. Intranuclear inclusion bodies are also present, and some cells contain both intracytoplasmic and intranuclear inclusions. (HE 600X) (Photo courtesy of: The Wildlife Conservation Society, Zoological Health, 2300 Southern Blvd., Bronx, NY 10460, http://www.wcs.org)*

intracytoplasmic inclusion bodies are also present. Rafts of sloughed epithelial cells (with occasional intranuclear inclusion bodies) admixed with keratin, necrotic cell debris and mixed bacteria often cover the affected mucosa. Underlying some epithelial lesions is accumulation of karyorrhectic debris in the submucosa, accompanied by mild basophilia and disruption of the fibrillar collagen architecture. Submucosal glands are frequently obliterated; these glands contain intraluminal sloughed epithelia (with occasional intranuclear inclusion bodies), necrotic cellular debris and mucinous material. Intranuclear inclusion bodies are also present in remaining, viable glandular epithelium. Scant mononuclear infiltrates are scattered throughout the submucosa and are predominantly perivascular.

**Contributor's Morphologic Diagnosis:** 1. Liver: Necrosis, acute, random, multifocal and individual cell, marked, with intranuclear inclusion bodies, necrotizing vasculitis, hemorrhage and hepatocellular vacuolar change.
2. Liver: Bacteremia, acute, moderate.
3. Esophagus: Necrosis, acute, multifocal, moderate, with intranuclear and intracytoplasmic inclusion bodies, multifocal erosions and ulcers, and submucosal gland necrosis.

**Contributor's Comment:** The submitted liver and esophagus exhibited necrosis with intranuclear inclusion bodies, lesions typical of herpesvirus infections across species. In addition to the tissues examined here, there was severe fibrinonecrotic ileitis and segmental necrosis in the remainder of the small intestines. These sites were heavily infiltrated by bacteria and loss of mucosal epithelium precluded identification of discrete inclusion bodies (sloughed epithelial cells occasionally harbored presumptive intranuclear inclusions). Intestinal lesions were potentially secondarily invaded by opportunistic bacteria following initial damage incurred from viral infection. As noted in the submitted tissue, bacteremia and septicemia followed.

Based on the presence of intranuclear inclusion bodies, tissue necrosis and the species affected, anatid herpesvirus 1 (AnHV-1) was suspected and molecular diagnostics were pursued. PCR performed on a sample of frozen liver amplified an appropriately sized PCR product which was sequenced and found to be identical to AnHV-1 (DNA polymerase gene).

Anatid herpesvirus 1 causes predominantly a gastrointestinal disease in waterfowl which is referred to as "duck plague" or "duck virus/viral enteritis" (DVE).[1,3,4] Disease severity depends on the strain of the virus and species infected.[2] Muscovy ducks, like the one in this case, are considered to be one of the more sensitive species, while mallard ducks (*Anas platyrhynchos*) are more resistant.[3] Many anseriform species, including geese and swan, are susceptible, and recently a crested and a common coot (*Fulica cristata* and *F. atria*, respectively) reportedly died as a result of DVE.[4] As with other herpes viruses, ducks surviving initial infection become latently infected and can intermittently shed the virus.[3,4]

Typical presenting signs for DVE include lethargy, polydipsia, emesis, bloody or watery diarrhea and prolapse of the phallus.[3,4] In many cases, especially in the more sensitive species, there may be no clinical signs prior to the animal being found dead.[3,4] Infection typically occurs via oral ingestion of the virus, which is shed in the feces and orally from infected ducks; ingestion of contaminated water is thought to be the major route of transmission.[3,4] Typical gross lesions include petechiae in

multiple organs, annular band necrosis and hemorrhage in the intestinal tract, ulcers and erosions in the esophagus (especially at the esophageal/proventriculus junction) and on the ventral surface of the tongue, and multifocal necrosis in the liver.[3,4] In addition to these findings, necrosis of lymphoid tissue and necrotizing vasculitis can be identified histologically.[1,3,4] Intranuclear inclusion bodies would be expected in areas of necrosis, including lymphocytes. Barr, et al[1] reported the presence of intracytoplasmic inclusion bodies in the esophagus and cloacal epithelium of DVE-affected Muscovy ducks.[1] Ultrastructurally, these inclusions were membrane-bound and contained enveloped virions.[1] Rare (and not present in all slides), variably sized eosinophilic intracytoplasmic inclusion bodies similar to those described in the above report were identified in the esophagus of this patient. Although other causes of intracytoplasmic inclusion bodies were not completely ruled out, they were considered less likely given the nature of the lesions, the findings in other organs and PCR identification of AnHV-1.

Approximately one week following the death of this duck, another Muscovy duck at the same facility was acutely lethargic one evening and found dead the following morning. Gross and histopathological lesions were similar to those reported here. This was the second DVE-related mortality event affecting ducks at our institutions in the past decade. The first was responsible for the death of four Muscovy ducks and at least two wild mallards. It is presumed that wild, latently infected ducks sharing waterways and housing with the Muscovies were responsible for the infection, but the possibility of latently infected permanent residents intermittently shedding the virus has not been fully investigated.

**JPC Diagnosis**: 1. Liver: Hepatitis, necrotizing, multifocal, moderate, with intranuclear viral inclusion bodies and necrotizing vasculitis.
2. Esophagus: Esophagitis, necrotizing, multifocal, moderate, with intranuclear and intracytoplasmic viral inclusion bodies and submucosal gland necrosis.

**Conference Comment**: The contributor provides a thorough summary of anatid herpesvirus 1 infection in anseriforms. Conference participants were intrigued by the presence of both intranuclear and intracytoplasmic viral inclusions in esophageal epithelium, a phenomenon more commonly associated with paramyxoviruses. Herpesviruses, which are DNA viruses that replicate in the host cell nucleus, generally produce intranuclear inclusions.[2] However, intracytoplasmic viral inclusions are observed with certain herpesvirus infections, as illustrated by this case. In addition to Anatid herpesvirus-1, cytomegaloviruses (in the subfamily *Betaherpesvirinae*) and Gallid herpesvirus-2 (Marek's Disease virus) can also be associated with intracytoplasmic viral inclusions in addition to the classic intranuclear inclusions.[1] Awareness of the possibility of observing intracytoplasmic inclusions in these herpesviral infections can help avoid misdiagnoses.[1]

**Contributing Institution**: Wildlife Conservation Society
Zoological Health
2300 Southern Blvd.
Bronx, NY 10460
www.wcs.org

**References:**

1. Barr BC, Jessup DA, Docherty DE, Lowenstine LJ. Epithelial intracytoplasmic Herpes viral inclusions associated with an outbreak of duck virus enteritis. *Avian Dis*. 1992;36:164-168.
2. MacLachlan NJ, Dubovi EJ. Herpesvirales. In: *Fenner's Veterinary Virology. 4th ed.* London, UK: Acadmic Press Elsevier; 2011:179-201.
3. Ritchie BW, Carter K. Avian Viruses Function and Control. Lake Worth, FL: Wingers Publishing, Inc; 1995:207-214.
4. Salguero FJ, Sanchez-Cordon PJ, Nunez A, Gomez-Villamandos JC. Histopathological and ultrastructural changes associated with herpesvirus infection in waterfowl. *Avian Pathol*. 2002;31:133-140.

**CASE III:** 11-1482 (JPC 4003259).

**Signalment:** Yearling, male, Harbor seal (*Phoca vitulina*).

**History:** This animal was found dead on a beach in the Pacific Northwest.

**Gross Pathology:** The animal was emaciated and featured corneal abrasions and numerous nasal mites.

**Laboratory Results:** PCR of pooled tissues proved negative for canine distemper virus and influenza virus and positive for *Apicomplexa*. No bacteria were recovered from the lung, lymph node, brain or spleen and there was heavy growth of *Escherichia coli* from the small intestine. Trace mineral and vitamin A analysis results of the liver proved within in house reference limits.

**Histopathologic Description:** Throughout the cerebellum, expanding the meninges, extending focally to segmentally throughout the molecular layer and expanding and disrupting the molecular and granular layers of numerous folia, there is multifocal to coalescing accumulations of lymphocytes and histiocytes with fewer plasma cells. In more severely affected areas, there is multifocal edema fluid with neovascularization, reactive endothelia, lymphoplasmacytic perivascular cuffing and edema. Randomly interspersed within the inflammatory infiltrate are numerous protozoa with multifocal karyorrhectic and pyknotic debris.

**Contributor's Morphologic Diagnosis:** Brain: Meningoencephalitis, severe, multifocally extensive, necrotizing, lymphohistiocytic, with numerous intralesional protozoa.

**Contributor's Comment:** Since 2000, increasing numbers of marine mammals have stranded within the Pacific Northwest with protozoal encephalitis. In the initial stages of this phenomenon, *Toxoplasma gondii* was the primary pathogen, however, more recently, *Sarcocystis neurona* has emerged as the dominant etiologic agent. Based on review of brain pathology, dual infections appear to have potentiated the pathogenicity of both parasites. Malnutrition, contaminant loads and other environmental stressors may have also potentiated the pathology of infections. The increase in *S. neurona* infections is attributed to the extension of opossums north, into Washington State and British Columbia.

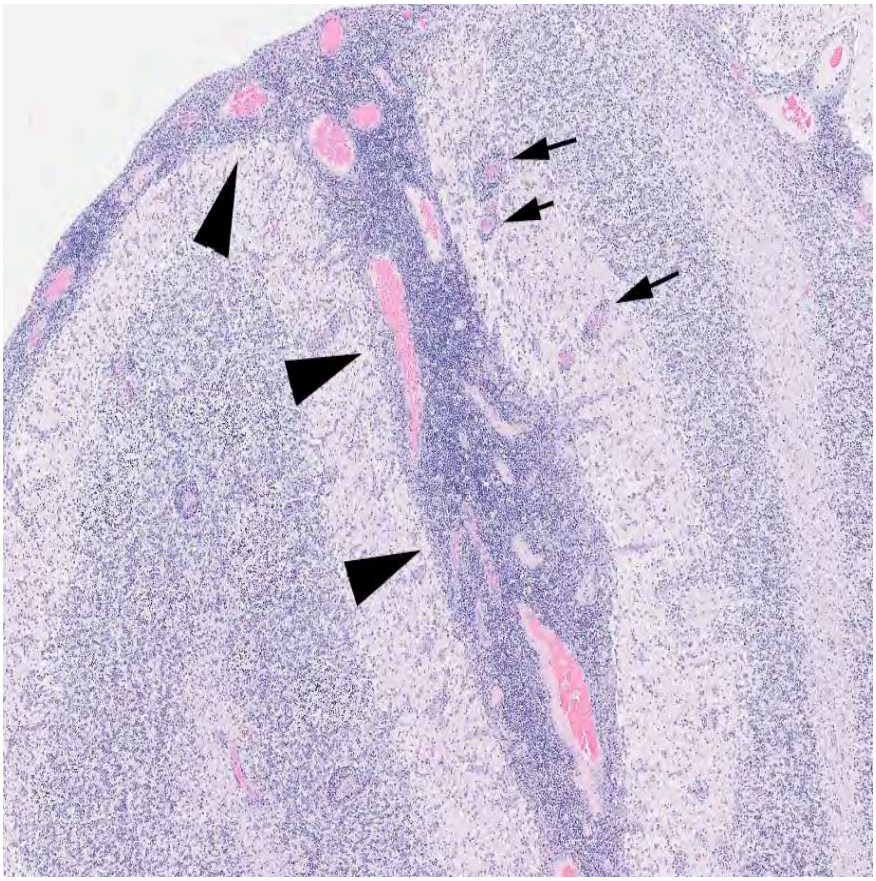

*3-1. Cerebellum, harbor seal: The meninges (arrowheads) and Virchow-Robins spaces (arrows) are expanded by a profound inflammatory infiltrate. (HE 40X)*

**JPC Diagnosis:** Cerebellum and brain stem: Encephalitis, necrotizing, multifocal to coalescing, severe, with diffuse lymphohistiocytic and neutrophilic meningitis, choroid plexitis, and numerous intracellular schizonts.

**Conference Comment:** Conference participants discussed the differential diagnosis for this case, and favored *Sarcocystis neurona;* however, since mature schizonts and merozoites of *Sarcocystis* are difficult to distinguish from *Toxoplasma*, we consulted with Dr. J.P. Dubey. Immunohistochemical staining with antibodies against *Sarcocystis neurona* performed by Dr. Dubey resulted in strong positive immunoreactivity in numerous schizonts. Furthermore, the diagnosis was confirmed by Dr. Dubey based on the morphology of the immature schizonts, as *S. neurona* immature schizonts are morphologically unique in that their nucleus becomes multilobed, eventually giving rise

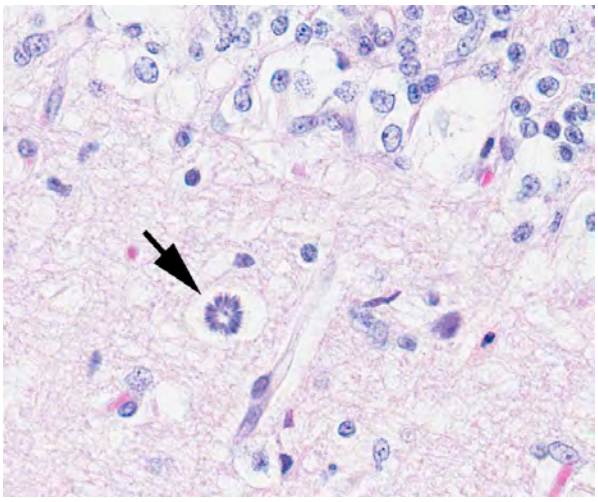

*3-2. Cerebellum, harbor seal: Areas of inflammation contain numerous 20 µm apicomplexan schizonts in which zoites reproduce by endopolygeny (arrow). (HE 400X)*

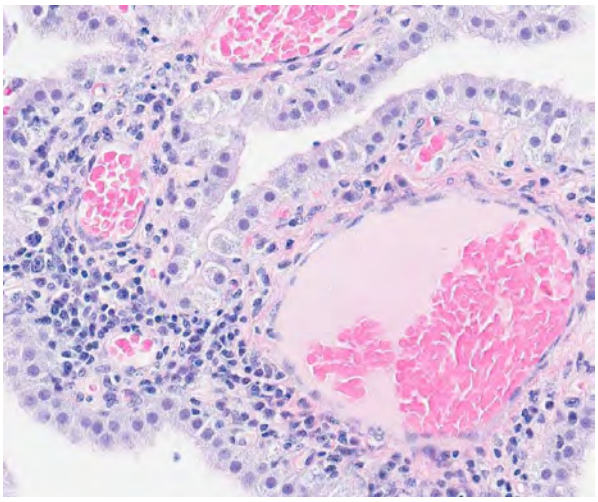

*3-3. Choroid plexus, harbor seal: There is a moderate lymphoplasmacytic choroid plexitis (a common finding in animals with inflammatory encephalitis). (HE 360X)*

to many merozoites, and often leaving a residual body. (J.P. Dubey, personal communication).

*S. neurona* is an apicomplexan, best known for causing equine protozoal myeloencephalitis (EPM), a severe neurologic disease in horses.[1] Opossums spread the disease by shedding sporocysts into the environment.[1] In addition to horses and sea mammals (sea otters, Pacific harbor seals), other animals including cats, striped skunks, and nine-banded armadillos can be infected with *S. neurona*; however, in these species, the sarcocysts tend to develop in muscle rather than the central nervous system.[1,2] Raccoons have also been reported to have myocarditis and encephalitis due to infection with *S. neurona*.[1]

**Contributing Institution**: Animal Health Center
1767 Angus Campbell Road
Abbotsford, BC, Canada, V3G 2M3

**References:**

1. Bowman DD. Protozoans. In: *Georgis' Parasitology for Veterinarians*. 9th ed. St. Louis, MO: Saunders Elsevier; 2009:104-105.
2. Dubey JP, et al. Toxoplasma gondii, Neospora caninum, Sarcocystis neurona, and Sarcocystis canis-like infections in marine mammals. *Vet Parasitol*. 2003;116 (4):275-96.

**CASE IV:** HN2633 (JPC 4003689).

**Signalment:** Juvenile, Whooper swan (*Cygnus cygnus*).

**History:** This wild swan was found weak at the northern lake of Japan in Jan, 2011. A local veterinarian euthanized the bird and detected influenza virus using rapid test kit. The carcass was transported to our university and dissected within the biosafety level 3 facility.

**Gross Pathology:** The bird was in relatively good nutritional condition. In pancreas, multiple hemorrhagic foci up to 8 mm were scattered.

**Laboratory Results:** Highly pathogenic avian influenza virus of H5N1 subtype was isolated from the brain, trachea, lungs and colon.

**Histopathologic Description:** Heart: Multifocal to coalescing myocardial necrosis and infiltration of inflammatory cells were scattered throughout the heart. The lesions consisted of coagulative necrosis of myocardial fibers admixed with lymphocytes, macrophages and mild hemorrhage. By immunohistochemistry, strong positive signals of influenza virus antigens were confirmed in myocardiocytes around the inflammatory lesions. A few organisms enclosed in cuticula in the heart were consistent with parasitic nematodes. The nematodes contained microfilaria-like structures in the viscera. Inflammatory reaction to the parasites was indiscernible.

**Contributor's Morphologic Diagnosis:** Heart: Myocarditis, necrotic and nonsuppurative, multifocal to coalescing, severe, influenza virus infection and parasitic nematode infection.

**Contributor's Comment:** The threat of highly pathogenic avian influenza virus (HPAI) of H5N1 subtype to humans as well as domestic and wild birds is of great concern to human public health and fowl industry. The first reported serious case of H5N1 influenza virus in Asia was in Hong Kong in 1997, and emerged in east and southeast Asian countries in 2003.[5] Since then, Japan has also suffered small outbreaks of H5N1 infection in domestic fowls. HPAI surveillance activity in poultry farm and wild migrating birds is important to control and predict the epidemics of HPAI. The present case was one of the birds likely on migration from southern Asian countries to Siberia.

Histopathological examination of the systemic organs from this bird revealed necrotic changes and nonsuppurative inflammation in the heart, pancreas and brain that were consistent with HPAI infection lesion.[6] Immunohistochemical analysis using anti-H5 subtype influenza virus polyclonal antibody also revealed the distribution of viral antigens in myocardium, necrotic foci

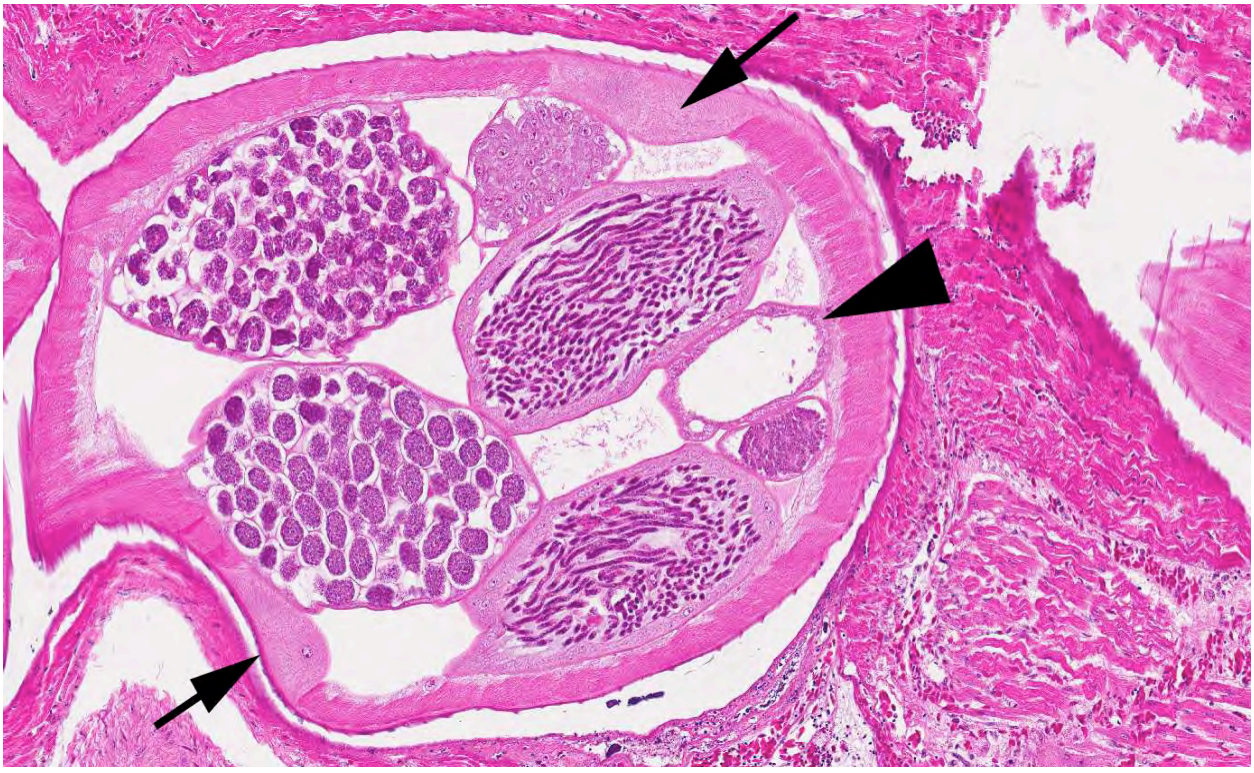

*4-1. Heart, swan: The myocardium contains numerous cross sections of an adult nematode measuring up to 100u in diameter, with a ridged cuticle, large lateral cords, a digestive tract with few multinucleated cells (arrowhead), ovaries with morulated eggs and a uterus with microfilariae (arrows). (HE 4X)*

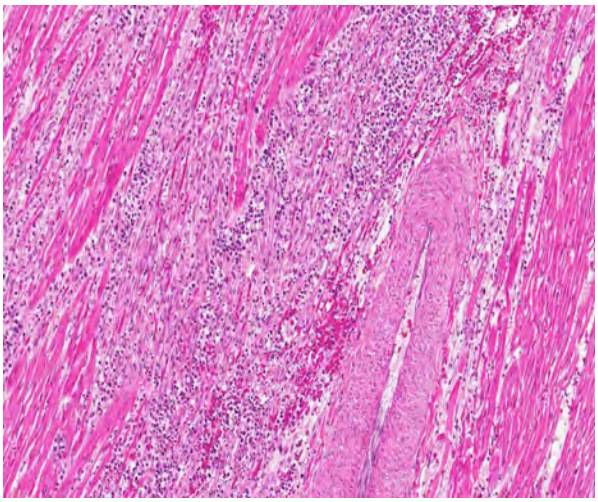

*4-2. Heart, swan: There are multifocal to coalescing areas of myofiber necrosis and loss with infiltration by large numbers of histiocytes, lymphocytes, and plasma cells, as well as scattered hemorrhage. In this particular case, necrosis may have resulted from either migration of parasites within the myocardium, or the concurrent infection with highly pathogenic avian influenza (or both, concurrently). (HE 160X)*

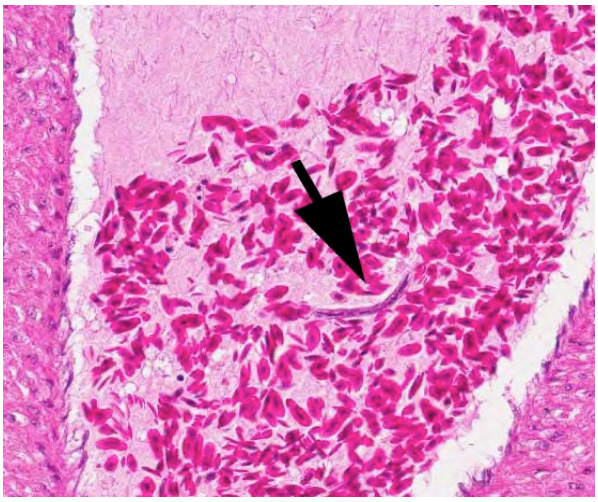

*4-3. Heart, swan: Coronary arterioles rarely contain microfilariae. (HE r00X)*

in pancreas and in astrocytes and neurons in the brain, suggesting systemic infection of influenza virus.

In domestic fowls, an experimental study found HPAI infection causes rapid viremia and produces vascular endothelial cell injury.[2,4] Necrotic and apoptotic changes of parenchymal cells of organs follow the endothelial damages. The most severely affected tissues are brain, heart, lungs and pancreas as well as primary and secondary lymphoid organs.[2,6] But the lesions vary from mild to severe, although the affected birds usually die shortly after systemic infection. The histopathological lesions in the present case were relatively severe.

Adult heartworms containing microfilariae in their uterus were found in the heart of the present case. The morphology of the parasites presumably identified as *Sarconema eurycerca*, a filarial nematode of the superfamily *Filariodea*. Several studies of *S. eurycerca* infection in wild swans and geese were reported.[1,7] Although mortality cases in wild birds are reported, the pathological significance of this worm is still not well understood. Grossly, an enlargement of the heart with dark red and white streaks due to the migration of adult worms in myocardium is described in previous reports. The heart failure is induced by myocardial necrosis when numbers of parasites infected. Hemorrhage, lymphocytic and histiocytic inflammation was multifocally observed. Migration of microfilaria into myocardium, which is accompanied with inflammation, is sometimes observed, but was not observed in the present case. The infection of heartworms may partly contribute to develop severe myocardial lesions, but the cause of death in this swan might be concluded as systemic influenza virus infection.

**JPC Diagnosis:** 1. Heart: Myocarditis, heterophilic and granulomatous, chronic, multifocal, moderate, with myofiber necrosis, atrophy and loss, with adult filarid nematodes and microfilaria.
2. Heart: Vasculitis, heterophilic and necrotizing, multifocal, with thrombosis and myofiber degeneration and necrosis.

**Conference Comment:** The contributor provides an informative summary of both HPAI and *Sarconema eurycerca* infection in this very interesting case. Conference participants discussed the two disease processes occurring simultaneously and speculated on the two distinct patterns of necrosis in the heart: The chronic lesions are attributed to adult filarid migration tracts while the granulomatous inflammation observed in some sections is associated with microfilaria. Although the relationship between the chronic myocardial lesions and the more acute vasculitis, thrombosis and coagulative necrosis are unclear, participants attributed the latter to infection with HPAI.

HPAI is in the family *Orthomyxoviridae*, genus *Influenzavirus A*. Influenza A viruses commonly infect horses, swine, and domestic poultry, as well as humans.[3] Wild birds, particularly ducks, shorebirds and gulls, are reservoir hosts for low-pathogenicity influenza A viruses; however, mink, seals, whales and dogs can also become infected. Influenza A viruses are currently classified into 16 hemagglutinin (H) and 9 neuraminidase (N) types. Gene reassortment results in numerous combinations of H and N subtypes; however, only a few combinations are important in naturally occurring infections in animals. Enzootic H7N7 and H3N8 viruses (previously called equine influenza viruses 1 and 2) cause respiratory disease in horses. Enzootic H1N1, H2N2, and H3N2

viruses affect swine. H3N8 and H3N2 viruses cause respiratory disease in dogs. Sporadic H10N4 viruses cause respiratory disease in mink. Sporadic H7N7 and H4N5 viruses cause disease in seals. In humans, H1N1, H2N2, H3N2, H5N1, H7N3, H7N7 and H9N2 viruses can all cause respiratory disease and virtually all of these types can be found in wild aquatic birds and domestic poultry. Of these, the H5 and H7 viruses can be associated with the high-pathogenicity phenotype. High pathogenicity is associated with changes in an amino acid sequence at the cleavage site of the hemagglutinin protein. These changes, which result in altered virulence, include the elimination of the glycosylation site, pH changes, and insertions or deletions in the amino acid sequence. While low pathogenicity subtypes are restricted to the intestinal and respiratory system in birds, highly pathogenic strains cause systemic disease characterized by viremia, endothelial injury and subsequent necrosis in multiple organs, as described by the contributor.[3]

Conference participants also discussed differential etiologic diagnoses for mononuclear myocarditis in birds including West Nile Virus, Newcastle Disease Virus, and protozoal myocarditis. As pointed out by the conference moderator, the presence of myocardial, pancreatic and/or hepatic necrosis in waterfowl should immediately raise the suspicion of HPAI infection.

**Contributing Institution**: Laboratory of Comparative Pathology
Department of Veterinary Clinical Sciences
Graduate School of Veterinary Medicine
Hokkaido University
Sapporo 060-0818, Japan
http://www.vetmed.hokudai.ac.jp/

**References:**

1. Irwin JC. Mortality factors in whistling swans at Lake St. Clair, Ontario. *J Wildl Dis*. 1975;11:8-12.
2. Kobayashi Y, Horimoto T, Kawaoka Y et al. Pathological studies of chickens experimentally infected with two highly pathogenic avian influenza viruses. *Avian Pathol.* 1996;25:285-304.
3. MacLachlan NJ, Dubovi EJ. Orthomyxoviridae. In: *Fenner's Veterianry Virology.* 4th ed. New York, NY: Elsevier; 2011:353-370.
4. Park CH, Ozaki H, Takada A et al. Primary target cells of virulent strains of type A influenza virus in chicken embryos. *Avian Pathol.* 2001;30:269-272.
5. Sims LD, Domenech J, Benigno C, et al. Origin and evolution of highly pathogenic H5N1 avian influenza in Asia. *Vet Rec.* 2005;157:159-164.
6. Swayne DE, Halvorson DA. Influenza. In: Saif YM, Barnes HJ, Fadly AM, Glison JR, McDougald LR, Swayne DE, eds. *Diseases of Poultry*. 11th ed. Ames, IA: Iowa State University Press; 2003:147-149.
7. Woo GH, Jean YH, Bak EJ, Kang S, Roh IS, Lee KH, et al. Myocarditis by nematodes infection, presumably Sarconema eurycerca, in a wild whooper swan (Cygnus Cygnus) in Korea. *J Vet Med Sci.* 2010;72:1233-1235.

**Joint Pathology Center**
**Veterinary Pathology Services**

## WEDNESDAY SLIDE CONFERENCE 2012-2013

# Conference 15

**20 February 2013**

**CASE I:** UFSM1 (JPC 4021297).

**Signalment:** 18-month-old, female, mixed breed, bovine (*Bos taurus*).

**History:** In a farm in southern Brazil there were 200 yearling calves (approximately 18-month-olds) of both sexes. During winter (July-August) 16 of those yearlings died within a one-month period (morbidity rate of 0.8%, lethality rate of 100%). Affected cattle had weakness, muscular tremors, apathy and death within 1-5 days of the onset of clinical signs. Some animals became very agitated and aggressive and those surviving for longer periods had icterus and occasionally photodermatitis. Very large numbers of 2-2.5 cm in length, black insect larvae were found at the pasture. The larvae formed closely packed masses on the ground and were observed crawling over the grass forming an orderly column of

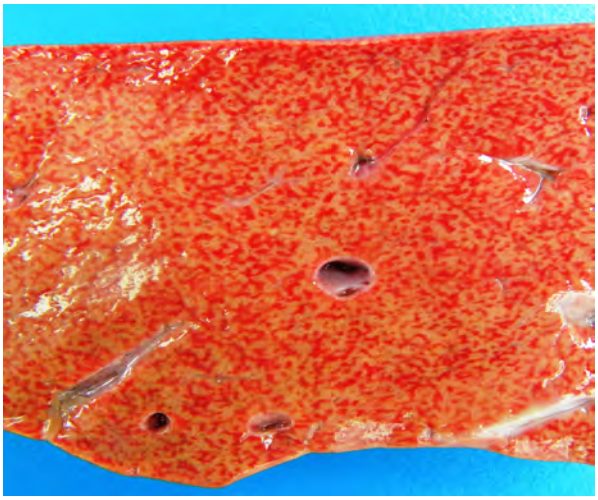

*1-1. Liver, ox: The liver was enlarged with rounded edges. The cut surface showed an accentuated lobular patter with -2 mm in diameter bright red depressed irregular areas surrounded by lighter (beige or tan) areas. Photo courtesy of: Departamento de Patologia, Universidade Federal de Santa Maria, 97105-900 Santa Maria, RS, Brazil. http://www.ufsm.br/lpv)*

*1-2. Very large numbers of 2-2.5 cm in length, black insect larvae were found at the pasture. The larvae formed closely packed masses on the ground and were observed crawling over the grass forming an orderly column of 10-15 cm long. (Photo courtesy of: Departamento de Patologia, Universidade Federal de Santa Maria, 97105-900 Santa Maria, RS, Brazil. http://www.ufsm.br/lpv)*

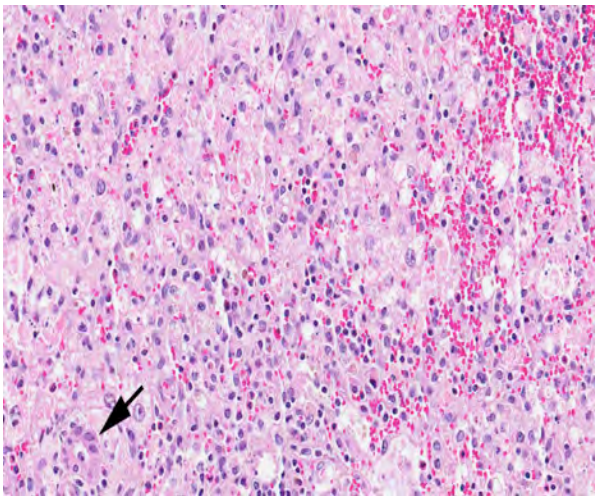

*1-3. Liver, ox: Classic massive necrosis, with necrosis of hepatocytes in all regions of the lobule. (HE 360X)*

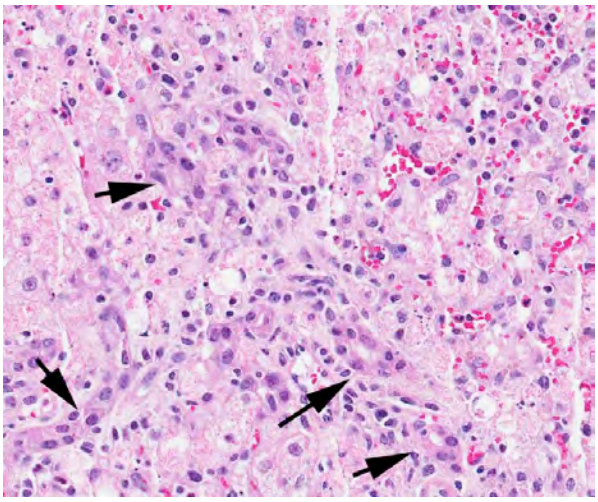

*1-4. Liver, ox: The few surviving hepatocytes are adjacent to portal triads, in which there is moderate ductular reaction (biliary hyperplasia). (HE 400X)*

10-15 cm long. Large numbers of these larvae were collected from this farm and subsequently identified as *Perreyia flavipes* Konow, 1899 (Hymenoptera: Pergidae).

**Gross Pathology:** One out of the 16 dead calves was necropsied. This calf died within 24 hours after the onset of clinical signs. Gross findings were consistent with an outbreak cause by an hepatotoxin and included ascites, petechiae and suffusion over the serosal surfaces of thoracic and abdominal cavities; the liver was somewhat enlarged (round edges) and mottled with an accentuation of the lobular pattern; this was best seen at cut surface as 1-2 mm in diameter bright red depressed irregular areas surrounded by lighter (beige or tan) areas. (The red areas would later be identified on histological examination as being centrilobular [periacinar]). There was edema of the gall bladder wall. Subendocardial and supepicardial petechiae and ecchymosis were also observed. Sawfly (*P. flavipes*) larval body fragments and heads were found in the rumen.

**Note**: The larvae collected from the pasture where deaths occurred were ground and orally fed to an unrelated calf of the same age (18-month-old) in one single dose of 20 g/kg/body weight. The calf developed clinical signs similar to the ones described above within 3 days after the administration of the larvae and died after a short period (approximately 24 hours) of the onset of clinical disease. The serum activity of liver enzymes was increased as measured before administration of the larvae and just prior the death of the experimental calf. Results of the two evaluated samples are within parenthesis (first value is from the pre-experimental sample and the second value is from the blood sampled just prior the death of the calf). Aspartate aminotransferase (73-804 U/L); gamma-glutamyl transferase (10-89 U/L); and alkaline phosphatase (54-404 U/L). The levels of total bilirubin were also elevated (3.46 mg/dL) and direct bilirubin elevation (2.98 mg/dL) accounted for this increase. Necropsy and histopathological findings on this experimental calf were similar to the ones observed in the spontaneous outbreak but were included in this submission.

**Histopathologic Description:** The main microscopic lesion was restricted to the liver and consisted of centrilobular (periacinar) to massive hepatocellular necrosis. In most lobules necrotic areas extended up to the portal triads where only a few viable hepatocytes remained. The lesion appeared diffusely and no preference for any hepatic lobe could be noticed. Hemorrhage occurred in centrilobular areas. Mild to moderate lymphocyte necrosis was seen in the splenic white pulp.

**Contributor's Morphologic Diagnosis:** Liver, centrilobular to massive hepatocellular necrosis, diffuse, acute, and severe.
Etiologic diagnosis: Toxic hepatopathy.
Etiology: ingestion of sawfly (*Perreyia flavipes*).

**Contributor's Comment:** Sawfly larval poisoning (SLP) is an acute hepatotoxicity of cattle caused by the ingestion of larval stage of insects of the suborder *Symphyta*, order *Hymenoptera*, commonly known as "sawfly." SLP has been described in cattle,[2,5,8,10,15,17,19,22] sheep,[5,14,21] and pigs[6;] there is one isolated report of SLP in a dog.[1] It is a remarkable disease since the toxin is present in the larvae of the insects.

In Australia, SLP is caused by the ingestion of the larvae of the sawfly *Lophyrotoma interrupta* (*Pergidae*, *Hymenoptera*), formerly referred also as *Pterigophorus analis*, *interrupts interrupta* and *Platysectra interrupta*.[8,17] The poisoning of cattle by eating *L. interrupta* (commonly referred to as Australian sawfly larva) has

been studied for over 70 years, since it was first described in the Maranoa district of southern Queensland in 1911[2,8,17,22] where it reportedly is responsible for an annual loss of 1 million Australian dollars (1981 values).[8] During 1972-1981 in Australia, 37 farms experienced 5,254 deaths during July to September and 1,800 deaths in cattle occurring in just one year were attributed to the intoxication.[4] Cattle were introduced in this area between 1862 and 1866 and the first suspected cases occurred in 1887 but the definite occurrence was only established in 1911.[22] Outbreaks in Australia are confined to districts where there are large forests of the silver leaf ironbark tree (*Eucalyptus melanoplhoia*), the main host for *L. interrupta*[2,8,11,12] and most deaths occurred between July and October and some deaths may occur after the dried-out remains of dead larvae are moistened by rain during summer.[4]

In Denmark, SLP was reported in sheep caused by the ingestion of the larvae of sawfly *Arge pullata* (Argidae), commonly referred as Danish sawfly larva which feed on birch trees (*Betula pendula*). This outbreak of SLP have been reported from the Danish Island of Sjelland where 50 sheep from a flock of 250 died 3 days after they were moved to the area infested by *A. pullata* larvae.[21] At this occasion, the disease was reproduced experimentally in goats that were fed larvae from this outbreak.[21]

The sawfly *Perreyia flavipes* Konow, 1899 (*Pergidae*: *Perreyiinae*) also referred as *Lophyroides flavipes* and *Brachytoma flavipes* have been reported from Argentina, Uruguay and Brazil in cattle,[5,15,19] sheep[5,14] and pigs[6] and the disease was reproduced in cattle, sheep[5] and pigs.[18] *P. flavipes* is commonly referred to as South American sawfly larva.

The economical importance of sawfly (*P. flavipes*) larval poisoning in South America can be evaluated if one considers that within a three-year period (1993-1995) at least 40 outbreaks of this intoxication occurred in Uruguay and that during just one year (1995) cattle losses exceeded 1,000 heads.[5] Mortality rates vary and are reported as 1.6%, 7.0% and 1.38% from one study[5] and 0.8%, 6.2% and 33% from another.[19]

D-amino acid-containing peptides have been found to the toxic principle in each sawfly involved in farm animal poisonings.[7,9,10] The octapeptide lophyrotomin is the major toxin in the larvae of Australian and Danish sawflies and is present in small amounts in the larvae of South American sawfly. The heptadecapeptide pergidin is the main toxin in the South American sawfly while small amounts of pergidin have been found in the other two species of toxic sawfly.[9]

One interesting environmental phenomenon related to sawfly occurred in Florida. The broad-leaf paper bark tree *Melaneuca quinquenervia* was introduced from Australia into Florida, USA, early in the 1900's, and has since then proliferated to such an extent as to be found in all 10 counties of Southern Florida in an area over 200,000 hectares where it causes considerable environmental and economic damage. Therefore the sawfly *Lophyrotoma zonalis* was introduced, again from Australia, as a possible biological control agent for this tree due to its ability to defoliate *M. quinquenervia*. However, this may turn out to be a dangerous practice since, although no cases of spontaneous poisonings in animals attributable to the ingestion of *L. zonalis* larvae have been detected either from Florida or Australia, the toxins lophyrotomin and a mixture of pergidin and val[4]-pergidin were demonstrated in *L. zonalis* larvae[12], making the larvae a possible threat to livestock. Furthermore, the toxic substances in *L. zonalis* larvae proved toxic to mice.[10]

The biological cycle of *P. flavipes* was studied in the laboratory[18] and it was determined that it develops along the whole year. Larvae appear in pasture from March on, when they are bright black and small, 1 mm in length, thus being not promptly observed. From March to August (autumn and winter in the south hemisphere) they measure 17-22 mm in length and are promptly detected. Under normal conditions full growth is reached in the late winter and early spring. They are ingested by cattle during this period. The reason that cattle eat the sawfly larvae is unknown. It has been suggested that this behavior reflects some form of nutritional deficiency (Roberts 1932), however, this remains unproven. Alternatively it has been suggested that some property of the sawfly may be involved in causing the animals to seek out and eat the larvae.[10] The nature of such attraction has not been determined, but it may also explain the existence of "toxic areas."[10] Larvae of *P. flavipes* feed on decomposing plant material, dry leaves and dried cattle manure. Larvae go through a series of changes until they pupate, when the insect penetrates 3-10 cm into the ground and form a bright black, leathery-like, 1x0.5 cm ovoid cocoon. Within the cocoon the larvae becomes white and remains in this stage from August to January when they emerge as adults. The adult insects are bright black and have a short life span: only 18-36 hours for females and 24-48 hours for males, time sufficient to start a new cycle. Females are 8-10 mm and males are 7.5-10 mm in length.[18]

The SLP is an acute condition in all affected species. The cattle most affected have weakness, muscular tremors, apathy, stupor and death within 2-5 days of the onset of clinical signs.[4,5,8,15] Some animals become very agitated and aggressive[5] and those cattle surviving for longer periods may show hepatogenous photodermatitis.[2,5] Some less affected cattle may recover.[2,5,17]

Necropsy findings include accentuation of the lobular hepatic pattern, edema of the gall bladder and serosal hemorrhages. Fragments of larvae (*P. flavipes*) can be

found in the rumen and omasum. The main histological lesion consists of centrilobular to massive liver necrosis and necrosis of lymphoid tissue.[5,15] Reportedly in cattle, necrosis of hepatocytes was most severe in the right lobe.[5] In our experience this is not an unusual finding in acute hepatotoxicosis in cattle, and we think it may be related to differences in the input of blood supply to different regions of the liver.

The acute centrilobular necrosis as seen associated to SLP is not specific of this condition and occurs in association with several other hepatotoxins, mainly phytotoxins, in farm animals.[16] Hepatocytes in the center of the lobule (zone 3) are more vulnerable to a toxic insult as compared with peripheral (zone 1) located hepatocytes because centrilobular hepatocytes have more abundant enzymes which act to transform liposoluble compounds in toxic substances and because centrilobular hepatocytes have lower levels of oxygen and glutathione peroxidase. Hepatocytes in the periphery of the lobule (zone 1) are more vulnerable to toxins of direct action due to the proximity of these periportal hepatocytes to the blood flow that arrives, but the portal vein and hepatic artery branches at the portal triads.[20] Interestingly, when the toxic principles of sawfly were administered to mice treated with lophyrotomin they developed periportal (zone 1) necrosis, and mice treated with pergidin developed centrilobular (zone 3) necrosis.[12] Regarding this aspect it is interesting to notice that a reduction in the sawfly-induced liver pathology associated as a consequence of the concurrent *Fasciola hepatica* infection was experimentally observed in lambs. A possible explanation for this phenomenon is as an inhibitory action of *F. hepatica* on the microsomal oxidative enzymes responsible by the biotransformation of the active principles within the larvae in toxic metabolites.[13] Other hepatotoxins that affect livestock in Brazil are in the included table.

The diagnosis in our case was based primarily in the clinical signs and pathological findings and on some epidemiological aspects. The aspects of the outbreak reported here are remarkably similar to SLP reported in cattle from Australia caused by *L. interrupta*[2,8,17] in sheep from Denmark caused by *Arge Pullata*[21] and in cattle and sheep from Uruguay[5] and cattle,[15,19] sheep,[14] and pigs[6] from Brazil caused by *P. flavipes*. Further evidence include the finding of fragments of the larvae in the fore-stomachs of the necropsied calf and the reproduction of the disease by feeding ground *P. flavipes* larvae collected from the site where the spontaneous outbreak occurred to a susceptible calf.

The neurologic clinical signs presented by cattle in this report affected by SLP are typical of hepatic encephalopathy. Cattle poisoned by the larvae *L. interrupta*[8] and sheep fed *Arge pulllata*[21] also show signs of hepatic encephalopathy, and the fatally poisoned calves presented increased plasma ammonia sufficient to account for the clinical signs.[8] Hepatic encephalopathy is common in ruminants and horses with hepatic failure.[3] Undetermined as yet are the specific metabolites that cause the neurologic dysfunction in hepatic encephalopathy, but increased concentrations of plasma ammonia derived from amines absorbed from the gastrointestinal tract may be responsible.[3] Normally, amines are absorbed from the intestines into the portal blood and metabolized by the liver. The toxic products may not be fully eliminated by severely damaged liver. However, abnormal ammonia concentrations are not the only possible cause of hepatic encephalopathy. An imbalance between inhibitory and excitatory amino acid neurotransmitters, -aminobutyric acid, and L-glutamate, respectively, and increased brain concentrations of endogenous benzodiazepines are other possible explanations.[3] Alternatively a low blood sugar can account for the neurological signs, and a fall in glucose was noticed in the fatally poisoned calves by *L. interrupta*.[8]

Widespread hemorrhages are prominent in some field cases of SLP, but they were not invariably present and their severity varied. Lengthened thrombin, activated thromboplastin times and reduced fibrinogen concentration have been reported in calves experimentally poisoned with the larvae of *Lophyrotoma interrupta*.[8] Hemorrhagic diathesis occurs terminally in animals with severe liver necrosis.[3] In these cases bleeding tendencies associated with hepatic failure may be due to impaired synthesis of clotting factors, reduced clearance of the products of the clotting process, and metabolic abnormalities affecting platelet function that affect normal clotting, individually or in combination. In acute liver failure (as is the case of liver failure in SLP) diminished synthesis of clotting factors with a short half-life, such as factors V; VII, IX, and X, impairs the ability of blood to coagulate. Diminished clearance of fibrin degradation products, activated coagulation factors, and plasminogen factors by the damaged liver also perturbs clotting. Metabolic disturbances resulting from liver failure can affect platelet function and lead to synthesis of abnormal fibrinogen, a condition termed dysfibrinogenemia.[3]

Due to the short course of the disease, jaundice and photosensitization were not common findings. An increased concentration of serum bilirubin has been seen in experimental sawfly larval poisoning of cattle and sheep.[8,21]

Tubular and degeneration of the renal epithelium tubular as described in cattle,[2,19] sheep,[14] and pigs[18] were not observed in our cases.

**JPC Diagnosis:** Liver: Necrosis, massive, diffuse.

**Table1. Acute hepatotoxicosis in farm animals in Brazil**

| Hepatoxin | Affected species | Toxic principle | Main lesion | Comments |
|---|---|---|---|---|
| **Plants** | | | | |
| *Xanthium* spp. | Cattle, sheep, pigs | Carboxyatractylosíde | Periacinar to massive necrosis | Poisoning in swine is associated with hypoglycemia and ascites |
| *Cestrum parqui* | Cattle | Carboxyatractylosíde | Periacinar necrosis | |
| *Cestrum corymbossum* var. *hirsutum* | Cattle | Not determined | Periacinar necrosis | Serosal hemorrhages, edema of the gall bladder wall. In natural conditions only causes acute poisoning. |
| *Cestrum intermedium* | Cattle | Not determined | Periacinar necrosis | Serosal hemorrhages, edema of the gall bladder wall. In natural conditions only causes acute poisoning. |
| *Sessea brasiliensis* | Cattle | Not determined | Periacinar necrosis | Serosal hemorrhages, edema of the gall bladder wall. In natural conditions only causes acute. Experimental small repeatedly administered doses can cause hepatic cirrhosis. |
| *Dodonea viscosa* | Cattle | Not determined | Periacinar necrosis | Serosal hemorrhages, edema of the gall bladder wall. In natural conditions only causes acute poisoning. |
| *Myoporum laetum* | Sheep | Furanosesquiterpenoid oils (ngaione) | Usually periacinar necrosis but variable zonal necrosis can occcur. | Other species can be affected but the in Brazil was only recognized in sheep. |
| *Cestrum intermedium* | Cattle | Not determined | Periacinar necrosis | Serosal hemorrhages, edema of the gall bladder wall. In natural conditions only causes acute poisoning. |
| *Cestrum laevigatum* | Cattle | Saponins, cestrumide | Periacinar necrosis | Serosal hemorrhages, edema of the gall bladder wall. In natural conditions only causes acute poisoning. Experimental small repeatedly administered doses can cause hepatic cirrhosis. |
| *Dodonea viscosa* | Cattle | Not determined | Periacinar necrosis | Serosal hemorrhages, edema of the gall bladder wall. In natural conditions only causes acute poisoning. |
| *Trema micanthra* | Goats and sheep | Not determined | Periacinar necrosis | Serosal hemorrhages, edema of the gall bladder wall. In natural conditions only causes acute poisoning. |
| *Vernonia molissima* | Catle and sheep | Not determined | Periacinar necrosis | There is also degeneration of renal tubular epithelium |
| *Vernonia rubricaulis* | Catle | Not determined | Necrose centrolobular | Outbreaks occur in the dry season |
| **Bacteria** | | | | |
| *Microcystis aeruginosa* | Cattle, sheep, horses, goats | Microcystins and oithers | Periacinar to massive necrosis | Multiple toxins present. Can also cause death by neuromuscular disturbances. This poisoning was not doccumented in farm animals in Brazil but there are evidences that it occurs |
| **Inscect larvae** | | | | |
| *Perreyia flavipeds* (sawfly) | Cattle, sheep and pigs | Pergidin and lophyrotomin | Periacinar to massive necrosis | Serosal hemorrhages, edema of the gall bladder wall. |
| **Mycotoxins** | | | | |
| Aflatoxin | Pigs, cattle | Bisfuranocoumarin compounds | Cnetrolobular necrosis (lipidosis) | Hemorrhages. Other species can be affected but the listed two are so more often in the country. Cattle are affecter as young and develop a chronic form with fibrosis, megalocytosis and bile duct hyperplasia |

**Conference Comment:** The contributor provides a very interesting and thorough discussion of sawfly larval poisoning. Conference participants discussed characteristics of the histological patterns of necrosis observed in acute toxicities such as this, noting that the patterns are very repetitive. Discussion focused on the extent of necrosis (centrilobular to massive) that is often a function of dose, as well as the presence of early ductular reaction that often occurs in response to hepatic damage. Ductular reaction is the phenomenon in which biprogenitor cells (cells that have the propensity to differentiate into either biliary epithelial cells or hepatocytes) proliferate in response to severe hepatic injury or nutritional deficits to form islands or small, crude tubules of small basophilic cells at the margin of the limiting plate. Ductular reaction is considered to be the hallmark of severe injury and may occur as early as 2-3 days after the toxic insult.[3]

Additionally, participants discussed the various toxins that can result in similar lesions of acute hepatic necrosis. The moderator provides the included table of agents involved in acute hepatic toxicity in cattle.

| Name | Toxic Principle |
|---|---|
| Blue-green algae | Microcystin-LR |
| Mushrooms: Amanita, Phalloides and others | Amatoxins |
| Cycads (Zamia sp.) | Methylazoxymethanol |
| Solanacae (Cestrum sp.) | Atractyloside |
| Compositae (Xanthium-cockleburr) | Carboxyatractyloside |
| Ulmaceae (Trema sp.-Poison peach) | Trematoxin |
| Myoporacae (Myoporum) | Ngaione (periportal) |
| Iron | |
| Sawfly larvae (Lophyrotoma sp.) | Lophyrotomin/pergidin |

**Contributing Institution**: Departamento de Patologia
Universidade Federal de Santa Maria, 97105-900
Santa Maria, RS, Brazil
http://www.ufsm.br/lpv

**References:**

1. Brummerstedt E, Kristensen E, Nielsen A, Bille-Hansen A. Death of a puppy after eating sawfly larvae. Case report. *Dansk-Veterrinaertids*. 1987;70:758-760.
2. Callow LL. Sawfly poisoning in cattle. *Qld J Agric Sci*. 1955;81:155-161.
3. Cullen JM. Liver, biliary system, and exocrine pancreas, hepatic failure. In: Zachary JF, McGavin MD, eds. *Pathologic Basis of Veterinary Disease*. 5th ed. St. Louis, MO Mosby: Elsevier; 2007:408, 414.
4. Dadswell LP, Abbott WD, Mckenzie RA. The occurrence, cost and control of sawfly larval (*Lophyrotoma interrupta*) poisoning of cattle in Queensland 1972/81. *Aust Vet J*. 1984;62:94-97.
5. Dutra F, Riet-Correa F, Mendez MC, Paiva N. Poisoning of cattle and sheep in Uruguay by sawfly (*Perreyia flavipes*) larvae. *Vet Hum Toxicol*. 1997;39:281-286.
6. Jonck F, Casagrande RA, Froehlich DL, Ribeiro Jr DP, Gava A. Intoxicação espontânea por larvas de *Perreyia flavipes* (Pergidae) em suínos no Estado de Santa Catarina. [Spontaneous poisoning by larvae of *Perreyia flavipes* (Pergidae) in pigs in the State of Santa Catarina.] Pesq *Vet Bras*. 2010;30:1017-1020. (In Portuguese, Abstract in English)
7. Kannan R, Oelrichs PB, Thamsborg ST, Willians DH. Identification of the octapeptide lophyrotomin in the European birch sawfly (*Arge pullata*). *Toxicon*. 1988;26:224-226.
8. McKenzie RA, Dunster PJ, Twist JO, Dimmock CK, Oelrichs PB, Rogers RJ, et al. The toxicity of sawfly larvae (*Lophyrotoma interrupta*) to cattle. *Qld. Dept. Prim. Ind. Bull*. 1985;QB85001:1-48.
9. Oelrichs PB, MacLeod JK, Seawright AA, Moore MR, Ng JC, Dutra F, Riet-Correa F, et al. Unique toxic peptides isolated from sawfly larvae in three continents. *Toxicon*. 1999;37:537-544.
10. Oelrichs PB, McLeod JK, Seawright AA, Grace PB. Isolation and identification of toxic peptides from *Lophyrotoma zonalis* (pergidae) sawfly larvae. *Toxicon*. 2001;39:1933-1936.
11. Oelrichs PB, Valley JV, McLeod JK, Cable J, Kiely D, Summers RE. Lophyrotomin, a new toxic octapeptide from the larvae of the sawfly, *Lophyrotoma interrupta*. *Lloydia*. 1977;40:209-214.
12. Oerlichs PB. Sawfly poisoning in cattle. *Qld Agric J*. 1982;108:110-112.
13. Olaechea FV, Thamsborg SM, Christensen NØ, Nansen P, Robles A. Interference with sawfly (*Arge pullata*) poisoning in *Fasciola hepatica*-infected lambs. *J Comp Path*. 1991;104:419-431
14. Raymundo DL, Bezerra Junior PS, Bandarra PM, Pedroso PMO, Oliveira EC, Pescador CA, et al. Spontaneous poisoning by larvae of *Perreyia flavipes* (Pergidae) in sheep. *Pesq Vet Bras*. 2008;28:169-173.
15. Raymundo DL, Bezerra Jr PS, Bandarra PM, Santos AS, Sonne L, Pavarini SP, et al. Intoxicação espontânea pelas larvas de *Perreyia flavipes* em bovinos no Estado de Santa Catarina, Brasil. *Ciência Rural*. 2009;39:163-166.
16. Rissi DR, Driemeier D, Silva MC, Barros RR, Barros CSL. Poisonous plants producing acute hepatic disease in Brazilian cattle. In: Panter KE, Wierenga TL, Pfister JA, eds. *Poisonous Plants: Global Research and Solutions*. Wallingford, UK: CAB International; 2007:72-76.
Roberts FHS. The cattle-poisoning sawfly (*Pterygophorus analis* Costa). *Qd Agric J*. 1932;37:41-52.
17. Soares MP, Quevedo PS, Schild AL. Intoxicação por larvas de *Perreyia flavipes* em bovinos na Região Sul do Rio Grande do Sul. [*Perreyia flavipes* larvae poisoning in cattle in southern Rio Grande do Sul, Brazil.] *Pesq Vet Bras*. 2008;28:169-173. (In Portuguese, Abstract in English)
18. Soares MP, Riet-Correa F, Smith DR, Pereira Soares M, Méndez MC, Brandolt AL. Experimental intoxication by larvae of *Perreyia flavipes* Konow, 1899 (Hymenoptera: Pergidae) in pigs and some aspects on its biology. *Toxicon*. 2001;39:669-678.
19. Stalker MJ, Hayes MA. Liver and biliary system: toxic hepatic disease. In: Maxie MG, ed. *Jubb, Kennedy, and Palmer's Pathology of Domestic Animals*. 5th ed. Vol. 2. Philadelphia, PA: Saunders Elsevier. 2007:372-378.
20. Thamsborg SM, Jørgensen RJ, Brummerstedt E. Sawfly poisoning in sheep and goats. *Vet Rec*. 1987;121:253-255.
21. Tryon H. Special cattle fatality in the Maranoa District, and its relation to the larvae of *Pterygophorus analis*, Costa. *Qld Agric J*. 1921;16:208-216.

**CASE II:** 01019006 (JPC 4017217).

**Signalment:** 8-day-old, male, miniature horse (foal), *(Equus ferus caballus)*.

**History:** Presented for complete necropsy following natural death. It had a reported clinical history of impaction.

**Gross Pathology:** The foal had a body condition score of 3/5 and was in fair post-mortem condition. The adipose tissue throughout the carcass was pale yellow (icterus). The liver contained numerous pinpoint pale tan and red-black foci throughout. Upon opening the elbow joints, minimal amounts of yellow, strand-like material was adherent to the cartilaginous surface of the humeral condyles and the radial fossa (fibrinosuppurative arthritis). The stomach contained a moderate amount of pale yellow, pasty material (digested milk), while the small intestines and cecum contained mild to moderate amounts of dark gray, opaque, viscous digesta. The large and small colon contained moderate amounts of yellow pasty feces throughout.

**Histopathologic Description:** Liver: The hepatic parenchyma is replaced by multifocal to coalescing round to oval aggregates of hepatic necrosis and inflammation. These areas are characterized by a central area of hepatocytes undergoing coagulative and liquifactive necrosis admixed with homogenous eosinophilic fibrillar material (fibrin) and neutrophils undergoing necrosis. The areas of hepatocellular necrosis are often surrounded by a dense layer of karyorrhectic and karyolytic nuclear debris from necrotic neutrophils. Hepatocytes can be observed at the periphery of these lesions that contain intracytoplasmic aggregates of rod-shaped bacteria.

**Contributor's Morphologic Diagnosis:** Marked acute multifocal random necrosuppurative hepatitis with intracytoplasmic bacilli.

**Contributor's Comment:** Tyzzer's disease was first described in laboratory rodents, but has been reported in a number of species as a naturally occurring disease.[3] The causative organism is *Clostridium piliforme*, formerly known as *Bacillus piliformis*. The organism is a gram-negative, obligate intracellular, spore-forming rod. Exposure is likely through the fecal-oral route with systemic dissemination taking place after infection establishes in the intestines. The liver and myocardium are primarily affected. Necrotizing enteritis can be seen in some laboratory animal species, most notably rodents

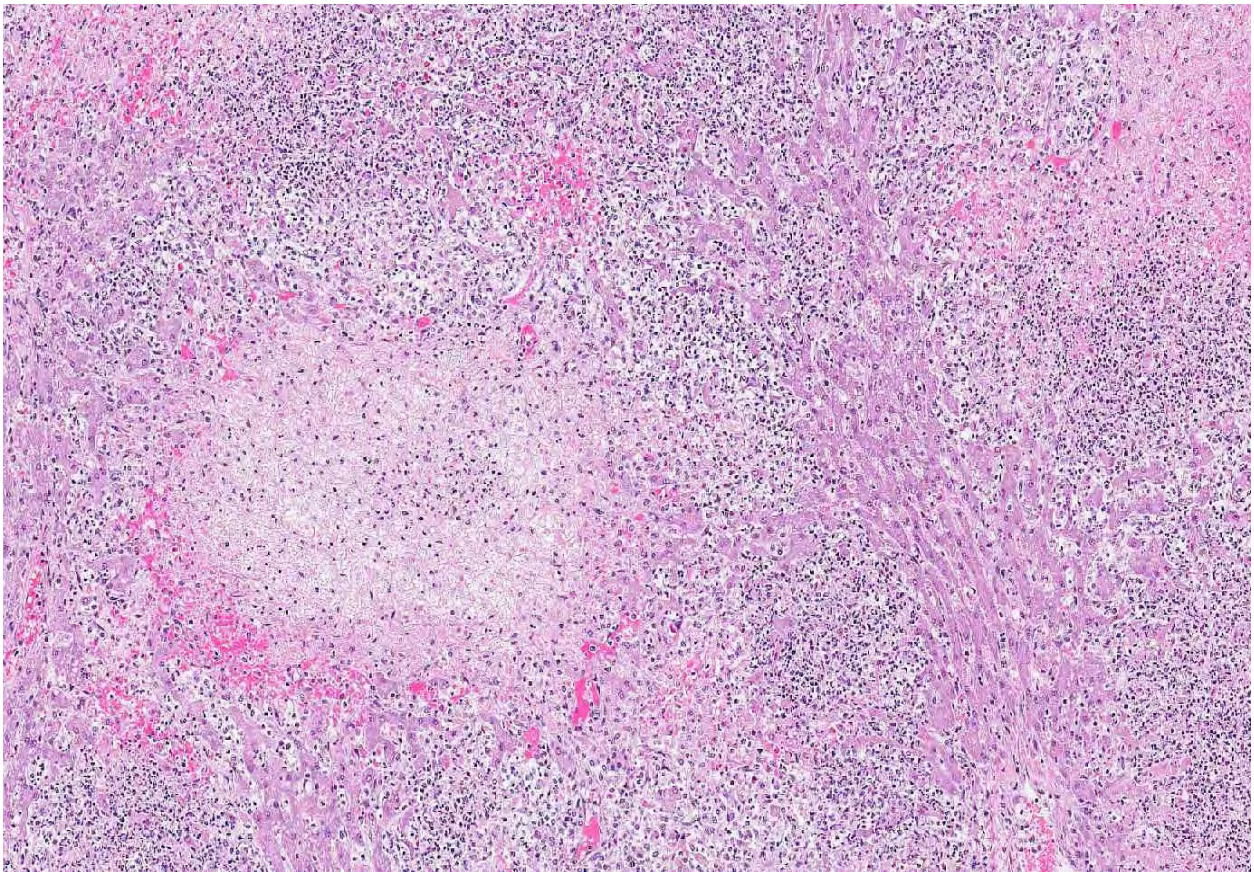

*2-1. Liver, miniature horse: Scattered throughout the liver are areas of coagulative necrosis, rimmed by hypercellular areas of lytic necrosis, and most peripheral, by intact hepatocytes. (HE 120X)*

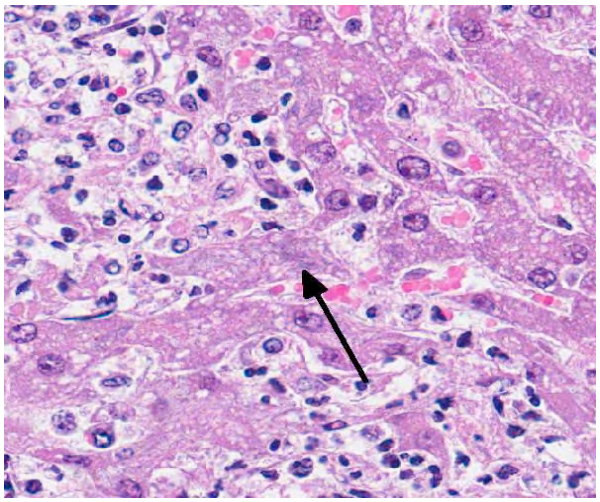

*2-2. Liver, miniature horse: At the periphery of necrotic areas, faintly stained outlines of filamentous rod-shaped bacilli (arrow) in a characteristic "haystack" or "pickup-stick" arranged may be seen in the cytoplasm of intact hepatocytes. (HE 120X)*

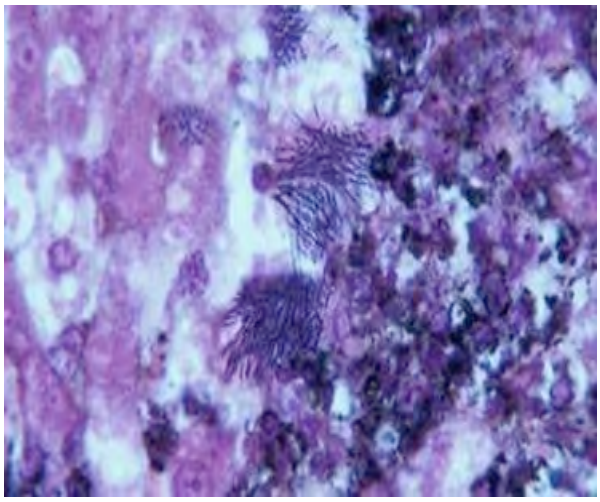

*2-3. Clostridium piliforme is best demonstrated with silver stains, such as Warthin-Starry stains, which or GMS with HE counterstains, as seen here. (GMS/HE 600X)*

and rabbits, with the distal small intestine primarily affected. Silver stains (e.g. Warthin-Starry or Gomori's methanamine silver) are useful in highlighting the bacteria.[3] Immunohistochemical or immunofluorescence staining can also be used to confirm the diagnosis.[1]

Foals from 7 to 42 days of age are primarily affected[1] and immunocompromised animals are predisposed to infection. The organism is not considered highly contagious and animals are typically affected sporadically in a given population. Infected animals can be found dead or may present for acute onset of non-specific clinical signs such as pyrexia, lethargy, anorexia and icterus. Typically elevations of hepatocellular leakage enzymes and hyperbilirubinemia take place.[3] Treatment of animals with confirmed disease is typically unrewarding.

**JPC Diagnosis:** Liver: Hepatitis, necrotizing and suppurative, multifocal to coalescing, severe, with intracytoplasmic filamentous bacilli.

**Conference Comment:** The contributor provides a good summary of *C. piliforme*, an atypical member of the genus *Clostridium*. Other members of the clostridia are large, Gram positive spore forming bacteria with straight or slightly curved morphology, in contrast to the filamentous, Gram negative spore forming *C. piliforme.*[2] Further differentiating *C. piliforme* from other clostridia is the fact that it does not possess characteristics that allow its inclusion into one of the three general categories of the other pathogenic members of the genus. These categories of clostridia are neurotoxic (*C. tetani, C. botulinum* types A-G), histotoxic (*C. chauvoei, C. septicum, C. novyi* types A and B, *C. perfringens* type A, *C. sordellii, C. hemolyticum)*, and enteropathogenic/enterotoxemia-producing (*C. perfringens* types A-E, *C. difficile, C. colinum, C. spiroforme*).[2]

Conference participants discussed the importance of recognizing both the pattern of necrosis (i.e. multifocal, random) as well as the inflammatory component in this section, and discussed the differential diagnosis for such lesions. The conference moderator provided the included table of common causes of bacterial hepatitis in various domestic animal species.

| **Organism** | **Species affected** |
|---|---|
| *Listeria monocytogenes* | Neonates: ruminants, foals, piglets |
| *Campylobacter fetus* | Lambs, foals, piglets |
| *Actinobacillus equilli/suis* | Foals/piglets |
| *Yersinia pseudotuberculosis* | Lambs, dogs, cats |
| *Francisella tularensis* | Lambs, cats |
| *Mannheimia hemolytica/ Histophilius somni* | Lambs |
| *Salmonella* spp. | Various |
| *Clostridium piliforme* | Foals, dogs |
| *Nocardia/Mycobacterium* | Various |

**Contributing Institution:** Department of Veterinary Biosciences
College of Veterinary Medicine
The Ohio State University
1925 Coffey Road
Columbus, OH 43210
http://vet.osu.edu/biosciences

**References:**

1. Van Der Lugt JJ. Tyzzer's disease. In: Coetzer JAW, Tustin RC, eds. *Infectious Diseases of Livestock.* Vol. 3. Capetown, South Africa: Oxford University Press Southern Africa; 2004:2089-2091.

2. Quinn PJ, Markey BK, Leonard FC, FitzPatrick ES, Fanning S, Hartigan PJ. Clostridium species. In: *Veterinary Microbioogy and Microbial Disease.* 2nd ed. Ames, IA: Wiley-Blackwell; 2011: Kindle edition.

3. Stalker MJ, Hayes MA. Liver and biliary system In: Maxie MG , ed. *Jubb, Kennedy and Palmer's Pathology of Domestic Animals*. 5th ed. Vol. 2. Philadelphia, PA: Elsevier; 2007:356.

**CASE III:** MS1104670 (JPC 4019870).

**Signalment:** Four-month old, female, athymic nude, mouse (*Mus musculus*).

**History:** Second mouse in cage to develop spontaneous emaciation and paresis.

**Gross Pathology:** Prior to euthanasia the animal is depressed. Mild splenomegaly and lymph node enlargement is present. The mesenteric lymph node is white and firm. Heart, lung, liver, GI and reproductive tract are grossly normal.

**Laboratory Results:** The fecal, kidney and mesenteric lymph node tissue samples are negative for MPV via PCR. The liver and mesenteric lymph node tissue samples are positive for MHV via RT-PCR.

**Histopathologic Description:** The liver has moderate, multifocal necrotizing and suppurative hepatitis. Some necrotic foci contain syncytial cells. Findings in other (not submitted) tissues include necrotizing splenitis and necrosis, variable suppuration and syncytial cells in the brain, bone marrow and lymph nodes, and the nasal cavity has necrosuppurative rhinitis.

**Contributor's Morphologic Diagnosis:** Hepatitis, necrotizing, moderate, multifocal with syncytial cells.

**Contributor's Comment:** This mouse is one in a group of other nude mice housed separately but near a room known to be positive for MHV and MPV. Of the known strains of MHV, this mouse likely presented with a polytropic strain, most notably with neurotropic characteristics. This mouse had characteristic necrotizing lesions with syncytial cells in multiple tissues, suggesting a polytropic strain of MHV.

Mouse hepatitis virus is a single-stranded, enveloped RNA virus of the family *Coronaviridae*. Approximately 25 strains or isolates of MHV have been described. Isolates can be divided into two biotypes with varying degrees of overlap: the respiratory (polytropic) and enterotropic strains.[3] Respiratory strains of MHV are extremely contagious and are transmitted primarily via aerosol, direct contact, and fomites. Once inhaled, the virus replicates in the nasal mucosa and subsequently spreads via the blood and lymphatics through cervical and mesenteric lymph nodes to multiple tissues.[1] Dissemination is more likely with more virulent strains of virus in infant mice without maternal antibody and in immunocompromised (particularly nude) mice. MHV has high morbidity and mortality in these groups. Immunocompetent mice may clear the infection in five to seven days post-infection with no carrier status. BALB/c mice are generally quite susceptible to MHV, whereas SJL mice are remarkably resistant. The spike protein (SP), responsible for viral entry, is a major determinant of

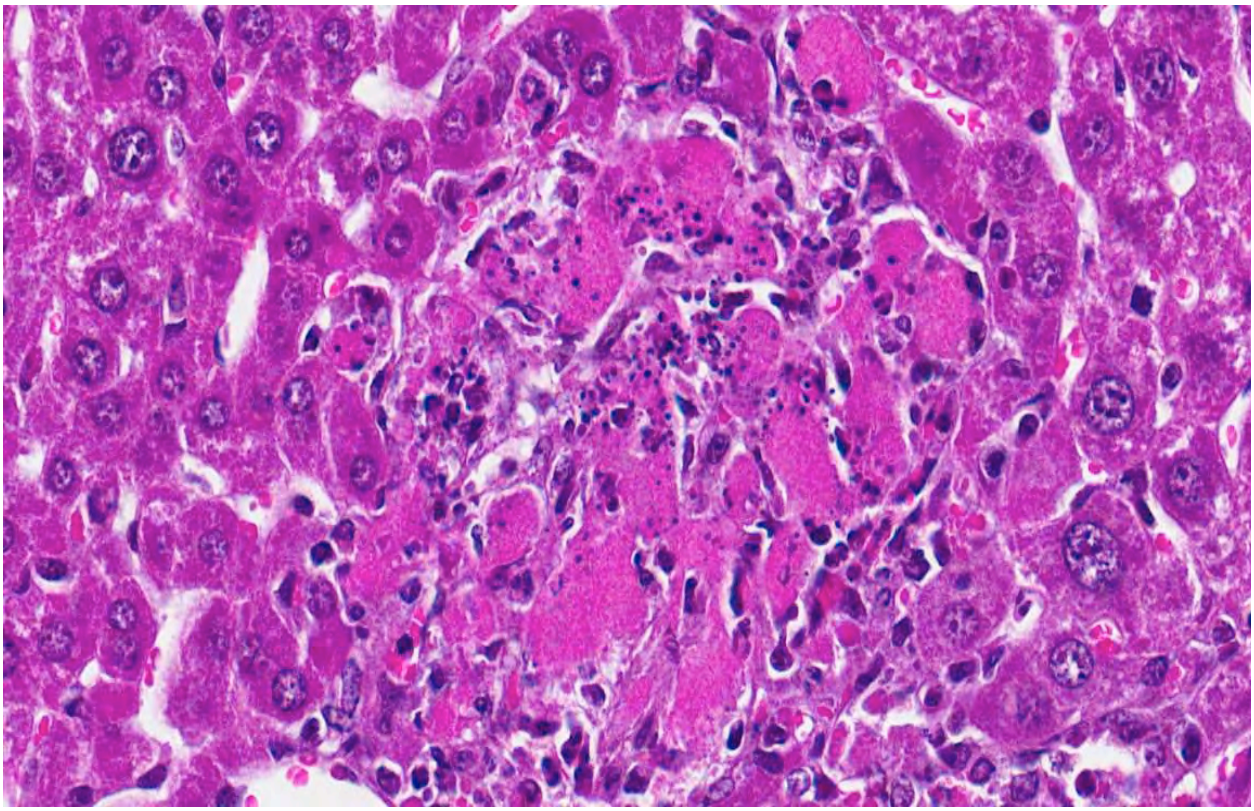

*3-1. Liver, mouse: Randomly scattered throughout the section of liver are numerous small foci of necrotic hepatocytes. (HE 400X)*

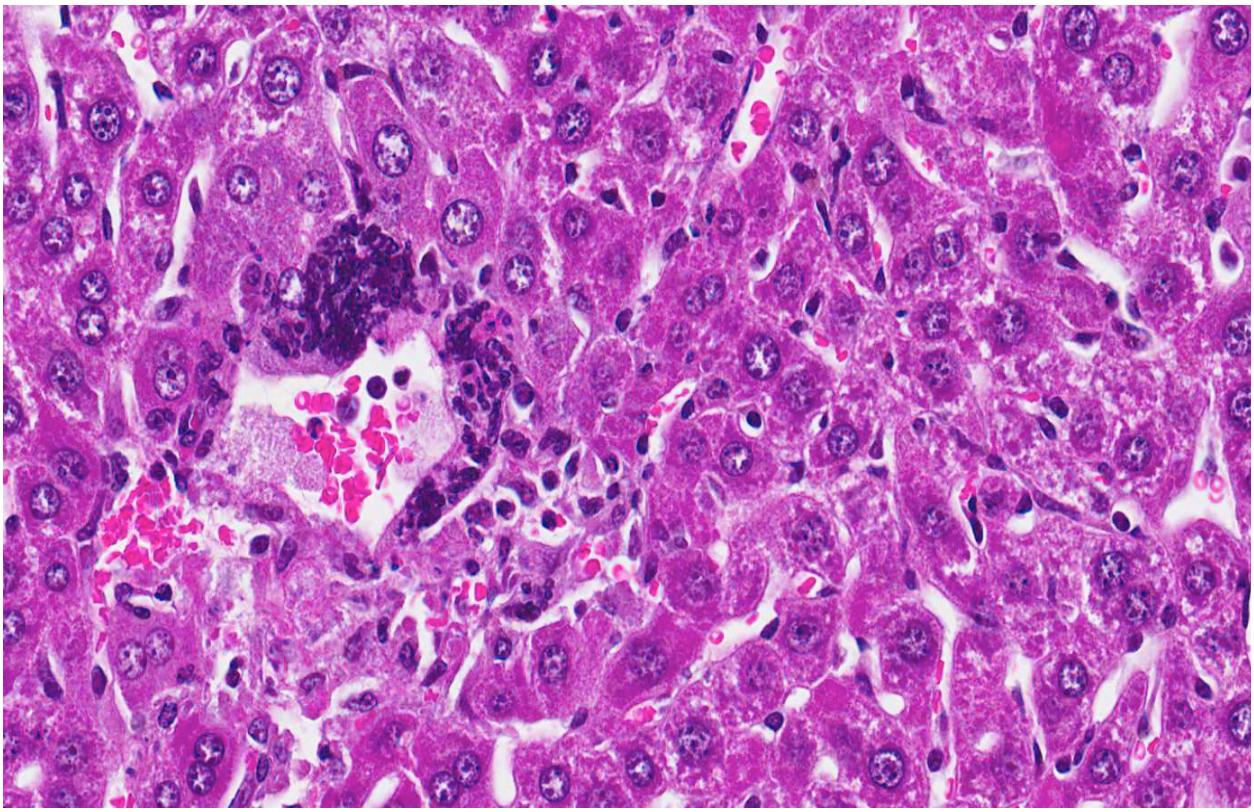

*3-2. Liver, mouse: Multinucleated hepatocellular viral syncytia are characteristic of infection by mouse polytropic coronavirus (mouse hepatitis virus). Necrotic syncytia are still recognizable in areas of hepatocellular necrosis. (HE 400X)*

tropism and virulence.[2] SP binds carcinoembryonic antigen-related cell adhesion molecule 1, CEACAM- 1 on either the cell surface or in endosomes. SP also mediates cell-to-cell fusion. The allelic form of CEACAM in a particular strain of mouse is a determinate of susceptibility. Strains that express CEACAM-1α such as Balb/C are susceptible. Strains that express CEACAM -1β such as SJL are resistant.[2] Disease severity is determined by thrombosis and coagulation necrosis due to induction of procoagulant activity by macrophages in susceptible mice.[5] T cell function is important for viral clearance depending on both CD8 activity and antibody and cytokine induction.[2]

Enterotropic strains of MHV selectively infect intestinal mucosal epithelium, with minimal to no dissemination to other organs, even in immunodeficient mice.[4] All stages and strains of mice are susceptible to enterotropic MHV infection, including SJL mice, which are resistant to polytropic MHV.[5] The severity of intestinal disease is associated with age-related intestinal mucosal proliferative kinetics, thus severe disease occurs only in infant mice.[4] Even in nude or SCID mice, disease can be minimal; however, hyperplastic colitis has been reported in nude mice.[5] Recovery from enterotropic MHV is T-cell dependent; persistent infections can occur in immunodeficient mice.[3]

Diagnosis is usually made via serology using an ELISA, but MHV may also be isolated in susceptible tissue culture cells. Differential diagnoses include Salmonellosis, Tyzzer's disease and reovirus infection.[5] Respiratory syncytial virus forms syncytial cells similar to MHV, but these cells are restricted to the pulmonary parenchyma.

**JPC Diagnosis:** Liver: Hepatitis, necrotizing, multifocal and random, moderate, with viral syncytia.

**Conference Comment:** The contributor provides a very good summary of mouse hepatitis virus (MHV). Conference participants discussed the polytropic nature of the respiratory strains of MHV. Despite being called a "hepatitis" virus, these viruses actually have a secondary tropism for a variety of cells and tissues other than the liver to include vascular endothelium, lymphoid tissue, hemopoietic tissue, and the central nervous system.[6] The majority of natural polytropic MHV infections are subclinical in immunocompetent mice; whereas infections in immunodeficient mice often result in wasting disease, neurologic signs and mortality. Interferon-gamma deficient mice infected with polytropic MHV develop a unique clinical presentation of granulomatous polyserositis and subsequent abdominal distention.[5,6] Participants also discussed the significance of MHV in laboratory mouse colonies, where its effects on research

resulting from immunomodulation can be particularly devastating.[5,6]

**Contributing Institution**: NIH, Division of Veterinary Resources, ORS, OD, Diagnostic Service Branch
Bldg. 28A/115
Bethesda, MD
http://www.ors.od.nih.gov

**References:**

1. Barthold SW, Smith AL. Viremic dissemination of mouse hepatitis virus-JHM following intranasal inoculation of mice. *Arch Virol*. 1992;112:35-44.
2. Bender SJ, Weiss SR. Pathogenesis of murine coronavirus in the central nervous system. *J Neuroimm Pharm*. 2010;5(3):336-354.
3. Compton SR, Barthold SW, Smith AL. The cellular and molecular pathogenesis of coronaviruses. *J Lab Animals*. 1993;43: 15-28.
4. Homberger FR. Enterotropic mouse hepatitis virus. *J Lab Anim*. 1997;31(2):97-115.
5. Percy DH, Barthold SW. Coronavirus infection: mouse hepatitis virus. In: *Pathology of Laboratory Rodents and Rabbits*. 3rd ed. Ames, IA: Blackwell Publishing; 2007:31-36.
6. Saif LJ. Coroniviridae. In: MacLachlan NJ, Dobovi EJ, eds. *Fenner's Veterinary Virology.* 4th ed. London, UK: Elsevier; 2011:404-406.

**CASE IV:** V11-30618 (JPC 4019134).

**Signalment:** Adult, male, sugar glider, (*Petaurus breviceps).*

**History:** The owner had seven sugar gliders. Two sugar gliders, one female and one male, became acutely lethargic, dehydrated, and were vomiting. The sugar gliders died and the male was presented for postmortem examination. The diet did contain cantaloupe that had been previously frozen and raw organic soybeans.

**Gross Pathology:** The liver was slightly enlarged with multiple pinpoint tan foci of necrosis. The lungs were mildly congested.

**Laboratory Results:** *Listeria monocytogenes* was isolated on bacterial culture of the liver.

**Histopathologic Description:** The liver contains numerous random multifocal to coalescing foci of necrosis filled with necrotic cellular debris and variable numbers of degenerate neutrophils. The margins of the necrotic foci contain variable numbers of gram-positive intracellular and extracellular rod-shaped bacteria. The necrotic foci occasionally extend into portal veins resulting in necrosis of the vascular wall and fibrin thrombi within the lumen. Throughout the liver, there are moderate numbers of hepatocytes that contain clear distinct cytoplasmic vacuoles consistent with lipid. There are moderate numbers of hepatocytes that contain golden-brown to yellow-green cytoplasmic granular pigment that is consistent with hemosiderin and bile.

**Contributor's Morphologic Diagnosis:** Liver: Severe multifocal and random necrotizing suppurative hepatitis with rare vascular necrosis and thrombosis and intracellular and extracellular gram-positive rod-shaped bacteria consistent with *Listeria monocytogenes.*

**Contributor's Comment:** *Listeria monocytogenes* is a gram-positive, intracellular, non-spore forming, facultative anaerobic, rod-shaped bacterium that causes the disease listeriosis.[2,5,6] It has the ability to infect and cause disease in multiple species including but not limited to humans, ruminants, pigs, horses, rabbits, chinchillas, and birds.[1,2,4,5,6,7,8,9] The bacterium is believed to be distributed worldwide with many animals and people (estimated up to 70% of people in some areas are carriers) being asymptomatic carriers.[2,6,7] In addition, the bacterium has been isolated from sewage, stream water, silage, and soil.[6]

Most incidents of listeriosis occur when the host ingests contaminated soil, water or food.[1,2,5,6,7] The bacterium is internalized into the host cell using the surface protein internalin, which interacts with E-cadherin on the host cells allowing the bacterium to cross the intestine, placenta, and blood-brain barrier.[1,2,5,7,9] Once inside the host cell, the bacterium lyse the phagocytic cell phagolysosome using a pore-forming protein called listeriolysin O and two phospholipases allowing it to gain access to the host cell cytoplasm. The bacterium then replicates within the host cell cytoplasm. *Listeria* has the ability to co-opt the host cell actin filaments using the bacterial surface protein ActA to help it migrate to the host cell membrane to induce pseudopod-like protrusions that can be transferred to another host cell. The host protection against *Listeria* appears to be mediated by IFN-γ production by NK cells and T-lymphocytes as host macrophages stimulated by IFN-γ phagocytose and kill *Listeria* while host macrophages that internalize *Listeria* coated by C3 become infected.[1]

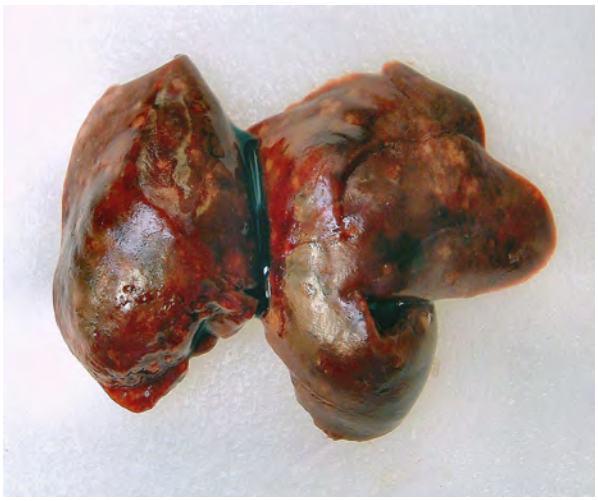

*4-1. Liver, sugar glider: The liver was slightly enlarged with multiple pinpoint tan foci of necrosis. (Photo courtesy of: The New Mexico Department of Agriculture Veterinary Diagnostic Services http://www.nmda.nmsu.edu/vds/)*

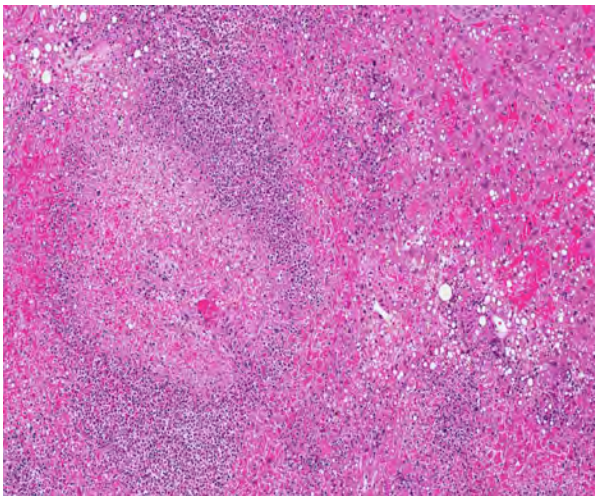

*4-2. Liver, sugar glider: There are numerous foci of coagulative necrosis bounded by areas of lytic necrosis scattered throughout the section. (HE 80X)*

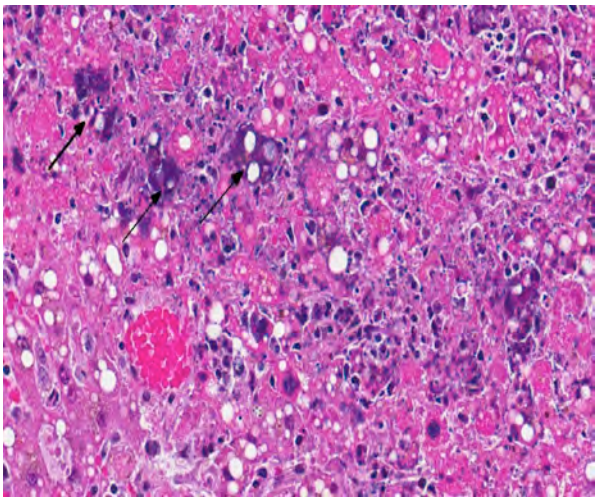

*4-3. Liver: Aggregates of 2-3 µm rod-shaped bacilli s are scattered throughout areas of lytic necrosis. (HE 320X)*

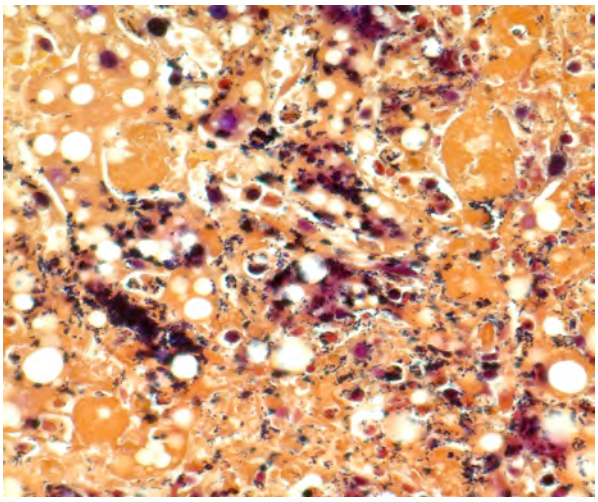

*4-4. In areas of lytic necrosis, a tissue Gram stain reveals numerous intra- and extracellular rod-shaped bacilli consistent with Listeria monocytogenes. (Gram 400X). (Photo courtesy of: The New Mexico Department of Agriculture Veterinary Diagnostic Services http://www.nmda.nmsu.edu/vds/)*

Severe disease caused by *Listeria monocytogenes* tends to manifest as three distinct syndromes in both animals and humans: abortion after infection of the pregnant uterus, septicemia with visceral abscesses, and meningoencephalitis.[1,2,9] The syndromes, particularly the neurologic and genital forms of listeriosis, rarely occur at the same time.[2] Abortions occur most commonly in cattle and sheep, but have also been reported in women and other species.[1,2] Encephalitic listeriosis occurs most commonly in ruminants while people tend to develop suppurative meningitis.[1,2] All species seem to be susceptible to septicemia with *Listeria*.[5]

In abortions, *Listeria* crosses the placenta and most likely results in fetal septicemia.[6] The gross lesions in the fetus often include severe placentitis and multiple pinpoint yellow foci in multiple organs, which are most prominent in the liver. However, the gross fetal visceral lesions are easily obscured by postmortem decomposition. The microscopic lesions in the fetal organs consist of foci of necrosis filled with degenerate neutrophils and macrophages surrounded by bacteria. Necrotizing enterocolitis with intralesional bacteria may be present. Meningitis can also be seen in the fetus. The microscopic placental lesions include necrosis of the cotyledonary villi with a suppurative exudate and many bacteria.

The neurologic form of listeriosis in ruminants is most often the result of feeding contaminated silage.[2,5,7,9] The bacteria travel via the trigeminal nerve and other sensory nerves to the brainstem possibly gaining entry to the nerves through wounds in the oral cavity. There usually are no gross lesions associated with neurologic listeriosis in ruminants. The microscopic lesions are limited to the brainstem. The microscopic lesions can range from small early lesions of accumulations of glial cells to severe encephalitis with macrophages, lymphocytes, plasma cells, neutrophils, and the formation of the characteristic microabscesses. Bacteria can be seen in some lesions.

The septicemic form of listeriosis most often occurs in neonates and young animals, but can occur in adult animals.[1,2,8,9] The gross and microscopic lesions consist of multifocal necrosis and microabscesses that can contain bacteria.[2] These lesions occur most frequently in the liver. Although the source of the bacterium is often not identified in septicemic cases, potential sources include contamination of the pregnant uterus by *Listeria* during gestation and the bacterium crossing the intestine after the animal ingesting contaminated soil, water or food.

In the fall of 2011, in multiple states including Colorado and New Mexico, a total of 146 persons were sickened, 30 people died, and one woman miscarried after eating cantaloupe contaminated with *Listeria monocytogenes*.[3] The sugar glider in this case was known to eat cantaloupe in its diet. *Listeria monocytogenes* has 11 different serotypes that can be distinguished from one another using molecular techniques. Using pulse field gel electrophoresis, the serotype of the *L. monocytogenes* isolated from the sugar glider was not the same as the serotype of the *L. monocytogenes* isolated from the cantaloupe associated with the listeriosis outbreak in people. Nevertheless, this case illustrates the "One Health" concept of the potential of infectious agents to infect veterinary species and humans that are sharing the same environment and ingesting the same food and water.

**JPC Diagnosis:** Liver: Hepatitis, necrotizing and suppurative, multifocal, severe, with vascular necrosis, thrombosis, and numerous intra and extracellular bacilli.

**Conference Comment:** The contributor provides an excellent review of listeriosis. Conference participants discussed the vascular lesions and described them as vascular necrosis due to local inflammation rather than a true vasculitis. Participants also commented on the necrotic areas, noting the core of lytic necrosis and inflammation surrounded by a corona-like ring of coagulative necrosis. There was speculation that such lesions could be due to either the local effects of listeriolysin O and phospholipase facilitating transfer of the bacteria across cell membranes resulting in coagulative necrosis in advance of inflammation; or to a locally released toxin directly resulting in cell death.

**Contributing Institution**: New Mexico Department of Agriculture Veterinary Diagnostic Services
1101 Camino De Salud NE
Albuquerque, NM 87102
http://www.nmda.nmsu.edu/vds/

**References:**

1. McAdam AJ, Sharpe AH. Infectious diseases. In: Kumar V, Abbas AK, Fausto N, Aster J, eds. *Robbins and Cotran Pathologic Basis of Disease*. 8th ed. Philadelphia, PA: Elsevier Saunders; 2010:361.
2. Maxie MG, Youssef S. Nervous system. In: Maxie MG, ed. *Jubb, Kennedy, and Palmer's Pathology of Domestic Animals*. 5th ed. Vol 1. Philadelphia, PA: Elsevier Saunders; 2007:405-408.
3. Multistate Outbreak of Listeriosis Linked to Whole Cantaloupes from Jensen Farms, Colorado. The Centers for Disease Control and Prevention Website. http://www.cdc.gov/listeria/outbreaks/cantaloupes-jensen-farms/120811/index.html. December 8, 2011 (Final Update). Accessed June 11, 2012.
4. Percy DH, Barthold SW. Rabbit. In: Percy DH, Barthold SW, eds. *Pathology of Laboratory Rodents and Rabbits*. 3rd ed. Ames, IA: Blackwell; 2007:278-280.
5. Quinn PJ, Markey BK, Leonard FC, FitzPatrick ES, Fanning S, Hartigan PJ. *Listeria* species. In: Quinn PJ, Markey BK, Leonard FC, FitzPatrick ES, Fanning S, Hartigan PJ, eds. *Veterinary Microbiology and Microbial Disease*. 2nd ed. Ames, IA: Wiley-Blackwell; 2011:217-221.
6. Schlafer DH, Miller RB. Female genital system. In: Maxie MG, ed. *Jubb, Kennedy, and Palmer's Pathology of Domestic Animals*. 5th ed. Vol 3. Philadelphia, PA: Elsevier Saunders; 2007:492-493.
7. Walker RL. *Listeria*. In: Hirsh DC, MacLachlan NJ, Walker RL, eds. *Veterinary Microbiology*. 2nd ed. Ames, IA: Blackwell; 2004:185-189.
8. Warner SL, Boggs J, Lee JK, et al. Clinical, pathological, and genetic characterization of *Listeria monocytogenes* causing sepsis and necrotizing typhlocolitis and hepatitis in a foal. *J Vet Diagn Invest*. 2012;24(3):581-586.
9. Zachary JF. Nervous system. In: Zachary JF, McGavin MD, eds. *Pathologic Basis of Veterinary Disease*. 5th ed. St. Louis, MO: Elsevier Mosby; 2012:845-846.

**Joint Pathology Center**
**Veterinary Pathology Services**

# WEDNESDAY SLIDE CONFERENCE 2012-2013

## Conference 16

**27 February 2013**

**CASE I:** PA5003 (JPC 4017810).

**Signalment:** Adult (age unspecified), male, rhesus monkey *(Macaca mulatta)*.

**History:** This adult male rhesus macaque had been infected 7 months previously with SIV and had a marked decrease in its CD4 cell counts. Prior baseline (pre-SIV infection) CT imaging had revealed a small, circumscribed, spherical, thick-walled air-filled cavitary lesion in the left lower lung lobe which had recently markedly expanded in size and was now associated with some adjacent parenchymal consolidation. An acid-fast organism was recovered from a recent gastric aspirate, although further identification/speciation was not performed. The animal was humanely sacrificed and presented immediately for post-mortem examination.

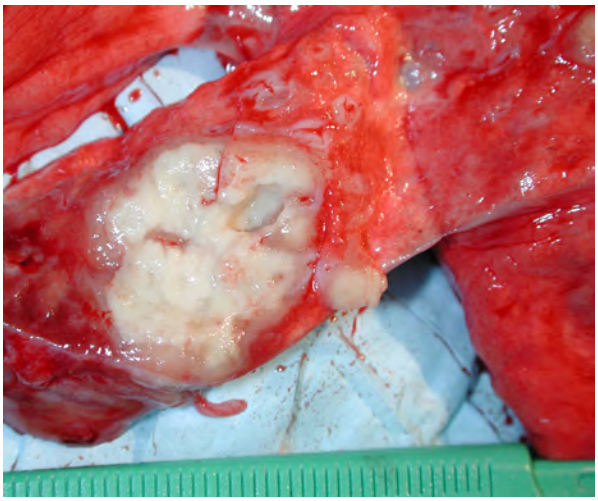

*1-1. At autopsy, there were marked fibrous adhesions between the left lower lobe and the diaphragmatic and lateral thoracic wall. Dissection revealed a well-demarcated are of necrosis and cavitation as seen here. (Photo courtesy of: The Division of Laboratory Animal Resources, S 1040 Biomedical Science Tower, University of Pittsburgh, Pittsburgh, PA 15668; http://www.dlar.pitt.edu/)*

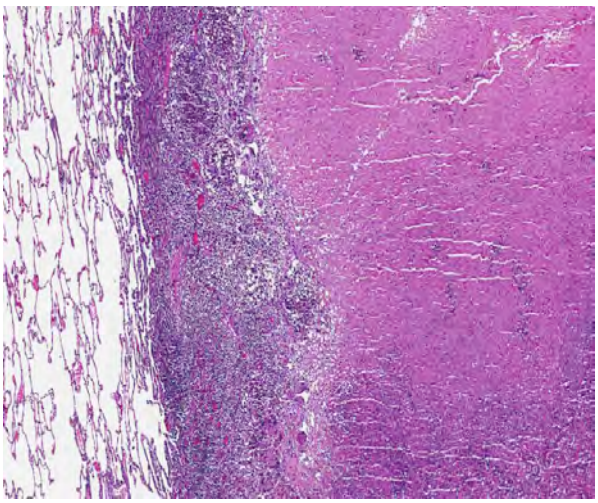

*1-2. Lung, rhesus monkey: A large peribronchiolar pyogranuloma replaces up to 50% in some sections. (HE 40X)*

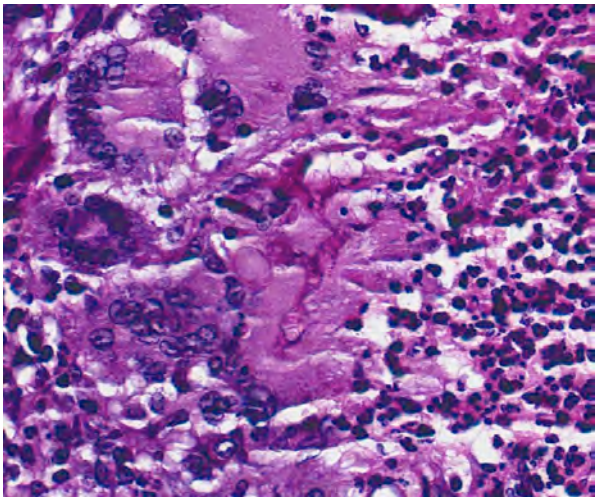

*1-3. Lung, rhesus monkey: At the periphery of the pyogranuloma, fungal hyphae with non-parallel walls measuring up to 12 µm in diameter are present within multinucleated macrophages of both the foreign body and Langhans' types. As is occasionally the case with zygomycete fungi, the hyphae in this case stain more prominently with hematoxylin and eosin than with silver stains. (HE 400X)*

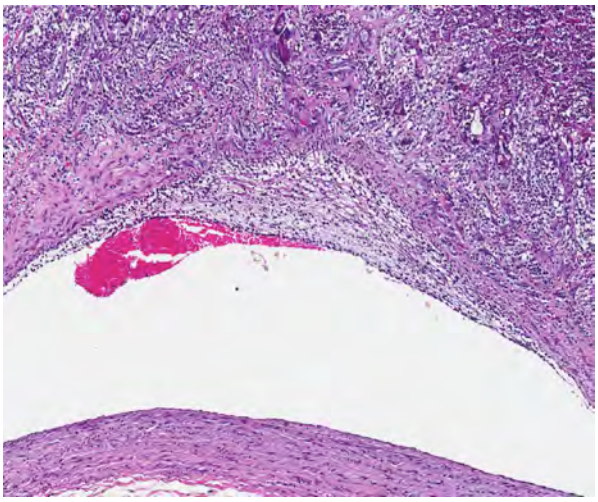

*1-4. Lung, rhesus monkey: There is a focally extensive granulomatous arteriolitis resulting from local extension of the pyogranuloma into an adjacent arteriole. (HE 400X)*

**Gross Pathology:** In the superior portion of the left lower lobe at the reflection of the anterior and posterior surfaces, there was a 3.5-4 cm area of firmness with associated marked fibrous adhesions to adjacent diaphragmatic and lateral thoracic wall surfaces. Some plum discoloration was noted in lung parenchyma superior to the lesion. On palpation the structure was somewhat softer centrally. On mid-central transection along the long axis there were small irregular areas of central cavitation within a large cream-colored necrotic core with a caseous texture. Peripherally, there was margination by an irregular, variable thickness rim of grey connective tissue. When excised in a para-sagittal plane there were multiple & coalescing small satellite nodules visible, generally with a similar appearance, although with less overt central necrosis. In the proximal portion of the right upper lobe, just distal to the hilum, there was a large (approximately 1.5 cm) nodular area of parenchymal firmness that was similar in transected appearance to the LLL lesion. No other areas of nodularity or consolidation were observed or palpated in other lung regions.

Clusters of enlarged, plump-appearing thoracic lymph nodes were present, especially in the left and right subclavicular and superior paratracheal regions. On transection, these showed partial effacement of normal cortical-medullary nodal architecture with cream-colored homogeneous tissue. However, no definitively recognizable granuloma structures were observable within them. Approximately 75% of the liver effaced by multifocal and coalescing expansile cream-colored solid but soft nodules. These ranged in size from several millimeters to several centimeters (coalescences). The spleen was enlarged to approximately 4 to 5 times its normal size. Visible centrally within the body was a 3 to 4 cm cream-colored soft mass. This lesion was mottled and soft centrally, suggesting early avascular necrosis. Other smaller solid cream colored masses were present within the splenic parenchyma. The right adrenal gland was massively enlarged (3 to 4 cm) and totally effaced by a similar appearing homogeneous cream colored mass and a 2 cm mass was present in the caudal pole of the right kidney. A large portion of one of the poles of the left adrenal gland was also replaced by a solid, grey-colored mass. Mesenteric lymph nodes were markedly enlarged, homogeneous and without normal-appearing central architecture. The GI tract was considered unremarkable grossly. No lesions were noted in the remainder of the abdominal viscera. Inguinal and axillary lymph nodes were enlarged 2-3 times normal size and had an appearance on cut surface similar to that described for the thoracic lymph nodes examined.

**Laboratory Results**: An acid-fast organism had been recently isolated from a gastric aspirate sample although it was not further speciated.

**Histopathologic Description:** The cavitary lung lesion consists of a massively ectatic and largely destroyed bronchus, as evidenced by the residual fragmented foci of bronchial wall (not visible in all slides). Filling this structure are massive amounts of amorphous, eosinophilic necrotic debris with evidence of early collagen fibril formation within. Easily visible in many areas are large numbers of fungal organisms. These structures are very pleomorphic, with broad, hyaline, ribbon-like, wide-angled branching, pauciseptate irregular hyphae. They often appear as large dilated structures, sometimes with central granular or vacuolated spherical content. Inflammation is abundant, especially along the margins of the cavity and is granulomatous or pyogranulomatous in

nature, consisting of large multinucleated giant cells, macrophages, degenerative neutrophils, eosinophils and a prominent but irregular margin of lymphoplasmacytic cells.

**Contributor's Morphologic Diagnosis:** Necrotizing granuloma(s), focally extensive or multifocal (depending on slide), with numerous visible hyphae, present within an extensively effaced and dilated bronchus (visible in some sections).

**Contributor's Comment**: A primary differential in this case of an SIV immunosuppressed animal with a cavitary lung lesion and isolation of an acid-fast organism on gastric aspiration (GA) was tuberculosis. Cultures of the lung lesions were negative for all *Mycobacterium* species including *M. tuberculosis,* although the monkey was positive for *M. avium* on Prmagam assay and the acid fast organism identified via GA likely originated from the gut. Concurrent disseminated lymphoma accounted for the enlargement and effacement of thoracic and peripheral lymph nodes as well as liver, spleen, kidney and adrenal lesions. Although frank, solid regions of lymphoma were not noted within lung, some of the lymphoid infiltrates surrounding the necrotizing granuloma(s) and in bronchial & vascular associated lymphoid tissue had a prominent component of more blastic appearing cells.

Pulmonary cavities are frequent manifestations of a wide variety of inflammatory processes involving the lung and considerable variation exists in the pathophysiology of their development. The term itself (cavity) has somewhat different pathological and radiological definitions, generally connoting air/gas filled spaces with definable walls of various thicknesses.[9] Other related and overlapping terms include lung abscess (a necrotizing lung infection characterized by pus or other inflammatory material filled cavity) and pulmonary mycetoma. The latter somewhat dated term is occasionally used to reference a fungal ball within a pre-existing lung cavity, although the designation mycetoma more properly refers to a chronic subcutaneous infection caused by actinomyces or fungus. In humans the list of conditions leading to cavitation is extensive.[3] Non-infectious entities potentially resulting in lung cavities include malignancies, rheumatologic diseases (especially Wegener's granulomatosis) and pulmonary infarction and necrosis. A variety of common bacterial infections (*S. pneumonia, H. influenza, Klebsiella pneumoniae*, etc) can cause cavitary pneumonias as well as less common agents such as *Nocardia, Actinomycosis, Burkholderia* (Melioidosis) and *Rhodococcus*. Mycobacterium, both tuberculous and non-tuberculous, are widely known to lead to cavitary change; in fact, *Mycobacterium tuberculosis* generally has the highest prevalence of cavities among persons with pulmonary disease of any infection.[3] Of parasitic causes of lung cavitation, *Echinococcus* and *Paragonimus* are the most commonly mentioned. Fungal etiologies also abound and include *Aspergillus* (often arising as fungal balls within a pre-existing cavity), *Histoplasma*, *Blastomyces*, *Coccidioides*, and *Pneumocystis*.

The fungus causing infection in this animal was identified by culture as *Cunninghamella bertholletiae.* This saprophytic, filamentous species is found primarily in soil and is one member of the *Zygomycetes* class of fungi, diseases from which are broadly referred to as zygomycosis.[2] Molds in this class are comprised of two fungal groups of primary medical importance – the orders *Mucorales* and *Entomophthorales*. Infections caused by *Mucorales* were formerly termed phycomycosis, a term no longer used.[7] *C. bertholletiae* is classified under this order and is the only member of its genus proven to be pathogenic. It has been increasingly reported as an emerging pathogen[4] causing disease in a wide range of immunosuppressed human patients with debilitating factors usually related to diabetes mellitus, corticosteroid treatment or granulocytopenia. Interestingly, T-cell dependent immunity does not play an essential role in the defense of this infection and AIDS patients are not particularly susceptible to these organisms.[5] Infection with *Cunninghamella* has rarely been reported in immunocompetent hosts.[10]

Although spontaneous zygomycosis is recognized not uncommonly in a variety of species,[8] naturally occurring *Cunninghamella* infections are not as widely reported in animals. However, murine models of the disease have been developed.

Whether the monkey in this case had a pre-existing primary cavitary lung lesion of some other pathogenesis (e.g. Trematode parasite, acariasis, etc) which subsequently became colonized after immunosuppression with this zygomycosis or the *Cunninghamella* arrived in conjunction with a primary cavity forming insult and remained contained until SIV infection is not clear – nor will the exact series of events ever be ascertainable. There was no morphological or culture evidence of concurrent infectious or parasitic agents.

**JPC Diagnosis:** Lung: Pyogranuloma, focally extensive, with fungal hyphae, rhesus monkey (*Macaca mulatta*), primate.

**Conference Comment:** As the contributor states in their excellent summary of *Cunninghamella bertholletiae*, naturally occurring infections with this zygomycete fungus are uncommon in animals, despite the ubiquitous nature of these fungi. In a recent report, the first case of *C. bertholletiae* in a marine mammal occurred in a 28-year-old female captive killer whale that died after a three-month history of gastrointestinal disease. Necropsy findings included numerous variably-sized rocks in the gastric compartments associated with ulceration, tubercule-like lesions in the lungs and multiple abscesses

in the pulmonary cavities. Microscopic examination revealed suppurative pneumonia associated with fungal hyphae and numerous bacterial colonies. *Cunninghamella bertholletiae*, as well as *Proteus mirabilis, Pseudomonas aeruginosa and Pseudomonas oryzihabitans* was cultured from the lesions. It is presumed this whale's infection with these opportunistic pathogens was secondary to immunosuppression, and it is hypothesized that the gastric lesions may have played a role in facilitating mycotic proliferation.[1]

In humans, *C. bertholletiae* has been shown to exhibit a higher pathogenicity and a poorer prognosis than infections with other members of the order *Mucorales*, specifically *Rhizopus* and *Mucor* species.[6] Neutrophils play an important role in the clearing of *C. bertholletiae* infection; thus its resistance to neutrophil-induced damage via IL-8 suppression accounts in part for its increased virulence. IL-8 is a potent chemotactic factor and thus its suppression results in a decrease in the number of neutrophils recruited. Other mechanisms of neutrophil suppression, including resistance to iron chelation, fungal mass, and modulation of TNF-alpha related responses, appear to enhance the virulence of this interesting zygomycete.[6]

**Contributing Institution**: Division of Laboratory Animal Resources
S 1040 Biomedical Science Tower
University of Pittsburgh
Pittsburgh, PA 15668
http://www.dlar.pitt.edu/

**References:**

1. Abdo W, Kakizoe Y, Ryono M, Dover SR, Fukushi H, Okuda H, et al. Pulmonary zygomycosis with *Cunninghamella* bertolletiae in a killer whale *(Orcinus orca)*. *J. Comp Pathol.* 2012;147(1):94-99.
2. Chayakulkeeree M, Ghannoum MA, Perfect JR. Zygomycosis: the re-emerging fungal infection. *Eur J Clin Microbiolo Infect Dis*. 2006;25:215-229.
3. Gadkowski LB, Stout JE. Cavitary pulmonary disease. *Clinical Microbiol Rev*. 2008;21(2):305-333.
4. Honda A, Kamei K, Unno H, Hiroshima K, Kuriyama TA. Murine model of zygomycosis by *Cunninhamella* bertholletiae. *Mycopathologia*. 1999;144:141-146.
5. Kamei K. Animal models of zygomycosis – *Agsidia*, *Rhizopus*, *Rhizomucor* and *Cunninhamella*. *Mycopathologia*. 2000;152:5-13.
6. Gomes MZR, Lewis RE, Kontoyiannis DP. Mucormycosis caused by unusual mucormycetes, non-*Rhizopus*, -*Mucor*, and -*Lichtheimia* species. *Clin Microbiol Rev*. 2011;24(2):411–445.
7. Migaki G, Schmidt RE, Toft JF, Kaufmann AF. Mycotic infections of the alimentary tract of nonhuman primates: a review. *Vet Pathol*. 1982;19:93-103.
8. Sondhi J, Gupta P, Sood N. Experimental zygomycosis in rabbits: clinicopathological studies. *Mycopathologia*. 1999;144:29-37.
9. Tuddenham WJ. Glossary of terms for thoracic radiology: recommendations of the nomenclature committee of the Fleischner society. *Am J Roentgenol*. 1984;143:509-517.
10. Zeilender S, Drenning D, Glauser FL, Bechard D. Fatal Cunninghamella bertholletia in an immunocompetent patient. *Chest 97*. 1990;1482-1483.

**CASE II:** 64354 (JPC 4019873).

**Signalment:** Two dams (seven- and four- month-olds) and three pups (one- month -olds), all females, NOD SCID Gamma (NOD.Cg-*Prkdc*$^{scid}$ *Il2rg*$^{tm1Wjl}$/SzJ; NSG), mice (*Mus musculus*).

**History:** Two-month history of high pup mortality and alopecia in NOD.Cg-*Prkdc*$^{scid}$ *Il2rg*$^{tm1Wjl}$/SzJ (NSG) mice. Original NSG mice purchased from Jackson Laboratory about one year previously had produced litters. Their offspring (F1 generation) also bred successfully; however, their pups (F2) developed alopecia at two weeks old, and had significant preweaning mortality. The few surviving pups eventually regrew hair at five to six weeks old and were used for breeding. Two breeding females from this second generation (F2), ages four and seven months, and three pups, all one month old, were submitted to Johns Hopkins Diagnostic Veterinary Pathology Service to evaluate the pup morbidity and mortality.

**Gross Pathology:** Gross examination of the pups and dams revealed variable, multifocal to coalescing, mild to marked alopecia over the dorsum, ventrum and face. The underlying skin was grossly normal, without obvious hyperkeratosis (flaking or scaly skin), erythema, or ulceration. No other gross abnormalities were identified in the pups.

Dam A (4 months old, 25.2 g) and Dam B (7 months old, 20.73 g), were in thin body condition, and had splenomegaly (0.13 and 0.18 g respectively). Dam B also had a grossly visible anterior mediastinal mass, approximately 1cm diameter, in the region of the thymus, with deep invasion into mediastinum and along parietal pleura.


*2-1. Haired skin, NSG mouse: Affected mice exhibit variable alopecia over the dorsum, ventrum and face. The underlying skin was grossly normal, without obvious hyperkeratosis, erythema, or ulceration. (Photo courtesy of: The Department of Molecular and Comparative Pathobiology, Johns Hopkins University, School of Medicine, 733 N. Broadway St., Suite 811, Baltimore, MD 21205; http://www.hopkinsmedicine.org/mcp/index.html)*

**Laboratory Results:** A PCR Rodent Infectious Agents (PRIA) panel was performed on pooled feces, skin and oropharyngeal swabs from the dams and three pups, and was positive for *Corynebacterium bovis* and *Staphylococcus xylosus.* This panel tests for over 35 common mouse microbial agents, including viruses, parasites, bacteria, and fungi.

Automated complete blood counts (CBC) were performed on Dams A and B and are displayed in the included chart.

| | Dam A | Dam B |
|---|---|---|
| WBC (K/µl) | 4.44 | 22.8 |
| NE (K/µl) | 2.64 | 12.8 |
| Ly (K/µl) | 0.99 | 4.11 |
| Eo (K/µl) | 0.25 | 1.79 |
| Ba (K/µl) | 0.02 | 0.17 |
| Mo (K/µl) | 0.54 | 3.92 |
| RBC (M/µl) | 7.91 | 10.44 |
| PLT (K/µl) | 800 | 440 |

**Histopathologic Description:** Skin (from Dam B): Sparsely haired, non-pigmented skin. Diffusely, there is marked orthokeratotic hyperkeratosis, and multifocal small, ~10 µm, 'dusty' intracorneal bacterial colonies within follicles and in superficial keratin. The bacteria are very small basophilic coccobacilli. Multifocally, there is mild but conspicuous thickening of the stratum spinosum up to 5 cell layers (acanthosis), and the superficial dermis contains low numbers of lymphocytoid mononuclear cells.

Transverse section of head, decalcified (from Dam A): Expanding the bone marrow and spilling out into the adjacent subdural space and meninges, and ventrally surrounding the pituitary and cranial nerves, is an unencapsulated, poorly delineated, neoplastic cellular infiltrate consisting of a monomorphic population of round cells (lymphocytes) multifocally coalescing into densely cellular sheets. Cytomorphology is somewhat compromised by demineralization of the head specimen; however, neoplastic lymphocytes are characterized by distinct cell borders, a moderate amount of eosinophilic granular cytoplasm, a round to oval centrally located nucleus, stippled chromatin, and occasionally 1-2 indistinct nucleoli. Mitoses are 0-1/HPF, and anisocytosis and anisokaryosis are minimal. There is multifocal minimal hemorrhage, and mild individual cell necrosis (pyknotic nuclei, and karyorrhectic debris).

**Contributor's Morphologic Diagnosis:** 1. Skin, dam: Hyperkeratosis, orthokeratotic, diffuse, marked with mild

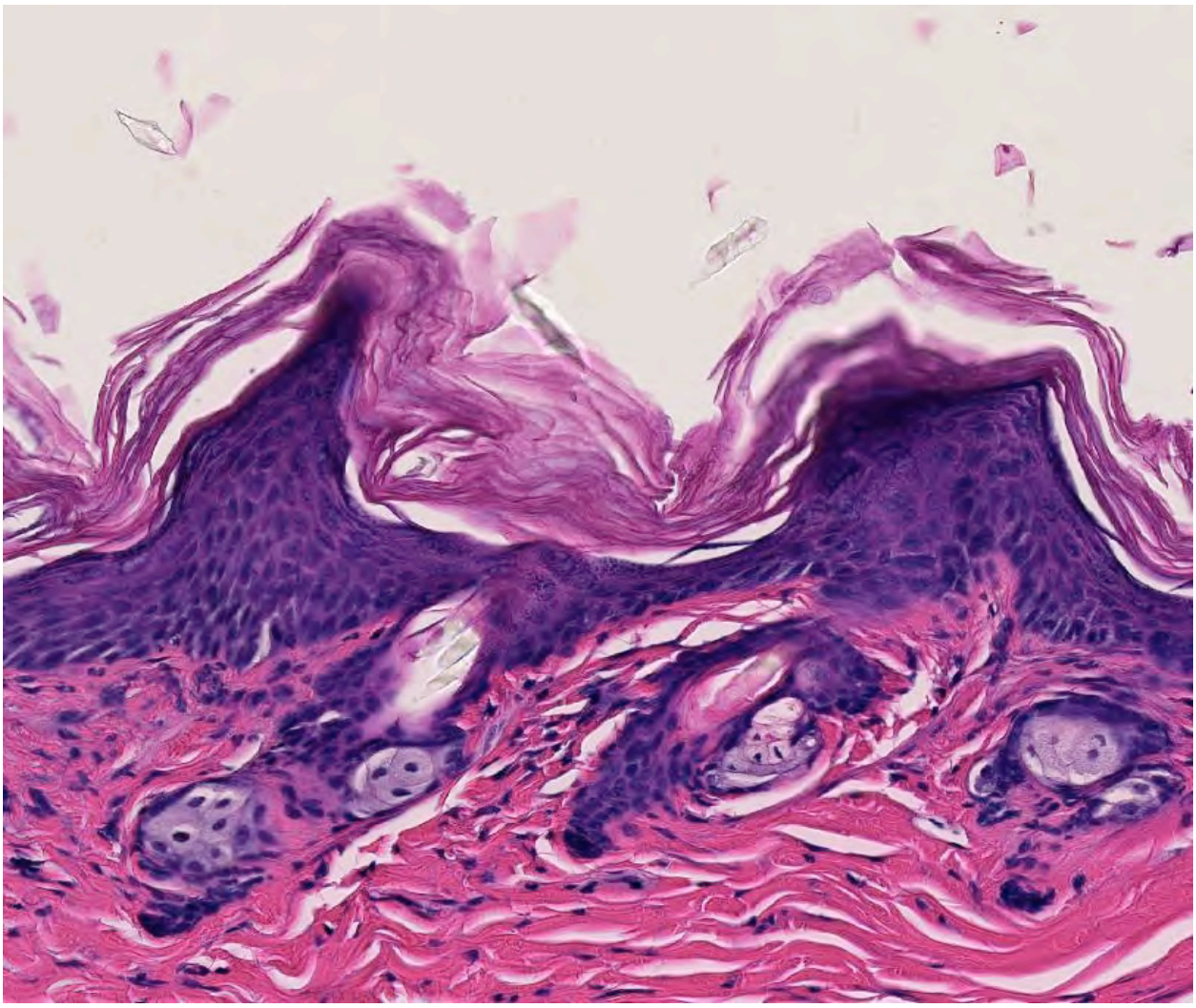

*2-2. Haired skin, NSG mouse: There is diffuse epidermal hyperplasia with marked orthokeratotic hyperkeratosis. (HE 320X)*

acanthosis, minimal non-suppurative dermatitis, and intracorneal bacterial colonies
2. Head, dam, bone marrow, meninges, subdural space: Lymphoma, leukemia.

**Contributor's Comment:** NOD.Cg-*Prkdc*$^{scid}$ *Il2rg*$^{tm1Wjl}$/SzJ, mice, commonly referred to as NSG, are a relatively new immunodeficient genotype that is becoming increasingly popular in biomedical research. NSG has a loss of function mutation in the IL-2 receptor gamma chain, bred onto the NOD-scid background. NSG mice are expected to be completely deficient in lymphocytes (B, T, and NK cells), have undetectable serum Ig, and disrupted cytokine signaling. Their lack of NK function, lack of leakiness, lymphoma resistance, and relatively good breeding performance confer important advantages over scid, NOD-scid and nude mice. NSG mice are becoming increasing popular in studies involving tumor transplantation (solid or hematogenous), hematopoietic engraftment, and infectious and autoimmune diseases.[2,7] They are highly susceptible to opportunistic infections.

In the current case, histopathology of pups combined with PCR results confirmed infection with *Corynebacterium bovis* in this NSG colony. The section on this slide is from the worst affected of the 2 dams. *Corynebacterium bovis*, the agent of "scaly skin disease" in mice, is a commensal and opportunistic bacterial agent that causes hyperkeratosis, pup mortality, and failure to thrive in susceptible mouse strains including immunodeficient nude, NOD SCID, and NSG mice.[1,2,3,7] Morbidity can be high, as transmission and persistence in the environment are associated with shedding of the infected keratin flakes.[8] Mortality is generally low, except in young/suckling mice.[8] Some immunocompetent mice may develop skin disease, but often harbor the bacteria without clinical signs, and thus serve as a reservoir, making it difficult to eradicate. Additionally, bacteria can persist in the environment, and

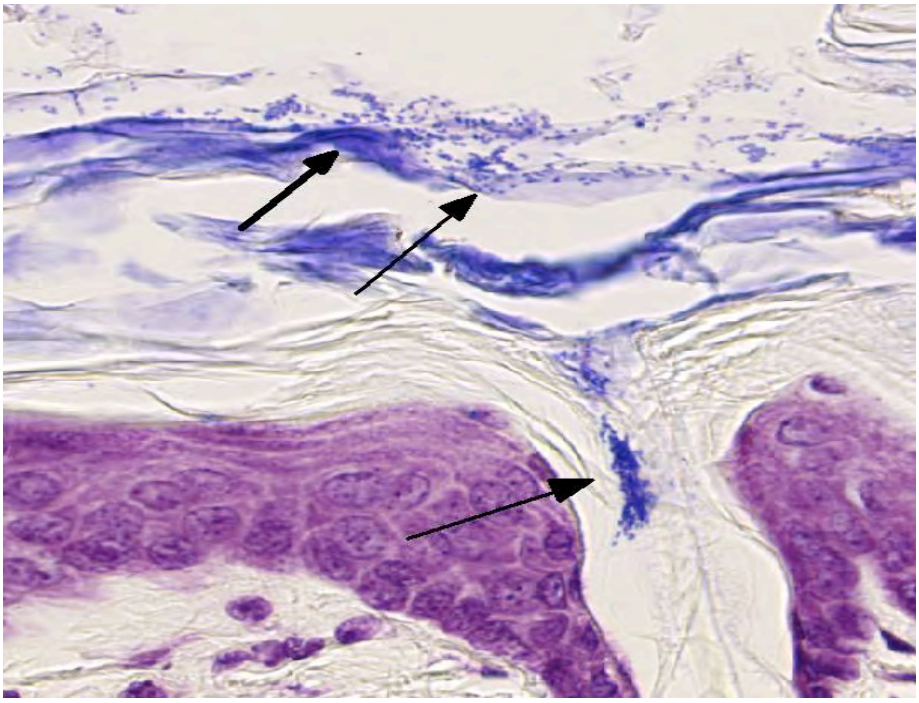

*2-3. Haired skin, NSG mouse: Within the hyperkeratotic scale and concentrated within follicles, there are numerous gram-positive 2-3 µm rod-shaped bacilli consistent with Corynebacterium bovis. (Gram 400X)*

can spread through sloughed keratin debris to other cage mates, or iatrogenically through handlers, which serve as a vehicle for transmission.[1,8] In addition to *C. bovis* infection, histologic evaluation of the gastrointestinal tract revealed a diverse enteric flora, including protozoa, corroborating the conventional microbial status of these animals. These findings strongly suggest that severely immunodeficient NSG mice require more stringent barrier conditions and microbial exclusion in order to thrive and be useful for research purposes.[10] The very mild dermatitis here was characterized as non suppurative, instead of lymphocytic or lymphoplasmacytic, because mice this genotype are expected not to have lymphocytes.

Interestingly, both submitted dams from this small group of breeding NSG mice had disseminated lymphoma with marrow and vascular involvement (leukemia). The head section is from Dam A. Cytomorphology, which is easier to assess in non-decalcified tissues, was consistent with a lymphoblastic lymphoma. Immunohistochemistry (on Dam A) was positive for CD3 and CD43, and negative for B220 and PAX5. These findings are consistent with T cell lymphoblastic lymphoma.[6] A similar presentation of lymphoma has been reported in the NOD.Cg-*Prkdc*$^{scid}$ *Il2rg*$^{tm1Sug}$/JicTac mouse, sometimes called NOG, which is also on a NOD.scid background but has a different loss of the function mutation in Il2rg.[5] These findings represent the first documented reports of lymphoma in NSG mice, which have been considered to be completely lymphocyte deficient, resistant to lymphocyte 'leakiness' and resistant to lymphoma.[7] Immune stimulation associated with *Corynebacterium bovis* and other agents encountered with less stringent barrier conditions may predispose to lymphoma, and may compromise the research value and

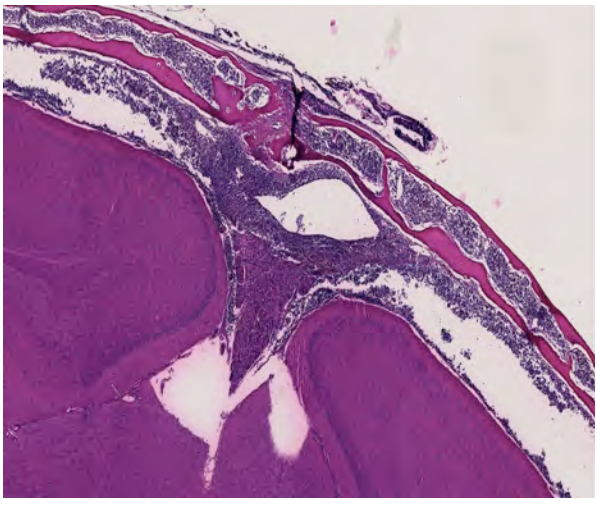

*2-4. A cross section of the skull demonstrates an infiltrate of neoplastic lymphocytes within the meninges and also infiltrating the marrow spaces of the overlying cranium. (HE 48X)*

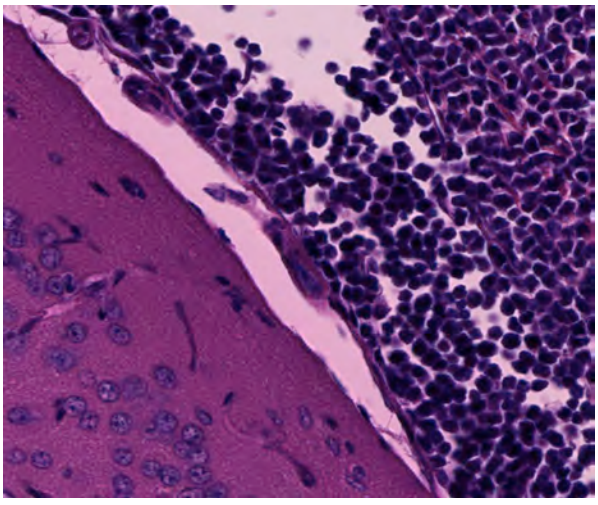

*2-5. Unfortunately, decalcification of the section precludes detailed analysis of cytomorphology of the neoplastic lymphocytes in the sections received by conference participants. (HE 400X)*

lifespan of immunodeficient mice.

**JPC Diagnosis:** 1. Haired skin: Hyperkeratosis, orthokeratotic, diffuse, moderate, with moderate epidermal hyperplasia and intracorneal bacilli.
2. Head, at level of hippocampus, cranial bone marrow, meninges, and tissues ventral to brain: Lymphocytic leukemia.

**Conference Comment:** Conference participants found this first report of lymphoma in NSG mice, so well described by the contributor, to be particularly interesting. While speculating on possible mechanisms, several questions arose, including the following: Could these neoplastic cells have arisen from a monocytic precursor? If so, what triggered the differentiation that resulted in expression of the identified markers? Are the circulating lymphocytes functional? It will be interesting to see future developments or any further reports of similar lesions in other NSG mice.

The use of various stains of *scid* mice in biomedical research originated from four littermates of the C.B-17 inbred strain that were found to lack IgM, IgG1, and IgG2a during a serum immunoglobulin quantitation study in 1983. These mice lacked both T and B lymphocytes because of a heritable recessive mutation, similar to a condition reported in humans.[9] *Scid* mice have a spontaneous loss-of-function mutation of the protein kinase, DNA activated, catalytic polypeptide (*Prkdc*) gene. Prkdc plays a role in repairing double-stranded DNA as well as in recombining the variable (V), diversity (D) and joining (J) segments of immunoglobulin and T cell receptor genes. Because of their inability to complete V(D)J gene recombination, T and B cells cannot mature; thus affected animals cannot develop cell mediated or humoral immune responses.

The penetrance of the *scid* mutation varies, and reduced penetrance can result in animals that are "leaky," developing immunoglobulin and T and B cells as they age.[3] Approximately 15% of *scid* mice have detectable serum Ig and functional T cells, and 15% of aged C.B17/Icr-*scid/scid* mice and 67% of 40-week-old NOD *scid/scid* mice develop thymic T-cell lymphomas.[9] Thus, as the contributor states, NSG mice, which are generally resistant to such "leakiness" are becoming increasingly popular in research. Nonetheless, the contributor provides a compelling argument that exposure to opportunistic pathogens may both circumvent the strain's natural resistance to leakiness, and contribute to the development of lymphoma; this case, therefore, underscores the importance of maintaining strict barrier conditions and microbial exclusion to preserve the research value of immunodeficient mice.

The relatively non-specific JPC histologic diagnosis of "lymphocytic leukemia" is based on the evaluation of hematoxylin- and eosin-stained sections available to conference participants. We believe that this diagnosis is attainable by conference participants; a more specific diagnosis of T-cell lymphoblastic leukemia would be appropriate if participants had access to non-decalcified sections and immunohistochemical studies performed by the contributor.

**Contributing Institution**: The Department of Molecular and Comparative Pathobiology
Johns Hopkins University
School of Medicine
733 N. Broadway St., Suite 811
Baltimore, MD 21205
http://www.hopkinsmedicine.org/mcp/index.html

**References:**

1. Burr HN, Lipman NL, White JR, Zheng J, Wolf FR. Strategies to prevent, treat, and provoke *Corynebacterium*-associated hyperkeratosis in athymic nude mice. *Journal of American Association for Laboratory Animal Science.* 2011;50:378-388.
2. Foreman O, Kavirayani AK, Griffey SM, Reader R, Shultz LD. Opportunistic bacterial infections in breeding colonies of the NSG mouse strain. *Vet Pathol.* 2011;48:495-499.
Jackson Laboratory Mouse Strain Data. *Scid* mice overview. http://jaxmice.jax.org/support/straindata/scid.html. Accessed 2 March 2013.
3. Jacoby RO, Fox JG, Davidson M. Biology and diseases of mice. In: Fox JG, Anderson LC, Loew FM, Quimby FW, eds. *Laboratory Animal Medicine*. 2nd ed. San Diego, CA; Elsevier Science. 2002:92-93.
4. Kato C, Fujii E, Chen YJ, Endaya BB, Matsubara K, Suzuki M, et al. Spontaneous thymic lymphomas in the non-obese diabetic/Shi-scid, IL-2R $\gamma^{null}$ mouse. *Laboratory Animals.* 2009;43:402-404.
5. Morse HC, Anver MR, Fredrickson TN, Haines DC, Harris AW, Harris NL, et al. Bethesda proposals for classification of lymphoid neoplasms in mice. *Blood.* 2002;100:246-258.
NOD.Cg-Prkdc$^{scid}$ Il2rg$^{tm1Wjl}$/SzJ. The Jackson Laboratory. Bar Harbor, ME. http://jaxmice.jax.org/literature/factsheet/SFS0001_005557.pdf, 2010
6. Scanziani E, Gobbi A, Crippa L, Giusti AM, Pesenti E, Cavalletti E, et al. Hyperkeratosis-associated coryneform infection in severe combined immunodeficient mice. *Laboratory Animals.* 1998;32:330-336.
7. Sudenberg JP, Shultz LD. The Severe Combined Immunodeficiency (scid) Mutation. JAX® Notes. 1993: 453. http://jaxmice.jax.org/jaxnotes/archive/453a.html. Accessed online on 2 March 2013.
8. Treuting PM, Clifford CB, Sellers RS, Brayton CF. Of mice and microflora: considerations for genetically engineered mice. *Veterinary Pathology.* 2012;49:44-63.

**CASE III:** 08-076G (JPC 3144240).

**Signalment:** Three-week-old, male, Mox-2 Cre transgenic mouse *(Mus musculus)*.

**History:** A mass was noted on left front leg.

**Gross Pathologic Findings:** A firm mass encompassed the left front leg from the shoulder to the paw (~2 cm in diameter).

**Histopathologic Description:** A cross-section of the left forelimb has an unencapsulated, expansile, and infiltrative mass expanding the dermis, extending into the subcutis, and replacing skeletal muscle. The mass is composed of densely-packed neoplastic cells haphazardly arranged as long and short interweaving streams and bundles within a minimal fibrovascular matrix. Neoplastic cells are predominantly spindle-shaped with some ovoid profiles; have abundant granular to fibrillar amphophilic cytoplasm; and prominent round to oval nuclei with marginalized chromatin and multiple magenta nucleoli. Many of these cells are quite long with a fairly consistent width, and fusiform nuclei (presumed strap cells). Neoplastic cells exhibit marked anisocytosis, anisokaryosis, and pleomorphism. Mitoses are numerous, varying between ~2 to ~10 per high-power field (40x). Multinucleated giant cells with abundant eosinophilic cytoplasm and 2 to 5 nuclei clustered at the periphery are frequently present (racket cells). Multifocal areas of the neoplasm are necrotic with hemorrhage and copious cytoplasmic and karyorrhectic debris. Small bundles of skeletal muscle entrapped by neoplastic cells are present at the periphery of the mass adjacent to sections of cortical bone. Mild edema (clear spaces) and moderate aggregates of lymphocytes and plasma cells multifocally expand the superficial dermis. The overlying epidermis has multiple variably sized ulcers with replacement by moderate amounts of degenerate neutrophils and eosinophilic debris. Small pockets of degenerate neutrophils are occasionally apparent within the stratum corneum.

**Contributor's Morphologic Diagnosis:** Left forelimb, skeletal muscle: Rhabdomyosarcoma.

**Contributor's Comment:** Spontaneous rhabdomyosarcomas in mice are rare with those of skeletal muscle occurring more often than those of the heart.[6] Rhabdomyosarcomas are typically induced experimentally via exposure to a variety of viruses, metals, and/or chemical carcinogens.[6] An investigation at the Jackson Laboratory identified 14 spontaneous well-differentiated rhabdomyosarcomas out of 10,000 mice, approximately 4 months old.[7] Landau et al[3] found a higher incidence of rhabdomyosarcomas (34% of controls); however, these mice were approximately 14 months old.

The mouse currently described was transgenic for the Mox-2 gene, which is an important regulator of vertebrate limb myogenesis.[4,8] Mox-2 is part of a cohort of genes important to normal myogenic differentiation. Historically, mice homozygous for a null mutation of Mox-2 have a developmental defect of the limb musculature, characterized by an overall reduction in muscle mass and elimination of specific muscles (www.jax.org).

Identification of strap cells may be difficult by light microscopy; however, phosphotungstic acid-hematoxylin (PTAH) stain is useful for identification of cross-

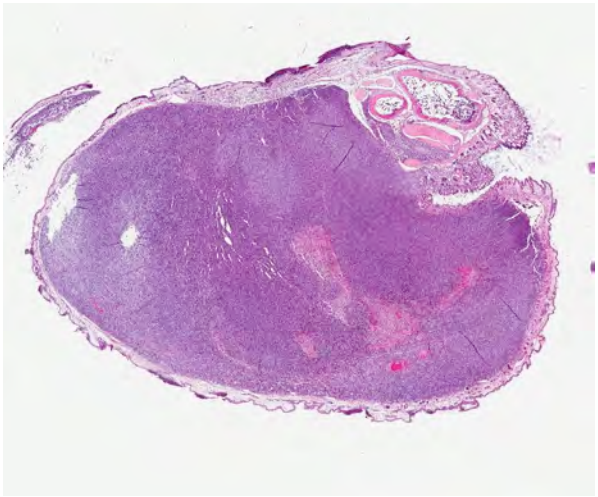

*3-1. Left forelimb, Mox-2 Cre transgenic mouse: The limb is expanded up to 10 times normal diameter by an infiltrative mesenchymal neoplasm. (HE 40X)*

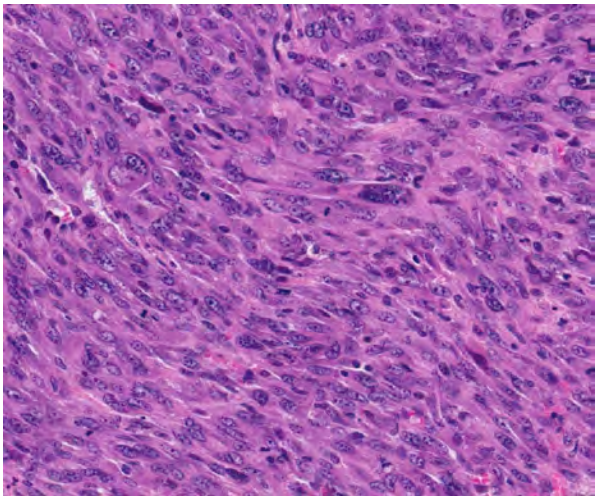

*3-2. Left forelimb, Mox-2Cre transgenic mouse: The neoplasm is composed of mildly pleomorphic spindle cells arranged in broad streams. Neoplastic cells exhibit occasionally large nuclei, and often multiple nuclei arranged along the long axis of the cell. Mitotic figures are common. (HE 320X)*

striations.[6,5] Malignant fibrous histiocytoma and leiomyosarcoma are differential diagnoses for rhabdomyosarcoma.[6] Immunolabels useful for differentiating these neoplasms include pan myosin, sarcomeric actin, desmin, actin, myosin, and smooth muscle actin.[7] The most useful antibodies are those that react with sarcomeric or smooth muscle actin.

**JPC Diagnosis:** Skeletal muscle, left forelimb: Rhabdomyosarcoma.

**Conference Comment:** Rhabdomyosarcomas (RMS) occur infrequently in domestic animals, as they do in mice. A recent publication reviewed the classification and pathogenesis of this diverse group of rare tumors, comparing canine rhabdomyosarcomas with those that occur in humans and with other canine soft tissue sarcomas.[1] Although in veterinary medicine rhabdomyosarcomas are often categorized as high grade soft tissue sarcomas, they are excluded from the soft tissue sarcoma grading scheme as recently proposed by Dennis et al.[2]

Diagnosis and classification is difficult due to their variation in phenotype, cellular morphology and age of onset. It is likely that some RMS are diagnosed as "undifferentiated sarcomas", "anaplastic sarcomas" or " poorly differentiated sarcomas", since skeletal muscle differentiation is not always evident by light microscopy. Therefore, immunohistochemistry can aid in the diagnosis. In addition to the immunolabels discussed by the contributor, MyoD1 and myogenin (early embryological transcription factors involved in mesoderm cell differentiation into myoblasts, myoblast proliferation and myoblast differentiation into myotubules) are associated with RMS of more undifferentiated cells.

Transmission electron microscopy can also aid in the diagnosis; however, EM is not helpful in classification, as several subtypes exhibit similar subcellular structures, including Z-lines, numerous mitochondria, myofilament tangles, and myosin-ribosome complexes.[1]

Canine classification of RMS is similar to the human classification of RMS, with the following subclasses:

- Embryonal, in which cells occur in different stages of development (from myoblast to myotubular) on a mucinous stroma. These occur in both juveniles and adults, and occur more frequently on the face, skull, within masticatory muscles, the oropharynx, trachea, axilla, scapula, perirenal, tongue, flank, leg, mammary gland, and hard palate. In the myotubular variant of embryonal RMS myotubule forms predominate; whereas large myoblast cells predominate in the rhabdomyoblastic variant and streams of plump spindle cells predominate in the spindle cell variant.[1]
- Botryoid RMS have a characteristic submucosal location and gross appearance that resembels grape-like masses. Histologically they appear as mixed round, undifferentiated myoblast cells and multinucleated myotubular cells on a mucinous stroma. These tend to occur in the urinary bladder or uterus in juveniles.[1]
- Alveolar RMS occur in juveniles and are usually found in the hip, maxilla, greater omentum or uterus. The classic variant is characterized by fibrous bands that divide small round cells into clusters and loose aggregates, while the solid variant is composed of closely packed cells with or without a thin fibrous septa.[1]
- Pleomorphic RMS typically occur in adult skeletal muscle. They are characterized by haphazardly arranged plump spindle cells with marked anisocytosis and anisokaryosis and bizarre mitotic figures.[1]

More studies are needed to determine if these classifications have prognostic significance in veterinary medicine.[1]

**Contributing Institution:** National Institute of Environmental Health Sciences
P.O. Box 12233
Research Triangle Park, NC 27709
http://ntp-server.niehs.nih.gov/

**References:**

1. Caserto BG. A comparative review of canine and human rhabdomyosarcoma with emphasis on classification and pathogenesis. *Vet Pathol Online First.* Published online 25 February 2013. Accessed online 2 March 2013.
2. Dennis MM, McSporran KD, Bacon NJ, Schulman FY, Foster RA, Powers BE. Prognostic factors for cutaneous and subcutaneous soft tissue sarcomas in Dogs. *Vet Pathol.* 2011;48(1):73-84.
3. Landau JM, Wang ZY, Yang GY, Ding W, Yang CS. Inhibition of spontaneous formation of lung tumors and rhabdomyosarcomas in A/J mice by black and green tea. *Carcinogenesis*. 1998;19:501-507.
4. Mankoo BS, Collins NS, Ashby P, Grigorieva E, Pevny LH, Candia A, et al. Mox2 is a component of the genetic hierarchy controlling limb muscle development. *Nature*. 1990;400:69-73.
5. Leininger JR. Skeletal muscle. In: Maronpot RR, ed. *Pathology of the Mouse.* St. Louis, MO; Cache River Press. 1999;640-642.
6. Mohr U, ed. *International Classification of Rodent Tumors, The Mouse*. Berlin, Heidelberg: Springer-Verlag. 2001;385, 386.
7. Sundberg JP, Adkison DL, Bedigian HG. Skeletal muscle rhabdomyosarcomas in inbred laboratory mice.

*Veterinary Pathology*. 1991;28:200-206.
8. Tiffin N, Williams, RD, Robertson D, Hill S, Shipley J, Pritchard-Jones K. WT1 expression does not disrupt myogenic differentiation in C2C12 murine myoblasts or in human rhabdomyosarcoma. *Experimental Cell Research*. 2003;287:155–165.

**CASE IV:** N47/09 (JPC 3149877).

**Signalment:** 8-year-old, castrated male, domestic short hair, feline *(Felis domesticus)*.

**History:** This cat was referred to the University Veterinary Hospital, University College Dublin with a two-month history of weight loss. It presented with periorbital alopecia, nasal discharge, pale mucus membranes and a heart murmur. Blood tests revealed a severe non-regenerative anaemia, neutropaenia and thrombocytopaenia.

**Gross Pathologic Findings:** The cat presented in poor body condition with pale mucus membranes. Focal areas of alopecia extended over both upper eyelids to the bases of both ears, and red crusted lesions were present over the upper eyelids and lateral canthuses (more extensive on the right). The right third eyelid was thickened and erythematous as were the nasal conchae. The nasal planum, particularly on the right, had a dry, crusty and flaky appearance. There was a small amount of serohaemorrhagic pericardial fluid. The mesenteric lymph nodes were enlarged and on sectioning contained mottled red and pale pink areas. The bone marrow was dark red in color and filled the marrow space.

**Histopathologic Description:** Multifocal ulcers covered by serocellular crust are present on the anterior surface of the eyelid. There is a moderate perifollicular and mural follicular inflammatory infiltrate consisting of macrophages, occasional neutrophils, lymphocytes and plasma cells along with a large numbers of mast cells. Hair follicles often contain mites. Multiple large areas of ulceration covered by a serocellular crust are apparent on the conjunctival surface of the eyelid and moderate neutrophilic and lymphocytic infiltration is apparent in the underlying mucosa. Epithelial cells immediately adjacent to the ulcerated areas are enlarged and occasionally contain large eosinophilic to amphophilic intra-nuclear inclusion bodies with marginated chromatin. There are accompanying necrotic 'ghost' epithelial cells.

Additional histological lesions include an ulcerative lymphoplasmacytic rhinitis and bone marrow hypercellularity with a reduced erythroid ratio (not submitted).

**Contributor's Morphologic Diagnosis:** 1. Severe acute ulcerative conjunctivitis with intralesional intranuclear inclusion bodies consistent with feline herpesvirus infection.
2. Subacute ulcerative folliculitis with intralesional mites suggestive of *Notoedres cati.*

**Contributor's Comment:** Feline herpesvirus 1 (FHV-1) is a common, worldwide infection of domestic cats of high morbidity and low mortality. A member of the alphaherpes virus subfamily, latency often develops after infection.[2,6] Up to 90% of tested cats are seropositive for this virus.[6]

Most cats are infected as kittens, developing conjunctivitis, corneal ulceration or rhinitis of varying severity depending on viral strain and host susceptibility. The virus replicates in epithelial cells at temperatures below 37° Celsius and so its preferential proliferation sites are peripheral locations such as ocular and nasal mucosa. The virus damages tissue by direct cytolysis during replication and secondarily by immune-mediated inflammation. Cytolysis results in corneal ulceration, conjunctivitis with ulceration and rhinitis with erosions. Immune-mediated injury is less common and results in stromal keratitis. In primary infections the most common presenting lesion is conjunctivitis.[2,7]

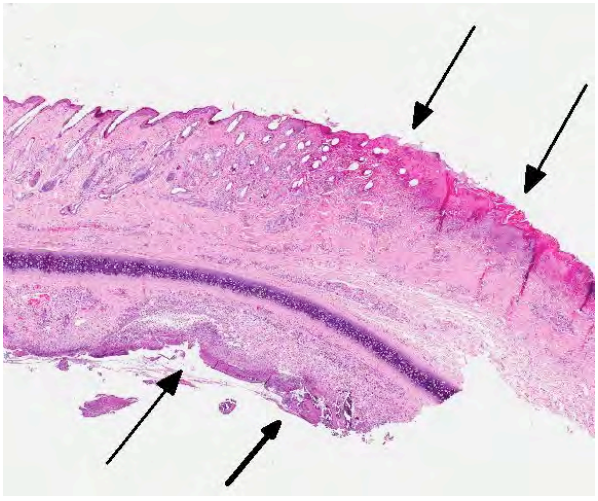

*4-1. Eyelid, cat: Foci of ulceration (arrows) are present within both the haired skin and conjunctival surface of the eyelid. (HE 4X)*

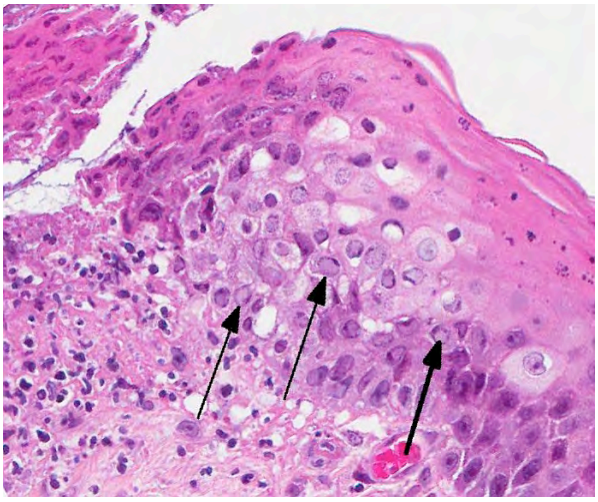

*4-2. Eyelid, conjunctival surface: At the edge of an area of ulceration, mucosal epithelial nuclei are enlarged by a smudgy, amphophilic intranuclear viral inclusion. (HE 400X)*

Up to 80% of infected cats go on to develop virus latency, typically in the trigeminal nerve, from which latency associated transcripts of FHV-1 have been demonstrated. More recently, evidence of persistent low-grade viral infection has been demonstrated in the cornea.[2,6,7] In approximately 50% of carriers, reactivation of infection can occur either spontaneously or during periods of stress or corticosteroid administration. Classically, this is associated with centrifugal spread of the virus from the trigeminal nerve along the sensory nerves to the original epithelial site of invasion. Upon reactivation, viral shedding recommences and this can be with or without recrudescence of clinical signs. With reactivation, the most common presenting clinical sign is conjunctivitis.[2]

*Notoedres cati* (feline scabies) is a rare, highly contagious ectoparasite of cats causing alopecia with adherent crusts around the head and ears, particularly the ear pinna. Histologically the parasite triggers superficial dermatitis with eosinophil-rich perivascular inflammation.[3]

**JPC Diagnosis:** 1. Eyelid: Blepharoconjunctivitis, ulcerative, focally extensive, severe with intranuclear viral inclusions.
2. Haired skin, eyelid follicles and sebaceous glands: Adult arthropod parasites, etiology consistent with *Demodex cati*.

**Conference Comment:** The contributor provides an excellent review of feline herpesvirus-1. Conference participants discussed the three most common clinical differential diagnoses for upper respiratory disease in cats, specifically feline viral rhinotracheitis (caused by FHV-1), feline calicivirus rhinitis (caused by feline calicivirus) and feline chlamydiosis (caused by *Chlamydophila felis*).[5] In general, feline viral rhinotracheitis manifests clinically as rhinitis, conjunctivitis and/or ulcerative keratitis; whereas, feline calicivirus often causes rhinitis, conjunctivitis, ulcerative gingivitis and stomatitis[5] and signs of *Chlamydophila felis* infection are often limited to rhinitis and conjunctivitis. Participants noted that these differences in presentation can be helpful in making a clinical diagnosis.

Dr. Chris Gardiner, JPC consultant in veterinary parasitology, believes these arthropods are more consistent with *Demodex* rather than *Notoedres cati* and provided by following justification: "…The mites in this specimen are elongate and found within the hair follicles; whereas, *Notoedres cati* mites are dorsoventrally flattened, similar to other members of the Family *Sarcoptidae,* and are typically observed in the stratum corneum.[1,4] Additionally, *Demodex* spp. are the only parasitic mites in which all four pairs of appendages originate together. *Notoedres* mites, on the other hand, have two pairs of two appendages that originate together separated by a space from another two pairs of two appendages that originate together." (C.H. Gardiner, personal communication).

**Contributing Institution**: UCD Veterinary Sciences Centre
UCD School of Agriculture
Food Science and Veterinary Medicine
University College Dublin
Belfield, Dublin 4
Ireland
www.ucd.ie

**References:**

1. Bowman, DD. Arthropods. In: *Georgis' Parasitology for Veterinarians.* 9th ed. St. Louis, MO: Saunders Elsevier; 2009:64-66.
2. Gaskell R, Dawson S, Ramford A, Thiry E. Feline herpesvirus. *Vet Res*. 2007;38:337-354.
3. Ginn PE, Mansell JEKL, Rakich PM. Skin and appendages. In: Maxie MG, ed. Jubb, Kennedy and Palmer's Pathology of Domestic Animals. 5th ed. vol. 1. Philadelphia, PA: Elsevier Saunders; 2007:721-722.
4. Hargis Am, Ginn PE. The integument. In: Zachary JF, McGavin MD, eds. *Pathologic Basis of Veterinary Disease.* St. Louis MO: Elsevier Mosby; 2012:1043.
5. Lopez A. Respiratory system, mediastinum, and pleurae. In: Zachary JF, McGavin MD, eds. *Pathologic Basis of Veterinary Disease.* St. Louis MO: Elsevier Mosby; 2012:473.
6. Maggs DJ. Update on pathogenesis, diagnosis and treatment of feline herpesvirus type 1. *Clin Tech Small Anim Pract*. 2005;20:94-101.
7. Wilcock BP. Eye and ear. In: Maxie MG, ed. *Jubb, Kennedy and Palmer's Pathology of Domestic Animals.* 5th ed. vol. 1. Philadelphia, PA: Elsevier Saunders; 2007:490-491.

**Joint Pathology Center**
**Veterinary Pathology Services**

# WEDNESDAY SLIDE CONFERENCE 2012-2013

## Conference 17

**06 March 2013**

---

**CASE I:** WSVL 08B4372 (JPC 3187132).

**Signalment:** Stillborn, late-term, male Red Angus calf *(Bos taurus)*.

**History:** A registered Red Angus seedstock and cow-calf operation in northern Wyoming recognized a distinctive syndrome of late-term abortions/stillbirths in 2008. It occurred after genetic disease was recognized in progeny of one bull's full brother on a property in Kansas. The

*1-1. This 8-month-old premature stillborn calf had a flat skull, impacted molars, short mandible (brachygnathia inferior), and a protuberant tongue. (Photo courtesy of: Wyoming State Veterinary Laboratory, 1174 Snowy Range Road, Laramie, WY 82072, http://wyovet.uwyo.edu/)*

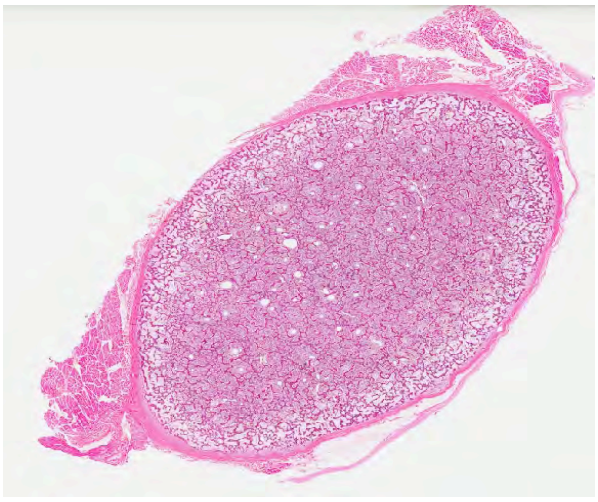

*1-2. Rib, Angus calf: The medullary cavity of this cross-section of rib is expanded and filled with anastomosing trabeculae of primary spongiosa. Lamellar cortical bone is markedly thinned – this finding suggests that the cross section was taken either at the metaphysis distal to the growth plate, or in the diaphysis, and that there is marked cortical osteopenia. (HE 40X)*

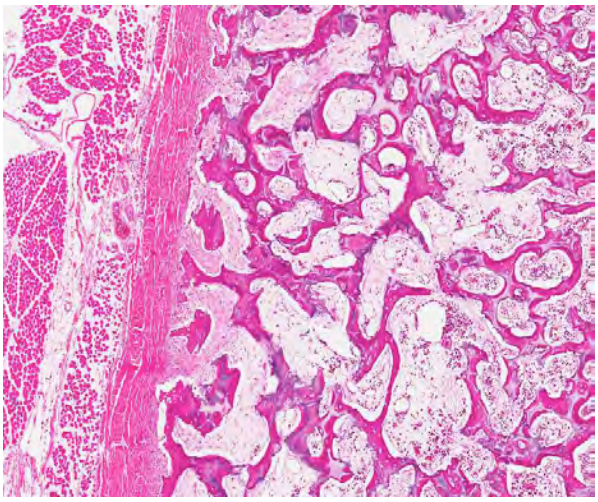

*1-3. Rib, Angus calf: Higher magnification of primary spongiosa subjacent to the cortex. The cortex is markedly osteopenic, and marrow spaces are hypocellular. (HE 320X)*

Wyoming rancher was concerned the bull he owned had the same trait, and bred one bull, BUF CRK Romeo L081, to 25 of his daughters. The goal was to establish that this valuable bull was free of the trait. Unfortunately, of 25 calves born to Romeo and his daughters in 2008, 5 were identical to malformed calves born to the bull's full brother in Kansas. All five were stillborn or premature (7 months – term).

**Gross Pathologic Findings:** This calf had a flat skull, impacted molars, short mandible (brachygnathia inferior), and a protuberant tongue. Gestational age was approximately 8 months.

**Laboratory Results:** Negative for bovine viral diarrhea virus by attempted virus isolation.

**Histopathologic Description:** Rib; persistent primary spongiosa, with empty resorption lacunae and scant osteoclasts.

**Contributor's Morphologic Diagnosis:** Osteopetrosis.

**Contributor's Comment:** Osteopetrosis has been recognized in the Angus breed since the 1960s, when a series of studies by Dr. Horst Leipold and colleagues documented the condition following an initial case report from New York.[2,5,6] The gross appearance of calves is distinctive. It is one of the few abortifacient inherited diseases in cattle that can be diagnosed with confidence over the telephone when concerned ranchers phone veterinarians or their diagnostic laboratory.

Gross diagnosis is established by splitting long bones and demonstrating persisting primary spongiosa in the medullary cavity. Histologically, osteoclasts are markedly reduced in number, in spite of the presence of resorption lacunae. In this section of rib there are scant osteoclasts. Where present, they are lightly stained with washed out vesicular nuclei.

The basis for the defect is a mutation in the anion exchanger protein coded for by SLC4A2 on chromosome 4. A similar mutation causes osteopetrosis in mice.[1,7] To date, no comparable mutation has been recognized in severe forms of osteopetrosis in children. Human osteopetrosis is classified morphologically into forms with reduced, normal or excessive numbers of osteoclasts. In Angus cattle it is likely that absence of the anion exchanger results in alkalinized cytoplasm, resulting in death of osteoclasts.[3] Death *in utero* is due to compression of the cerebral cortex with posterior herniation of cerebellum as a result of osseous crowding in the cranial vault.[4] An important diagnostic rule out is osteopetrosis due to *in utero* infection with bovine viral diarrhea virus. In this instance this and other calves sired by the bull were negative for BVDV.

**JPC Diagnosis:** Bone, rib: Persistent primary cartilaginous spongiosa with osteoclastopenia.

**Conference Comment:** The contributors published an excellent report of the calves in this case, with gross and histopathologic descriptions as well as comparisons with osteopetrosis conditions in humans.[4] Although, as the contributor explains, osteopetrosis can be caused by several genetic mutations, all affected individuals share similar clinical characteristics (increased skeletal mass, increased likelihood of fractures and neurological complications).[4]

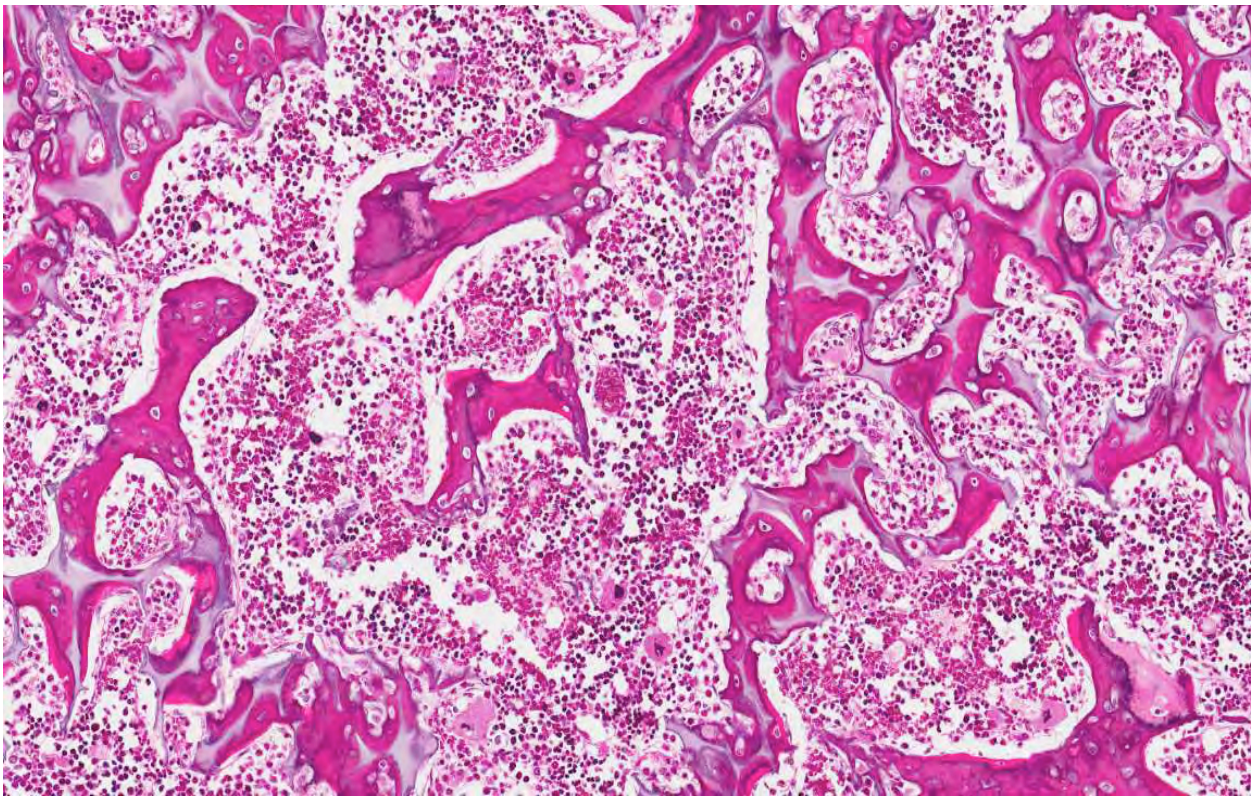

*1-4. Rib, Angus calf: Primary spongiosa have scalloped edges, however, they are largely devoid of osteoblasts, and Howship's lacunae are empty. The presence of retained cartilage cores identifies these trabeculae as primary spongiosa. (HE 400X)*

The distinctive gross appearance of affected calves identified by the contributor are:

- compression of cerebral hemispheres with herniation of the cerebellar vermis into the foramen magnum
- dorsoventrally compressed brain with a concave depression in the parietal cortex
- thickened parietal bone
- mildly proptosis
- protruding tongue
- brachygnathia inferior
- restricted movement of temporomandibular joints
- loose, misaligned, not fully erupted inscisors
- misaligned and unerupted molars
- abnormally smooth cranial calvarium surface with prominent bilaterally symmetrical bony ridges at the frontal-parietal synchondrosis and a corresponding depression in the temporoparietal cortex
- 1-2 cm fontanelle between frontal and parietal bones
- bilaterally symmetrical transverse ledge of bone at the frontal–sphenoid synchondrosis that involved the orbital wing of the sphenoid bone[4]

Distinctive histologic findings are:

- trabecular bone with cores of hyaline cartilage
- rare osteoclasts in long bones, with numerous osteoclasts in the skull
- significant reduction or absence of retinal ganglion cells
- axonal loss and gliosis in the optic nerves and optic chiasm
- chromatolysis and neuronal atrophy in nuclei of the medulla oblongata (facial, vestibulocochlear, and hypoglossal nuclei, and red nuclei)
- atrophy of muscles of the tongue and larynx
- axonal swelling and Wallerian degeneration in pyramidal tracts and medial longitudinal fasciculus perivascular paraventricular corpora amylacea in the thalamus, basal nuclei, and midbrain with similar but larger structures in the choroid plexus of the third ventricle
- calcified vessel walls and mineralization of neuropil associated with the corpora amylacea
- reduced Purkinje cell numbers (but no other histologically identifiable cortical atrophy in compressed parietal cortex or in herniated cerebellum)
- disorganized mixture of cementum, dentin, enamel and trabecular bone in teeth (particularly around apical foramina within the intra-alveolar portion of premolars)
- mineralized and ossified connective stroma in the tooth chamber

- periodontal hemorrhage
- increased ratio of acellular to cellular cementum[4]

Interestingly, 4 of the 10 affected calves in this report were heterozygous for the *SLC4A2* mutation. The heterozygous calves were born alive, survived 1-7 days post birth and had milder brain lesions than the homozygous calves.[4]

Conference participants noted that the cortex in the examined sections appears thin. Since we are unclear as to the level at which these sections were taken, we cannot fully evaluate this cortical thinning. It was speculated that the sections may be through the cutback zone, in which case the cortex would be expected to be discontinuous and thin.

**Contributing Institution:** Wyoming State Veterinary Laboratory
1174 Snowy Range Road
Laramie, WY 82072
http://wyovet.uwyo.edu/

**References:**

1. Josephsen K, Praetorius J, Frische S, et al. Targeted disruption of the Cl-/HCO3- exchanger Ae2 results in osteopetrosis in mice. *Proc Natl Acad Sci USA*. 2009;106:1638-1641.
2. Leipold HW, Huston K, Dennis SM, Guffy MM. Hereditary osteopetrosis in Aberdeen Angus Calves. I. Pathological changes. *Ann Génét Sél Anim*. 1971;3:245-253.
3. Meyers SN, McDaneld TG, Swist SL, et al. A deletion mutation in bovine SLC4A2 is associated with osteopetrosis in Red Angus cattle. *BMC Genomics*. 2010;11:337.
4. O'Toole D, Swist S, Steadman L, Johnson GC. Neuropathology and craniofacial lesions of osteopetrotic Red Angus calves. *Vet Pathol*. 2012;49:746.
5. Thompson K. Diseases of bones and joints. In: Maxie MG, ed. *Pathology of Domestic Animals.* 5th ed. Vol. 1. Edinburgh, Scotland: WB Saunders; 2007:38-40.
6. Thomson RG. Failure of bone resorption in a calf. *Vet Pathol*. 1966;3:234-246.
7. Wu J, Glimcher LH, Aliprantis AO. HCO3-/Cl- anion exchanger SLC4A2 is required for proper osteoclast differentiation and function. *Proc Natl Acad Sci USA*. 2008;105:16934-16939.

**CASE II**: A11-650 (JPC 4017812).

**Signalment:** 4-year-old, male intact, rhesus macaque (*Macaca mulatta*).

**History:** This animal was born and maintained as a specific pathogen free (SPF) animal within the NEPRC colony. Over a one-week period, a hard swelling, approximately 40 cm in diameter, developed over the left shoulder and biceps. Radiographs revealed a lytic bone mass within the left humerus with 1-2 areas of metastasis to the lungs; bone biopsy of the left humerus was non-diagnostic and revealed only reactive bone. Based on the rapid growth of the bony mass and poor prognosis based on the presence of pulmonary metastasis, humane euthanasia was elected.

**Gross Pathologic Findings:** The proximal and middle left humerus is swollen to five times normal size and on cross section has been replaced by a large 12 x 8 cm multilobular, fleshy, white to red friable mass that is variably gritty to hard on cross section. The neoplasm also infiltrates and surrounds the shoulder joint and the articulation of the humerus and radius. Scattered throughout the lungs, most numerous in the caudal right lung lobe, are approximately two dozen 1 to 4 cm diameter firm, pale nodules.

**Laboratory Results:** Chemistry panel revealed elevated ALP and LDH, hypoalbuminemia and hypoproteinemia.

**Histopathologic Description:** Lung: Arising within the pulmonary parenchyma are multiple well-demarcated nodules of neoplastic spindle-shaped cells arranged in sheets and cords that surround and are producing abundant osteoid. The nodules are variable in appearance with some having more osteoid than others. The neoplastic cells have abundant eosinophilic cytoplasm and large, round to ovoid nuclei with finely stippled chromatin and often prominent nucleoli. There is marked cellular and nuclear atypia with numerous mitotic figures (>5/hpf), many of which are bizarre. The nodules of neoplastic tissue are rimmed by a thick layer of fibrous connective tissue and are often traversed by numerous small blood vessels.

**Contributor's Morphologic Diagnosis:** Lung: Metastatic osteoblastic osteosarcoma.

**Contributor's Comment:** Histologically, this tumor is consistent with an osteosarcoma (OSA) arising from the left humerus, with extensive metastases to the lungs. Although this tumor can arise from any bone (and rarely extraosseous sites), the proximal humerus is one of the most common sites for this neoplasm to occur, along with the distal femur and proximal tibia.[2] The histomorphology of this tumor (marked cellular atypia and extraordinarily high mitotic rate) is consistent with the extraordinarily rapid growth of a severely dysplastic and invasive metastatic neoplasm with numerous areas of lymphatic invasion and metastasis. Based on the amount of osteoid, this is considered a productive osteoblastic osteosarcoma.

Different subsets of OSA include those that produce osteoid (bone) (productive osteoblastic type), bone and cartilage (compound or combined type), are anaplastic with little extracellular osteoid production (poorly differentiated type), or rarely may form blood filled cysts lined by malignant osteoblasts (telangiectatic type).[2,5] Of these, osteoblastic (progressing to anaplastic) and

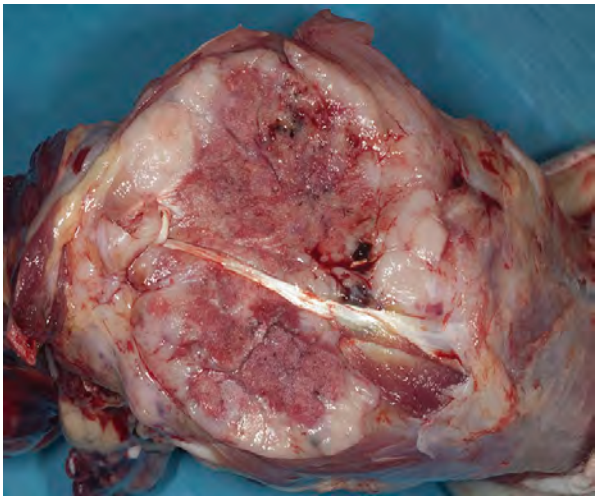

*2-1. Humerus, rhesus macaque: The left humerus is swollen to 5x normal size and on cross section has been replaced by a large 12 x 8 cm multilobular, friable mass which is gritty on cut section. (Photo courtesy of: New England Primate Research Center, Harvard University Medical School, One Pine Hill Drive Southborough, MA 01772, http://www.hms.harvard.edu/nerprc/)*

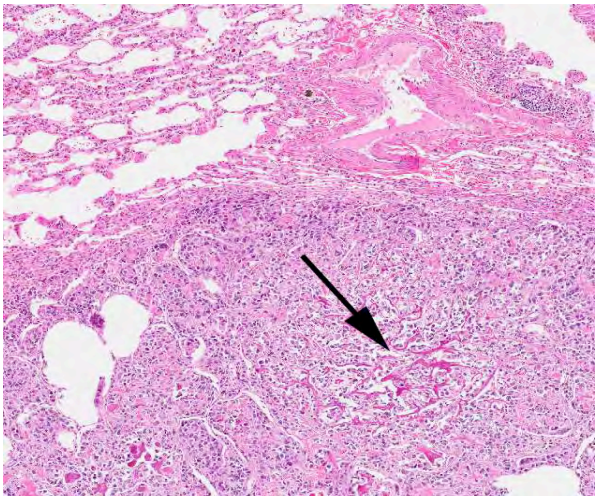

*2-2. Lung, rhesus macaque: The sections contain multiple nodules of an infiltrative, moderately cellular neoplasm producing trabeculae of osteoid (arrow). (HE 40X)*

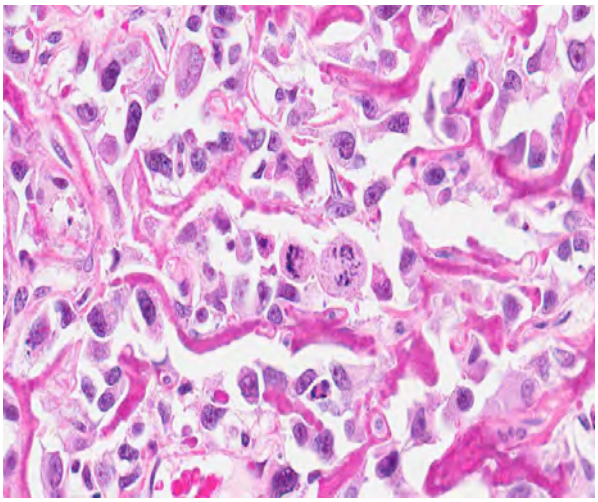

*2-3. Lung, rhesus macaque: Neoplastic osteoblasts, which in this nodule (but interestingly, not a second neoplastic nodule in this section of lung), exhibit anisokaryosis, multinucleation, and a high mitotic rate. (HE 400X)*

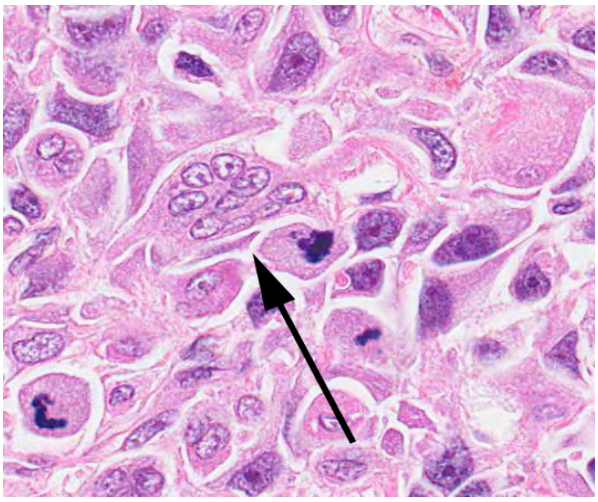

*2-4. Lung, rhesus macaque: Rarely, osteoclasts (arrow) are present throughout the neoplasm (which is common in osteosarcoma), and should be differentiated from multinucleated neoplastic cells. (HE 400X)*

combined type OSAs have been previously reported in rhesus macaques.[1,3] Based on the paucity of reported cases, little is known about the prognosis of these bony tumors in non-human primates.

Differential diagnoses for the grossly lytic lesion included bacterial or fungal osteomyelitis, which was deemed less likely given the radiographic evidence of pulmonary nodules. Specific infectious agents reported to cause osteomyelitis in non-human primates include *Salmonella enteritidis*, *Mycobacterium tuberculosis*, *Coccodiodes immitis*, and *Histoplasma duboisii*.[4] In addition, other neoplasms such as multiple myeloma, chondroblastoma, or other metastatic tumors could be considered. In this case, the bone biopsy revealed only reactive bone and was uninformative in distinguishing between neoplastic and inflammatory causes of bony lysis; this is a common issue with non-diagnostic specimens that miss the primary lesion.

Specific predisposing genetic mutations for the development of OSAs have not been reported in non-human primates, but several have been identified in dogs and humans. These include hereditary mutation in retinoblastoma (Rb) as well as sporadic mutations in p53, both common tumor suppressor genes. Mutations leading to overexpression of the p53 ubiquitin ligase MDM2 or decreased expression of the p14 gene product lead to increased p53 degradation and have been associated with OSA development. In addition, alterations in other genes include HER2/neu overexpression correlated with decreased survival and RECQL4 in the human Rothmund-Thomson Syndrome.[6]

**JPC Diagnosis:** Lung: Osteosarcoma, metastatic.

**Conference Comment:** As the contributor notes in the excellent discussion, OSA occurs in dogs and humans, as well as non-human primates. Additionally, it is fairly common in cats, but rare in other domestic species.[2] Conference participants compared and contrasted OSA in primates and dogs, with the following table provided by the conference moderator:

| | Primates | Dogs |
|---|---|---|
| Occurrence | Rare | Common |
| Age | Young | Old |
| Sites | Away from the elbow and towards the knee | Away from the elbow and towards the knee, except distal tibia > proximal* |
| Prognosis | 87% survival | Dismal |

*The moderator stressed an important caveat to the popular memory device "away from the elbow and towards the knee" (i.e., proximal humerus, distal radius, distal femur, proximal tibia) for common sites for canine OSA, noting that the distal tibia is actually more commonly affected than the proximal tibia.[2]

Discussing hereditary predispositions for developing osteosarcoma, the contributor brings up the interesting topic of tumor suppressor genes. Tumor suppressors such as RB and p53 are part of an intricate regulatory system in which they act to halt cellular proliferation in response to genetic damage. Active (i.e., hypophosphorylated) RB controls the cell cycle at the gap between mitosis and DNA synthesis (i.e., G1-S transition) by complexing with E2F transcription factors and recruiting chromatin-remodeling factors (e.g., histone deacetylases and histone methyltransferases), thereby inhibiting transcription of genes whose products are necessary for DNA synthesis in the S phase. When RB is inactivated via phosphorylation

by the cyclin D-cyclin-dependent kinase (CDK) 4, cyclin D-CDK6 and cyclin E-CDK2 complexes, it releases E2F, which then activates the transcription of genes required for the S phase, and the cell cycle continues. Further regulation of this checkpoint occurs when growth inhibitors stimulate CDK inhibitors such as p16 (p16/INK4A) and p21 to inactivate the cyclin D-CDK complexes, leading to activated RB and subsequent cell cycle arrest. Thus, the G1-S checkpoint can be dysregulated by mutations in the genes that control the phosphorylation of RB: *RB1*, *CDK4*, and genes that encode cyclin D and p16.[7]

Tumor suppressor p53 is known as the "guardian of the genome" due to its critical role in regulating the cell cycle both at the G1-S and G2-M checkpoints. In healthy cells, p53 is quickly degraded by the ubiquitin pathway via MDM2; however, when DNA damage is sensed by ataxia-telangiectasia mutated (ATM) and ataxia-telangiectasia and Rad3 related (ATR) proteins, p53 undergoes post-transcriptional modifications causing it to be released from MDM2. Additionally, p14, another INK4A protein transcribed from the same gene as p16, has a protective effect on p53 by binding to and inhibiting MDM2. Once released from MDM2, p53 activates the transcription of numerous genes that cause cell cycle arrest and repair or apoptosis. Although p53 induces hundreds of genes, some of the key players include p21, which mediates cell cycle arrest by binding cyclin-CDK complexes and thus activating RB; GADD45, which aids in DNA repair; and BAX, which promotes apoptosis. If the DNA damage is successfully repaired, p53 up-regulates MDM2 transcription, which leads to its own destruction. If the DNA cannot be repaired, the cell becomes senescent (i.e., undergoes permanent, irreversible cell cycle arrest) or undergoes apoptosis. Similar to RB, mutations that cause loss of function in p53 or in the genes coding for proteins involved in the p53 pathway can disrupt this vital checkpoint and promote tumorigenesis.[7]

**Contributing Institution:** New England Primate Research Center
http://www.hms.harvard.edu/nerprc/

**References:**

1. Beam SL. Combined-type osteosarcoma in a rhesus macaque. *Vet Pathol*. 2005;42(3):74-7.
2. Carlson CS, Weibrode SE. Bones, joints, tendons, and ligaments. In: McGavin MD, Zachary JF, eds. *Pathologic Basis of Veterinary Disease*. 5th ed. St. Louis, MO: Elsevier; 2012:959.
3. Gliatto JM, Bree MP, Mello NK. Extraosseous osteosarcoma in a nonhuman primate (*Macaca mulatta*). *Journal of Medical Primatology*. 1990;19(5):507-13.
4. Pritzker KPH, Kessler MJ. Arthritis, muscle, adipose tissue, and bone diseases of nonhuman primates. In: Abee CR, Mansfield K, Tardiff S, Morris T, eds. In: *Nonhuman Primates in Biomedical Research, Vol. 2: Diseases*. 2nd ed. St. Louis, MO: Elsevier; 2012:664.
5. Slayter MV, Boosinger TR, Pool RR, Dammarch J, Misdorp W, Larsen S. *Histological Classification of Bone and Joint Tumors of Domestic Animals.* World Health Organization. 2nd series. Vol. 1. Washington, DC: Armed Forces Institute of Pathology, American Registry of Pathology;1994.
6. Hansen MF. Genetic and molecular aspects of osteosarcoma. *Journal of Musculoskeletal and Neuronal Interactions*. 2002;2(6):554-560.
7. Stricker TP, Kumar V. Neoplasia. In: Kumar V, Abbas AK, Fausto N, Aster JC, eds. *Robbins and Cotran Pathologic Basis of Disease*. 8th ed. Philadelphia, PA: Saunders Elsevier; 2010:kindle edition, location 12860 of 92558.

**CASE III**: 09-1057 (JPC 3134056).

**Signalment:** Nine-year-old, female spayed, Greyhound, *(Canis familiaris)*.

**History:** The dog presented for a 2-month history of vomiting and diarrhea and later anorexia, which were partially responsive to antibiotics. She also had a history of left forelimb lameness. Ultrasound revealed a thickened gastric wall with loss of layering and enlarged gastric lymph nodes. Cytology on ultrasound-guided fine needle aspirate of the stomach revealed a gastric carcinoma. Radiographs of the left front limb revealed multiple radiolucent medullary lesions. On the day of euthanasia, the dog developed left hind limb lameness.

**Gross Pathologic Findings:** The dog weighed 23 kg, had a body condition score of 3/5 and was in fair postmortem condition. An area measuring 9cm x 3cm had been removed post mortem from the antrum, pylorus, and duodenum for purposes of tumor tissue banking. The tissue remaining at the pyloric-duodenal junction was 5 to 7 mm thick, firm and white to gray on cut surfaces. The pancreas was nodular, firm and up to 8 mm thick with multifocal areas of hemorrhage. There was a mild to moderate amount of petechiae and ecchymoses throughout the small and large intestinal mucosa. Three of the lymph nodes adjacent to the stomach were 1.3 to 1.5 cm in diameter, firm, dark red on the capsular surface and tan on section. Multiple round, white, soft to hard nodules (3 to 4 mm in diameter) were present throughout the medulla of the left humerus.

**Histopathologic Description:** Tissue is from the diaphysis of the left humerus. The lesions are most marked in the medullary cavity with marked infiltration with solid to occasionally acinar carcinoma associated with marked reactive fibrosis and marked reactive woven bone. Marrow cavity not involved with reactive woven bone or reactive fibrosis has mixed fatty and hematopoietic marrow. In some sections, there is tumor infiltrate into this mixed marrow without reaction. Not present on all slides is invasion of tumor into the cortex with variable cortical bone lysis, cortical bone necrosis and periosteal reactive woven bone formation. Neoplastic cells are not apparent in the periosteal lesion.

**Contributor's Morphologic Diagnosis:** Left humerus: moderately differentiated, metastatic, solid carcinoma (presumed of gastric origin based on post mortem

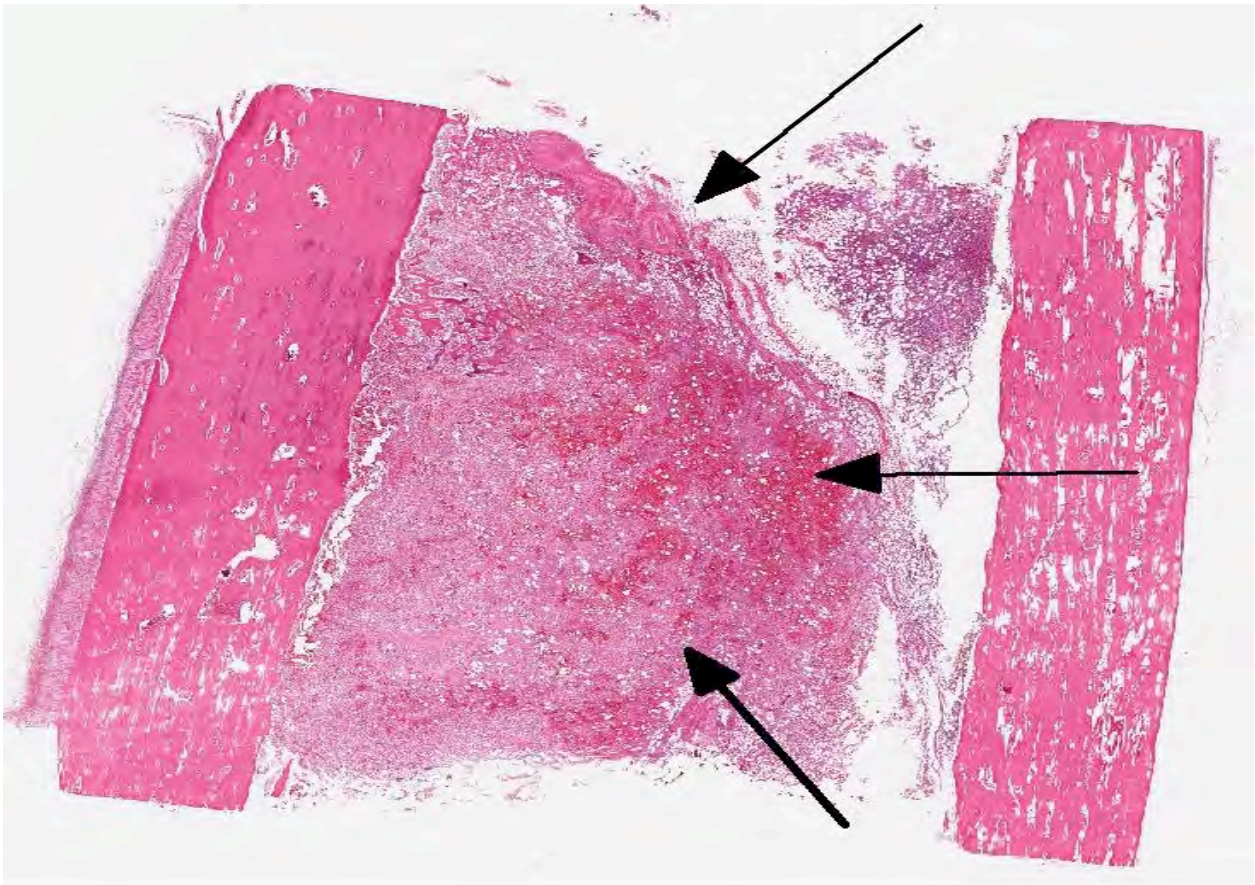

*3-1. Humerus, dog: Within the diaphysis, extending to the subperiosteum, is an infiltrative, moderately cellular, well-demarcated neoplasm which effaces marrow elements, and multifocally infiltrates the cortical lamellar bone. (HE 4X)*

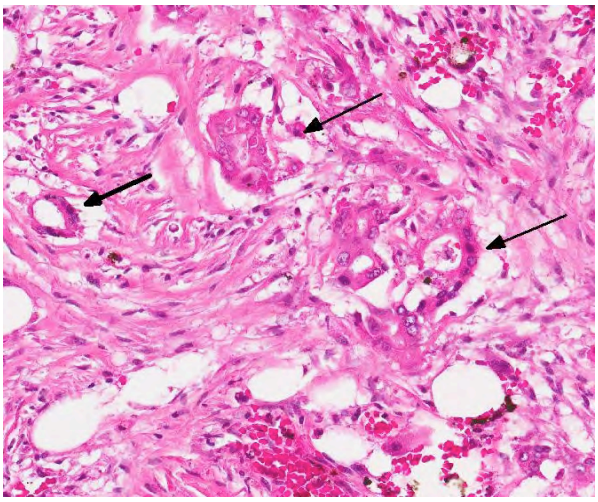

*3-2. Humerus, dog: Neoplastic cells are arranged in nests and poorly formed acini (arrows), amidst a marked desmoplastic response. (HE 320X)*

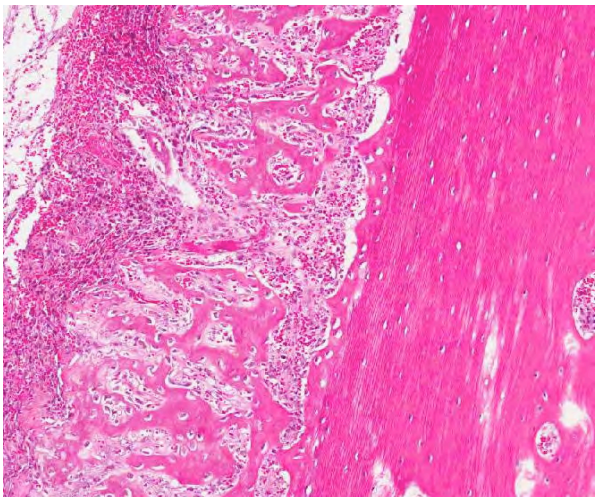

*3-3. Humerus, dog: The periosteum is elevated by diffusely radiating spicules of woven bone that are perpendicular to the lamellar cortical bone. (HE 400X)*

findings) with marked medullary reactive fibrosis and woven bone formation, variable cortical bone lysis and variable periosteal woven bone formation.

**Contributor's Comment:** Carcinoma was confirmed in the stomach and based on pattern of infiltrate/absence of other primary tumors, metastatic gastric carcinoma was found in pancreas, gastric lymph nodes and left humerus. The clinical findings relevant to the left rear leg were unexplained (no lesions were apparent in the left rear leg grossly or microscopically).

Mammary gland and prostatic carcinoma are the major origin of metastatic carcinoma to bone in humans. Such metastatic pattern in spontaneous animal disease is rare.[4] Most carcinoma metastatic to bone cause lysis; prostatic carcinoma in dog and man can be associated with osteoblastic metastases. The mechanisms by which prostatic tissue induces reactive woven bone is unclear but seems to have an endothelin-dependent mechanism. PtH-rp and prostaglandins are likely not involved.[3] In the current case, the radiographic appearance of the lesions in the humerus were that of medullary lysis. It is difficult to explain the discrepancy between the microscopic appearance of a productive process in the medullary cavity and the radiographic interpretation of a lytic one. It is possible that because of reduced superimposition of bone, the cortical lysis (present in some sections) gave the appearance of medullary lysis radiographically. In a series of 19 dogs with skeletal metastatic carcinoma, most dogs were presented for veterinary care because of clinical signs relating to the skeletal metastasis and not the primary carcinoma.[2] In 58% of the dogs, a primary site of the carcinoma was not determined. Most skeletal metastases are in axial skeleton and proximal long bones.

**JPC Diagnosis:** Long bone: Adenocarcinoma, metastatic.

**Conference Comment:** As the contributor states, metastasis of carcinoma to bone is rare in dogs relative to humans. Interestingly, malignant pilomatricomas appear predisposed to metastasize to bone in dogs.[1] During a review of 13 reported cases of canine malignant pilomatricoma, Carroll et al. identified seven neoplasms which metastasized to or extended into bone (sites included vertebrae, ribs, mandible, maxilla and femur). In humans, tumor metastasis to bone is most common in well-vascularized sites (axial skeleton, proximal aspect of long bones and ribs), where the microenvironment provides "fertile soil" for solid carcinomas.[1] For example, once human breast cancer metastasizes to bone, it produces colony stimulating factor 1, parathyroid hormone related protein, and tumor necrosis factor alpha. The resulting activation of nuclear factor kappa B ligand stimulates osteoclast formation and activation. Osteoclast degradation of bone matrix releases insulin-like growth factor 1, transforming growth factor beta and bone morphogenic proteins, which promotes survival of metastatic cells and stimulates parathyroid hormone related protein synthesis, thus resulting in a positive feedback loop of metastatic growth and osteolysis. Other factors that have been found to promote metastasis to bone in humans include chemokines in bone that attract circulating receptor-bearing tumor cells, cytokines that bind tumor cells bearing E-cadherin and laminin, and the presence of tumor associated macrophages. It is unclear if these factors play a role in the tendency of canine malignant pilomatricoma to metastasize to bone.[1]

**Contributing Institution**: Department of Veterinary Biosciences
The Ohio State University
1925 Coffey Road
Columbus, Ohio 43210
http://vet.osu.edu/biosciences.htm

**References:**

1. Carroll EE, Fossey SL, Mangus LM, Carsilo ME, Rush LJ, McLeod CG, Johnson TO. Malignant Pilomatricoma in 3 Dogs. *Vet Pathol.* 2010;47(5)937-943.
2. Cooley DM, Waters DJ. Skeletal Metastasis as the initial clinical manifestation of metastatic carcinoma in 19 dogs. *J Vet Intern Med*. 1998;12:288-293.
3. LeRoy BE, Sellers RS, Rosol TJ. Canine prostate stimulates osteoblast function using the endothelin receptors. *Prostate*. 2004;59:148-156.
4. Rosol TJ, Tannehill-Gregg SH, LeRoy BE, Mandle S, Contag CH. Animal models of bone metastasis. *Cancer*. 2007;97(3 Suppl):748-757.

**CASE IV:** 12-2197-6 (JPC 4019352).

**Signalment:** 4-year-old, castrated male, Bullmastiff dog (*Canis lupis familiaris)*.

**History:** Dog had a lump on the lateral aspect of L elbow for an unknown period of time. Punch biopsy sent to a diagnostic laboratory resulted in a suspected diagnosis of chondroma. Dog continued to be lame and the owners elected amputation.

**Gross Pathology:** Received an elbow joint, which had an ulcerated firm mass, measuring approximately 5 x 5 cm, over the lateral aspect. The ulceration was from the site of the previous punch biopsy. On section, the mass was cavitated; continuous with the elbow joint space; filled with variably-sized, smooth, white, hard masses. Sections of the mass were placed into decalcification to allow sectioning. Fluid injected into the joint space opposite the mass drained out through the section area of the mass suggesting the mass communicated with the joint space.

**Histopathologic Description:** The mass consists of numerous nodules consisting of well-differentiated hyaline cartilage arising from the synovial membrane and occasionally found within it. Residing within the lacunae are mature and well-differentiated chondrocytes. The nuclei are round and eccentric and consist of homogeneous dark purple chromatin. There is a moderate amount of eosinophilic cytoplasm, often containing small basophilic granules. The cells have irregular, almost spiculated cellular margins. Often these nodules show evidence of endochondral ossification. The synovium is markedly thickened and infiltrated with lymphocytes and plasma cells. The overlying fibrous capsule is also thickened by numerous reactive fibroblasts.

**Contributor's Morphologic Diagnosis:** 1. Synovial osteochondromatosis.
2. Synovial hyperplasia with lymphocytic plasmacytic synovitis.

**Contributor's Comment:** Synovial osteochondromatosis (SOC) is a condition described infrequently in dogs.[1,2,3,4,5,9] and rarely in cats[7], horses[8], pigs[13], great horned owls[6,10] and a red tailed hawk.[10] It is characterized by the formation of small intra- or periarticular cartilaginous or osseous nodules. Histologically, the cartilaginous lobules are hypercellular and can show features of nuclear and cellular atypia which can complicate the diagnosis, particularly if only small samples are taken. Compared to the condition in humans, relatively little is known about the pathogenesis of the disease in dogs. The majority of the descriptions in veterinary medicine are based on case reports of individual dogs.[1,2,3,4,5,9]

In humans, SOC is considered to be a metaplastic condition rather than a neoplastic disease.[11] There are however, at least two case reports of malignant transformation of synovial osteochondromatosis to chondrosarcoma in dogs.[1,2]

Based on the description of the condition in humans numerous subcategories have been described. These include chondromatosis where the nodules are strictly cartilaginous in nature and osteochondromatosis where some of the nodules have undergone endochondral ossification as in this case. They are further subdivided based upon the suspected origin as either primary or secondary. SOC is defined as being secondary when

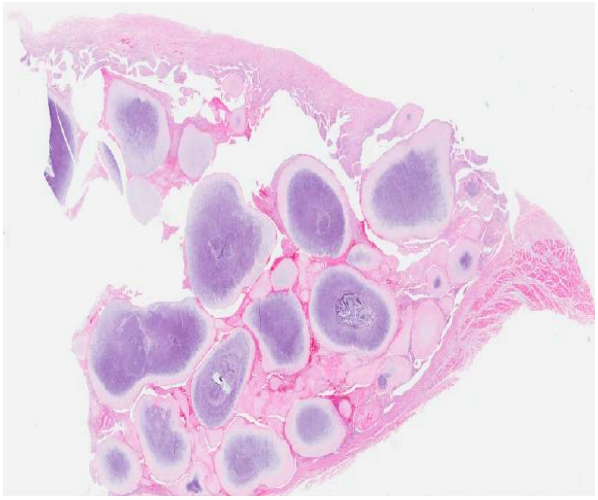

*4-1. Elbow joint, dog: The joint capsule is markedly expanded by numerous nodules of hyaline cartilage scattered throughout a proliferative synovium. (HE 10X)*

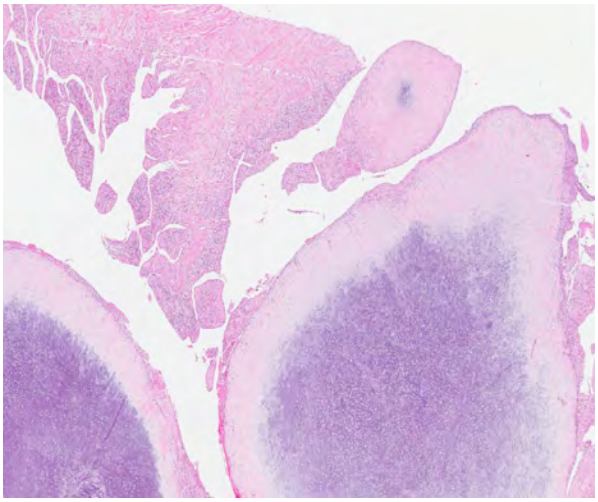

*4-2. Elbow joint, dog: Cartilage nodules are surrounded by villar proliferation of synovium. The proliferative synovium contains an infiltrative of large numbers of lymphocytes and plasma cells. (HE 200X)*

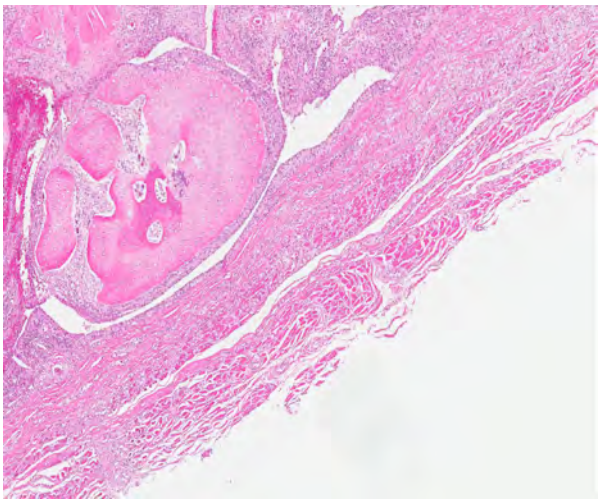

*4-3. Elbow joint, dog: Rarely, cartilaginous nodules exhibit osseous differentiation, reminiscent of endochondral ossification. (HE 350X)*

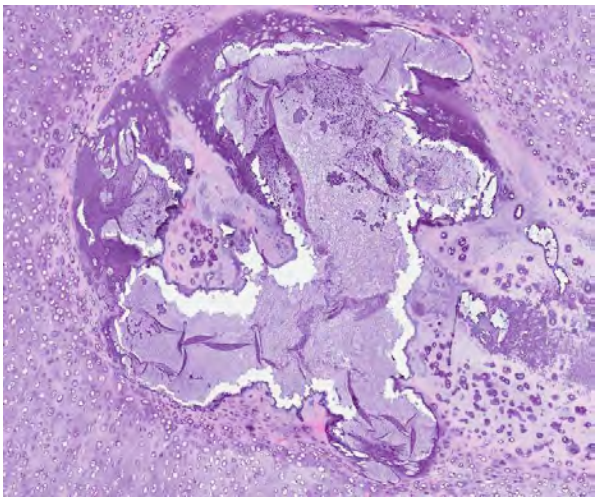

*4-4. Elbow joint, dog: Occasionally cartilaginous nodules, exhibit central areas of chondronecrosis. (HE 400X)*

there is a preexisting history of joint trauma or chronic mechanical irritation, while primary SOC is an idiopathic condition.[12] In this case, there was no previous history of joint injury or disease and careful examination of the articular surfaces of the joints did not reveal any sign of disease suggesting that this is a primary SOC.

There are limited numbers of cases describing the treatment of this condition; those that do exist suggest that removal of the nodules and partial synovectomy may improve the clinical signs, although radiographic reoccurrence of nodules was noted in some of these cases.[4]

**JPC Diagnosis:** Synovium: Cartilaginous nodules, multiple, with marked proliferative and lymphocytic synovitis.

**Conference Comment:** The contributor provides an excellent summary of this uncommon condition. Conference participants considered both primary and secondary synovial chondromatosis as differential diagnosis for this case, and discussed differences between the two. The moderator provides the included table for comparison:

| | Primary synovial chondromatosis | Secondary synovial chondromatosis |
|---|---|---|
| Occurrence | Rare | Fairly common |
| Joints affected | Single | Multiple |
| Degenerative joint disease | Mild | Severe |
| Number of nodules | More | Fewer |

Participants also considered chondroma and chondrosarcoma as potential diagnoses; however, most agreed that a chondroma would more likely present as a single, discrete mass rather than as multiple nodules, and chondrosarcoma would likely not appear so well-demarcated or demonstrate such a repeatable and orderly appearance within each nodule.

The classification of primary synovial chondromatosis is controversial, as there is evidence of both a reactive process and a metaplastic/proliferative process.[1] Recent cytogenic studies demonstrate that in human primary osteochondromatosis, a subpopulation of mesenchymal stem cells undergo clonal proliferation, suggesting a benign neoplastic process.[1]

**Contributing Institution**: Department of Veterinary Pathology
Western College of Veterinary Medicine and Prairie Diagnostic Services
52 Campus Drive
University of Saskatchewan
Saskatoon, Saskatchewan
S7N 5B4, Canada
www.usask.ca/wcvm/vetpath

**References:**

1. Aeffner F, Weeren R, Morrison S, Grundmann INM, Weisbrode SE. Synovial osteochondromatosis with malignant transformation to chondrosarcoma in a dog. *Vet Pathol.* published online 27 January 2012.
2. Díaz-Bertrana C, Durall I, Rial JM, Franch J, Fontecha P, Ramis A. Extra- and intra-articular synovial chondromatosis and malignant transformation to chondrosarcoma. *Vet Comp Orthop Traumatol*. 2010;4:277-283.

3. Edinger DT, Manley PA. Arthrodesis of the shoulder for synovial osteochondromatosis. *J Small Anim Prac.* 1998;39:397-400.
4. Flo GL, Stickle RL, Dunstan RW. Synovial chondrometaplasia in five dogs. *J Am Vet Med Assoc.* 1987;191:1417-1422.
5. Gregory SP, Pearson GR. Synoval osteochondromatosis in a Labrador retriever bitch. *J Small Anim Prac.* 1990;31:580-583.
6. Howard MO, Nieves MA, Miles KG. Synovial chondromatosis in a Great Horned Owl (*Bubo virginianus*). *J Wildlife Dis*. 1996;32:370-372.
7. Hubler M, Johnson KA, Burling RT, Francis DF, Ratcliffe RCC. Lesions resembling osteochondromatosis in two cats. *J Small Anim Pract*. 1986;27:181-187.
8. Kirk MD. Radiographic and histologic appearance of synovial osteochondromatosis of the femorotibial bursae in a horse: a case history report. *Vet Radiol*. 1982;23:167-170.
9. Smith TJ, Baltzer WE, Lohr C, Steiger-Vanegas SM. Primary synovial osteochondromatosis of the stifle in an English Mastiff. *Vet Comp Orthop Traumatol*. 2012;2:1-7.
10. Stone EG, Walser MW, Redig PT, Rings B, Howard DJ. Synovial chondromatosis in raptors. *J Wildlife Dis*. 1999;35:135-140.
11. Thompson K. Diseases of joints. In: *Jubb, Kennedy and Palmer's Pathology of Domestic Animals*. 5th ed. 2007;130-136.
12. Villacin AB, Brigham LN, Bullough PG. Primary and secondary synovial chondrometaplasia. *Hum Path*. 1979;10:439-451.
13. Zimmerman W, Kircher P, Hani H. Synovial osteochondromatosis in swine: a case report. *Schwiez Arch Tierheilkd*. 2000;142:289-291.

**Joint Pathology Center**
**Veterinary Pathology Services**

# WEDNESDAY SLIDE CONFERENCE 2012-2013

## Conference 18

**13 February 2013**

---

**CASE I:** M09-03439/ 3429 (JPC 3139508).

**Signalment:** 4-year-old, female Anglo Nubian goats *(Capra aegagrus hircus)*.

**History:** Four out of twenty-five stud goats from a herd in Northern NSW died suddenly after displaying ataxia, tachycardia, dilated pupils, pyrexia (38.2C), head tilt and stargazing. The submitting clinician necropsied one animal, and found a "diffuse white pattern in the liver." No other changes were reported. The entire brain and sections of liver were submitted. There was a recent introduction of new hay.

**Histopathologic Description:** There is extensive centrilobular necrosis with replacement hemorrhage. Hepatocytes at the margins of the necrotic zones contain multiple fine vacuoles. Occasional cytosegresomes are

*1-1. Liver, goat: Centrilobular hemorrhage is prevalent at subgross inspection. (HE 40X)*

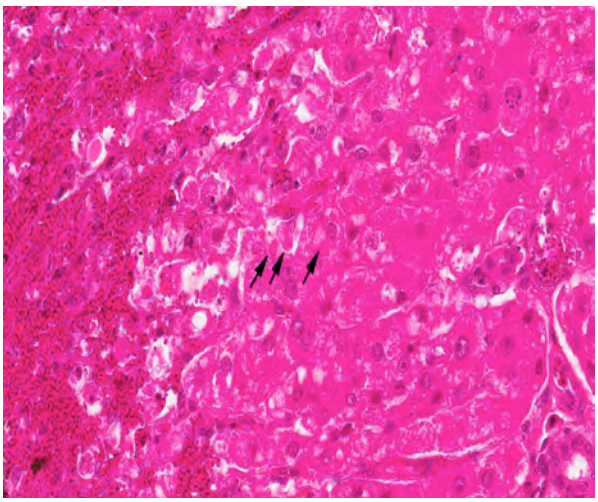

*1-2. Liver, goat. A range of degenerative (cytoplasmic vacuolation, cytosegresome formation - arrows) and necrotic changes (individualized, rounded up, hypereosinophlic granular cytoplasm, and karyorrhexis) are present with remaining hepatocytes in centrilobular and midzonal areas. At left, hemorrhage obscures necrotic hepatocytes within the lobule's center. (HE 400X)*

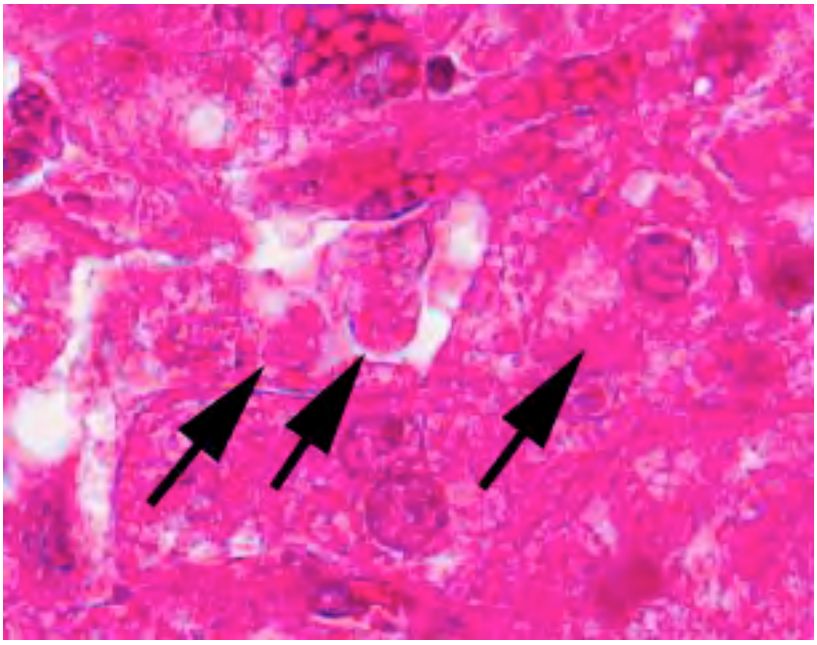

*1-3. Liver goat: Cytosegresomes are autophagic vacuoles induced in hepatocytes by a wide range of sublethal insults. (HE 400X)*

noted, and individualized, shrunken hepatocytes are scattered through the section. There is mild to focally moderate hepatocytic cellular size variation, with an increase in mitotic figures. Larger bile ducts are frequently lined by hyperplastic epithelium, and there are multiple zones with increased numbers of intraepithelial lymphocytes.

**Contributor's Morphologic Diagnosis:** 1. Hepatic necrosis, centrilobular, severe, coalescing, acute.
2. Mild biliary epithelial hyperplasia.

**Contributor's Comment:** The submitting veterinarian made a note that a number of potential poisonous plants were present in the fields, including a heavy growth of *Trema tomentosa* (formerly *Trema aspera*), more commonly known as poison peach.

Poison peach is a large leafy shrub or small tree distributed along Eastern and Northern Australia, extending into New Guinea. It grows mainly in moist open forest, and is considered a pioneer species – frequently becoming a dominant growth following deforestation. Cattle and sheep readily eat the leaves when access is given. In Australia, leaves and fine stems have been shown to be toxic to many livestock species - presumably due to the presence of a glycoside named "trematoxin," which acts as a hepatic toxin.[2] Death due to its ingestion has been reported in Australia in cattle, sheep, horses and camels. Experimentally, toxicity can be easily induced in rabbits and guinea pigs. The submitters have been unable to find any description of toxicity in the literature.

Its relative, *Trema micrantha*, is widely dispersed in Central and South America. It is also a pioneer species and is being considered as a prime candidate in replantings and restoration of degraded forest land. The tree contains toxins which induce a profound hypoglycaemia in rats, and some trials have been carried out touting this agent as an alternative treatment for diabetes mellitus in humans.[4] One reference (in Portuguese) was found citing toxicity in cattle[4] and experimentally in rabbits[6], both of which suggest pathological changes similar, if not identical, to those seen in *Trema tomentosa.* Toxicity in livestock induced by *T. micrantha* appears to be more prevalent in Brazil, explaining the tendency for more recent reports to be in the non-English literature.

The differential diagnosis for this histological pattern in ruminants should include the common suspects of microcystin (blue green algae), green cestrum (*Cestrum* spp.), and noogoora burr (*Xanthium pungens*). The chinaberry or white cedar tree (*Melia azedarach)* contains four teranortriterpenes (meliatoxins A1, A2, B1 and B2), which can variably lead to massive central necrosis; however, these changes are less uniform that those noted above.[3]

**JPC Diagnosis:** Liver, centrilobular hepatocytes: Degeneration and necrosis, diffuse, acute, with marked hemorrhage.

**Conference Comment:** We have seen several examples of various types of hepatic toxicity in this year's conferences. The liver is a common site of toxic injury, as it is exposed to numerous ingested substances through the portal blood. There are six categories of hepatotoxic liver injury, based on the cellular targets of the injurious substances. The most common mechanism involves biotransformation by the cytochrome p-450 system that results in toxic metabolites. Because cytochrome p-450 is most abundant in the centrilobular areas, the result is centrilobular necrosis, as in this case of poison peach toxicity. The second category is characterized by the formation of adducts between drugs and cellular enzymes, other proteins or nucleic acids that act as antigens that, once recognized by the immune system, trigger an inflammatory response against the hepatocytes or biliary epithelium that contain them. A third category involves toxins (such as retained or excess bile acids) that trigger apoptosis of hepatocytes either by direct stimulation of pro-apoptotic pathways or immune mediated events that release TNF-alpha or activate Fas apoptosis pathways.

The fourth category of hepatic toxicity is caused by the disruption of calcium homeostasis by cell membrane damage or disruption of enzymes responsible for maintaining intracellular calcium concentrations. This disruption leads to increased intracellular calcium, which activates proteases that damage actin filaments such that further damage to cell membranes results. The fifth category of toxic injury to the liver manifests as intracellular cholestasis, as the pumps that secrete bile into the canaliculi can be disrupted by certain chemicals (such as estrogen, erythromycin) or by hepatocellular injury that affects the canalicular pumps or actin filaments around the canaliculi. Finally, the sixth category of hepatic toxicity is hepatocellular injury and death due to mitochondrial damage. Mitochondrial damage can result in hepatocyte injury, apoptosis or necrosis via several mechanism, including release of reactive oxygen species, decreased ATP, and decreased beta-oxidation of lipids leading to microvesicular steatosis (lipid accumulation), or release of cytochrome-c which triggers apoptosis.[1]

The distribution of hepatocellular injury reflects the mechanism and cellular targets of the toxin. Toxins that require bioactivation by cytochrome p-450 metabolism result in centrilobular or paracentral (periacinar) degeneration and necrosis. Midzonal degeneration and necrosis are uncommon lesions, but have been reported with aflotaxicosis in pigs and horses. Periportal hepatocellular injury occurs with cholestasis-related injury or toxins that do not require cytochrome p-450 metabolism (e.g. white phosphorous).[1] Other mechanisms, such as toxins that cause mitochondrial or cellular membrane damage, may result in a more diffuse distribution of injury.

**Contributing Institution**: Veterinary Laboratory
Department of Primary Industries
New South Wales
Woodbridge Rd
Menangle, NSW 2568
Australia
www.dpi.nsw.gov.au

**References:**

1. Cullen JM, Brown DL. Hepatobiliary system and exocrine pancreas. In: McGavin MD, Zachary JF, eds. *Pathologic Basis of Veterinary Disease*. 5th ed. St. Louis, MO: Elsevier Mosby; 2012:437-439.
2. Oelrichs PB. Isolation and purification of trematoxin from Trema aspera. *Phytochemistry*. 1968:7:1691-1693.
3. Oelrichs PB, Hill MW, Vallely PJ, et al. Toxic tetranortriterpenes of the fruit of Melia azedarach. *Phytochemistry*. 1983;22:531-534.
4. Schoenfelder T, Cirimbelli TM, Citadini-Zanette V. Acute effect of Trema micrantha (Ulmaceae) on serum glucose levels in normal and diabetic rats. *Journal of Ethnopharmacology*. 2006;107:456-459.
5. Traverso SD, Correa AMR, Schmitz M, et al. Experimental poisoning by Trema micrantha (Ulmaceae) in cattle. *Pesquisa Veterinaria Brasileira*. 2004;24:211-216.
6. Traverso SD, Driemeier D. Experimental Trema micrantha (Ulmaceae) poisoning in rabbits. *Veterinary and Human Toxicology*. 2000;42:301-302.

**CASE II:** D1395000028 (JPC 3174953).

**Signalment:** Nine-week-old, male, Sprague-Dawley rat *(Rattus norvegicus)*.

**History:** This rat was administered 400 mg/kg gentamicin subcutaneously once daily on days 1, 2 and 3 to induce renal tubular injury. Serum and urine were collected on day 4 for urinalysis and serum chemistry analysis; pertinent data is listed in the tables below. The rat was euthanized and necropsied 48 hours after administration of the last dose of gentamicin.

**Gross Pathologic Findings:** Kidneys were bilaterally pale on gross examination.

**Laboratory Results:**

| **Serum chemistry** | **Normal** | **Day 4** | **Day 5** |
|---|---|---|---|
| BUN, mg/dL | 7 - 27 | 30 | 103 |
| Creatinine, mg/dL | 0.4 – 1.8 | 0.8 | 3.0 |
| Phosphorus, mg/dL | 2.1 – 6.3 | 9.5 | 13.0 |
| | | | |
| **Urinalysis** | | **Day 4** | **Day 5** |
| Specific gravity | | 1.010 | 1.016 |
| Protein, mg/dL | | <100 | 300-500 |

**Histopathologic Description:** The slide contains one section of kidney. There is widespread degeneration and necrosis of the proximal convoluted tubules of the cortex. Frequently, the cytoplasm of the degenerate and necrotic cells contains discrete, variably sized, hyaline granules to globules (hyaline droplets). There are rare attempts at epithelial restitution characterized by more squamous-appearing epithelial cells which have spread to cover denuded basement membrane. Necrotic epithelial cells are hypereosinophilic with pyknotic or karyolytic nuclei (coagulation necrosis) and are individualized and desquamating into the tubular lumen. There is often complete dissolution of necrotic epithelial cells into fine, eosinophilic granular cellular debris which fills the tubular lumen. The interstitium is multifocally expanded by scant clear space (interstitial edema). There is widespread proliferation of interstitial cells in the cortex predominantly surrounding glomeruli but also seen scattered between tubules. Admixed with the proliferating interstitial cells are low numbers of lymphocytes and histiocytes. Distal convoluted tubules in the cortex are more apparent with large vesicular nuclei and increased cytoplasmic basophilia. Increased numbers of mitotic figures, large vesicular nuclei and cytoplasmic basophilia are also seen in tubular epithelial cells within the outer and inner medullary stripe. Many tubules of the outer stripe are lined by epithelial cells which have intense hyaline cytoplasmic droplet formation. Scattered tubules within the outer and inner medullary stripe and papilla contain proteinaceous fluid (hyaline casts), granular eosinophilic debris, desquamated necrotic cells or cellular debris (cellular casts) and/or deeply basophilic to purple granular material (mineral).

**Contributor's Morphologic Diagnosis:** 1. Acute diffuse degeneration and necrosis of the cortical proximal tubules with cytoplasmic hyaline droplet formation.
2. Cortical interstitial cell proliferation with mild lymphohistiocytic interstitial nephritis.

**Contributor's Comment:** Gentamicin is almost exclusively filtered by the glomerulus and excreted unchanged by the kidney. Nephrotoxicity results from reabsorption and accumulation of gentamicin in proximal convoluted tubule (PCT) epithelial cells.[8] Gentamicin is a cationic molecule that binds anionic phospholipids in the brush border of the PCT epithelial cells with endocytotic uptake leading to its lysosomal sequestration. Binding of gentamicin to the anionic phospholipid membranes impairs the hydrolysis of phosphatidylcholine in the bilayer by sphingomyelinase and other phospholipases and results in lysosomal phospholipidosis.[7] There is an increase in size and number of phagolysosomes, which are ultrastructurally called myeloid bodies. Myeloid bodies are membrane bound vesicles characterized internally by electron-dense, concentrically whorled membranes (myelin figures) and membrane fragments, and may contain altered cellular organelles including mitochondria. There is also loss of microvilli and cytoplasmic blebbing of the apical PCT.[3]

There are several hypotheses as to the mechanism of PCT cell necrosis in gentamicin-induced nephrotoxicity. Gentamicin changes lysosomal membrane permeability which may result in lysosomal enzyme leakage and necrosis.[9] There are several examples of PCT lysosomal overload resulting in toxicity such as in the unique male rat α2u-globulin nephropathy, Bence-Jones nephropathy and nitrilotriacetic acid nephrotoxicity. It has been suggested that gentamicin is toxic through non-lysosomal targets including disruption of ion transport and enzyme release at the apical and basolateral membranes.[9] Recent studies have indicated free radicals are important mediators of damage in gentamicin nephrotoxicity. Gentamicin has been shown to enhance the generation of superoxide anion and hydrogen peroxide by mitochondria. Gentamicin has also been shown to lead to the release of iron from renal cortical mitochondria and to enhance generation of hydroxyl radicals which are produced by the superoxide anion and hydrogen peroxide in the presence of a metal catalyst, in this case iron. Free radical scavengers and metal chelators have been shown to ameliorate gentamicin-induced renal injury.[1]

On gross examination the kidneys may be pale and enlarged. Microscopically, acute tubular necrosis is restricted to the S1 and S2 segments (pars convoluta) of the PCT, though hyaline droplets are prominent

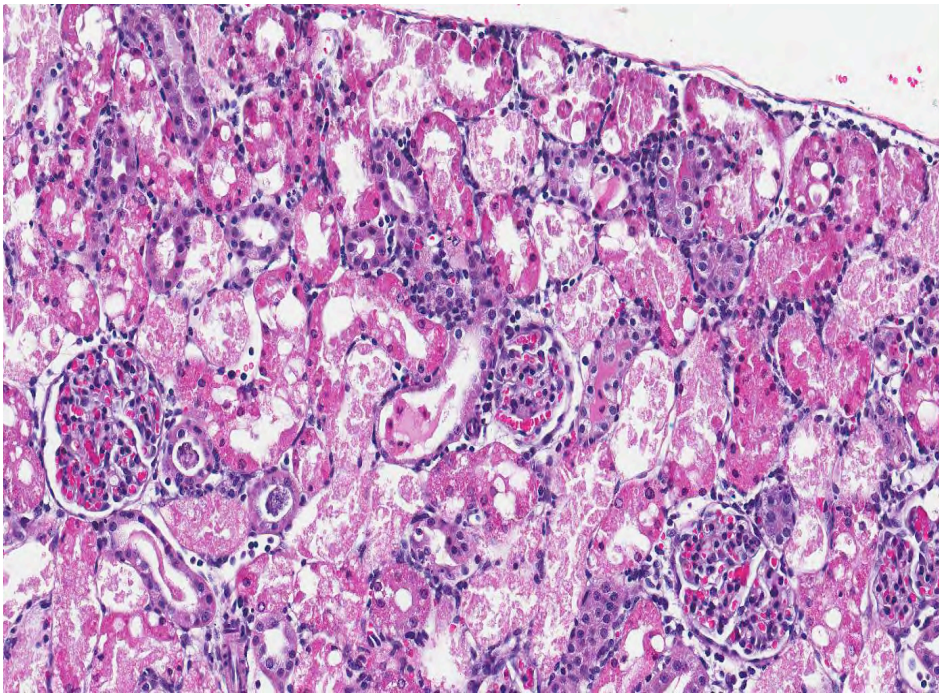

*2-1. Kidney, Sprague-Dawley rat: Throughout the cortex, proximal convoluted tubular epithelium exhibits extensive degeneration and necrosis. (HE 60X)*

throughout all segments of the proximal tubule.[9] Clinically gentamicin toxicity results in the inability to concentrate urine, polyuria, glucosuria, proteinuria, phospholipiduria and increased serum BUN and creatinine.[8] Dysfunction of the PCT results in decreased uptake of glucose, organic bases and low molecular weight protein resulting in their excretion in the urine. Phospholipiduria results in phospholipid-rich myeloid bodies that are shed from the damaged microvillar surfaces of the PCT and can be seen in the urine sediment.[3]

Proximal tubule intracytoplasmic hyaline droplet formation may be associated with accumulation of $\alpha$2u-globulin. This is a gender specific phenomenon and is only seen in mature male rats. These hyaline droplets represent an accumulation of secondary lysosomes containing α2u-globulin and/or albumin within the cytoplasm. Under toxicologic and pathologic conditions hyaline droplets may also consist of other proteins (e.g. histiocytic sarcoma associated hyaline droplets contain lysozyme).[6] Hyaline droplet formation is thought to occur through two mechanisms: increased endogenous protein production or interference with lysosomal enzyme-mediated hydrolysis occurring in the renal epithelial cell. It has been reported that lysosomal bodies in the PCT of rats autofluoresce[5]; the hyaline droplets in the PCT of this rat demonstrate this phenomenon. A Mallory's Heidenhain or chromotrope-aniline-blue stain is used to visualize the α2u-globulin component and PAS is used to demonstrate the albumin component of the hyaline droplets in this case.[4,5,7] As a highly exaggerated dose of gentamicin was used in this study to enable a rapid development of necrosis, specific evidence of

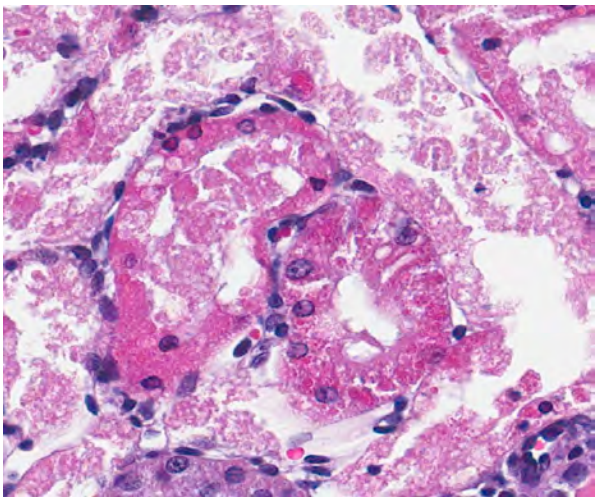

*2-2. Kidney, Sprague-Dawley rat: Sublethal injury to proximal convoluted tubule epithelium by aminoglycosides often results in an accumulation of brightly eosinophilic lysosomes filled with phosphopids, as a result of the drug's antagonistic effect on cellular phospholipases. (HE 400X)*

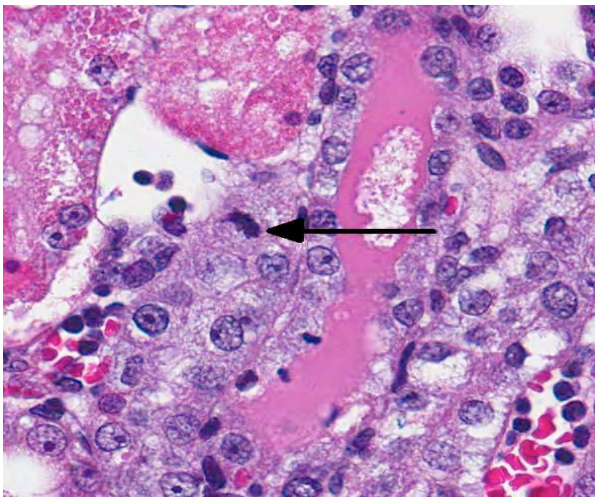

*2-3. Kidney: Regenerating tubules exhibit cytoplasmic basophilia, enlarged nuclei with vesicular chromatin, and often, mitotic figures (arrow). (HE 400X)*

phospholipidosis in H&E section are not apparent in this case. However, a Baker's stain in frozen section or a toluidine blue stain of plastic section could be anticipated to dramatize the phospholipidotic accumulations and debris.

Gentamicin nephrotoxicity can be reversible. Regeneration of PCT epithelium progresses even with continued dosing of gentamicin. It is thought that regenerating epithelium is more resistant to toxicity than mature PCT epithelium.[8] However, over chronic time frames in toxic exposures, even at doses that do not cause necrosis, increased cell turnover can be demonstrated and exacerbation of lesions of chronic progressive nephropathy may be the longer term consequence.

**JPC Diagnosis:** Kidney, proximal convoluted tubules: Degeneration, necrosis and regeneration, with abundant protein casts.

**Conference Comment:** The kidney is a major site of drug-induced injury, primarily because approximately one quarter of the cardiac output is delivered to the kidneys, where substances in the blood are filtered, biotransformed, and concentrated. Toxins or toxic metabolites can then result in renal cell damage and death in a variety of ways. Renal epithelial cells can be damaged directly, as often occurs in proximal convoluted tubules after intracellular biotransformation converts a drug to reactive metabolites. Alternatively, reactive metabolites can be generated in the tubular filtrate, causing renal tubular epithelial necrosis upon reabsorption. Some nephrotoxins cause vasoconstriction and ischemia-related cell death.[10]

Because of their unique mechanisms of toxicity, different drugs affect different specific segments of the nephron, which may assist in narrowing the differential diagnosis in a diagnostic setting. The proximal convoluted tubule is the most commonly-affected segment; numerous drugs cause injury here, including gentamicin, cyclosporine, and cisplatin. The distal tubules are damaged by cyclosporine, sulfadiazine, and amphotericin B, among others. The collecting duct is affected by amphotericin B and acyclovir, and the loop of Henle can be damaged by chronic exposure to analgesics. Glomerular damage can be caused by doxorubicin, gold and penicillamine.[2]

Conference participants discussed serum biomarkers of renal injury such as serum creatinine and blood urea nitrogen, which despite lacking sensitivity, are commonly used to detect renal damage, and are elevated in severe renal disease, as in this case. Serum creatinine, the standard biomarker for glomerular filtration rate, increases only after substantial injury, and is affected by both systemic production and tubular secretion of creatinine. Blood urea nitrogen is also used to measure renal function, but it can be affected by many factors, including urea production by the liver; in addition to being filtered by the glomerulus, it is also reabsorbed by other parts of the nephron.[2] For these reasons, recent research through the Predictive Safety Testing Consortium has been aimed at identifying second-generation biomarkers for acute kidney injury in both laboratory animal models and humans. The goal is to identify markers for early detection of renal injury as well as localization of the injury. Although none have yet shown sufficient specificity and sensitivity for clinical use, several markers have been proposed, including the following:[2]

- Kidney injury molecule-1 (KIM-1), interleukin-18 (IL-18), and fatty acid binding protein-liver type (L-FABP) which are increased with damage to proximal tubules
- Neutrophil gelatinase-associated lipocalin (NGAL) and clusterin, which are associated with damage to proximal and distal tubules
- Osteopontin, which is associated with damage to proximal tubules, loops of Henle and distal tubules
- Cystatin C, which is associated with damage to glomeruli and proximal tubules

Histopathology remains the gold standard for identifying renal injury; however, these or other biomarkers may prove to reliably detect kidney injury in both experimental animals and in a clinical setting.[2]

**Contributing Institution:** Millennium: The Takeda Oncology Company
35 Landsdowne Street
Cambridge, MA 02139
http://www.mlnm.com/

**References:**

1. Baliga R, Ueda N, Walker PD, Shah SV. Oxidant mechanisms in toxic acute renal failure. *Drug Metab Rev*. 1999;31:971-997.
2. Bonventre JV, Vaidya VS, Schmouder R, Feig P, Dieterle F. Next-generation biomarkers for detecting kidney toxicity. *Nat Biotechnol*. 2010;28:436-440.
3. Cheville N. *Ultrastructural Pathology: The Comparative Cellular Basis of Disease*. 2nd ed. Ames, Iowa: Wiley-Blackwell; 2009.
4. de Rijk EP, Ravesloot WT, Wijnands Y, van Esch E. A fast histochemical staining method to identify hyaline droplets in the rat kidney. *Toxicol Pathol*. 2003;31:462-464.
5. Hard GC. Some aids to histological recognition of hyaline droplet nephropathy in ninety-day toxicity studies. *Toxicol Pathol*. 2008;36:1014-1017.
6. Hard GC, Snowden RT. Hyaline droplet accumulation in rodent kidney proximal tubules: an association with histiocytic sarcoma. *Toxicol Pathol.* 1991;19:88-97.

7. Haschek WM, RC, Wallig WA. Handbook of Toxicologic Pathology, Two-Volume Set, 2 ed. San Diego, CA: Academic Press; 2002.
8. Maxie MG. *Jubb, Kennedy and Palmer's Pathology of Domestic Animals*. Philadelphia, PA: Elsevier Saunders; 2007.
9. Mingeot-Leclercq MP, Tulkens PM. Aminoglycosides: nephrotoxicity. Antimicrob Agents *Chemother*. 1999;43:1003-1012.
10. Newman SJ. The urinary system. In: McGavin MD, Zachary JF, eds. *Pathologic Basis of Veterinary Disease*. 5th ed. St. Louis, MO: Elsevier Mosby; 2012:602-603.

**CASE III:** 09/191 (JPC 3148216).

**Signalment:** Seven-year-old, male, German shepherd, *Canis familiaris*, dog.

**History:** At presentation to the clinic at the Norwegian School of Veterinary Science, the dog had a one-week history of anorexia, vomiting and diarrhea. Clinical examination showed below normal body condition, dehydration, listlessness and necrotic ulcers of oral mucosa.

**Gross Pathologic Findings:** Perianal skin was contaminated with dark feces. From mid-jejunum and aborally the intestinal content was dark. There was mineralization of pleura between ribs 2, 3 and 4, on vocal cords and subintimally in the pulmonary artery and vein. The endocardium of the left atrium was hyperemic and mildly rugous. The kidneys were moderately swollen with a moist cut surface and cortical pale radiating stripes.

**Laboratory Results:** Serum samples showed hyperkalemia, hypoglycemia and severely elevated creatinine (2900 µmol/L). Blood gas analysis showed severe metabolic acidosis (pH 7.1).

In serum collected on the day of presentation at the clinic ethylene glycol or glycolic acid was not detected. Fresh renal tissue collected at the time of necropsy showed presence of glycolic acid.

**Histopathologic Description:** Multifocally renal tubules are moderately dilated and commonly show a flattened attenuated epithelium. There is mild tubular epithelial hydropic degeneration and necrosis characterized by hypereosinophilic cytoplasm and pyknotic and karyorrhectic nuclei. Many proximal tubules show epithelial loss and contain dark, basophilic, birefringent material (von Kossa positive calcium deposits) filling the space delineated by intact tubular basement membranes. Some tubules contain hyaline or granular casts. The granular casts are characterized by eosinophilic granular material (cytoplasmic debris) and basophilic finely granular material (nuclear debris and calcium deposits). Some tubular epithelial cells show mitosis (regeneration). There is a moderate amount of intratubular sheaves and bundles of faintly yellow material showing birefringence in polarized light (crystals of calcium oxalate). Some tubular epithelial cells contain intracytoplasmic brown pigment (hemosiderin), and rarely intranuclear eosinophilic inclusions (incidental finding). Focally there is a mild interstitial infiltration of lymphocytes and fewer plasma cells. Bowman's space is focally moderately dilated, ands show sloughing of parietal epithelium.

**Contributor's Morphologic Diagnosis:** 1. Kidney: Tubular degeneration, necrosis and loss with intratubular calcium deposits and calcium oxalate crystals.
2. Kidney: Nephritis, interstitial, lymphoplasmacytic, multifocal, mild.

**Contributor's Comment:** A diagnosis of sub-acute ethylene glycol (EG) poisoning was confirmed by the detection of glycolic acid.

EG poisoning commonly occurs in dogs and cats after accidental ingestion of antifreeze solution. Cats are more susceptible than dogs, but dogs are more commonly affected.[3] EG is readily absorbed from the intestinal tract, but is in itself of low toxicity. While most EG is eliminated in the urine, some is metabolized by alcohol dehydrogenase to glycoaldehyde and its metabolites glycolic acid (GA), glyoxylate and oxalate. EG is rapidly metabolized while GA accumulates in plasma, and is

*3-1. Intestine, dog: The jejunum and aboral GI tract contained dark contents. (Photo courtesy of the Norwegian School of Veterinary Science, Departments of Basic Sciences and Aquatic Medicine, POB 8146 Dep N-0033, Oslo, Norway; www.nvh.no)*

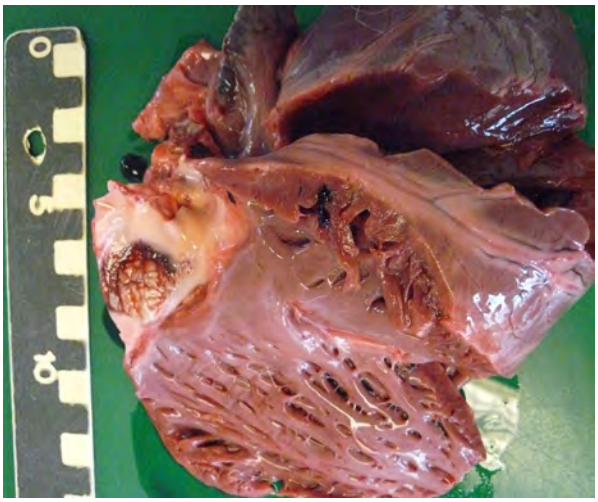

*3-2. Heart, dog: There was mineralization subintimally in the pulmonary artery and vein. The endocardium of the left atrium was hyperemic and mildly rugose. (Photo courtesy of the Norwegian School of Veterinary Science, Departments of Basic Sciences and Aquatic Medicine, POB 8146 Dep N-0033, Oslo, Norway; www.nvh.no)*

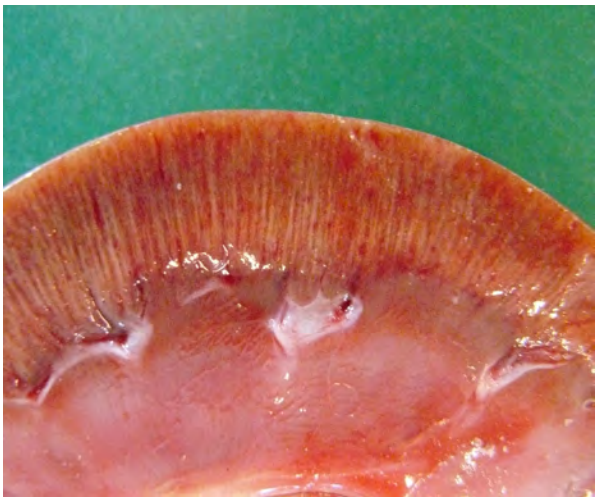

*3-3. Kidney, dog: The kidneys were moderately swollen with a moist cut surface and cortical pale radiating stripes. (Photo courtesy of the Norwegian School of Veterinary Science, Departments of Basic Sciences and Aquatic Medicine, POB 8146 Dep N-0033, Oslo, Norway; www.nvh.no)*

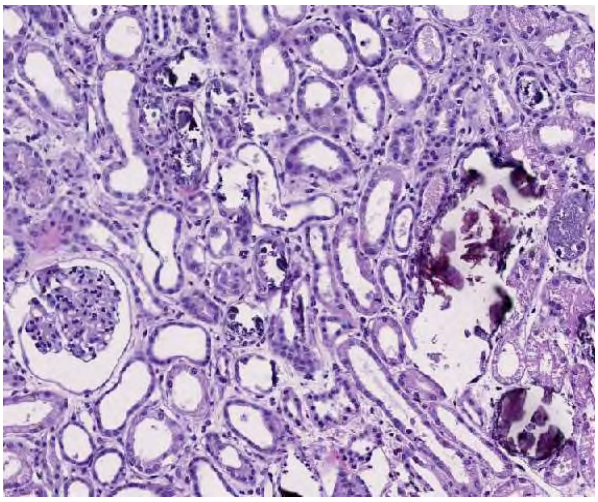

*3-4. Kidney, dog: Diffusely, tubules are ectatic and lined by attenuated epithelium and often contains crystalline mineral. Bowman's space is also multifocally dilated. (HE 40X)*

detectable for a longer time period.[2] Glycoaldehyde and glyoxylate have been considered to be the primary nephrotoxic metabolites.[3] However, recent studies show that the calcium oxalate crystals might be most important for the renal toxicity.[4]

EG toxicity may progress through three stages. The first stage of EG toxicity is characterized by central nervous depression. The second stage is characterized by metabolic acidosis and is seen 12-24 hours after ingestion, and GA is the major contributor to this. The third stage includes oxalic acid excretion, nephropathy and eventual renal failure.[2,3]

Renal failure is due to toxic tubular necrosis and a renal edema that compromises the intrarenal blood flow. Tubular changes are most severe in proximal tubules and range from hydropic degeneration to necrosis to regeneration. The characteristic calcium oxalate crystals may be found in tubular lumina, in tubular cells and in the interstitium. While few calcium oxalate crystals may be seen in chronic tubular obstruction, large numbers of these crystals in renal tubules are virtually pathognomonic for EG poisoning.[3]

**JPC Diagnosis:** Kidney, proximal convoluted tubules: Degeneration and necrosis, diffuse, moderate, with abundant intratubular protein, mineral and numerous oxalate crystals, mild multifocal interstitial hemorrhage and edema.

**Conference Comment:** Conference participants discussed the diagnostic histopathologic findings and pathogenesis, as so well described by the contributor, in this example of a classic disease. In addition, participants considered the clinicopathologic findings associated with EG toxicity. The reported metabolic acidosis and hyperkalemia in this case correlate well with the diagnosis of EG toxicosis. A brief discussion of typical clinicopathologic findings in EG toxicosis follows.

Acid-base homeostasis is tightly regulated by major buffers such as hemoglobin and the bicarbonate buffer system as well as by minor buffers that include inorganic phosphate and plasma proteins.[5] The bicarbonate buffer system plays a major role in acid-base regulation and acts through the equilibrium reaction $H_2O + CO_2 \leftrightarrow H_2CO_3 \leftrightarrow H^+ + HCO_3^-$ to control the amount of hydrogen ions in (and thus the pH of) the blood.[1,5] The ratio of $HCO_3^-$/ $H_2CO_3$ determines the blood pH: An excess of acid (acidosis) leads to a decrease in blood pH (acidemia); whereas an excess of base (alkalosis) causes an increase in blood pH (alkalemia).[1] Disturbances in acid-base status are classified as either metabolic or respiratory, based on the underlying mechanism. Metabolic acidosis, the most common acid-base disturbance, is due to the production of acid by a pathologic metabolic processes.[5] Decreased plasma $HCO_3^-$ (or serum $TCO_2$ concentrations, which is another way of measuring $HCO_3^-$) indicate metabolic acidosis.[1] In most species, plasma $HCO_3^-$ or serum $TCO_2$ concentrations of 15 to 20 mmol/L is interpreted as moderate metabolic acidosis; whereas in the dog and cat, 12 to 17 mmol/L is consistent with moderate metabolic acidosis. Severe metabolic acidosis occurs when plasma $HCO_3^-$ or serum $TCO_2$ concentrations are less than 15 mmol/L in most species and less than 12 mmol/L in the dog and cat.[1]

Common causes of metabolic acidosis include the following[1,5]:

- loss of bicarbonate (such as occurs with severe diarrhea, or decreased synthesis and loss of NaHCO3 by the renal tubules)
- excess in organic acids (titration acidosis)

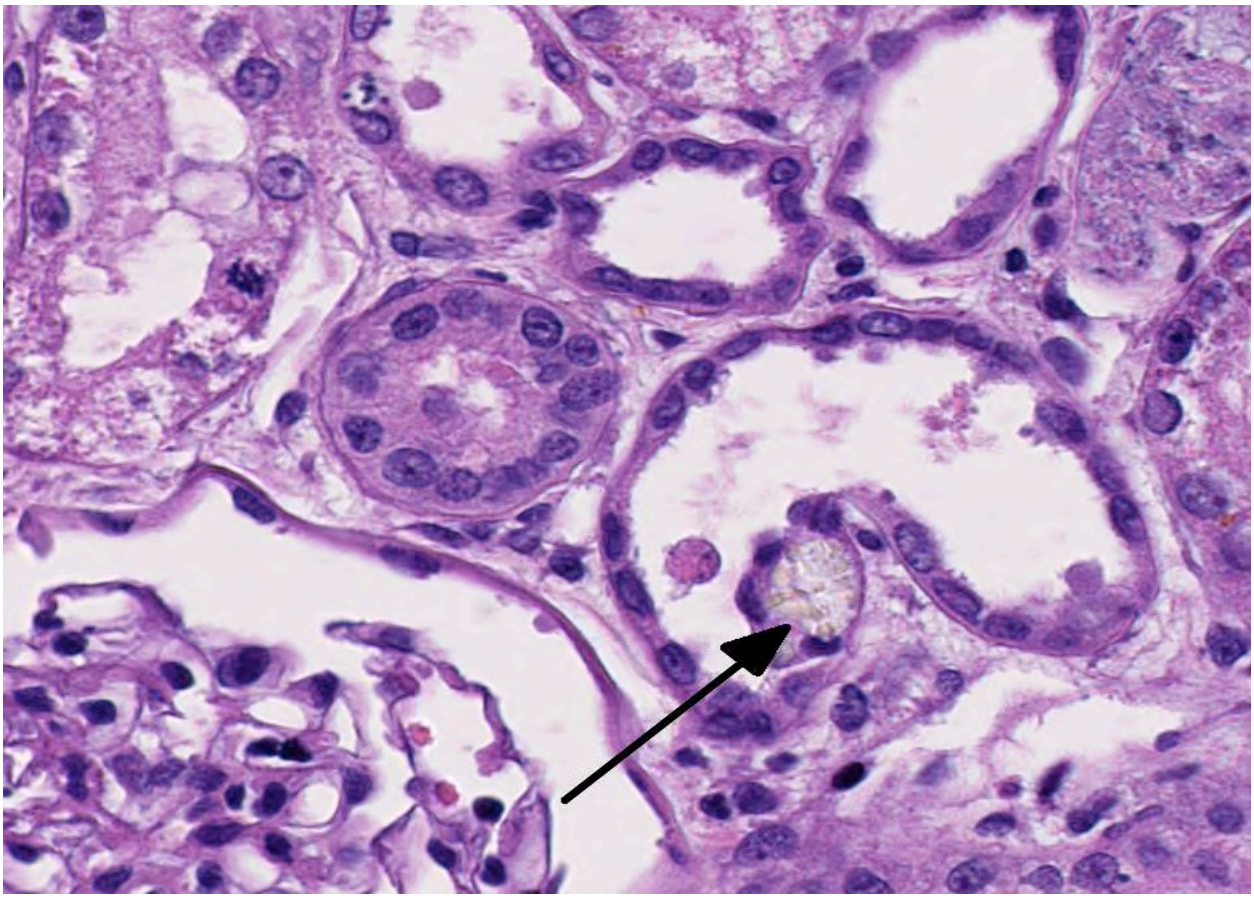

*3-5. Kidney, dog: Occasionally, tubules contain an oval, fan- or prism-shaped birefringent oxalate crystal within the lumen (arrow). Additional changes such as necrosis (upper right), and regeneration (characterized by mitoseswithin epithelial cells at upper left) are present in this field. (HE 400X)*

- lactic acidosis (from anaerobic glycolysis in hypoxia and shock; or excessive bacterial catabolism of carbohydrates)
- ketoacidosis (acetoacetic acid and beta-hydroxybutyric acid in diabetic ketoacidosis, starvation or ketosis of ruminants)
- renal failure (uremic acids)
- acid toxicities (e.g. ethylene glycol toxicity)

As in this case, metabolic acidosis associated with EG toxicity is due to the EG metabolite, glycolic acid. Hyperkalemia, also as observed in this case, results from acidosis, as an excess of hydrogen ions causes a shift of potassium ions from intracellular to extracellular space. Additionally, oliguria in the acute renal failure stage prevents excretion of potassium by the kidneys.[1]

In addition to these findings, EG toxicity is also often accompanied by a high anion gap, due to the presence of the salt of the organic acid.[1] Although not reported in this case, hypocalcemia is often observed in cases of EG toxicity; although renal disease can cause hypocalcaemia by a variety of mechanisms, in EG toxicosis, it is likely due to the sequestration of calcium in the formation of calcium oxalate crystals.[1]

**Contributing Institution**: Norwegian School of Veterinary Science
Departments of Basic Sciences and Aquatic Medicine
POB 8146 Dep N-0033
Oslo, Norway
www.nvh.no

**References**

1. George JW, Zabolotzky SM. Water, electrolytes, and acid base. In: Latimer KS, ed. *Duncan & Prasse's Veterinary Laboratory Medicine Clinical Pathology.* 5th ed. Ames, Iowa: Wiley-Blackwell; 2011:1145-171, 430.
2. Hess R, Bartels MJ, Pottenger LH. Ethylene glycol: an estimate of tolerable levels of exposure based on a review of animal and human data. *Arch Toxicol*. 2004;78:671-680.
3. Maxie M, Newman S. Urinary system. In:Maxie MG, ed. *Jubb, Kennedy & Palmer's Pathology of Domestic Animals*. Vol. 2. Edinburg, Scotland: Saunders Elsevier; 2007:425-522.

4. McMartin K. Are calcium oxalate crystals involved in the mechanism of acute renal failure in ethylene glycol poisoning? *Clin Toxicol*. 2009;47:859-869.
5. Weiser G. Laboratory of acid-base disorders. In: Thrall MA, Weiser G, Allison RW, Campbell TW, eds. *Veterinary Hematology and Clinical Chemistry.* Ames, Iowa: Wiley-Blackwell; 2012: Kindle edition, location *17216 of 37098.*

**CASE IV:** N1113774 (JPC 4022572).

**Signalment:** A 16-month-old male Sprague-Dawley rat (*Rattus norvegicus).*

**History:** Shortly after arrival from the vendor, this aged male rat began T-maze training on a memory task to test cognitive loss with aging. Two weeks later the laboratory notified the veterinary staff of a mass on the ventral surface of the rat's neck. Physical examination of the ventral neck revealed, a 2 x 2 firm, non-mobile mass. A fine needle aspirate (FNA) collected from the mass consisted of neutrophils and macrophages. Two weeks treatment with oral enrofloxacin resulted in no change in the size of the mass; therefore, the rat was anesthetized for surgical excision of the mass. The right submandibular lymph node was removed with the mass. Excision was incomplete due to the location of the mass and approximation to the trachea, etc.
The biopsy revealed that the tumor was a high grade, poorly-differentiated adenocarcinoma and the rat was euthanized and submitted for necropsy.

**Gross:** Lung: There are numerous, multifocal, white, firm neoplastic masses encompassing approximately 50% of the lung lobes. Complete atelectasis of one lung lobe is observed and the distal surface of the right caudal lung lobe is adhered to the diaphragm.

**Histopathologic Description:** Submandibular salivary gland: The specimen consists of multiple lobules of submandibular salivary glands that are partially effaced and replaced by 2.5 cm unencapsulated irregular mass which extends into the surrounding soft tissues and to the limits of the section. The mass is comprised of irregular epithelial cells that infrequently form irregular ducts or acini. Density of tumor cells varies throughout the mass. Many anaplastic spindle-shaped tumor cells are also present. The neoplastic epithelial cells have marked nuclear pleomorphism, frequent prominent nucleoli and indistinct cell borders. Large foci of necrosis, scattered foci of hemorrhage and variable numbers of mitotic figures vary by field. Excision does not appear to be complete.

Review of a Masson's trichrome-stained section of tumor revealed that the neoplastic epithelial cells were negative for collagen while the desmoplastic tissue response was positive for collagen.

**Morphologic Diagnosis:** Submandibular salivary gland: Adenocarcinoma: high grade, poorly- differentiated.

**Other significant microscopic findings (not submitted):** Haired Skin, Incision Site of Tumor Removal: There are numerous small clusters to large foci (0.4 CM) of neoplastic cells similar in appearance to the primary tumor described in the biopsy report above scattered within the dermis and subcutis.

Lung, Thymus (none visible): There is a metastatic neoplastic process admixed with hemorrhage and inflammation that effaces and replaces at least 50% of the lung. The neoplastic cells are similar in appearance to those described for the salivary gland mass above, with the exception of a greater epithelial cell component. Clusters and islands of neoplastic cells are frequent within alveoli. Hemorrhage, fibrin and inflammatory cells (macrophages) predominate within adjacent alveolar spaces.

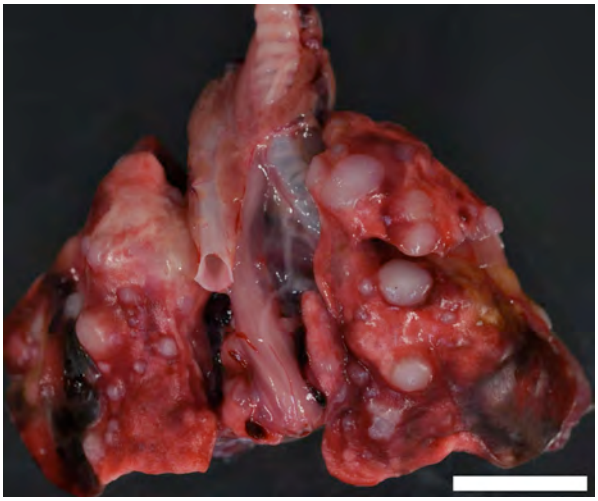

*4-1. Lung: There are numerous, multifocal, white, firm neoplastic masses encompassing approximately 50% of the lung lobes. Complete atelectasis of one lung lobe is observed and the distal surface of the right caudal lung lobe is adhered to the diaphragm. (Photo courtesy of: The Section of Comparative Medicine Yale University School of Medicine, New Haven, CT)*

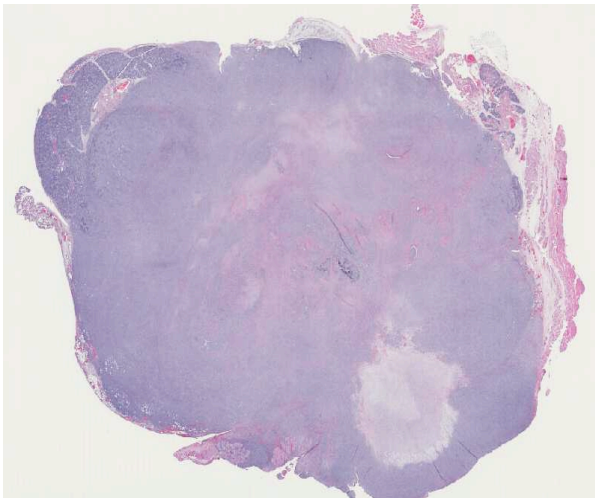

*4-2. Submandibular salivary gland, rat: The submandibular salivary gland is effaced by a large neoplasm with multiple areas of necrosis. Normal salivary tissue is at upper left, with infiltration of skeletal muscle and adipose tissue around the rest of the periphery. (HE 0.63X)*

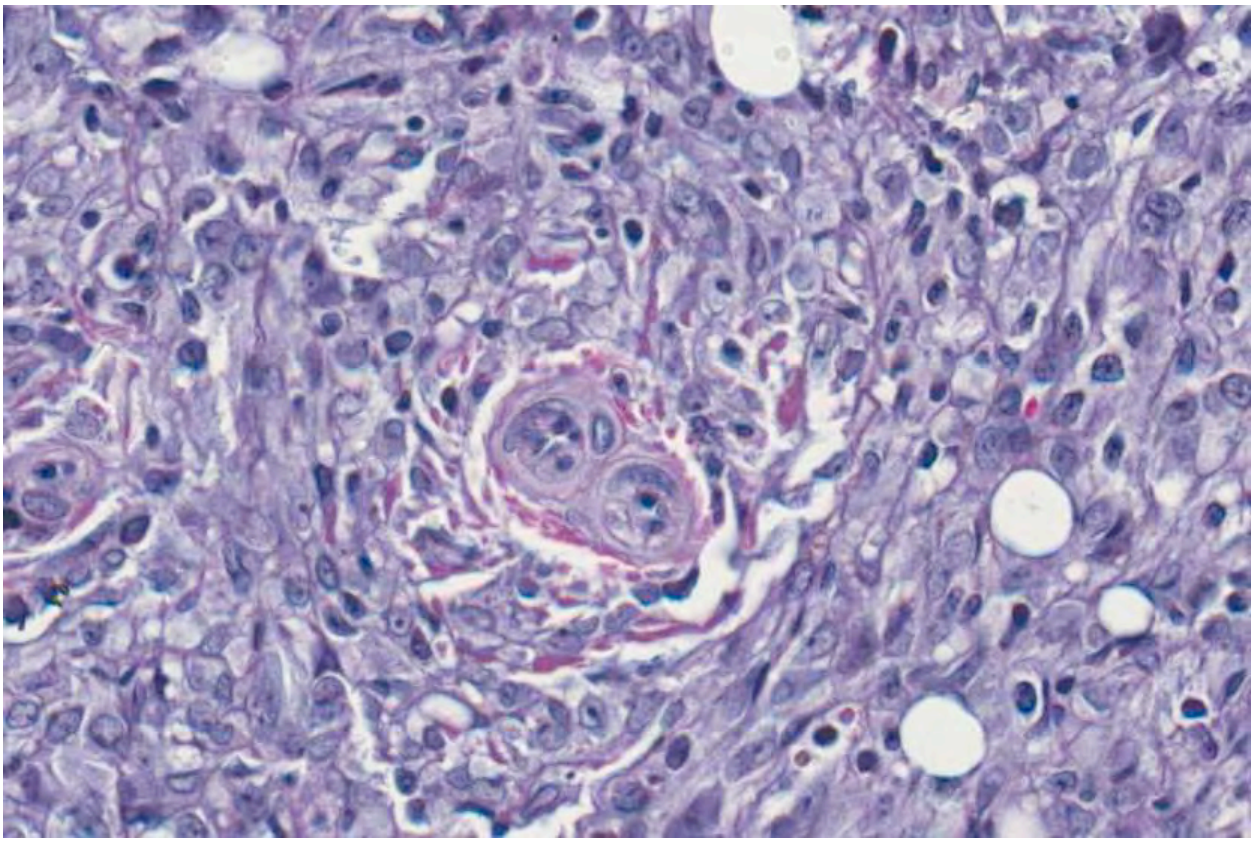

*4-3. Submandibular salivary gland, rat: Neoplastic cells are spindle to polygonal with variably distinct cell border, eosinophilic to granular (zymogen) cytoplasm, and supported on a fine fibrovascular stroma in some area. Tumor cells appear to be forming acinar structures that have a clear lumen multifocally. (HE 400X)*

Liver, Kidney, Adrenal Gland, Spleen, Pancreas: Within the one visible adrenal gland, 75% of the cortex and medulla are effaced and replaced by neoplastic cells similar in appearance to those described for the salivary gland above. There is bilateral mild to moderate chronic progressive glomerulonephropathy.

**Contributor's Comment:** Primary tumors of the major salivary glands are rare in humans, and the majority (>85%) are benign.[1,2,4,8,10,20,22,24] The incidence rate for both malignant and benign tumors is most common in patients between 50-70 years of age, but can occur at any age. There is also a wide geographic diversity of salivary gland tumor prevalence and frequency.[2,11,21] For example, it is reported that Canadian Eskimos have a greater prevalence (14/11,500/9years) of developing salivary gland carcinomas as compared to any other geographic group and they have a 100% mortality rate.[11] The majority of these tumors are undifferentiated lymphoepithelioma-like tumors found in mixed salivary glands.[21] Whereas in Denmark, they have a low prevalence of salivary gland carcinomas with an average of 1.1/100,000/year and the most common type is a parotid gland carcinoma.[2]

Benign salivary gland tumors tend to occur more commonly in females, whereas malignant tumors are more prevalent in males.[10] Malignant salivary gland tumors can be diagnosed using the World Health Organization (WHO) classification system.[22] In general, mucoepidermoid carcinomas account for over 50% of malignant salivary gland tumors in humans, while adenocarcinomas were reported in only 12% of the cases. Tumors have been documented in all three major salivary glands, as well as in minor salivary glands; however, the most common site in humans is the parotid gland and the second most common being the submaxillary gland.[2,4,10,20,22]

In humans, submandibular gland tumors account for 5-15% of all salivary gland tumors and less than 1% of all malignant head and neck tumors, however, over 50% are malignant.[1] Malignant submandibular adenocarcinomas in humans tend to have areas of necrosis and hemorrhage with irregular and ill-defined margins that infiltrate growth into surrounding tissues. They tend to form nests or islands of tumor cells and have a widespread ductal differentiation. Clinically, over 20% of patients have reported pain and facial weakness associated with the mass.[14] Most tumors have progressed to high grade by the time they are diagnosed; therefore, these malignant

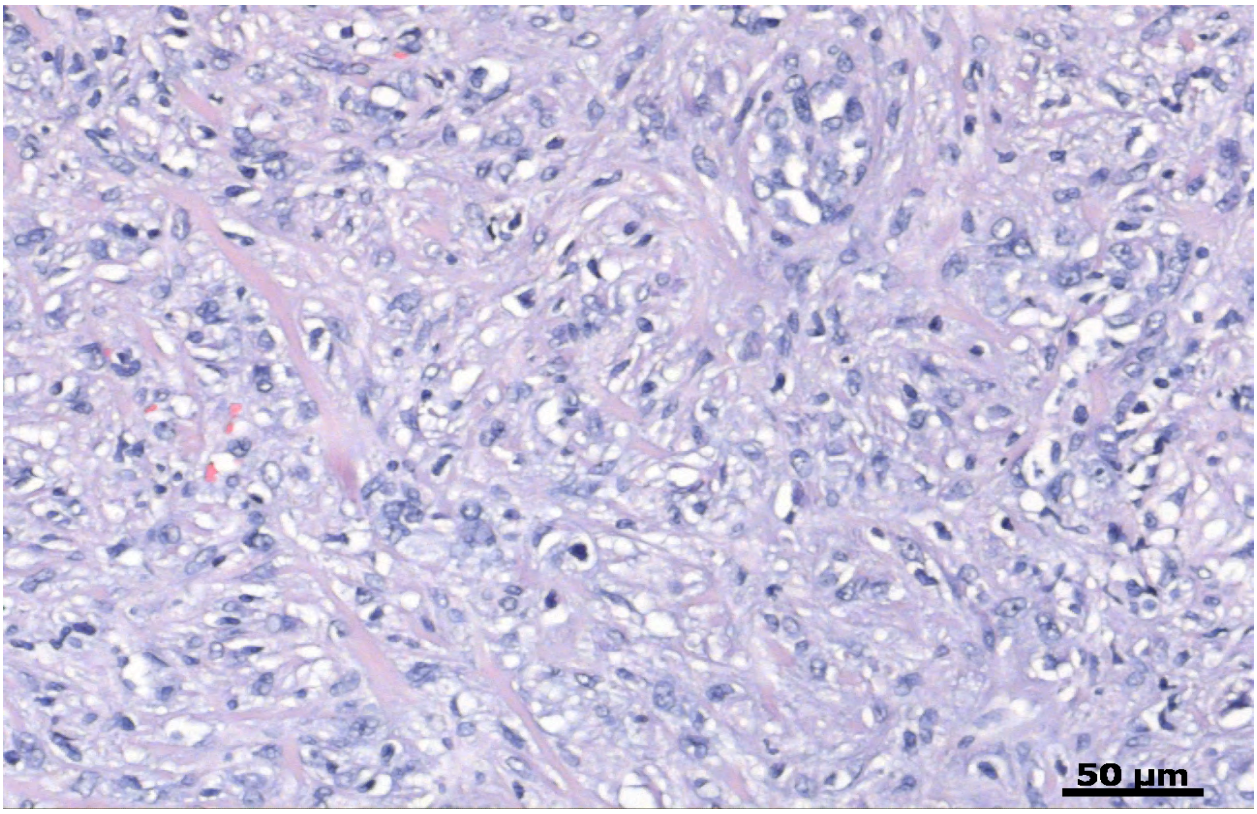


*4-4. Submandibular salivary gland, rat: Within large areas of the neoplasm there are broad streams and bundles of spindle cells. Whether this population represents a phenotypic variation of a single population of neoplastic cells, or a second population within the neoplasm was a major source of discussion in this case. (Photo courtesy of: The Section of Comparative Medicine, Yale University School of Medicine, New Haven, CT)*

submandibular salivary adenocarcinomas have a poor prognosis in humans.

Primary salivary gland tumors are also rare in domestic animals and have been reported in dogs[9,17], cats[13], lions[5], and cows.[3] In dogs, the most common salivary gland neoplasms are adenocarcinomas and carcinomas. There are two reports that describe rare cases in dogs, a malignant fibrous histiocytoma in a boxer[9] and another report of an osteosarcoma of the mandibular salivary gland in a collie.[17] Primary salivary gland tumors in cats are commonly carcinomas found in the minor salivary glands, rather than the parotid gland.[13] A single case of a high-grade mucoepidermoid carcinoma of the mandibular salivary gland has been reported in a lion.[5] There have also been three cases of parotid gland carcinomas reported in cows, two of which were pleomorphic carcinomas, and one was a squamous cell carcinoma.[3] Primary salivary gland tumors are also rare in rodents.[6,7,12,15,16,18,19,23] There has also been a single report of a Mongolian Gerbil developing a pleomorphic sarcoma of the salivary gland[18], and a ground squirrel with an adenocarcinoma of a minor salivary gland.[23] Mice very rarely develop salivary gland tumors, but myoepitheliomas have been reported to occur spontaneously in certain inbred strains of mice.

Spontaneous primary salivary gland tumors are also rare in rats, but may be chemically induced.[15,25] A study during carcinogenesis in rat submandibular glands showed that histopathology and immunohistochemistry is a useful tool for tumor histiogenesis.[15] Submandibular salivary gland adenocarcinomas in rats are poorly differentiated, show local invasion, and, in most cases, incite a significant desmoplastic response.[7] They should also exhibit the same characteristics seen in human salivary glands, including nests or islands of tumor cells, and tumor-grade specific nuclear and mitoses characteristics. In this case, the rat demonstrated a significant amount of irregular epithelial cells, marked nuclear pleomorphism, prominent nucleoli, large area of necrosis, scattered foci of hemorrhage, a variable number of mitotic figures, with a desmoplastic tissue response. All of these characteristics are consistent with a diagnosis of a high grade submandibular salivary gland adenocarcinoma. Metastasis to the lungs and adrenal gland also indicates that this was a high-grade tumor with a poor prognosis.

**JPC Diagnosis:** Submandibular salivary gland: Carcinoma, poorly-differentiated.

**Conference Comment:** The contributor does an excellent job of summarizing salivary gland tumors in

humans and animals. We agree that this neoplasm is both a high grade malignancy and poorly-differentiated; however, we prefer a more general diagnosis of poorly-differentiated salivary gland carcinoma. In this case, we considered diagnoses of salivary gland adenocarcinoma and myoepithelial carcinoma, as conference participants discussed whether or not the spindle cells represent either a desmoplastic response to tumor invasion or perhaps, a neoplastic component in itself. Immunophenotyping of the spindle cell population revealed a diffuse, strong cytoplasmic immunoreactivity for vimentin and scattered cytoplasmic immunoreactivity for both smooth muscle actin and calponin, (a myoepithelial cell marker). In addition to the poorly-differentiated tumor cell morphology, additional features of malignancy include local invasion into the surrounding adipose and skeletal muscle, areas of necrosis and neoplastic thrombi within blood vessels. Also present and of descriptive interest are individual and clusters of mast cells within the neoplasm, as well as ductal hyperplasia within the preexisting, entrapped salivary gland.

**Contributing Institution**: Section of Comparative Medicine
Yale University School of Medicine
New Haven, CT

**References:**

1. Bhattacharyya N. Survival and prognosis for cancer of the submandibular gland. *J Oral Maxillofac Surg*. 2004;62:427-430.
2. Bjorndal K, Krogdahl A, Therkildsen MH, Overgaard J, Johansen J, Kristensen CA, et al. Salivary gland carcinoma in Denmark 1990-2005: a national study of incidence, site and histology. Results of the Danish Head and Neck Cancer Group (DAHANCA). *Oral Oncol*. 2011;(47):677-682.
3. Bundza A. Primary salivary gland neoplasia in three cows. *J Comp Pathol*. 1983;93:629-632.
4. Cho KJ, Ro JY, Choi J, Choi SH, Nam SY, Kim SY. Mesenchymal neoplasms of the major salivary glands: clinicopathological features of 18 cases. *Eur Arch Otorhinolaryngol*. 2008;(265 Suppl 1): S47-56.
5. Dorso L, Risi E, Triau S, Labrut S, Nguyen F, et al. High-grade mucoepidermoid carcinoma of the mandibular salivary gland in a lion (Panthera leo). *Vet Pathol*. 2008;45:104-108.
6. Ishikawa Y, Nishimori K, Tanaka K, Kadota K. Naturally occurring mucoepidermoid carcinoma in the submandibular salivary gland of two mice. *J Comp Pathol*. 1998;118:145-149.
7. Nishikawa S, Sano F, Takagi K, Okada M, Sugimoto J, Takagi S. Spontaneous poorly differentiated carcinoma with cells positive for vimentin in a salivary gland of a young rat. *Toxicol Pathol*. 2010;38:315-318.
8. Pang B, Leong CC, Salto-Tellez M, Petersson F. Desmoplastic small round cell tumor of major salivary glands: report of 1 case and a review of the literature. *Appl Immunohistochem Mol Morphol*. 2011;19:70-75.
9. Perez-Martinez C, Garcia Fernandez RA, Reyes Avila LE, Perez-Perez V, Gonzalez N, Garcia-Iglesias MJ. Malignant fibrous histiocytoma (giant cell type) associated with a malignant mixed tumor in the salivary gland of a dog. *Vet Pathol*. 2000;37:350-353.
10. Pinkston JA, Cole P. Incidence rates of salivary gland tumors: results from a population-based study. *Otolaryngol Head Neck Surg*. 1999;120:834-840.
11. Schaefer O, Hildes JA, Medd LM, Cameron DG. The changing pattern of neoplastic disease in Canadian Eskimos. *Can Med Assoc J*. 1975;112:1399-1404.
12. Slavin BG, Paule WJ, Bernick S. Morphological changes in the submandibular gland of aging rats. *Gerodontology*. 1989;8:53-58.
13. Sozmen M, Brown PJ, Eveson JW. Salivary duct carcinoma in five cats. *J Comp Pathol*. 1999;121:311-319.
14. Spiro RH, Huvos AG, Strong EW. Adenocarcinoma of salivary origin. Clinicopathologic study of 204 patients. *Am J Surg*. 1982;144:423-431.
15. Sumitomo S, Hashimura K, Mori M. Growth pattern of experimental squamous cell carcinoma in rat submandibular glands--an immunohistochemical evaluation. *Eur J Cancer B Oral Oncol*. 1996;32B: 97-105.
16. Sundberg JP, Hanson CA, Roop DR, Brown KS, Bedigian HG. Myoepitheliomas in inbred laboratory mice. *Vet Pathol*. 1991;28:313-323.
17. Thomsen BV, Myers RK. Extraskeletal osteosarcoma of the mandibular salivary gland in a dog. *Vet Pathol*. 1999;36:71-73.
18. Toyoda T, Tsukamoto T, Cho YM, Onami S, Takasu S, Shi L, et al. Undifferentiated sarcoma of the salivary gland in a Mongolian gerbil (Meriones unguiculatus). *J Toxicol Pathol*. 2011;24:173-177.
19. Tsunenari I, Yamate J, Sakuma S. Poorly differentiated carcinoma of the parotid gland in a six-week-old Sprague-Dawley rat. *Toxicol Pathol*. 1997;25:225-228.
20. Vargas PA, Gerhard R, Araujo Filho VJ, de Castro IV. Salivary gland tumors in a Brazilian population: a retrospective study of 124 cases. *Rev Hosp Clin Fac Med Sao Paulo*. 2002;57:271-276.
21. Wallace AC, Macdougall JT, Hildes JA, Lederman JM. Salivary gland tumors in Canadian Eskimos. *Cancer.* 1963;16:1338-1353.
22. Barnes L. Tumors of the salivary glands. In: Barnes L, Eveson JW, Reichart P, Sidransky D, eds. *World Health Organization (WHO): The WHO Classification of Head and Neck Tumours. Pathology and Genetics of Head and Neck Tumours*. Lyon, France: International Agency for Research on Cancer (IARC) Press. 2005:209-281.
23. Yamate J, Yamamoto E, Nabe M, Kuwamura M, Fujita D, Sasai H. Spontaneous adenocarcinoma immunoreactive to cyclooxygenase-2 and transforming growth factor-beta1 in the buccal salivary gland of a

Richardson's ground squirrel (Spermophilus richardsonii). *Exp Anim.* 2007;56:379-384.
24. Yin WH, Guo SP, Yang HY, Chan JK. Desmoplastic small round cell tumor of the submandibular gland--a rare but distinctive primary salivary gland neoplasm. *Hum Pathol*. 2010;41:438-442.
25. Zaman A, Kohgo T, Shindoh M, Iizuka T, Amemiya A. Induction of adenocarcinomas in the submandibular salivary glands of female Wistar rats treated with 7,12-dimethylbenz(a)anthracene. *Arch Oral Biol*. 1996;41:221-224.

**Joint Pathology Center**
**Veterinary Pathology Services**

# WEDNESDAY SLIDE CONFERENCE 2012-2013

## Conference 19

**20 March 2013**

---

**CASE I:** 10-85188 (JPC 3165182).

**Signalment:** 10-year-old Holstein-Friesian cow from a dairy herd *(Bos Taurus)*.

**History:** This cow presented to the large animal teaching hospital with a history of being off feed and having decreased milk production. A swelling in the subcutis of her left ventral abdomen was noted. This cow had a history of clinical mastitis in the left front quarter, and was being treated with intravenous antibiotics including sulfadimethoxine and oxytetracycline. Heart sounds were muffled, and multiple "comet tails" were noted on ultrasound examination of the thorax.

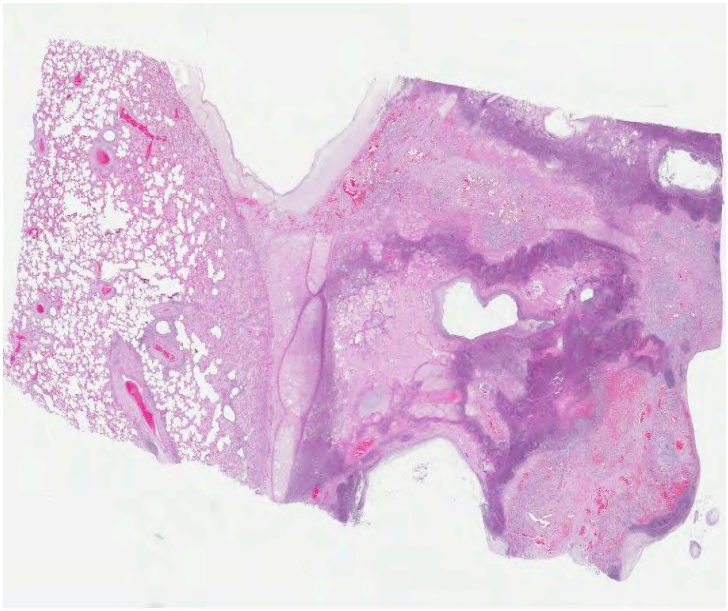

*1-1. Lung, ox: Subgross examination of the section of tissue shows confluent areas of necrosis at right delineated by dense basophilic bands of necrotic leukocytes, as well as marked expansion of interlobular connective tissue and lymphatics by marked edema and polymerized fibrin. (HE 0.63X)*

**Gross Pathologic Findings:** There is a moderately increased amount of blood-flecked foam in the distal 1/2 of the trachea and bronchial tree. The lungs contain approximately 100, 0.5 cm to 1 cm, firm, round, red-brown nodules with caseous or purulent centers; these nodules are evenly distributed through all lung lobes. Additionally, there are smaller numbers of subpleural and randomly distributed foci comprising solitary or multiple closely apposed or coalescing, 1 to 2 cm diameter, air-filled bullae surrounded by firm white tissue and lined by green-black, tenacious necrotic material and scattered, variably sized, velvety, white to brown plaques.

**Histopathologic Description:** Obliterating over 50% of the lung parenchyma in the examined section is a focally extensive, empty space bounded by a dense band of fungal hyphae embedded in eosinophilic, amorphous to granular necrotic material and fibrin. Fungal hyphae stain relatively poorly with PAS and GMS, and are characterized by nonparallel

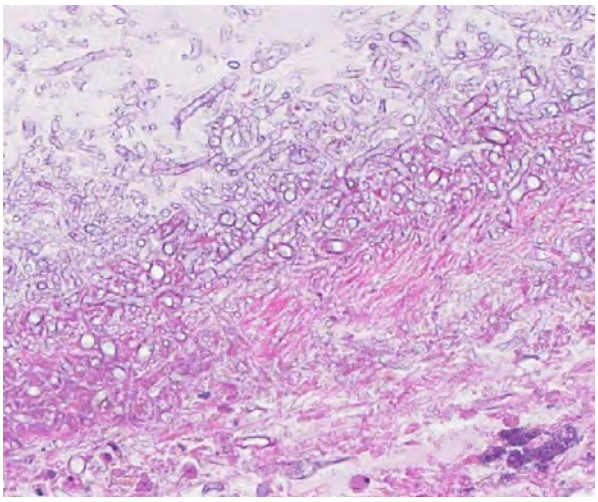

*1-2. Lung, ox: Within necrotic areas, and focally, within the wall of a large vessel, there are numerous clusters of pauciseptate 6-10 µm diameter fungal hyphae with non-parallel walls and bulbous dilations which seen in negative relief. (HE 300X)*

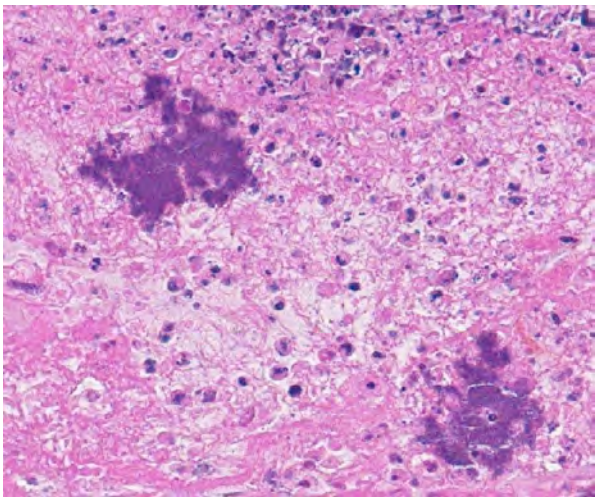

*1-3. Lung, ox: Also within necrotic areas, there are numerous large colonies of 1-2 µm bacilli, consistent with the Truperella cultured at autopsy. (HE 400X)*

walls, a lack of septa, irregular, non-dichotomous branching at right angles, and occasional bulbous dilatations. The adjacent pulmonary parenchyma is characterized by lytic or coagulative necrosis, multifocal hemorrhage, granulation tissue, and florid infiltrates of viable and degenerate neutrophils with fewer macrophages, eosinophils, lymphocytes and plasma cells. Within this surrounding tissue are many large colonies of gram positive short rods. Bronchiolar epithelium is multifocally attenuated or eroded, and airway lumina rarely contain proteinaceous material admixed with small numbers of degenerate inflammatory cells. In less affected areas of the lung, alveolar spaces are filled by edema, fibrin, and foamy macrophages and bronchioles are spared.

**Contributor's Morphologic Diagnosis:** Pneumonia, necrosuppurative, chronic-active, multifocal, severe, with intralesional fungal hyphae consistent with zygomycetes and gram positive rods. (*Arcanobacterium pyogenes* and *Rhizomucor* spp. [not further classified] were cultured from the lung).

**Contributor's Comment:** The class *Zygomycetes* is divided into the orders *Mucorales* and *Entomophthorales*. Members of the order *Mucorales* tend to cause disseminated disease characterized by angioinvasion, while members of the *Entomophthorales* tend to cause localized subcutaneous granulomas.[2] Mucormycosis generally manifests as subcutaneous, systemic or rhinocerebral infections.[2] The main portal of entry in bovine mucormycosis is reported to be the gastrointestinal tract; however, a recent report of 194 slaughtered feedlot steers with granulomatous lymphadenitis and intralesional fungal hyphae noted that no evidence of gastrointestinal disease or systemic spread was present in any of the animals, and that other portals of entry could not be completely ruled out.[1] Zygomycetes are cosmopolitan and ubiquitous, and at least one member of the genus *Rhizopus*, *R. pusillis*, is thermophilic.[1] The presence of broad, infrequently septate hyphae with irregular branching is characteristic of these fungi and can be seen in routine H & E stains, but visualization is greatly augmented by the periodic acid-Schiff reaction or Gomori's methanamine silver stain. In the present case, because *Arcanobacterium pyogenes* (but not fungi) were cultured from the mammary gland, it is likely that the bacterial mastitis was the primary source of an embolic pneumonia that was further complicated by aerogenous zygomycete infection. There was no gross or histological evidence of fungal infection in any other tissue, including mammary gland and gastrointestinal tract.

**JPC Diagnosis:** Lung: Pleuropneumonia, necrosuppurative, chronic, focally extensive, severe, with vasculitis, numerous colonies of bacilli and fungal hyphae.

**Conference Comment:** The contributor provides a good summary of the fungal aspect of this mixed infection. Conference participants debated on the bacterial agent; based on the combination of lytic and coagulative necrosis observed, some participants considered *Mannheimia or Mycoplasma*. These entities were ruled out, however, as neither of them would be present in large colonies as seen in this slide. Recently *Arcanobacterium pyogenes* (formerly *Actinomyces pyogenes* and *Corynebacterium pyogenes)* has undergone another taxonomic reclassification and subsequent name change and is now known as *Trueperella pyogenes.* Based on phylogenetic and chemotaxonomic differences, the genus *Arcanobacterium* was divided into two genera--*Arcanobacterium* and a novel genus, *Trueperella.* *T. pyogenes* is the type species for this new genus.[4] Both

genera are in the family *Actinomycetaceae*, a diverse group of gram positive bacteria that also includes the genera *Actinomyces* and *Actinobaculum*.[3] *T. pyogenes* is an opportunistic pathogen that clinically causes abscesses, mastitis, suppurative pneumonia, endometritis, pyometra, arthritis and umbilical infections in cattle, sheep and pigs. Its pathogenicity is due to several virulence factors, primarily pyolysin, a hemolytic exotoxin that lyses neutrophils, macrophages and other cell types. Additionally, they produce neuraminidases, adhesins, extracellular matrix-binding proteins and fimbriae. *T. pyogenes* produces proteases as well, but their role in pathogenicity is yet to be determined. Other members of veterinary importance in the family *Actinomycetaceae* include: *Actinomyces bovis* (lumpy jaw in cattle), *Actinomyces speci*es (pyogranulomatous mastitis in pigs and poll evil and fistulous withers in horses), *Actinomyces viscosus* (cutaneous pyogranulomas in dogs and horses, proliferative pyogranulomatous pleuritis in dogs, abortion in cattle), *Actinobaculum suis* (cystitis and pyelonephritis in pigs), and *Actinomyces hordeovulneris* (cutaneous and visceral abscessation, pleuritis, peritonitis, and arthritis in dogs).[3]

**Contributing Institution:** Auburn University
Department of Pathobiology
College of Veterinary Medicine
166 Greene Hall
Auburn, AL 36849

**References:**

1. Ortega J, et al. Zygomycotic Lymphadenitis in Slaughtered Feedlot Cattle. *Vet Pathol*. 2010;47(1): 108-115.
2. Ginn P, Mansell JEKL, Rakich PM. In: Maxie MG, ed. *Jubb, Kennedy and Palmer's Pathology of Domestic Animals*. Vol. 1. 5th ed. Philadelphia, PA; Saunders Elsevier: 2007;707-8.
3. Quinn PJ, et al. Actinobacteria. In: *Veterinary Microbology and Microbial Disease.* 2nd ed. Ames, Iowa: Wiley Blackwell; 2011, Kindle edition, location 6945 of 35051.
4. Yassin AF, Hupfer H, Siering C, Schumann O. Comparative chemotaxonomic and phylogenetic studies on the genus Arcanobacterium Collins et al. 1982 emend. Lehnen et al. 2006: proposal for Trueperella gen. nov. and emended description of the genus Arcanobacterium. *Int J Syst Evol Microbiol.* 2011;61:1265-74.

**CASE II:** A10-6475 (JPC 3164432).

**Signalment:** Four-year-old, spayed female domestic medium hair cat (*Felis catus),* feline.

**History:** The history described facial dermatitis that progressed over a four-month period to generalized erythema and crusting of the pinnae, paws, dorsum, legs, and ventrum. Euthanasia was elected due to progressive deterioration of the cat.

**Gross Pathologic Findings:** The body was in good postmortem condition. Thick sheets of exfoliated keratin or tan to yellow exudate covered regions of alopecia and erythema on the legs, ventral and lateral abdomen and thorax, dorsum, muzzle, and pinnae. The residual hair coat was easily epilated and often entrapped thick layers of keratin. The cranial mediastinum contained a 5.5 x 3 x 2 cm, pale red to tan mass. The mass contained multiple cystic structures that were separated by soft pale red parenchyma and filled with translucent pale yellow to blood-tinged fluid.

**Histopathologic Description:** There was severe, diffuse, compact, orthokeratotic to parakeratotic hyperkeratosis that covered the epidermis and extended into most follicular infundibula which often lacked hair shafts. The epidermis was moderately to markedly acanthotic with prominent rete pegs. The epidermis was segmentally eroded to ulcerated and covered by thick serocellular crusts admixed with colonies of gram positive cocci. There were scattered individual necrotic keratinocytes in the stratum spinosum, and less frequently in the stratum basale and stratum granulosum. Lymphocytes were multifocally exocytosed into the stratum basale and the deep layers of the stratum spinosum. The dermis was moderately inflamed with a perivascular distribution of mast cells, plasma cells, and fewer lymphocytes. Sebaceous glands were diffusely atrophied.

**Morphologic Diagnosis:** Skin: Epidermal hyperkeratosis and acanthosis with apoptotic keratinocytes, lymphoplasmacytic perivascular dermatitis, and sebaceous gland atrophy.

**Contributor's Comment:** The mediastinal mass was composed of dense aggregates of small to medium-sized lymphocytes that were surrounded by sheets of larger polygonal to round cells with moderate to abundant pale eosinophilic cytoplasm, ovoid to indented hypochromic nuclei, and 0-1 basophilic nucleoli. These larger polygonal cells demonstrated cytoplasmic immunoreactivity for pancytokeratin, facilitating the diagnosis of a thymoma. Thymomas arise from thymic epithelial cells and are classified as lymphocytic, epithelial, or mixed based on the ratio of epithelial cells to lymphocytes.[4] Thymomas are exceedingly rare in cats and are seen most often in middle-aged to older animals. Several immune mediated conditions in humans, dogs, and cats have been associated with thymomas, including myasthenia gravis, polymyositis, and various dermatoses.[6]

Thymoma-associated exfoliative dermatitis is an uncommon condition that has been reported in cats and rabbits.[1,5,6] This disorder is thought to be a paraneoplastic syndrome that results from the failure of the neoplastic thymus to eliminate autoreactive T lymphocytes that target epidermal keratinocytes.[3,5] The association between exfoliative dermatitis and thymomas has been supported clinically by the alleviation of cutaneous lesions following surgical removal of the thymoma.[5]

*2-1. Thick sheets of exfoliated keratin or tan to yellow exudate covered regions of alopecia and erythema on the legs, ventral and lateral abdomen and thorax, dorsum, muzzle, and pinnae. (Photo courtesy of: The Purdue University Department of Comparative Pathobiology, 725 Harrison St., West Lafayette, IN 47905)*

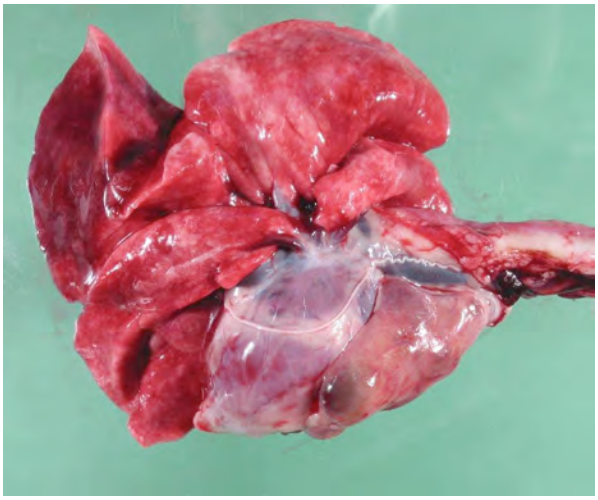

*2-2. The cranial mediastinum contained a 5.5 x 3 x 2 cm, pale red to tan mass. The mass contained multiple cystic structures that were separated by soft pale red parenchyma and filled with translucent pale yellow to blood-tinged fluid. (Photo courtesy of: The Purdue University Department of Comparative Pathobiology, 725 Harrison St., West Lafayette, IN 47905)*

*2-3. This slide contains two tissues, a multicystic thymic mass (left), and a section of hyperkeratotic haired skin (right). (HE 0.63X)*

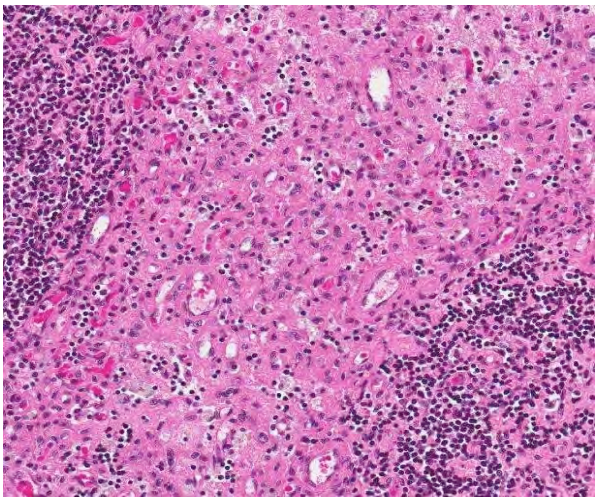

*2-4. Thymus, cat: The thymic neoplasm is composed of poorly defined sheets of epithelial cells which surround and separate remaining islands of thymic lymphocytes. (HE 280X)*

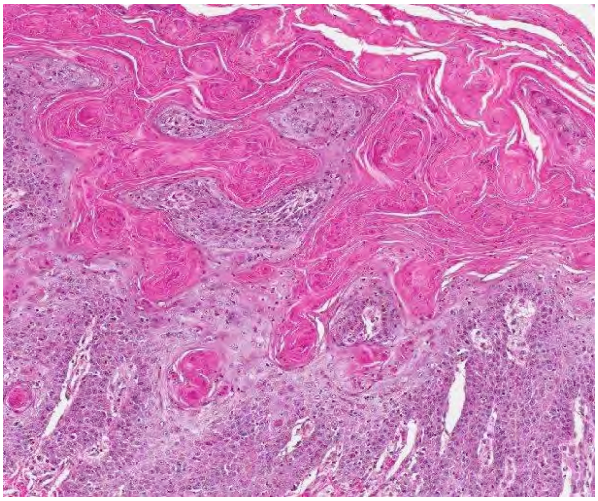

*2-5. Haired skin, cat: The epidermis exhibits marked parakeratotic hyperkeratosis which extends down into follicular ostia. There is profound epidermal hyperplasia, acanthosis, and spongiosis, with formation of deep rete ridges and a cell-poor infiltrate at the dermal-epidermal junction. (HE 240X)*

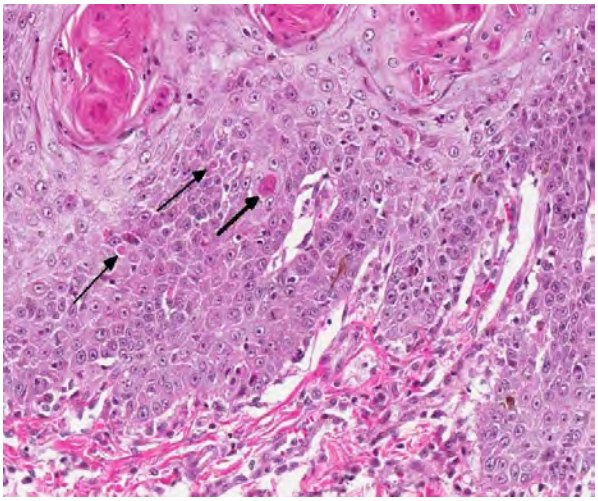

*2-6. Haired skin: There are necrotic keratinocytes (arrows) at all levels of the epidermis. (HE 360X)*

The cutaneous lesions of erythema and exfoliation of keratin are often first noted on the head, neck, and pinnae, but progressively become more generalized.[3] Alopecia is commonly seen as a sequela to the exfoliative dermatitis.[3] Clinical differentiation from other exfoliative dermatoses can be achieved by skin biopsies and a diagnosis of thymoma via thoracic radiographs and fine needle aspirates of the mass.[3]

The typical histopathologic lesions of thymoma-associated exfoliative dermatitis include severe parakeratotic to orthokeratotic hyperkeratosis, acanthosis, mild transepidermal apoptosis, sebaceous gland atrophy, and cell-poor interface dermatitis.[3,5] An alternative diagnosis to consider is the hyperkeratotic form of erythema multiforme.[3] Both conditions can exhibit marked hyperkeratosis and variable degrees of interface dermatitis, but transepidermal apoptosis is often more severe in erythema multiforme.[3]

**JPC Diagnosis:** 1. Thymus: Thymoma.
2. Haired skin, auricular pinna: Epidermal hyperplasia and hyperkeratosis, diffuse, marked, with multifocal keratinocyte necrosis and mild cell-poor lymphoplasmacytic interface dermatitis.

**Conference Comment:** In an informative summary of this rare condition, the contributor notes that thymoma-associated exfoliative dermatitis is typically characterized by parakeratosis and a cell-poor interface dermatitis;

however, in a review of five cats with this paraneoplastic condition, Rottenberg et al also observed examples of cell-rich skin lesions.[5] Conference participants discussed the use of the terms "cell-poor" and "cell-rich" in defining and categorizing various types of interface dermatitis. Interface dermatitis refers to conditions in which an inflammatory infiltrate abuts and/or obscures the dermoepidermal junction; it is classified based on the dominant inflammatory cell type involved (i.e. neutrophilic, lymphocytic, lymphohistiocytic, etc.), and can be further described as either cell-poor or cell-rich. Cell-poor interface dermatitis is characterized by a sparse infiltrate of inflammatory cells along the dermoepidermal junction, whereas its cell-rich counterpart – also referred to as lichenoid interface dermatitis -- comprises a heavy band-like inflammatory infiltrate which can obscure the epidermal basal layers. In humans, cell-poor interface dermatitis is associated with conditions such as erythema multiforme, systemic lupus erythematous, dermatomyositis, mixed connective tissue disease, graft-versus-host disease, morbilliform viral exanthema, and morbilliform drug reactions. Cell-rich interface dermatitis is observed in cases of idiopathic lichenoid disorders, discoid lupus erythematous, lichenoid and granulomatous dermatitis, lichenoid purpura, and lichenoid and fixed drug reactions.[2]

**References:**

1. Florizoone K. Thymoma-associated Exfoliative Dermatitis in a Rabbit. *Veterinary Dermatology.* 2005;16:281-284.
2. Crowson AN, Magro CM, Mihm Jr MC. Interface Dermatitis. *Archives of Pathology & Laboratory Medicine*. 2008;132(4):652-666.
3. Gross TL. Ihrke PJ. Walder EJ, et al. *Skin Diseases of the Dog and Cat*. 2nd ed. Ames, IA: Blackwell Science Ltd; 2005:68-70, 78-79.
4. Jacobs RM. Messick JB. Valli VE. Tumors of the hemolymphatic system. In: Meuten DJ, ed. *Tumors in Domestic Animals*. 4th ed. Ames, IA: Blackwell Publishing Professional; 2002:165-166.
5. Rottenberg S, Tscharner CV, Rossje RJ. Thymoma-associated Exfoliative Dermatitis in Cats. *Vet Pathol.* 2004;41:429-433.
6. Scott DW, Yager JA, Johnston KM. Exfoliative Dermatitis in Association with Thymoma in Three Cats. *Feline Pract.*1995;23:8-13.

**CASE III:** AFIP Case 1 (JPC 4018760).

**Signalment:** Fetus, female, Thoroughbred, *Equus caballus*, horse.

**History:** No history was provided.

**Gross Pathology:** A fetus with a crown-rump length of 61 cm was submitted with attached fetal membranes. There were hundreds of multifocal, white to yellow, irregular, slightly raised, soft, 25mm and 100mm in diameter plaques that often had a ring or pinwheel shape with a clear centre on the skin. The plaques concentrated around the head, particularly around the eyes, and the trunk but also extended along the back, tail, and limbs.

Disseminated throughout the lung lobes were hundreds of 20-50mm diameter, multifocal, firm, off-white to yellow nodules. On the cut section, the nodules were homogenous, off-white and often markedly friable centrally with a thin capsule.

The stroma of the chorioallantois was diffusely variably thickened and expanded by dark red to yellow gelatinous material. The surface of the chorion was mottled with well-demarcated red and tan areas. The chorion was covered by very thin multifocal to coalescing plaques of yellow, friable, foul smelling material. There was abundant, clumped, loosely adhered, tan to yellow material along the amnion, often tracking along blood vessels.

**Histopathologic Description:** Chorioallantois: There is marked, locally extensive necrosis of the chorionic villi that occasionally extends deeply, extending the full thickness of the stroma. Within the affected areas, there is a loss of the normal architecture with extensive areas of necrotic cellular debris, fibrin, and degenerate neutrophils. Layered within the surface debris are numerous 5-10 µm diameter, septate, branching fungal hyphae with non-parallel walls. Large clusters of neutrophils extend deeply into the areas of more viable stroma, and are often admixed with cellular debris and small numbers of lymphocytes, macrophages, and plasma cells. Inflammatory cells expand the walls of deep vessels. Vascular luminal fibrin thrombi are frequent. The allantoic epithelium is multifocally irregularly thickened (proliferation) and is occasionally cystic. Allantoic epithelial cells have abundant often heavily vacuolated cytoplasm. Cellular debris is scattered within the more affected areas.

Haired skin: There is marked diffuse orthokeratotic hyperkeratosis. Embedded within the layers of keratin are aggregates of cellular debris and fungal hyphae as in the placenta. Within the superficial dermis, there is a marked, diffuse infiltrate of lymphocytes and plasma cells.

Lung (slide not provided): Randomly scattered throughout the lung are multifocal, nodular areas of inflammation that efface the normal architecture and often engulf adjacent vessels. The centers of the nodules are composed of liquefactive necrosis surrounded by a rim of epithelioid macrophages and multinucleated giant cells admixed with fibrin and hemorrhage. Peripherally, there are moderate numbers of lymphocytes and plasma cells admixed with cellular debris. Entrapped vessels have walls replaced by fibrin and cellular debris. Within the necrotic areas, there are branching clear spaces that are suspicious for fungal hyphae.

**Contributor's Morphologic Diagnosis:** Placenta: Marked, multifocal to coalescing necrotizing placentitis with intralesional fungal hyphae and vasculitis.

*3-1. The equine fetus was covered by numerous multifocal, white to yellow, irregular, slightly raised, soft, 25 and 100mm in diameter plaques, most commonly around the eyes and trunk. (Photo courtesy of: University of Glasgow, School of Veterinary Medicine, Bearsden Rd, Glasgow, UK G611QH, http://www.gla.ac.uk/schools/vet/)*

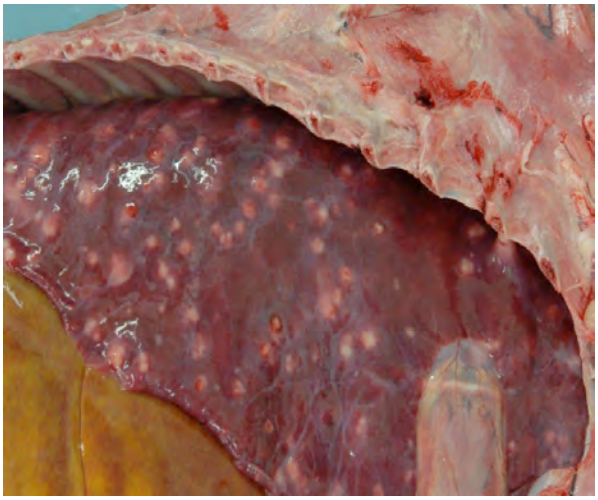

*3-2. Disseminated throughout the lung lobes were hundreds of 20-50mm diameter, multifocal, firm, off-white to yellow nodules. (Photo courtesy of: University of Glasgow, School of Veterinary Medicine, Bearsden Rd, Glasgow, UK G611QH, http://www.gla.ac.uk/schools/vet/)*

*3-3. The chorioallantosis was thickened with a mottled red-tan appearance. The chorion was covered by thin plaques of yellow, friable, foul-smelling material. (Photo courtesy of: University of Glasgow, School of Veterinary Medicine, Bearsden Rd, Glasgow, UK G611QH, http://www.gla.ac.uk/schools/vet/)*

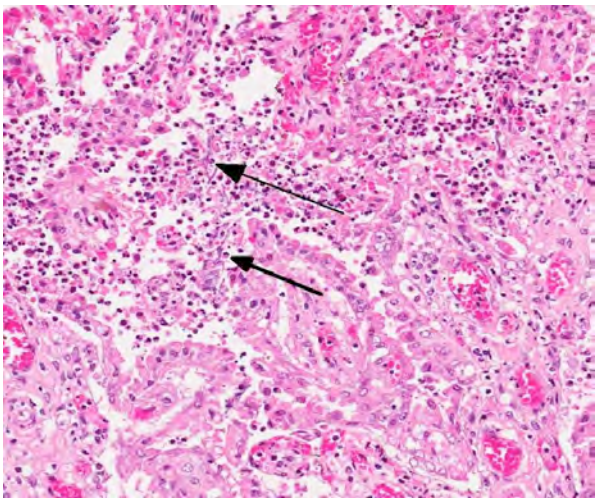

*3-4. Placenta, chorion: Chorionic villi are separated by abundant necrotic debris and aggregates of numerous 4um wide, pigmented, septate, non-dichotomous, parallel wall, acute angle branching fungal hyphae (arrows). (HE 320X)*

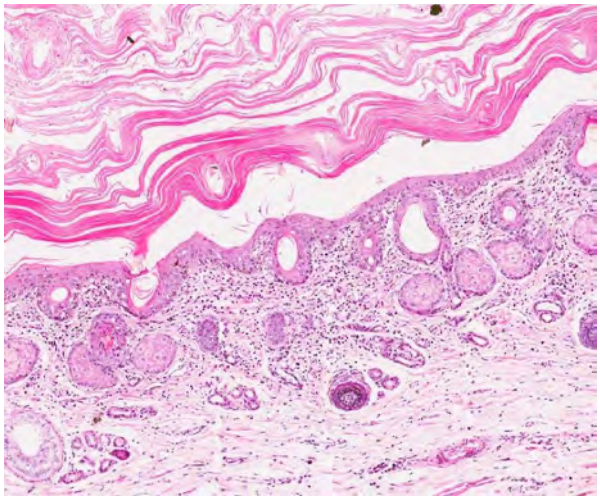

*3-5. Haired skin: Fetal skin exhibits marked orthokeratotic hyperkeratosis, overlying a markedly inflamed dermis. (HE 240X)*

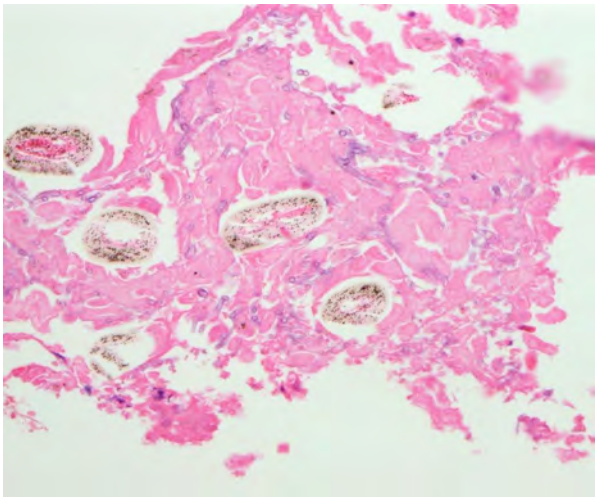

*3-6. Embedded within the hyperkeratotic scale overlying the skin are aggregates of cellular debris and fungal hyphae as in the placenta. (Photo courtesy of: University of Glasgow, School of Veterinary Medicine, Bearsden Rd, Glasgow, UK G611QH, http://www.gla.ac.uk/schools/vet/)*

Dermatitis: Marked, multifocal dermatitis with orthokeratotic hyperkeratosis and intralesional fungal hyphae.
Lung: Marked, multifocal granulomatous pneumonia.

**Contributor's Comment:** Differentials for abortion in horses include a wide variety of maternal, mechanical (vascular), toxic, and infectious causes. Of these causes, placental disease is the most common cause of abortion in horses.[2] The most common pathogens isolated from the placenta of aborted fetuses are *Streptococcus* spp., *Leptospira* spp., *Escherichia coli,* nocardioform actinomycetes, *Pseudomonas aeruginosa, Enterobacter agglomerans*, and *Klebsiella pneumoniae*.[2]

Mycotic placentitis is less common than bacterial placentitis in horses and typically results in a regionally extensive placentitis centered on the cervical star, reflecting the ascending nature of the infection.[2,3] Abortion due to mycotic placentitis occurs more commonly in late gestation and results from placental failure.[3] Mycotic dermatitis is a common concurrent finding. Pulmonary lesions, as seen in this case, are uncommon and are thought to occur as a result of aspiration of contaminated amniotic fluid. Systemic dissemination is rarely seen in the fetus.[4] *Aspergillus* spp. are the most common fungal organisms isolated from aborted fetuses.[2] In this case, the morphology of fungal

hyphae is highly suggestive of *Aspergillus* spp.; however, cultures are required for definitive diagnosis.

**JPC Diagnosis:** 1. Placenta: Placentitis, necrotizing and suppurative, diffuse, moderate, with focal infarction, vasculitis, fibrinoid change, and moderate numbers of fungal hyphae.
2. Haired skin, eyelid: Dermatitis, lymphoplasmacytic, diffuse, mild, with marked epithelial hyperkeratosis and intracorneal fungal hyphae.

**Conference Comment:** As the contributor states, there are numerous causes of failure of equine pregnancy. In addition to the bacterial and fungal etiologic agents described by the contributor, other infectious causes include viruses such as equine herpesvirus 1 (EHV-1), EHV-3 (equine coital exanthema) and EHV-4, as well as equine viral arteritis virus.[1] EHV-1 is an important cause of abortion; its classic histopathologic lesion is focal necrosis in the liver, and necrosis in other organs is often seen as well. It is often associated with pneumonia, and fibrin casts in the trachea are characteristic of EHV-1 infection. EHV-3 and EHV-4 cause similar lesions, but are not as common. Equine viral arteritis often results in no fetal lesions, as fetal death is likely due to anoxia secondary to myometritis. Bacterial-associated abortion in horses is associated with placentitis, and although fetal sepsis probably plays a major role, macroscopic and microscopic fetal lesions are rare.[1]

There are many noninfectious causes of pregnancy failure in horses, some of which include: twinning, umbilical cord anomalies, endometrial fibrosis, premature placental separation, and fetal thyroid hyperplasia and musculoskeletal disease.[1] Twinning results in a decreased surface area of chorionic villi, since villi do not develop in the areas where the two placentas come into contact. In these cases, death is thought to be due to placental insufficiency. Equine umbilical cord anomalies such as excessive or inadequate length and torsion can also result in failure of pregnancy. Endometrial fibrosis, usually a result of past endometriosis, precludes adequate maternofetal interface, thus resulting in either failure of the mare to become pregnant or an inability to carry the fetus to term. Premature placental separation results in a detachment of the caudal part of the chorioallantois from the uterus and a tearing across the body of the placenta instead of at the cervical star. Fetal anomalies are rare in horses; however, in some regions foals abort due to thyroid hyperplasia and musculoskeletal disease, characterized by microscopic thyroid hyperplasia but no macroscopic gland enlargement. Prognathia, flexural deformities, joint laxity, and tendon ruptures can occur in this syndrome.[1]

Although not as common, there have also been several abortion storms in mares associated with eastern tent caterpillars (ETC), referred to as mare reproductive loss syndrome (MRLS), the pathogenesis for which has not been fully elucidated. Current hypotheses propose either a bacterial invasion and bacteremia occurrence secondary to injury from ingested ETC-related toxins or from mechanical damage to the gastrointestinal mucosa by setae ("hairs") on the ETC.[5]

**Contributing Institution**: University of Glasgow
School of Veterinary Medicine
Bearsden Rd
Glasgow, UK G611QH
http://www.gla.ac.uk/schools/vet/

**References:**
1. Foster RA. Femal reproductive system and mammary gland. In: Zachary JF, McGavin MD, eds. *Pathologic Basis of Veterinary Disease*. St. Louis, MO: Elsevier Mosby; 2012:1109-1111.
2. Hong CB, Donahue JM, Giles RC Jr, Petrites-Murphy MB, Poonacha KB, Roberts AW, et al. Equine abortion and stillbirth in central Kentucky during 1988 and 1989 foaling seasons. *J Vet Diagn Invest*. 1993;(4):560-6.
3. Hong CB, Donahue JM, Giles RC Jr, Petrites-Murphy MB, Poonacha KB, Roberts AW, et al. Etiology and pathology of equine placentitis. *J Vet Diagn Invest*. 1993; (1):56-63.
4. Schlafer DH, Miller RB. Female genital system. In: Maxie MG, ed. *Pathology of Domestic Animals*. 5th ed. Edinburgh, UK: Saunders Elsevier; 2007:508-509.
5. Sebastian MM, Bernard WV, Riddle TW, Latimer CR, Fitzgerald TD, Harrison LR. REVIEW paper: mare reproductive loss syndrome. *Vet Pathol*. 2008;45(5): 710-22.

**CASE IV:** 12-1821 (JPC 4017807).

**Signalment:** Three-year-old, intact female cat *(Felis catus).*

**History:** This was a feral cat submitted from a spay-neuter project in southern CA. The history was 'unknown death'. The submitter wished to rule out viral disease and poisons.

**Gross Pathology:** The carcass was in good post mortem condition but poor body condition, with minimal fat stores, prominent ribs and decreased muscle mass. The most significant lesions were in the lungs. All lung lobes did not collapse and were expanded by multiple coalescing, slightly firm, tan nodules. Tracheobronchial lymph nodes were 4 times normal size. An impression smear of the nodules showed numerous macrophages filled with 2-4 µm yeasts.

All other organs including liver and spleen were considered to be grossly within normal limits.

**Laboratory Results:** After DNA extraction from the paraffin block, the D1D2 region of the 28S ribosomal RNA gene was amplified by PCR using universal fungal primers. When this PCR amplicon was directly sequenced, the sequence most closely matched that of *Ajellomyces capsulatus* (*Histoplasma capsulatum*) (>99 % sequence identity with GenBank acc # AB176473 and others ) when compared with sequences in GenBank.

**Histopathologic Description:** The architecture of over 80% of the lung in all evaluated sections was distorted by dense sheets of abundant inflammatory infiltrate composed of many epithelioid macrophages that expand the interstitium and fill the alveoli and bronchioles. Mixed with the macrophages were fewer lymphocytes, fibrin and edema residue. Macrophages were commonly distended by 8 to 20 intracytoplasmic yeast bodies that were round, 3 to 4 µm diameter and had a basophilic center surrounded by a 2 µm halo. Multifocally large areas of the lung were replaced by eosinophilic cellular debris, karyorrhectic debris and degenerate cells (necrosis). Small scattered areas were interrupted by hemorrhage.

The tracheobronchial lymph nodes (not submitted) were expanded by sheets of epithelioid macrophages, many of which contained similar yeast bodies. Organisms were further demonstrated by Gomori methenamine silver and periodic acid-Schiff on lung and lymph node. Fewer, scattered macrophages with intracellular yeasts were identified in the liver and spleen with special stains.

**Contributor's Morphologic Diagnosis:** Bronchopneumonia, histiocytic, focally extensive to coalescing, severe with multifocal necrosis and intralesional, intracytoplasmic yeasts.

**Contributor's Comment:** Histoplasmosis is a non-contagious infectious disease of man and animals caused by the dimorphic fungus *Histoplasma capsulatum* var. capsulatum.[3] It is a soil-born infection often associated with exposure to soil contaminated either with bird or bat feces. Although affecting both man and animals, it is not considered a zoonotic disease.[7] It is distributed world-wide but is considered endemic in the Ohio, Mississippi and St. Lawrence River Valley. However, any area with the right conditions can produce cases, such as the reported outbreak in dogs and cats in the Rio Grande Valley of Texas.[2] In that report, exposure was attributed to urbanization of rural land once occupied by chicken farms, and to a local bat cave. Local irrigation made


*4-1. When the thorax of this cat was opened, lung lobes did not collapse and were expanded by multiple coalescing, slightly firm, tan nodules. (Photo courtesy of the Department of Veterinary Microbiology and Pathology, College of Veterinary Medicine, Washington State University, Pullman, WA 99164-7040 http:// www.vetmed.wsu.edu)*


*4-2. Lung, cat: Tracheobronchial lymph nodes were 4 times normal size. (Photo courtesy of the Department of Veterinary Microbiology and Pathology, College of Veterinary Medicine, Washington State University, Pullman, WA 99164-704 http:// www.vetmed.wsu.edu)*

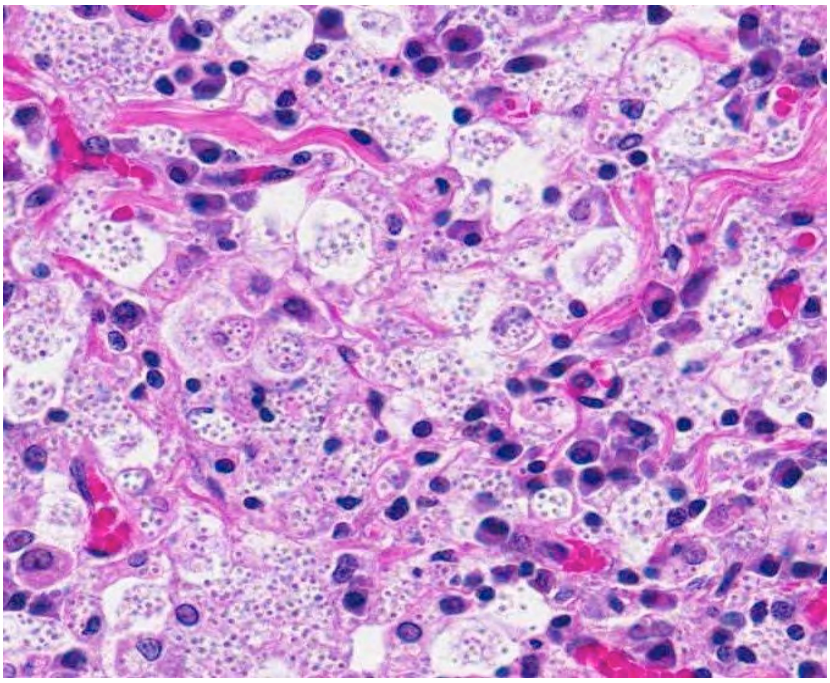

*4-3. Lung, cat: Alveoli and airways are filled with innumerable macrophages, which contain multiple intracytoplasmic 4 µm round yeasts, consistent with Histoplasma capsulatum. (HE 400X)*

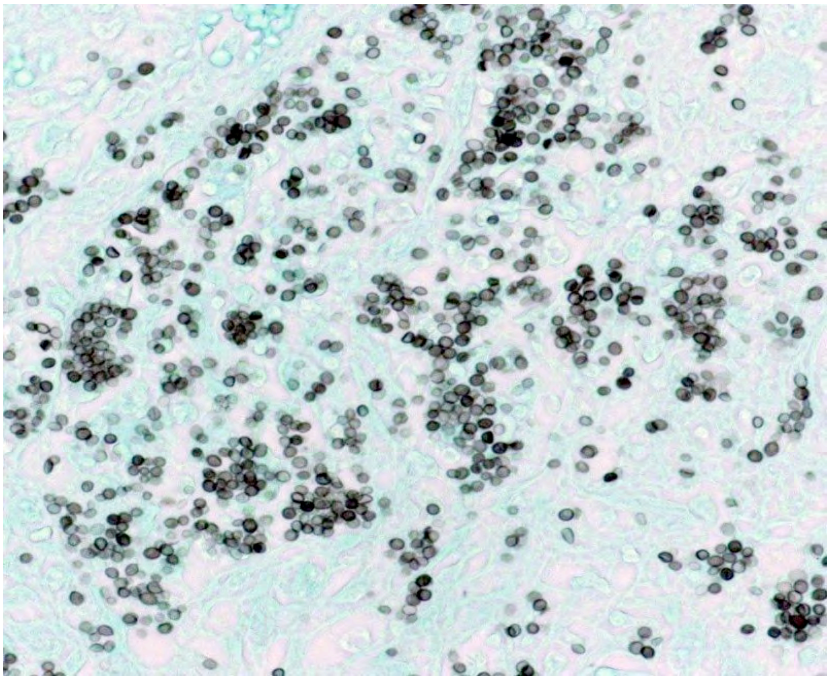

*4-4. A silver stain demonstrates the numerous yeasts present within macrophages. H. capsulatum is also demonstrated well by periodic acid-Schiff stains. (GMS 400X)*

conditions ripe for fungal growth, even in the arid southwest. In endemic areas many people and animals are exposed but few develop clinical disease.[5] Risk factors include extremes in age and immunosuppression. The travel history was not available for the cat in this report, so it was not determined if the cat traveled from an endemic area or if exposure was local. The FeLV/FIV status of this cat was unknown, but as a feral animal it presumably was at high risk for exposure to immunosuppressive viruses and potentially high doses of infectious agent.

Inoculation is by inhalation of spores from contaminated soil. The spores are then taken up by pulmonary macrophages and spread to local lymph nodes and, often, throughout the body. Respiratory disease is most common, but the frequency of gastrointestinal lesions in animals suggests that oral inoculation is also possible.[7] Localized infections in the skin and eye are also reported[1]; disseminated disease is invariably fatal. Clinical signs include fever, malaise and respiratory distress; hepatic and splenic enlargement are present if the disease is disseminated. Debilitated patients are often anemic and maybe be terminally leukopenic.[7] Gross lesions are dependent upon the extent of dissemination in the body. The lesions illustrated in the lungs and lymph nodes of this cat are a classic presentation of the respiratory lesions of histoplasmosis in cats.[1,2] Histologically, the organisms are easily distinguished from other dimorphic fungi (*Cryptococcus neoformans*, *Blastomyces dermatitidis* and *Coccidioides immitis*) by their size and obligate intracellular location.

The pathogenesis of the disease is best characterized in people.[3] Once phagocytized by pulmonary macrophages, the conidia convert to the yeast form and disseminate within the reticuloendothelial system. Dendritic cells present antigen to T lymphocytes and within 2-3 weeks, cell mediated immune responses stimulate cytokine dependent killing of yeast by effector macrophages. In the absence of effective cell-mediated immunity (as in HIV-AIDS patients), fungus disseminates and leads to terminal illness. In the immunocompetent human host infections are most often inapparent, with occasional acute or chronic localized manifestations.[5] Localized chronic pulmonary infections are often mistaken clinically for neoplasia. The pathogenetic factors that determine inapparent and clinical disease in

animals is less well characterized, but presumably involves similar cell mediated immune mechanisms.[7]

Diagnosis can be made by fine needle aspirates or impression smears, confirmed by histopathology and may be verified by culture or PCR. Fungal culture, however, is a risk to laboratory personnel, as the chlamydospores of the mycelial phase are highly infective.[7]

**JPC Diagnosis:** Lung: Pneumonia, interstitial, granulomatous, multifocal to coalescing, severe with numerous intrahistiocytic yeasts.

fungi, *Sporothrix schenckii, Histoplasma capsulatum* var. duboisii and *Histoplasma farciminosum* cause disease less frequently. Another fungal pathogen, *Cryptococcus neoformans*, can also be considered dimorphic, although it rarely appears in its filamentous form, and more often is found in its yeast form. *Candida albicans* can also exist as yeast or hyphae and pseudohyphae; however, its mold form occurs in animal tissues and its yeast form occurs in the environment.[4] The included table summarizes differential diagnoses for fungal yeast infections:[4,6]

| | *Blastomyces dermatitidis* | *Coccidioides immitis* | *Histoplasma capsulatum* | *Histoplasma farciminosum* | *Sporothrix schenckii* | *Cryptococcus neoformans* |
|---|---|---|---|---|---|---|
| Disease | Blastomycosis | Coccidioidomycosis | Histoplasmosis | Epizootic lymphangitis | Sporotrichosis | Cryptococcosis |
| Species most affected | Dogs, humans | Dogs, horses, cats, humans | Dogs, cats, humans | Horses | Horses, cats, dogs, humans | Cats, horses, humans |
| Organs affected | Lungs, skin, metastasis to other tissues | Lungs, metastasis to bones, skin, and other tissues | Lungs, metastasis to other organs | Skin, lymphatic vessels, lymph nodes | Skin, lymphatic vessels | Nasal cavity, lungs, brain, eye, skin |
| Tissue morphology | Large (8 to 10 µm), broad-based unipolar budding yeast cells | Large (10 to 80 µm) spherules with numerous 2 to 5 µm endospores | Small (1 to 5 µm) narrow base budding yeast cells **var. duboisii are larger (5 to 20 µm)* | Small (1 to 5 µm) narrow base budding yeast cells | Small (2 to 5 µm) narrow base budding yeast cells | Small (4 to 8 µm) narrow base budding, thick-walled yeast surrounded by a large 5 to 10 µm gelatinous capsule |

**Conference Comment:** The contributor provides an excellent review of the dimorphic fungus, *Histoplasma capsulatum*. The two forms of dimorphic fungi include the mold form which occurs in the environment and the yeast form which forms in animal tissues.[4] Several species of dimorphic fungi are opportunistic pathogens in domestic animals, the most common of which are *Histoplasma capsulatum* var. capsulatum, *Blastomyces dermatitidis* and *Coccidioides immitis.* Other dimorphic

**Contributing Institution**: Department of Veterinary Microbiology and Pathology
College of Veterinary Medicine
Washington State University
Pullman, WA 99164-7040
www.vetmed.wsu.edu

**References:**

1. Brilhante RSN, Coehlo CGV, Sidrim JJC, et al. Feline histoplasmosis in Brazil: Clinical and laboratory aspects and a comparative approach of published reports. *Mycopathologica*. 2012;173:193-197.

2. Kabali S, Koschmann JR, Robertstad GW, et al. Endemic canine and feline histoplasmosis in El Paso, Texas. *J Med and Vet Mycol*. 1986;24:41-50.

3. Knox KS, Hage CA. Histoplasmosis. *Proc Am Thoracic Soc*. 2010;7:169-172.

4. Quinn PJ, et al. Actinobacteria. In: *Veterinary Microbology and Microbial Disease.* 2nd ed. Ames, Iowa: Wiley Blackwell; 2011, Kindle edition, location 17002 of 35051.

5. McKinsey DS, McKinsey JP. Pulmonary histoplasmosis. *Sem in Resp and Critical Care Med*. 2011;32:735-744.

6. University of Adelaide Mycology Online. Dimorphic Systemic Mycoses, http://www.mycology.adelaide.edu.au/Mycoses/Dimorphic_systemic /. Accessed online on 28 March 2013.

7. Valli VEO. The hematopoietic system. In: Maxie MG, ed. *Jubb, Kennedy and Palmer's Pathology of Domestic Animals*. 5th ed. Vol. 3. Edinburgh, Scotland: Elsevier; 2007:299-301.

**Joint Pathology Center**
**Veterinary Pathology Services**

# WEDNESDAY SLIDE CONFERENCE 2012-2013

## Conference 20

**03 April 2013**

---

**CASE I:** S2011-0023 (JPC 4019875).

**Signalment:** 7-year-old Maltese bitch *(Canis familiaris)*.

**History:** A 7-year-old Maltese bitch that had been ovariohysteretomized at age 6 years was found by the owner to bear a nodular mass at the right 2nd mammary gland in the past two weeks. Upon clinical examination, the mass was subcutaneous, solid, firm, and movable near the right second mammary gland. Malignant mammary tumor was suspected and lumpectomy was recommended. The tumor mass was removed one week later.

**Gross Pathology:** Grossly, the mass was approximately 3.0 x 3.0 cm and appeared light red on the cut surfaces.

**Histopathologic Description:** Mammary gland: Within the interlobular connective tissue, separating and surrounding pre-existing and mildly hyperplastic

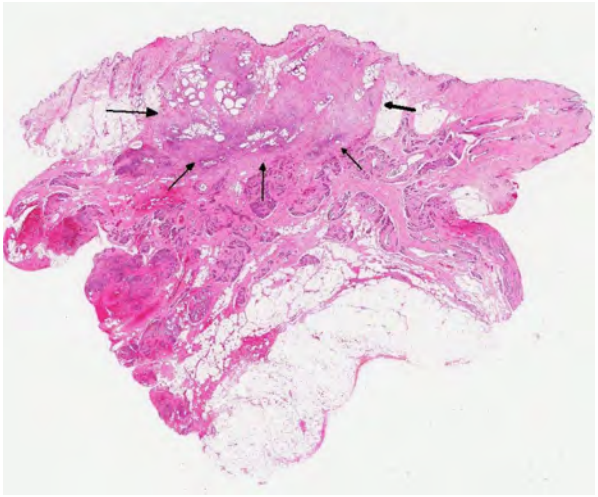

*1-1. Mammary gland, dog: There is a poorly demarcated, infiltrative neoplasm within the superficial dermis (arrows). Surrounding the mass are numerous densely basophilic mammary ducts. (HE 0.63X)*

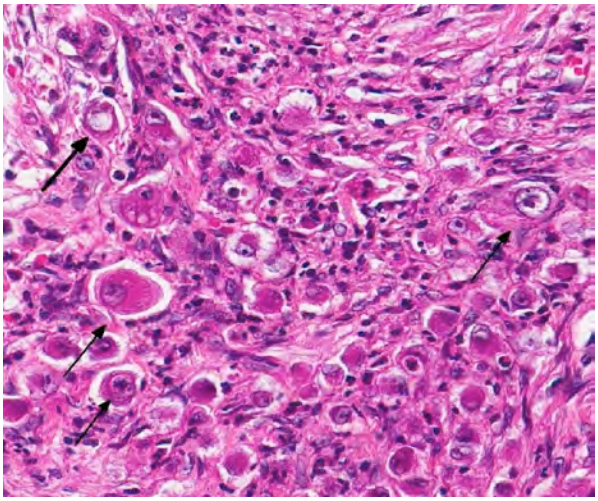

*1-2. Mammary gland, dog: Within the mass, neoplastic cells (arrow) show marked pleomorphism, and are scattered individually throughout the desmoplastic stroma. Neoplastic cells show no predilection to recapitulate mammary gland. (HE 288X)*

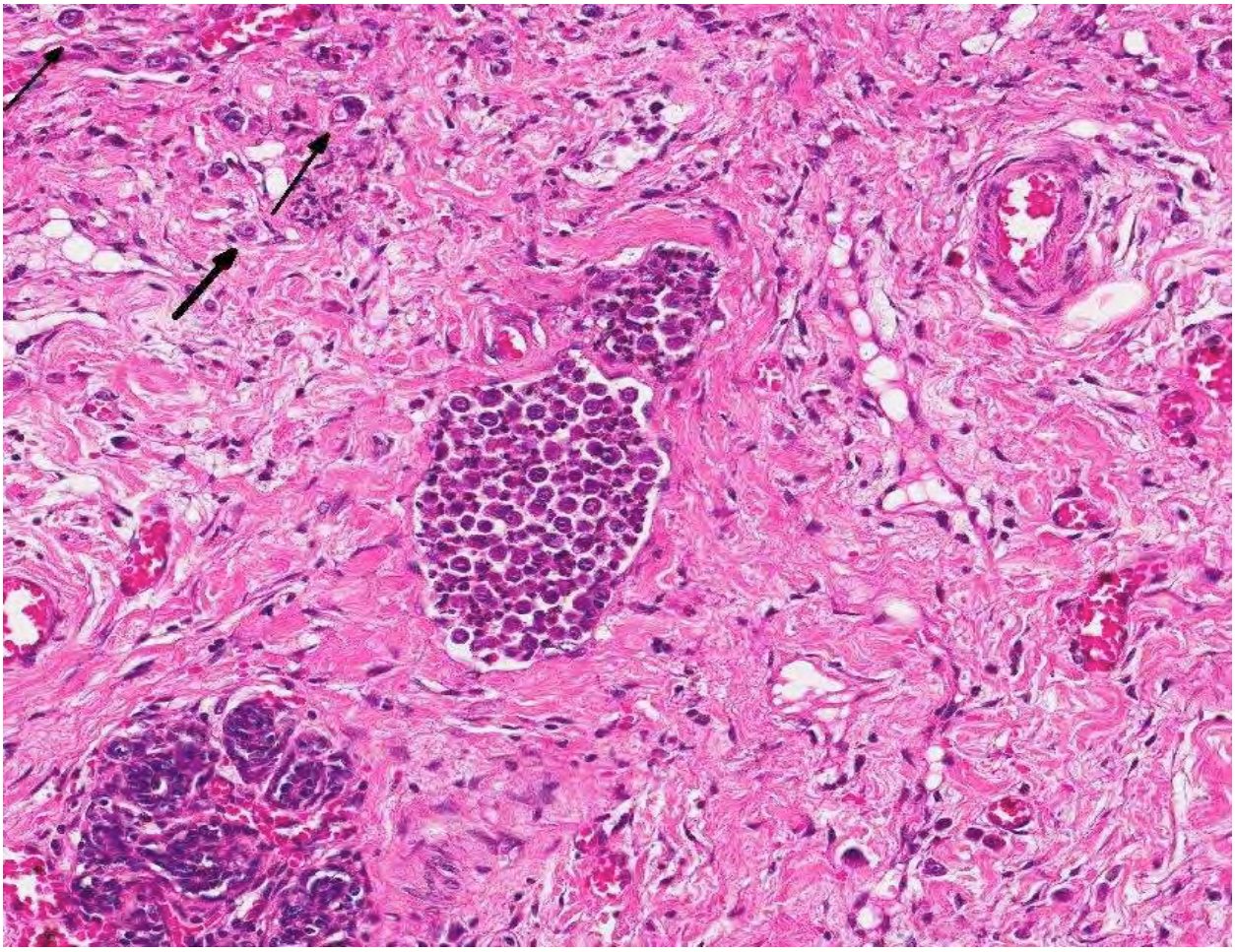

*1-3. Haired skin, mammary gland: Pleomorphic neoplastic cells fill dilated lymphatics adjacent to the primary mass. The primary contains numerous individualized neoplastic cells (arrows). Hyperplastic mammary ducts are present below. (HE 288X)*

ducts, there is a poorly cellular, infiltrative, unencapsulated, poorly demarcated neoplasm. In a large portion of the neoplasm, neoplastic cells line mammary ducts, proliferating up to 5 cells deep and expanding the ductal lumen. Neoplastic cells are polygonal with distinct cell borders and a moderate amount of eosinophilic cytoplasm. Nuclei are irregularly round with finely stippled chromatin and 1-2 large eosinophilic nucleoli. There is moderate anisocytosis and anisokaryosis. Mitotic figures average 1/400x field. Apoptotic cells are common within ducts, and many ducts lined with neoplastic cells contain low numbers of neutrophils admixed with cellular debris, and ducts are surrounded by low to moderate numbers of lymphocytes, with fewer plasma cells, histiocytes, and hemosiderin-laden macrophages. Within the superficial dermis, neoplastic cells have escaped ducts, and are distributed in an individualized fashion, rarely forming nests and acini on a dense fibrous stroma. In this area, neoplastic cells range up to 50 μm in diameter, exhibit marked anisokaryosis, and are often separated and surrounded by dense bands of fibrous connective tissue, and in some areas, plump myofibroblasts. They often fill and expand lymphatics, and surrounding tissue is often edematous.

**Contributor's Morphologic Diagnosis:** Canine mammary anaplastic carcinoma.

**Contributor's Comment:** Canine mammary tumors are the most common neoplasm in female dogs, and anaplastic carcinoma is the most malignant form. The occurrence of anaplastic carcinomas is uncommon; no case has ever been reported in Taiwan.

The present case is a 7-year-old Maltese bitch with a history of ovariohysterectomy performed a year before the tumor occurrence. No other external abnormalities were observed. Lumpectomy rather than mastectomy was performed. This bitch was still alive at the time this manuscript was prepared (8 months post-surgery) despite the malignant features observed on histopathology. Continuous follow up for "two year survival" will be interesting.

Classification of canine mammary tumors has been complicated and debatable. The earliest classification scheme for canine and feline mammary tumors was seen in 1961, in Moulton's *Tumor in Domestic Animals.* The classification at that time was fairly simple; however, over the years, the classification scheme has further advanced to more detailed and complex ones, including the 1974 WHO edition of International Histological Classification of Tumors of Domestic Animals, and the 1999 Armed Forces Institute of Pathology's classification. In 2011, a new classification scheme was proposed.[2]

**JPC Diagnosis:** Mammary gland: Anaplastic mammary carcinoma.

**Conference Comment:** Of the canine mammary tumors, anaplastic carcinomas are the most malignant, and thus carry the worst prognosis. As illustrated so well in this case, anaplastic carcinomas often exhibit diffuse invasion of interlobular connective tissue and elicit a marked desmoplastic response with concomitant proliferation of myofibroblasts. Lymphatic invasion and metastasis to regional lymph nodes and lung is also common. Interestingly, pulmonary metastasis appears radiographically as an interstitial pattern, rather than a nodular one.

As the name implies, neoplastic cells are pleomorphic, round to polygonal, with moderate to abundant eosinophilic cytoplasm, and round to oval nuclei which are sometimes indented. Neoplastic cells are often individualized or grouped in small nests. Features of malignancy include frequent multiple prominent nuclei, severe anisokaryosis and anisocytosis and a high mitotic rate; occasional multinucleated neoplastic cells are also present.[1]

Conference participants discussed use of the term "inflammatory carcinoma," which should not be used as a morphologic diagnosis, as it refers to a clinical entity that can be associated with several types of malignant mammary carcinomas, including anaplastic carcinomas. The hallmark histologic lesion for this condition is invasion of neoplastic emboli into dermal lymphatics[2] and despite the name, and the clinical appearance of a reddened mammary neoplasm, which is warm to the touch, there is often little to no microscopic inflammation associated with the neoplasm.

In addition, inflammatory carcinomas are highly angiogenic.[1] Tumor angiogenesis can be accomplished via several mechanisms, including production of vessels through endothelial precursor cells from the bone marrow or from endothelial cells in preexisting vessels, by sprouting angiogenesis, by intussusceptive angiogenesis, and by vessel co-option. More recently, a new mechanism, vasculogenic mimicry (VM) has been identified. Vasculogenic mimicry consists of the *de novo* generation of microvascular channels by genetically deregulated aggressive tumors cells without participation of endothelial cells. The resulting channels are not true blood vessels, although they function to distribute plasma and blood cells to the neoplasm, and are thought to play a role in metastasis. VM has been identified in several types of malignant tumors in humans, including inflammatory breast carcinoma and ductal breast carcinoma, as well as in several types of inflammatory mammary carcinomas in dogs, with its occurrence seen most frequently in anaplastic carcinomas. Highly malignant neoplastic cells in canine mammary cancer have been observed to resemble endothelial cells that histologically, immunohistochemically, and ultrastructurally resembled VM as described in human tumors. Specifically, the endothelial-like cells (ELCs) in VM are positive for epithelial markers and for the same markers used for the rest of the tumor cells may be positive for vimentin, but negative for smooth muscle actin and desmin, and show absence of specific immunoreaction with endothelial markers. Ultrastructurally, ELCs lack Weibel-Palade bodies (which are characteristic of endothelial cells) and have desmosomes (the type of junctions between epithelial cells) instead of fascia occludens (endothelial cell- to-cell junctions). Tumor and/or blood cells contained in the channels formed by ELCs are not inside a vacuole as in emperipolesis or phagocytosis; instead, they are inside an actual space formed by the cytoplasmic membranes of ECLs. It is thought that ECLs can also form channels that mimic lymph vessels rather than blood vessels; however, further studies are needed to identify the mechanisms of cancer cells developing channels of VM as well as confirm the presence of lymphatic VM.[1]

**Contributing Institution**: Animal Technology Institute of Taiwan
Division of Animal Medicine
P.O. Box 23, Chunan, Miaoli, 350 Taiwan

**References:**

1. Clemente M, Perez-Alenza MD, Illera JC, Pen˜a L. Histologic, immunologic and ultrastructural description of vasculogenic mimicry in canine mammary cancer. *Vet Pathol*. 2010;47(2):265–274.
2. Goldschmidt M, Pen˜a L, Rasotto R, Zappulli V. Classification and grading of canine mammary tumors. *Vet Pathol.* 2011:48(1):117-131.

**CASE II:** FMVZ USP Case II (JPC 4019407).

**Signalment**: 15-month-old, intact female cat (*Felis catus)*.

**History**: A 15-month-old, female cat of indeterminate breed with history of good general condition presented with multiple ulcerated necrotic nodular skin lesions in the nasal planum, ears, forelimbs, cervical and lumbosacral regions. The cat had been treated orally with itraconazole for a few weeks based on isolation of *Sporothrix schenckii* from lesions. After approximately six weeks the cat was sent to necropsy.

**Gross Pathology**: The animal was in poor body condition, weighting less than 2 kg, with reduced amounts of internal body fat. On the right cheek, ears, cervical region, digits of both forelimbs and in the lumbosacral region there were multiple nodular and ulcerative gummy reddish skin lesions measuring 1 to 7 cm in diameter. The ulcerated skin lesions were covered by hemorrhagic crusts and had irregular edges. Cut surfaces of lesions were white to yellowish, irregular, friable and well demarcated nodules or plaques.

**Laboratory Results**: Skin fragments collected during gross examination resulted in growth of *Sporothrix schenckii* in Sabouraud's dextrose agar.

**Histopathologic Description:** Histopathologic evaluation of sections of the forelimb nodule revealed on low power a nodular to diffuse dermatitis that extended into the deep dermis. The overlying epidermis of the sample was intact and atrophic. The superficial dermis was edematous and in the deep dermis there were epithelioid macrophages intermingled with rare lymphocytes, plasma cells and neutrophils. At higher magnification myriads of small, 2 to 6 µm diameter, elongated or dot-like, cigar-shaped to oval yeasts consistent with *Sporothrix schenckii* were observed. The organisms were pink in periodic acid–Schiff stain (PAS) and lie in vacuoles often grouped within macrophages, but were also free in the tissue. The blood vessels within the lesion were dilated and congested.

**Contributor's Morphologic Diagnosis**: Skin: Dermatitis, nodular to diffuse, granulomatous, marked, with myriads of cigar-shaped to oval *Sporothrix schenckii* yeast, undefined breed, cat.

**Contributor's Comment:** Sporotrichosis is an ergodermatosis anthropozoonotic or saprozoonotic dermatopathy caused by the thermally dimorphic fungus *Sporothrix schenckii*, whose main sources of infection are domestic cats, plants and soil. *Sporothrix schenckii* is distributed worldwide, and at present it is rare in Europe, but frequent in the Americas, Africa, Japan, and Australia. The main areas of endemicity are located in Japan, India, Mexico, Brazil, Uruguay, and Peru. In Latin America, it is the most common subcutaneous mycosis in humans.

*S. schenckii* belongs to the kingdom Fungi and is a eukaryotic organism that has no mobility, is heterotrophic, and presents chitin on its cell wall. For several years, this fungus was included in division *Eumycota*, subdivision *Deuteromycotina*, class *Hyphomycetes*, order *Moniliales*, and family *Moniliaceae*. After a substantial fungal taxonomy revision, this fungus was replaced in division *Ascomycota*, class *Pyrenomycetes*, order *Ophiostomatales*, and family *Ophiostomataceae*.

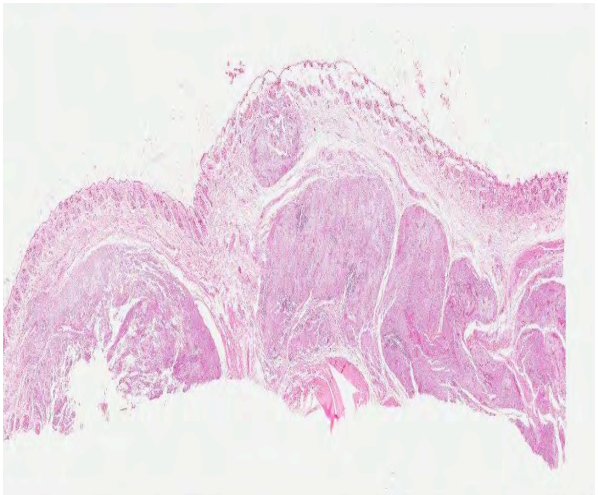

*2-1. Haired skin, cat: The dermisis is expanded by multifocal to coalescing granulomas which extend from the dermis into the subcutis. (HE 0.63X)*

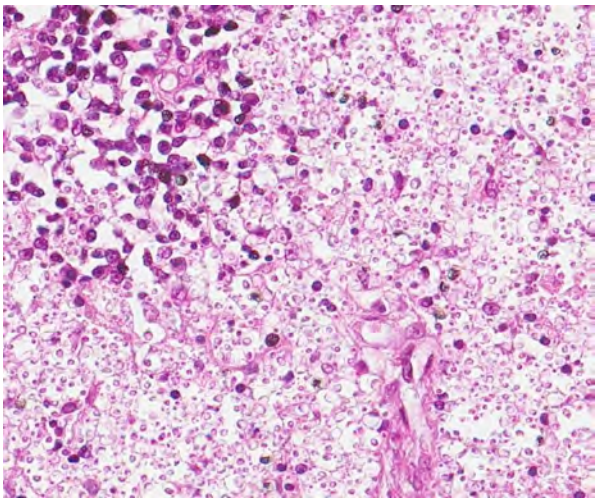

*2-2. Haired skin, cat: Within the granulomas, macrophages are greatly expanded by abundant mildly pleomorphic 5-8 µm yeast with a clear capsule, consistent with Sporothrix schenkii. There are small nodules of lymphocytes and plasma cells scattered through the granulomas (upper left). (HE 400X)*

*S. schenckii* must not be considered a single species. A recent molecular study demonstrated that *S. schenckii* is a complex of cryptic species, denominated the *S. schenckii* complex. Within this complex, at least five species are considered of interest due to their pathogenic potential. Gene sequencing has revealed the following six species in the complex: *S. albicans*, *S. brasiliensis*, *S. globosa*, *S. luriei*, *S. mexicana* and *S. schenckii*. These cryptic species were further subdivided into a number of smaller groups that appear to be reproductively isolated in nature. This suggests not only that the existing *S. schenckii* populations are in the process of divergence but also that all of the resulting lineages are undergoing separation into distinct taxa. In Brazil there are four species recognized as pathogens for human and animals: *S. albicans*, *S. brasiliensis*, *S. luriei*, and *S. schenckii*.

Although the genetic separation is considerable among the three major monophyletic clades (i.e., the Spanish clade, the Brazilian clade, and the clade made up of the rest of the South American isolates), each of them shows a high level of clonality. Primitive populations were probably isolated by the separation of the continents, and the formation of natural barriers facilitated their speciation as they became adapted to hosts endemic to the different regions. However, although geographical separation of the main clades is clearly evident, the different genotypes present within them are not related to geography, which seems to indicate that there has been interbreeding within these isolated populations.

In the environment, at temperatures ranging from 25 to 30°C, *S. schenkii* grows as filamentous mold; it forms white to cream-colored colonies which become brown to black in weeks and produces dark or hyaline conidia arranged along hyphae with a bouquet-like appearance. In the wild, the fungus is a saprophyte on living and decaying vegetation. Soil is fundamental for mycelium development. At 37°C, *S. schenkii* grows as yeast-like cell.

*S. schenckii* virulence factors are thermotolerance and the ability to synthesize melanin that enhances resistance to macrophage phagocytosis, allowing the

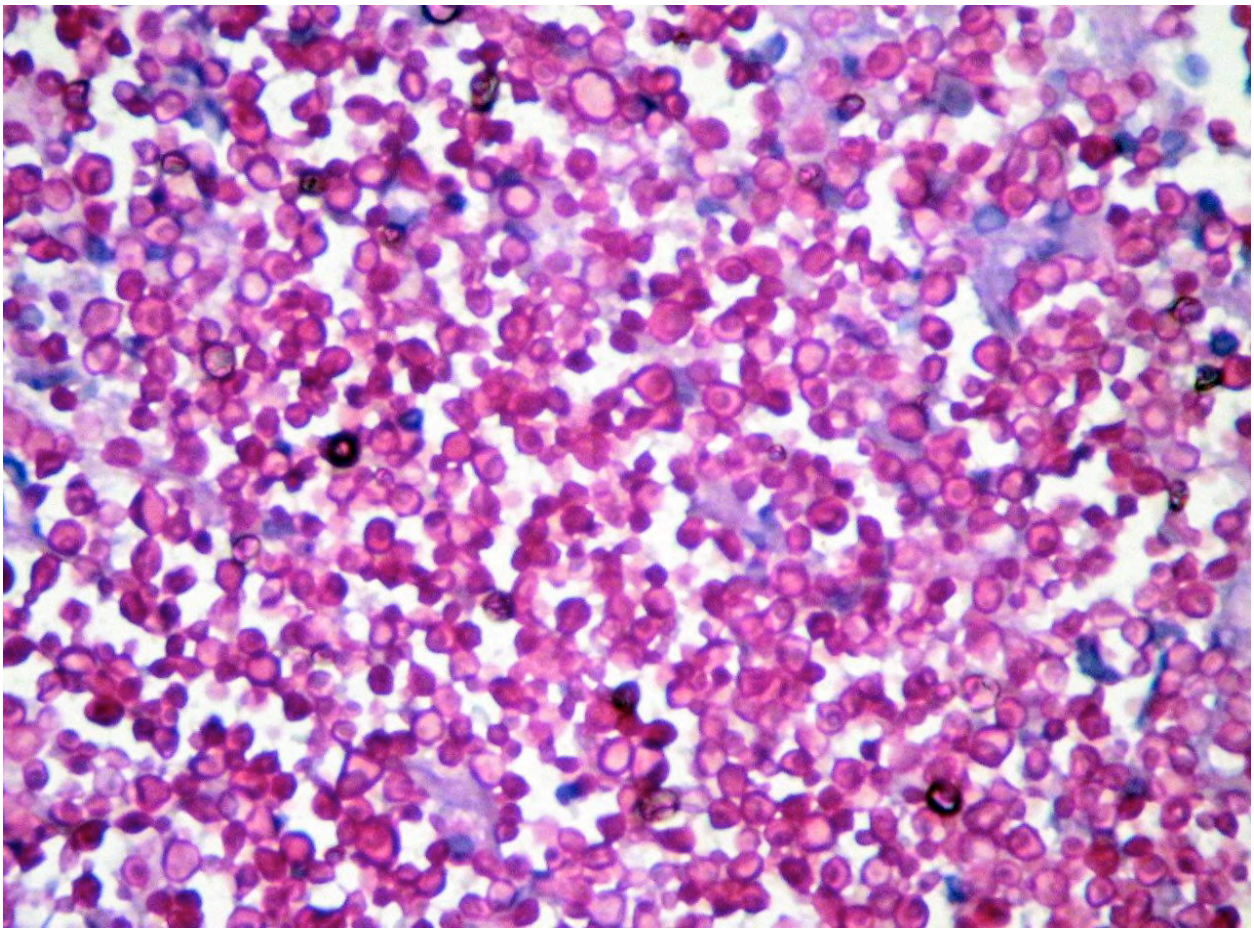

*2-3. Haired skin, cat: A periodic acid-Schiff preparation highlights the yeast cell wall. (PAS 400X) (Photo courtesy of: the Faculdade de Medicina Veterinária e Zootecnia da Universidade de São Paulo, Av. Prof. Dr. Orlando Marques de Paiva, 87, CEP 05508 270, Cidade Universitária, São Paulo/ SP – Brasil.)*

first steps of infections in mammalian hosts; melanization also promotes the formation of multifocal granuloma. Another virulence factor is expression of integrins or adhesion lectin-like molecules that recognize fibronectin from the host. The fibronectin adhesins are located on the surface of yeast cell and the existence of these adhesins would favor adherence to host tissues and fungal dissemination. Components of the *S. schenckii* cell wall that act as adhesins and immunogenic inducers, such as a 70-kDa glycoprotein, are apparently specific to this fungus and they seem to participate in adhesion to the dermal extracellular matrix. The main glycan peptido-rhamnomannan cell wall component is the only *O*-linked glycan structure known in *S. schenckii*, and it causes depression of immune response until the sixth week of infection. Yeast cells also synthesize ergosterol peroxide that is a protective mechanism to evade reactive oxygen species during phagocytosis and may represent a virulence factor.

Differences in virulence between clinical and environmental strains were reported, but no correlation was found with the different clinical forms of sporotrichosis. In several *in vitro* antifungal susceptibility studies of clinical isolates of *S. schenckii*, a wide range of susceptibility to different drugs has been demonstrated. This suggests that these isolates could represent different species. If true, knowledge of their various responses to antifungal agents would be critical for appropriate patient management.
Classically, the infection is acquired through traumatic implantation of *S. schenckii* present in organic matter. The most frequent clinical presentations are the cutaneous and subcutaneous forms with or without regional lymphatic involvement. But, inhalation of the conidia can lead to pulmonary infection which, rarely, may also spread to bones, eyes, central nervous system and viscera. Another mode of transmission is through animal bites and scratches.

Sporotrichosis usually occurs in isolated cases or in small family or professional outbreaks. Epidemics are rare and, when they occur, are commonly related to a single source of infection. Interhuman transmission is rare and human sporotrichosis has sporadically been related to the scratch or bite of infected animals. The role of felids in the transmission of the mycosis to humans has, however, gained importance. There was no description of epizootics before a cat-transmitted epidemic was reported in Rio de Janeiro, Brazil, in 1980. Since then, successive reports of epizootics from different geographical regions have characterized a new risk group for acquisition of sporotrichosis, composed of cat owners and veterinarians.

It should be noted that the highest number of cases that occurred during Rio de Janeiro epizootics were in an area characterized by underprivileged socioeconomic conditions and precarious health services. The typical human patients were female, mainly housewives, which is normal if we consider that members of this group are those most frequently exposed to the fungus because they care for cats. Some authors explained the wide dissemination of the disease with factors related to the behavior of cats which, although cohabiting with human beings, do not always stay in the house but also circulate in the neighborhood, often getting involved in fights with other animals and coming into contact with soil and plants.

It is possible that environmental factors, increased urbanization, and improved diagnostics partly explain the alterations in the profile of the disease. Furthermore, since sporotrichosis is not a reportable disease in most countries, such as Brazil, there is little information on the incidence, and the known data are those generated by case publications.

Following inoculation, the fungus penetrates into deeper layers of tissue where it converts into the yeast like form (37°C). It can remain in the dermis and subcutaneous tissue at the inoculation site, spread up to regional lymphatics and produce lymphangitis and lymphadenitis, or disseminate systemically through blood vessels. Furthermore, in cats, the high frequency of respiratory signs and pulmonary and nasal mucosal lesions, in addition to the isolation of *S. schenckii* from bronchoalveolar lavage and from the lungs of necropsied animals, suggests the epidemiologic importance of the inhalation route in the infection. Multiple skin lesions can occur because of self-trauma, grooming, and hematogenous dissemination from the lungs or perhaps from the initial skin lesion.

The lesions are characterized by a wide variety of morphologies: nodules, tubercles, pustules, cysts, gummy lesions, ulcers, vegetative lesions, and plaques, accompanied or not by lymphangitis.

Virulence is one of the factors thought to play a role in the development of sporotrichosis, but there are discordant results concerning disease evolution in experimental sporotrichosis with *S. schenckii.* Clinical isolates from cutaneous and disseminated infection indicate that host immune responses also substantially participate in the progress of sporotrichosis. The immunological mechanisms involved in prevention and control of *S. schenckii* infections are still not very well understood. However, they probably include both humoral and cellular responses, which appear to be triggered by distinct antigens. Surface cell antigens, especially some lipids, inhibit the phagocytosis process; while the humoral response is induced by secreted fungal proteins, the exoantigens are not involved in the cellular response. The innate immune

response also plays a role in the pathogenesis of sporotrichosis.

The classification of clinical presentations used for humans includes several forms: lymphocutaneous, fixed cutaneous, mucocutaneous, extracutaneous, and disseminated. These categories are difficult to transpose to sporotrichosis in dogs and cats because they frequently have more than one of these forms simultaneously. Although the cutaneous lymphatic form is the most frequently seen clinical presentation in humans, this is not the case with cats and dogs. The most common lesions in dogs and cats are skin nodules and ulcers, with frequent mucosal involvement. The initial lesions are firm subcutaneous nodules that slowly soften, generally draining purulent or seropurulent content, and progress to form exudative ulcers with slightly elevated well-defined rims. In addition, dogs and cats may have extracutaneous, mainly respiratory signs, such as sneezing, nasal discharge, and dyspnea, followed by lymphadenomegaly. Other clinical signs that may be observed are anorexia, vomiting, weight loss, cough, fever, and dehydration.

According to the location of the lesions, sporotrichosis can be classified into three forms in animals. The primary cutaneous form consists of multiple scattered raised alopecic, ulcerated, crusted nodules or plaques that remain confined to the point(s) of entry of the organism. It is thought that this form results from a high degree of host immunity, preventing spread of infection. Nodules may become ulcerated and associated with seropurulent exudate and crust formation. The normal grooming behavior of cats may result in autoinoculation and spread of lesions to distant sites. The cutaneous form may have a very chronic course. An unusual case of sporotrichosis in a dog consisted of otitis externa characterized by multiple cutaneous nodules which persisted for more than five years.

The cutaneous-lymphatic form involves the skin, subcutaneous tissue, and associated lymphatics. Lesions begin as firm round nodules at the site of entry, usually on an extremity, and spread proximally along lymphatics. Lymphatic vessels become thick and corded and a series of secondary nodules forms as the infection progresses. The nodules may break open and discharge seropurulent material. Lesions may cavitate and expose extensive areas of underlying muscle and bone. Regional lymphadenopathy is common. This is the most common form in horses. Lesions generally involve the proximal forelimbs, chest, and thigh but usually no regional lymph node involvement is evident. Dogs usually have the cutaneous or cutaneous-lymphatic form. The head, pinnae, and trunk are involved most frequently. In cats, lesions are usually located on the head, distal limbs, and base of the tail. The initial draining puncture wounds may be indistinguishable from cat-inflicted fight wound infections.

The extracutaneous/disseminated form may involve a single extracutaneous tissue, such as osteoarticular sporotrichosis, or multiple internal organs. It develops as a sequela to cutaneous lymphatic infection or following inhalation of the fungus. The disseminated form of sporotrichosis occurs most frequently in cats, and no immunosuppressive factors are usually identified. In experimentally induced sporotrichosis in cats, organisms were shown by culture to have disseminated to viscera in 50% of the cases. Cats with disseminated sporotrichosis are often febrile, depressed, and anorexic.

In cats, as the case described, unlike humans, the low frequency of typical formed granulomas and the richness of fungal elements found in the histopathology of the skin demonstrate the increased susceptibility of animals to *S. schenckii.* Some investigators believe that the severity of feline sporotrichosis can be related to immunosupression caused by co-infection with feline immunodeficiency virus (FIV) or feline leukemia virus (FeLV), although reports of co-infection with FIV/FeLV and *S. schenckii* are very rare which renders this hypothesis unlikely.

Microscopically, sporotrichosis is usually a nodular to diffuse pyogranulomatous or granulomatous inflammatory reaction involving the dermis and subcutaneous fat. The epidermis is acanthotic or ulcerated. Neutrophils, epithelioid macrophages, multinucleated giant cells, and fewer lymphocytes and plasma cells can form discrete granulomas or extensive sheets of inflammation replacing dermal and subcutaneous tissues. Fibrosis is variable, and necrosis may be extensive. Yeast(s) surrounded by a stellate radial corona of brightly eosinophilic material (asteroid body/Splendore-Hoeppli reaction) are seen in some cases. The yeasts appear as round, oval, or elongated ("cigar"-shaped) single or budding cells which measure 2-6 µm or more in diameter for the round and oval forms.

Although *S. schenckii* may be seen in tissue with the routinely used hematoxylin and eosin (H&E) stain, other special stains such as Gomori methenamine silver (GMS) or periodic acid-Schiff (PAS) can be employed to enhance fungal detection. Atypical *S. schenckii* cells can appear spherical and surrounded by a PAS-positive capsule, resembling *Cryptococcus* cells.

Isolation of the fungus from the nails and oral cavity of cats supports evidence indicating that transmission can occur through a scratch or bite, while isolation from

the nasal fossae and cutaneous lesions indicates the possibility of infection through secretions. Sporotrichosis can be diagnosed through a correlation of clinical, epidemiological, and laboratory data. Laboratory analysis for the determination of sporotrichosis includes direct examination of specimens such as tissue biopsy specimens or pus from lesions. In case of disseminated infections, other specimens, such as sputum, urine, blood, and cerebrospinal and synovial fluids can be analyzed, depending on the affected organs.

The differential diagnoses should be considered in accordance with the diversity of clinical forms and the morphology of the lesions. The main differential diagnosis is cutaneous leishmaniasis, cryptococcosis, mycobacterioses and skin neoplasias. Sporotrichosis can also mimic cutaneous bacterial infections, sarcoidosis, lupus vulgaris, tuberculosis, and scrofuloderma, among others in humans. These conditions should be differentiated by history, areas of endemicity, and lab tests.

Sodium iodide (NaI) or potassium iodides (KI) were considered the drugs of choice in human and canine sporotrichosis; however, serious adverse effects have limited their use. Itraconazole (ITZ) is considered the drug of choice in feline and human sporotrichosis treatment because of its greater effectiveness and safety when compared to other antifungal agents. Sporotrichosis in cats is more difficult to treat than in dogs, requiring a prolonged period of therapy. The number of affected noncontiguous anatomic regions, the general medical condition, and the degree of compromise to the immune system influence the treatment outcome. The cooperation and persistence of the owners is instrumental in attempting a successful response to therapy. When sporotrichosis is not treated for an adequate time, it often recurs, usually with respiratory signs. In these cases the clinical cure is difficult; respiratory signs are associated with treatment failure and death. There is a report of ITZ-resistant strains of *S. scherenkii*.

People handling cats with potential sporotrichosis should follow biosecurity measures. In addition, separation of sick cats from other animals in the same environment is indicated. Care must be taken to avoid cuts or penetrating injuries when working with infected cats, and protective outerwear should be worn. Proper physical restraint or sedation of noncooperative patients must be done to allow complete examination of lesions and the collection of biologic material for laboratory analysis.

Decontamination and cleaning of cages or transport containers must be done with hypochlorite (1%), diluted 1:3 in water, for at least 10 minutes. If possible, sun drying is also beneficial. Examination tables should be cleaned after contact with infected animals and disinfected with sodium hypochlorite solution (1%), followed by alcohol 70% for at least 10 minutes using disposable paper towels. Additionally, floors and walls must be cleaned and disinfected daily with sodium hypochlorite solution (1%). For public health purposes and to control epidemic cat-transmitted sporotrichosis, an effective and viable therapeutic regimen applied to cats under field conditions is necessary.

Moreover, public awareness programs on sporotrichosis prophylaxis are required, encouraging the following: responsible ownership, castration, cremation of dead cats, confinement of cats inside the home, limitation of the number of cats per household, regular cleaning of the dwelling, and proper health care for the animals.

This case is interesting because of the possibility of dealing with an ITZ resistant strain. Even if other possibilities (like inadequate treatment) cannot be excluded, such cases deserve special attention because of the discussed antropozoonotic potential and epidemic situation in some cities.

**JPC Diagnosis:** Haired skin: Dermatitis, pyogranulomatous, multifocal to coalescing, severe with numerous intrahistiocytic yeasts.

**Conference Comment:** The contributor provides a very thorough and informative summary of sporotrichosis. Conference participants compared the histopathologic findings in this case with those found in cases of dermatitis associated with *Histoplasma capsulatum,* noting the lesions and organisms can be very similar in appearance. As the contributor states, sporotrichosis can also mimic leishmaniasis, cryptococcosis, and mycobacterioses, as well as other non-infectious conditions. Therefore, participants noted that, although histopathology is a useful auxiliary test for sporotrichosis, the gold standard for definitive diagnosis of *Sporothrix schenckii* remains culture, as was performed in this case.

**Contributing Institution:** Faculdade de Medicina Veterinária e Zootecnia da Universidade de São Paulo
CEP 05508 270
Cidade Universitária
São Paulo/SP - Brasil

**References**:

1. Barros MB, de Almeida Paes R, Schubach AO. *Sporothrix schenckii* and Sporotrichosis. *Clin Microbiol Rev.* 2011;24(4):633-54.
2. Carlos IZ, Sassa MF, Sgarbi DBG, Placeres MCP, Maia DCG. Current research on the immune response

to experimental sporotrichosis. *Mycopathologia*. 2009;168:1-10.
3. Ginn PE. Mansell JEKL, Rakich PM. Skin appendages: Fungal diseases of skin. In: Maxie MG, ed. *Jubb, Kennedy and Palmer's Pathology of Domestic Animals*. 5th ed. Vol 1. New York, NY: Elsevier Saunders; 2007:694 -708.
4. Lopes-Bezerra LM. *Sporothrix schenckii cell call peptidorhamnomannans*. *Frontiers in Microbiology*. 2011;2(243):1-4.
5. Marimon R, Gene J, Cano J, trilles L, Lazera MS, Guarro J. Molecular Phylogeny of *Sporothrix schenckii*. *J Clin Microbiol*. 2006;44(9):3251–3256.
6. Marimon R, Cano J, Gene J, Sutton DA, Kawasaki M, Guarro J. *Sporothrix brasiliensis*, *S. globosa*, and *S. mexicana*, Three New *Sporothrix* Species of Clinical Interest. *J Clin Microbiol*. 2007;45(10):3198–3206.
7. Oliveira DC, Lopes PGM, Spader TB, Mahl CD, Tronco-Alves GR, Lara VM, et al. Antifungal Susceptibilities of *Sporothrix albicans*, *S. brasiliensis*, and *S. luriei* of the *S. schenckii* Complex Identified in Brazil. *J Clin Microbiol*. 2011;49(8):3047–3049.
8. Schubach AO, Barros MB, Wanke B. Epidemic sporotrichosis. *Current Opin Infectious Dis.* 2008;21 (2):129-133.
9. Schubach TMP, Menezes RC, Wanke B. Sporotrichosis. In: Greene CE, ed. *Infectious Diseases of the Dog and Cat*. 4th ed. Philadelphia, PA: Saunders; 2011:645-650.

**CASE III:** T12 20790 (JPC 4019451).

**Signalment:** 8-year-old, female spayed Jack Russell mix *(Canis familiaris)*.

**History:** The referring veterinarian described pustule formation progressing to ulceration in the axillary and inguinal regions, ventral abdomen and around the vulva.

**Gross Pathologic Findings**: NA.

**Histopathologic Description:** Haired skin: There are multiple focal plaque-like lesions alternating with small areas of normal skin. The epidermis is characterized by mild parakeratosis that often spans several hair follicles. The epidermis has mild to moderate thickening with apoptotic cells present in high numbers in all levels. Some of the apoptotic cells are surrounded by lymphocytes (satellitosis). Numerous intraepithelial or exocytosing lymphocytes are present. There is vacuolation along the basal layer with moderate pigmentary incontinence. These changes extend into the infundibular portion of the hair follicle sheaths. A mild diffuse interface and perivascular infiltrate of lymphocytes, plasma cells and histiocytes is present. Several hair follicles are in growth arrest and contain keratin plugs. Sebaceous glands are small and absent from a few follicles. In the area of the isthmus of the follicles with small or absent sebaceous glands, there is pyogranulomatous inflammation and vacuolation. Apocrine glands are mildly dilated. No fungal organisms are detected in routinely stained sections. A small colony of bacteria is associated with hair in the ostia of a single follicle. Rare coccoid bacteria are noted in the surface keratin debris.

**Contributor's Morphologic Diagnosis:** Haired skin: Dermatitis, interface, subacute, multifocal, moderate with apoptosis, mild parakeratotic hyperkeratosis, folliculitis and adnexal destruction (sebaceous gland)

**Contributor's Comment:** The clinical history, lesion distribution and histologic lesions are consistent with erythema multiforme (EM). The two major differential diagnoses for immune-mediated skin disease with interface dermatitis and apoptosis are erythema multiforme (EM) and all forms of lupus erythematosus (LE). The apoptosis observed in LE tends to be limited to the basal cell layer where vacuolation also occurs. The classic lesion in EM is apoptosis involving any cellular layer of the epidermis along with lymphocyte satellitosis.[4] There are usually aggregates of lymphocytes and histiocytes along the dermal-epidermal junction. Vacuolation and apoptosis of the basal cell layer occur, and there is variable pigmentary incontinence. Areas of ulceration are typically associated with additional infiltrates of neutrophils, eosinophils and plasma cells.

Erythema multiforme is a relatively uncommon skin disease reported in dogs, cats, horses and cattle that has been associated with a number of different triggers.[2,3] The pathogenesis of EM is not completely understood; however, this disease is thought to be a T-cell-mediated hypersensitivity reaction against a variety of antigens including drugs, viruses, bacteria and food substances.[1,3,5-9] EM has also been described as a paraneoplastic condition associated with a variety of tumor types.[1,4,10]

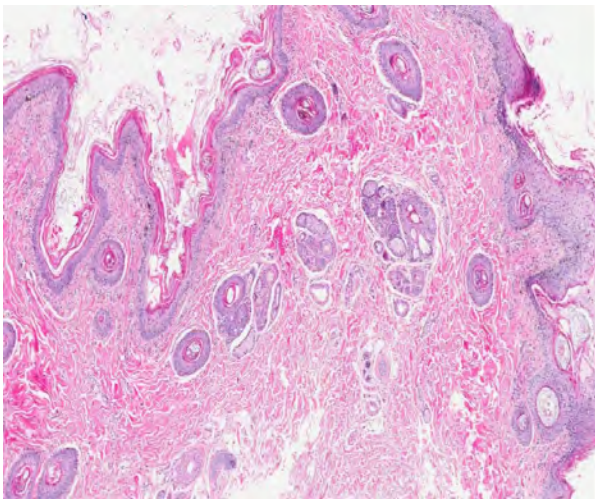

*3-1. Haired skin, dog: The epidermis is diffusely hyperplastic and hyperkeratotic. The parakeratotic hyperkeratosis extends into hair follicles. (HE 4X)*

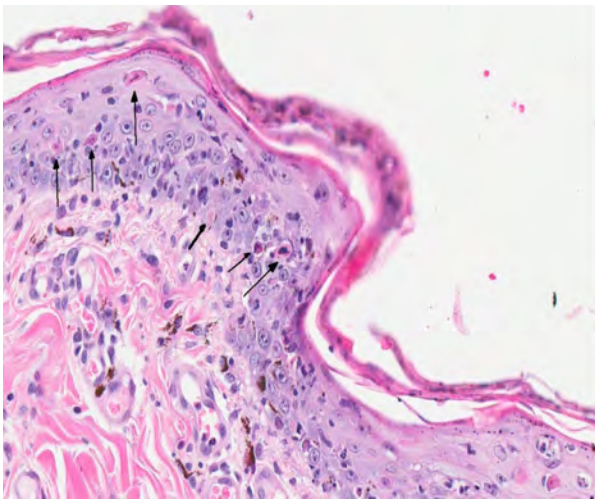

*3-2. Haired skin, dog: There are numerous apoptotic epithelial cells within all levels of the epidermis (arrows) and follicular infundibulum (not pictured). The epidermis is hyperplastic and hyperkeratotic. The dermal-epidermal interface is blurred and contains lymphocytes, histiocytes, plasma cells, and melanomacrophages (thick arrow). (HE 40X)*

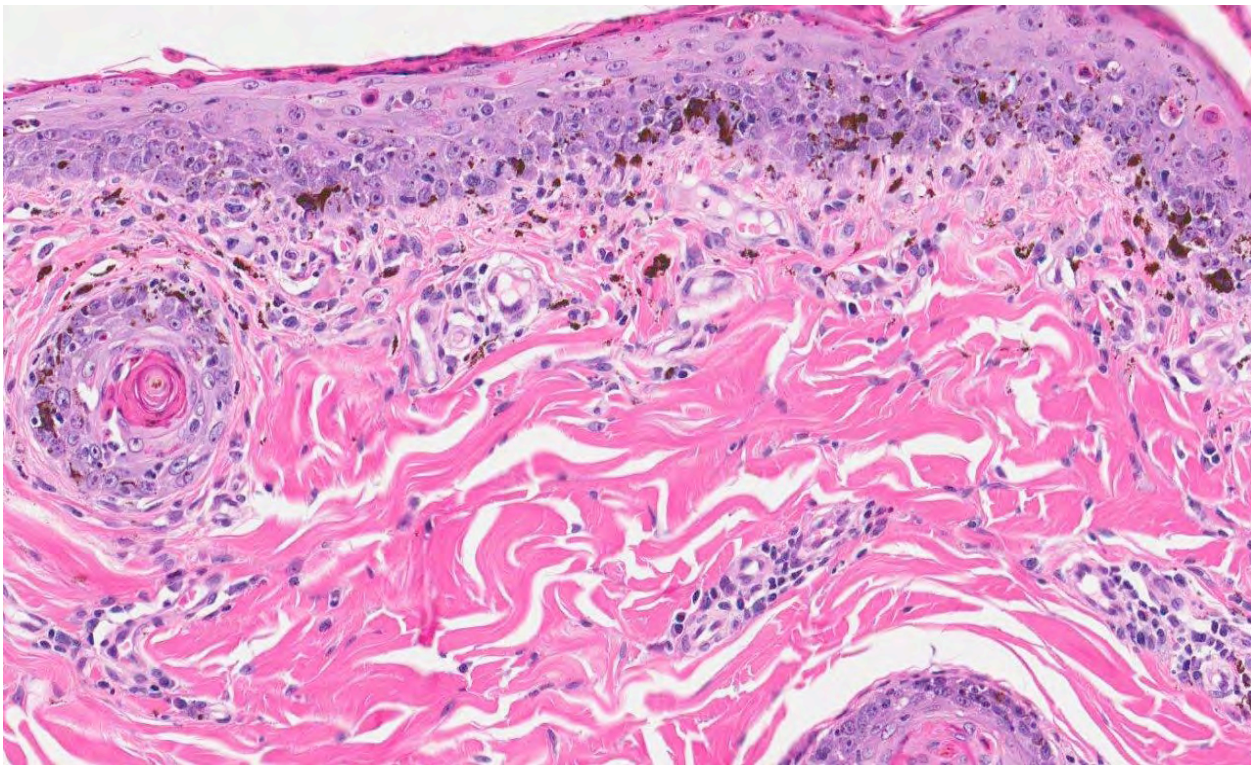

*3-3. Haired skin, dog: There is a mild interface dermatitis composed of low numbers of lymphocytes, histiocytes, plasma cells, and macrophages at the dermal epidermal junction as well as hair follicles. Melanomacrophages in the subjacent dermis ("pigmentary incontinence") attest to damage of the basal layer. Apoptotic keratinocytes are scattered throughout the epidermis. (HE 400X)*

The most commonly incriminated drugs include trimethoprim-potentiated sulfonamides, penicillins and cephalosporins.[4,7,8] The dog in this case was medicated with trimethoprim-sulfa for cystitis prior to the onset of the cutaneous lesions.

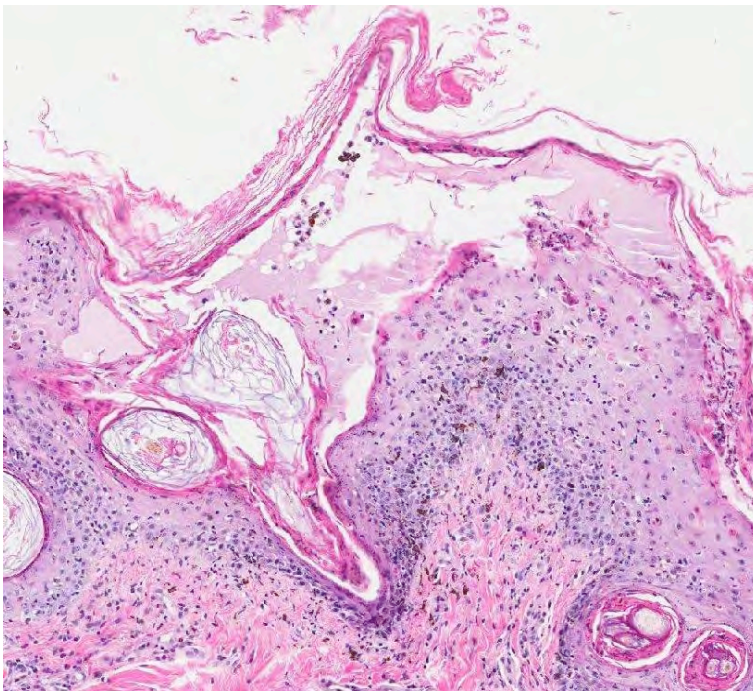

*3-4. Haired skin, dog: Suprabasilar clefting is present. Apoptotic keratinocytes are scattered at all levels thought the epidermis. (HE 360X)*

Clinically, dogs present with an acute onset of erythematous annular macules, elevated circular plaques and papules that are most commonly involve the glabrous skin of the inguinal and axillary regions.[4] Mucocutaneous junctions, oral mucosa, ears and paw pads are also commonly affected. Two classifications for EM have been adopted from human nomenclature. EM minor includes patients with no more than one mucosal surface affected and <10% of the body surface affected. EM major is used for cases in which more than one mucosal surface and between 10% to 50% of the body surface is affected. A third syndrome, Stevens-Johnson syndrome, is reserved for patients with >50% of the body surface affected.

**JPC Diagnosis:** Haired skin: Apoptosis, transepidermal, epidermal and follicular, multifocal, with necrosis, hydropic degeneration, subepidermal clefting, orthokeratotic hyperkeratosis, and neutrophilic and lymphohistiocytic interface dermatitis.

**Conference Comment:** As the contributor notes in the above informative summary, EM is thought to be a T-cell mediated hypersensitivity in which the host's cellular immune response is directed against keratinocyte-associated antigens. Such reactions have been reported to be associated with certain drugs, bacterial infections (staphylococcal folliculitis, pseudomonal otitis externa), food products, and epitheliotropic viral infections. In particular, conference participants discussed the association between EM and canine parvovirus type 2b (CPV-2b). There have been a few cases of EM reported in dogs associated with CPV-2b infection, including in a 2-month-old Great Dane puppy and, more recently, a litter of English Setter puppies.[2,6] It has been suggested that infection of stem cells and transient amplifying keratinocytes occurs following hematogenous dissemination of CPV-2b, thus leading to initiation of EM. The recent report suggests that, along with the multiple other possible initiating factors, CPV-2b should be considered as a potential initiator of EM in dogs.[6]

**Contributing Institution:** University of Georgia
Tifton Veterinary Medical Diagnostic Laboratory

**References:**

1. Elmore S, Basseches J, Anhalt GJ, Cullen JM, Olivry T. Paraneoplastic pemphigus in a dog with splenic sarcoma. *Vet Pathol*. 2005;42:88-91.
2. Favrot C, Olivry T, Dunston SM, et al. Parvovirus infection of keratinocytes as a cause of canine erythema multiforme. *Vet Pathol*. 2000;37:647–649.
3. Ginn PE, Mansell JEKL, Rakich PM. The skin and appendages. In: Maxie MG, ed. *Jubb, Kennedy and Palmer's Pathology of Domestic Animals.* 5th ed. Vol. 1. New York, NY: Elsevier Saunders; 2007:656.
4. Gross TL, Ihrke PJ, Walder EM, Affolter VK. Interface diseases of dermal-epidermal junction. In: *Skin Disease of Dogs and Cats: Clinical and Histopathologic Diagnosis.* 2nd ed. Oxford, UK: Blackwell Science Ltd; 2005:52-68.
5. Itoh T, Nibe K, Kojimoto A, Mikawa M, Mikawa K, Uchida K, et al. Erythema multiforme possibly triggered by food substances in a dog. *J Vet Med Sci*. 2006;68(8):869-871.
6. Woldemeskel M, Liggett A, Ilha M, Saliki JT, Johnson LP. Canine parvovirus-2b–associated erythema multiforme in a litter of English Setter dogs. *J Vet Diagn Invest*. 2011;23:576-580.
7. Nuttall TJ, Malham T. Successful intravenous human immunoglobulin treatment of drug-induced Stevens-Johnson syndrome in a dog. *J Small Anim Pract*. 2004;45:357-361.
8. Scott DW, Miller WH, Griffin CE. Immune mediated disorders, erythema multiforme. In: *Muller and Kirk's Small Animal Dermatology.* 6th ed. Philadelphia, PA: Saunders; 2001:729-740.
9. Scott DW. Erythema multiforme in a dog caused by a commercial nutraceutical product. *J Vet Clin Sci*. 2008;1:16–21.
10. Scott DW, Miller WH. Erythema multiforme in dogs and cats: Literature review and case material from the Cornell University College of Veterinary Medicine (1988–96). *Vet Dermatol.* 1999;10:297–309.
11. Tepper L, Spiegel IB, Davis GJ. Diagnosis of erythema multiforme associated with thymoma in a dog and treated with thymectomy. *J Amer Anim Hosp Assoc*. 2011;47:e19-e25.

**CASE IV:** A2011-01 (JPC 4002941).

**Signalment:** 10-year-old, spayed female mixed breed, canine *(Canis familiaris)*.

**History:** This animal had a cutaneous mass removed from the inter-scapular region three years previously which was diagnosed as a malignant pilomatricoma. The animal presented recently with labored breathing and was euthanized due to numerous pulmonary soft-tissue opacities radiographically. Portions of lung were submitted for histopathology.

**Gross Pathology**: In multifocal to coalescing regions, there is extensive replacement of the pulmonary parenchyma by soft, pale tan to red, variably necrotic masses.

**Histopathologic Description:** The normal pulmonary architecture is extensively effaced by neoplastic epithelial cells, necrosis, and debris. The basaloid cells are arranged in coalescing cords and clusters supported by a fibrovascular to inflammatory stroma. The cells have indistinct cell borders and small amounts of eosinophilic cytoplasm and central round to ovoid nuclei with coarse, irregular chromatin and prominent nucleoli. There are scattered foci of squamous differentiation. The cells exhibit moderate to marked anisocytosis and anisokaryosis. Mitoses are common and range from 3-10 per 40X field. The cell clusters occasionally have central necrosis or central keratinized "ghost cells." Tumor emboli are common in vessels and lymphatics.

**Contributor's Morphologic Diagnosis:** Lung: Metastatic pilomatricoma.

**Contributor's Comment:** Pilomatricoma is a benign cutaneous tumor that arises from the germinative cells of the follicular matrix, or hair bulb exhibiting only matrical differentiation.[1,2,4] It is an uncommon neoplasm of dogs and comprises approximately 1% of canine skin tumors.[1,3] Pilomatricomas most commonly occur on the back, neck, thorax, and tail. The tumors are generally well-delineated, firm, multilobular intradermal masses that often contain areas of grey-white chalky material on cut section.[2] Young, adult dogs are typically affected. Poodles, Kerry Blue Terriers, Old English Sheepdogs, Soft-coated Wheaten Terriers, and other breeds with continuously growing coats are over-represented which is believed to be related to the continuously-growing coat and subsequently greater numbers of mitotically active anagen follicles in these breeds.[1,4]

The histological features include a well-delineated dermal and/or subcutaneous epithelial tumor composed of multiple, variably sized cystic structures supported by a collagenous stroma. The structures are lined with several layers of basaloid keratinocytes which

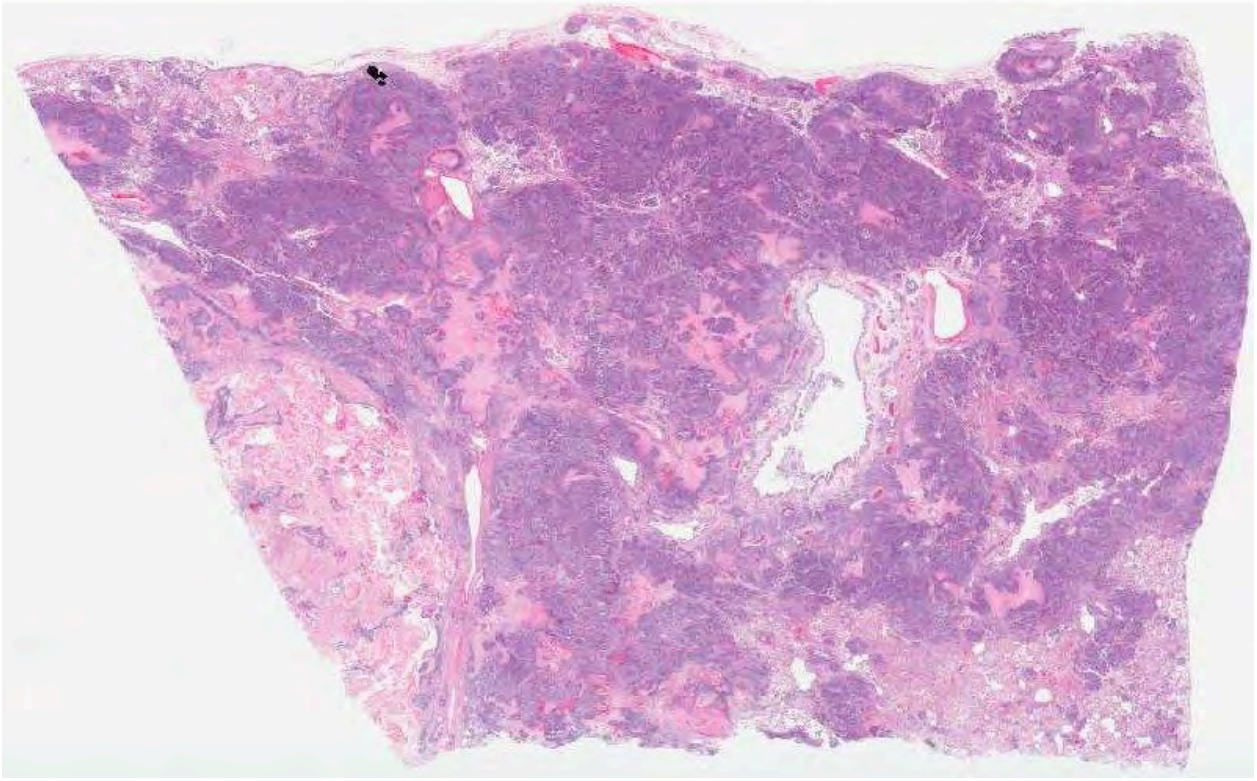

*4-1. Lung, dog: 85% of the section is effaced by an infiltrative, densely cellular neoplasm. (HE 0.63X)*

resemble the matrix cells of the anagen hair bulb with a moderate to high mitotic activity. Scattered squamous differentiation can be seen. As the neoplastic epithelial cells differentiate towards the center of the lesion they exhibit matrical keratinization ("ghost" or "shadow" cells) and the center of the cysts accumulate large aggregates of ghost cells and debris. The central debris can degenerate and become mineralized with foci of osseous metaplasia.[2,4]

Malignant pilomatricomas are rare and can be distinguished from the benign variety by their poorly delineated, infiltrative nature, increased mitotic activity, and increased ratio of basaloid cells to keratinized ghost cells. Lymphatic invasion is often evident along the periphery of the lesion. Metastasis has been reported to local lymph nodes, bone, and lung.[1,2,3]

**JPC Diagnosis:** Lung: Metastatic pilomatricoma.

**Conference Comment**: Recently, Martano et al. reported on the histopathological and immunophenotypic characteristics of malignant pilomatricoma with metastasis to bone in an 11-year-old mongrel dog.[5] Malignant pilomatricoma was diagnosed in an ulcerated mass from the dog's neck and a nodular bone mass, based on the histopathological features of irregularly-shaped, lobulated islands of basaloid cells undergoing abrupt keratinization to shadow cells, a high mitotic rate, and nuclear atypia, as well as metastasis to bone. Anti β-catenin immunohistochemistry revealed strong nuclear immunoreactivity of neoplastic basaloid cells, with few transitional cells exhibiting membrane-bound immunoreactivity. In humans, although the extent of membrane, cytoplasmic and nuclear expression of β-catenin varies in most skin tumors, basaloid cells in pilomatricoma and malignant pilomatricoma usually demonstrate intense diffuse nuclear immunoreactivity with β-catenin antibody. Furthermore, pilomatricoma in humans are often associated with deregulation of the Wnt/β-catenin pathway due to mutations in the *CTNNB1* gene. In normal cells, β-catenin can be located at the cell surface where it links E-cadherin to the actin cytoskeleton to create cell-to-cell junctions. Cytosolic β-catenin is phosphorylated by the APC-AXIN-GSK3β destruction complex, and subsequently destroyed via ubiquitination (known as the APC/ β-catenin pathway).[6] Wnt signaling blocks the destruction complex, allowing β-catenin to accumulate and translocate to the nucleus, where it complexes with transcription factors that up-regulate transcription of c-*MYC, cyclin D1,* and other genes that increase cellular proliferation. Dysregulation of the APC/ β-catenin pathway has been found to play a role in the development of several neoplasms, including colon tumors and hepatocellular carcinomas in addition to pilomatricomas.[5,6] Based on the findings in this study, Martano et al. suggest that, similar to humans, β-catenin is involved in the pathogenesis of malignant pilomatricoma in dogs, and therefore may be a useful diagnostic marker.[5]

**Contributing Institution:** TVMDL
PO Box 3200
Amarillo, TX 79116-3200
tvmdl.tamu.edu

**References:**

1. Carroll EE, Fossey SL, Mangus LM, Carsillo ME, Rush LJ, McLeod CG, Johnson TO. Malignant pilomatricoma in 3 dogs. *Vet Path*. 2010;47(5): 937-943.
2. Goldschmidt MH, Hendrick MJ. Tumors of the skin and soft tissue: "Pilomatricoma" and "malignant pilomatricoma". In: *Tumors in Domestic Animals*. 4th ed. Ames, Iowa: Iowa State Press; 2002:61-63.
3. Gross TL, Ihrke PJ, Walder EJ, Affolter VK. Malignant pilomatricoma. In: *Skin Diseases of the Dog and Cat, Clinical and Histopathologic Diagnosis.* 2nd ed. Ames, Iowa: Blackwell Publishing; 2005:637-638.
4. Gross TL, Ihrke PJ, Walder EJ, Affolter VK. Pilomatricoma. In: *Skin Diseases of the Dog and Cat, Clinical and Histopathologic Diagnosis.* 2nd ed. Ames, Iowa: Blackwell Publishing; 2005:624-625.
5. Martano M, et al. Malignat pilomatricoma with multiple bone metastases in a dog: Histological and immunohistochemical study. *Exp Ther Med*. 2013;5(4): 1005–1008.
6. Stricker TP, Kumar V. Neoplasia. In: KumarV, Abbas AK, Fausto N, Aster JC, eds. *Robbins and Cotran Pathologic Basis of Disease*. 8th ed. Philadelphia, PA: Saunders Elsevier;2010:292-294.

**Joint Pathology Center**
**Veterinary Pathology Services**

## WEDNESDAY SLIDE CONFERENCE 2012-2013

# Conference 21

**10 April 2013**

**CASE I:** 11120715 (JPC 4020064).

**Signalment:** 20-month-old, Charolais bull, *Bos taurus.*

**History:** The bull presented to Veterinary Teaching Hospital with 7-day history of acute onset blindness. This patient is the most severely affected of 12 bulls exhibiting clinical signs (from total of 20). All bulls are housed on separate, but adjacent lots. The water source is pond and associated creek. The animals are fed 15-25lbs/head/day of a mixture of distiller's grain, corn gluten, corn, soybean hulls and wheat ration with a small amount of hay (native grass). Some of the bulls were treated with thiamine, Nuflor, banamine and a multivitamin injection. There was no response to therapy. This patient was euthanized and submitted for necropsy to investigate cause of disease in herd.

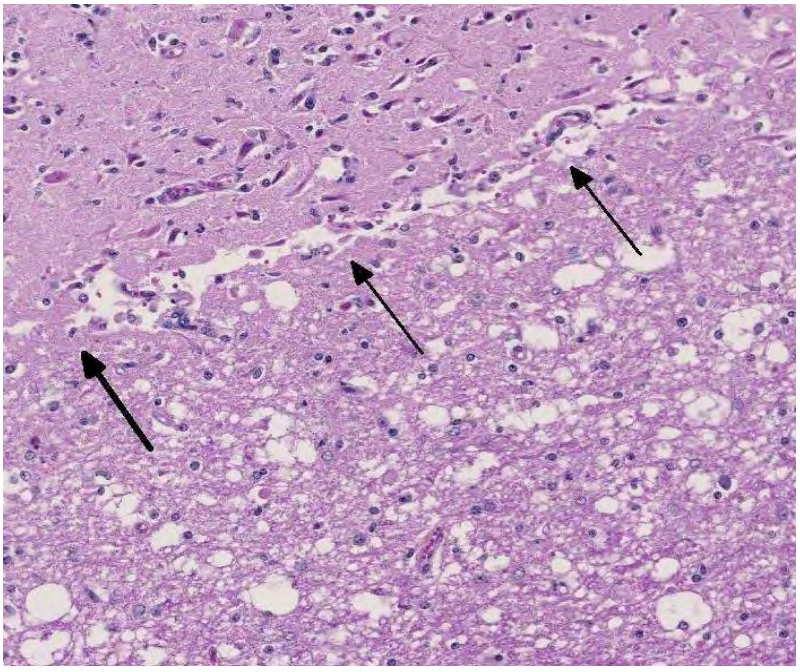

*1-1. Ox, cerebrum: Scattered throughout the superficial cortex, there are focally extensive areas of laminar necrosis, with adjacent vacuolation of neuropil. (HE 116X)*

**Gross Pathology:** Necropsy is performed on a 20 month-old (per history), white, 640 kg, Charolais bull in good body condition with no appreciable autolysis. Following comprehensive examination of the carcass and all major organ systems, there are no significant gross lesions (including the brain).

**Laboratory Results:**
Feed analysis, sulfur, 4200ppm
Water analysis, sulfates, <7mg/L
Blood lead, negative

**Histopathologic Description:** Histologic changes were confined to the cerebrum and overlying meninges. Within the deep cortical lamina, and segmentally, extending out to affect the more superficial laminae, the neuropil is

moderately to markedly vacuolated and rarefied (necrosis) with infiltration of the neuropil by moderate to marked numbers of small glial cells, moderate numbers of gitter cells and fewer gemistocytic astrocytes. Cortical neurons are shrunken, angular, and hypereosinophilic with pyknotic nuclei (necrosis) and are often cuffed by glial cells (satellitosis). Vessels within the affected areas are lined by plump, hypertrophied endothelial cells and are frequently cuffed by large macrophages. The overlying meninges are infiltrated by low to moderate numbers of large, perivascular to diffusely distributed macrophages and mildly expanded by edema.

**Contributor's Morphologic Diagnosis:** 1. Cerebrum: Severe, subacute, locally extensive laminar cortical (neuronal) necrosis (polioencephalomalacia).
2. Meninges: Mild to moderate histiocytic meningitis.

**Contributor's Comment:** Histologic lesions in the cerebrum of this bull were characteristic of nutritional polioencephalomalacia (PEM).

Nutritional PEM has traditionally been associated with thiamine (vitamin B1) deficiency in numerous animal species, particularly small carnivores and ruminants. While the pathogenesis and direct association with thiamine deficiency is well established in carnivores, the pathogenesis remains somewhat more obscure in ruminants who may be thiamine responsive early in disease, but often have striking PEM without a demonstrable deficiency in tissue thiamine, or blood transketolase levels.

In the early 1980s, nutritional PEM was first associated with elevated sulfur levels in a group of cattle in Missouri receiving sulfated feeds to limit feed consumption and has since been demonstrated in cattle, sheep, and goats receiving elevated sulfur from a variety of feed materials including sulfated feeds (calcium sulfate), high-protein forage (alfalfa), corn meal by-products, molasses based liquid feeds, sulfur containing plants, such as genus Brassica, and excessively sulfated water.[1]

The pathogenesis of sulfur-related PEM is related to ruminal microbes reducing ingested sulfur to highly toxic hydrogen sulfide, which then interferes with cellular energy metabolism.[2] Presumptively, the continuous energy requirement of cerebral neurons make them particularly susceptible. Additionally, sulfite, an intermediate in sulfate reduction, can cleave thiamine;[1] however, the contribution of this phenomenon to PEM in ruminants is not well established given the typically normal thiamine levels in these animals.

Clinical course in ruminants ranges from acute, characterized by acute cortical blindness, depression, dullness to recumbency, convulsions, opisthotonos, coma and death, to more subacute, characterized primarily by blindness and ataxia. Grossly cerebral edema, swelling, pallor and softening of the cerebrum with variable laminar paleness of the gray matter at the junction between gray and white is seen in acute deaths and tissues may autofluoresce under UV light. If survival is prolonged gross changes may progress to yellow-brown discoloration and cavitation of the gray matter and the tissue will fail to autofluoresce.[2] Histologic lesions of PEM may be somewhat varied in their distribution, being more pronounced in the cerebral cortices of ruminants, and in periventricular nuclei of carnivores. Laminar cortical necrosis of neurons especially within the deeper laminae with malacia is classic. This change is also seen in cases of lead toxicity, hypoxia, and water deprivation-salt intoxication.[1]

Unlike in ruminants, the pathogenesis of nutritional PEM in carnivores (Chastek paralysis) is well established. Thiamine is an essential dietary vitamin in carnivores, and cases of PEM are associated with ingestion of high levels of thiaminase containing fish diets (cats) or consumption of excessively heated meats that destroy thiamine (dogs). Less commonly, consumption of the food preservative sulfur dioxide has been documented. The course of disease and clinical signs are similar to ruminants, with lesions more typically present bilaterally and symmetrically in the brain stem nuclei, most commonly the inferior colliculi. Less commonly the cerebral cortex and cerebellar vermis may be affected. Vascular dilation and hemorrhage may be a prominent feature.[3]

The clinical disease, histopathologic lesions and demonstration of elevated sulfur levels in the feed support a classic sulfur-related PEM in this bull. The source of sulfur is most likely the corn by-products (distiller's grain) that can contain excessively high sulfur. The National Research Council states the daily requirement for adult beef cattle is 1500-2000 ppm sulfur within the ration with a daily maximum tolerated dietary dose of 0.4% (4000 ppm).[4]

**JPC Diagnosis:** Brain, cerebrum, cortex: Necrosis, laminar, multifocal, with diffuse spongiosis.

**Conference Comment:** Conference participants discussed the causes of PEM in ruminants, as reviewed by the contributor in the above comments. Participants further discussed causes of polioencephalomalacia in other veterinary species, noting that the term "polioencephalomalacia" is generally used to describe softening in the cerebrocortical grey matter with a laminar distribution. There are several conditions associated with this pattern of necrosis, which is also referred to as "laminar cortical necrosis" or "cerebrocortical necrosis." It is a characteristic lesion due to hypoxia/ischemia, such as that caused by feline ischemic encephalopathy due to aberrant migration of *Cuterebra* larva and neonatal maladjustment syndrome of foals, salt poisoning in swine,

lead poisoning in cattle, and cyanide poisoning in a variety of species.[1]

**Contributing Institution**: Department of Veterinary Pathobiology
Center for Veterinary Health Sciences
Oklahoma State University
Rm 250 McElroy Hall
Stillwater, OK 74078 USA
www.cvhs.okstate.edu

**References:**

1. Maxie MG, Youssef S. Nervous system. In: Maxie MG, ed. *Pathology of Domestic Animals.* 5th ed. Vol. 1. Philadelphia, PA: Elsevier Ltd, 2007;336-356.
2. Gould DH. Update on sulfur-related polioencephalomalacia. *Vet Clin North Am Food Anim Pract*. 2000;6:481-496, vi-vii.
3. Summers B, Cummings JF, Delahunta A. Degenerative diseases of the central nervous system. In: *Veterinary Neuropathology*. St. Louis, MO: Mosby; 1995:277-280.
4. Nutrient requirements of beef cattle/Subcommittee on Beef Cattle Nutrition, Committee on Animal Nutrition, Board on Agriculture, National Research Council.—7th ed. Washington, DC., USA: National Academies Press, 2000;60-61. [http://www.ag.ndsu.edu/pubs/ansci/beef/eb74w.htm ]

**CASE II**: 40282/14C (JPC 4019898).

**Signalment:** 8-year-old female, Irish Sport Horse, *Equus caballus*, horse.

**History:** Unilateral left epistaxis for two months, pallor of oral and conjunctival mucosa, anorexia.

**Gross Pathology:** Necropsy revealed dried blood on the muzzle, pallor of conjunctival and oral mucosa, bloody and foamy tracheal and bronchial edema, atrophy of the left laryngeal muscles, bloody content in the stomach, and, on the caudodorsal wall of the medial compartment of the left guttural pouch, a proliferative and hemorrhagic lesion with erosion and thrombosis of the internal carotid artery.

**Laboratory Results:** Microbiological culture of the proliferative lesion of the guttural pouch was positive for *Aspergillus fumigatus*.

**Histopathologic Description:** Guttural pouch, internal carotid artery and nerves: The guttural pouch mucosa is severely and diffusely eroded and ulcerated and is replaced by a thick coagulum of fibrin, necrotic debris, degenerate neutrophils and hemorrhage.

The necrotic process extends into, and replaces, up to one third of the internal carotid artery wall and extends within the lumen forming a thrombus. Palisading on the surface of the coagulum and in association with the necrotic material there are myriad 5 to 8 µm thick, septate, dichotomously branched, PAS-positive fungal hyphae with parallel walls, often associated with abundant brown pigment and numerous bacterial colonies. The remaining two thirds of the arterial wall are characterized by diffuse erosion of the endothelium, severe thickening of the intimal, medial and adventitial layers due to fibroblasts, myofibroblasts and muscular cells proliferation, deposition of collagenous and mucinous extracellular matrix, multifocal fibrin deposition, edema and a multifocal inflammatory infiltrate mainly composed of karyolytic and karyorrhectic neutrophils associated with cellular and nuclear debris (necrosis).

The necrotic process extends also into the subepithelial connective tissue where it is associated with a severe and multifocal to coalescent inflammatory infiltrate composed of neutrophils, macrophages, eosinophils, lymphocytes,

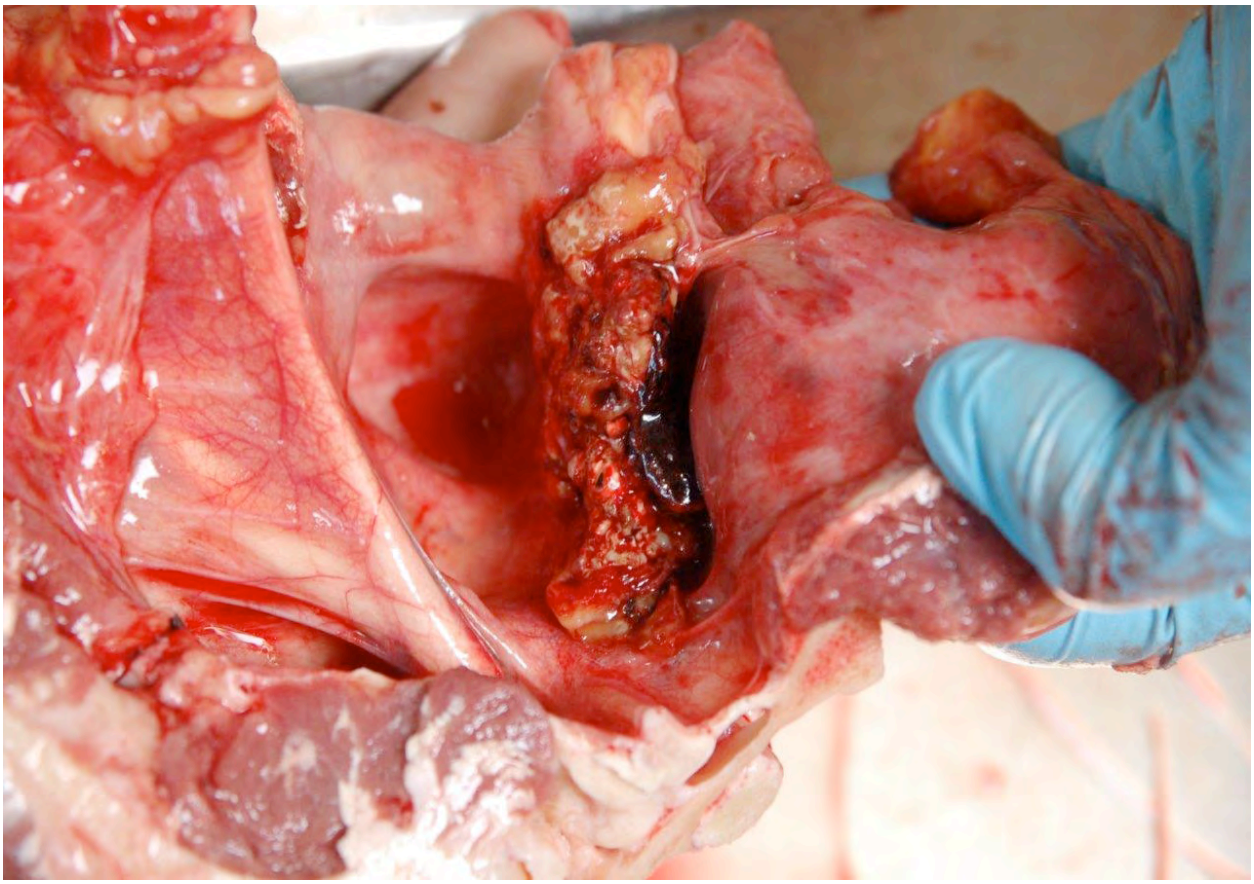

*2-1. Horse, guttural pouch: The edge of the guttural pouch is thickened by abundant granulation tissue which is covered by a thick mat of fibrin and necrotic tissue. There is thrombosis of the internal carotid artery (not visible in the photo). (Photo courtesy of the Department of Comparative Biomedicine and Food Science (BCA), University of Padua, Viale dell'Università 16, 35020 Legnaro, Padova – Italy. http://www.bca.unipd.it/)*

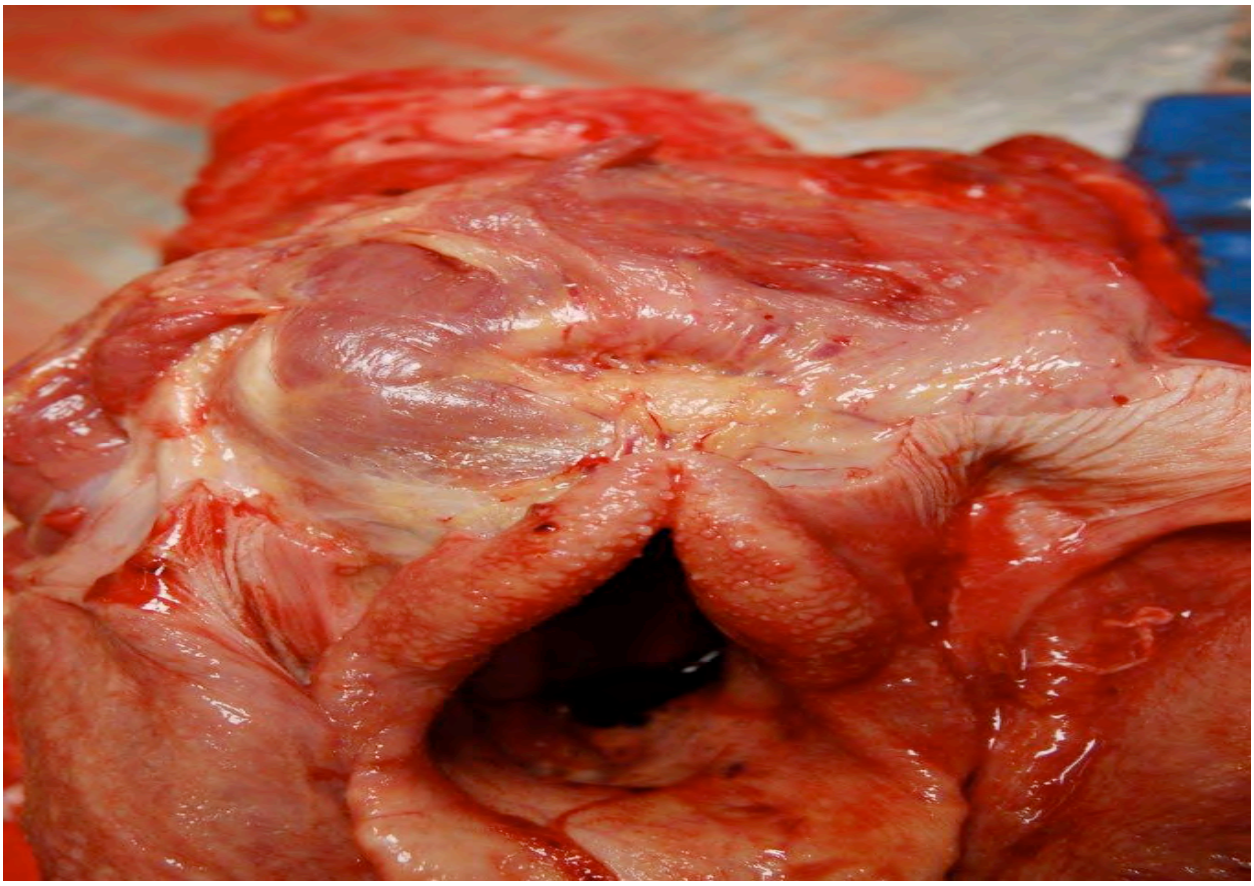

*2-2. Horse, guttural pouch: There is atrophy of the left cricoarytenoideus muscle (laryngeal hemiplegia), as well as diffuse lymphofollicular largyngitis. (Photo courtesy of the Department of Comparative Biomedicine and Food Science (BCA), University of Padua, Viale dell'Università 16, 35020 Legnaro, Padova – Italy. http://www.bca.unipd.it/)*

plasma cells with occasional fungal hyphae. There is severe and diffuse edema and multifocal hemorrhages. There is multifocal thrombosis.

The nerves within the subepithelial connective tissue are characterized by loss of myelin sheaths, spheroid formation, multifocal areas of coagulative necrosis associated with karyolytic and karyorrhectic neutrophils, macrophages, lymphocytes and plasma cells and severe multifocal hemorrhages.

**Contributor's Morphologic Diagnosis:** 1. Guttural pouch: Eustachitis, severe, diffuse, chronic, ulcerative, fibrino-necrotizing, suppurative and macrophagic with intralesional fungal hyphae and bacterial colonies.
2. Internal carotid artery: Arteritis, severe, chronic, fibrino-necrotizing, suppurative and proliferative with thrombus formation and fungal hyphae.
3. Nerves: neuritis, severe, multifocal chronic, suppurative and necrotizing with demyelination and multifocal hemorrhages, *Equus caballus*, horse.

**Contributor's Comment:** Guttural pouch mycosis is a rare fungal disease of the upper respiratory tract of horses.[1,4,11] There is no apparent age, sex, breed or geographic predisposition to this disease although it is seen most frequently in stabled horses in temperate climates during the warmer months of the year and is seldom recorded in warmer climatic regions. Guttural pouch mycosis shows no predilection for either the right or the left guttural pouch.[1,6,7,8,10,11]

The pathogenesis has not been ascertained; however, it has been speculated that the mucous membrane layer of the guttural pouch is disrupted by trauma, local inflammation, a primary bacterial infection, or all three. This disruption allows opportunistic fungi that are present in the normal equine airway, such as *Aspergillus* spp., to invade into the deeper tissues, including local arteries and nerves.[5] Different species of *Aspergillus* can be isolated such as *A. fumigatus, A. versicolor, A. nidulans* and *A. niger*, but *A. fumigatus* is the most frequently isolated.[10]

The clinical signs of guttural pouch mycosis can be explained by the fact that fungal growth, and the inflammation associated with it, has a predilection for the roof of the medial and, occasionally, the lateral compartments of the guttural pouch. This area is anatomically associated with the external and internal carotid arteries, internal maxillary artery,

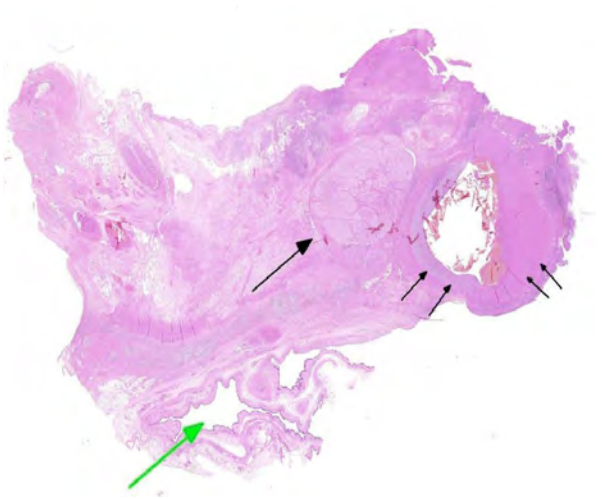

*2-3. Horse, guttural pouch: The section contains a section of the guttural pouch (green arrow), a large nerve (black arrow), and the internal carotid artery (multiple small arrows). (HE 0.63X)*

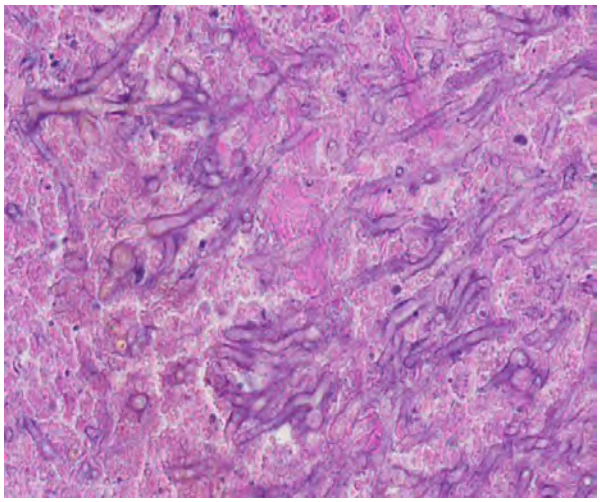

*2-4. Horse, guttural pouch: Within the necrotic wall of the thrombosed internal carotid artery, there are numerous fungal hyphae which exhibit parallel walls, septae, and dichotomous branching. (HE 400X)*

glossopharyngeal nerve (cranial nerve IX), vagus nerve (X), spinal accessory nerve (XI), hypoglossal nerve (XII), sympathetic nerves, and stylohyoid bone.[1,4,6,7,10,11] Due to this close association, a horse with guttural pouch mycosis can show signs of epistaxis, dysphagia, parotid pain, abnormal head posture, nasal discharge, head shyness, abnormal respiratory noise, sweating and shivering, Horner's syndrome, colic, tongue atrophy and facial paralysis.[1,4,6,7,10,11]

Radiographs and clinical pathologic analyses have been determined to be of little value, as radiographic change with guttural pouch mycosis is minimal and clinical pathologic analyses typically will show an anemia, only if a recent significant bleeding episode has occurred.[11]

Gross pathologic examination of the mycotic guttural pouch characteristically reveals a yellow-brown to black mottled dry diphtheritic membrane with dry, dull white fungal plaques growing on it.[1] This membrane and fungal plaques are typically adhered to the tissues of the roof of the medial pouch and found in association with the internal carotid artery, with possible extension onto the roof of the lateral pouch and ventrally to the stylohyoid bone.[6]

If untreated, spontaneous resolution of guttural pouch mycosis has been observed but it may also result in fatal hemorrhage or irreversible neurological signs.[9] Medical treatment generally gives unsatisfactory and doubtful results.[8,9] Therefore, a surgical treatment option is still recommended and is usually successful even though progression of the disease has been described after surgical treatment.[5,8,9] Surgical treatment consisting of a vascular occlusion for prevention of hemorrhage is the recommended procedure and the occlusion must be performed on the cardiac and cerebral sides of the lesion to prevent haemorrhage.[3,5,8,9,12] Complications reported with this technique include recurrence of moderate to profuse epistaxis and retrograde infection.[8,9]

**JPC Diagnosis:** Guttural pouch: Eustachitis, fibrinosuppurative and necrotizing, diffuse, severe, with multifocal arteriolar and venous vasculitis and thrombosis, necrotizing neuritis, and numerous fungal hyphae.

**Conference Comment**: Guttural pouches are ventral diverticulae of the auditory tubes in equids. Bacterial infection of the guttural pouch is referred to as guttural pouch empyema, and is most often caused by *Streptococcus equi* or other streptococci. Compared to guttural pouch empyema, guttural pouch mycosis tends to feature more extensive inflammation that invades deeper tissues, and thus leads to more severe complications. In addition to the extension into the nerves and arteries described above, guttural pouch mycosis may also result in osteitis and fusion of the stylohyoid and petrous temporal bones.[2]

Conference participants considered the report of left laryngeal muscle atrophy in this horse, and speculated it may be due to damage to the left recurrent laryngeal nerve from extension of the guttural pouch mycosis. In horses, laryngeal paralysis is usually a left-sided hemiplegia caused by idiopathic degeneration of the left recurrent laryngeal nerve. Although it is thought that neuritis due to extension from guttural pouch disease may play a role in laryngeal paralysis, the extent to which this occurs has yet to be determined. Other possible, but unproven, causes of laryngeal hemiplegia are trauma, vitamin deficiency, or neurotoxins. Bilateral laryngeal paralysis is more often due to hepatic encephalopathy and general anesthesia.[2]

There is some slide variation, with some slides exhibiting the described neuritis, which is considered to be secondary to the profound inflammation in surrounding tissue.

**Contributing Institution**: Department of Comparative Biomedicine and Food Science (BCA)University of Padua
Viale dell'università 16, 35020 Legnaro, Padova – Italy
http://www.bca.unipd.it/

**References**

1. Archer RM, Knight CG, Bishop WJ. Guttural pouch mycosis in six horses in New Zealand. *N Zeal Vet J*. 2012;60(3):203–209.
2. Caswell J, Williams KJ. Respiratory System. In: Maxie MG, ed. *Jubb, Kennedy and Palmer's Pathology of Domestic Animals*. 5th ed. Vol. 2. Philadelphia, PA: Elsevier Ltd, 2007;537-538.
3. Delfs KC, Hawkins JF, Hogan DF. Treatment of acute apistaxis secondary to guttural pouch mycosis with transarterial nitinol vascular occlusion plugs in three equids. *JAVMA*. 2009;235(2):189-193.
4. Dixon PM, McGorum BC, Railton DI, Hawe C, Tremaine WH, Pickles K, et al. Laryngeal paralysis: a study of 375 cases in a mixed-breed population of horses. *Eq Vet J*. 2001;33(5):452-458.
5. Ernst NS, Freeman DE, MacKay RJ. Progression of mycosis of the auditory tube diverticulum (guttural pouch) after arterial occlusion in a horse with contralateral temporohyoid osteoarthropathy. *JAVMA*. 2006;229(12):1945-1948.
6. Hunter B, Nation PN. Mycotic encephalitis, sinus osteomyelitis, and guttural pouch mycosis. *Can Vet J*. 2011;52(12):1339-41.
7. Kipar A, Frese K. Hypoglossal neuritis with associated lingual hemiplegia secondary to guttural pouch mycosis. *Vet Path*. 1993;30(6):574-6.
8. Lepage OM, Perron MF, Cador JL. The mystery of fungal infection in the guttural pouches. *Vet J*. 2004;168: 60–64.
9. Lepage OM, Piccot-Crèzollet C. Transarterial coil embolisation in 31 horses (1999-2002) with guttural pouch mycosis a 2-year follow-up. *Eq Vet J*. 2005;37(5): 430-434.
10. Ludwig A, Gatineau S, Reynaud MC, Cadore´ JL, Bourdoiseau G. Fungal isolation and identifiaction in 21 cases of guttural pouch mycosis in horses. *Vet J*. 2005;169 (3):457-61.
11. Millar H. Guttural pouch mycosis in a 6-month-old filly. *Can Vet J*. 2006;47(3):259-61.
12. Yoshikazu M, Yu N, Yutaka M. Occlusion of the internal carotid artery by means of microcoils for preventing epistaxis caused by guttural pouch mycosis in horses. *J Vet Med Sci*. 1999;61(3):221-5.

**CASE III**: 12-26 (JPC 4019359).

**Signalment:** 1-year-old male quarter horse (*Equus caballus*).

**History:** The body of a 1-year-old quarter horse colt was submitted for postmortem examination. The animal had been observed the day before and was reported to be healthy. The next day the colt was found dead with no evidence of a struggle. No other animals on the premises were sick.

**Gross Pathology:** Received the body of a 1-year-old, bay, quarter horse colt for postmortem examination. The body was in good nutritional condition and there was evidence of dehydration. Mild autolysis was noted. Over the left side and dorsal aspect of the thorax, there were locally extensive areas of subcutaneous hemorrhage and edema. Within the thoracic cavity, there were multifocal to coalescing ecchymoses located immediately below the costal pleura. The trachea contained a moderate amount of stable white froth consistent with pulmonary edema. The lungs had failed to completely collapse and multifocal areas of hemorrhage were noted on the pleural surface and within the pulmonary parenchyma. Foci of pulmonary hemorrhage measured up to 0.8 cm in diameter. Within the pericardial sac approximately 10 ml of serosanguinous fluid was noted. On the epicardial surface of the heart, there were innumerable petechiae. On the endocardial surface, extensive ecchymotic hemorrhage was noted in both the right and left ventricles. On the capsular surface of the spleen, numerous petechiae were noted. The liver was diffusely congested. Bilaterally the renal medulla was dark red and congested. Multifocally and randomly distributed within the renal cortices there were numerous, 1-3 mm, white foci.

**Laboratory Results:** 4+ *Actinobacillus equuli* isolated from the kidney.

**Histopathologic Description:** Kidney: Randomly scattered within the cortex and occasionally extending into the medulla, there is a severe inflammatory process characterized by the presence of numerous microabscesses. The inflammation frequently centers on and effaces the glomeruli and is seen to extend into the adjacent tubules and interstitium. Glomeruli, which remain intact, are characterized by congestion, and numerous bacterial emboli and fibrin microthrombi within the glomerular capillaries. This is further accompanied by necrosis, hemorrhage and marked neutrophilic inflammation resulting in the formation of abscesses. In some areas the bacterial colonies and neutrophilic inflammation extend into the adjacent proximal tubules and there is degeneration and necrosis of the tubular epithelium. Focally suppurative inflammation extends into the renal capsule (not present in every slide). The bacterial colonies are large and are characterized by a myriad of 1X2 µm coccobacilli. While bacterial emboli are most prominent within glomerular capillaries they are also observed within intertubular capillaries. Marked medullary congestion is a feature. Gram stain reveals the presence of innumerable gram-negative coccobacilli.

Similar bacterial emboli were noted in many other organs including the liver, lung, spleen, lymph nodes, brain and spinal cord consistent with septicemia (not shown in this slide).


*3-1. Lung, quarter horse: The lungs had failed to completely collapse and multifocal areas of hemorrhage were noted on the pleural surface and within the pulmonary parenchyma. Petechiae were also seen on the thoracic pleura and pericardium. (Photo courtesy of the Diagnostic Services Unit, University of Calgary Veterinary Medicine, Clinical Skills Building, 11877 85 St. NW, Calgary AB T3R 1J3, http://vet.ucalgary.ca/*

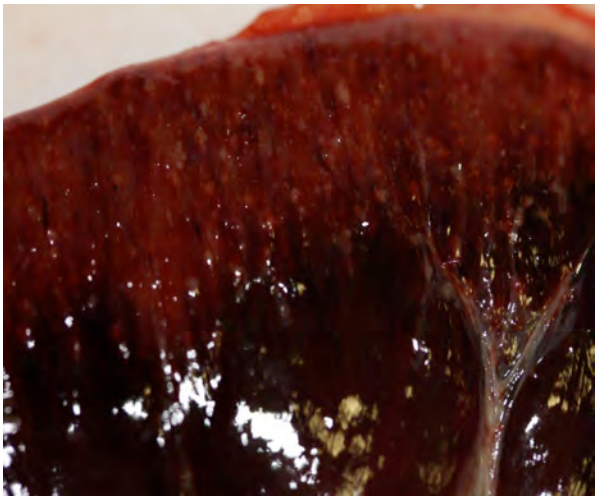

*3-2. Kidney, quarter horse: Bilaterally the renal medulla was dark red and congested. Multifocally and randomly distributed within the renal cortices there were numerous, 1-3 mm, white foci. (Photo courtesy of the Diagnostic Services Unit, University of Calgary Veterinary Medicine, Clinical Skills Building, 11877 85 St. NW, Calgary AB T3R 1J3, http://vet.ucalgary.ca/*

*3-3. Kidney, quarter horse: Scattered throughout the cortex, and to a lesser extent in the medulla, there are numerous microabscesses, often centered on glomeruli. (HE 0.63X)*

**Contributor's Morphologic Diagnosis:** Nephritis, suppurative, embolic, acute, severe with intralesional coccobacilli.

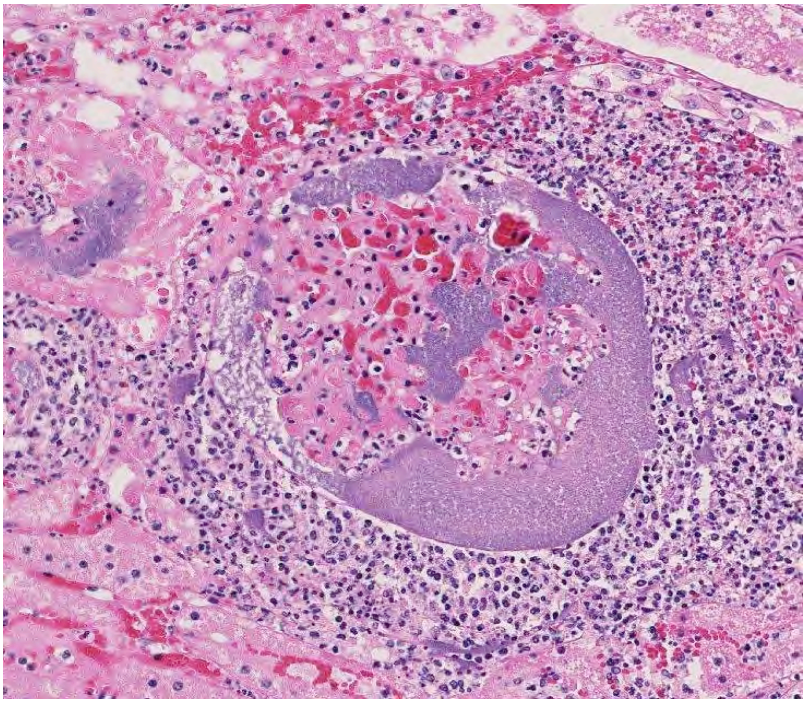

*3-4. Kidney, quarter horse: Large colonies of bacilli (Actinobacillus equuli) fill Bowman's capsule and are present in surrounding areas of necrosis and suppurative inflammation. (HE 280X)*

**Contributor's Comment:** Actinobacillosis, also known as sleepy foal disease, is an acute and highly fatal septicemia of newborn foals caused by *Actinobacillus equuli*. In many countries it is the most important cause of equine neonatal deaths.[6,9] *A. equuli* is a small, nonmotile, gram-negative, pleomorphic rod. This is a diverse species with at least 28 different antigenic groups.[2] Certain strains of *A. equuli* form part of the normal flora of the gastrointestinal and respiratory tracts of horses.[3,4] There is a high degree of strain variability within horse populations and within individual horses over time. It is currently unknown whether there are specific strains of *A. equuli* with greater virulence for foals and/or adult horses or whether such strains are common inhabitants of the equine gastrointestinal and respiratory tracts.[4]

Typically actinobacillosis is a disease of newborn foals and the pathogenesis of the infection remains speculative. It is postulated that one of the main sources of infection is from the gastrointestinal or respiratory tracts of the mare, although some foals may be infected in utero via placental transmission of the


*3-5. Kidney, quarter horse: A tissue Gram stain discloses of the gram-negative nature of the bacilli, compatible with A. equuli. (Photo courtesy of the Diagnostic Services Unit, University of Calgary Veterinary Medicine, Clinical Skills Building, 11877 85 St. NW, Calgary AB T3R 1J3, http:// vet.ucalgary.ca/*

organism resulting in abortion. The majority of foals are likely infected at or during parturition through inhalation, ingestion, or via the umbilicus.[3] Colostrum deprivation is often implicated in cases of actinobacillosis in the early neonatal period; therefore, components of the colostrum from the mare are thought to be passively protective to the foal.[3,8]

Foals may either die of acute fulminating septicemia in the early neonatal period or survive for several days allowing the organism to localize to multiple organ systems. Aborted foals and those with fulminating septicemia generally do not have distinctive gross lesions at postmortem. Animals that survive 2-4 days post-infection often develop miliary microabscesses and fibrinopurulent arthritis. Microabscesses, which are of embolic origin, are most easily observed in the renal cortices and are characterized by the presence of numerous, 1-3 mm, white foci.[6,9] In fact, *A. equuli* is the most common cause of embolic suppurative nephritis in horses. Typical histopathologic features in the kidney include the presence of numerous bacterial colonies within the glomerular and intertubular capillaries admixed with hemorrhage, necrotic debris and intense suppurative inflammation. The inflammation frequently obliterates the glomerulus.[9]

While the lesions in the current case are classical for infection with *A. equuli*, the unusual feature in this case is the older age of the horse. As previously mentioned, actinobacillosis is primarily a disease of neonatal foals and the organism is seldom of significance in older horses.[6,9] Although infections in adult horses are uncommon, cases of arthritis, endocarditis, orchitis, periorchitis, pleuropneumonia and enteritis have been reported.[4] In addition, both acute and chronic forms of *A. equuli* peritonitis have been described in adult horses. In acute infections, horses present with abdominal pain, ileus, lethargy and inappetance. In chronic cases, weight loss is the most common clinical signs. The source of infection has not been identified, but some have postulated that migrating strongyle larvae from the intestinal tract may play a role. Although *A. equuli* peritonitis is a rare disease in horses, clinicians and pathologists need to be aware of this condition as it is potentially treatable.[4,6]

While *A. equuli* is typically recognized as an opportunistic pathogen of horses, historically *A. equuli* has also been recognized as a rare opportunistic pathogen of pigs. The infection in pigs has been typically associated with abortion, septicemia and polyarthritis.[8] Interestingly, there have been two recent reports of *A. equuli* associated disease in pigs in North America and one outbreak was associated with a high level of morbidity and mortality in sows as the result of septicemia.[7,10] While in foals the primary source of infection is believed to be the mare, there is conflicting evidence concerning the role of the adult horse as a source of infection in pigs.[10] Furthermore, it has been suggested that the rarity of *A. equuli* infections in North American pigs may be the result of the separation of pigs and horses in modern farming systems.[5] A single report of *A. equuli* septicemia has been reported in the human medical literature.[1]

**JPC Diagnosis**: Kidney: Nephritis, embolic and suppurative, multifocal, severe, with numerous large colonies of bacilli.

**Conference Comment:** *Actinobacillus* species are within the family *Pasteurellaceae.* Most of the bacteria in this family are commensal, often colonizing the mucosal tissues of both humans and animals; however, there are several species of *Actinobacillus* that are of importance in veterinary medicine, including the following pathogens:[5] Two subspecies of *Actinobacillus* equuli have been identified, *A. equuli* subsp. *equuli*, and *A. equuli* subsp. *haemolyticus*.[2] The former appears to be pathogenic, while the latter's pathogenicity appears to be associated with its expression of a repeats-in-structural toxin (RTX) called Aqx, which is cytotoxic for equine leukocytes. RTX toxins, which are expressed by many species in the family *Pasteurellaceae,* are pore-forming proteins that, when present in high concentrations, bind to $\beta_2$-integrins and cause cell lysis and necrosis or, when present in low concentrations, lead to apoptosis by inducing apoptotic signaling cascades. Ultimately, the cellular destruction results in inflammation and disease. RTX toxins bind to specific $\beta_2$-integrins, such as CD18, and therefore play an important role in the host and host cell specificity of pathogenic *Pasteurellaceae*.[2]

| ***Actinobacillus* species** | **Associated species: disease** |
|---|---|
| *A. lignieresii* | Cattle: Lesions in the tongue, lymph nodes, rumen, and skin<br>Sheep: Lesions in the skin<br>Pigs: Granulomatous mastitis |
| *A. pleuropneumoniae* | Pigs: Pleuropneumonia |
| *A. suis* | Piglets, foals: Septicemia, pneumonia<br>Pigs, horses: Pneumonia |
| *A. equuli* | Foals: Septicemia<br>Piglets: Septicemia<br>Pigs: Arthritis, enteritis<br>Calves: Enteritis<br>Mares: Abortion |
| *A. seminis* | Rams: Epididymitis<br>Lambs: Polyarthritis |

**Contributing Institution**: Diagnostic Services Unit
University of Calgary Veterinary Medicine
Clinical Skills Building
11877 85 St. NW
Calgary AB T3R 1J3
http://vet.ucalgary.ca/

**References:**

1. Ashhurst-Smith C, Norton R, Thoreau W, et al. *Actinobacillus equuli* septicemia: an unusual zoonotic infection. *J Clin Microbiol*. 1998; 36:2789-2790.
2. Frey J. The role of RTX toxins in host specificity of animal pathogenic *Pasteurellaceae*. *Veterianry Microbiology. 2011;153:51-58.*
3. Matthews S, Dart AJ, Dowling BA, et al. Peritonitis associated with *Actinobacillus equuli* in horses: 51 cases. *Aus Vet J*. 2001;79:536-539.
4. Patterson-Kane JC, Donahue JM, Harrison LR. Septicemia and peritonitis due to Actinobacillus equuli infection in an adult horse. *Vet Pathol*. 2001;38:230-232.
5. Quinn PJ, et al. Actinobacillus. In: *Veterinary Microbology and Microbial Disease.* 2nd ed. Ames, Iowa: Wiley Blackwell; 2011, Kindle edition, location 10980 of 35051.
6. Radostits OM, Gay CC, Blood DC, Hinchcliff KW. *Veterinary Medicine: A Textbook of the Diseases of Cattle, Sheep, Pigs, Goats and Horses*. Edinburgh, UK: WB Saunders Company Ltd; 2000.
7. Ramos-Vara JA, Wu CC, Mitsui I, et al. Metritis, valvular endocarditis, and septicemia by *Actinobacillus equuli* in a gilt in the United Sates. *Vet Pathol*. 2008;45:495-499.
8. Rycroft AN, Garside LH. *Actinobacillus* species and their role in animal disease. *Vet J*. 2000;159: 18-36.
9. Schlafer DH, Miller RB. Female genital system. In: Maxie MG, ed. *Jubb, Kennedy and Palmer's Pathology of Domestic Animals*. 5th ed. Edinburgh, UK: Saunders Elsevier; 2007:431-563.
10. Thompson AB, Postey RC, Snider T, et al. *Actinobacillus equuli* as a primary pathogen in breeding sows and piglets. *Can Vet J*. 2010;51:1223-1225.

**CASE IV:** TAMU-1 2012 (JPC 4019888).

**Signalment:** 8-month-old male black and white Micro Pig (*Sus scofra*).

**History:** Wilber presented with dyspnea from potential aspiration. He has had CNS deficits for 2 months, since overeating at Thanksgiving. Recently, he was treated for a facial abscess. Profound hypoglycemia, hypokalemia, depression, bradycardia and hypothermia were recorded. He seizured and went into cardiac arrest.

**Gross Pathology:** Mild pneumonia was detected in this emaciated, 2.3kg pig. Animal had hydrocephalus.

**Histopathologic Description:** A section of the thinned cerebral cortex is presented. A laminar pattern of neuronal necrosis and loss is seen. Remaining is a neuropil of gliosis with astrocytes activated microglia and scattered oligodendroglia. Gitter cells are scattered and also form nests about aciculate "cholesterol clefts." Foci of calcified debris and cells and arterioles with a rim of calcium at the medial/intimal interface are noted. Scattered mononuclear cells infiltrate with a few neutrophils and thin cuffs of mononuclear cells are noted. Remaining neuropil is often rarified or has microcavitation (edema) with rare spheroids.

**Contributor's Morphologic Diagnosis:** Chronic encephalopathy with laminar cortical necrosis; hydrocephalus ex vaccuo.

**Cause:** Potato chip binging, salt intoxication.

**Contributor's Comments:** Micro pigs are one of a recent proliferation of pocket pets to appear on the market. Sometimes called "teacup pigs" because when born they can fit in a teacup, they grow to be the height of a medium-sized dog and weigh as much as 65 pounds.

This is a unique lesion and becomes intriguing when you are told that little Wilber loved potato chips, and at Thanksgiving was waylaid by a bag of Lays. He survived the "salt intoxication" with deficits for 2 months. The gross images of his brain demonstrate injected cerebral vessels and cortex collapse. On cross section, the laminar necrosis is seen nicely. While the morphologic can be followed by a chain of descriptors, this is an encephalopathy. Calcification of neuropil necrosis is common, but the pattern of vessel calcification is interesting. The nests of Gitter cells with cholesterol clefts are reminiscent of lipogranulomas. The mononuclear cells are mostly macrophages like is seen in cases of chronic polioencephalopathy and many infarcts; therefore, encephalitis is probably not a valid morphologic. I am not aware of a similar case being described although a comment on similar chronic lesions is in texts.[5] One must wonder if seizures have a role in developing some of the cortical necrosis.

Salt poisoning of young pigs is well known in its acute form and occurs when high salt diets are given when inadequate water is available.[2,5] Upon the later consumption of water, the salt in the cortical tissues cannot be cleared before water enters to cause the laminar necrosis. Evidence of presumed previous eosinophil cuffing is nowhere to be seen at this time. It is thought that eosinophil cuffs are associated/induced by sodium excess in tissues but may not be seen and cuffs are not present several days after survival.[2,5] Laminar necrosis in cases of salt intoxication does not fluoresce (JFE).

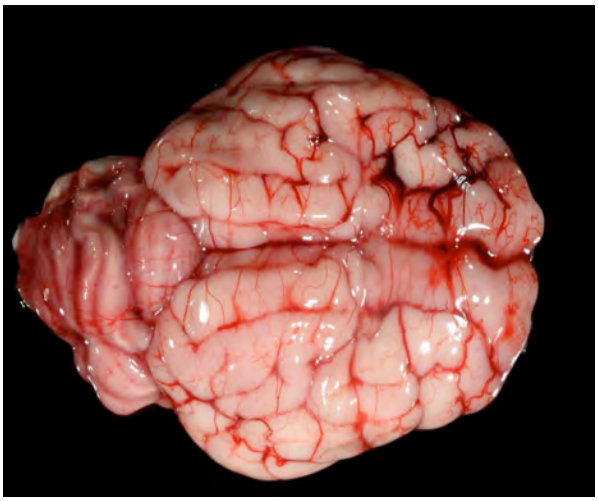

*4-1. Cerebrum, micropig: The cerebrum displays mild flattening of the gyria and a loss of sulcal depth, as well as multifocal cloudiness of the meninges. (Photo courtesy of the Deptartent of Veterinary Pathobiology, College of Veterinary Medicine and Biomedical Sciences,Texas A&M University, College Station, TX 77843-4467)*

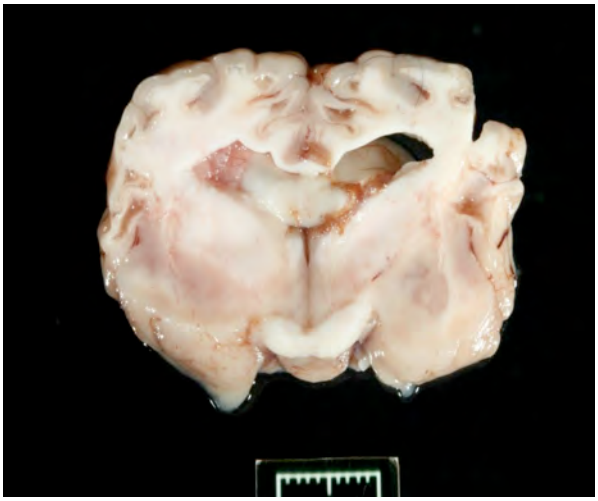

*4-2. Cerebrum, micropig: There is diffuse thinning of the superficial gray matter, as well as mild dilation of the lateral ventricles as a result of hydrocephalus ex vacuo. (Photo courtesy of the Deptartment of Veterinary Pathobiology, College of Veterinary Medicine and Biomedical Sciences, Texas A&M University, College Station, TX 77843-4467)*

Swine are considered the most sensitive species to salt intoxication.[3] Potato chips have been reported before in this disease in pigs and survivors with CNS deficits are reported.[2,4] It has been shown that diets high in salt lead to increased salt in the pig brain with the highest concentrations being in the cerebral and cerebellar hemispheres.[1,6]

**JPC Diagnosis:** 1. Brain, cerebrum: Necrosis, cortical, laminar, with multifocal cholesterol clefts and spongiosis, Micro Pig, porcine.
2. Brain, cerebrum, arteries and veins: Mineralization, diffuse, moderate, with multifocal fibrinoid necrosis.

**Conference Comment:** Conference participants found the proposed etiology in this case of great interest, especially since there was no report of concurrent water deprivation. Although in the face of water deprivation, salt toxicity can occur in pigs with the intake of normal salt amounts (0.25-1%), much higher salt levels (up to 13%) can be tolerated as long as water intake is adequate.[4] It would be interesting to know if Wilber did in fact have a reduced water intake in conjunction with his potato chip binge. Additionally, some participants noted the absence of eosinophils that are often observed in swine salt toxicity; however, as the contributor states, although eosinophilic cuffs around vessels in the cerebral cortex usually develop within 48 hours, they tend to no longer be present after three to four days.[6] Conference participants found the mural mineralization and occasional fibrinoid necrosis of the vessels (not visible on all slides) interesting, but could not determine the cause.

For an acute case of salt toxicity in a pig, participants are urged to review conference 22, case 1 from the 2008-2009 WSC.

**Contributing Institution:** Dept. of Veterinary Pathobiology
College of Veterinary Medicine and Biomedical Sciences
Texas A&M University
College Station, TX 77843-4467

**References:**

1. Adejumo DO, Okunlola OO. Mineral profile and dietary mineral supplements on the concentration of high sodium crystalloid solution for treatment of hypernatremia in a Vietnamese pot-bellied pig. *JAVMA*. 1996;209:1268-70.
2. Fountaine JH, Gashe DG, Oehme FW. Experimental salt poisoning (water deprivation syndrome) in swine. *Vet Toxicol*. 1975;17:5-8.
3. Heydarpour F, Derakhshandeh J, Fekri A, Heydarpour P. Salt poisoning blindness in wistar rat, rabbit, and pig. *Toxicol & Environmental Chemistry*. 2008;90:1035-42.
4. Holbrook TC, Barton MH. Neurologic dysfunction associated with hypernatremia and dietary indiscretion in Vietnamese pot bellied pigs. *Cornell Vet*. 1994;84:67-76.
5. Summers BA, Cummings JF, de Lahunta A. *Veterinary Neuropathology*. 1995;254-5.
6. Wells GAH, Lewis G, Hawkins SAC, Don PL. Evaluation of brain chloride determinations in the diagnosis of water deprivation salt intoxication in pigs. *Vet Rec*. 1984;114:631-635.

**Joint Pathology Center**
**Veterinary Pathology Services**

## WEDNESDAY SLIDE CONFERENCE 2012-2013

# Conference 22

**17 March 2013**

---

**CASE I:** 48081 (JPC 4019425).

**Signalment:** 7-year-old, female spayed, domestic shorthair cat (*Felis catus*).

**History:** The cat had a history of acute onset of seizures with concurrent circling to right and a left menace deficit. Based on the MRI characteristics of rim enhancement and large amounts of perilesional edema, right thalamic abscess, neoplasia and granuloma were the top differential diagnoses. There was initially a good response to antibiotics and phenobarbital, and the cat was lost to follow-up for several months. The cat represented 14 months later, and demonstrated no response to repeat steroids, therefore, the owner elected euthanasia. An MRI was obtained prior to euthanasia revealing a large, right thalamic mass.

**Gross Pathology:** External examination of the brain from the dorsal and ventral aspects reveals asymmetric enlargement of the right cerebrum, involving the right

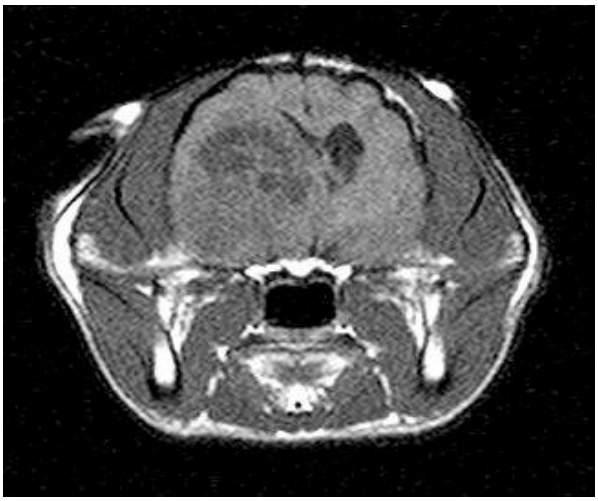

*1-1. MRI of cerebrum at level of thalamus, cat: An MRI was obtained prior to euthanasia revealing a large, right thalamic mass. (Photo courtesy of the Department of Pathology, Animal Medical Center, 510 East 62nd St. New York, NY 10065. http:// www.amcny.org/)*


*1-2. Cerebrum, cat: At necropsy, there was asymmetric enlargement of the right cerebrum. (Photo courtesy of the Department of Pathology, Animal Medical Center, 510 East 62nd St. New York, NY 10065. http:// www.amcny.org/)*


*1-3. Cerebrum at level of thalamus, cat: Upon sectioning of the fixed brain, there is a 2 cm diameter, large, firm, tan to light yellow, gelatinous, cystic mass extending from the right cerebrum to the midbrain, expanding the pyriform lobe and compressing the right lateral and third ventricles and causing a midline shift. (Photo courtesy of the Department of Pathology, Animal Medical Center, 510 East 62nd St. New York, NY 10065. http:// www.amcny.org/)*

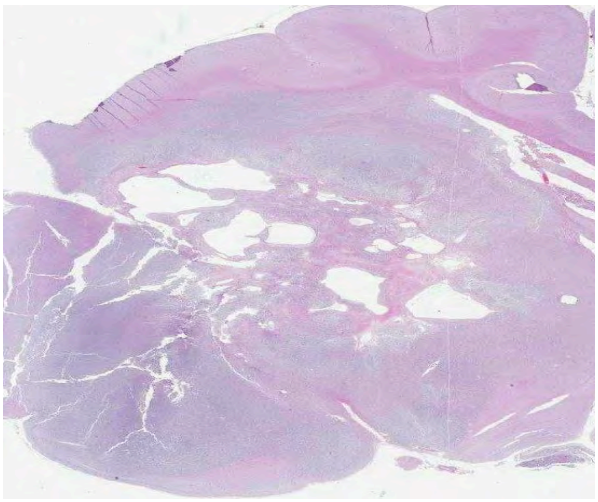

*1-4. Cerebrum at level of thalamus, cat: Subgross image of tissue corresponding to Figure #3. (Photo courtesy of the Department of Pathology, Animal Medical Center, 510 East 62nd St. New York, NY 10065. http:// www.amcny.org/) (HE 0.63X)*

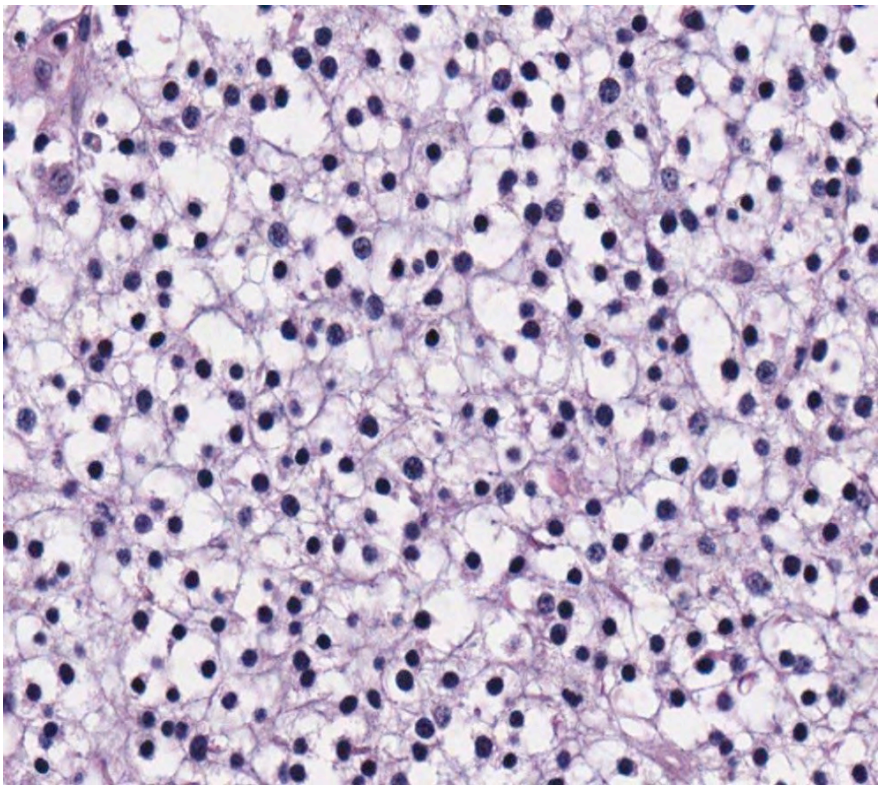

*1-5. Cerebrum at level of thalamus, cat: Neoplastic cells form a characteristic "honeycomb" or "chicken-wire" arrangement, considered the result of artifactual retraction of cytoplasm. (Photo courtesy of the Department of Pathology, Animal Medical Center, 510 East 62nd St. New York, NY 10065. http:// www.amcny.org/) (HE 400X)*

pyriform lobe. Upon sectioning of the fixed brain, there is a 2 cm diameter, large, firm, tan to light yellow, gelatinous, cystic mass extending from the right cerebrum to the midbrain. The mass compresses the right lateral and third ventricles, causing a midline shift, with marked expansion of the pyriform lobe and obliteration of basal nuclei.

**Laboratory Results:** Cytology of the mass did not reveal any inflammatory cells.

**Histopathologic Description:** A section of the brain including the cerebral cortex and thalamus is examined at the level of the body and crura of fornix, basal nuclei, third ventricle and pituitary gland (not all slides contain pituitary gland). Within the thalamus, white matter of the pyriform lobe and cerebral cortex of the temporal lobe, extending to involve the grey matter, there is a poorly demarcated, infiltrative, densely cellular neoplasm, consisting of round to polygonal cells forming sheets and cords amongst an eosinophilic fibrovascular to amphophilic myxomatous stroma. Neoplastic cells are mildly pleomorphic, with variably distinct cell borders, clear (perinuclear halo) to lightly stained vacuolated eosinophilic cytoplasm,

and round, central nuclei. Nuclei are typically hyperchromatic, with indistinct chromatin and nucleoli. Mild anisokaryosis is observed, up to two fold. There are zero mitoses in ten high power fields. In some regions of the neoplasm, cell borders are prominent ("fried egg" or "honeycomb" pattern). Multifocally, vessels are conspicuous, characterized by prominent endothelial hypertrophy and proliferation (glomeruloid vessels). Clear, cystic spaces are dispersed throughout the center of the neoplasm, and a focus of hemorrhage is present in some slides. Within these regions, the white matter parenchyma is rarefied (edema), containing swollen axons (spheroids) and glial cells, including Gitter cells and gemistocytic astrocytes. Remnant neurons from the infiltrated neuroparenchyma and reactive glial cells are scattered throughout the neoplastic populations. In the section of pituitary gland, there is mild acidophil hyperplasia. Mild endothelial hypertrophy is present in the small vessels of the adjacent and contralateral cerebral cortex.

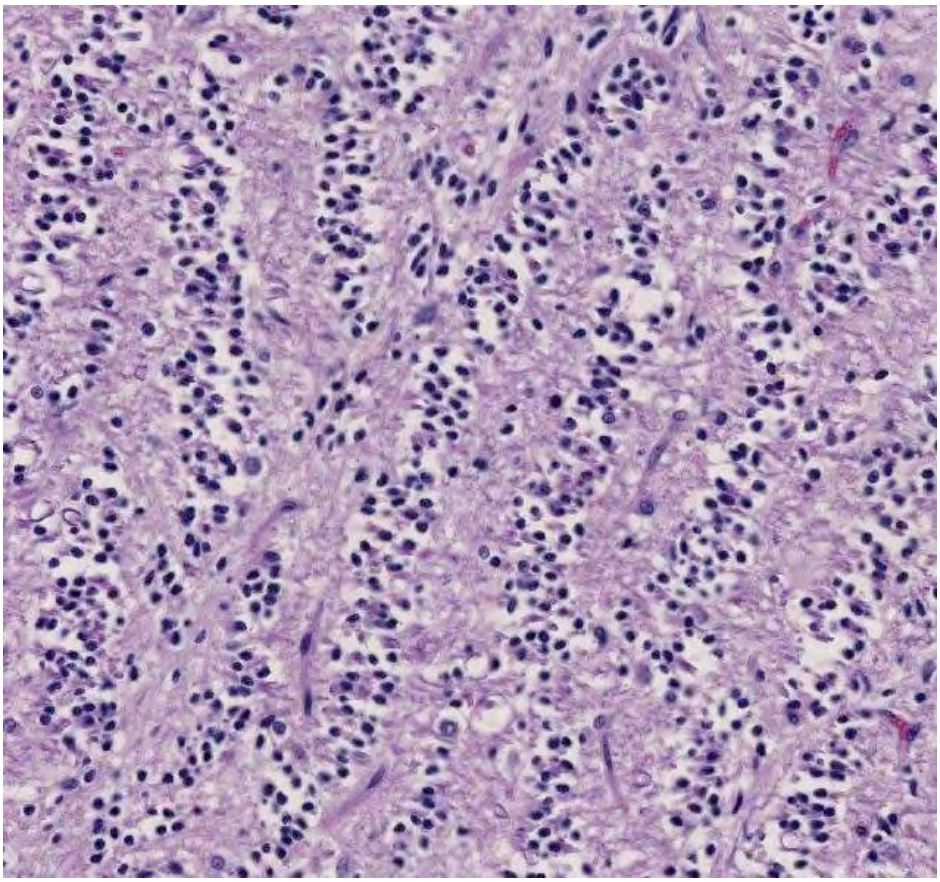

*1-6. Cerebrum at level of thalamus, cat: In some areas of the neoplasm, nuclei are arrayed in characteristic "tiger striping" formations. (HE 400X)*

**Contributor's Morphologic Diagnosis:** Brain (thalamus): Oligodendroglioma with intralesional and peripheral edema and gliosis.
Pituitary gland: Mild acidophil hyperplasia.

**Contributor's Comment:** Oligodendroglioma is a primary central nervous system neoplasm composed of oligodendrocytes, the myelin producing cells of the central nervous system (CNS). In cats, glial tumors are reported to be the fourth most common CNS neoplasm, preceded by meningioma, lymphoma and, in one study, pituitary neoplasms.[5,6] In a retrospective study of 160 cases of feline intracranial neoplasia, six oligodendrogliomas were reported, the median age for which was 9.3 years. Seizures were the most common clinical sign, along with altered consciousness, aggression, circling and ataxia in 2 cats.[6] A study analyzing tumor types and seizure patterns in 61 cats found that generalized seizures (vs partial seizures) were most common in cats with intracranial neoplasia. In that study, the highest incidence of seizures occurred with astrocytomas (33%), with a high overall incidence of seizures with all glial cell tumors (26.7%).[5] Oligodendrogliomas can occur in all areas of the white matter of the cerebrum, brainstem, and interventricular septum.[3,4,7] Feline oligodendrogliomas in the aforementioned larger case series were most commonly found in the temporal lobes, and all were located in the ventral portion of the brain, consistent with previous reports of this tumor in the deeper structures of the cerebral hemisphere.[5] In dogs, this tumor is more common in brachycephalic breeds.[3,4,6,7]

Macroscopic features of oligodendrogliomas range from soft and gelatinous to firm and they are frequently grey to pink-red, varying from well demarcated to poorly demarcated.[3,4,7] Neoplastic oligodendrocytes are typically uniform in cellular and

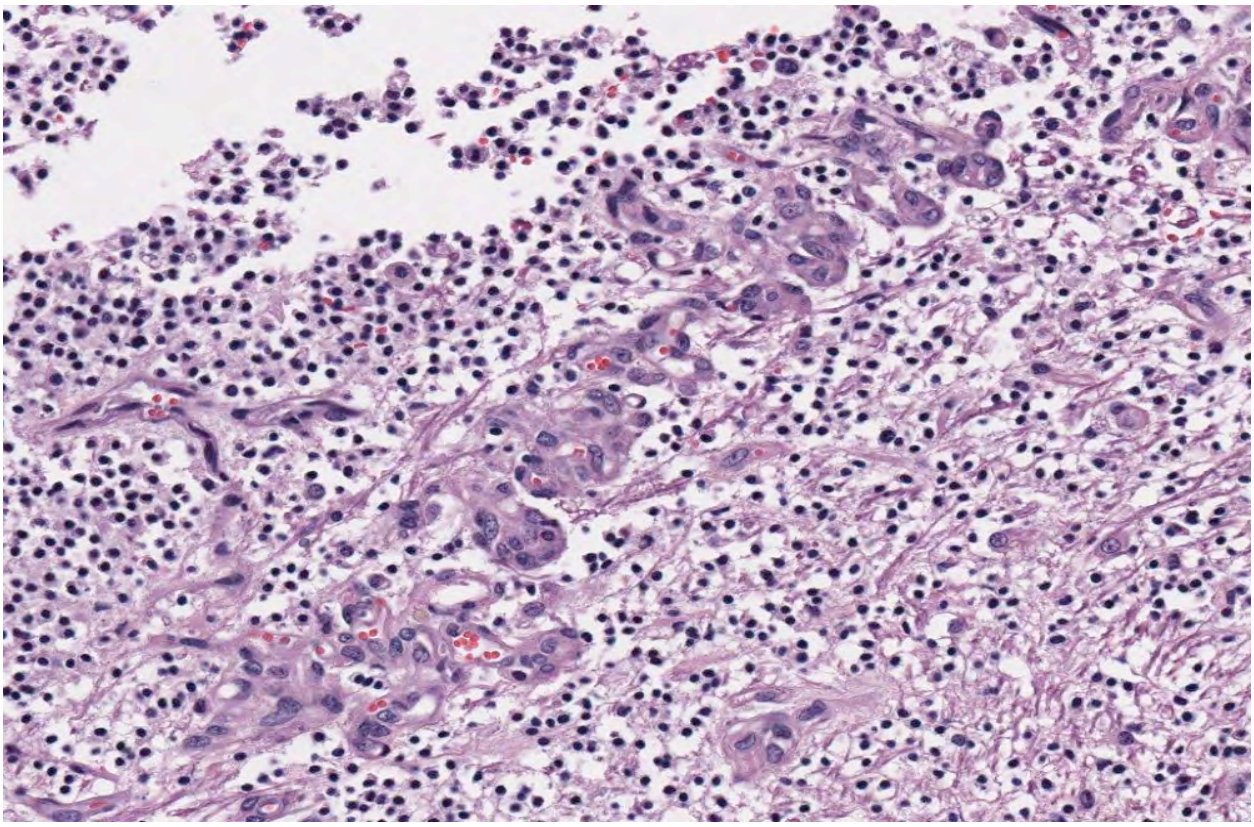

*1-7. Cerebrum at level of thalamus, cat: Multifocally, vessels are conspicuous, characterized by prominent endothelial hypertrophy and proliferation (a.k.a "glomeruloid vessels"). (Photo courtesy of the Department of Pathology, Animal Medical Center, 510 East 62nd St. New York, NY 10065. http://www.amcny.org/) (HE 400X)*

nuclear size and shape, with rare mitoses. Characteristic features of this neoplasm include the clear to lightly stained cytoplasm (perinuclear halo) and a distinct cell membrane.[3,4,7] Autolysis is thought to lend to the "fried egg" or "honeycomb" appearance of the neoplastic cells.[1,3] Mucinous cystic degeneration, edema, cavitation and rarely mineralization can occur, and necrosis is rare. Prominent branching capillary proliferation forms a "chicken wire" vascular pattern.[3,4] At the margins of the tumor, neoplastic cells may be arranged in chains (as in this case), reminiscent of interfascicular oligodendrocytes.[3,4,7] Perivascular cuffing and satellitosis of neurons with neoplastic cells may occur in infiltrated grey matter.[4] Anaplastic oligodendrogliomas are characterized by nuclear pleomorphism, high cellularity, a high mitotic index, prominent vascularization, intratumoral necrosis and rarely, calcification.[1,4,7] The initial MRI findings of rim enhancement and perilesional edema could not differentiate neoplasia from inflammatory conditions including abscess and granuloma. A report detailing clinical and pathologic features of oligodendrogliomas in two cats found heterogenous contrast enhancement and hyperintensity of proton weighted (PW) and T2 weighted images and either iso or hypointensity on T1 weighted images in both cases.[1] Post contrast ring enhancement has been reported with CT scans of canine oligodendrogliomas.[1]

Some human oligodendrogliomas express S-100 protein and the Leu-7 marker, but this expression pattern is not specific for oligodendrogliomas.[3] Immunoreactivity for GFAP may indicate the presence of early transitional glial cell forms.[3] Normal oligodendrocytes do not express GFAP, but immunoreactivity for GFAP can be demonstrated in up to 50% of human oligodendrogliomas, which may be due to reactive gemistocytic astrocytes.[1] A case series of two cats with oligodendrogliomas identified minigemistocytic astrocytes or gliofibrillary oligodendrocytes in one cat. These cells may represent a transitional form between neoplastic oligodendrocytes and astrocytes and appear identical to oligodendroglioma cells, but have a thin perinuclear rim of GFAP positive cytoplasmic staining.[1] GFAP immunohistochemistry was not performed in this case. Detection of smooth muscle actin expression in the glomeruloid vascular proliferation is a distinctive feature of anaplastic oligodendrogliomas of dogs.[1]

**JPC Diagnosis:** Brain, cerebrum at level of midbrain: Oligodendroglioma.

**Conference Comment:** The contributor's adept summary includes a brief discussion of patterns of immunohistochemical expression in oligodendrogliomas. Recently, Ide et al. explored several markers to identify characteristic immunohistochemical profiles for each of the eight types of canine neuroepithelial tumors (i.e. astrocytic tumors, oligodendroglial tumors, other gliomas, ependymal tumors, choroid plexus tumors, neuronal and mixed neuronal–glial tumors, embryonal tumors, and pineal parenchymal tumors).[2] They found that in oligodendrogliomas, the majority of cells were positive for doublecortin (DCX) but negative for glial fibrillary acidic protein (GFAP). Furthermore, benign oligodendrogliomas contained few nestin-positive cells compared to anaplastic oligodendrogliomas, which contained many nestin-positive cells. Two anaplastic oligodendrogliomas displayed positivity for Beta III tubulin. All cases of oligodendrogliomas were negative for neurofilament (NF), cytokeratin AE1/AE3, or cytokeratin 18. DCX plays a major role in neuroblast migration during cerebral cortex development. GFAP is an intermediate filament protein of mature astrocytes; nestin is an intermediate filament protein of immature astrocytes; NF is a marker for mature neurons; beta III tubulin is used to identify early neuronal differentiation; cytokeratin AE1/AE3 is used to identify many high- and low-molecular weight cytokeratins; and cytokeratin 18 is a simple epithelial cytokeratin.[2] As for expression of proliferation/ apoptosis markers in oligodendrogliomas, the following results were found: Generally, the percentage of Ki-67-positive cells were low, with the exception of two cases; p53 expression by more than 10% of tumor cells was observed in one case; there were higher numbers of Bcl-2 positive tumor cells in comparison to Bcl-xL-positive cells, and no cells showed positivity for epidermal growth factor receptor (EGFR), c-erbB2 (aka HER-2 or neu), phosphoextracellular signal-regulated kinase 1/2 pERK1/2, phospho-Akt (pAkt), or cleaved caspase 3.[2]

**Contributing Institution:** Animal Medical Center
510 East 62nd St.
New York, NY 10065
www.amcny.org/

**References:**

1. Dickinson PJ, Keel MK, Higgins RJ, Koblik PD, Lecouteur RA, Naydan DK, et al. Clinical and pathologic features of oligodendrogliomas in two cats. *Vet Pathol*. 2000;37:160-167.
2. Ide, Uchida K, Kikuta F, Suzuki K, Nakayama H. Immunohistochemical Characterization of Canine Neuroepithelial Tumors. *Vet Pathol*. 2010;47(4) 741-750.
3. Koestner A, Bilzer T, Fatzer R, Schulman FY, Summers BA, Van Winkle TJ. Oligodendroglioma. In: *Histological Classification of Tumors of the Nervous System of Domestic Animals*. 2nd series. Vol. V. Washington, DC: Armed Forces Institute of Pathology; 1999:19-20.
4. Summers BA, Cummings JF, DeLahunta A. Oligodendroglial tumors. In: *Veterinary Neuropathology*. St. Louis, MO: Mosby-Year Book Inc; 1995:370-373.
5. Tomek A, Cizinauskas S, Doherr M, Gandini G, Jaggy A. Intracranial neoplasia in 61 cats: localisation, tumour types and seizure patterns. *J Feline Med Surg*. 2006;8(4):243-53.
6. Troxel MT, Vite CH, Van Winkle TJ, Newton AL, Tiches D, Dayrell-Hart B, et al. Feline intracranial neoplasia: retrospective review of 160 cases (1985-2001). *J Vet Intern Med*. 2003;17(6):850-9.
7. Zachary JF. Nervous system. In: McGavin MD, Zachary JF, eds. *Pathologic Basis of Veterinary Disease*. 4th ed., St Louis, MO: Mosby Elsevier; 2007:951.

**CASE II**: 10-548 (JPC 3164843).

**Signalment:** 13-year-old, female, Thoroughbred horse (*Equus caballus*).

**History:** A rostral mandibular mass on the right side was noted in July 2009. Biopsy samples were non-diagnostic, showing small fragments of new bone formation with a uniform spindle cell population that may have been consistent with reactive new bone or neoplasia, though the cells were not overtly malignant. Radiographs showed an aggressive, lytic, bony lesion, and neoplasia was considered a likely differential. The horse appeared comfortable at this time. She was euthanized eight months later when the mass was perceived to be painful and she had difficulty prehending food.

**Gross Pathologic Findings:** The right rostral mandible is expanded by an 8 x 8 cm, well-demarcated, spherical mass with a smooth but slightly irregular surface. Cut surface of the mass is composed of firm, tan tissue with multifocal regions of cavitation (often with hemorrhage), bone lysis and mineralization. The right mandibular incisors are loose. There is a sharp demarcation between the mass and normal mandibular bone.

**Laboratory Results:** Cultures (aerobic and anaerobic) collected at the initial identification of the mass were negative.

**Histopathologic Description:** Mandibular mass: Surrounding scant remaining islands of pre-existing mandibular bone is an irregularly multilobulated, densely cellular neoplasm. Lobules are composed of sheets of cells and are separated by moderate fibrovascular stroma. The neoplastic cells are round to polygonal with indistinct cell borders and contain a scant to moderate amount of pale eosinophilic cytoplasm that surrounds a central nucleus. The nuclei are round to oval, and sometimes reniform with coarsely clumped chromatin and rarely have 1-3 small nucleoli. Larger nuclei sometimes have a vesicular appearance to their chromatin. Within the densely cellular lobules, cells are haphazardly arranged with occasional perivascular pseudo-rosettes and rare rosettes (Homer-Wright). There is moderate

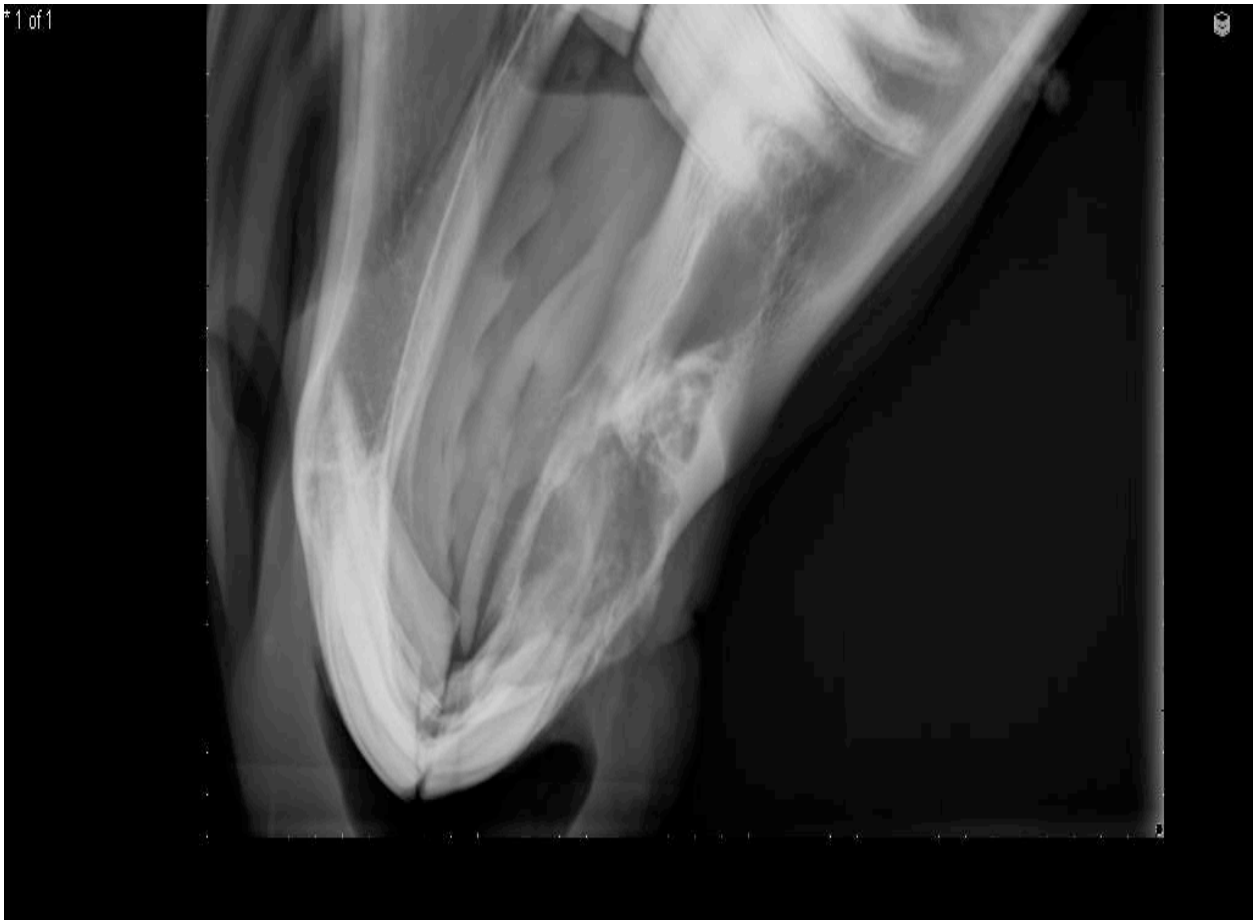


*2-1. Radiograph of mandible, horse: This radiograph of a 13-year-old TB mare, taken eight months prior to autopsy, shows a lytic lesion of the right rostral mandible. (Photo courtesy of: Department of Population Health and Pathobiology, NCSU College of Veterinary Medicine, 4700 Hillsborough St. Raleigh, NC 27606. http://www.cvm.ncsu.edu)*

*2-2. Mandible, horse: The right rostral mandible is expanded by an 8 x 8 cm, well-demarcated, spherical mass with a smooth but slightly irregular surface. (Photo courtesy of: Department of Population Health and Pathobiology, NCSU College of Veterinary Medicine, 4700 Hillsborough St. Raleigh, NC 27606. http://www.cvm.ncsu.edu)*

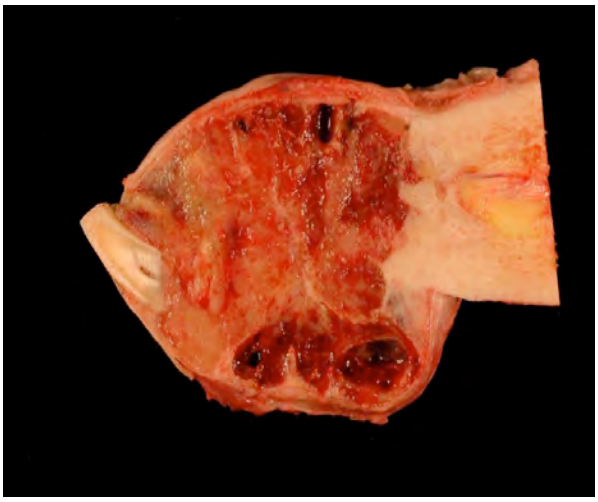

*2-3. Mandible, horse: The cut surface of the mass is composed of firm, tan tissue with multifocal regions of cavitation (often with hemorrhage), bone lysis and mineralization. (Photo courtesy of: Department of Population Health and Pathobiology, NCSU College of Veterinary Medicine, 4700 Hillsborough St. Raleigh, NC 27606. http://www.cvm.ncsu.edu)*

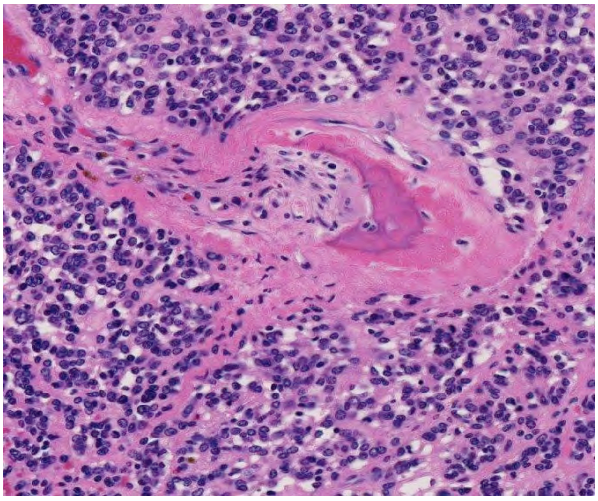

*2-4. Mandible, horse: The neoplasm, which effaces mandibular bone, is composed of poorly defined streams and bundles of primitive neuroepithelium. (HE 280X)*

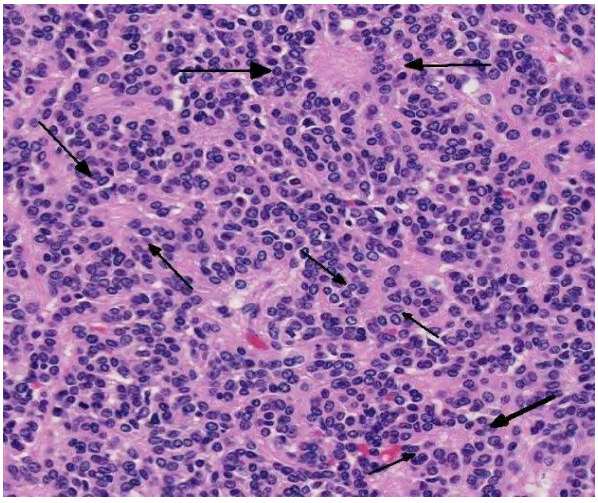

*2-5. Mandible, horse: Throughout the neoplasm, neoplastic cells form rare Homer-Wright rosettes (arrows). (HE 320X)*

anisocytosis and anisokaryosis and 6 mitotic figures per 10 high power fields are observed.

Immunohistochemically, the tumor cells show diffuse, strong staining for glial fibrillary acidic protein (GFAP), and moderate positive reactivity for vimentin and S100. About 60% of the neoplastic cells have weak to moderate cytoplasmic staining for neuron-specific enolase, and about 30% of cells have weak staining for synaptophysin.

**Contributor's Morphologic Diagnosis:** Peripheral primitive neuroectodermal tumor.

**Contributor's Comment:** Peripheral primitive neuroectodermal tumors (pPNET) are similar to the Ewing's sarcoma family of tumors (EFT). In man, there are three main types of tumors in this group including the intraosseous pPNET (Ewing's sarcoma), the extraosseous pPNET, and the thoracopulmonary Askin's tumor.[3] These tumors are rarely reported in animals, but there is a recent case reported in a camel, a few reports in dogs, and one in a Colobus monkey.[1,4,5] In people, the intraosseous tumors are most common in the long bones, but about 10% of them are reported in the skull. Of the primary tumors in the skull, approximately 10% are in the jaw bones, either the mandible or the maxilla.[3] The recently described

camel pPNET had a primary vertebral mass with hepatic metastases.[5]

The pPNETs are often highly aggressive tumors composed of primitive small round cells of putative neuroectodermal phenotype, and generally occur outside the nervous system.[3,5] They often present in nests or sheets of poorly differentiated small round cells with scant cytoplasm and may have rosette or pseudorosette formation. In people, a diagnosis of EFT is strengthened with positive reactivity for MIC2 (CD99) which is not available in veterinary species, and all EFTs in people stain with neuron-specific enolase (NSE).[1,3] Variable staining for synaptophysin and S-100 has been reported in human pPNETs.

Immunohistochemistry in the few reported veterinary cases of pPNET has been somewhat inconsistent with positive triple neurofilament staining reported in one case, and variably positive or negative staining for vimentin, NSE, synaptophysin, and glial fibrillary acidic protein (GFAP).[1,4,5] The variation in reported immunohistochemistry has been postulated to be due to the variable differentiation of the neural crest progenitor cells (neuronal, ependymal, and glial).[5] Our case of a pPNET in a horse mandible most closely resembles the immunohistochemical pattern described in the recent case report in the camel with positive vimentin, GFAP, and NSE staining.

This case is also interesting because the mass was initially noted approximately eight months prior to euthanasia with no evidence of metastases at the time of necropsy, but these tumors are typically aggressive growths that often metastasize.

**JPC Diagnosis:** Bone, mandible: Primitive neuroectodermal tumor.

**Conference Comment:** As the contributor states, peripheral primitive neuroectodermal tumors (pPNET) have rarely been reported in horses; another case was recently reported in a two-year-old paint horse gelding with multiple lobulated masses bilaterally filling the scrotal cavities, extending through the inguinal canals and along the peritoneal cavity, and infiltrating both kidneys as well as the liver, spleen, mesenteric lymph nodes, mesentery and diaphragm. Histomorphological

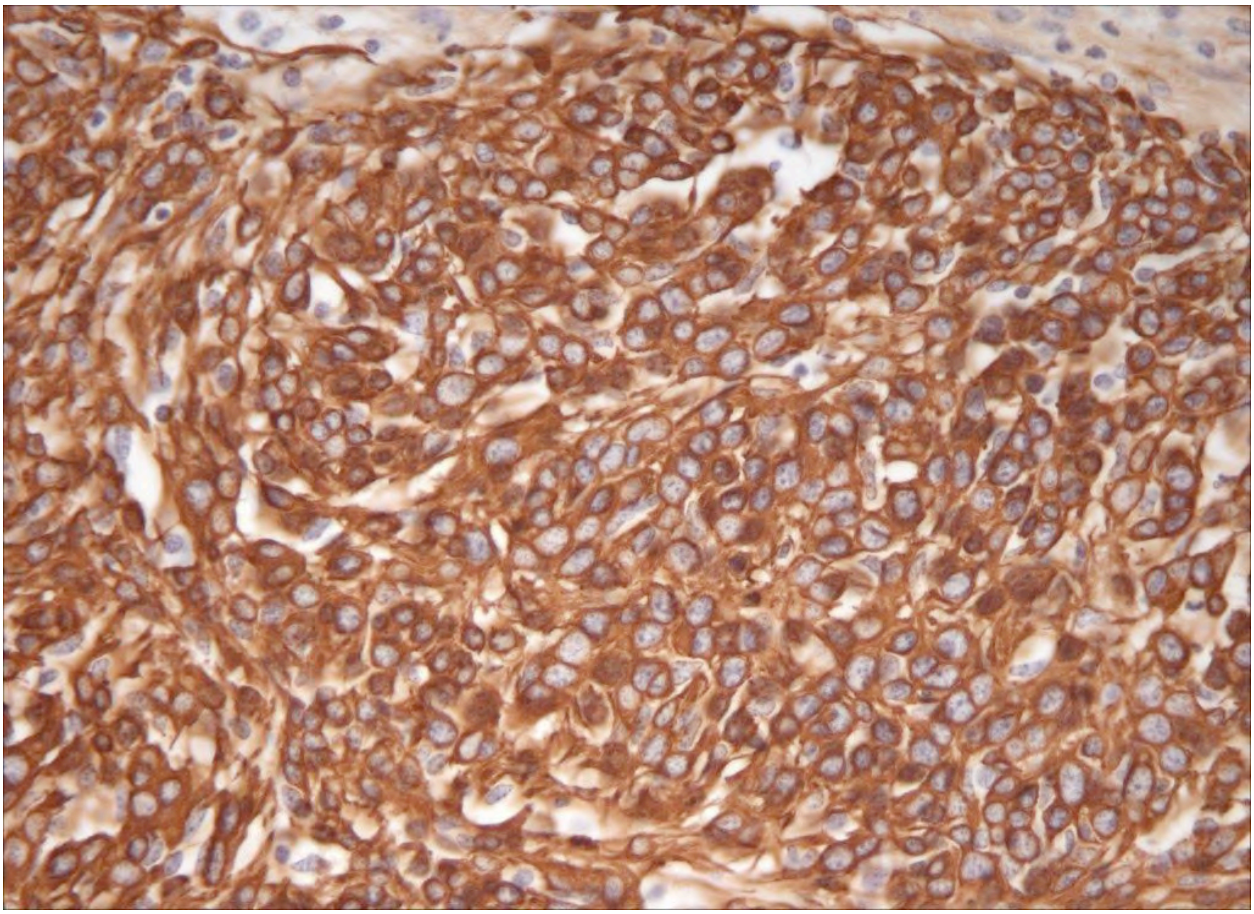

*2-6. Mandible, horse: Neoplastic cells exhibit strong cytoplasmic immunoreactivity for glial fibrillary acid protein. (Photo courtesy of: Department of Population Health and Pathobiology, NCSU College of Veterinary Medicine, 4700 Hillsborough St. Raleigh, NC 27606. http://www.cvm.ncsu.edu) (anti-GFAP, 400X)*

and immunohistochemical findings were consistent with a pPNET; the neoplastic cells were positive for synaptophysin, S-100, GFAP, NSE, and neurofilament protein (NFP), but negative for muscle-specific actin. Interestingly, in this gelding there appeared to be no bony involvement, whereas most pPNETs reported in veterinary literature, including the mandibular mass presented here, have significant bony involvement.[2]

**Contributing Institution**: North Carolina State University – College of Veterinary Medicine
Department of Population Health and Pathobiology
NCSU College of Veterinary Medicine
4700 Hillsborough St.
Raleigh, NC 27606
www.cvm.ncsu.edu

**References:**

1. De Cock HE, Busch MD, Fry MM, Mehl M, Bollen AW, Higgins RJ. A peripheral primitive neuroectodermal tumor with generalized bone metastases in a puppy. *Vet Pathol.* 2004;41:437-41.
2. Facemire PR, Facemire LM, Honnold SP. Peripheral primitive neuroectodermal tumor in a two-year-old paint horse. *Vet Diagn Invest.* 2012; 24:794.
3. Hadfield MG, Quezado MM, Williams RL, Luo VY. Ewing's family of tumors involving structures related to the central nervous system: a review. *Pediatr Dev Pathol*. 2000; 3:203-10.
4. Long PH, Schulman FY, Koestner A, Fix AS, Campbell MK, Cameron KN. Primitive neuroectodermal tumor in a two-month-old black and 5 white Colobus monkey. *Vet Pathol*. 1998; 35:64-7.
5. Weiss R, Walz PH. Peripheral primitive neuroectodermal tumour in a lumbar vertebra and the liver of a dromedary camel (Camelus dromedarius). *J Comp Pathol*. 2009; 141:182-6.

**CASE III**: V148/12 (JPC 4019895).

**Signalment:** A newborn, female lamb (*Ovis aries*) of unknown breed.

**History:** The sheep was born alive and died perinatally with a body weight of 5.3 kg. The animal originated from an area in the southeast of North Rhine-Westfalia, district of Siegen in Germany, which is approximately 50 km apart from the town of Schmallenberg.

**Gross Pathology:** Gross pathological findings consisted of torticollis, cerebellar hypoplasia, and hydranencephaly.

**Laboratory Results:** Central nervous system and blood samples were positive for Schmallenberg virus-specific genome fragments RTqPCR.

**Histopathologic Description:** Frontal cerebral cortex: The cerebrum shows a bilateral focally extensive reduction of the thickness of the dorsal cortex (0.5 to 1 mm) associated with cystic cavities (pores). Within the pores multiple fine strands of residual pre-existing nervous tissue are present. The affected cerebral cortex displays a severe, diffuse loss of the gray and white matter with widespread destruction of tissue architecture and accumulation of cellular debris (karyorrhectic, karyolytic and pyknotic cells) consistent with liquefactive necrosis. In addition, a low amount of irregular shaped, acellular, dark basophilic, coarsely granular material (mineralization) up to 30 µm in diameter is found scattered throughout the cortex. A moderate diffuse neuronal loss with neuronal degeneration characterized by hypereosinophilic, chromatolytic, shrunken and pyknotic neurons is found. Furthermore, few round to oval cells with a diameter up to 25 µm, eccentric nuclei and foamy, eosinophilic cytoplasm (Gitter cells) as well as plump astrocytes containing a homogenous, eosinophilic cytoplasm (gemistocytes) are present throughout the pores. The cerebral cortex shows a diffuse and moderate capillary proliferation with prominent vessels associated with endothelial swelling (neovascularisation). Both lateral ventricles are moderately distended (up to 0.7 mm in diameter). Predominantly the gray and white matter of the ventral parts of the cerebral cortex display a moderate to severe, multifocal perivascular cuffing (up to 20 layers) and diffuse meningeal infiltration of lymphocytes and macrophages. Diffusely slight parenchymatous infiltrates are dominated by lymphocytes. In addition, rod-shaped microglial cells/ macrophages (microgliosis) and astrocytes (astrogliosis) are present.

**Contributor's Morphologic Diagnosis:** Frontal cerebral cortex, bilateral, focally extensive liquefactive necrosis, severe, subacute to chronic, with cystic cavities, and meningoencephalitis, lympho-histiocytic, multifocal, subacute, moderate to severe.

**Contributor's Comment:** Since autumn 2011, a new emerging arthropod-borne, negative stranded ssRNA Orthobunyavirus, termed Schmallenberg virus (SBV), was detected in Europe.[11] Virus prevalence has been reported in Germany, The Netherlands, France, Belgium, Luxembourg, United Kingdom, Italy, and Spain.[7] SBV had significant economic relevance due

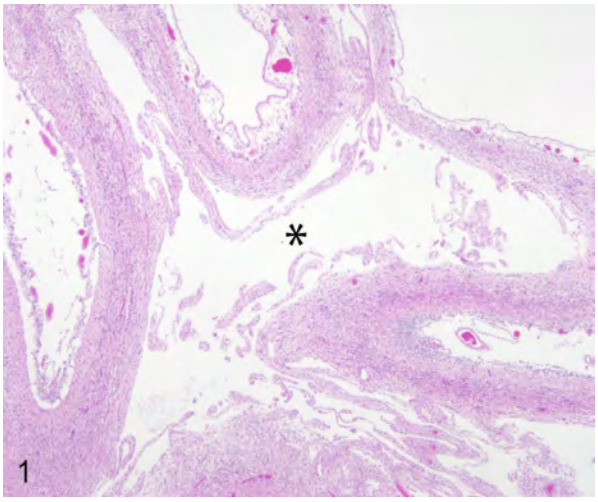


*3-1. Cerebrum, lamb: Cerebral cortex of a naturally SBV-infected sheep shows widespread necrosis of the cerebral cortex with pore formation (asterisk). A thin cerebral cortex and tissue remnants of the cortex are visible as fine strands. (Photo courtesy of: Department of Pathology, University of Veterinary Medicine Hannover, Buenteweg 17, D-30559 Hannover, Germany. http://www.tiho-hannover.de/kliniken-institute/institute/institut-fuer-pathologie/) (HE)*

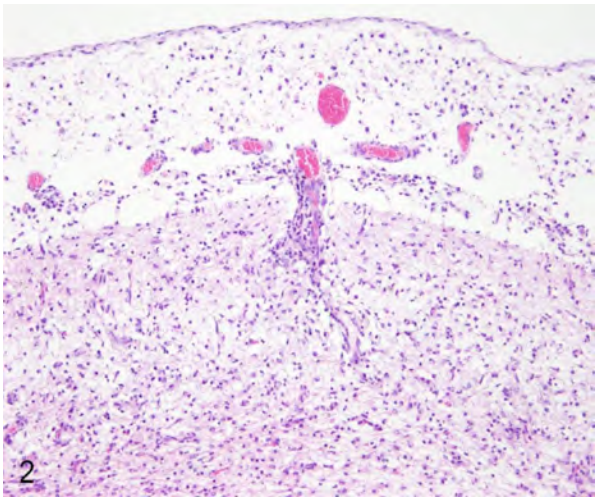


*3-2. Cerebral cortex of a naturally SBV-infected sheep shows lymphohistiocytic meningoencephalitis, astro- and microgliosis and neuronal loss. (Photo courtesy of: Department of Pathology, University of Veterinary Medicine Hannover, Buenteweg 17, D-30559 Hannover, Germany. http://www.tiho-hannover.de/kliniken-institute/institute/institut-fuer-pathologie/) (HE)*

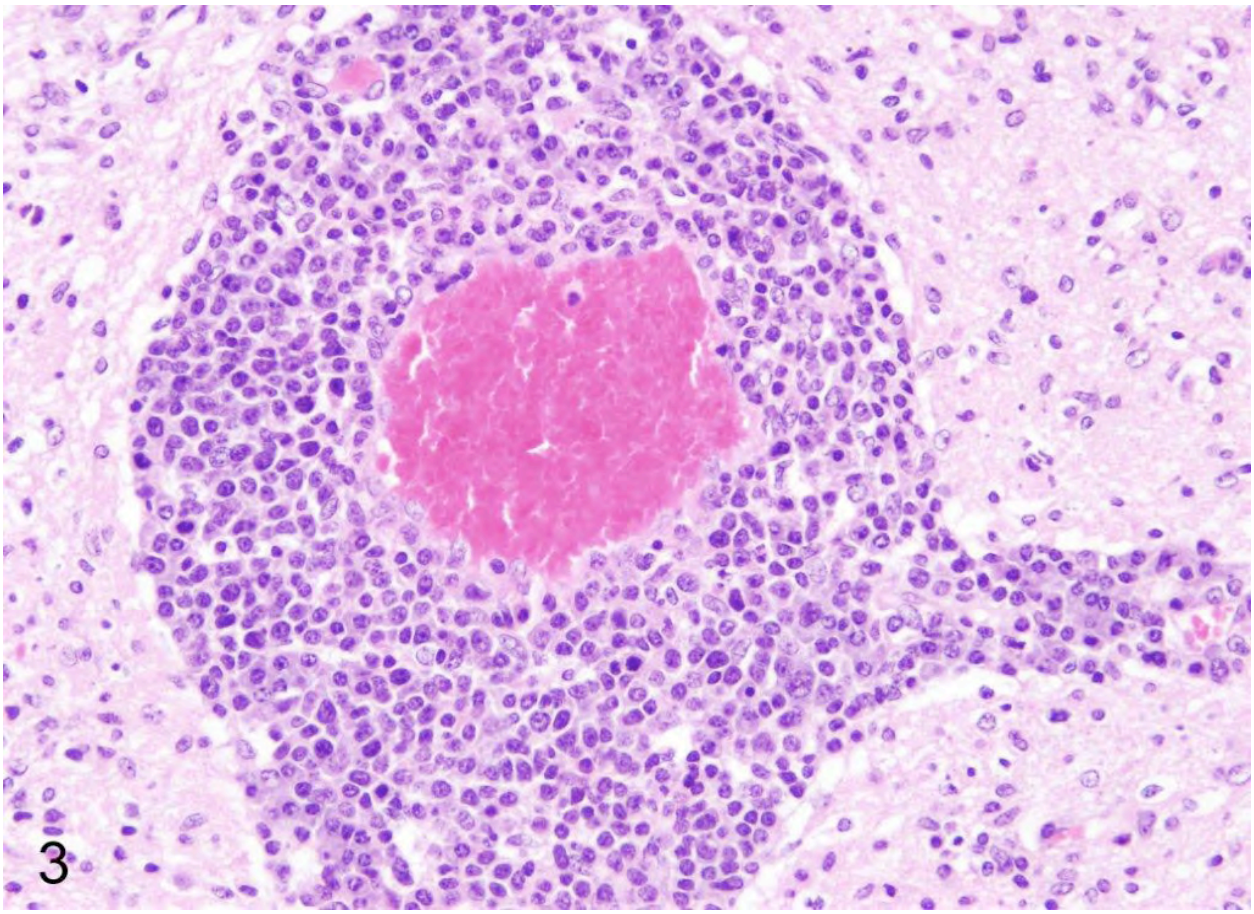


*3-3. Virchow-Robin spaces contain multifocally up to 20 layers of lymphocytes and macrophages in the cerebral cortex of an SBV-infected sheep. (Photo courtesy of: Department of Pathology, University of Veterinary Medicine Hannover, Buenteweg 17, D-30559 Hannover, Germany. http://www.tiho-hannover.de/kliniken-institute/institute/institut-fuer-pathologie/) (HE)*

to reduced milk yield, fever, and diarrhea in pregnant dairy cows and particularly due to abortions, and malformations of newborn ruminants.[11] Clinical signs in adult ruminants were usually limited up to a period of three weeks and affected animals recovered subsequently completely.[8] The virus was named after the town Schmallenberg in western Germany, because the first identification of the virus succeeded in samples of cattle housed next to this town. Similar to other Orthobunyaviruses, like Akabane virus, SBV causes malformations in newborn ruminants due to a prenatal infection. Macroscopically, malformations comprise arthrogryposis, vertebral malformations, brachygnathia inferior as well as various central nervous system (CNS) malformations like hydranencephaly, porencephaly, internal hydrocephalus, cerebellar hypoplasia and micromyelia in lambs, goat kids and calves.[10] Until now, it is not known how exactly SBV arrived in Germany, but parallels were made to the epidemiology of Blue tongue virus, which emerged first in Europe in 2006 and is also transmitted via arthropods.[17] Possible routes of SBV entry to Europe are insects and/or animals in aircrafts or import of cut flowers from Africa.[17]

Based on metagenomic analysis,[11] SBV belongs to a group of teratogenic viruses causing arthrogryposis and hydranencephaly (AG/HE). These malformations in cattle caused by Akabane virus represent an entity called "*enzootic bovine arthrogryposis and hydranencephaly*".[20]

Until now the pathogenesis of SBV infection is not fully understood. Due to a genetic relationship to other viruses of the genus *Orthobunyavirus*, a similar pathogenesis is suggested.[12] Furthermore, the SBV-induced pathology cannot be differentiated from infections with Akabane virus[12] which requires an identification at the molecular level with PCR.[11] Appropriate samples for the detection of viral nucleotides by means of this technique are external placental fluid, umbilical cord, cerebrum, and spinal cord.[2] Placental fluid and umbilical cord samples can be taken easily without necropsy. The central nervous system is accessible in animals submitted for necropsy without placental fluid and only umbilical cord

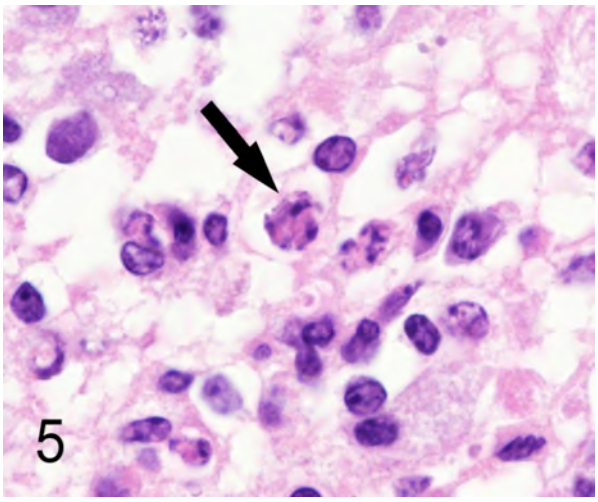


*3-4. Thin cortical areas of a SBV-infected sheep contain necrotic neurons with karyorrhexis and karyolysis (arrow). (Photo courtesy of: Department of Pathology, University of Veterinary Medicine Hannover, Buenteweg 17, D-30559 Hannover, Germany. http://www.tiho-hannover.de/kliniken-institute/institute/institut-fuer-pathologie/) (HE)*

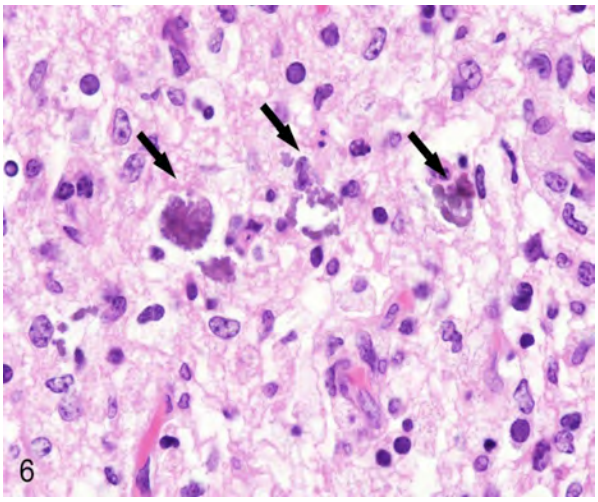


*3-5. Cortical liquefactive necrosis of a SBV-infected sheep displays multifocal deposition of basophilic, coarse granular, extracellular material (arrows). (Photo courtesy of: Department of Pathology, University of Veterinary Medicine Hannover, Buenteweg 17, D-30559 Hannover, Germany. http://www.tiho-hannover.de/kliniken-institute/institute/institut-fuer-pathologie/) (HE)*

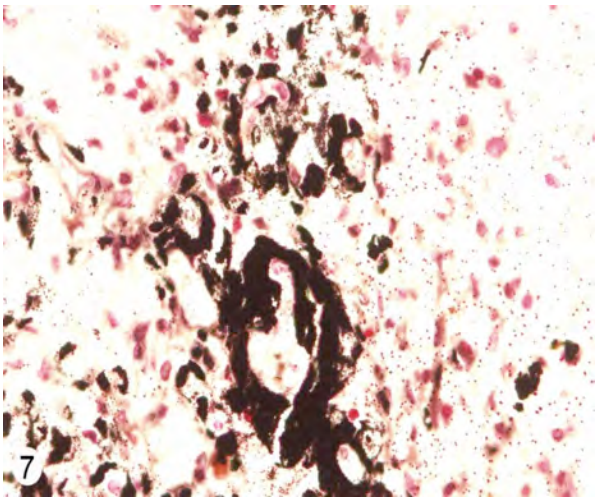


*3-6. Remaining cortical tissue of a SBV-infected sheep displays multifocally moderate to severe mineralizations, which stained black with von Kossa's stain. (Photo courtesy of: Department of Pathology, University of Veterinary Medicine Hannover, Buenteweg 17, D-30559 Hannover, Germany. http://www.tiho-hannover.de/kliniken-institute/institute/institut-fuer-pathologie/) (Von Kossa)*

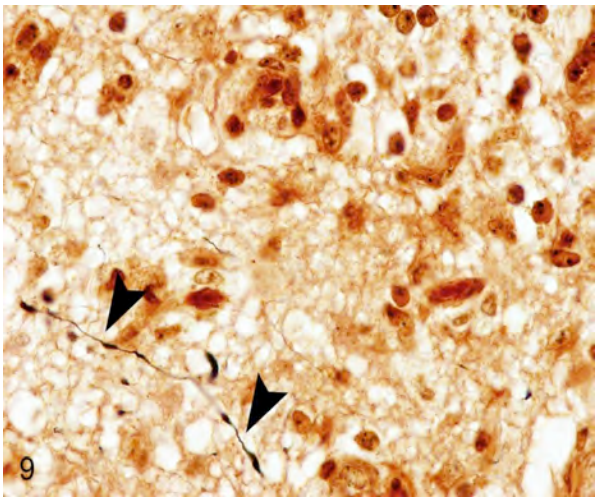


*3-7. The cerebral cortex of an SBV-infected sheep displays reduced axonal density in areas with necrosis, inflammation and mineralization. Only few remaining silver impregnated axons are visible (arrowheads). (Photo courtesy of: Department of Pathology, University of Veterinary Medicine Hannover, Buenteweg 17, D-30559 Hannover, Germany. http://www.tiho-hannover.de/kliniken-institute/institute/institut-fuer-pathologie/) (Bielchowsky silver impregation)*

remnants.[2] Spleen, cartilage, placental fluid from the stomach, and meconium rarely revealed a positive PCR result in SBV-infected animals and therefore these samples should be avoided for virus detection.[2] In addition, placenta and placental fluid of SBV-infected animals contain huge amounts of virus.[2] So far the host range of SBV seems to be restricted to ruminants and there is no evidence of a zoonotic risk.[6]

A recent study compared genomic RNA of SBV with Sathuperi and Shamonda viruses indicating that all viruses belong the genus *Orthobunyavirus* and that SBV originates from a re-assortment of Sathuperi and Shamonda virus.[26]

In general, climate change is suggested to be the most important factor for the occurrence of arthropod-borne virus-infections in Europe.[9] SBV is supposed to be transmitted by arthropods, but the high numbers of initial SBV infections in Europe suggest additional routes of transmission, e.g. direct contact, fecal-oral route or aerosols.[1]

**Table 1: Overview on virus infections, their pathology in offspring after natural transmission, susceptible species and the transmission mode representing possible etiological differentials of Schmallenberg virus infection.**

| Virus | Disease name | Gross findings | Histology | Species | Transmission |
|---|---|---|---|---|---|
| **Schmallenberg virus**[4,10,11] Orthobunyavirus, Bunyaviridae | | Arthrogryposis, vertebral malformations, brachygnathia inferior, hydran- and porencephaly, internal hydrocephalus, cerebellar hypoplasia, micromyelia | Lymphohistiocytic meningoencephalomyelitis, CNS malacia, gliosis, muscular hypoplasia | Ruminants: sheep, goats, cattle, bisons | Arbovirus: mosquitos and midges: e. g. *Culex obsoletus*, *Culex dewulfi* |
| **Akabane virus**[3,13,15,16,18,22] Orthobunyavirus, Bunyaviridae | Enzootic bovine arthrogryposis and hydranencephaly; congenital arthrogryposis-hydranencephaly syndrome (CAHS) | Arthrogryposis, vertebral malformations, hydranencephaly, CNS cyst formation | Non-suppurative encephalomyelitis, neuronal loss in the spinal cord, muscular dysplasia | Herbivores: cattle, horses, donkeys, sheep, goats, camels, buffaloes, pigs | Arbovirus: mosquitos and midges, eg. *Culex sp., Aedes sp., Culicoides imicola* |
| **Bovine virus diarrhea virus**[20] Pestivirus, Flaviviridae | | Cerebellar hypoplasia, mummification, runting, microencephaly, hydranencephaly, hydrocephalus, microphthalmia, cataract, brachygnathism, thymic aplasia, hypotrichosis, alopecia, pulmonary hypoplasia | perivascular non-suppurative meningeal infiltration, CNS malacia, hypomyelinogenesis, retinal degeneration, optic neuritis, myocarditis, | Cattle, sheep, goat, pig, | Excretions, inhalation, ingestion, semen, contaminated embryo transfer fluid |
| **Blue tongue virus**[19,20] Orbivirus, Reoviridae | | Porencephaly, hydranencephaly, hydrocephalus, subcortical cysts, cerebellar dysgenesis, runting | Necrotizing meningoencephalitis, interstitial pneumonia, mononuclear cells in kidney and liver | Sheep, wild ruminants, camelids, cattle, zoo carnivores[14] | Arbovirus: *Culicoides sp.* |
| **Border disease virus**[20] Pestivirus, Flaviviridae | Border disease Condition: "hairy shaker" | Embryonic death, mummification, fleece abnomalities, runting, cerebellar hypo- and dysplasia, micro-, por- and hydranencephaly, leukoencephalomalacia, micro-myelia, starvation, cardiac abnormalities, rarely: arthrogryposis, kyphoscoliosis | Dys- and hypomyelination | Sheep, goats, pigs, cattle | Oral, conjuctival, intranasal, genital, semen |
| **Cache valley virus, syn. Bunyamwera virus**[5,20] Orthobunyavirus, Bunyaviridae | | Arthrogryposis, hydrocephalus, hydranencaphaly, microcephaly, vertebral malformations, cerebellar hypoplasia, micromelia, porencephaly | Necrosis and loss of neuropil and motor neurons, myositis, poorly developed myocytes | Sheep, deer, caribou, pigs, horses, cattle, raccoons, foxes, man | Arbovirus: *Culicoides sp., Culiseta sp., Anopheles sp.* |
| **Chuzan virus**, **syn. Palyamvirus**[20] Orbivirus, Reoviridae | | Hydranencephaly, cerebellar hypoplasia, hydrocephalus, microcephaly | | Cattle | Arbovirus: *Culicoides oxystoma* |
| **Classical swine fever virus**[20] Pestivirus, Flaviviridae | Hog cholera | Mummification, runting, stillbirth, pulmonary hypoplasia, pulmonary artery malformation, micrognathia, arthrogryposis, cerebellar hypoplasia, microcephaly, defective myelination | Necrotizing vasculitis in CNS, intestine, skin, lymphoid depletion, endothelial degeneration, valvular fibrosis, portal fibrosis (liver), interstitial pneumonia, neuronal degeneration | Pigs, cattle, sheep, goats | Excretions, ingestion |
| **Rift valley fever virus**[20,23] Phlebovirus, Bunyaviridae | | Intra-uterine fetal death | Hepatic necrosis, acidophilic intranuclear inclusions, cholestasis, degeneration of lympho-cytes, heart muscle and renal tubules | Sheep, cattle, goats, man | Arbovirus: *Aedes sp., Culex sp.* |
| **Wesselsbron virus**[20] Flavivirus, Flaviviridae | | Mummification, hydranencephaly, arthrogryposis, hydrops amnii, porencephaly, cerebellar hypoplasia | Non-suppurative meningoencephalomyelitis, eosinophilic, intranuclear inclusions, liver: degeneration, necrosis, Kupffer cell hyperplasia, hepatitis, hyper- and inflammation of bile ducts | Sheep, cattle, man | Arbovirus |
| **Aino virus, syn. Shuni virus**[3,21,25] Orthobunyavirus, Bunyaviridae | Arthrogryposis-hydranencephaly syndrome (CAHS) | Hydranencephaly, arthrogryposis, cerebellar hypoplasia | Necrotizing encephalopathy, perivascular cuffing with lymphoid cells, neuronal mineralization | Cattle, sheep | Arbovirus: *Culicoides brevitarsis, Culex tritaeniorhynchus* |

Interestingly, in the present case the lambs' CNS showed liquefactive necrosis with porencephaly and additional non-suppurative inflammation. Studies with the closely related Akabane virus showed that the virus crosses the placenta after viremia and replicates in fetal cells of the central nervous system. The virus prefers rapidly dividing cells and causes damage to neurons.[24] Depending on the time point of infection, CNS pathology varies. According to Akabane virus infection, it is suggested that transplacental SBV infection at early stages of gestation causes severe brain lesions, like hydranencephaly due to a widespread loss of neuronal tissue. The severity of brain damage is less extensive, if the infection occurs to a later time point of gestation. Infection during the 2nd trimester may result in a more focal necrosis of the CNS characterized by porencephaly. This porencephaly can be associated with a meningoencephalitis.[20] Assuming that Akabane virus and SBV have a similar pathogenesis, an infection during the 2nd trimester is suggested in the present case. Our study revealed that only 20% (12 out of 58 animals) of all RTqPCR positive tested CNS samples of ruminants (lambs, goat kids and calves) showed meningoencephalitis with or without CNS malformations.[10] Infiltration of lymphocytes and macrophages showed a perivascular pattern. Furthermore, gitter cell formation and neuronal necrosis were present. For further characterization of the lesions several special stains were applied including von Kossa´s stain, Luxol fast-blue stain, and Bielschowsky´s silver impregnation. Intralesional amorphous basophilic material stained positive with a von Kossa stain indicating intralesional mineralization, which was found multifocally in the thin cortical areas of the pore. Demyelination was shown as reduced staining intensity in the cortex containing pores. Bielschowsky´s silver impregnation was used to investigate the extent of axonal alterations. The amount of positive axons was reduced.

The included table lists possible etiological differentials of SBV infection. The described histopathological lesions are not characteristic for a particular virus. The etiology has to be proven with other methods, e.g. molecular techniques, like PCR. Further epidemiological information as well as the geographical area (e.g. Asia, Europe, USA) of occurrence have to be considered. The table summarizes information of naturally infected animals; results of experimentally infected animals were not included.

**JPC Diagnosis:** Brain, cerebrum: Necrosis, liquefactive, bilateral, focally extensive, with marked gliosis, mineralization, spheroid formation, lymphohistiocytic meningoencephalitis and hydrocephalus ex vacuo.

**Conference Comment:** The contributor provides an excellent and thorough description of this emerging Orthobunyavirus. Conference participants commented on the presence of band-like areas of microvascular proliferation (increased vascular pattern) present in the section, and speculated that these were likely due to collapse of the parenchyma, vessel dilation, and a compensatory induction of new vessel formation secondary to the release of cytokines and factors [i.e. vascular endothelial growth factor (VEGF)] associated with the inflammatory response and hypoxic conditions within these areas of parenchymal collapse.

**Contributing Institution**: Department of Pathology
University of Veterinary Medicine Hannover
Buenteweg 17
D-30559 Hannover
Germany
http://www.tiho-hannover.de/kliniken-institute/institute/institut-fuer-pathologie/

**References:**

1. Scenarios for the future spread of Schmallenberg virus. *Veterinary Record.* 2012;170:245-246.
2. Bilk S, Schulze C, Fischer M, Beer M, Hlinak A, Hoffmann B. Organ distribution of Schmallenberg virus RNA in malformed newborns. *Veterinary Microbiology*. 2012:159:236-8.
3. Brenner J, Tsuda T, Yadin H, Chai D, Stram Y, Kato T. Serological and clinical evidence of a teratogenic Simbu serogroup virus infection of cattle in Israel, 2001-2003. *Vet Ital.* 2004;40:119-123.
4. Conraths F, Beer M, Peters M. "Schmallenberg-Virus": Eine neue Infektionskrankheit bei Wiederkäuern. *Tierärztliche Umschau*. 2012;5:147-150.
5. Edwards JF, Livingston CW, Chung SI, Collisson EC. Ovine arthrogryposis and central nervous system malformations associated with in utero Cache Valley virus infection: spontaneous disease. *Veterinary Pathology.* 1989;26:33-39.
6. Eurosurveillance editorial team: European Food Safety Authority publishes its second report on the Schmallenberg virus. *Euro Surveillance.* 2012;17: pii=20140.
7. Garigliany MM, Hoffmann B, Dive M, Sartelet A, Bayrou C, Cassart D, et al. Schmallenberg virus in calf born at term with porencephaly, belgium. *Emerging Infectious Diseases.* 2012;18:1005-1006.
8. Gibbens N. Schmallenberg virus: a novel viral disease in northern Europe. *Vet Rec.* 2012;170:58.
9. Gould EA, Higgs S, Buckley A, Gritsun TS. Potential arbovirus emergence and implications for the United Kingdom. *Emerging Infectious Diseases.* 2006;12:549-555.
10. Herder V, Wohlsein P, Peters M, Hansmann F, Baumgärtner W. Salient lesions in domestic ruminants infected with the emerging so-called Schmallenberg

Virus in Germany. *Veterinary Pathology*. 2012;49(4): 588-91.
11. Hoffmann B, Scheuch M, Höper D, Jungblut R, Holsteg M, Schirrmeier H, et al. Novel orthobunyavirus in cattle, Europe, 2011. *Emerging Infectious Diseases*. 2012;18:469-472.
12. Höper D, Wernike K, Eschbaumer M, Conraths F, Hoffmann B, Schirrmeier H, et al. "Schmallenberg-Virus" - Ein neues Virus in Europa. *Deutsches Tierärzteblatt*. 2012;4:500-505.
13. Huang CC, Huang TS, Deng MC, Jong MH, Lin SY. Natural infections of pigs with akabane virus. *Veterinary Microbiology*. 2003;94:1-11.
14. Jauniaux TP, De Clercq KE, Cassart DE, Kennedy S, Vandenbussche FE, Vandemeulebroucke EL, et al. Bluetongue in Eurasian lynx. *Emerging Infectious Diseases*. 2008;14:1496-1498.
15. Konno S, Moriwaki M, Nakagawa M. Akabane disease in cattle: congenital abnormalities caused by viral infection. Spontaneous disease. *Veterinary Pathology*. 1982;19:246-266.
16. Kono R, Hirata M, Kaji M, Goto Y, Ikeda S, Yanase T, et al. Bovine epizootic encephalomyelitis caused by Akabane virus in southern Japan. *BMC Vet Res*. 2008;4:20.
17. Kupferschmidt K. Infectious disease. Scientists rush to find clues on new animal virus. *Science*. 2012;335:1028-1029.
18. Lee JK, Park JS, Choi JH, Park BK, Lee BC, Hwang WS, et al. Encephalomyelitis associated with akabane virus infection in adult cows. *Veterinary Pathology*. 2002;39:269-273.
19. Maclachlan NJ, Drew CP, Darpel KE, Worwa G. The pathology and pathogenesis of bluetongue. *Journal of Comparative Pathology*. 2009;141:1-16.
20. Maxie M, Youssef S. Jubb, Kennedy, and Palmer's Pathology of Domestic Animals. 5th ed. Vol. 1-3. Philadelphia, PA: Saunders Elsevier; 2007.
21. Noda Y, Uchinuno Y, Shirakawa H, Nagasue S, Nagano N, Ohe R, et al. Aino virus antigen in brain lesions of a naturally aborted bovine fetus. *Veterinary Pathology*. 1998;35:409-411.
22. Parsonson IM, McPhee DA, Della-Porta AJ, McClure S, McCullagh P. Transmission of Akabane virus from the ewe to the early fetus (32 to 53 days). *Journal of Comparative Pathology*. 1988;99:215-227.
23. Rippy MK, Topper MJ, Mebus CA, Morrill JC. Rift Valley fever virus-induced encephalomyelitis and hepatitis in calves. *Veterinary Pathology*. 1992;29:495-502.
24. St. George T, Kirkland P. Diseases caused by Akabane and related Simbu-group viruses. In: Coetzer J, Tustin R, eds. Infectious Diseases of Livestock. 2nd edition. eds. 2nd ed. Oxford, UK: Oxford University Press; 2004:1029-1036.
25. Uchinuno Y, Noda Y, Ishibashi K, Nagasue S, Shirakawa H, Nagano M, et al. Isolation of Aino virus from an aborted bovine fetus. *Journal of Veterinary Medical Science*. 1998;60:1139-1140.
26. Yanase T, Kato T, Aizawa M, Shuto Y, Shirafuji H, Yamakawa MT. Genetic reassortment between Sathuperi and Shamonda viruses of the genus Orthobunyavirus in nature: implications for their genetic relationship to Schmallenberg virus. *Archives of Virology*, 2012;157(8):1611-6.

**CASE IV:** E884/12 (JPC 4019397).

**Signalment:** 9-year-old, spayed female, Basset hound, dog, (*Canis lupus familiaris)*.

**History:** The dog had generalized seizures, intermittent tremor, high amplitude myoclonia and altered behavior since a few weeks. The seizures were controlled with antiepileptic drugs over a period of 4 weeks prior to euthanasia.

**Gross Pathology:** Only the formalin fixed brain of the animal was obtained and no gross lesions were noted.

**Histopathologic Description:** Brain, cerebral cortex: Multifocally and haphazardly distributed within the white and gray matter, nerve cell bodies, axons, dendrites and occasional the neuropil contain large, up to 20 µm in diameter, round, basophilic to amphophilic inclusions. Nerve cell bodies are enlarged up to 40 µm in diameter by the inclusions and most nuclei are compressed or displaced to the periphery. Inclusions have a homogeneous core with a more faintly staining radiating periphery and are PAS-positive, also accentuating their structure. Multifocally neurons contain fine granular golden-brown pigment in their cytosol (lipofuscin). Additionally, there is mild, multifocal satellitosis and mild diffuse increase in microglia.

**Contributor's Morphologic Diagnosis:** Brain, cerebral cortex: Polyglucosan (Lafora) bodies, diffuse, numerous with mild multifocal satellitosis and microgliosis.

**Contributor's Comment:** Lafora disease (LD) is a rare autosomal recessive disorder that was first described in humans in 1911 by a Spanish neurologist named Gonzalo Rodríguez Lafora. Clinically, this neurologic disorder is characterized by early onset during adolescence of symptoms including stimulus-sensitive grand mal tonic-clonic, absence, visual and myoclonic seizures. The disease then rapidly progresses to dementia, psychosis, cerebellar ataxia, dysarthria, amaurosis, mutism, muscle wasting and respiratory failure leading to death within 10 years after onset.[2,12,17] It is most commonly seen in populations and parts of the world where there is a high rate of consanguinity.[4]

Histopathologically, LD is characterized by the presence of pathognomonic inclusions named Lafora bodies (LB) especially in the brain, spinal cord and other tissues such as skin, liver, cardiac and skeletal muscle.[2] In the central nervous system LB are localized mostly in the perikarya. These inclusions can become very large, leading to cell death.[1]

LB are carbohydrate storage products that are composed of polyglucosans, which are abnormally formed glycogen molecules that resemble starch. This polyglucosans are poorly branched which makes them insoluble leading to the formation of the characteristic intracellular inclusions.[14]

In most cases this disorder is caused by mutations in one of two different genes, EPM2A and EPM2B (also known as NHLRC1) which encode the proteins laforin and malin, respectively.[3,11] Laforin is a glycogen phosphatase which plays an important role in glycogen metabolism and is involved in dephosphorylation of complex carbohydrates such as amylopectin and glycogen and thus preventing the soluble glycogen molecules from becoming insoluble polyglucosans.[9] Malin on the other hand is an E3 ubiquitin ligase that is believed to target laforin catalyzing its polyubiquitination and thus its degradation. However, the specific role of malin in this process is yet to be determined.[9]

In the dog LD has been reported in the Basset Hound, Miniature Wirehaired Dachshund, Poodle and Beagle also.[8,18] In these animals progressive myoclonus is associated with the presence of intraneuronal storage of complex polyglucosans forming the so-called LB.[8]

LB in the dog appear as spherical basophilic to amphophilic, mostly intracytoplasmatic inclusions with peripheral radiating filaments; their size may vary from 5 to 20 µm and can be localized in the dendrites, axons or perikarya (unlike in humans).[2] LB may be found anywhere along the neuroaxis and retinal ganglion cells but in dogs with neuronal disease they are most common in the Purkinje cells and neurons of the caudate, thalamic and periventricular nuclei.[18] LB are PAS positive, diastase resistant, stain positively with Best's carmine, methenamine silver, and Weil's.[7] In electron microscopy, they are not membrane bound and are composed of fibrillary and electron-dense, sometimes granular components in varying proportions. They are often associated with rough endoplasmic reticulum and Golgi. LB present as accumulations of insoluble complex glycoprotein polymers that need to be distinguished from other types of polyglucosan bodies such as Lafora-like bodies, corpora amylacea, and amylopectin bodies.[14] The distinction between LB and other inclusions is performed based on clinical features and tissue distribution of the inclusions.[15]

Corpora amylacea are inclusions that are formed in normal aging cells and are chemically and histochemically indistinguishable from LB. Corpora amylacea can be found in axons and astrocytic processes but not in the perikarya, unlike LB.[15]

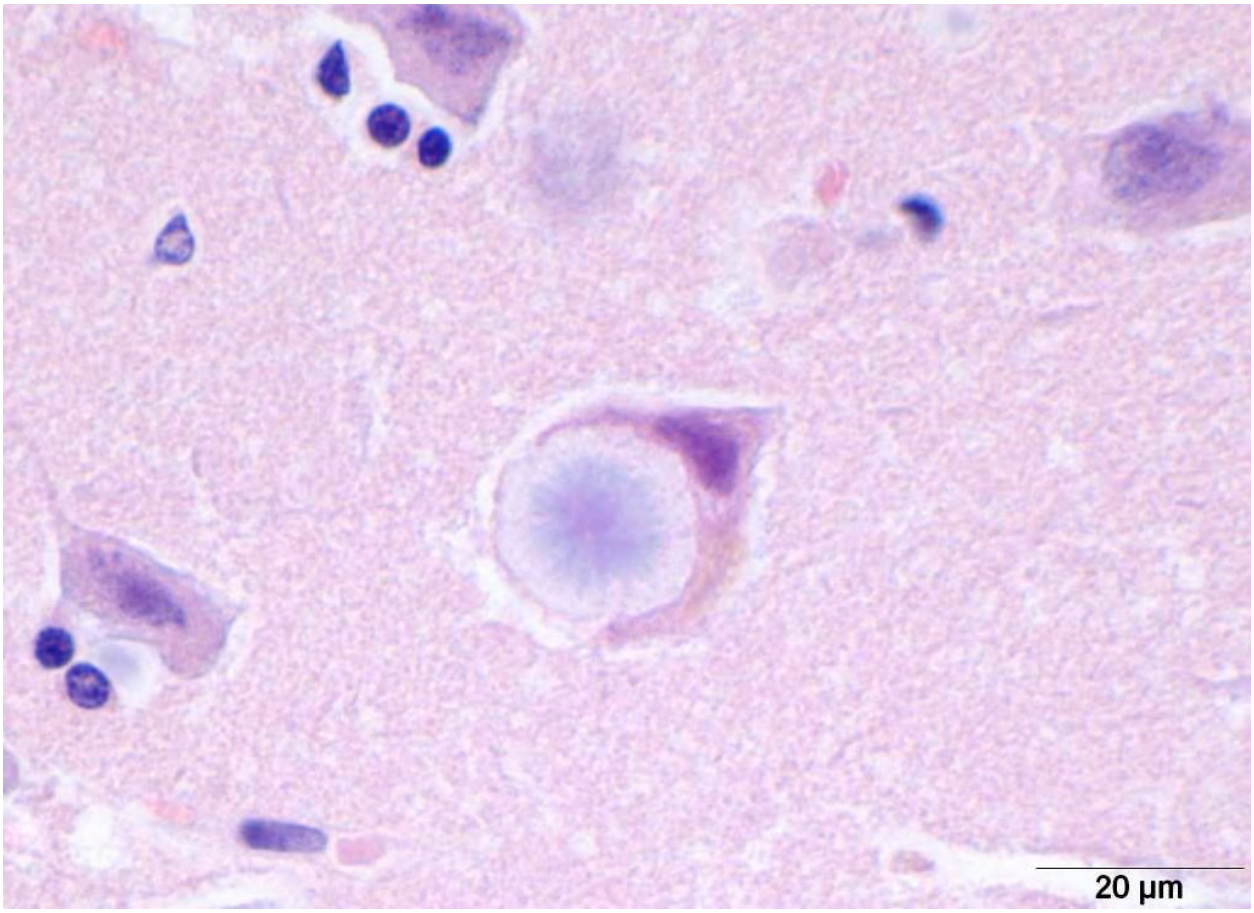


*4-1. Cerebral cortex, dog: Within the white and gray matter, nerve cell bodies, axons, and dendrites contain large, basophilic to amphophilic inclusions ranging up to 20 µm in diameter. (Photo courtesy of: Institute of Veterinary Pathology, Freie Universitat Berlin, Robert-von-Ostertag-Straße 15, Building 12 14163 Berlin, Germany, http://www.vetmed.fu-berlin.de/en/einrichtungen/institute/we12) (HE)*

Amylopectin bodies are formed in patients with glycogen storage disease type IV or glycogen branching enzyme deficiency.[19,20] They result from accumulation of abnormal polysaccharides and are mostly indistinguishable from LB in terms of morphology and distribution and thus the clinical presentation of the disease should be used in their distinction.[19,20]

Lafora-like bodies are also very similar in their morphology and distribution but are observed in normal aged animals without neurologic symptoms.[19]

In cases of LD, typically LB are also found in skeletal muscle samples where they lie between myofibrils or beneath the sarcolemma and therefore muscle biopsies can be used for the diagnosis of the disease.[15] In the case presented here, a biopsy of the cranial tibial muscle was submitted for histopathological analysis and accumulations of PAS positive, diastase resistant, brightly staining material forming focal intraparenchymal subsarcolemmal accumulations consistent with LB were found in the skeletal muscle fibers.

The canine counterpart of LD seems to be associated with a mutation in the *EPM2B* gene, more precisely a dodecamer expansion in the gene.[10] This mutation was observed in 5% of Miniature Wirehaired Dachshunds in England.[10]

The presence of LB associated with neurologic disease has also been documented in cats and cows.[5,16] A recent report described a Lafora´s-like disease in a fennec fox (*Vulpes zerda*)[7] and another report demonstrated LB in the brain of an aged captive raccoon (*Procyon lotor*).[6]

**JPC Diagnosis**: Brain, cerebrum, frontal lobes: Polyglucosan bodies, intraneuronal, numerous.

**Conference Comment:** As the contributor states in this informative summary of Lafora's disease, the genetic mutation in dogs involves the *EPM2B* gene. Recently a DNA test for the autosomal recessive mutation that identifies "clear," "carrier," and "affected" dogs has been developed and is currently available in the United Kingdom.[13]

**Contributing Institution:** Department of Veterinary Pathology
Freie Universität Berlin, Germany
http://www.vetmed.fu-berlin.de/en/einrichtungen/institute/we12/index.html

**References:**

1. Andrade DM, Ackerley CA, Minett TS, et al. Skin biopsy in Lafora disease: genotype-phenotype correlations and diagnostic pitfalls. *Neurology.* 2003;61:1611-1614.
2. Andrade DM, Turnbull J, Minassian BA. Lafora disease, seizures and sugars. *Acta* Myol. 2007;26:83-86.
3. Chan EM, Young EJ, Ianzano L, et al. Mutations in NHLRC1 cause progressive myoclonus epilepsy. *Nat Genet.* 2003;35:125-127.
4. Delgado-Escueta AV, Ganesh S, Yamakawa K. Advances in the genetics of progressive myoclonus epilepsy. *Am J Med Genet.* 2001;106:129-138.
5. Hall DG, Steffens WL, Lassiter L. Lafora bodies associated with neurologic signs in a cat. *Veterinary Pathology.* 1998;35:218-220.
6. Hamir AN. Spontaneous lesions in aged captive raccoons (Procyon lotor). *J Am Assoc Lab Anim Sci.* 2011;50:322-325.
7. Honnold SP, Schulman FY, Bauman K, et al. Lafora's-Like Disease in a Fennec Fox (Vulpes Zerda). *J Zoo Wildlife Med.* 2010;41:530-534.
8. Jubb KVF, Kennedy PC, Palmer NC. *Pathology of Domestic Animals*. 5th ed. Philadelphia, PA: Saunders Elsevier; 2007;898.
9. Knecht E, Aguado C, Sarkar S, et al. Impaired autophagy in Lafora disease. *Autophagy*. 2010;6:991-993.
10. Lohi H, Young EJ, Fitzmaurice SN, et al. Expanded repeat in canine epilepsy. *Science.* 2005;307:81-81.
11. Minassian BA, Ianzano L, Delgado-Escueta AV, et al. Identification of new and common mutations in the EPM2A gene in Lafora disease. *Neurology.* 2000;54:488-490.
12. Minassian BA. Lafora's disease: towards a clinical, pathologic, and molecular synthesis. *Pediatr Neurol.* 2001;25:21-29.
13. Sainsbury R. DNA scrrening for Lafora's disease in miniature wire-haired dachshunds. *Vet Rec*. 2011;169:292.
14. Sakai M, Austin J, Witmer F, et al. Studies in myoclonus epilepsy (Lafora body form). II. Polyglucosans in the systemic deposits of myoclonus epilepsy and in corpora amylacea. *Neurology.* 1970;20:160-176.
15. Schoeman T, Williams J, van Wilpe E. Polyglucosan storage disease in a dog resembling Lafora's disease. *J Vet Intern Med.* 2002;16:201-207.
16. Simmons MM. Lafora Disease in the Cow. *Journal of Comparative Pathology* 1994;110:389-401.
17. Singh S, Ganesh S. Lafora progressive myoclonus epilepsy: a meta-analysis of reported mutations in the first decade following the discovery of the EPM2A and NHLRC1 genes. *Hum Mutat.* 2009;30:715-723.
18. Summers BA, Cummings JF, de Lahunta A. *Veterinary Neuropathology*. 1st ed. St. Louis, MO: Mosby: 1995:527.
19. Suzuki Y, Akiyama K, Suu S. Lafora-like inclusion bodies in the CNS of aged dogs. *Acta Neuropathol*. 1978;44:217-222.
20. Suzuki Y, Ohta K, Kamiya S, et al. Topographic distribution pattern of Lafora-like bodies in the spinal cord of some animals. *Acta Neuropathol*. 1980;49:159-161.

**Joint Pathology Center**
**Veterinary Pathology Services**

# WEDNESDAY SLIDE CONFERENCE 2012-2013

## Conference 23

**1 May 2013**

---

**CASE I:** V13-1511 (JPC 4028574 ).

**Signalment:** 11-year-old, male castrated Shih Tzu, canine *(Canis familiaris)*.

**History:** Presented with glaucoma OS. Increased IOP OS, significantly deceased tear production OU and moderate to severe pigmentary keratitis OU. Unable to view intraocular structures OU.

**Gross Pathology:** Entire globe, anterior lens luxation with fusion of lens to cornea and loss of lens structure.

**Histopathologic Description:** None provided.

**Contributor's Morphologic Diagnosis:** Eye: End stage globe with: corneal vascularization and pigmentation; lens luxation, rupture and fusion to cornea; anterior chamber collapse; synechia of iris to caudal lens; chronic retinal atrophy and detachment and optic nerve cupping.

**Contributor's Comment:** Lens displacement refers to a change in position of the lens from its normal anatomical location and can be partial (subluxation) or

*1-1. Eye, dog: The globe is mildly enlarged with anterior displacement of the lens and detachment of the retina. (HE 0.63X)*

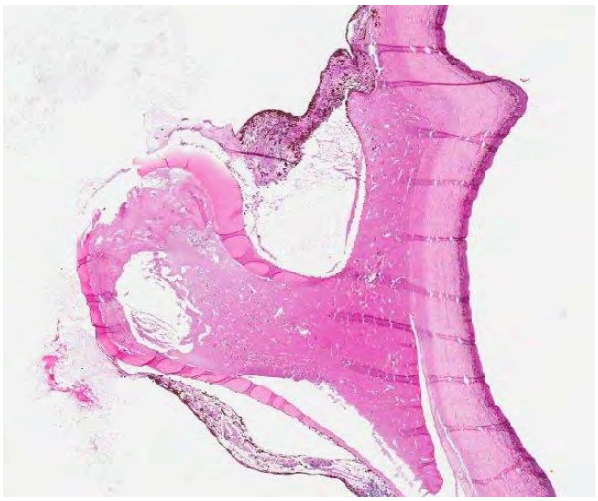

*1-2. Eye, dog: The lens is flattened in an anterior-posterior direction, and present completely within the anterior chamber, where it is attached to the posterior aspect of the cornea (anterior synechia). (HE 15X)*

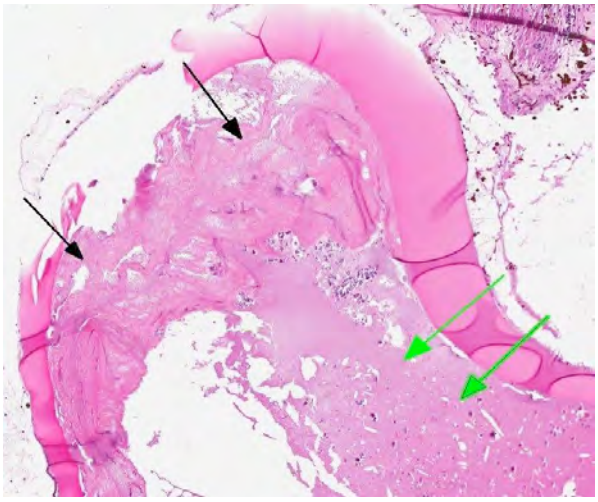

*1-3. Eye, dog: Internal changes within the lens include liquefaction and mineralization of lens fibers (green arrows), and fibrous metaplasia of lens fibers at the posterior aspect. (HE 60X)*

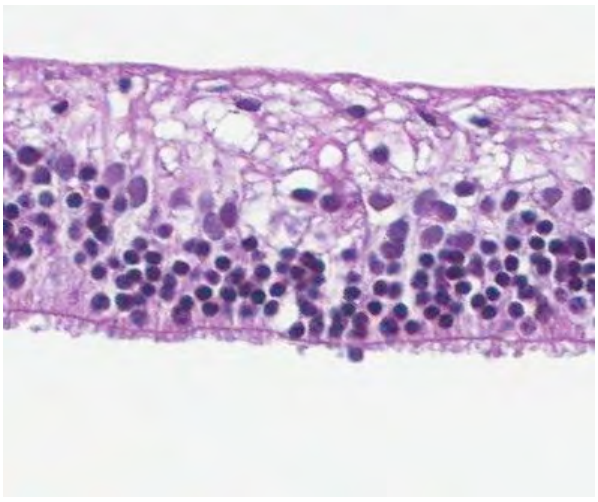

*1-4. Eye, dog: There is diffuse marked atrophy of the detached retina, with loss of the ganglion cell layer, inner nuclear and plexiform layers (consistent with glaucoma), and photoreceptor layer. (HE 85X)*

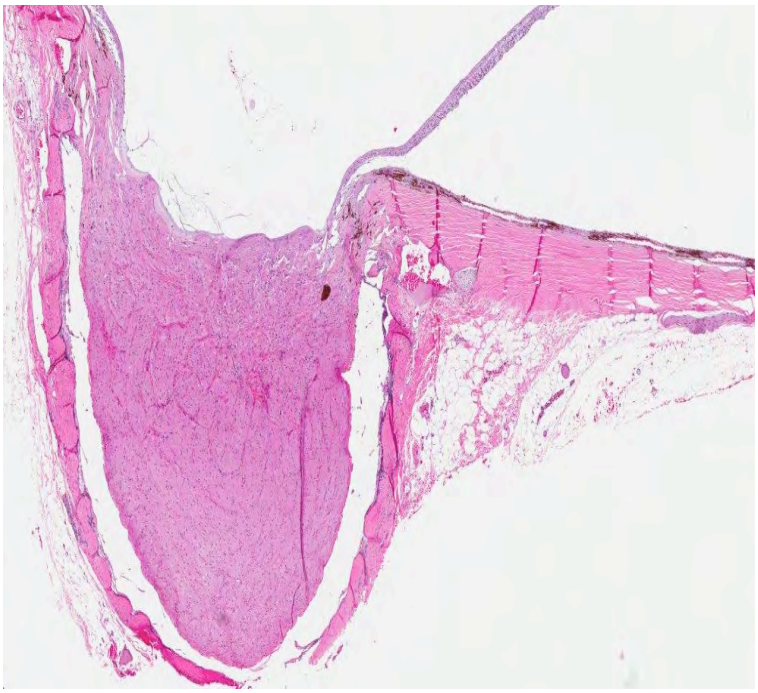

*1-5. Eye, dog: There is cupping of the optic nerve, also consistent with chronic increased intraocular pressure. (HE 25X)*

complete (luxation). This condition affects several species and is a well-documented clinical disease in dogs. Primary lens displacement (PLD) occurs spontaneously, and it is likely due to an inherited defect in the lens zonules. This defect leads to spontaneous rupture of the lens zonules inducing initial lens instability that may eventually result in luxation of the lens. Secondary lens displacement occurs when the zonules are disrupted by a prior or concomitant disease such as glaucoma, cataracts, uveitis, or trauma. In these cases, the zonules are not defective, but rather damaged by the underlying disease, and they break down causing lens instability.[1] A recent study found ADAMTS17 mutation associated with primary lens luxation is widespread among breeds.[3,7]

If the zonular disinsertion is partial and the lens still rests in the patella fossa of the anterior vitreous, it is described as a posterior subluxation. If the zonular disinsertion is total, with migration of the lens posteriorly onto the floor of the vitreous, or anteriorly through the pupil, into the anterior chamber, the lens is described as luxated. Pathogenesis of sequelae involve the distortion of the visual optics, physical irritation by the displaced lens to retina, anterior uvea, and/or cornea, and pupillary block by the lens itself of the adherent vitreous with resultant secondary glaucoma. Luxated lenses become cataractous if they are not already, likely due to altered nutrition.

Primary luxation occurs in the terrier breeds; dogs are usually middle-aged and the condition is always bilateral although not necessarily concurrently so. The affected eye may present with iridodonesis, an aphakic crescent, and irritation manifested by redness, blepharospasm, and tearing if the lens is subluxated; IOP may be variable. Anterior luxation is characterized by visualization of the lens equator and obscuration of the pupil; IOP will usually be elevated and if it is not, it soon will be. Posterior luxations are diagnosed by observing a deep anterior chamber with a concavity to the iris surface, and the lens on the floor of the posterior segment; IOP

is usually not elevated. Examine fellow eyes closely; iridodonesis may be present and dilation may reveal an aphakic crescent. Dilation may turn an innocuous posterior subluxation into an emergent anterior luxation. In cats, the majority of luxations occur secondary to chronic uveitis; secondary glaucoma is uncommon compared to the dog, related to the deep feline anterior chamber and the liquefaction of the vitreous that accompanies chronic inflammation.

Primary lens displacement has been documented to be heritable in many terrier breeds as well as Tibetan Terriers, Border Collies, and Shar-Peis. PLD is invariably a bilateral condition, albeit usually not simultaneous. When a patient presents with one eye affected, the fellow eye may vary in presentation from no apparent instability to early signs of instability such as iridodensis, phacodonesis, and vitreal herniation, to clear evidence of subluxation or complete luxation. The reported time to displacement in the fellow eye varies from days to years. Lens displacement often leads to vision- threatening complications, of which glaucoma is the most common and can occur regardless of lens position (anterior, posterior, or subluxated). Other reported complications include retinal detachment and uveitis.[4]

**JPC Diagnosis:** Eye: Anterior lens luxation, with corneal adhesions, anterior and posterior synechiae, drainage angle occlusion, retinal detachment and atrophy, and optic nerve degeneration and excavation.

**Conference Comment:** There is significant slide variation in this case, with not all slides exhibiting all the described changes.

Conference participants discussed the difficulty in determining primary versus secondary lens luxation from histology alone, concluding that similar lesions can be seen in both. As the contributor notes, primary luxation of the lens is due to rupture of the lens zonules, which function to keep the lens in its normal position between the ciliary processes. The zonular fibers are made of microfibrils (primarily the glycoproteins fibrillin-1 and fibrillin-2). Genetic abnormalities in genes coding for fibrillin-1 have been shown to cause lens displacement in humans and possibly in cattle.[6] A truncating gene mutation in *ADAMTS17* on CFA03 has been found to be associated with the development of primary lens displacement in 17 dog breeds; however, its mode of inheritance and penetrance have yet to be fully elucidated.[2] Primary lens displacement in dogs appears to be affected by both dose and age (i.e. heterozygotes are affected later in life than homozygotes, and penetrance increases with age), which is consistent with an additive allelic model.[2] *ADAMTS17* is a member of the secreted metalloproteinase family of proteins which bind extracellular matrix; it is believed to play a role in the formation of crystalline lens zonules and connective tissue. Mutations in *ADAMTS17* cause abnormalities similar to Weill-Marchesani syndrome (WMS) in humans. WMS, which is associated with mutations in a related gene (*ADAMTS10*), as well as *FBN1*, is a rare connective tissue disorder in which patients develop eye and skeletal abnormalities.[5]

**Contributing Institution**: Tri Service Research Lab
4141 Petroleum Road
Fort Sam Houston, TX 78234

**References** :

1. Alario AF, Pizzirani S, Pirie CG. Histopathologic evaluation of the anterior segment of eyes enucleated due to glaucoma secondary to primary lens displacement in 13 canine globes. *Vet Ophthalmol.* 2012;(4):doi 10.1111.
2. Gharahkhani P, O'Leary C, Duffy D, Bernays M, Kyaw-Tanner M. Primary lens luxation in Australian Tenterfield and Miniature Bull Terriers is due to an old *ADAMTS17* mutation and is an additive trait. *The Open Genomics Journal.* 2012;5:7-13.
3. Gould D, Pettitt L, McLaughlin B, Holmes N, Forman O, Thomas A, Ahonen S, Lohi H, O'Leary C, Sargan D, Mellersh C. ADAMTS17 mutation associated with primary lens luxation is widespread among breeds. *Veterinary Ophthalmology*. 2011;14, 6, 378–384.
4. Gelatt K, MacKay E. Secondary glaucomas in the dog in North America. *Veterinary Ophthalmology.* 2004;7:245–259.
5. Morales J, Al-Sharif L, Khalil DS, Shinwari JMA, Bavi P, Al-Mahrouqi RA, et al. Homozygous mutations in ADAMTS10 and ADAMTS17 cause lenticular myopia, ectopia lentis, glaucoma, spherophakia, and short stature. *Am J Hum Genet*. 2009;85(5):558–568.
6. Morris RA, Dubielzig RR. Light-microscopy evaluation of zonular fiber morphology in dogs with glaucoma: secondary to lens displacement. *Vet Ophthalmol.* 2005;8(2)81-44.
7. Sargan DR, Withers D, Pettiite I, Squire M, Gould DJ, Mellersh CS. Mapping the mutation causing lens luxation in several terrier breeds. *Journal of Heredity*. 2007:98(5):534–538.

**CASE II**: JPC012 (JPC 4020974).

**Signalment:** One month old, intact male Dorper lamb (*Ovis aries*).

**History:** This lamb was smaller than normal at birth and showed poor weight gain while nursing. The owner noticed that it became weak with labored breathing and increased lung sounds. Antibiotic treatment (oxytetracycline) was initiated, but the animal was found dead five days later.

**Gross Pathology:** Approximately 70-80% of the lungs contained moderately well-demarcated, often confluent, firm, white-tan nodular areas, with only a small portion of the dorsal-caudal regions unaffected. On section, many bronchi were filled with a white-tan material. No thymic tissue was identified. No other abnormalities were noted.

**Laboratory Results:** *Nocardia* sp. was isolated from the cut surface of affected lung.

**Histopathologic Description:** Lung: Filling or effacing up to 75% of alveoli and bronchioles are multifocal to coalescing, variably sized and shaped pyogranulomas characterized by central areas of necrotic cellular debris, high numbers of degenerate and necrotic neutrophils and macrophages, and mineralization surrounded by variable mixtures of neutrophils, large macrophages, fewer lymphocytes and multinucleated giant cells. Adjacent, less affected airways and alveoli are often compressed and contain congestion and hemorrhage, fewer numbers of inflammatory cells and multifocal areas of edema and/or basophilic-staining material (mucus). On H&E stained sections, faintly-staining, fine filamentous organisms can be seen sporadically at the margins of the necrotic areas.

Special stains revealed numerous, approximately 1 micron thick, beaded to filamentous and occasionally branching, gram-positive (Brown & Brenn) and variably acid-fast (Fite-Faraco) bacteria within areas of inflammation.

**Contributor's Morphologic Diagnosis:** Lung: Pyogranulomas, multifocal and coalescing, marked, with necrosis, mineralization and numerous branching, filamentous gram-positive and acid-fast bacteria, lamb (*Ovis aries*).

**Contributor's Comment:** *Nocardia* spp. are ubiquitous, saprophytic, aerobic bacteria that are commonly associated with opportunistic infections in animals and people characterized by pyogranulomatous inflammation. The organisms are observed as long, thin, beaded filaments with frequent right-angle branching that are said to have a "Chinese character" pattern. They can be easily overlooked on standard H&E stained sections and are better demonstrated with special stains including Gomori methenamine silver (GMS), Gram stains and modified acid-fast stains such as Fite-Faraco.[9]

The primary differential diagnosis for pulmonary nocardiosis includes infections with *Actinomyces* and some atypical mycobacteria.[9] Actinomycosis is more commonly associated with sulfur granules and Splendore-Hoeppli material, and the organisms are not acid fast.[10] Atypical mycobacteria are much shorter beaded bacilli and do not exhibit true branching.

*Nocardia* are commonly found in the environment, particularly soil enriched with decayed organic matter.

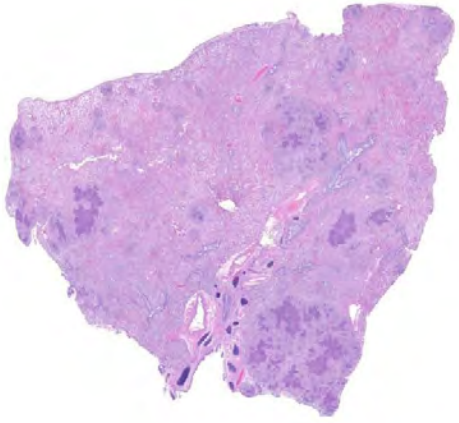

*2-1. Lung, sheep: Randomly scattered throughout the lung, there are numerous foci of inflammation which compress the adjacent hypercellular pulmonary parenchyma. (HE 0.63X)*

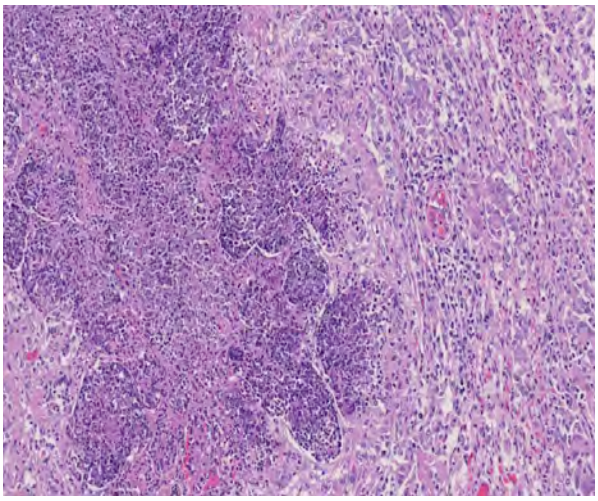

*2-2. Lung, sheep: Within inflammatory foci, alveoli are filled with large numbers of degenerate neutrophils and cellular debris; there is central septal necrosis. (HE 168X)*

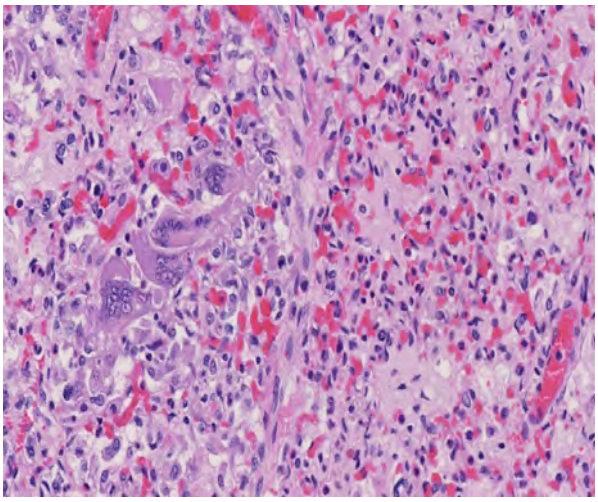

*2-3. Lung, sheep: Occasional multinucleated giant cell macrophages are scattered throughout the parenchyma adjacent to inflammatory foci. (HE 180X)*

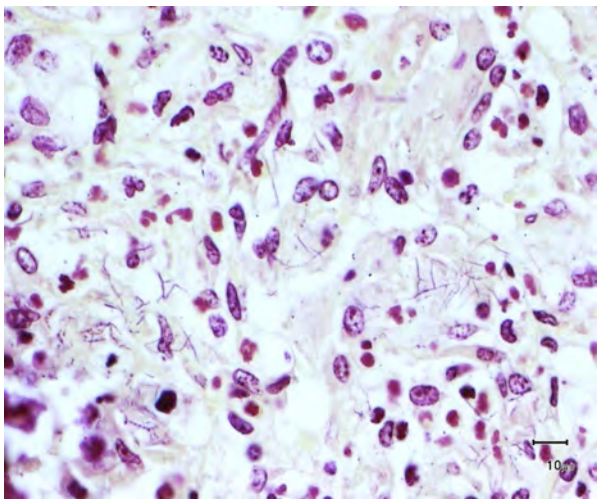

*2-4. Lung, sheep: A tissue Gram stain reveals moderate numbers of 1um diameter, filamentous, occasionally beaded gram-positive bacteria within inflammatory foci. (Photo courtesy of: Covance Laboratories, Inc, Madison, Wisconsin, USA. http://www.covance.com/products/nonclinical/toxicology/risk-assessment/index.php) (Brown-Brenn, 400X)*

Routes of infection include inhalation, inoculation, and ingestion. In people, *Nocardia* are generally considered pathogenic bacteria with relatively low virulence. With the exception of cutaneous disease, human infection is typically opportunistic, occurring more commonly in the elderly and people with compromised T cell-mediated immunity, as with prolonged steroid treatment or HIV infection.[6] In the present case, it is not clear if the absence of a normal appearing thymus at necropsy was due to a primary condition predisposing the animal to infection (thymic hypoplasia) or a secondary response to the severe infection (thymic atrophy).

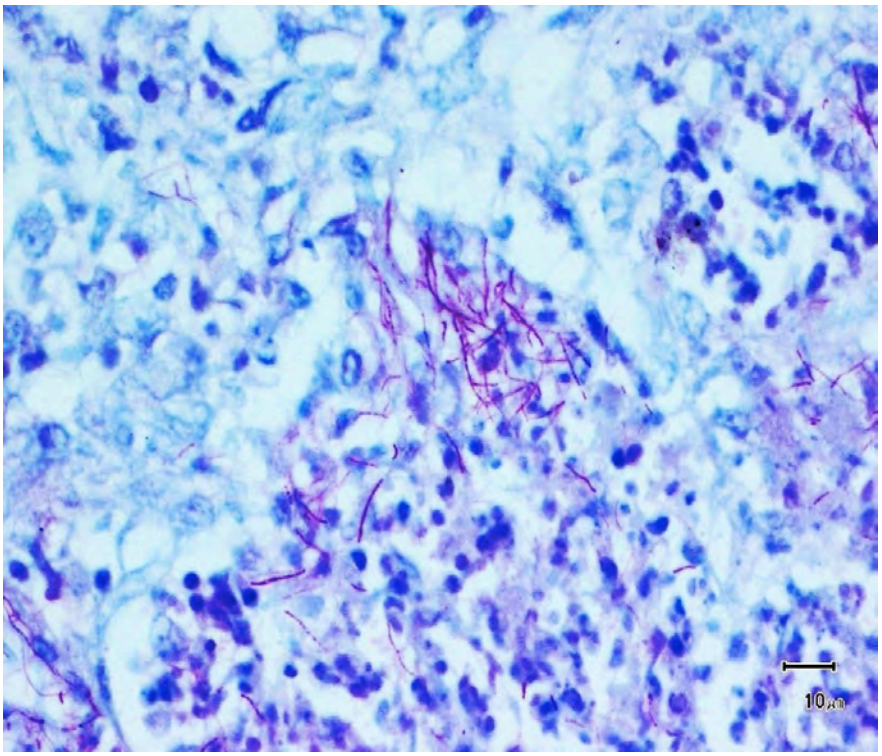

*2-5. Lung, sheep: An acid-fast stain reveals moderate numbers of 1µm diameter, filamentous, occasionally beaded, variably acid-fast bacteria within inflammatory foci. (Photo courtesy of: Covance Laboratories, Inc, Madison, Wisconsin, USA. http://www.covance.com/products/nonclinical/toxicology/risk-assessment/index.php) (Brown-Brenn, 400X)*

Nocardiosis is an important cause of pneumonia, pleuritis and empyema in dogs, particularly hunting/sporting dogs in which, following inhalation or ingestion of plant material, migrating grass awns can contaminate the pleural spaces with bacteria resulting in a putrid "tomato soup-like" hemorrhagic pyothorax. In most other species, pulmonary nocardiosis more closely resembles the nodular pyogranulomatous and necrotizing inflammation observed in this lamb. *Nocardia* infections have been infrequently reported in primates, cats, horses, cattle and marine mammals.[1,2,5,8] In cattle, infections have been associated with mastitis, pneumonia, dermatitis, placentitis with abortion, and disseminated disease.[1] *Nocardia* infections in other ruminants are apparently very uncommon, but have been reported in sheep, goats, llama,

bison and reindeer.[3,7,10] Nocardiosis is reportedly a significant and often fatal disease in marine mammals.[8] Pinnipeds, particularly hooded seals, and cetaceans appear to be prone to a systemic form of infection which typically involves the lung and thoracic lymph nodes and, to lesser extent, brain and skin.

**JPC Diagnosis:** Lung: Pneumonia, pyogranulomatous, multifocal to coalescing, severe, with numerous filamentous gram-positive, acid-fast bacteria.

**Conference Comment:** In addition to discussing nocardiosis in the various species so well described by the contributor, conference participants also discussed the so-called "nocardioform" placentitis associated with equine abortion. Nocardioform placentitis can be caused by several genera of gram positive, branching actinomycetes that share similarities with *Nocardia* species, including the following: *Crossiella equi, Amycolatopsis kentuckyensis, Amycolatopsis lexingtonensis, Amycolatopsis pretoriensis, Streptomyces atriruber,* and *Streptomyces silaceus*.[4] Clinically, nocardioform placentitis presents as late gestation abortion, stillbirth, prematurity or full term but weak foals. Grossly, a thick, light brown exudate is often observed in the chorion at the bifurcation of the horns of the affected placenta. The organisms do not reach the fetus; thus fetal lesions are those of placental insufficiency. Recently, nocardioform placentitis resulted in a record number of equine abortions in the 2011 foal crop in Kentucky. The most prominent actinomycetes found in this series of third trimester abortions were *Amycolatopsis* spp. and *Crosiella equi*; fewer *Streptomyces, Microbacterium, Nocardia* and *Allokutzneria* species were identified.[4]

**Contributing Institution**: Covance Laboratories, Inc
Madison, Wisconsin, USA
http://www.covance.com/products/nonclinical/toxicology/risk-assessment/index.php

**References:**

1. Bawa B, Bai J, Whitehair M, Purvis T, et al. Bovine abortion associated with *Nocardia farcinica*. *J Vet Diagn Invest.* 2010;22(1):108-11.
2. Bolon B, Buergelt CD, Cooley AJ. Abortion in two foals associated with *Nocardia* infection. *Vet Pathol.* 1989;26(3):277–278.
3. Chang CD, Boosinger TR, Dowling PM, et al. Nocardiosis in a llama. *J* Vet Diagn Invest. 1993;5(4): 631-4.
4. Erol E, Sells SF, Williams NM, Kennedy L, Locke SJ, Labeda DP, et al. An investigation of a recent outbreak of nocardioform placentitis caused abortions in horses. *Vet Microbiol*. 2012:17;158(3-4):425-30.
5. Klumpp SA, McClure HM. Nocardiosis, lung. In: Jones TC, Mohr U, Hunt RD, eds. *Monographs on Pathology of Laboratory Animals: Nonhuman Primates II*. Berlin and New York: Springer-Verlag; 1993:99–103.
6. McAdam AJ, Sharpe AH. Infectious diseases. In: Kumar V. Abbas A. Fausto N, eds. *Robbins and Cotran: Pathologic Basis of Disease*. 8th edition. Philadelphia, PA: Elsevier Saunders; 2010:362-363.
7. Pal M. *Nocardia asteroides* as a cause of pneumonia in a buffalo calf. *Review of Scientific Technical Office International Des Epizootics*. 1997;16:881-884.
8. St. Leger JA, Begeman L, Fleetwood M, et al. Comparative pathology of nocardiosis in marine mammals. *Vet. Pathol.* 2009;46:299–308.
9. Travis WD, Colby TV, Koss MN, et al. Lung Infections. *Atlas of Nontumor Pathology. Non-neoplastic Disorders of the Lower Respiratory Tract.* Washington, DC: American Registry of Pathology; 2002:557-563.
10. Vemireddi V, Sharma A, Wu CC, et al. Systemic nocardiosis in a reindeer (*Rangifer tarandus tarandus*), *J. Vet. Diagn. Invest*. 2007;19(3):326-329.

**CASE III**: AR12-0051 (JPC 4017933).

**Signalment:** Adult male Sprague-Dawley rat, *Rattus norvegicus*.

**History:** This transgenic rat for the mouse Ren2 gene was found dead.

**Gross Pathology:** The small intestinal mesenteric arteries were diffusely dark red, nodular, tortuous and measured up to 5mm in diameter. Both kidneys had many 0.5mm round indentations on their surfaces.

**Histopathologic Description:** The renal changes are consistent with an end stage kidney with polyarteritis nodosa and hypertensive arterial disease. The renal capsule is irregularly indented throughout. The underlying interstitium has tubular loss with replacement by fibrous connective tissue and infiltration by lymphocytes and plasma cells. The glomerular mesangium is regularly thickened by pale eosinophilic amorphous material, the tufts are large and prominently segmented, and periglomerular fibrosis is prominent. Occasional glomeruli are shrunken, have synechia or are sclerotic. The cortical renal tubules are dilated, up to 1mm across, by eosinophilic amorphous material, and are lined by attenuated epithelium. Tubular epithelial cells are occasionally swollen with vacuolated cytoplasm, and some have hypereosinophilic cytoplasm and pyknotic nuclei. The tunica media of medium-sized arteries is thickened by concentric rings of excessive smooth muscle and sometimes fibrous connective tissue, and the walls are infiltrated by lymphocytes and fewer macrophages. Hypereosinophilic amorphous material obscures the tunica media in some slides (fibrinoid change).

**Contributor's Morphologic Diagnosis:** 1. Glomerulonephropathy, diffuse, chronic, severe with tubular proteinosis and interstitial lymphocytic nephritis and fibrosis (chronic progressive nephropathy).
2. Arteritis, segmental, chronic, moderate to severe, lymphohistiocytic with fibrinoid change, kidney (polyarteritis nodosa).
3. Smooth muscle hyperplasia, segmental, chronic, moderate, arterial tunica media, kidney (hypertensive change).

**Contributor's Comment:** This case demonstrates three histological renal lesions in a hypertensive rat: chronic progressive nephropathy (CPN), polyarteritis nodosa and hypertensive arterial disease. CPN is a common age-related lesion most common in males, with increased incidences in Sprague-Dawley and Fischer 344 rats. Grossly, the renal cortices are irregular and pitted, as in this case. The kidneys may be enlarged, pale and have linear streaks in the cortex and medulla. Histologically, glomerular changes include basement membrane and mesangial thickening, segmental sclerosis, and synechia. Tubules are regularly dilated, protein-filled, and lined by flattened epithelial cells. Interstitial fibrosis and inflammation are common. Advanced cases may also have secondary hyperparathyroidism with metastatic calcification in the kidneys, gastric mucosa, lungs and/or tunica media of larger arteries. Late-stage CPN has been associated with hypertension and polyarteritis nodosa.[7]


*3-1. Mesentery, Ren2 transgenic rat: Mesenteric arteries in the region of the small intestine are diffusely dark red, nodular, tortuous and measure up to 5mm in diameter. (Photo courtesy of: Wake Forest University Health Sciences, Animal Resources Program, Medical Center Boulevard, Winston-Salem, NC 27157 http://www.wfubmc.edu/schoolofMedicine/schoolofMedicine_default.aspx?id=26651*

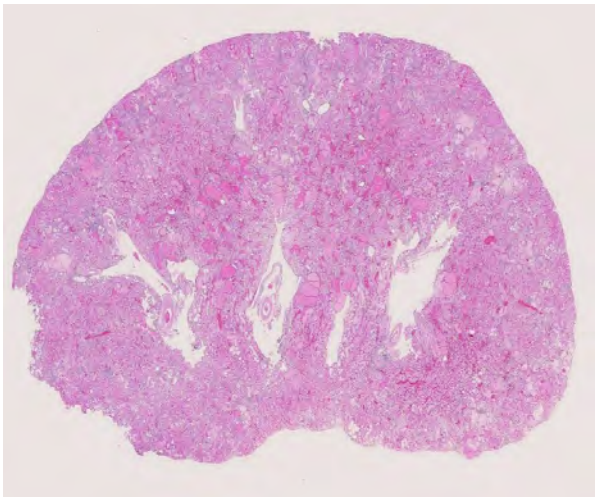

*3-2. Kidney, Ren2 transgenic rat: At the subgross level, the marked ectasia of tubules and pitted capsule are evident, suggesting chronic progressive nephropathy. (HE 0.63X)*

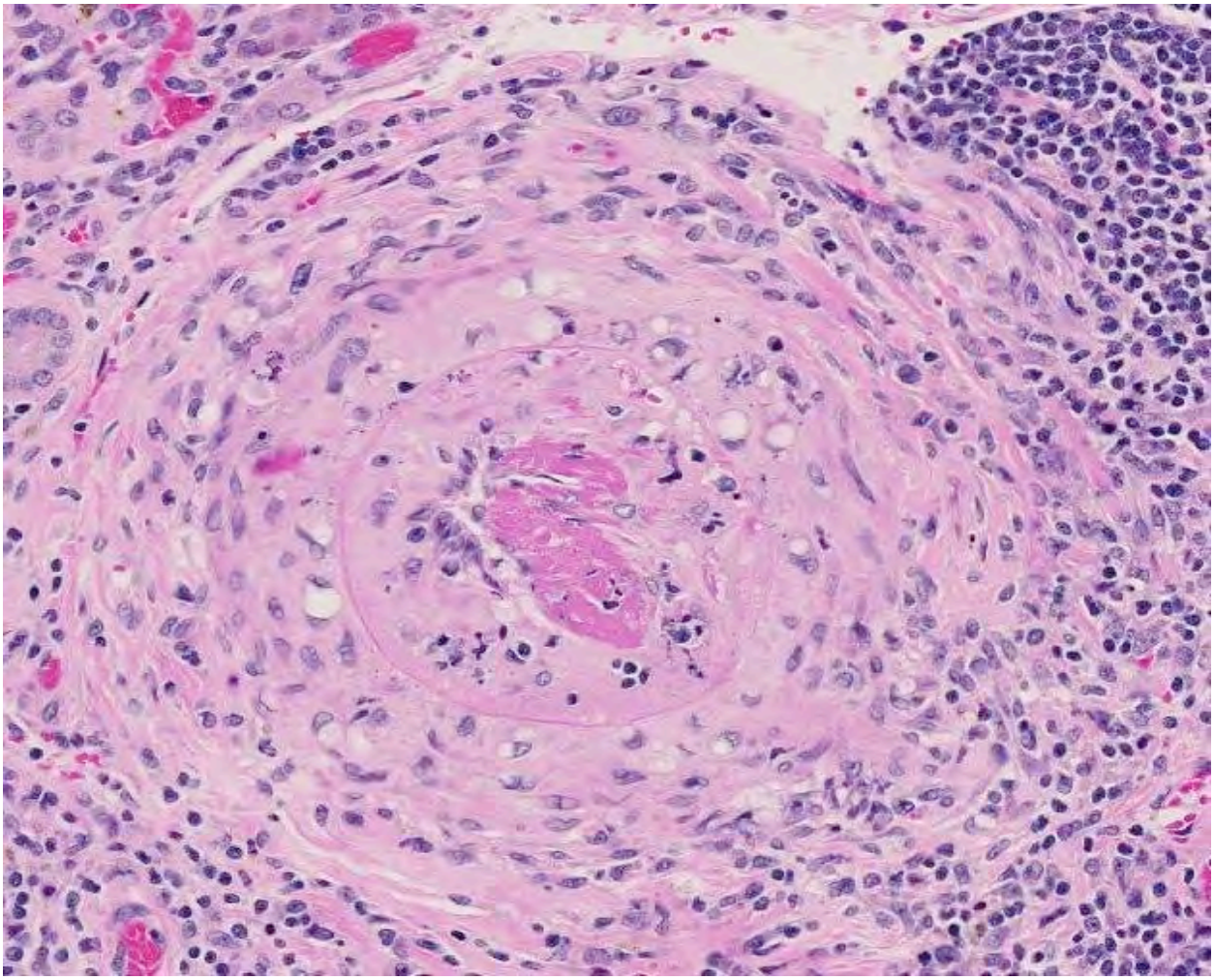

*3-3. Kidney, Ren2 transgenic rat: Multifocally, the intima of renal arterioles is expanded by bright eosinophilic protein, and the intima and media are infiltrated by neutrophils admixed with cellular debris (fibrinoid necrosis). Additionally, there is lamellar fibrosis of the tunica adventitia, suggesting prolonged hypertension. (HE 144X)*

Similar to CPN, polyarteritis nodosa is a chronic progressive degenerative disease occurring most frequently in aged Sprague-Dawley rats, spontaneous hypertensive rats, and rats with late-stage chronic nephropathy. At necropsy the mesenteric vessels are often enlarged, tortuous and segmentally thickened, as in this case. Polyarteritis nodosa is characterized histologically by fibrinoid degeneration and thickening of the tunica media of medium-sized arteries with infiltrating mononuclear cells and fewer neutrophils. The lumina may vary in size and have thromboses, some of which may recanalize. Polyarteritis nodosa has also been reported in mice,[7] cats,[1] dogs,[11] pigs,[2,4] cynomolgus macaques[9] and foxes.[6] Although the cause is uncertain, the lymphohistiocytic inflammation suggests it may have an immune-mediated basis.[4,7,9]

The rat is a common animal model of hypertension. Spontaneously hypertensive Wistar rats, Dahl-salt sensitive rats, transgenic mREN2 rats, and rats administered deoxycorticosterone acetate (DOCA) in combination with a high salt diet are the most common models.[3,8] In all of these models, the hypertensive animals have impaired endothelium-dependent relaxation and vascular remodeling which lead to increased vascular resistance and renal damage.[3,8] Severe end-organ damage involving the heart, brain and kidney is only seen in a subset of animals within some models. This rat was transgenic (TGR[mREN2] 27), with over-expression of the mouse Ren-2 gene which increases renin activity. Renin catalyzes the conversion of angiotensinogen to angiotensin I, which is then converted to angiotensin II by angiotensin-converting enzyme. Angiotensin II causes vasoconstriction and increased blood pressure. Hypertensive changes are further exacerbated by angiotensin II-induced aldosterone secretion which increases mineralocorticoid levels and sodium reabsorption, thus increasing blood volume osmotically and further increasing blood pressure.[10]

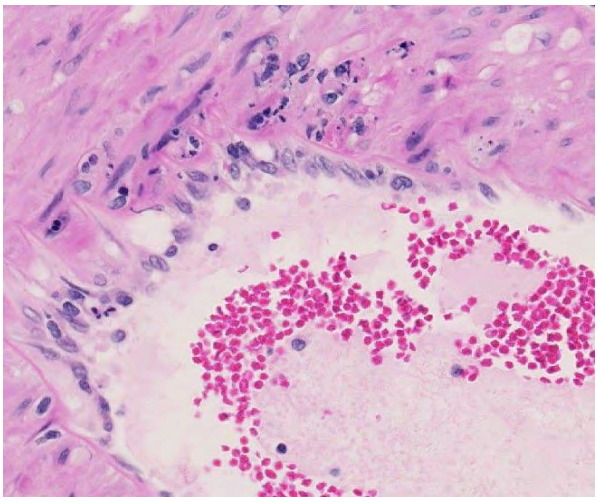

*3-4. Kidney, Ren2 transgenic rat: Less affected arterioles contain degenerate neutrophils admixed within the inner tunica media. (HE 144X)*

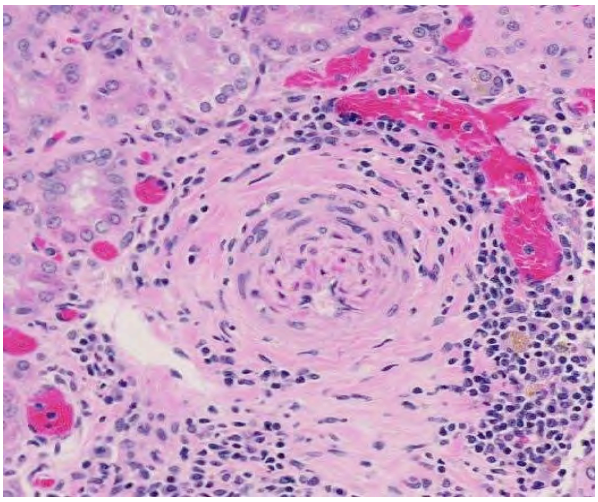

*3-5. Kidney, Ren2 transgenic rat: Lamellar fibrosis of the tunica adventitia is a common finding in hypertension. (HE 168X)*

**JPC Diagnosis:** 1. Kidney, arteries: Arteritis, proliferative and necrotizing, multifocal, severe, with fibrinoid necrosis.
2. Kidney, arteries: Arteriosclerosis, multifocal, moderate.
3. Kidney: Glomerulonephritis, diffuse, with tubular degeneration, necrosis and regeneration, proteinosis, and chronic interstitial nephritis.

**Conference Comment**: The contributor provides an excellent summary of the various changes observed in this animal model of hypertension. Veterinary species are not as commonly affected with idiopathic (essential) hypertension as humans; however, several species, including cats and dogs, develop systemic hypertension which is often secondary to other conditions. In the cat, hypertension is often associated with hyperthyroidism and chronic renal failure; whereas in the dog, it is more likely to be associated with chronic renal failure, hyperadrenocorticism, or pheochromocytomas.[5]

Conference participants discussed the vessel wall changes observed in this case, noting that hypertension results in several pathologic changes in the walls of small arteries and arterioles, including two types of arteriolosclerosis: hyaline and hyperplastic. Small blood vessels in hyaline arteriolosclerosis exhibit a homogeneous, eosinophilic thickening of the wall and narrowing of the lumen due to endothelial cell damage and the subsequent increased vascular permeability and plasma protein leakage into the vessel wall. Hyperplastic arteriolosclerosis, on the other hand, is characterized by a concentric, laminated thickening of the wall ("onion skinning") and narrowing of the lumen which is due to smooth muscle cell hyperplasia and reduplication of basement membranes. Hyperplastic arteriolosclerosis can also be associated with fibrinoid necrosis in the vessel walls.[10]

**Contributing Institution**: Wake Forest University Health Sciences
Animal Resources Program
Medical Center Boulevard
Winston-Salem, NC 27157
http://www.wfubmc.edu/schoolofMedicine/schoolofMedicine_default.aspx?id=26651

**References:**

1. Altera KP and Bonasch H. Periarteritis nodosa in a cat. *J Am Vet Med Assoc*. 1966;149(10):1307-11.
2. Elling F. Nutritionally induced necrotizing glomerulonephritis and polyarteritis nodosa in pigs. *Acta Pathol Microbiol Scand A*. 1979;87A(1-6): 387-392.
3. Dornas W, Silva ME. Animal models for the study of arterial hypertension. *J Biosci*. 2011;36(4): 731-737.
4. Hélie P, Drolet R, Germain MC, Bourgault A. "Systemic necrotizing vasculitis and glomerulonephritis in grower pigs in southwestern Quebec." *Can Vet J*. 1995;36(3):150–154.
5. Miller LM, Van Vleet JF, Gal A. Cardiovascular system and lymphatic vessels. In: McGavin MD, Zachary JF, eds. *Pathologic Basis of Veterinary Disease*. 5th ed. St. Louis, MO: Elsevier Mosby; 2012:552.
6. Nordstoga K, Westbye K. Polyarteritis nodosa associated with nosematosis in blue foxes. *Acta Pathol Microbiol Scand A*. 1976;84(3):291-296.
7. Percy, DH, Barthold SW. Rat. In: Pathology of Laboratory Rodents and Rabbits. 3rd ed. Ames, Iowa: Blackwell Publishing; 2007:125-206.
8. Pinto YM, Paul M, Ganten D. Lessons from rat models of hypertension: from Goldblatt to genetic engineering. *Cardiovasc Res*. 1998;39:77-88.

9. Porter BF, Frost P, Hubbard GB. Polyarteritis Nodosa in a Cynomolgus Macaque (Macaca fascicularis). *Vet Pathol*. 2003;40(5):570-573.
10. Schoen FJ. Blood Vessels. In: *Robbins and Cotran Pathologic Basis of Diseases*. 8th ed. Philadelphia, PA: Saunders Elsevier; 2010:487-528.
11. Scott-Moncrieff JC, Snyder PW, Glickman LT, Davis EL, Felsburg PJ. Systemic necrotizing vasculitis in nine young beagles. *J Am Vet Med Assoc*. 1992;201 (10):1553-1558.

**CASE IV:** V08-10649 (JPC 3141626).

**Signalment:** 10-year-old castrated male Belgian, equine *(Equus caballus)*.

**History:** A 10-year-old Belgian gelding was euthanized following progressively worsening neurological signs, including severe ataxia, gait abnormalities, and sudden loss of balance with falling. The horse owner determined this was a severe safety risk for the handlers tending the horse. Originally, this horse was diagnosed positive for equine protozoal myeloencephalitis (EPM) eight months earlier. Despite appropriate medical treatment, clinical signs progressively deteriorated. This horse was insured and the insurance carrier requested a necropsy.

**Gross Pathology:** This 10-year-old Belgian gelding appeared to be in good external condition and estimated weight was 2,500 to 2,700 pounds. An unexpected flow of cerebrospinal fluid (CSF) was observed upon separation of the atlanto-occipital junction. Similarly, a large volume of CSF poured out of the lateral ventricles upon incising the cerebral hemispheres. The CSF was yellow to light tan, and cloudy to slightly turbid. An ovoid mass was found bridging the midline and extending into both right and left lateral ventricles, with loose attachment to the floor of the left lateral ventricle. The mass was 9.5 x 5.0 x 2.75 cm, yellow/ivory to grey/tan with a smooth shiny surface, except for an area of roughened surface corresponding to a loose attachment to the floor of the left lateral ventricle. On cut surface, the mass was solid and colored similar to the surface described above. Both lateral ventricles were moderately dilated resulting in moderate internal hydrocephalus.

**Histopathologic Description:** This brain mass was made up of a well-differentiated, somewhat irregularly oriented fibrous and fibrovascular supporting tissue network filled with irregular variable-sized palisading bundles or "sheaves" of needle-like cholesterol clefts along with variable mixed inflammation. Inflammatory cells present included histiocytes/ macrophages, lymphocytes, plasma cells, neutrophils, and fewer eosinophils. Patchy edema and hemorrhage was present within the mass and many macrophages contained hemosiderin pigment. Binucleate and cytomegalic plasma cells were randomly observed within the inflammation.

Changes in cerebral cortical tissue (slides not included) surrounding the dilated lateral ventricles included rarefaction and loss of nerve cell bodies immediately peripheral to the lateral ventricle space. In a number of sections, there was complete loss of the nerve cell body layer and neuropil collapse resulting in an appearance of increased blood vessels somewhat like a line of irregular granulation tissue. Random areas of spongy degeneration were noted in cortical white matter about the dilated ventricles. Additionally, the meninges sometimes contained a few inflammatory cells, predominately histiocytes, lymphocytes, and/or neutrophils.

**Contributor's Morphologic Diagnosis:** Brain mass: Cholesterol granuloma, right and left lateral ventricles, cerebrum, Belgian, equine.

**Contributor's Comment:** This case demonstrates the sometimes perplexing situation for clinical practitioners and veterinary pathologists alike, when a horse is presented for evaluation of what is often loosely referred to as an "equine neurological case." Many of these cases may be relatively long-standing and may have been previously diagnosed, erroneously or not, with a specific neurological disease (in this case, equine protozoal encephalomyelitis [EPM]).

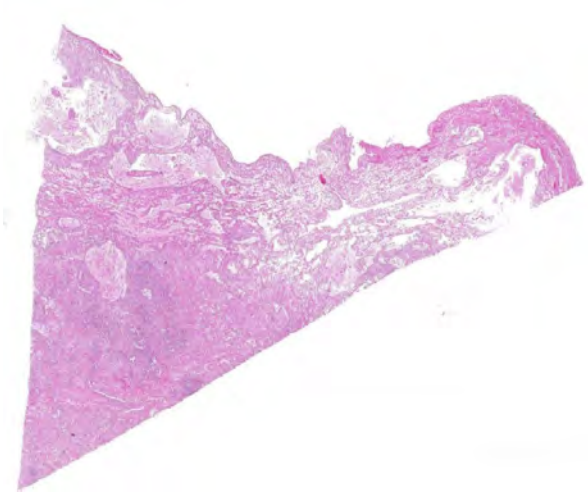

*4-1. Lateral ventricle, horse: Section from a yellow to grey tan mass found on the floor of the lateral ventricle. (HE 6.3X)*

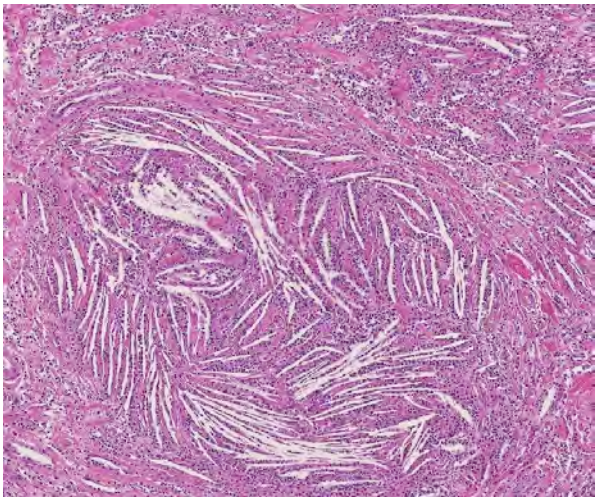

*4-2. Lateral ventricle, horse: Acicular cholesterol cleft are a diagnostic feature of cholesterol granulomas in the horse. (HE 60X)*

Additionally, some cases may have been treated for a specific disease with or without improvement. At the time the veterinary pathologist receives the case, most likely some set of events or changes in the clinical state of the horse have taken place that warrant euthanasia of the horse.

Knowing the above chain of events is likely in many cases, then, the veterinary pathologist should preface the undertaking of an equine neurological case necropsy, with a set of all possible differential diagnoses, in addition to any previous clinical diagnosis. Many equine neurological cases, and particularly CNS cases, have overlap of signs. Even if a case has a diagnosis confirmed by reliable clinical testing, as in this case, that particular diagnosis may not be the cause of the recent chain of events that brought about the euthanasia of the horse. Finally, there are some equine neurological cases that may be a "rule out diagnosis." Botulism is one disease that always should come to mind as an example of this. Because the levels of botulinum toxin required to affect and even kill a horse are so low that current modes of testing may be unable to detect, the pathologist should always have a conversation with the horse owner and clinical veterinarian, about any and all of the details of environment and husbandry that could possibly lead to a final rule-out diagnosis of botulism.

Clearly then, cholesterol granulomas should be considered as a differential diagnosis in any equine neurological case, especially those in older horses with predominantly CNS signs. In fact, it has been reported that 15-20% of old horses have cholesterol granulomas, although many may be present in the absence of clinical signs.

Cholesterol granulomas and cholesteatoma have been used in veterinary literature to describe the lesion diagnosed in this case.[2,3,4,6,7] There is some disagreement of sorts as to whether cholesteatoma should be used to describe this brain lesion, specifically found in old horses.[2] Cholesteatoma is a term also used to describe a nodular mass in the middle ear, although this aural cholesteatoma has not been reported in horses.[5] It may be a prudent move to

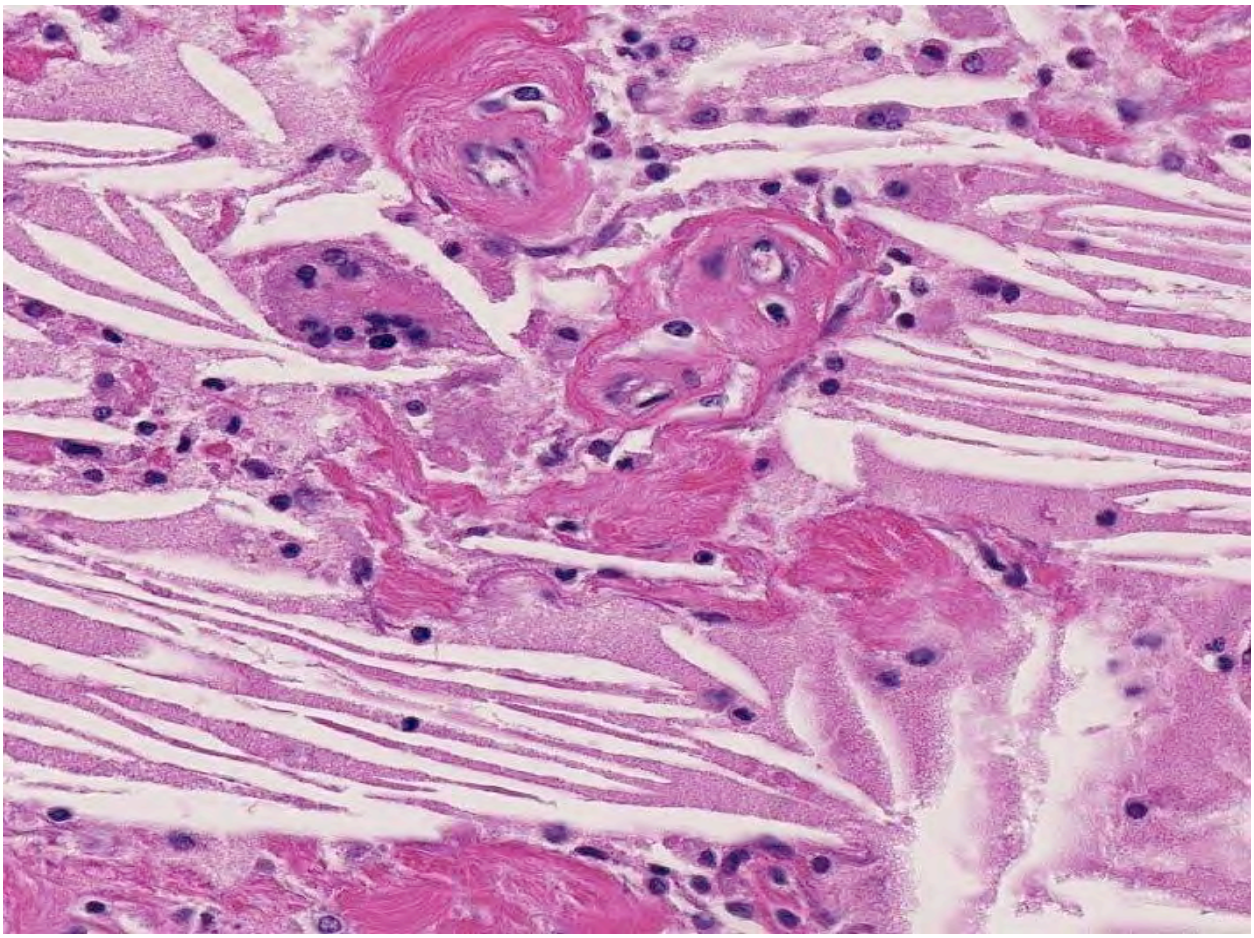

*4-3. Lateral ventricle, horse: The cholesterol granuloma is largely composed of mature collagen, large numbers of epithelioid macrophages and lymphocytes, and rare plasma cells and multinucleated giant cell macrophages. In this mass, vessels are surrounded by moderate amounts of fibrous connective tissue. (HE 220X)*

restrict the use of cholesterol granulomas only to describe this specific entity of aged horses, rather than use cholesteatoma interchangeably with cholesterol granuloma.

Despite this sort of disagreement of terminology for equine cholesterol granulomas, the mechanism of development is basically agreed upon.[2,3,4,6,7] The exact underlying pathogenesis, however, seems to be uncertain.[7] Equine cholesterol granulomas are often described as an aging or degenerative phenomenon.[2,3,5,7] Repeated episodes of hemorrhage and/or chronic intermittent congestion, edema and congestive hemorrhage in the choroid plexuses are believed to be the pathological processes responsible for development of cholesterol granulomas of older horses.[2,3] Erythrocytes are likely the source of the cholesterol.[6] It is when hemorrhage results in formation of a hematoma, subsequently becoming organized, followed by breakdown of red blood cells to release cholesterol that the granuloma develops.[2] Cholesterol accumulation, both extracellular and within macrophages, is observed and the cholesterol itself stimulates a "foreign body response" or "giant cell reaction,"[6] resulting in developing and progressive granulomatous inflammation and fibrovascular "organization."[2,3,4,6,7] Whether this is or can result from a single event or requires multiple episodes is speculative, but likely the larger cholesterol granulomas develop because of multiple events of this type.

Small cholesterol granulomas may remain clinically silent and are discovered incidentally. The larger cholesterol granulomas produce clinical CNS signs and signs can be variable and progressive. Most, if not all, of the effects of large cholesterol granulomas are caused by blockage of interventricular foramen resulting in development of internal hydrocephalus and progressive degeneration and compression atrophy of the cerebral hemispheres. Inflammation in the brain itself is usually minimal and represented as small infiltrates of macrophage, lymphocytes, and neutrophils in the meninges. It may be fortunate that even though the occurrence of cholesterol granulomas in old horses is reported to be 15-20%, the majority are found in the fourth ventricle; and, development of hydrocephalus, the usual cause of clinical signs, is limited to those in the lateral ventricles that can by location block the interventricular formen causing hydrocephalus.[3]

**JPC Diagnosis:** Ventricle (left lateral, per contributor): Cholesterol granuloma (cholesteatoma).

**Conference Comment:** Conference participants discussed the typical gross and histopathologic findings as well the pathogenesis of cholesterol granulomas, all of which are discussed in the contributor's excellent summary. Conference participants also used this case as an opportunity to review the anatomy of the ventricular system of the brain. There is one lateral ventricle within each cerebral hemisphere, each of which communicates with the third ventricle through an interventricular foramen. The third ventricle is a narrow chamber that lies along the midline, between the two thalami in the diencephalon; it communicates with the fourth ventricle in the hindbrain through the mesencephalic aquaduct. The fourth ventricle communicates with the central canal of the spinal cord and the subarachnoid space via lateral recesses and apertures. This system of cavities through which cerebrospinal fluid (CSF) flows is lined by ependymal epithelial cells. *Tela choroidea*, (an area in which nervous tissue is absent and pia mater contacts the ependymal cells directly) forms a portion of the floor of the lateral ventricles and roof of the third and fourth ventricles. It gives rise to the choroid plexuses, which are composed of ependymal cells and microvascular proliferations. The choroid plexuses project into each ventricle, where they produce CSF via secretion and ultrafiltration.[1]

**Contributing Institution:** NMDA – Veterinary Diagnostic Services
P.O.Box 4700
Albuquerque, NM 87196-4700
http://www.nmda.nmsu.edu/animal-and-plant-protection/veterinary-diagnostic-services

**References:**

1. Fletcher TF. Spinal cord and meninges. In: Evans HE, ed. *Miller's Anatomy of the Dog*. 3rd ed. Philadelphia PA: Saunders Elsevier; 1993:824-826.
2. Jones TC, Hunt RD, King NW. The nervous system. In: *Veterinary Pathology*. 6th ed. Baltimore, MD: Lippincott Williams & Wilkins; 1997:1286, 1291-2.
3. Jubb KVF, Kennedy PC, Palmer N. Nervous system. In: Maxie MG, ed. *Pathology of Domestic Animals*. Vol. 1. Philadelphia, PA: Elsevier Saunders, 2007:345-6.
4. McGavin DM, Zachary JF. *Pathologic Basis of Veterinary Disease*. 4th ed. St. Louis, MO: Mosby; 2007:47, 922.
5. McGavin, Carlton & Zachary. The nervous system. In: *Thomson's Special Veterinary Pathology*. 3rd ed. St. Louis, MO: Mosby; 2001:448-449.
6. Moulton JE. Tumors in Domestic Animals, 3rd ed. Berekley, CA: University of California Press, 1990:647.
7. Summers B, Cummings J, de Lahunta A. Neuropathology of aging. In: *Veterinary Neuropathology*. St. Louis, MO: Mosby; 1995:49-53.

roots and intramuscular nerves and the dorsal root ganglia due to neurofilamentous accumulations. This lesion may be accompanied by Wallerian degeneration in peripheral nerves and associated denervation muscle atrophy. It is uncertain how these changes relate to the metabolic deficits present in primary hyperoxaluria or whether they represent a concurrent genetic defect.[3,7]

Primary hyperoxaluria must be distinguished from secondary disease due to exposure to large amounts of oxalates or increased absorption of dietary oxalic acid from the intestinal tract. In companion animals, acute oxalate nephrosis is typically seen in cases of ethylene glycol poisoning. In large animals, oxalate-rich plants are generally the source of toxicity.[8] Histologically, renal changes due to ethylene glycol toxicity are indiscernible from those present in cases of feline primary hyperoxaluria. A distinction between feline primary hyperoxaluria and oxalate toxicity is made on the basis of clinical history and supporting clinicopathological information (e.g. L-glyceric aciduria).

**JPC Diagnosis:** 1. Kidney: Tubular degeneration and necrosis, diffuse, marked, with regeneration, mineralization, and numerous intratubular oxalate crystals.
2. Kidney: Nephritis, interstitial, lymphoplasmacytic, multifocal to coalescing, mild, with fibrosis.

**Conference Comment:** The contributor provides an excellent synopsis of primary hyperoxaluria (PH). Given only the species of origin in advance of the conference, participants correctly determined that this was a young animal based on the occasional presence of hypercellular "fetal" glomeruli in the section. While most participants included PH in their differential diagnoses, ethylene glycol toxicosis was considered the most likely etiology. In addition to reviewing the pathogenesis of PH, conference participants discussed the pathogenesis of ethylene glycol toxicosis in depth. The main focus of the discussion was the clinicopathologic aberrations typical of ethylene glycol toxicosis, including titrational metabolic acidosis, hyperkalemia, hyperphosphatemia, hypocalcemia, and calcium oxalate monohydrate crystalluria.[9] A detailed review of ethylene glycol toxicosis and its associated clinicopathologic consequences is available elsewhere in these proceedings (i.e., Conference 18, Case III).

Finally, participants discussed toxic plants as the usual cause of oxalate nephrosis in ruminants. A partial listing of oxalate-containing plants implicated in such cases follows:[8]

| Scientific Name | Common Name |
|---|---|
| *Halogeton glomeratus* | Halogeton |
| *Sarcobatus vermiculatus* | Greasewood |
| *Rheum rhaponticum* | Rhubarb |
| *Oxalis cernua* | Soursob |
| *Rumex* spp. | Sorrel, dock |

**Contributing Institution**: Department of Anatomic Pathology
Biomedical Sciences
College of Veterinary Medicine
T4 018 Veterinary Research Tower
Cornell University
Ithaca, NY 14853
http://www.vet.cornell.edu/biosci/pathology/services.cfm

**References:**

1. Bobrowski AE, Langman CB. The primary hyperoxalurias. *Semin Nephrol*. 208;28:152-162.
2. Danpure CJ, Jennings PR, Mistry J, Chalmers RA, McKerrell RE, Blakemore WF, et al. Enzymological characterization of a feline analogue of primary hyperoxaluria type 2: a model for the human disease. *J Inherit Metab Dis*. 1989;12:403-14.
3. De Lorenzi D, Bernardini M, Pumarola M. Primary hyperoxaluria (L-glyceric aciduria) in a cat. *J Feline Med Surg*. 2005;7:357-361.
4. Goldstein RE, Narala S, Sabet N, Goldstein O, McDonough SP. Primary hyperoxaluria in cats is caused by a mutation in the feline GRHPR gene. *J Heredity*. 2009;100:S2-S7.
5. Gülbahar MY, Kaya A, Gölen I. Renal Oxalosis in a Calf. *Turk J Vet Anim Sci*. 2002;26:1197-1200.
6. Hoppe B, Beck BB, Miller DS. The primary hyperoxalurias. *Kidney Int*. 2009;75:1264-1271.
7. Maxie MG, Youssef S. Nervous system. In: Maxie MG, ed. *Jubb, Kennedy and Palmer's Pathology of Domestic Animals*. 5th ed. Philadelphia, PA: Elsevier Saunders; 2007:375.
8. Maxie MG, Newman SJ. Urinary system. In: Maxie MG, ed. *Jubb, Kennedy and Palmer's Pathology of Domestic Animals*. 5th ed. Philadelphia, PA: Elsevier Saunders; 2007:468-473.
9. George JW, Zabolotzky SM. Water, electrolytes, and acid base. In: Latimer KS, ed. *Duncan & Prasse's Veterinary Laboratory Medicine Clinical Pathology*. 5th ed. Ames, Iowa: Wiley-Blackwell; 2011:145-171, 430-432.

**Joint Pathology Center**
**Veterinary Pathology Services**

# WEDNESDAY SLIDE CONFERENCE 2012-2013

# Conference 24

**8 May 2013**

---

**CASE I:** 09-123996 (JPC 3170126).

**Signalment:** Three-month-old, female domestic shorthair cat (*Felis catus*).

**History:** The kitten came from a breeding colony at the College of Veterinary Medicine, Cornell University.

**Gross Pathologic Findings:** The kidneys are bilaterally enlarged; each measures approximately 4 x 3 x 2.5 cm. On section, the parenchyma exudes a small amount of clear fluid. Dozens of pinpoint to linear white foci are scattered throughout the cortex and medulla (tubular crystalluria).

**Histopathologic Description:** Kidney (1 section): Frequent tubules within the cortex and, to a lesser extent, the medulla, are occluded by linear crystalline material arranged into radiating sheaths. Crystals are translucent, clear to blue and birefringent bright white under polarized light (oxalate crystals). Cortical tubules are irregularly ectatic and variably lined by flattened, attenuated epithelium with hypereosinophilic cytoplasm and pyknotic nuclei (degeneration and necrosis) or, rarely, by plump, basophilic cells that are haphazardly stacked (regeneration). Scattered tubules additionally contain karyorrhectic debris and droplets of homogenous, eosinophilic material (protein). Small numbers of lymphocytes, plasma cells and neutrophils multifocally infiltrate the cortical and medullary interstitium and fine threads of fibroblasts occasionally dissect between tubules (fibrosis).

**Contributor's Morphologic Diagnosis:** 1. Kidney: Moderate, diffuse, subacute tubular necrosis and ectasia with multifocal tubular epithelial regeneration and many intratubular oxalate crystals.
2. Mild, multifocal lymphoplasmacytic and neutrophilic interstitial nephritis.

**Contributor's Comment:** This kitten was bred as a feline model of primary hyperoxaluria; the histologic features of the examined section of kidney are characteristic of this disease. Primary hyperoxaluria (PH) is best described in humans but has also been reported in cats, dogs and cattle.[2,3,4,5] In humans PH is a rare, autosomal recessive inherited disease that is classified as either type I (PH1) or type II (PH2) based on mutations of the respective genes alanine: glyoxylate aminotransferase (*AGT*) and glyoxylate reductase/ hydroxypyruvate reductase (*GRHPR*), and their associated biochemical deficits. Up to 83 *AGT* mutations have been associated with PH1 and 13 mutations of *GRHPR* have been identified in cases of PH2; these mutations reduce or eliminate activity of the hepatic enzymes AGT and GRHPR.[1] Consequently, increased glyoxalate and hydroxypyruvate are available for conversion by lactate dehydrogenase to oxalate and, in the case of

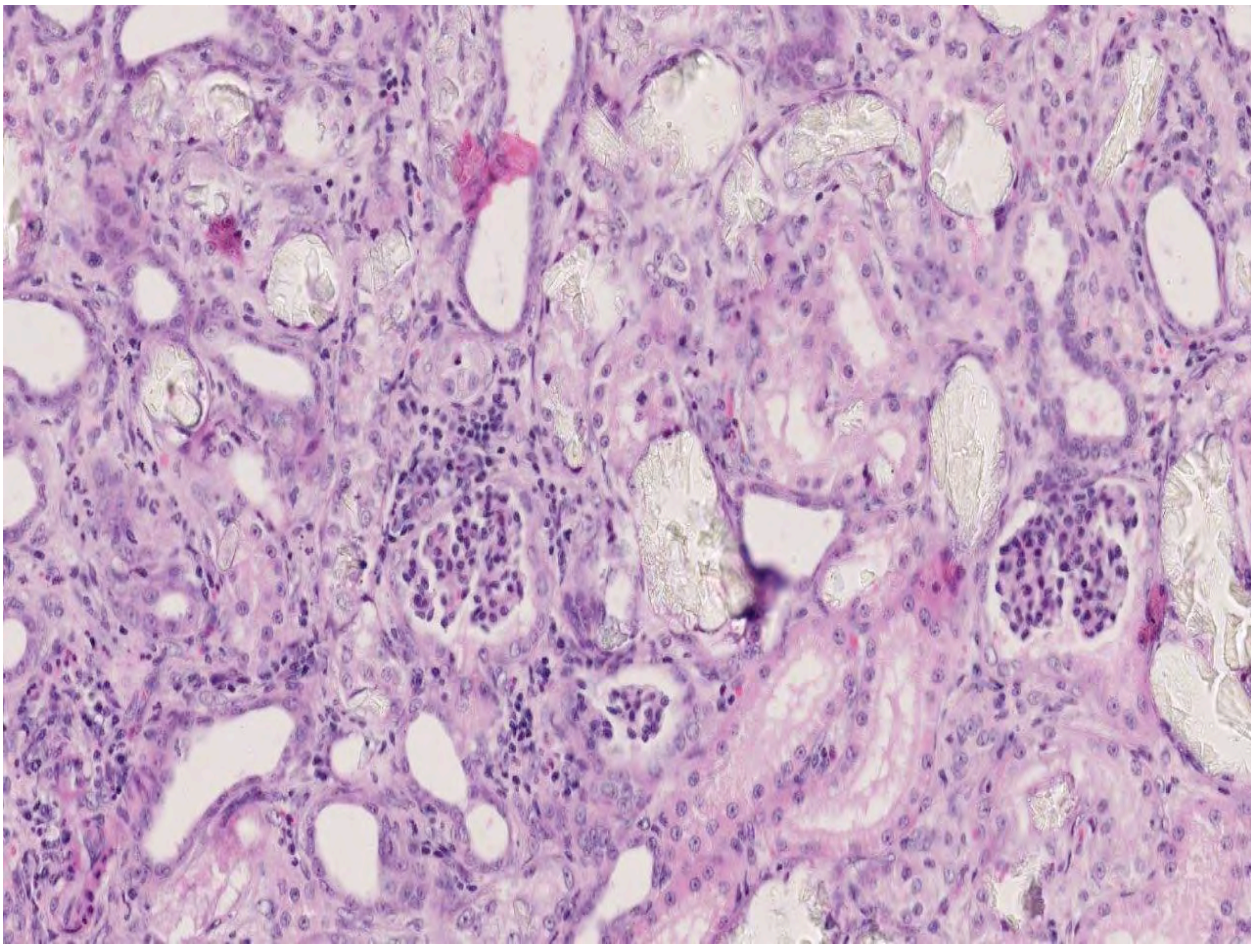

*1-1. Kidney, cat: In this section of kidney from a 3-month-old kitten (note immature glomeruli) ectatic tubules contain numerous fan-shaped, birefringent oxalate crystals. Tubules are multifocally lined by attenuated epithelium and plump basophilic epithelium (regenerating epithelium). There is moderate interstitial fibrosis and lymphocytic interstitial inflammation. (HE 168X)*

PH2, L-glyceric acid. The resultant errors in glyoxylate metabolism lead to markedly increased serum and urinary oxalate concentrations. Patients with PH2 also have L-glyceric aciduria as GRHPR mutations disrupt the hydroxypyruvate reductase pathway leading to production of L-glycerate in hepatocyte cytoplasm.[2,6] Mammals cannot metabolize oxalate, which is primarily excreted through the kidneys. In PH, oxalate binds with free calcium ions forming insoluble crystals; once the urine is super-saturated calcium oxalate crystals are deposited in renal tubules and, to a lesser extent, the renal interstitium. As renal excretion of oxalate declines, systemic deposition of calcium oxalate occurs and the retina, myocardium, central nervous system, skin, bone and blood vessel walls may be involved. Clinical disease in humans manifests by recurrent oxalate urolithiasis and nephrocalcinosis leading to end-stage renal failure and death, if untreated. Diagnosis is usually made when disease is already advanced; patients require dialysis and combined kidney and liver transplantation.[6]

A naturally occurring disease in cats, clinically similar to PH2 in humans, has been described in several instances.[2,3,4] As with humans, the disease is autosomal recessive and typically affects kittens between five and nine months of age. Affected animals develop acute renal failure with increased urinary oxalate and L-glyceric acid levels. Histologically, abundant oxalate crystals are present within renal tubules and occasionally Bowman's spaces, accompanied by acute tubular necrosis and, variably, mild interstitial fibrosis.[3] Also consistent with human PH2, *GRHPR* mutation has been associated with the feline disease in cats from one colony.[4] A point mutation in the acceptor site of intron 4 was identified and correlated with a frameshift and premature stop codon in RNA transcripts from affected cats.

Several distinct differences exist in the clinical presentation of feline primary hyperoxaluria and PH2 in humans. Human PH2 is typically diagnosed in adults when renal changes are chronic; stone formation is usually less severe than that observed in

PH1, which may present in infancy. By contrast, feline PH presents in young animals and is characterized by severe, acute disease. Concurrent neurologic lesions may accompany renal disease in cats and are histologically typified by swelling in the proximal axons of spinal motor neurons, ventral

**CASE II**: 1984511 (JPC 4017822).

**Signalment:** 5-month-old male Boxer, dog (*Canis lupus familiaris*).

**History:** The puppy was presented with a two- to three-month history of waxing and waning occurrence of inappropriate mentation, visual difficulties and lethargy. The clinical neurologist concluded that the animal had multifocal disease of the thalamocortex and brainstem, which was thought somewhat worse on the right side. Due to a poor prognosis, the puppy was euthanized. The brain was removed and portions submitted for rabies testing, which was negative, prior to postmortem examination of the rest of the body.

**Gross Pathology:** The puppy weighed 10.5 kg, had adequate fat stores, and, at the time of somatic necropsy after rabies testing, was severely autolyzed. No other gross findings were noted.

**Laboratory Results:** Negative rabies IFA at the public health department laboratory.

**Histopathologic Description:** Brain: The gray matter and immediately adjacent white matter of the medulla, excluding the vagal and hypoglossal nuclei, contain numerous lacey, irregularly interconnected, unstained vacuoles that are well defined. At the edges of some affected areas astrocytes possess enlarged, pale homogeneous nuclei. The gray matter of the caudate nucleus, globus pallidus, peri-aqueductal gray matter, parts of the reticular formation, thalamus and hypothalamus are similarly affected, with much less change in the cerebrum and cerebellum.
Liver: The hepatic lobules are mildly reduced in size. Although thin-walled veins are present in the largest portal areas near the capsule of the liver, none are apparent in the portal triads comprising the liver parenchyma.

**Contributor's Morphologic Diagnosis:** 1. Brain: Spongiform encephalopathy, gray matter, with astrocytic nuclear hypertrophy (Alzheimer type II astrocytes).
2. Portal vein hypoplasia, liver.

**Contributor's Comment:** Hepatoencephalopathy occurs in the presence of liver injury or, as in this case, if the liver is bypassed due to a portosystemic shunt.[1] Prominent histopathological changes found in encephalopathy that accompanies liver failure include Alzheimer's type II astrocytosis (i.e. enlarged astrocytes with pale, large nuclei and prominent nucleoli) and pronounced astrocytic swelling, leading to spongiform change. Hepatoencephalopathy can result from acute or chronic liver failure, including that resulting from portocaval shunts, and is considered to result from accumulation of toxic substances, principally ammonia, but impaired detoxification during liver failure results in increased blood levels of several toxic compounds.

In acute liver failure, spongiform encephalopathy may lead to increased intracranial pressure. Studies suggest that intracranial hypertension complicates 25% of acute liver failure cases in humans but only 9% of those with subacute liver failure. In acute liver failure, an arterial ammonia concentration greater than 150 µmol/L predicts a greater likelihood of dying from brain herniation.[1] Spongiform change can be found in a variety of species, with the exception of the horse.

Of the compounds that escape detoxification by the failing liver, ammonia most easily crosses the blood-brain barrier. Although other compounds contribute, ammonia is accepted as the central cause of hepatoencephalopathy. It is considered that astrocyte dysfunction is central to ammonia toxicity in hepatoencephalopathy, and that functional neuronal changes are secondary. Astrocytic end processes surround capillaries in the CNS. Normally, this would ensure that any toxin entering the brain, such as ammonia, would be immediately metabolized, protecting other CNS cells from damage. In acute liver failure, increased brain ammonia concentrations affect transit of electrolytes and water across cell membranes, and cause astrocyte swelling, with cytotoxic brain edema. Primary alteration of the blood brain barrier results in vasogenic edema as well. Opening of the blood-brain barrier is thought to further exacerbate aberrant neuronal transmission and entry of toxins besides ammonia. Immunohistochemical staining with GFAP demonstrates some astrocytes with dense robust processes, while others near vacuoles stain poorly. CD18 reagent revealed multifocal clusters of large cells, with microglial morphology in affected tissue.

Astrocytes perform a number of other important metabolic supportive functions for neurons, including supplying them with GSH, the main cytosolic antioxidant.[2] Significant reduction in the activities of glutathione peroxidase and superoxide dismutase enzymes occur in the brain of rats exposed to ammonium acetate.[1]
Astrocytes also control GABAergic and glutamatergic activities at the synapse, especially terminating excitotoxic action in the synaptic cleft. Astrocytes take up glutamate, metabolizing it to glutamine that is transported back to excitatory

neurons for neurotransmitter metabolism. In hepatoencephalopathy, there is correlation between astrocyte swelling and glutamine concentration. When the urea cycle is dysfunctional in the brain, ammonia is detoxified through its condensation with glutamate to form glutamine. Increased ammonia concentrations lead to mitochondrial permeability transition, and the loss of mitochondrial transmembrane potential.[1] Astrocytes also utilize glycolysis to produce lactate as a neuronal energy source.

There are additional roles for inflammation in hepatoencephalopathy. In advanced stages of acute liver failure, the brain produces a number of pro-inflammatory cytokines such as tumor necrosis factor-α (TNF-α), interleukin (IL)-1β and IL-6.

**JPC Diagnosis:** 1. Liver: Venous hypoplasia, portal and central, diffuse, marked, with arteriolar hyperplasia, lymphangiectasia, and mild lobular and hepatocellular atrophy.
2. Cerebral cortex, gray matter: Spongiform change, multifocal to coalescing, marked, with Alzheimer type II astrocytosis and microgliosis.

**Conference Comment:** Conference participants readily ascribed the lesions in the cerebral cortex to hepatoencephalopathy, and recognized the salient diagnostic features of a portosystemic shunt (PSS) in the liver. Attendees briefly reviewed canine congenital PSS, which are usually caused by a single large anomalous connection between the portal venous and systemic venous circulation. Intrahepatic shunts are most common in large-breed dogs and usually consist of a patent fetal ductus venosus in the left hepatic division. Extrahepatic shunts, more common in small-breed dogs and cats, usually consist of a direct shunt from the portal vein, gastric vein, or splenic vein to the caudal vena cava (i.e., portocaval shunt), or to the azygous vein (i.e., portoazygous shunt). Importantly, congenital PSS do not result in portal hypertension, whereas other congenital vascular anomalies, such as congenital arteriovenous fistulae, primary hypoplasia of the portal vein, and hepatoportal microvascular dysplasia, do cause portal hypertension, and can thus lead to ascites and the development of acquired portosystemic shunts.[3]

The conference moderator led a review of the serum biochemistry abnormalities typical of PSS with hepatic atrophy. Fasting and postprandial serum bile acid concentrations are elevated for at least two reasons: 1) portal blood has a high concentration of bile acids, and bypasses the liver, which in health removes approximately 95% of bile acids from portal blood; and 2) hepatic atrophy that follows chronic shunting causes loss of hepatic functional mass, impairing the liver's ability to clear bile acids from the blood. Hyperammonemia, as discussed by the contributor, is also usually present in PSS because ammonia bypasses the liver, where hepatic urea cycle enzymes catalyze its conversion to urea. Consequently, animals with PSS may develop ammonium biurate crystalluria, as ammonium biurate precipitates in alkaline urine. With chronicity and the development of hepatic atrophy, loss of hepatic functional mass may result in hypoalbuminemia, hypoglycemia, hypocholesterolemia and/or decreased blood urea nitrogen (BUN) concentrations. Levels of cholestatic markers (e.g. alkaline phosphatase, gamma glutamyltransferase) and hepatocellular

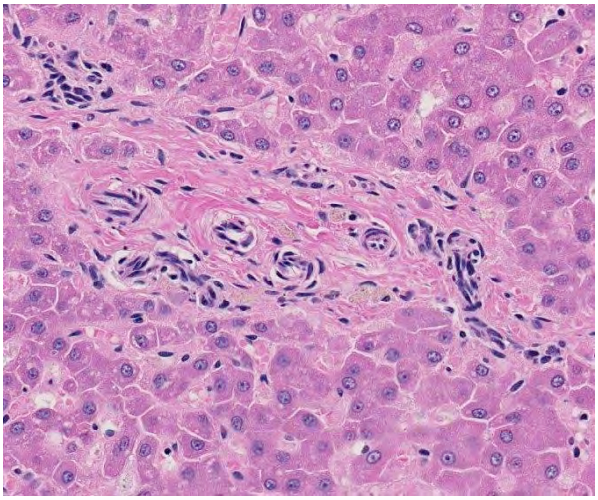

*2-1. Liver, 5-month-old Boxer: Portal areas contain numerous cross sections of hepatic arterioles, without a single portal vein. Surrounding hepatocytes are decreased in size (atrophy). These changes are characteristic of microvascular dysplasia. (HE 220X)*

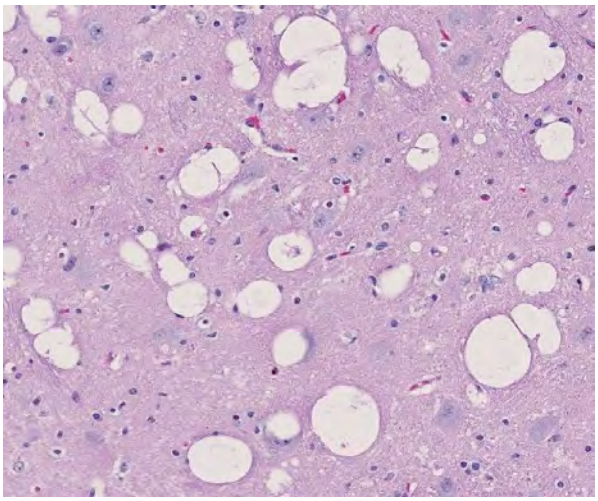

*2-2. Cerebrum, 5-month-old Boxer: The grey matter contains numerous clear discrete vacuoles (spongiosis). (HE 100X)*

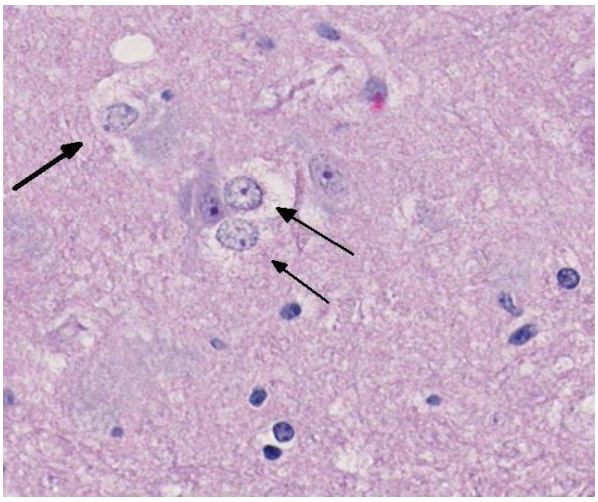

*2-3. Cerebrum, 5-month-old Boxer: Within the spongiotic section of the cerebrum, there are moderate numbers of astrocytes with moderate amounts of amphophilic cytoplasm and large, vesicular nuclei (Alzheimer's Type II astrocytes). (HE 140X)*

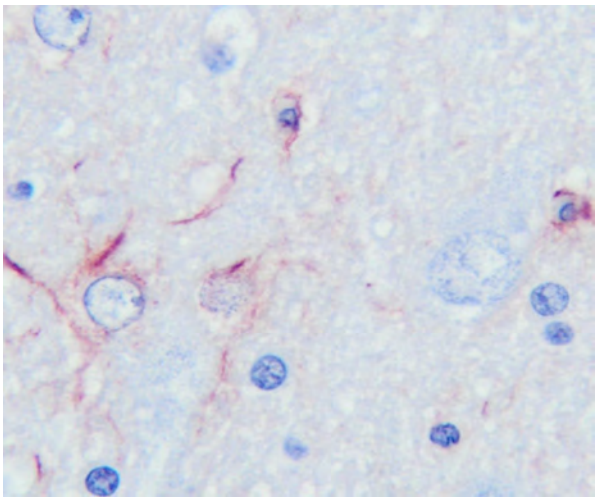

*2-4. Cerebrum, 5-month-old Boxer: Alzheimer's Type II astrocytes exhibit poor staining with glial fibrillary acidic protein> (HE 280X). (Photo courtesy of: The Veterinary Medical Diagnostic Laboratory and Department of Veterinary Pathobiology, University of Missouri, http://www.cvm.missouri.edu/vpbio)*

leakage enzymes (e.g. alanine transaminase, aspartate transaminase, sorbitol dehydrogenase, glutamate dehydrogenase) are usually within reference intervals. Animals with PSS may have microcytic anemia of unknown cause.[4]

**Contributing Institution**: Veterinary Medical Diagnostic Laboratory and Department of Veterinary Pathobiology
University of Missouri
http://www.cvm.missouri.edu/vpbio

**References:**

1. Seyan AS, Hughes RD, Shawcross DL. Changing face of hepatic encephalopathy: role of inflammation and oxidative stress. *World J Gastroenterol.* 2010;16:3347-3357.
2. Sidoryk-Wegrzynowicz M, Wegrzynowicz M, Lee E. Bowman AB, Aschner M. Role of astrocytes in brain function and disease. *Toxicol Pathol.* 2011;13:115-123.
3. Stalker MJ, Hayes MA. Liver and biliary system. In: Maxie MG, ed. *Jubb, Kennedy and Palmer's Pathology of Domestic Animals*. 5th ed. Philadelphia, PA: Elsevier Saunders; 2007:2:302-304.
4. Bain PJ. Liver. In: Latimer KS, ed. *Duncan & Prasse's Veterinary Laboratory Medicine Clinical Pathology*. 5th ed. Ames, Iowa: Wiley-Blackwell; 2011:227, 415-417.

**CASE III**: S1269/08 (JPC 3138060).

**Signalment:** 17-year-old gelded Westfalian warmblood, horse (*Equus caballus*).

**History:** The horse had an eight-week history of pneumonia. Physical examination revealed a reduced nutritional status, and a purulent exudate was detected within the trachea. Microbiological investigation yielded growth of *Aspergillus fumigatus* within the tracheal fluid. Based on the thoracic radiography results, a granulomatous pneumonia was suspected. Due to unsuccessful treatment, the horse was eventually euthanized for animal welfare reasons.

**Gross Pathologic Findings:** The horse was in a reduced nutritional condition. Necropsy revealed that the main lesions were restricted to the lung. Lung parenchyma was interspersed with multiple large, bulging, coalescent, tan to white and firm nodules of fibrosis affecting all lobes. The patchy areas of fibrosis had predominantly distinct borders to the adjacent normal appearing lung tissue. The cut surfaces of the nodules were homogeneously tan to white. Numerous subpleural hyperemic blood vessels and emphysema of the cranial lung lobes were additionally detected. The bronchial lymph nodes were noticeably enlarged. Furthermore, the trachea revealed a streaky redness of mucosa.

**Laboratory Results**: Lung: DNA of both equine herpesvirus type 5 (EHV-5) and EHV-2 was detected using standard PCR analysis.
Tracheal fluid: mild growth of *Candida* species.

**Histopathologic Description:** The lung fibrosis resulted in a vast interstitial expansion and eventually led to a complete remodeling of the lung architecture and formation of abnormal cystic airspaces (honeycombing). These airspaces were lined by a cuboidal epithelium. According to the

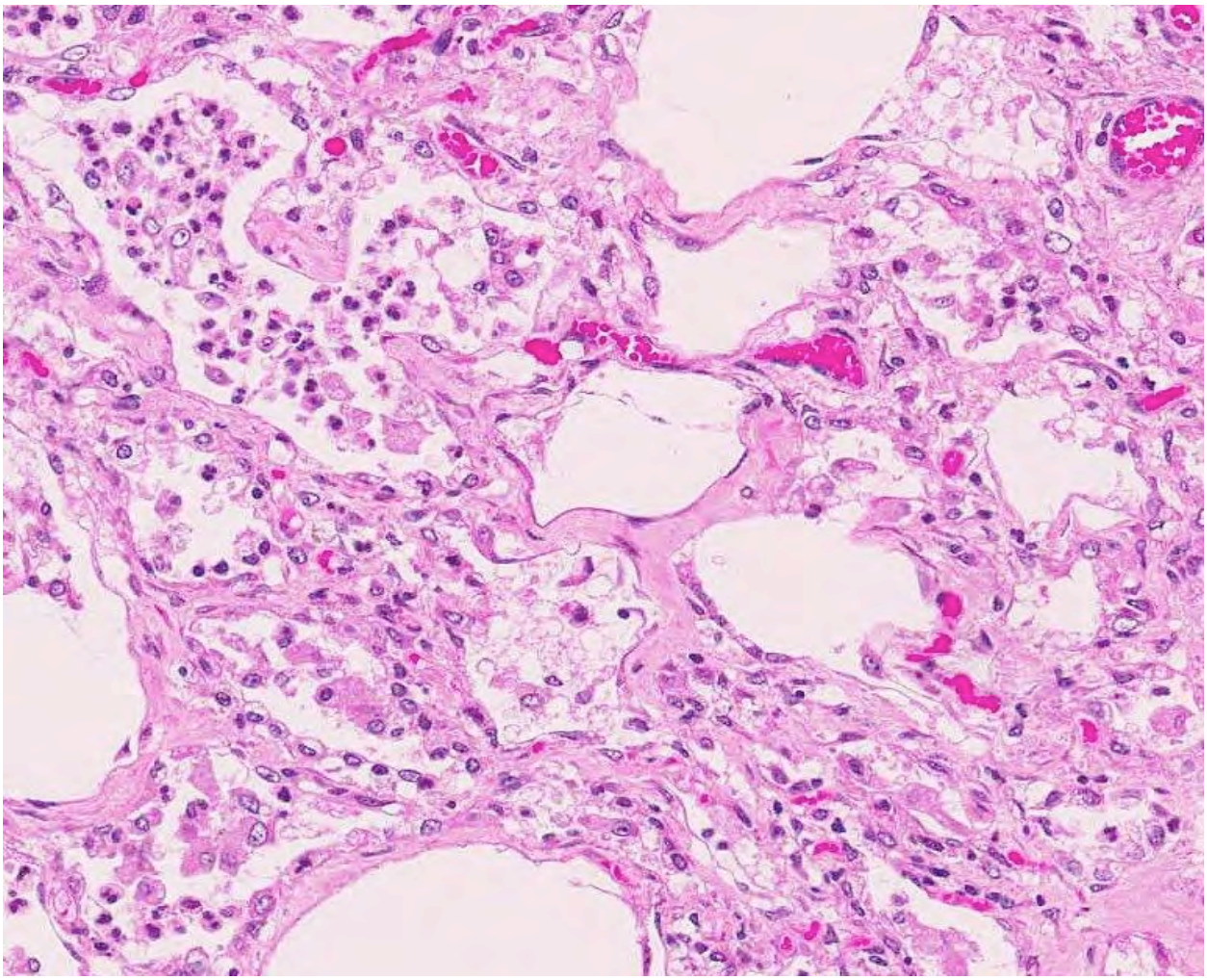

*3-1. Lung, horse: Diffusely throughout the section, alveolar septa are thickened up to ten times by a combination of mature collagen (center), plump fibroblasts, and type II pneumocytes hyperplasia. Alveolar spaces contain moderate numbers of neutrophils and macrophages. (HE 256X)*

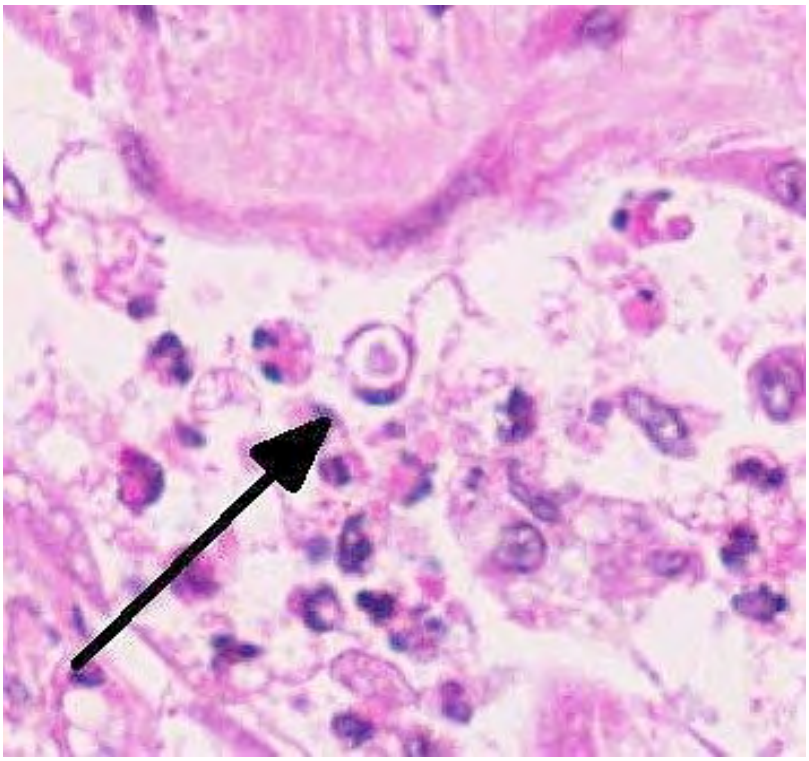

*3-2. Lung, horse: Within alveolar spaces, macrophage nuclei occasionally contain a single 4µm eosinophilic viral inclusion surrounded by a clear halo. (HE 400X)*

gross findings, the nodular lesions were sharply demarcated from normal parenchyma. The interstitium was infiltrated by numerous inflammatory cells including lymphocytes, plasma cells and neutrophils as well as some eosinophils and multinucleated giant cells. The bronchioli, alveoli, and abnormal cystic airspaces were filled with numerous large vacuolated macrophages and neutrophils. Occasionally, some multinucleated giant cells were detected. Within lung areas with chronic inflammatory lesions, a few enlarged intraluminal macrophages were found that showed eosinophilic intranuclear inclusion bodies (Cowdry type A). Some lung areas revealed a marked alveolar edema and hyperplasia of type II pneumocytes. Special stains for bacteria and fungi yielded negative results. The bronchiolar lymph nodes were severely hyperplastic. Acute hemorrhages were found within submucosal and muscular layers of the trachea. No inflammation and no pathogenic agents were detectable within the tracheal mucosa using special staining methods.

**Contributor's Morphologic Diagnosis**: Lung: Equine multinodular pulmonary fibrosis (EMPF).

**Contributor's Comment**: Equine multinodular pulmonary fibrosis (EMPF) is a chronic and fibrosing interstitial lung disease in adult horses that results in characteristic lung lesions. The disease was first recognized in 2005 by Williams et al.[1] and further cases in the USA and Europe have recently been described.[2-5] In all reported cases, the disease was associated with an infection of EHV-5, which belongs to the genus percavirus that is actually classified within the gammaherpesvirus subfamily.[6] A co-infection with EHV-2 was detected in several cases, but it seems not to be associated with EMPF.[2,3,5] In horses suffering from EMPF, the lung lesions differ significantly from other interstitial fibrosis in lung diseases due to their nodular pattern, the parenchymal remodeling with honeycombing and the presence of intranuclear viral inclusion bodies within intraluminal macrophages. Other noxa, such as thermal and chemical injury, toxic gases, ingested toxins, endotoxins, pneumoconiosis, uremia and chronic left heart failure could be excluded in the present case as cause for interstitial pneumonia. The pathogenesis of EMPF is unclear at the moment.

**JPC Diagnosis:** Lung: Fibrosis, interstitial, diffuse, severe, with histiocytic and neutrophilic alveolitis, type II pneumocyte hyperplasia and rare eosinophilic intrahistiocytic intranuclear viral inclusions.

**Conference Comment:** As noted by the contributor, Koch's postulates have not yet been fulfilled to definitively establish EHV-5 as the etiology of EMPF. Moreover, asinine herpesvirus-5 (AHV-5) has also been detected by PCR either alone, or in combination with EHV-5, in some cases of EMPF, suggesting that other herpesviruses may be involved in the pathogenesis of the disease. An analogous human condition, idiopathic pulmonary fibrosis (IPF) is similarly attributed to an array of potential causes, including pneumocyte injury, abnormal fibroplasia, inflammation, and the excessive deposition of extracellular matrix proteins. As with EMPF, gammaherpesviruses have been implicated in the pathogenesis and/or exacerbation of IPF, as well as IPF-like lesions in mice.[7]

Conference participants discussed the importance of the cytokine milieu in driving macrophage activation and expression, and speculated that, based on the degree of fibroplasia that typifies EMPF, alternative (M2) activation of macrophages is most

likely to predominate in this condition. Monocytes exposed to the signature cytokines of Th2 lymphocytes (i.e., IL-4 and IL-13) undergo alternative (M2) activation to mature into a fibrotic phenotype and produce polyamines that drive cell proliferation, and proline and TGF-β that drive collagen production.[8]

Other notable gammaherpesviruses of importance in animals were briefly reviewed, including those associated with IPF-like lesions in the lungs of mice (i.e., Murine herpesvirus-68), urogenital carcinomas in California sea lions (i.e., Otarine herpesvirus-1), and malignant catarrhal fever in ruminants (i.e., Alcelaphine herpesvirus-1, Alcelaphine herpesvirus-2, Hippotragine herpesvirus-1, Ovine herpesvirus-2, Caprine herpesvirus-2 and MCFV-white tailed deer).

**Contributing Institution:** Institute of Veterinary Pathology
Ludwig-Maximilians-University Munich
Veterinaestrasse 13
D-80539
Munich Germany
www.patho.vetmed.uni-muenchen.de

**References:**

1. Williams KJ, Jackson CA, Scott MA, Robinson NE, Derksen FJ, Macs R, et al. Multinodular equine pulmonary fibrosis: a newly recognized herposvinis associated respiratory disease of horses. ACVP/ASVCP meeting. *Vet Pattie'*. 2005;42:716.
2. Williams KJ, Maes R, Del Piero F, Lim A, Wise A, Bolin DC, et al. Equine multinodular pulmonary fibrosis: a newly recognized herpesvirus-associated tihtotic lung disease. *Vet Pathol*. 2007;44:849-862.
3. Hart KA, Barton MH, Williams KJ, Flaminio MJBF, Howerth EW. Pulmonary fibrosis, pancytopenia and equine herpesvirus-5 infection in a Thoroughbred gelding. *Equine Vet Educ*. 2008;20:470-6.
4. Wong DM, Belgrave RL, Williams KJ, Del Piero F, Alcott CJ, Bolin SR, et al. Multinodular pulmonary fibrosis in five horses. *J Am Vet Med Assoc*. 2008;232:898-905.
5. Poth T, Niedermaier G, Hermanns W. Equine multinodular pulmonary fibrosis (EMPF) in association with an EHV-5 infection in 5 horses. *Wien Tierailt1 Monatsschr*. 2009;96:203-8.
6. McGeoch DJ, Rixon FJ, Davison AJ. Topics in herpesvirus genomics and evolution. *Virus Res*. 2006;117:90-104.
7. Back H, Kendall A, Grandon R, Ullman K, Treiberg-Berndsson L, Stahl K, et al. Equine multinodular pulmonary fibrosis in association with Asinine herpesvirus type 5 and Equine herpesvirus type 5: a case report. *Acta Veterinaria Scandinavica*. 2012;54:57.
8. Ackermann MR. Inflammation and healing. In: Zachary JF, McGavin MD, eds. *Pathologic Basis of Veterinary Disease*. 5th ed. St. Louis, MO: Elsevier; 2012: 128-130.

**CASE IV:** 10L-3893 (JPC 4002755).

**Signalment:** 18-month-old, female, Cavalier King Charles Spaniel, dog (*Canis familiaris*).

**History:** 48-hour history of hematochezia, icterus and collapse with marked anemia (PCV 7%) with regeneration. Prior to presentation the referring veterinary surgeon removed a gastric metallic foreign body, an identification tag, via gastrotomy.

**Gross Pathology:** There was moderate to severe icterus observed throughout the subcutis, sclera and visceral adipose tissue. The cut surfaces of both kidneys were diffusely very dark red. The urinary bladder contained a small volume of red-tinged urine (pigmenturia). The pancreas was diffusely pale and nodular, and on the cut surface there were multifocal, variably sized (~2 mm – 1 cm), dark red, approximately spherical to irregularly shaped, soft foci (necrosis). The descending colon and rectum contained a moderate amount of soft, red-tinged fecal material (evidence of hematochezia).

**Laboratory Results:**

Haematology - PCV 7%
- degenerative left shift
- reticulocytes 5%

Biochemistry - urea 45.7 mmol/l (3.5 – 6.0)
- creatinine 243 µmol/l (20 – 110)
- ALP 497 U/l (0 – 100)
- ALT 136 U/l (7 – 50)

APTT -123 seconds (8 -12)

Tissue chemical analysis

| Test | Units (Wet weight) | Ref range (normal) | Ref (toxic) | CASE |
|---|---|---|---|---|
| **Zinc (Liver)** | **ppm** | **30-70** | **204-436** | **165** |
| **Zinc (Kidney)** | **ppm** | **16-30** | **190-295** | **141** |

**Histopathologic Description:** Kidney: Multifocally within renal tubular lumina throughout the cortex and medulla, there is moderate to marked accumulation of eosinophilic material which varies from coarsely granular to hyaline or crystalloid (hemoglobin). Similar coarsely granular, eosinophilic material is also present within vascular lumina, and no intact erythrocytes are observed. Multifocally, tubular epithelial cells are expanded by mild to moderate accumulation of cytoplasmic eosinophilic material (hemoglobin). There are focal areas where tubular epithelial cells appear hypereosinophilic with nuclei exhibiting clumped chromatin or karyorrhexis (acute tubular necrosis). There are mild, multifocal infiltrates of lymphocytes (mild, tubulo-interstitial nephritis). There is focally mild accumulation of coarsely granular eosinophilic material within the urinary space of glomeruli.

Pancreas: Throughout the exocrine pancreas there are multifocal, variably sized (2-5 mm), irregularly shaped, moderately well demarcated areas characterized by hypereosinophilia of the acinar cells and disruption of acinar architecture (necrosis). The centers of these foci exhibit disorganized accumulations of proteinaceous and nuclear debris with some nuclei exhibiting pyknosis and karyorrhexis, with few scattered acinar cells remaining. Multifocally at the periphery of these foci and within sub-capsular connective tissue are variable numbers of neutrophils. Pancreatic lobules are separated by mildly edematous interstitium. Peripancreatic and interstitial adipose tissue often contains foci of amorphous basophilic to amphophilic material with numerous macrophages with vacuolated cytoplasm (foamy) with neutrophils and spindloid cells with plump, ovoid nuclei (fat necrosis).

Some sections also contain a small amount of unaltered duodenum.

**Contributor's Morphologic Diagnosis:** 1. Kidney – multifocal to diffuse, moderate intratubular and intravascular hemoglobin accumulation with hemoglobin cast formation, with mild, multifocal acute tubulonecrosis and mild, multifocal, chronic, lymphocytic tubulo-interstitial nephritis.
2. Pancreas – multifocal, severe, acute pancreatic necrosis with mild acute neutrophilic pancreatitis and fat necrosis.

**Contributor's Comment:** The pathological changes confirmed the clinical suspicion of acute hemolytic anemia by demonstrating marked intratubular and intravascular accumulation of hemoglobin; the hyaline hemoglobin casts being a typical presentation. Staining of sections of kidney with Dunn-Thompson's stain confirmed the hyaline tubular casts to be hemoglobin. There were also areas of mild acute tubulonecrosis and inflammation. Acute pancreatic necrosis was also demonstrated. These findings, together with the history of prior removal of a metallic gastric foreign body, lead to the presumptive diagnosis of zinc intoxication, which was confirmed by the markedly raised levels of zinc in the liver and kidney. Although the zinc levels in liver and kidney post-

mortem are below the reference toxic range, it has been shown in similar cases that after removal of the offending foreign body, zinc levels decline rapidly, and it is considered likely that in this case tissue levels would have been higher whilst the foreign body was present in the stomach.[11]

Zinc intoxication has been reported in the USA on several occasions since the mid 1980s, often as a consequence of ingestion of zinc-containing coins;[4] there have also been cases reported in Europe.[1,2] In a review of 19 cases, the most common presenting clinical signs included hemolytic anemia, gastrointestinal disturbances and pigmenturia.[4] Acute pancreatic necrosis (acute pancreatitis) has been reported previously in only two dogs.[8,11] Zinc toxicity may result from ingestion of zinc-containing metallic foreign bodies as the acidic pH of gastric secretions liberates zinc which facilitates absorption, it is bound to albumin and macroglobulins where it is transported to the liver before being distributed to pancreas, kidney and spleen.[3]

The mechanism underlying the zinc-associated hemolysis is not completely elucidated. Suggested mechanisms include oxidative injury due to inhibition of glutathione reductase or enzymes of the hexose-monophosphate pathway,[5] however, oxidative stress often leads to Heinz body formation in erythrocytes, and in the aforementioned review, only 33% of cases exhibited Heinz body formation, suggesting other mechanisms may also be present.[4] During clinical examination, biochemical analysis revealed azotaemia in this case, and histological examination of the kidneys revealed scattered areas of acute tubulonecrosis. Zinc is not considered to be a direct nephrotoxin, but the marked hemolysis and intratubular accumulation of hemoglobin is likely to have lead to hemoglobinuric nephrosis. In this condition, while hemoglobin is not a primary nephrotoxin it is thought to lead to an ischemic necrosis through other mechanisms such as hypotension.[6] The extended activated partial thromboplastin time is of uncertain pathogenesis, but it has been hypothesized that zinc may inhibit certain coagulation factors, e.g. VIII, IX, XI and XII.[7]

The mechanism underlying the acute pancreatic necrosis is similarly poorly defined. Zinc has been shown to be concentrated in the pancreas of the dog, [8] and to cause acute acinar cell necrosis and pancreatitis in mice.[9] The pancreas plays an important part in zinc homeostasis and contains high levels of metallothionein (MT). In studies on zinc-induced pancreatitis in mice, pretreatment with non-toxic doses of zinc protect the pancreas from a toxic dose if given 24 hours prior to the toxic dose, apparently by induction of MT which is able to sequester excess zinc.[9,10] If the pretreatment is given 2 hours prior to the toxic dose or no pretreatment is given, however, the toxic mechanism in mice appears to be related to free zinc ions or zinc bound to low molecular weight proteins, and there is no increase in the MT-bound fraction.[10] These studies also showed that pre-treatment of the mice with a trypsin inhibitor before zinc challenge attenuated the signs of pancreatitis, i.e. serum amylase activity, suggesting that zinc-induced pancreatitis may be related to activation of trypsinogen. The underlying mechanism remains unclear, although there has been speculation over the role of oxidative stress in the pancreas.[10]

**JPC Diagnosis:** 1. Pancreas: Acinar degeneration and necrosis, acute, multifocal to coalescing, marked with edema, necrosis and saponification of peripancreatic adipose tissue.
2. Kidney, tubules: Degeneration and necrosis, acute, diffuse, marked, with tubulorrhexis, edema and many intratubular protein and hemoglobin casts.

**Conference Comment:** The contributor provides an excellent review of zinc toxicosis. The submitted section of kidney provides for an edifying contrast with Case I from this conference. While both sections feature abundant tubular degeneration and necrosis, a key difference is the presence of tubulorrhexis in this case. Tubulorrhexis, or necrosis of the tubular epithelial cells accompanied by rupture or loss of the basement membrane, is often a consequence of ischemic damage. Its presence in this case supports the idea, noted by the contributor, that ischemia is at least part of the mechanism underlying hemoglobinuric nephrosis. In addition to providing clues to the mechanism of tubular damage, the presence of tubulorrhexis has important implications for the ability of the tubule to respond to injury. Although glomeruli are essentially incapable of regeneration, tubular epithelial cells can regenerate and reepithelialize the tubule following injury as long as the basement membrane remains intact, as was evidenced in case 1. Intact basement membranes not only form an effective barrier system for defense against injury and infectious agents; they also form the scaffolding for tubule reepithelialization.[12]

Zinc toxicosis uniformly topped conference participants' differential diagnoses based on the combination of pancreatic and renal lesions evident in this case. Other common causes of hemoglobinuric nephrosis include immune-mediated hemolytic anemia in dogs, red maple leaf toxicosis in horses, babesiosis in dogs and cattle, leptospirosis in cattle, and chronic copper toxicosis in sheep.[12] In

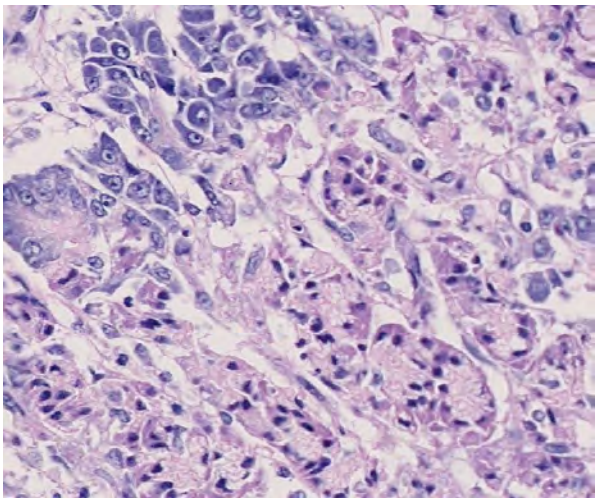

*4-1. Pancreas, dog: There is extensive necrosis of pancreatic acinar tissue. Adjacent viable pancreatic acini show degenerative changes, including disorganization of acinar architecture and loss of zymogen granules. (HE 284X)*

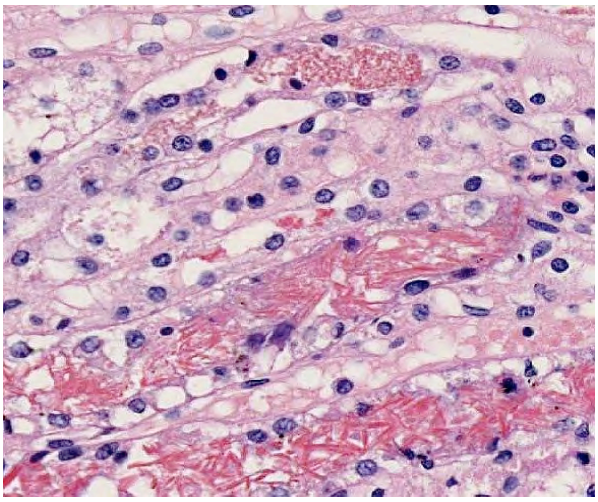

*4-2. Kidney, dog: Throughout the kidney (here in the medulla), tubular lumina are filled with a bright red granular material (hemoglobin) which forms granular (top), and specular arrangements. (HE 284X)*

intravascular hemolysis, free hemoglobin is bound by an α2-globulin carrier, haptoglobin; hemoglobin-haptoglobin complexes are cleared by the liver, preventing loss of hemoglobin in the urine. Haptoglobin is usually present in sufficient quantities to bind hemoglobin up to 150 mg/dL. Since hemoglobin causes pink to red discoloration of plasma at much lower concentrations (i.e. 50-100 mg/dL), plasma discoloration precedes the development of hemoglobinuria. When haptoglobin becomes saturated, excess hemoglobin dissociates into dimers, which pass freely through the glomerulus, and are absorbed by the proximal convoluted tubule and catabolized to iron, bilirubin, and globin. Excess unabsorbed hemoglobin passes into the urine, causing hemoglobinuria.[13]

Conference participants briefly reviewed the differential diagnosis for causes of red-brown urine with a positive occult blood test: hematuria, hemoglobinuria, and myoglobinuria. Hematuria usually clears with centrifugation; the presence of erythrocytes in the urine sediment and absence of clinical or laboratory evidence of hemolytic anemia or muscle disease are also supportive of the diagnosis. Neither hemoglobin nor myoglobin will clear upon centrifugation of urine; however, the addition of saturated ammonium sulfate solution will clear the urine sample by precipitating hemoglobin. Clinical evidence of intravascular hemolysis and the presence of pink to red discolored plasma further support the diagnosis. Saturated ammonium sulfate will not clear myoglobin from the urine, and the plasma should remain clear.[14]

**Contributing Institution:** School of Veterinary Science

University of Liverpool
Crown Street
Liverpool
L69 7ZJ
United Kingdom
www.liv.ac.uk/vets/index.htm

**References:**

1. Bexfield N, Archer J, Herrtage M. Heinz body haemolytic anaemia in a dog secondary to ingestion of a zinc toy: a case report. *Vet J*. 2007;174:414-417.
2. Gandini G, Bettini G, Pietra M, Mandrioli L, Carpene E. Clinical and pathological findings of acute zinc intoxication in a puppy. *J Small Anim Pract*. 2002;43:539-542.
3. Garland T. Zinc. *Veterinary Toxicology - Basic and Clinical Principles*. Oxford, UK: Elsevier; 2007.
4. Gurnee CM, Drobatz KJ. Zinc intoxication in dogs: 19 cases (1991-2003). *J Am Vet Med Assoc*. 2007;230:1174-1179.
5. Luttgen PJ, Whitney MS, Wolf AM, Scruggs DW. Heinz body hemolytic anemia associated with high plasma zinc concentration in a dog. *J Am Vet Med Assoc*. 1990;197:1347-1350.
6. Maxie MG, Newman SJ. Urinary system. In: Maxie MG, ed. *Jubb, Kennedy and Palmer's Pathology of Domestic Animals*. Edinburgh, UK: Elsevier; 2007:425-522.
7. Meurs KM, Breitschwerdt EB, Baty CJ, Young MA. Postsurgical mortality secondary to zinc toxicity in dogs. *Vet Hum Toxicol*. 1991;33:579-583.
8. Mikszewski JS, Saunders HM, Hess RS. Zinc-associated acute pancreatitis in a dog. *J Small Anim Pract*. 2003;44:177-180.

9. Onosaka S, Tetsuchikawahara N, Min KS. Paradigm shift in zinc: metal pathology. *Tohoku J Exp Med*. 2002;196:1-7.
10. Tetsuchikawahara N, Min KS, Onosaka S. Attenuation of zinc-induced acute pancreatitis by zinc pretreatment: Dependence on induction of metallothionein synthesis. *Journal of Health Science*. 2005;51:379-384.
11. Weingart C, Kohn B. Zinc intoxication in a Yorkshire Terrier due to Euro cent ingestion. *Schweiz Arch Tierheilkd*. 2009;151:75-81.
12. Newman SJ. The urinary system. In: Zachary JF, McGavin MD, eds. *Pathologic Basis of Veterinary Disease*. 5th ed. St. Louis, MO: Elsevier; 2012:600-602, 632.
13. Brockus CW. Erythrocytes. In: Latimer KS, ed. *Duncan & Prasse's Veterinary Laboratory Medicine Clinical Pathology*. 5th ed. Ames, Iowa: Wiley-Blackwell; 2011:12-13.
14. Tripathi NK, Gregory CR, Latimer KS. Urinary system. In: Latimer KS, ed. *Duncan & Prasse's Veterinary Laboratory Medicine Clinical Pathology*. 5th ed. Ames, Iowa: Wiley-Blackwell; 2011:262.

**Joint Pathology Center**
**Veterinary Pathology Services**

# WEDNESDAY SLIDE CONFERENCE 2012-2013

## Conference 25

**15 May 2013**

---

**CASE I:** A12-3507 (JPC 4017798).

**Signalment:** 11-year-old Saddlebred gelding, horse, *Equus caballus.*

**History:** This horse was referred to Purdue University Veterinary Teaching Hospital after being rescued from a barn fire. The horse had been treated with intranasal oxygen by firefighters, with dexamethasone and furosemide by the attending veterinarian. Of four other horses in the barn, two died and two remained stable.

On admission, the horse had marked respiratory distress (manifested by nostril flaring, increased abdominal efforts, and cyanotic mucous membranes) and evidence of pulmonary edema

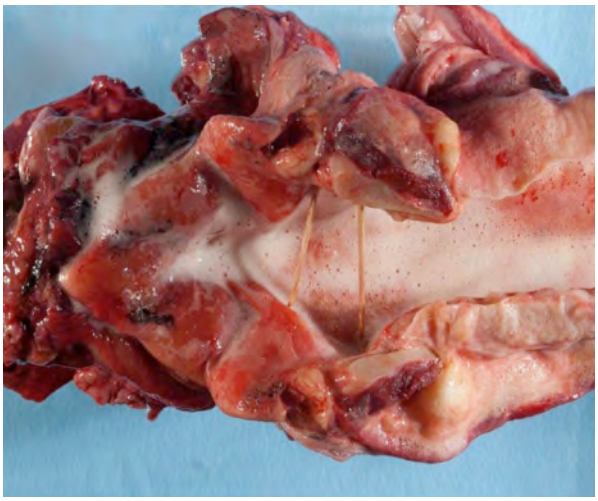

*1-1. Larynx, horse: The larynx was diffusely thickened by edema with streaks and there are specks of black granular material on the mucosal surface. The lumen contains abundant froth. (Photo courtesy of: Purdue University Department of Comparative Pathobiology, 725 Harrison St., West Lafayette, IN 47907 (http://www.vet.purdue.edu/cpb/)*

*1-2. Lung, horse: The lungs were heavy, wet, and non-collapsing. On cut section, abundant clear colorless to red frothy fluid flowed from the airways and pulmonary parenchyma. Aggregates of black fibrillar to granular specks were in the pulmonary parenchyma and tracheobronchial lymph nodes. (Photo courtesy of: Purdue University Department of Comparative Pathobiology, 725 Harrison St., West Lafayette, IN 47907 (http://www.vet.purdue.edu/cpb/)*

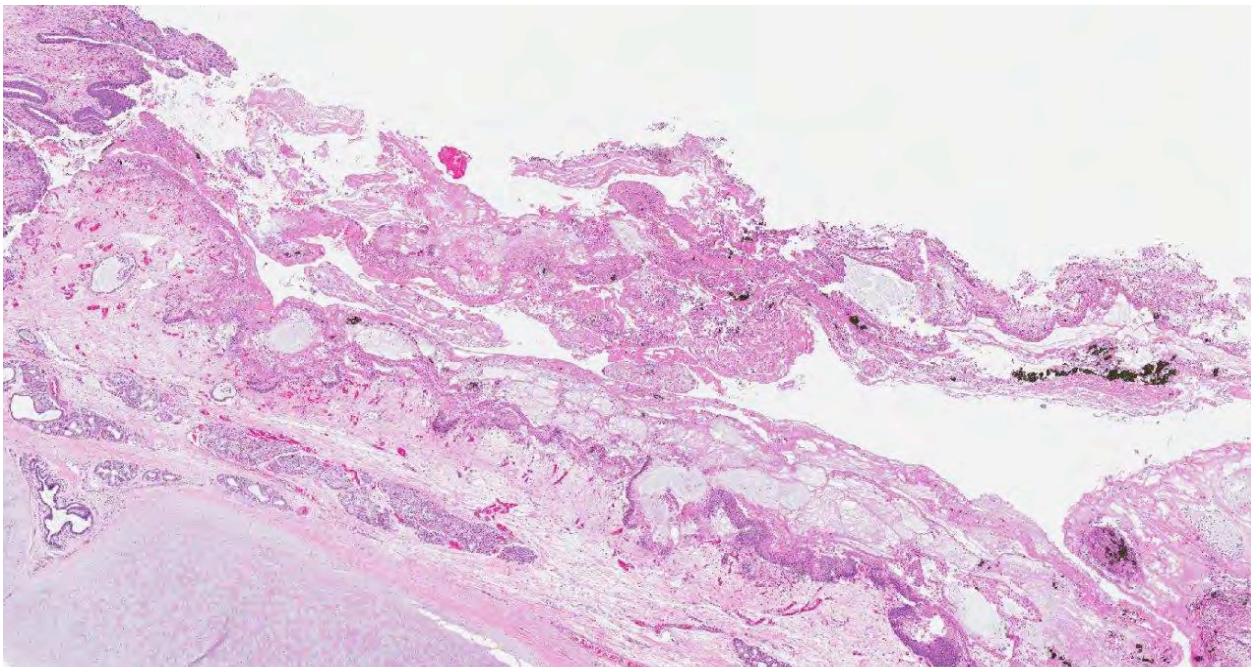

*1-3. Larynx, horse: There is partial- to full-thickness necrosis of the laryngeal epithelium (normal at extreme left). The submucosa is markedly edematous. (HE 15X)*

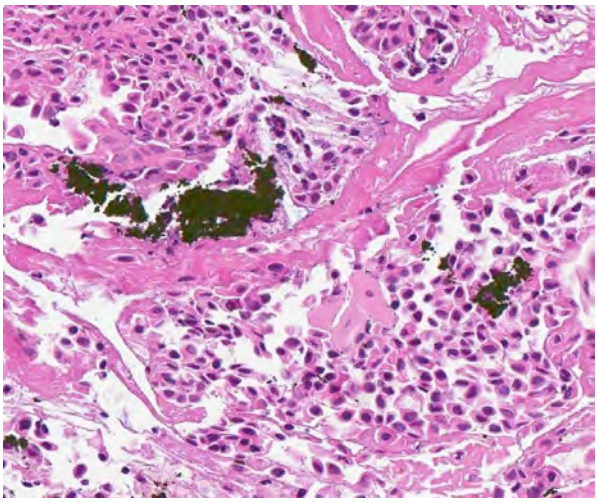

*1-4. Larynx, horse: The sloughed and necrotic epithelium contains multifocal aggregates of dark granular carbon particles (soot). (HE 232X)*

(frothy nasal discharge and bilateral crackles on thoracic auscultation). It also had tachycardia with hypovolemia and marked hypoxemia. Despite supportive treatment, the horse's condition did not improve, so it was humanely euthanized.

**Gross Pathology:** The nasal and pharyngeal mucosa was diffusely thickened, dark red to green, wet, and glistening with streaks or mats of black granular material. The larynx was diffusely thickened by edema with streaks or specks of black granular material on the mucosal surface. The tracheal lumen was filled with clear frothy fluid; tracheal submucosa was diffusely expanded with transparent yellow edema fluid. The lungs were heavy, wet, and non-collapsing. On cut section, abundant clear colorless to red frothy fluid flowed from the airways and pulmonary parenchyma. Aggregates of black fibrillar to granular specks were in the pulmonary parenchyma and tracheobronchial lymph nodes. The pericardium contained approximately 50 ml of serosanguineous fluid.

**Histopathologic Description:** Pharyngeal and laryngeal mucosa is eroded or ulcerated with fibrinosuppurative exudate, free erythrocytes and carbon particle accumulation. The propria-submucosa is expanded by poorly stained edema fluid and variably sized aggregates of neutrophils. Blood vessels are distended with blood. Lymphatic vessels and some glands and ducts contain numerous neutrophils and macrophages. The remaining epithelial lining has a few necrotic ciliated epithelial cells with pyknosis and hypereosinophilic cytoplasm. In the lung (not included in the submitted slide), bronchi and bronchioles were partially or totally obstructed by thick, amphophilic mucus mixed with black carbon particles, numerous leukocytes, including neutrophils, mast cells, and eosinophils, and sloughed epithelial cells. The associated bronchial/bronchiolar epithelium was multifocally attenuated

or sloughed. The interlobular septa were diffusely expanded by poorly stained edema fluid.

**Contributor's Morphologic Diagnosis:** Necrotizing pharyngitis and laryngitis with intralesional carbon particles.

**Contributor's Comment:** Inhalation of smoke and associated gases in a closed space can cause severe acute respiratory injury, which is a major cause of death in fires.[2,4,5,6] The severe acute respiratory injury that occurs in barn fires can be explained through three pathophysiological mechanisms; direct thermal injury, carbon monoxide intoxication, and chemical irritation.[4,6] Thermal injury causes local edema, necrosis, inflammation and upper airway obstruction by direct insult to the microvasculature and coagulation of tissue.[6] Carbon monoxide, which is produced by incomplete combustion, leads to delayed or interrupted oxygen delivery due to low blood oxygen content, which can lead to pulmonary vasoconstriction and hypoxia.[4,6] The severity of the chemical insult depends on the burned products, which may include hydrogen cyanide, hydrochloric acid, sulfuric acid, or aldehydes. These compounds initially induce mucosal hyperemia, but as long as the carbon particles containing the chemical remain on the mucosal surface, they can cause severe inflammation and mechanical pressure resulting in peribronchial edema or mucosal sloughing and necrosis. The damage to respiratory mucosal epithelium also results in decreased mucociliary transport and clearance of bacteria or foreign material in the airways.[4,6]

**JPC Diagnosis:** Pharyngeal and laryngeal mucosa: Necrosis, multifocal to coalescing, with marked edema and numerous aggregates of carbon particles.

**Conference Comment:** Conference participants found tissue identification somewhat difficult, as much of the respiratory epithelium has been effaced by necrosis. Discussion centered on classification and morphology of direct thermal injury. Direct thermal burns are classified into the following categories based on the depth of their involvement: superficial burns are restricted to the epidermis; partial thickness burns involve the dermis; and in full thickness burns there is damage to subcutaneous tissue or underlying muscle tissue. Grossly, partial-thickness burns are pink, blistered, and painful; whereas full thickness burns are white, charred, and non-painful due to the destruction of nerve endings in the tissue. As seen in this case, thermal burns are characterized histologically by coagulative necrosis that is often sharply demarcated from vital tissue.[3]

Conference participants also discussed the phases of injury associated with smoke inhalation, noting that during the early phase (first 24 hours) of smoke inhalation, there is acute pulmonary insuffiency due to bronchoconstriction and upper airway damage. This is followed within the next 24 to 72 hours by the middle phase, characterized by the development of pulmonary edema and laryngeal reflux. The pulmonary edema obstructs nasal passages and can lead to pneumonia. During the late phase, bronchopneumonia develops and worsens due to several factors, including the loss of protective barriers such as mucociliary clearance and surfactant as well as the blockage of effective inflammatory response owing to compromised blood flow in the area.[3]

**Contributing Institution**: Purdue University
Animal Disease Diagnostic Laboratory: http://www.addl.purdue.edu/
Department of Comparative Pathobiology: http://www.vet.purdue.edu/cpb/
Purdue University Department of Comparative Pathobiology
725 Harrison St.
West Lafayette, IN 47907

**References:**

1. Hanson RR. Management of burn injuries in the horse. *Vet Clin North Am Equine Pract.* 2005;21:105-123.
2. Kirkland KD, Goetz TE, Foreman JH, Francisco C, Baker GJ. Smoke inhalation injury in a pony. *J Vet Emerg Crit Care. 1993;* 3:83-89.
3. Kumar V, Abbas AK, Fausto N, Aster JC. Environmental and nutritional diseases. In: Kumar V, Abbas AK, Fausto N, Aster JC, eds. *Robbins and Cotran Pathologic Basis of Disease*. 8th ed. Philadelphia, PA: Saunders Elsevier; 2010: 421-422.
4. Marsh PS. Fire and smoke inhalation injury in horses. *Vet Clin North Am Equine Pract.* 2007;23:19-30.
5. McFarlane D. Smoke inhalation injury in the horse. *J Equine Vet Sci.* 1995;15(4):159-162.
6. Norman TE, Chaffin MK, Johnson MC, et al. Intravascular hemolysis associated with severe cutaneous burn injuries in five horses. *J Am Vet Med Assoc.* 2005;226(12):2039-2043.

**CASE II**: TP 11 089 (JPC 4020070).

**Signalment:** 1.5-year-old male non-castrated colony beagle, dog (*Canis familiaris)*.

**History:** The dog was received from the provider when it was eight months old. Until the onset of clinical signs, it was never part of a toxicology study. One month before euthanasia, this dog presented with bloody stool, which was refractory to metronidazole and fenbendazole. Colonoscopy revealed multiple erosive lesions in distal colon.

**Gross Pathologic Findings:** Body condition was thin. There were small amounts of adipose tissue in the subcutis and abdomen. Mesenteric and submandibular lymph nodes were slightly enlarged and red. The cecum had numerous, sometimes coalescing, 0.3 to 0.6 cm diameter erosions-ulcers in the mucosa. Similar findings were observed in the distal colon, 5 to 12 cm cranial to the anus, where the mucosa was thickened, reddened and numerous 0.3 to 0.8 cm erosions-ulcers were present.

**Histopathologic Description:** Multifocally expanding the mucosa of the colon, separating mucosal crypts and extending into the submucosa, there is a dense inflammatory infiltrate composed of large numbers of macrophages and fewer neutrophils, and occasional lymphocytes and plasma cells. These macrophages have abundant eosinophilic cytoplasm and occasionally contain pale eosinophilic, variably sized vacuoles, bacillary bacteria or cellular debris in the cytoplasm. Along the mucosal surface, there are multiple erosions of the epithelium, with the presence of numerous bacillary bacteria, and associated with necrotic cellular debris in the mucosal and apical lamina propria. Colonic crypts are often dilated with desquamated and necrotic cellular debris, and lined by flattened epithelium. Additionally, there are focal hemorrhages at the apical portion of the mucosa. Numerous foamy macrophages are separating the basal crypts from the muscularis mucosa and are present in the submucosa, surrounding mucosa associated lymphoid tissue. Frequently in the crypts, there are numerous spirochetes.

In the cecum (not submitted), findings are similar as described above.

Macrophages infiltrating the colonic mucosa and submucosa are PAS-positive (data not shown). Immunohistochemical stains using polyclonal anti-*Escherichia coli* antibody highlighted numerous bacillary bacteria present free in the upper lamina propria and in the cytoplasm of macrophages.

**Contributor's Morphologic Diagnosis:** Colon and cecum: Marked, multifocal to coalescing, chronic histiocytic typhlocolitis, with intralesional *Escherichia coli*.

**Contributor's Comment:** Canine histiocytic ulcerative colitis is an idiopathic, probably multifactorial, inflammatory condition of the cecum, colon and rectum of dogs. This condition was first described by Van Kruiningen et al. (1965),[9] after observing chronic hemorrhagic diarrhea in a Boxer colony, which was characterized as a granulomatous colitis with resemblance to Whipple's disease. Subsequent reports led to the use of the term of canine histiocytic ulcerative colitis (CHUC), which has since gained general acceptance.[6] CHUC has been distinctively recognized in Boxers and the related French bulldogs. Nevertheless, this condition has also

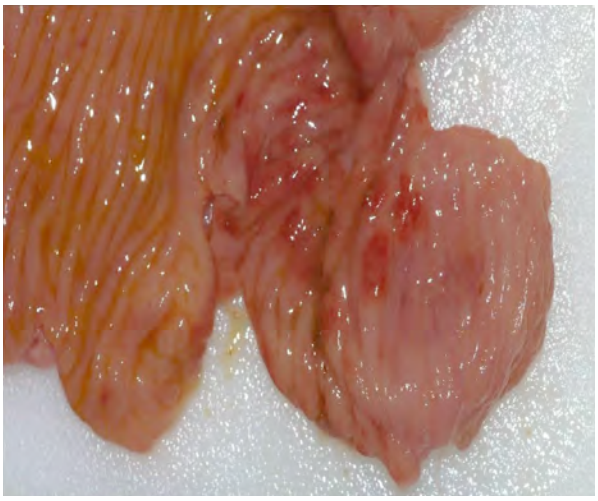

*2-1. Cecum, dog: The cecum had numerous, sometimes coalescing, 0.3 to 0.6 cm diameter erosions/ulcers in the mucosa. (Photo courtesy of: Pfizer Inc., Global Research and Development, Groton/New London Laboratories, Eastern Point Road MS 8274-1330,Groton, CT (www.pfizer.com)*

*2-2. Colon, dog: Similar findings were observed in the distal colon, 5 to 12 cm cranial to the anus, where the mucosa was thickened, reddened and numerous 0.3 to 0.8 cm erosions-ulcers were present. (Photo courtesy of: Pfizer Inc., Global Research and Development, Groton/New London Laboratories, Eastern Point Road MS 8274-1330,Groton, CT (www.pfizer.com)*

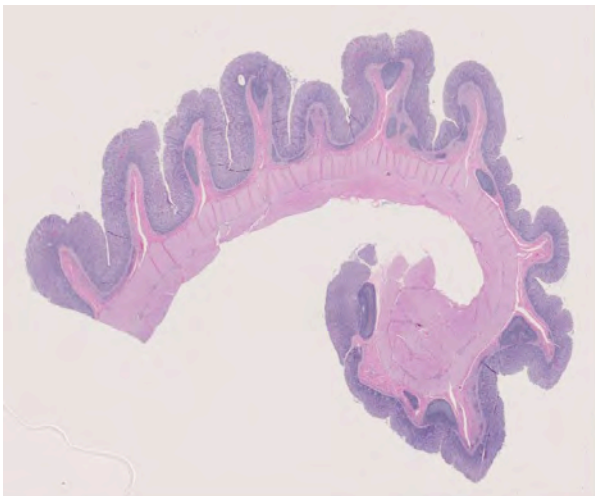

*2-3. Colon, dog: The colonic mucosa is moderately thickened, and a thick band of histiocytes expands the mucosa, separating glands, and the submucosa, surrounding and separating lymphoid tissue. (HE 140X)*

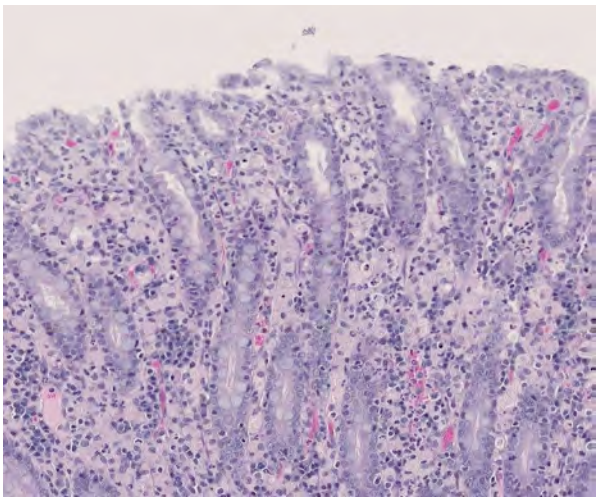

*2-4. Colon, dog: The multifocally eroded mucosa is expanded by moderate numbers of foamy histiocytes and fewer neutrophils which separate mucosal glands. (HE 240X)*

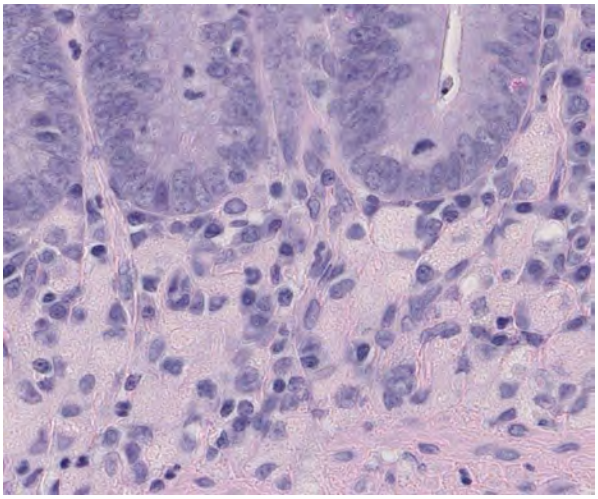

*2-5. The submucosa is expanded by a thick layer of histiocytes ranging up to 20 µm with abundant granular cytoplasm. The overlying crypts are hyperplastic as shown by numerous mitotic figures (HE 400X)*

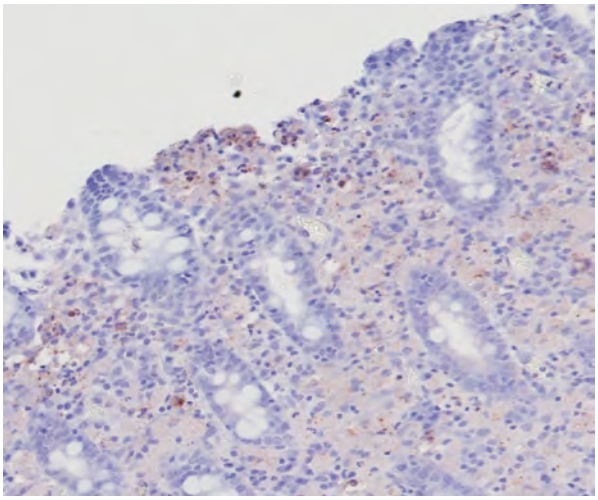

*2-6. Colon, dog: Immunohistochemical stains using polyclonal anti-Escherichia coli antibody highlighted numerous bacillary bacteria present free in the upper lamina propria and in the cytoplasm of macrophages. (Photo courtesy of: Pfizer Inc., Global Research and Development, Groton/New London Laboratories, Eastern Point Road MS 8274-1330,Groton, CT www.pfizer.com)*

been described in a Doberman pinscher, a Mastiff and one Alaskan malamute.[7] Here, we report the first case of CHUC in a colony Beagle dog.

Grossly, the colon of affected dogs is thickened, folded and perhaps dilated, with focal areas of scarring. On the mucosa, the lesion varies from red, frequently raised areas to patchy or coalescing ulcers. Histologically, it is characterized by a dense inflammatory infiltrate in the mucosa and submucosa, composed mainly by large numbers of foamy, PAS-positive macrophages which contain phagocytized necrotic cellular debris and bacteria. Additionally, there is distortion of the normal glandular architecture and decreased numbers of goblet cells. Ulceration, which does not progress beyond the submucosa, arises from the superficial epithelial erosion and destruction of the basement membrane.[1] Resultant clinical signs consist of large bowel diarrhea, tenesmus, hematochezia and marked weight loss.[4]

The inflammatory infiltrate of the colonic mucosa and submucosa was further characterized in an immunohistochemical study. German et al (2000) found increased IgG plasma cells, plus PAS, CD3, L1 and MHC class II positive cells in the lamina propria, in conjunction with increased enterocyte MHC II class expression, and decreased goblet cell numbers in the epithelium. These findings are similar to those of human ulcerative colitis and might suggest a similar pathogenesis at a cellular level.[3]

The exact cause of this condition remains unknown, and a multi-factorial etiology is highly suspected. In an ultrastructural study, it was concluded that CHUC was probably caused by a lipid-rich, ribosome-rich, coccoid to coccobacillary organism that possesses a cell membrane and range from 100 to 500 nm in size. This agent was suspected to be a *Chlamydia*-like organism.[10] In more recent reports, the infectious agent hypothesis was again brought to attention, since dogs completely recover after treatment with enrofloxacin.[2,4] In one study, there was demonstration of *E. coli* in 100% of the examined colonic samples with a polyclonal antibody, strongly associating this organism to the disease. In the same study, there was a comparison of this entity with granulomatous leptomeningitis of Beagle dogs, and malakoplakia and xanthogranulomatous cholecystitis in man, in which *E. coli* has also been incriminated, together with abnormal lysosomal function.[11] In 2009, Mansfield et al. observed remission of CHUC in Boxer dogs in correlation with the eradication of invasive intramucosal *E. coli*, further supporting the causal involvement of *E.coli* in the development of the disease in susceptible Boxer dogs.[5]

**JPC Diagnosis:** Colon: Colitis, histiocytic, multifocal, moderate, with glandular hyperplasia.

**Conference Comment:** In addition to reviewing the contributor's excellent summary of canine histiocytic ulcerative colitis (CHUC), conference participants discussed the use of the term "histiocytic" versus "granulomatous," noting that "histiocytic" is preferred in this condition, as the lesions lack the epithelioid macrophages and multinucleated giant cell macrophages that are characteristic of granulomatous inflammation. The comparison between human inflammatory bowel disease (IBD), which encompasses both Crohn's disease and ulcerative colitis, and CHUC is interesting. Human IBD is thought to be the result of a combination of defects affecting the host's interaction with intestinal microbes as well as intestinal epithelial dysfunction and abnormal immune responses.[8] Additionally, in humans, Crohn's disease is thought to be associated with a TH-1 response; whereas ulcerative colitis has been suggested to be a TH-2 mediated disease.[8] This may not be clear-cut, however, as polymorphisms of the IL-23 receptor have been shown to be protective against both Crohn's disease and ulcerative colitis, suggesting there may also be involvement of a TH-17 response in both conditions. Furthermore, anti-TNF therapy has been effective in some human patients with ulcerative colitis, indicating that a TH-1 response may play a role in ulcerative colitis as well.[8] As the contributor notes, similar to IBD in humans, a multifactorial etiology is suspected in CHUC, although neither has yet to be fully elucidated. Participants noted some slide variation with some slides exhibiting crypt abscesses and/or crypt herniation absent in other slides.

**Contributing Institution**: Pfizer Inc.

Global Research and Development
Groton/New London Laboratories
Eastern Point Road MS 8274-1330
Groton, CT
Phone: 860-441-4498
www.pfizer.com

**References:**

1. Brown CC, Baker DC, Barker IK. Alimentary system. In: Maxie MG, ed. *Jubb, Kenedy and Palmer's Pathology of Domestic Animals*. 5th ed. Vol 2. Philadelphia, PA: Elsevier; 2007:112-114.
2. Davies DR, O'Hara AJ, Irwin PJ, Guilford WG. Successful management of histiocytic ulcerative colitis with enrofloxacin in two Boxer dogs. *Aust Vet J*. 2004;82:58-61.
3. German AJ, Hall EJ, Kelly DF, Watson ADJ, Day MJ. An immunohistochemical study of hisitiocytic ulcerative colitis of Boxer dogs. *J Comp Path*. 2000;122:163-175.
4. Hostutler RA, Luria BJ, Johnson SE, Weisbrode SE, Sherding RG, Jaeger JQ, et al. Antibiotic-responsive histiocytic ulcerative colitis in 9 dogs. *J Vet Intern Med*. 2004;18:499-504.
5. Mansfield CS, James FE, Craven M, Davies DR, O'Hara AJ, Nicholls PK, et al. Remission of Histioytic ulcerative colitis in boxer dogs correlates with eradication of invasive intramucosal Escherichia coli. *J Vet Intern Med.* 2009;23:964-969.
6. Sander CH, Langham RF. Canine histiocytic ulcerative colitis. A condition resembling Whipple's disease, colonic histiocytosis and malakoplakia in man. *Arch Pathol*. 1968;85:94-100.
7. Stokes JE, Kruger JM, Mullaney T, Holan K, Schall W. Histiocytic ulcerative colitis in three non-boxer dogs. *J Am Anim Hosp Assoc*. 2001;37:461-465.
8. Turner JR. The Gastrointestinal tract. In: Kumar V, Abbas AK, Fausto N, Aster JC, eds. *Robbins and Cotran Pathologic Basis of Disease.* 8th ed. Philadelphia PA: Saunders Elsevier; 2010:807-813.
9. Van Kruiningen HJ, Montali RJ, Strandberg JD, Kirk RW. A granulomatous colitis of dogs with histologic resemblance to Whipple's disease. *Path Vet*. 1965;2:521-544.
10. Van Kruiningen HJ. The ultrastructure of macrophages in granulomatous colitis of Boxer dogs. *Vet Pathol.* 1975;12:446-459.
11. Van Kruiningen HJ, Civco IC, Cartun RW. The comparative importance of E. coli antigen in granulomatous colitis of Boxer dogs. *APMIS*. 2005;113:420-425.

**CASE III**: 1/10 (JPC 3165170).

**Signalment:** 8-year-old female spayed German shepherd dog, *Canis familiaris*.

**History:** The dog developed acute weakness and vomiting. On clinical examination, the dog presented with pale mucous membranes, superficial breathing and abdominal distension. Abdominal radiographs revealed a moderate abdominal effusion. Cytology of abdominal fluid contained elevated numbers of red blood cells and rare mesothelial reactive cells, suggestive of hemoperitoneum. On exploratory laparotomy a primary splenic ruptured mass was observed and splenectomy was performed. The mass was diagnosed as hemagiosarcoma by histology. To prevent metastatic spread, post-operative chemotherapy with a combination protocol of doxorubicin and cyclophosphamide administered every 3 weeks for a total of 6 treatments was administered after suture removal. The cumulative dose of doxorubicin was lower than 240 mg/m². After the sixth treatment the dog was referred for sudden onset of general weakness. Heart failure with atrial fibrillation rapidly followed and the animal died spontaneously.

**Gross Pathologic Findings:** At necropsy severe dilation of left and right ventricles was observed. The myocardial wall was generally paler than normal with thin, white, longitudinal streaks beneath the epicardium. Mild pulmonary edema and hyperemia of major internal organs were present. The entire heart was collected for histopathology.

**Laboratory Results:** Complete blood count, liver and renal panels and electrocardiography were performed before each treatment. All parameters were within normal limits for the entire duration of chemotherapy.

**Histopathologic Description:** Sections from the ventricular free walls, interventricular septum, and left papillary muscle are provided. All samples provided have similar changes with variable severity: randomly distributed, degenerated cardiomyocytes are present single or in groups admixed with morphologically normal myocytes. Single cells or small groups of cardiomyocytes are characterized by intracytoplasmic, one to multiple, smooth-contoured, empty vacuoles ranging from 4 to 36 μm in diameter (vacuolar degeneration-Adria cells). In these cells, when visible, the nucleus is displaced to the periphery. Occasionally, scattered myocytes contain a perinuclear area of homogenous, pale eosinophilic cytoplasm, with loss of central cross striations (myofibril loss, myocytolysis). Scattered hypereosinophilic, angulated myocytes and fragmented myofibers are also evident. Cardiomyocytes are multifocally separated by mild interstitial edema and occasional microhemorrhages. Areas of myocardial fibrosis with minimal numbers of lymphocytes and plasma cells may be present in some sections.

**Contributor's Morphologic Diagnosis:** Moderate, multifocal chronic myocardial vacuolar degeneration and mild chronic interstitial edema and fibrosis.

**Contributor's Comment:** Myocardial vacuolar degeneration ("Adria" cells), myocytolysis, interstitial edema and fibrosis are considered characteristic findings of doxorubicin-induced cardiomyopathy.[6,8] Doxorubicin (DOX) is known to be a dose-limiting cardiotoxic compound able to induce an irreversible dilated cardiomyopathy in several species including canine and human.[1,3,5] Congestive heart failure and death have been documented during the treatment but also months after the completion of chemotherapy in many species. Despite its toxicity, DOX is largely used alone or in combination in order to treat several neoplastic entities including hemangiosarcoma in dogs.[6] In humans, the incidence of DOX-induced cardiomyopathy is approximately 1.7% and the mortality rate once dilation is initiated reaches 50% of patients.[8]

Toxicity is related to the total cumulative dose administered, as well as to the acute peak concentration levels of the compound. Increased risk of DOX cardiotoxicity has also been correlated with young age, concurrent administration of additional chemotherapy compounds and viral diseases. Retrospective studies of human patients have revealed that more than 4% of patients who receive a cumulative dose of 500-550 mg per square meter of surface area develop congestive heart failure. The incidence rises to more than 18% over 551-600 mg/m².[8] Based on several clinical studies limiting the cumulative dose to less than 450 mg/m² is the best line of defense against DOX cardiotoxicity. Alternative methods have been the concurrent administration of antioxidants, iron chelators, use of DOX analogues. However, none of the approaches have had major success. Recently, combined administration of the hematopoietic cytokines EPO, G-CSF and TPO has prevented DOX cardiomyopathy in animal models.[8] In this dog, a standard chemotherapy protocol for canine hemangiosarcoma with a cumulative dose of DOX lower than 240 mg/m² (recommended to minimize chronic cardiac toxicity) was used.[3] Myocardial vacuolization is described in early and chronic toxicity with a wide range of and from 122 to 265 mg/ m² body surface area (BSA) in clinical cases.[3] The overall cumulative dose causing fatal cardiomyopathy is therefore controversial, and dogs are generally considered more sensitive to cardiotoxic effects of doxorubicin than humans, where cardiomyopathy and congestive heart failure are reported to occur at a total dose greater than 550mg/ m² BSA.[2]

Prognosisis very poor in human patients that develop cardiomyopathy within four weeks after administration of

DOX and the majority die within two weeks after onset of symptoms.[8] Among long survivors after DOX therapy, several develop heart failure six to ten years after conclusion of chemotherapy. The late-onset cardiotoxic effects of conventional anthracycline therapy highlight the need of lifelong monitoring the cardiac status in human patients. Several techniques (i.e. radionuclide angiography assessment of left ventricular ejection fraction, electrocardiography and echocardiographically derived ejection fraction) have been proven to be poor indicators of early changes and subclinical myocardial injury.[3,8] Serial endomyocardial biopsies are currently considered the most sensitive and specific indicators of doxorubicin-induced injury.[8] Biopsies are examined by electron microscopy and graded applying a semiquantitative scoring system[1] based on the percentage of myocytes affected by myofibrillar loss and cytoplasmic vacuolization. Ultramicroscopic markers including myofibril loss, retention of sarcoplasmic reticulum and cytoplasmic vacuolation are utilized to grade injury on a scale of 1 to 3; biopsy samples in which fewer than 5% of cells have typical changes are given a grade 1 while those with changes over 36% are graded 3, the highest severity.[8] This grading shows a linear correlation with left ventricular function determined by radionuclide angiocardiography and is helpful for clinical determination of continuation of DOX therapy.[8]

In veterinary medicine, no sensitive predictor tests are currently available to monitor patients treated with doxorubicin. Herman and co-workers (1981) observed that plasma enzymes CPK (creatine phosphokinase), LDH (Lactate Dehydrogenase) and SGOT (Serum Glutamic Oxaloacetic Transaminase) were not reliable indicators of slowly progressive cardiac damage. Similarly to human patients, sequential echocardiograms and EKGs (electrocardiogram) are not considered sensitive predictors for canine cardiomyopathy since no consistent correlation between the severity of rhythm disturbance and the pathologic myocardial changes have been observed.[2] Myocardial biopsies in dogs, although not routinely performed due to their invasiveness, have been experimentally proven to be a sensitive test to monitor the early doxorubicin-associated cardiotoxicity.[7]

Because DOX cardiotoxicity is dose dependent, it has been used to experimentally induce heart failure in different animal species such as dog, sheep, goats and rodents.[5] DOX is delivered by intravenous and intracoronary injections at small doses to induce heart failure without systemic toxicity. Experimental DOX heart failure develops via bilateral enlargement, ventricular wall thinning with decreased cardiac output. This model has been utilized to study several treatments for cardiac failure however the model has several limitations: the degree of left ventricular dysfunction varies, is characterized by high incidence of arrhythmias, high cost of multiple intracoronary injections and the irreversible and progressive heart damage.[5]

The mechanism of action of DOX and other antracycline compounds on tumor cells are still a matter of controversy. Suggested mechanisms are: intercalation into the DNA molecule leading to inhibition of transcription, generation of reactive oxygen species leading to lipid peroxidation and DNA damage, DNA binding and alkylation, DNA cross-linking, interference with DNA unwinding and helicase activity, inhibition of topoisomerase II and induction of apoptosis.

Anthracycline compounds including DOX, produce reactive oxygen species (ROS) interacting with mitochondrial enzymes. ROS are produced in vitro by high concentration of DOX that binds to iron forming DOX-iron complexes that bind to DNA and induce production of partially reduced oxygen compounds. These radicals can damage DNA via strand break formation. However, high concentrations of DOX seem necessary and antioxidant compounds do not diminish DOX cytotoxicity.[8]

The mechanism of DOX-cardiomyopathy remains unclear but seems different from the one underlying DOX's anti-tumour activity. Most studies support the view that increase in oxidative stress evidenced by increases in ROS and lipid peroxidation play a key role along with reduction in antioxidant levels and sulfhydryl groups.[3,6] Other associated mechanisms proposed have been: inhibition of protein and DNA synthesis, lysosomal and mitochondrial changes, alteration of sarcolemmal Ca2+ transport, attenuation of adenylate cyclase, ATPase activities, imbalance in myocardial electrolytes and several others.[8] Also, DOX downregulates the expression of cardiac-specific genes including contractile proteins (alpha-actinin, myosin light and heavy chains, troponin I, desmin), and sarcoplasmic reticulum proteins. The reduction of myocardial contractility can be directly associated with reduction in muscle proteins. DOX additionally induces apoptosis of endothelial cells and cardiomycytes contrary to its cystostatic effect in tumor cells. This latest mechanism seems related to p53 activation. However, the role of apoptotic pathways in DOX cardiotoxicity is still controversial.[8]

Transcriptional profiling via genome wide transcriptome analysis has been utilized to determine early cardiac response to DOX in a rat model perfused with DOX leading only to mild cardiac dysfunction.[9] The main characteristics of cardiomyocyte reprogramming were the repression of transcripts involved in cardiac stress response and stress signaling, modulation of genes with cardiac remodeling capacity and upregulation of energy related pathways. This latest research supports the hypothesis that blunted response to stress and reduced

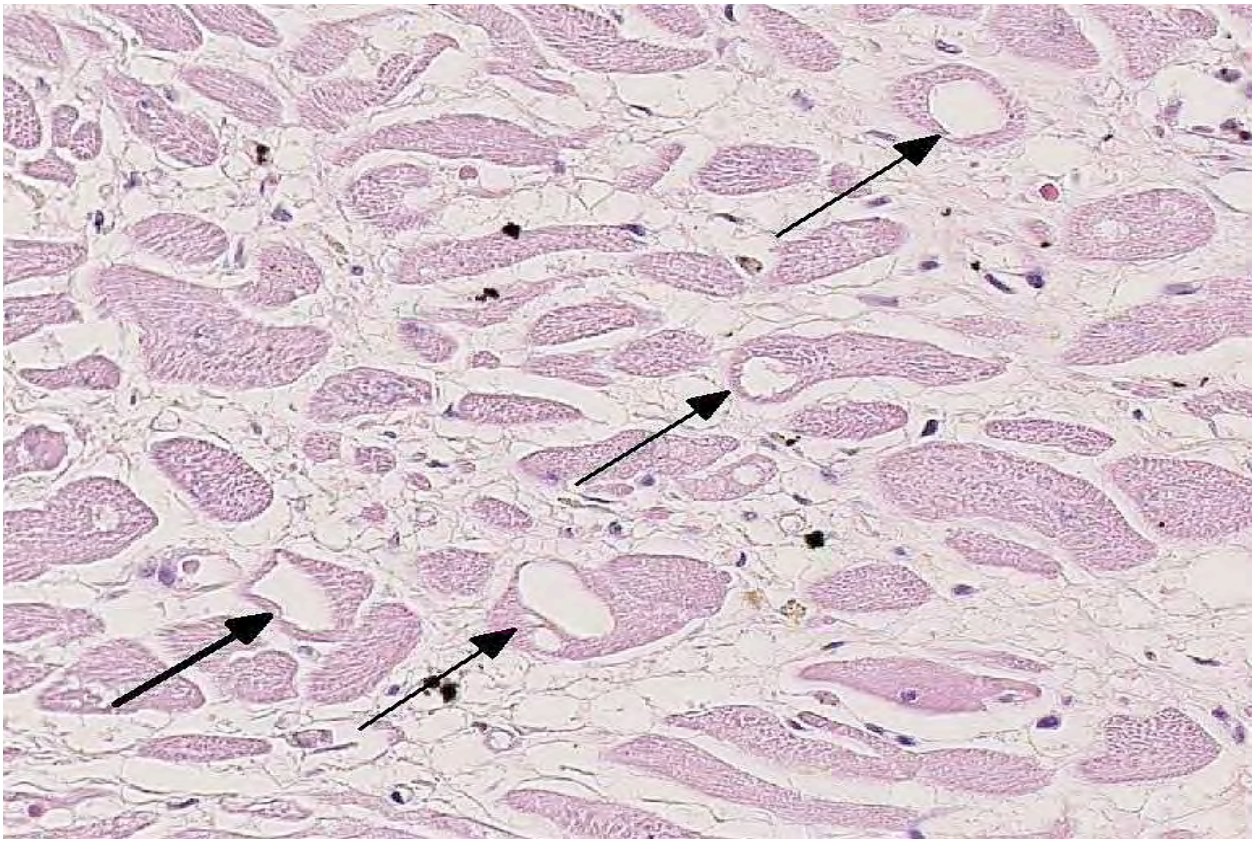

*3-1. Heart, dog: Scattered throughout the mildly edematous myocardium, occasional myocytes contain one to multiple discrete clear vacuoles ("adria cells"). (HE 240X)*

"danger signalling" are prime components of DOX toxicity and can drive to cardiomyocyte damage.[9]

**JPC Diagnosis:** Heart, cardiomyocytes: Degeneration, multifocal, mild, with intracytoplasmic vacuolation and rare myocardial fibrosis.

**Conference Comment:** The contributor provides an excellent review of doxorubicin cardiotoxicity. Conference participants discussed the severity of the lesions in this section, favoring the term "mild" to describe both the vacuolar degeneration and fibrosis. This spurred a discussion of the general correlation of clinical cardiac disease and severity of myocardial injury as observed histologically. This correlation is often poor, as a small lesion at a critical site within the heart can lead to death, while even more extensive lesions, if not affecting a critical area, are sometimes asymptomatic. Furthermore, it is not uncommon for animals that die peracutely from cardiac failure to show no detectable microscopic abnormalities.[5]

**Contributing Institution:** Dipartimento di Patologia Animale, Igiene e Sanita' Pubblica Veterinaria
Sezione di Anatomia Patologica e Patologia Aviare
Facolta' di Medicina Veterinaria
Milano - Italy
http://www.anapatvet.unimi.it/

**References**

1. Billingham ME, Bristow MR. Evaluation of anthracycline cardiotoxicity: predictive ability and functional correlation of endomyocardial biopsy. *Cancer Treatment Symposia*. 1984;3:71-76.
2. Gralla EJ, Fleischman RW, Luthra YK, Stadnicki SW. The dosing schedule dependent toxicities of adriamycin in beagle dogs and rhesus monkeys. *Toxicology*. 1979;13:263-73.
3. Mauldin GE, Fox PR, Patnaik AK, Bond BR, Money SC, Matus RE. Doxorubicin-induced cardiotoxicosis. Clinical features in 32 dogs. *J Vet Inter Med*. 1992;6:82-88.
4. Miller LM, Van Vleet JF, Gal A. Cardiovascular system and lymphatic vessels. In: Zachary JF, McGavin MD, eds. *Pathologic Basis of Disease*. 5th ed. St Louis, MO: Elsevier Mosby; 2012:555.
5. Monnet E, Chachques JC. Animal models of heart failure: what is new? *Ann Thorac Surg*. 2005;79:1445-1453.
6. Ogilvie GK, Powers BE, Mallinckrodt CH, Withrow J. Surgery and doxorubicin in dogs with hemangiosarcoma. *J Vet Intern Med*, 1996;10:379-84.
7. Sparano BM, Gordon G, Hall C, Iatrapoulos MJ, Noble JF. Safety assessment of new anticancer compound,

mitoxantrone, in Beagle dogs: comparison with doxorubicin. II. Histologic and ultrastructural pathology. *Cancer Treat Rep*. 1982;66:1145-1158.
8. Takemura G, Fujiwara H. Doxorubicin-induced cardiomyopathy from the cardiotoxic mechanisms to management. *Prog Cardiovasc Dis*. 2007;49:330-352.
9. Tokarska-Schlattner M, Lucchinetti E, Zaugg M, Kay L, Gratia S, Guzun R, et al. Early effects of doxorubicin in perfused heart: transcriptional profiling reveals inhibition of cellular stress response genes. *Am J Physiol Regul Integr Comp Physiol*. 2010;298: R1075-1088.

**CASE IV:** 09 848 41 (JPC 3164206).

**Signalment**: Young male dog, *Canis familiaris.*

**History**: The dog was inoculated experimentally with *Leptospira interrogans* serovar *icterohaemorrhagiae.* The animal was euthanized for human reasons.

**Histopathologic Description**: The liver is affected by a diffuse and severe lesion which is characterized by a dissociation of hepatocytes and hepatic plates (degeneration with loss of intercellular junction systems). Many hepatocytes have a hypereosinophilic cytoplasm and a karyorrhectic nucleus (individual hepatocyte necrosis). However, a number of hepatocytes are binucleated or show mitotic figures (hepatic proliferation). The sinusoids wall is not visible (endothelial cells lysis) and Kupffer cells show erythrophagocytosis (recent hemorrhages).

In portal tracts, bile ducts are distended by an amphophilic mucinous substance (moderate bile duct mucostasis). The wall of centrolobular veins is infiltrated by a few lymphocytes and neutrophils (discrete lymphocytic and neutrophilic transparietal vasculitis).

**Contributor's Morphologic Diagnosis:** Liver: Hepatitis, degenerative, diffuse, acute, severe, with hepatocytes dissociation and individual necrosis, moderate bile duct mucostasis, and centrolobular discrete lymphocytic and neutrophilic vasculitis.

**Etiology:** *Leptospira interrogans* serovar *icterohaemorrhagiae.*

Special stain: **A Warthin-Starry stain was negative.**

**Contributor's Comment:** Leptospirosis is a zoonosis of worldwide distribution, caused by infection with antigenically distinct serovars of the motile spirochete bacterium *Leptospira interrogans sensu lato*.[2,3,4] Leptospirosis has been identified as one of the emerging infectious diseases.[4] *Leptospira* organisms are thin, flexible, filamentous bacteria made up of fine spirals with hook- shaped ends. More than 200 different serovars have been identified in the *Leptospira interrogans* complex.[3] Canine leptospirosis was first described in 1899. Prior to 1960, serovars *icterohemmorrhagiae* and *canicola* were believed to be responsible for most clinical cases of canine leptospirosis. After a bivalent serovar-specific vaccine against *canicola* and *icterohemmorrhagiae* came into widespread use, the incidence of "classic" leptospirosis in dogs appeared to

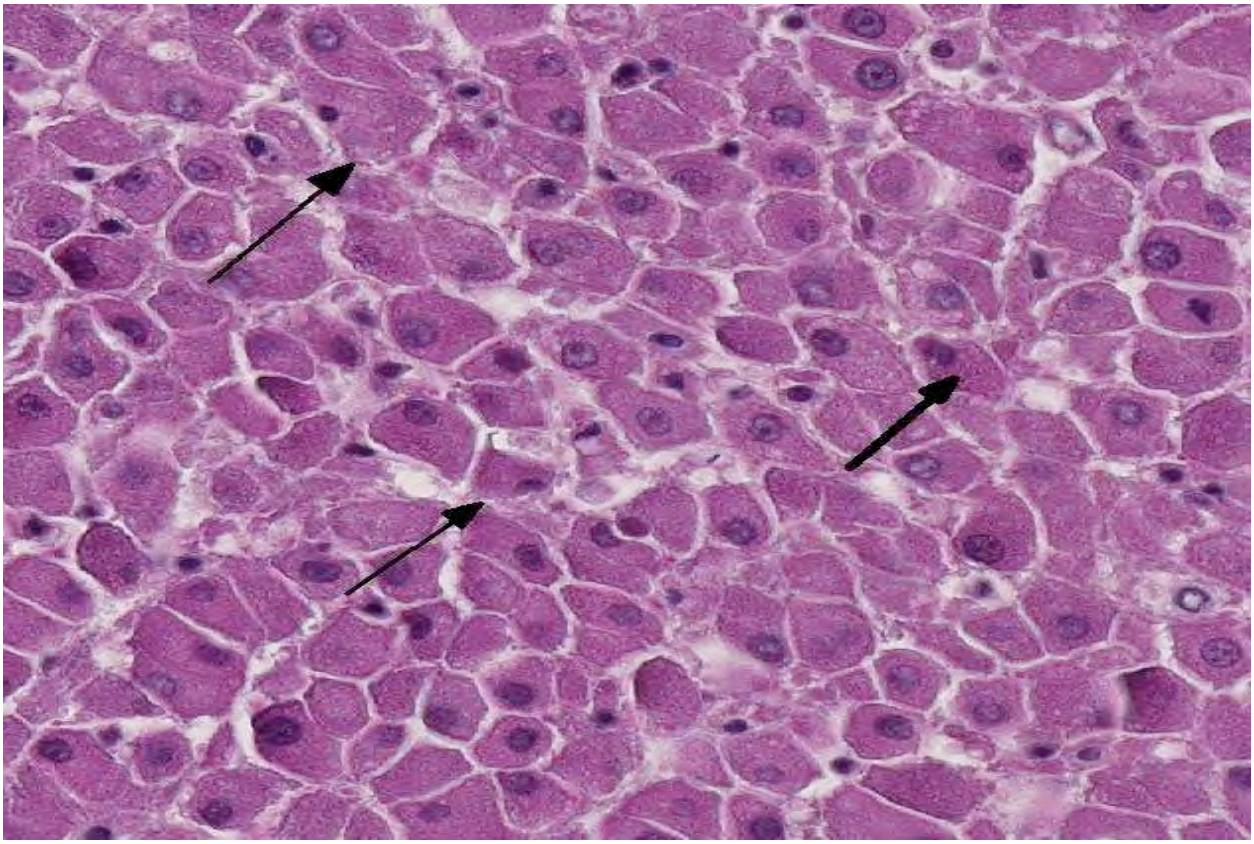

*4-1. Liver, dog: Diffusely throughout the section, there is loss of hepatic plate architecture. Heptaocytes are individualized, rounded up, and exhibit single cell necrosis (smudgy nuclei, pyknosis). (HE 256X)*

have decreased. However, these vaccines did not induce immunity against other serovars, leading to a relative increase in the incidence of disease attributed to other serovars.[3] Leptospirosis can be transmitted directly between hosts in close contact through urine, venereal routes, placental transfer, bites, or ingestion of infected tissues. Recovered dogs can excrete organisms in urine intermittently for months to four years after infection. Indirect transmission happens more often, occurring through exposure of susceptible animals to a contaminated environment (e.g., soil, food or bedding). Water contact is the most common means of spread, and habitats with stagnant or slow moving warm water favor organism survival. Leptospires in contaminated water invade the host through skin wounds or through intact mucous membranes. Once in a susceptible host, leptospires begin to multiply as early as one day after entering the blood vascular space. They invade many organs, including the kidneys, liver, spleen, central nervous system, eyes and genital tract.[3]

Clinical signs associated with leptospirosis vary and depend on the serovar and the host. In maintenance hosts, leptospirosis generally is characterized by a low serological response, relatively mild acute clinical signs, and a prolonged renal carrier state which may be associated with chronic renal disease. In incidental hosts, leptospirosis can cause severe disease, associated with high titers of agglutinating antibody, and has a short or negligible renal carrier state. The clinical signs observed vary with the susceptibility of the host and with the infecting serovar. In general, young animals are more seriously affected than adults.[1,2] Clinical signs reported in dogs with leptospirosis include fever, inappetence, vomiting, abdominal pain, diarrhea, polyuria/polydipsia, myalgia, jaundice, epistaxis, hematuria and reproductive failure.[1,2] Signs of hepatic and renal dysfunction and of coagulation defects usually predominate in dogs with leptospirosis. The severity of clinical signs depends on the age and immunocompetence of the host, the environmental factors affecting the organisms, the serovar involved and its virulence, and the infecting dose. Younger dogs (less than six months) are more severely affected and develop more signs of hepatic dysfunction. A majority of leptospiral infections in dogs are subclinical. The peracute form is characterized by massive leptospiremia, causing shock and often death with few premonitory signs. Less severe infections are characterized by fever, anorexia, vomiting, dehydration, increased thirst and reluctance to move.[3]

Renal colonization occurs in most infected animals because the organism replicates and persists in renal tubular epithelial cells, even in the presence of neutralizing antibodies. Acute impairment of renal function may result from decreased glomerular filtration caused by swelling that impairs renal perfusion. Renal function in some dogs that survive acute infections may return to normal within several weeks, or chronic compensated polyuric renal failure may develop.[3]

The liver is another major organ damaged during leptospirosis. The degree of icterus in both canine and human leptospirosis usually corresponds to the severity of hepatic necrosis. In contrast, the icterus, hemoglobinemia and hemoglobinuria which develop in cattle with leptospirosis result from a specific hemolytic toxin produced by serovar pomona.

Tissue edema and disseminated intravascular coagulation may occur rapidly and result in acute endothelial injury and hemorrhagic manifestations. *Leptospira* lipopolysaccharides stimulate neutrophil adherence and platelet activation, which may be involved in inflammatory and coagulatory abnormalities.[3] Benign meningitis is produced when leptospires invade the CNS; however, it is not as common as in humans. Uveitis is occasionally present. Abortion and infertility resulting from transplacental transmission of leptospires associated with serovar *bataviae* infection have been described. Pulmonary manifestations include labored respiration and coughing. Interstitial pneumonia has been documented as the cause in humans, whereas lung changes in dogs with leptospirosis are associated with pulmonary hemorrhage most likely due to endothelial damage and vasculitis.[3]

Laboratory abnormalities usually include leukocytosis, thrombocytopenia, increased serum urea and creatinine, electrolyte disturbances, bilirubinemia and increased serum hepatic enzyme activities. Coagulation parameters may be altered in severely affected animals. Urinalysis abnormalities include bilirubinuria, sometimes glucosuria, proteinuria and increased numbers of granular casts, leukocytes and erythrocytes in the sediment.[3]

Establishment of a diagnosis is important because animals can serve as reservoirs and pose potential zoonotic risks.[1]

The diagnosis of leptospirosis can be accomplished by several techniques. Detection of antibodies using the microscopic agglutination test (MAT) is the most common diagnostic method; however, other methods to detect antibodies, such as immune- fluorescent assays or enzyme-linked immunosorbent assay (ELISA), have been used.[2,3] Application of silver stains, or immunohistochemical stains to tissue sections are effective for detection of leptospires or leptospiral antigens in the renal tubules and interstitium of the kidney and liver. Low sensitivity is a disadvantage of this diagnostic technique. Leptospires are often present in small numbers in affected tissues, particularly in chronic leptospirosis or in dogs treated with antibiotics.

Serological studies should also be conducted.[2] Bacteriologic culture of blood, urine, or tissue specimens

is the definitive method for the diagnosis of leptospirosis. Leptospiremia occurs early in the clinical course of leptospirosis and is usually of short duration and low level. Therefore, blood is only useful for culture in the first few days of clinical illness and before antibiotic therapy. Leptospires are usually present in the urine of animals with leptospirosis four to ten days after the onset of clinical signs. Culture of leptospires is difficult, time-consuming and requires specialized culture medium. However, isolation of the organism allows definitive identification of the infecting serovar.[2]

The spectrum of human disease caused by leptospires is extremely wide, ranging from subclinical infection to a severe syndrome of multi-organ infection with high mortality.[4] Leptospirosis is presumed to be the most widespread zoonosis in the world. The source of infection in humans is usually either direct or indirect contact with the urine of an infected animal. The incidence is significantly higher in warm-climate countries than in temperate regions; this is due mainly to longer survival of leptospires in the environment in warm, humid conditions.[4]

The clinical presentation of leptospirosis is biphasic, with the acute or septicemic phase lasting about a week, followed by the immune phase, characterized by antibody production and excretion of leptospires in the urine. Most of the complications of leptospirosis are associated with localization of leptospires within the tissues during the immune phase and thus occur during the second week of the illness.[4] A comparison of the prevalence of anti-leptospiral antibodies with the prevalence of clinical signs indicates that subclinical infections are relatively common.[2]

**JPC Diagnosis:** Liver: Hepatitis, necrotizing, multifocal, random, with suppurative cholangitis, severe hepatocellular dissociation and single cell necrosis.

**Conference Comment:** As the contributor states in this interesting review, leptospiruria may persist in an infected animal for months to years. It is believed that down-regulation or differential expression of *Leptospira* antigenic surface proteins and possibly the binding of complement regulatory proteins (i.e. plasma factor H) allow the leptospires to evade the host immune system. Although the virulence factors associated with leptospires have not been fully elucidated, it appears that their toxic components are associated with outer membrane proteins rather than the secretion of specific toxins. Attachment to the host cell is likely mediated by fibronectin-binding protein on the bacterial surface that binds to host extracellular matrix proteins. Infection of the host cell is via receptor-mediated endocytosis. Pathogenic species of *Leptospira* contain sphingomyelinases and other hemolysins, which may play roles in erythrocyte and endothelial cell membrane damage that results in hemolytic anemia, jaundice, hemoglobinuria and hemorrhage observed in acute leptospirosis. Once in the bloodstream, leptospires evade phagocytosis; the mechanism for this is thought to be induction of macrophage apoptosis. Leptospires are cytochemically gram negative bacteria; however, they differ from other gram negative organisms in several ways, including the following: The LPS of leptospires is not as endotoxic as other gram-negative bacteria; and leptospires, unlike other gram negative organisms, activate the host immune response through TLR-2 rather than TLR-4 pathway.

Conference participants discussed the serovars of *Leptospira interrogans* that commonly affect domestic animals and humans. The included chart summarizes these serovars and their hosts (both maintenance and incidental), as well as associated clinical conditions:[4]

* Adapted from Quinn PJ, Markey BK, Leonard FC, Hartigan P, Fanning S, FitzPatrick ES. *Veterinary Microbiology and Microbial Disease*. 2nd ed.

**Contributing Institution:** Ecole Nationale Veterinaire D'Alfort
Unite d'histologie et d'Anatomie Pathologique
7, avenue du General De Gaulle 94704 Maisons-Alfort cedex FRANCE

**References:**

1. Birnbaum N, Barr SC, Center SA, Schermerhorn T, Randolph JF, Simpson KW. Naturally acquired leptospirosis in 36 dogs: serological and clinicopatholoical features. *J. Small Anim. Pract*. 1998;39:231- 236.
2. Bolin CA. Diagnosis of leptospirosis: a reemerging disease of companion animals. *Semin. Vet. Med. Surg*. (Small Anim.) 1996;11:166- 171.
3. Hartmann K, Creene GE. Diseases caused by systemic bacterial infection. In: *Textbook of Veterinary Internal Medicine.* 6th ed. St. Louis, MO: Elsevier Saunders; 2005;616- 619.
4. Levett P. Leptospirosis. *Clin. Microbiol. Rev*. 2001;14: 296- 326.
*Quinn PJ, Markey BK, Leonard FC, Hartigan P, Fanning S, FitzPatrick ES. *Veterinary Microbiology and Microbial Disease.* Ames, IA: Wiley; 2011: *Kindle Edition,* location 13471 of 35051.